

Power Systems

Morteza Nazari-Heris
Somayeh Asadi
Behnam Mohammadi-Ivatloo *Editors*

Planning and Operation of Multi-Carrier Energy Networks

 Springer

Power Systems

Electrical power has been the technological foundation of industrial societies for many years. Although the systems designed to provide and apply electrical energy have reached a high degree of maturity, unforeseen problems are constantly encountered, necessitating the design of more efficient and reliable systems based on novel technologies. The book series Power Systems is aimed at providing detailed, accurate and sound technical information about these new developments in electrical power engineering. It includes topics on power generation, storage and transmission as well as electrical machines. The monographs and advanced textbooks in this series address researchers, lecturers, industrial engineers and senior students in electrical engineering.

****Power Systems is indexed in Scopus****

More information about this series at <http://www.springer.com/series/4622>

Morteza Nazari-Heris • Somayeh Asadi
Behnam Mohammadi-Ivatloo
Editors

Planning and Operation of Multi-Carrier Energy Networks

 Springer

Editors

Morteza Nazari-Heris
Department of Architectural Engineering
Pennsylvania State University
University Park, PA, USA

Somayeh Asadi
Department of Architectural Engineering
Pennsylvania State University
University Park, PA, USA

Behnam Mohammadi-Ivatloo
Faculty of Electrical and Computer
Engineering
University of Tabriz
Tabriz, Iran

Department of Energy Technology
Aalborg University
Aalborg East, Denmark

ISSN 1612-1287

ISSN 1860-4676 (electronic)

Power Systems

ISBN 978-3-030-60085-3

ISBN 978-3-030-60086-0 (eBook)

<https://doi.org/10.1007/978-3-030-60086-0>

© Springer Nature Switzerland AG 2021

This work is subject to copyright. All rights are reserved by the Publisher, whether the whole or part of the material is concerned, specifically the rights of translation, reprinting, reuse of illustrations, recitation, broadcasting, reproduction on microfilms or in any other physical way, and transmission or information storage and retrieval, electronic adaptation, computer software, or by similar or dissimilar methodology now known or hereafter developed.

The use of general descriptive names, registered names, trademarks, service marks, etc. in this publication does not imply, even in the absence of a specific statement, that such names are exempt from the relevant protective laws and regulations and therefore free for general use.

The publisher, the authors, and the editors are safe to assume that the advice and information in this book are believed to be true and accurate at the date of publication. Neither the publisher nor the authors or the editors give a warranty, expressed or implied, with respect to the material contained herein or for any errors or omissions that may have been made. The publisher remains neutral with regard to jurisdictional claims in published maps and institutional affiliations.

This Springer imprint is published by the registered company Springer Nature Switzerland AG
The registered company address is: Gewerbestrasse 11, 6330 Cham, Switzerland

Preface

Nowadays, the high integration rate of interconnecting energy technologies in energy systems has been increased, such as combined heat and power plants, natural gas-fired power plants, power to gas technology, hydropower plants, and water desalination systems. Accordingly, the design and operation of multi-carrier networks should be studied, taking into account the operational and technical constraints of each interconnecting element between energy systems and the network constraints of each energy system. Hence, studying the optimal design and operation of multi-carrier energy networks associated with different kinds of energy carriers such as gas, power, heating, cooling, and water carriers is of great importance for attaining more effective and promising operation of such networks, and has received significant attention of researchers. The operation of multi-carrier energy networks considering various interconnecting elements is improved in different studies regarding economic and environmental viewpoints. The consideration of interconnecting elements in the operation of multi-carrier energy networks is a realistic framework since the constraints of all of the energy networks as well as the interconnecting elements are considered in the operation and design of such systems. Also, the multi-carrier energy storage facilities such as the power to gas systems and pumped storage technology are effective in improving the operation of multi-carrier energy systems because one form of energy can be converted to another form when the load demand is low, and it can be used in supplying the load demand of an energy carrier in on-peak hours. The book *Planning and Operation of Multi-Carrier Energy Networks* aims to discuss the recent developments and contribution of optimal design and operation of multi-carrier energy networks in both aspects of providing a comprehensive review on the title and proposing new models of operation and design of such systems.

The book covers theoretical background and experimental analysis of the multi-carrier energy networks with concentrations on gas, power, heating, cooling, and water carrier, special and professional fields of integrated energy systems. The authors focus on the optimal design and operation of multi-carrier energy systems. Thus, the studied challenging issues in this book can provide effective and promising

solutions for the optimal design and operation of energy systems. The authors try to study the optimal design and operation of multi-carrier energy networks with concentrations on the integration of various energy carriers as well as interconnecting elements between such systems. The application and study cases are selected, with as many realistic cases around the world are investigated. The authors hope the current book helps undergraduate and graduate students, researchers, and engineers, trying to evaluate the concept of multi-carrier energy networks based on theoretical aspects and application case studies. The topics covered in this book are presented in the following:

- Overview on the operation of multi-carrier energy networks
- The role of demand response programs and energy storage facilities in optimal operation of multi-carrier energy networks
- Operation of multi-carrier energy networks by modeling the uncertain parameters
- Introduction to planning and sizing of multi-carrier energy networks
- Network expansion planning of multi-carrier energy systems by modeling the uncertain parameters
- Risk-constrained planning of multi-carrier energy systems

University Park, PA
University Park, PA
Aalborg East, Denmark

Morteza Nazari-Heris
Somayeh Asadi
Behnam Mohammadi-Ivatloo

Contents

1	Introduction and Literature Review of Cost-Saving Characteristics of Multi-carrier Energy Networks	1
	Jaber Fallah Ardashir and Hadi Vatankhah Ghadim	
2	Introduction and Literature Review of the Operation of Multi-carrier Energy Networks	39
	Mehrdad Ghahramani, Milad Sadat-Mohammadi, Morteza Nazari-Heris, Somayeh Asadi, and Behnam Mohammadi-Ivatloo	
3	An Optimal Operation Model for Multi-carrier Energy Grids	59
	Mohammad Saadatmandi, Seyed Mehdi Hakimi, and Pegah Bahrevar	
4	Energy Markets of Multi-carrier Energy Networks	87
	Seyed Mahdi Kazemi-Razi and Hamed Nafisi	
5	Optimal Operation of Multi-carrier Energy Networks Considering Demand Response Programs	121
	Mehrdad Setayesh Nazar and Alireza Heidari	
6	Optimal Scheduling of Hybrid Energy Storage Technologies in the Multi-carrier Energy Networks	143
	Morteza Zare Oskouei, Hadi Nahani, Behnam Mohammadi-Ivatloo, and Mehdi Abapour	
7	A Decomposition-Based Efficient Method for Short-Term Operation Scheduling of Hydrothermal Problem with Valve-Point Loading Effects	159
	Elnaz Davoodi and Behnam Mohammadi-Ivatloo	

8	Optimal Scheduling of Electricity-Gas Networks Considering Gas Storage and Power-to-Gas Technology	179
	Amir Talebi and Ahmad Sadeghi-Yazdankhah	
9	Uncertainty Modeling in Operation of Multi-carrier Energy Networks	195
	Manijeh Alipour, Mehdi Jalali, Mehdi Abapour, and Sajjad Tohidi	
10	Optimal Planning and Design of Multi-carrier Energy Networks	209
	Hamid HassanzadehFard, Arezoo Hasankhani, and Seyed Mehdi Hakimi	
11	Risk-Constrained Generation and Network Expansion Planning of Multi-carrier Energy Systems	235
	Mehrdad Setayesh Nazar and Alireza Heidari	
12	Uncertainty Modeling in Operation of Multi-carrier Energy Networks	257
	Mohammad Salehimaleh, Adel Akbarimajd, Khalil Valipour, and Abdolmajid Dejamkhooy	
13	Network Expansion Planning of Multi-carrier Energy Systems	339
	Fazel Mohammadi	
	Index	361

Chapter 1

Introduction and Literature Review of Cost-Saving Characteristics of Multi-carrier Energy Networks



Jaber Fallah Ardashir and Hadi Vatankhah Ghadim

1.1 Introduction

Economics has always been one of the most important factors in human-made systems which are directly related to different communities and groups in society. From costs of design, execution, operation, and planning of systems to challenges in grids like energy wastages, low efficiency, and inevitable costs of outages at any level, all are considered in the economic analysis of an energy system. Efforts on decreasing these costs while maintaining and enhancing other parameters of the system like stability, reliability, and resiliency have continued since the appearance of these systems until now.

With a closer look at the shares of different fuels participating in electricity generation, we can see that natural gas, coal, and nuclear energy are currently keeping the highest share in energy generation systems. After them, wind and hydropower, biomass, solar, petroleum, and other supplies are used in the system [1]. Due to the percentages of participation mentioned in Fig. 1.1, we can easily understand that natural gas is currently the most popular fuel for energy generation and that is why most of the energy hubs are usually integrated with the gas network [2]. The reason will be explained in the upcoming sections. But what is important is that coal and petroleum fuels had a decreasing trend of penetration in energy supply in recent years, reducing from 48% in 2008 to 27% in 2018 for coal and from 1.12% in 2008 to 0.6% in 2018 for petroleum. With the appearance of eco-friendly multi-carrier systems, this trend can go down even faster, creating an ideal vision of a green energy system.

Multi-carrier energy systems (MESs) are an innovative solution for solving a different variety of problems that are currently present in energy networks. Cost-

J. Fallah Ardashir (✉) · H. Vatankhah Ghadim
Department of Electrical Engineering, Tabriz Branch, Islamic Azad University, Tabriz, Iran
e-mail: j.fallah@iaut.ac.ir; stu.hadivghadim@iaut.ac.ir

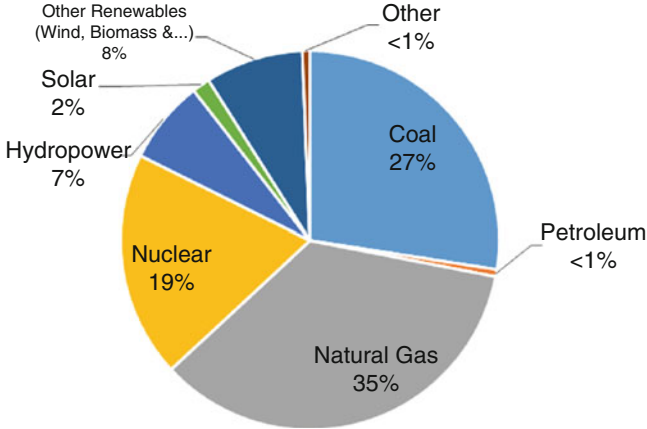


Fig. 1.1 Renewable energy share in the United States—2018 [1]

saving specifications of MES have always been considered a trending subject in studies and as a great compelling economic reason for planning and implementing this system.

1.2 Alternative Resources and Supply-Side Technologies

Conventional power plants that usually work with fossil fuels might seem suitable for electric energy systems because of their low-cost fuels but the harm that they cause to the environment and challenges they create in urban design have made them no more rational choices. Besides, innovations in renewable power units and studies on new approaches in maintaining the power we need have shown us a new path to the future of the energy systems. In this section, different solutions are discussed and their probable role in MES is considered economically.

1.2.1 Renewable Energy Resources (Solar, Wind, Geothermal, Biomass)

To understand the difference which implementing renewables will make in energy economics, a comparison between the cost of renewables and non-renewables seems necessary. To ensure the reliability of this comparison, many factors like fuel costs which generally consist of discovery, extraction, refinery, emission control, and distribution; inevitable expenses of tax and fee; and externality costs considering environmental, civil, unpredicted human, or natural incidents like war or natural disasters should be considered. After all, the result will be just slightly more accurate

to be used in future planning because there will be always some issues that are never considered in calculations and will show up at the stage of execution.

1.2.1.1 Solar Energy-Based Technologies

Solar energy has always been an attraction for the studies to enhance efficiency, decrease the production cost of harvesters like photovoltaic cells, etc. Although there were some flaws in the previous technologies which caused the increase in the final cost of the energy per kilowatt, nowadays high-tech tools and devices have improved the quality of energy produced within each of the cells or plants and decreased the total cost of them. Because of the innovations in the production of extractors like photovoltaic and solar thermal plants, the cost faced a downward trend, especially in the recent decade.

To understand the change which implementing solar plants will make in the total cost of a multi-carrier system, a comparison between the cost per production unit of solar plants and typical coal plant is made in Table 1.1 [3]. To calculate the total cost, there is a need to compute the total cost of a power plant consisting of the building cost plus annual operation and maintenance costs per life span which will be as below:

$$\begin{aligned}
 & \text{TOC}(\$/\text{KW}) + [\text{Fuel} (\$/\text{KW.yr}) + \left(\frac{\text{Var.O\&M}(\$/\text{KWh}) \times 24(\text{h}) \times 335^*(\text{day})}{1000} \right) \\
 & + \text{Fix.O\&M} (\$/\text{KW.yr})] \times \text{Life span}(\text{yr}) = \text{Total BOM cost} (\$/\text{KW})
 \end{aligned}
 \tag{1.1}$$

TOC: Total overnight cost

O&M: Operation and maintenance

BOM: Building, operation, and maintenance

*Because of sparing 30 days (1 month) for overhaul process in power plants, the period of a year is considered 335 days.

As it is seen, the total BOM cost of a power plant with solar photovoltaic technology is lower than a coal power plant. In contrast, a solar thermal power

Table 1.1 Financial information of solar and coal-fired power units

Technology	Total overnight cost (TOC) \$/KW	Fuel cost \$/KW.yr	Fixed O&M cost \$/KW.yr	Variable O&M cost \$/MWh	Life span (yr)	Total BOM cost \$/KW
Solar PV	1331	0	15.19	0.0	20	1634.8
Solar thermal	7191	0	85.03	0.0	20	8891
Ultra-super-critical coal	3661	154.52	40.41	4.48	50	15,208.46

plant might not be an economical choice to build in an energy network. But what is not mentioned in this table is that there are some effective regional specifications which make the thermal power plant construction inevitable. Importing cost of coal, higher emission taxes, and limitations in the construction of coal plants may force the state or private investors to build solar thermal plants.

It is obvious that the construction of a solar photovoltaic plant will reduce the costs of investment and operation up to 68% in equal time intervals and sizing. This number could add up by involving new technologies which will be discussed further in Sect. 1.2.4.

1.2.1.2 Wind Energy-Based Technologies

Wind power stations which are popular as wind farms use the power of the wind to rotate the turbines in order to generate electricity. Usually, the onshore turbines have different challenges with the offshore ones, and as a result, they have different costs, but this has not made wind farms one of the most expensive and inefficient power plants. Actually, due to a study in the United States Department of Energy (DOE), wind farms are producing the electricity much cheaper than the conventional or clean-tech coal power plants and gas-fired power plants, with a rate of approximately 5 cents per kilowatt which, with state subsidies, becomes 2 cents per kilowatt.

China, India, and the United States host the world's largest wind farms, mostly onshore, while countries with limited shore capacity are investing in offshore technologies like the UK or Japan. Gansu Wind Farm, located in China, is reaching its initial goal set in 2012 to generate 20,000 MW by 2020. Besides, the UK owns the largest offshore wind farm with a capacity of 660 MW [4]. According to studies on wind farms in Europe, Europe can be able to power the entire planet by installing about an additional 11 million onshore turbines over an area of 5 million square kilometers across its terrain. Of course, this is an ambitious project, but the same findings suggest that if accurate studies of the environmental conditions as well as the wind atlas of lands are carried out, the potential for wind energy production is both technically and economically high.

Environmental concerns about wind farms will be discussed in Sect. 1.5 but what is obvious is that use of wind farms will eliminate the expenditure of fuel and will decrease the total cost of the electricity generation. To analyze the economic benefits of the wind farms, a comparison between it and a wind farm is shown in Table 1.2 [3]. Detailed shares of a wind power plant breakdown costs, from planning until the operation, are also shown in Fig. 1.2.

1.2.1.3 Geothermal Energy-Based Technologies

Despite the high initial cost of investing in geothermal power plants, these plants have very low operating costs and can be managed. Many factors contribute to the initial investment costs, including drilling costs, thermal and boiler installations,

Table 1.2 Financial information of wind and coal-fired power units

Technology	Total overnight cost (TOC) \$/KW	Fuel cost \$/KW. yr	Fixed O&M cost \$/KW. yr	Variable O&M cost \$/MWh	Life span (yr)	Total BOM cost \$/KW
Wind onshore	1319	0	26.22	0	20	1843.4
Wind offshore	5446	0	109.54	0	20	7636.8
Ultra-super-critical coal	3661	154.52	40.41	4.48	50	15,208.46

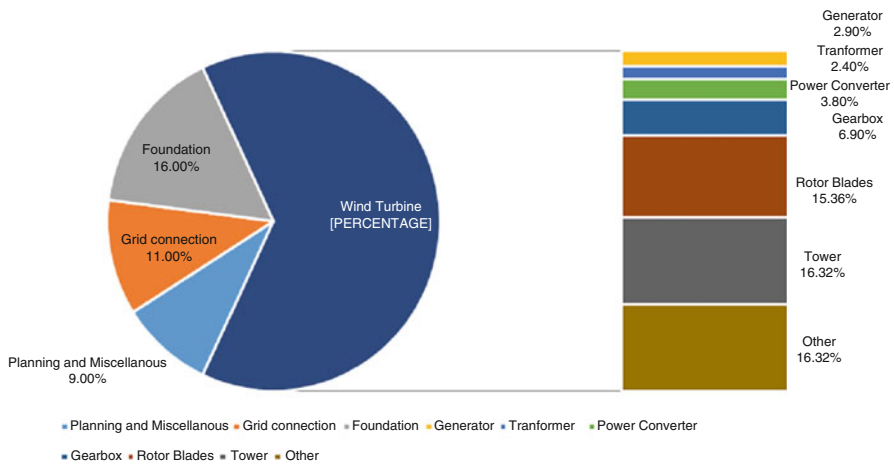


Fig. 1.2 Capital cost breakdown for a typical onshore wind power system and turbine [5]

disposal system, construction of underground and on-ground facilities, project development costs, and network linking costs. A brief pie chart of the probable percentages for each of the mentioned costs and further is available in Fig. 1.3.

In more realistic calculations, the costs of a geothermal plant will depend on the technology which it uses, the capacity or quantity of wells it contains, and other crucial geothermal circumstances. But after all, it is undeniable that these power plants are invulnerable to price changes since they do not need fuel. An economic comparison between a typical geothermal plant and a coal-fired plant is detailed in Table 1.3 [3].

As it is obvious, the overall life span costs of a geothermal plant are much less than those of the coal power plant, even in an equal time interval.

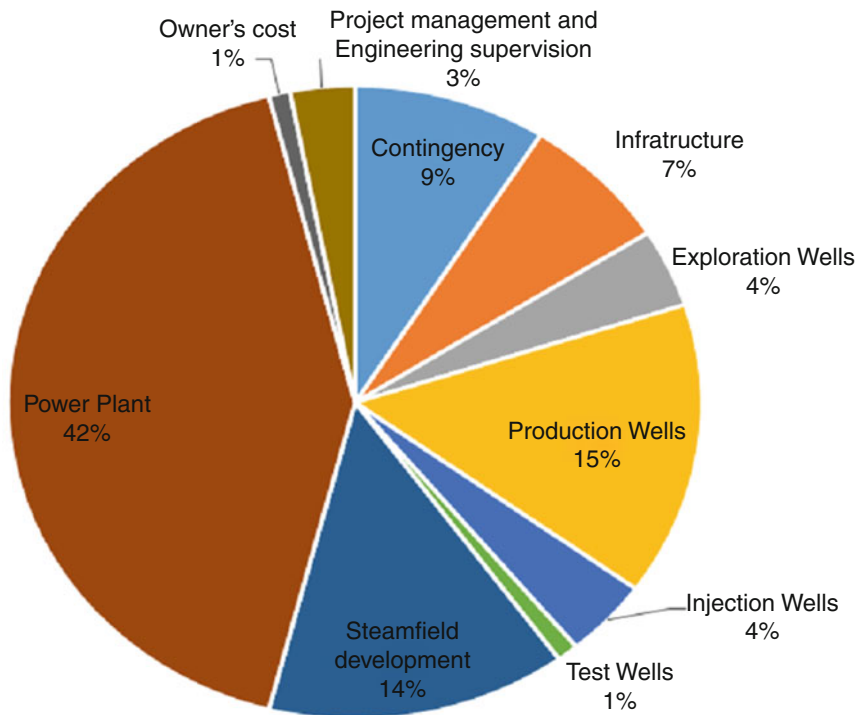


Fig. 1.3 Total probable cost breakdown for an installed geothermal power plant [6]

Table 1.3 Financial information of geothermal and coal-fired power unit

Technology	Total overnight cost (TOC) \$/KW	Fuel cost \$/KW. yr	Fixed O&M cost \$/KW. yr	Variable O&M cost \$/MWh	Life span (yr)	Total BOM cost \$/KW
Geothermal	2680	0	113.29	1.16	30	6358.492
Ultra-super-critical coal	3661	154.52	40.41	4.48	50	15,208.46

1.2.1.4 Biomass Energy-Based Technologies

Unlike wind, solar, and hydropower, biomass requires raw materials as fuel for its power plant, which must be produced or collected, transported, and stored. The economy of biomass power plants is heavily dependent on the fuel supply chain at an economic cost, as well as the technology used in these power plants. The cost of the equipment used in the power plant may depend on the area of construction of the power plant, the type of power plant fuel, and the production capacity and storage of fuel in the nature around the power plant. Fixed O&M costs include labor, scheduled

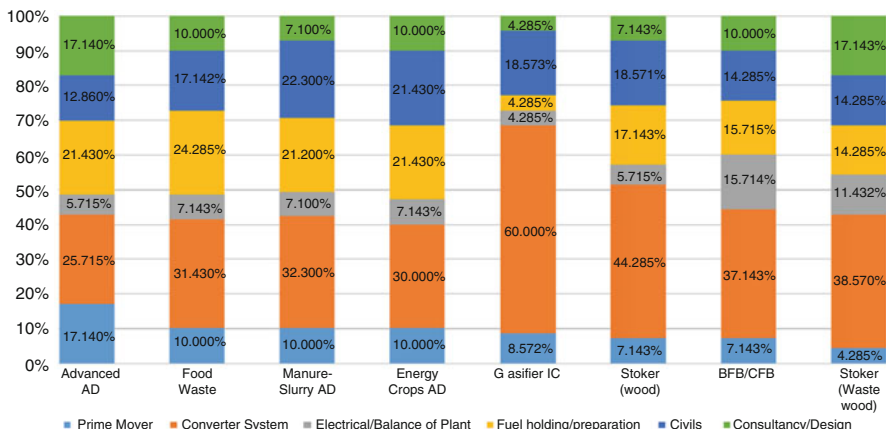


Fig. 1.4 Capital cost breakdown for biomass power generation technologies [7]

maintenance, and replacement of power plant equipment and power plant components (boilers, gas supply facilities, etc.) and, of course, power plant insurance costs.

The size of the plant is inversely related to the fixed O&M costs, meaning that the larger the plant, the lower the fixed O&M costs per kilowatt. The reason for this is the effect of the scale of the power plant unit on the economy and especially the employed labor force index at that time. The variable costs of O&M depend on the output of the power plant and are usually expressed in dollars per kilowatt-hour. These costs include non-biomass fuel costs, ash disposal, unpredicted maintenance operations, replacement of equipment and tools, as well as additional service costs. In some studies, fixed and variable O&M costs are combined and expressed, so accurate data on these costs may not be available separately. A comparison of total breakdown costs between different biomass technologies is shown in Fig. 1.4.

To analyze the biomass technologies with coal-fired power units, data for different cost groups are available in Table 1.4 [3]. As it is seen, prior three technology groups of biomass will have higher total BOM costs in comparison with USC plant per year. This surplus could be decreased or even be eliminated in stations which have access to affordable fuel supply like India. What is obvious is that landfill gas biomass plants are a great opportunity to generate electricity at a lower price and in a slightly eco-friendly way.

1.2.2 Gas Power Units

The natural gas-fired power plant is a thermal power generation unit that uses natural gas as its main fuel to generate steam and eventually electricity. Currently, gas power units have almost 25% of generation share in the world which, with lower gas prices in high oil and gas cases, could be almost about 51% in 2050 due to EIA annual

Table 1.4 Financial information of biomass and coal-fired power units

Technology	Total overnight cost (TOC) \$/KW	Fuel cost \$/KW.yr	Fixed O&M cost \$/KW.yr	Variable O&M cost \$/MWh	Life span (yr)	Total BOM cost \$/KW
Biomass (BFB/CFB/stoker)	2800	45.007	126	4.2	25	7919.375
Biomass (gasifiers)	3250	43.415	146.25	3.7	25	8735.325
Biomass (anaerobic digestion)	1975	125.47	79	4.2	25	7930.95
Landfill gas	1557	69.433	20.02	6.17	25	5728.794
Ultra-supercritical coal	3661	154.52	40.41	4.48	50	15,208.46

Table 1.5 Annual total fuel consumption of gas-fired power units

Year	Annual total consumption for electricity generation (million m ³)				Natural gas price (\$/m ³)
	State share (million m ³)	Private share (million m ³)	Commercial share (million m ³)	Industrial share (million m ³)	
2008	195,268.53				0.316
	77,308.79	102,286.02	945.87	14,727.85	
2018	306,721.2				0.124
	157,191.96	132,031.53	1490.88	16,006.83	

report of energy 2019. These power plants are also responsible for the significant amount of global greenhouse gas emissions which ends with the known threat for this planet, global warming. Gas power units could be used as a compensating generation to bring the balance to network with variable renewable plants and higher demands in the network.

In a study in 2018, the amount of natural gas which is consumed in the United States for electricity generation was increased by about 57.1% and the price of gas for this purpose was decreased by about 60.75% compared with 2008 data. Besides the advances in technologies related to gas-fired power plants, low cost of fuel and higher dispatch ability in critical situations make the presence of gas power plants in energy network rational. This is why we have been seeing increases in the consumption shares of different consumer groups in recent years (Fig. 1.8). Extended analysis about the relation of gas consumption and gas price per unit is mentioned in Figs. 1.5, 1.6, 1.7, and 1.8 (data driven from [1, 8]):

To understand the importance of gas-fired power plants' presence in energy networks, as mentioned in Eq. (2.1), there will be a comparison between gas-fired generation technologies and coal power units. The results are in Table 1.6 [3]:

Fig. 1.5 Average natural gas price comparison in 2008 and 2018—eia.gov [1, 8]

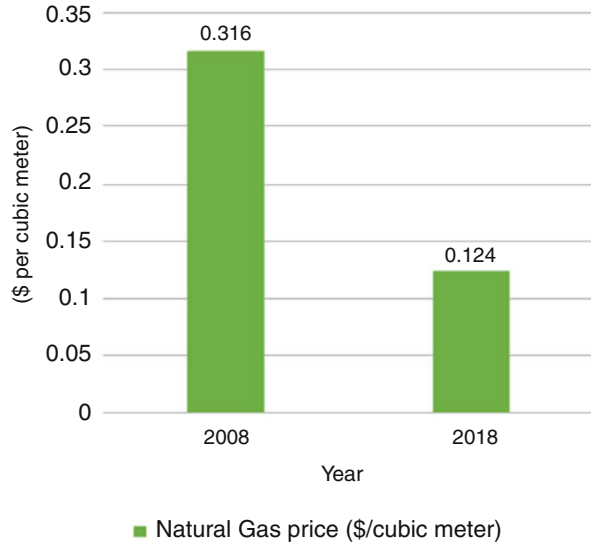
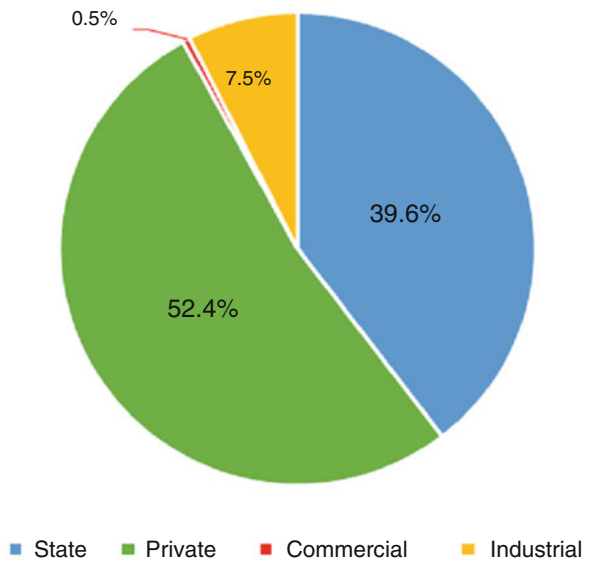


Fig. 1.6 Natural gas consumption shares for electricity generation in 2008 [8]



1.2.3 Hydro Technologies

Hydropower plants have many positive points, including the following:

- As the fuel of these plants is water, it is accounted for as clean energy resources.
- Hydropower plants bring energy independence to any region with water resources.

Fig. 1.7 Natural gas consumption shares for electricity generation in 2018 [1]

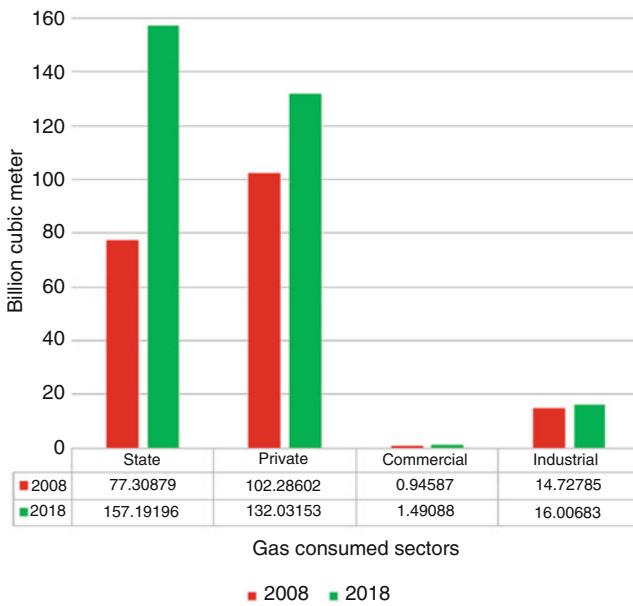
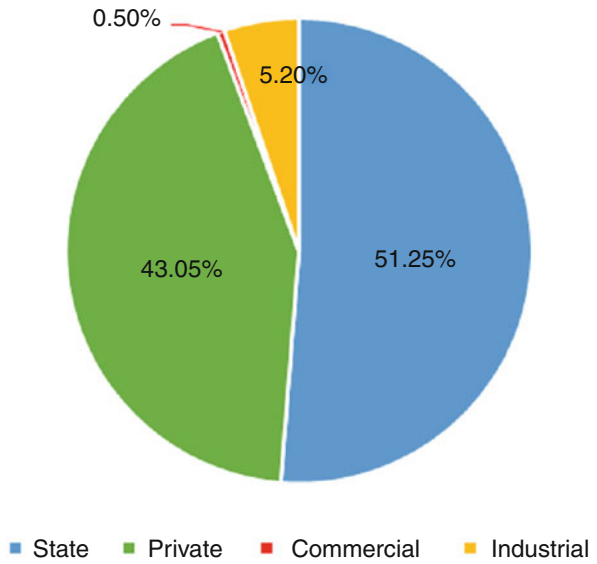


Fig. 1.8 Consumption of natural gas for electricity generation purpose divided by sector-year [1, 8]

Table 1.6 Financial information of gas-fired and coal-fired power units

Technology	Total overnight cost (TOC) \$/KW	Fuel cost \$/KW.yr	Fixed O&M cost \$/KW.yr	Variable O&M cost \$/KWh	Life span (yr)	Emission costs ^a \$/KW.yr	Total BOM cost \$/KW
Single-shaft combined cycle	1079	282.14	14.04	2.54	30	83.8773	13,093.367
Multi-shaft combined cycle	954	282.14	12.15	1.86	30		12,747.651
Internal combustion turbine	1746 ^b	282.14	35.01	5.67	30		15,144.423
Industrial frame combustion turbine	710	282.14	6.97	4.48	30		12,980.195
Ultra-super-critical coal	3661	154.52	40.41	4.48	50		25,282.58

^aCongressional Budget Office (CBO) regulated carbon tax at \$25 per metric ton on most emissions of greenhouse gases in the United States (H.R.6463, US 115th Congress 2017-2018/CBO-Budget options 2018-54,821). The data for emission costs are calculated on this basis. For the gas-fired technologies an average of 0.4173 kg per kilowatt hours is estimated (eia.gov)

^bDue to TOC tolerance in different sizing of internal combustion engines, an average value is calculated (eia.gov)

- Because of the water cycle driven by the sun, hydropower plants are considered as renewable power plants which make them reputable and reasonable.
- In a specific kind of hydropower plant (impoundment plants), recreational benefits are also available for the community.
- Their ability in instant power injection to network in critical situations like disruptions, disturbances, and outages makes them a reliable backup power choice.

Additionally, flood control and water supply for farms, cities, and ponds are the other benefits of these power plants. To have a detailed image of the total costs of a hydropower plant, a figure which represents the detailed costs with both percentages and exact numbers of the 500 megawatt greenfield hydropower project is available in Fig. 1.9.

To analyze the economic advantages of hydropower, there should be a comparison between the costs of a hydropower plant and a coal power unit. The data for each of the technologies are listed in Table 1.7 (data driven from [3, 9]):

As seen, the total BOM cost of hydropower plants is lower than a coal power plant in a year interval. It is obvious that because of the higher life span of hydropower plants—which are normally up to 100 years—the overall lifetime total BOM cost of hydropower plants will be slightly more than a coal power unit per kilowatt. Implementing these power plants to an energy network could decrease

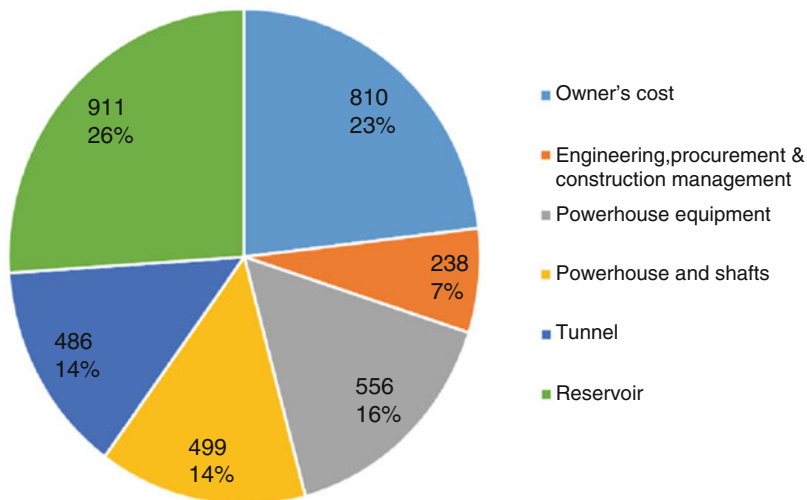


Fig. 1.9 Cost breakdown of an indicative 500 mw greenfield hydropower project in the United States (values in \$/KW) [9]

Table 1.7 Financial information of hydro and coal-fired power units

Technology	Total overnight cost (TOC) \$/KW	Fuel cost \$/KW.yr	O&M cost \$/KW.yr	Total BOM cost \$/KW.yr
Large-scale hydro-power plant	2100	0	97.875	2197.875
Small-scale hydro-power plant	3100	0	139.5	3197.875
Conventional hydro-power plant	2752	0	52.805	2804.805
Ultra-supercritical coal	3661	154.52	76.43	3891.95

the investment costs while the fuel costs have already been omitted from expenditures, which results in significant economic benefits.

1.2.4 Innovative Technologies

Improvements in current technologies of generation units often resulted in intensity reduction of adverse characteristics in them. In this section, a brief review of innovative technologies for power stations is given and how the advances can help to decrease overall operational costs is also explained.

Table 1.8 Efficiency of different generation technologies

Technologies	Efficiency (%)
Ultra-supercritical coal (USC)	39.5
USC with 30% carbon capture and sequestration (CCS)	35
USC with 90% CCS	27.3
Combined cycle—single shaft	53
Combined cycle—multi-shaft	53.5
Combined cycle with 90% CCS	47.9
Internal combustion engine	41.3
Combustion turbine—aeroderivative	37.4
Combustion turbine—industrial frame	34.5
Advanced nuclear	32.6
Ocean thermal energy	51
Biomass	25.3
Geothermal	37.3
Landfill gas	40

Coal- and gas-fired power plants have already taken the attention of researchers as a great opportunity to increase the overall efficiency of the energy system. Nowadays, these power plant technologies are usually equipped with carbon capture and sequestration (CCS) technology in order to reduce the CO₂ emission intensity in them, which will cause the overall operational cost reduction. CCS includes three main steps which are as below:

- Capturing CO₂ from fossil fuel power plants or industrial complexes
- Transportation of CO₂ in pipelines toward the facility
- Injection of CO₂ into deep underground layers of earth, which is an approach of storing

The stored gas cannot climb up the way to surface because it is injected beneath the nonporous rock layer, between the porous layer of earth. This technology is very important because it can reduce a significant amount of greenhouse gases released by power and industrial utilities and it can be accounted as a great approach toward green energy. Just in the United States, 40% of annual CO₂ emission is by energy section which can be decreased by up to 36% by deploying CCs on fossil fuel power plants. Right now this technology can reduce up to 90% of emission gas, which for a 500 MW coal-fired power plant could be equal to 2,700,000 tons of CO₂ annually, equivalent to 62 million trees planted and grown in 10 years.

Other technologies in renewable energy fields are also interesting. New approaches on building PV panels can provide cheaper energy with higher efficiency (like Sunrgi Xtreme which can provide solar energy with 5 cents per kWh—cheaper than a gas power plant which can supply with 7–10 cents per kWh—and with 37.5% efficiency, 1366 Technologies which can provide solar power with an unbelievable price, 1 cent per kWh, nano-wired PV panels with 40% efficiency). In wind

turbines, new technologies suggested increasing the length of blades in order to improve the torque for more efficiency and making it eco-friendly by reducing the risk of collision with birds due to lower speed of rotation. Although most of these projects and innovations are not commercialized and some results may change in a real operational environment, what is same in all of them is their goal to reduce the production cost while increasing efficiency.

1.3 Energy Exchange and Demand-Side Technologies

Energy conversion is the process of converting energy from a form to another. In fact, all of the power plants work with this principle. Fossil fuel plants transform the potential energy of coal to electricity, renewable generators convert wind or sun radiation to electricity, and even fuel cells use energy conversion to maintain electricity from chemicals. The important point in considering energy conversion is that if this conversion is cost effective or not. Effectiveness could be described by many points of view like economic, social, or even environmental. Innovations in electrical storage systems along with the appearance of improved power plant facilities and clean energy infrastructure have made this subject more attractive for researchers. As there is no ideal incident in the electricity generation, transmission, distribution, and consumption, there will always be some losses with the converting process which defines its efficiency. Increasing efficiency will result in more converted energy, which, at here, means the increased capacity of electricity generation, transmission, distribution, and consumption. In this section, innovative solutions for energy conversion and their effect on demand-side regulations are discussed.

1.3.1 Heat Exchange

Heat exchange refers to the action of converting heat to electrical energy in terms of electrical systems. The action is somehow known as steam energy in thermal power stations, making the turbines rotate and produce power. Combustion engine power plants, combined cycle plants (CC), combined heat and power (CHP) and combined cooling, heat, and power plants (CCHP), ventilating technologies like absorbing chillers and ocean thermal energy conversion (OTEC), and so on are all considered as heat exchange technologies. In the previous section, the total costs of producing energy from any available fuel have been analyzed and comparisons were made.

The issue will be interesting when we can also examine the thermal efficiency of power plants. In this case, the best decision can be made by considering the costs and thermal efficiency. However, in the following sections we will see that in addition to these two characteristics, other parameters also play a role in the decision to optimize

energy production in a multi-carrier energy network. At first, in order to understand what is thermal efficiency, some definitions need to be mentioned.

Heat rate is an acceptable tool to determine the thermal efficiency of power plants that use heat exchange technologies. It is actually the heat energy usage of any power plant to generate kilowatt-hour electricity and it is indicated as British thermal unit per kilowatt-hour (Btu/KWh). In order to get the efficiency percentage from the heat rate, the value of kilowatt-hour electricity needs to be converted to an equal amount of Btu (1KWh = 3412 Btu) and multiplied by 100. This number should be divided by the heat rate value in order to find efficiency:

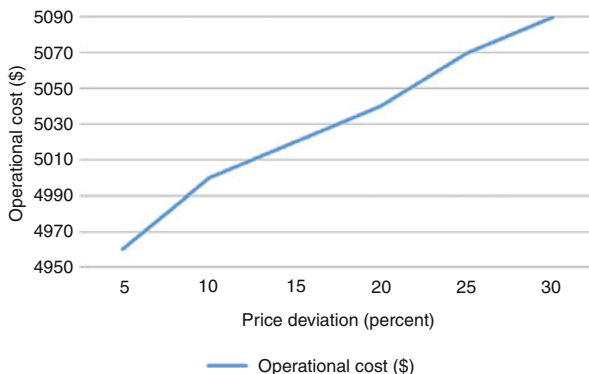
$$\frac{3412 \text{ (Btu)}}{\text{Heat rate (Btu/KWh)}} \times 100 = \text{Thermal efficiency} \quad (1.2)$$

According to the table given, it can be understood that the thermal efficiency of combined cycle gas power plants, as well as OTEC, geothermal, and landfill, is higher than the efficiency of improved coal power plants. This becomes more tangible when compared to other traditional coal-fired power plants around the world. The higher the thermal efficiency, the higher the power efficiency of the plant, and the more energy it delivers compared to the same volume of fuel. This generally increases the overall efficiency of the power plant complex and thus increases the production capacity of the energy system.

CHP units are a practical solution for providing electrical and heat demand of consumers [10]. These units can recover the heat waste during the process of the generation which can increase their overall efficiency up to 90%. The emission of CO₂ or other pollutant gases is decreased by a maximum of 18% using CHP units. They are capable of providing a reliable and secure supply of energy in a system. The heat generation cost of CHP units is much less than other generators, which makes it a suitable option for heat production. In a study done by Nazari-Heris et al. (2018) [11], short-term scheduling of heat and power integrated grid is analyzed. In the test grid, a robust optimization method and scenario-based modeling approach were implemented in order to confront the uncertainties of load demand and energy market price. The result of this study shows that the increase in the robust budget can cause more costs in the operation of the system while maintaining the robust action of the system. On the other hand, the price deviation can also create a difference in operational costs. The lower it comes, the lower the system will cost to operate. A detailed diagram is shown in Fig. 1.10.

For CHP and CCHP power plants, however, the situation is slightly different. In calculating the electrical efficiency of these power plants, other factors must be considered, namely heat and cold. The technology used in these power plants can be one of the gas technologies mentioned in the table given, or micro-turbines or even fuel cells. What is important here is that even the heat output of this plant, which is usually wasted in other power plants, can be used for heating homes and other consumer groups. Of course, by installing absorption chillers in the air outlet of these power plants, hot air can be considered as the inlet of the chiller to produce cold air

Fig. 1.10 Impact of price deviation on operational costs considering average robust budget [11]



without the need for electrical energy, providing desired air-conditioning for consumers. As a result, in addition to 45% electrical efficiency, these power plants also have a 40% efficiency in cooling and heating.

1.3.2 Power to Gas (P2G)

Conversion of power to gas is one of the solutions for energy grid to decrease costs, although implementation of such systems is currently expensive. P2G facilities permit electricity storage in a gas form (typically hydrogen) and maintain the fuel for transportation or even household usages like cooking and heating. Power-to-gas technology is based on the conversion of energy into hydrogen gas, which is obtained from the process of water electrolysis [12]. Plenty of methods are introduced for this technology to study the probable uncertainties that are included in different case studies like information-gap decision theory and Monte Carlo simulation [13, 14]. The resulting gas can be injected into the gas network or used for transportation purposes. There are many examples of these systems around the world. Germany is using the technology as part of its “Energiewende” project to reduce its energy shortage in the winter. In Italy, hydrogen storage technology has been used to supply the fuel needed for hydrogen vehicles as well as for maintaining network balance.

The resulting hydrogen can be used in power plants and provides sufficient heat to generate energy, so power plants can use existing equipment to generate energy and save additional costs for optimizing the plant and developing it for low-emission targets. Another purpose of this technology is to convert the power to methane. This process is done by mixing the hydrogen gas outlet of power to hydrogen systems with carbon dioxide. If the pressure of methane is maintained, it could be injected in the gas distribution grid.

Methane from these processes is also known as carbon neutral due to the consumption of carbon dioxide in the production of methane and the completion

Fig. 1.11 Economic benefits resulting from implementing P2G storage facility in renewable energy system

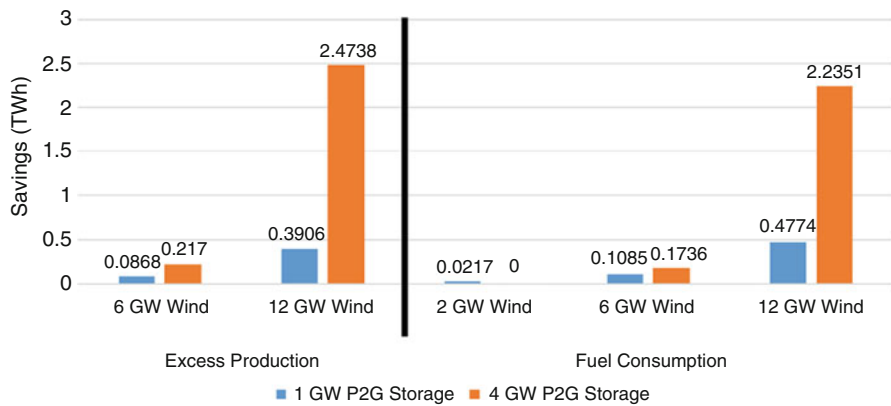
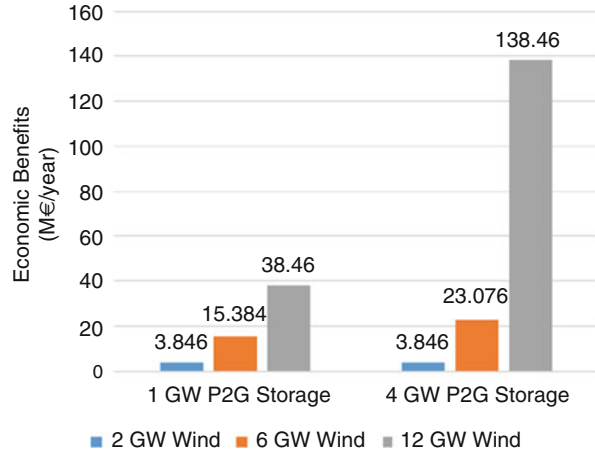


Fig. 1.12 Savings in excess electricity production and fuel consumption in comparison with the base state

of the production cycle and consumption of this greenhouse gas, and in addition to its use in gas power plants as fuel, it can also be used for urban heating to meet other needs. In a study of economic benefits on the energy system of Germany [15], the integration of renewable energy facilities and P2G storage facility is analyzed. The result shows that integrating wind energy with P2G could bring a minimum of 3.84 million € and a maximum of 138.46 million € per year economic benefit (Fig. 1.11).

Besides, savings in energy production excess and fuel consumption is significant. In a system with wind farms and P2G storage, the savings could be a minimum of 86.7 GWh and a maximum of 2.5 TWh in production excess and a minimum of 21.7 GWh and a maximum of 2.23 TWh in fuel consumption. The detailed chart for different capacities is available in Fig. 1.12.

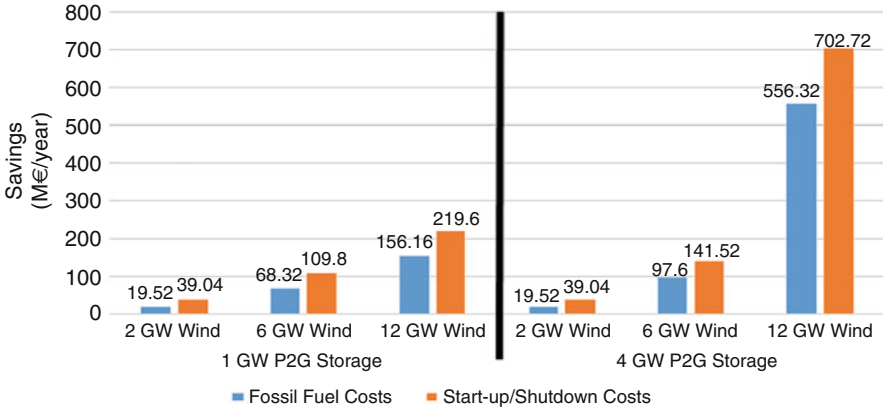


Fig. 1.13 Economic effects of P2G + wind system on fuel and startup/shutdown costs of fossil fuel plants

Also, the usage of P2G storage technology can prevent several undesired startups or shutdowns of fossil fuel power plant system during the demand peak which results in the decrease of the fuel costs and startup/shutdown costs of power plants (Fig. 1.13).

Despite all the benefits mentioned above, these processes, and therefore the fuels that result from them, can also have negative points. Every energy conversion has energy losses. In this case, too, about 42–58% of energy is wasted when converting energy from electricity to hydrogen and during hydrogen gas methanation. Assuming that the methane gas from this process is used in a combined cycle power plant with 60% efficiency, the total efficiency of the power to gas technology (the total efficiency of the electricity-to-electricity conversion cycle) will be about 30%. There are some solutions to increase the efficiency of this conversion cycle like recovering the heat of the water electrolysis process [16]. Accordingly, the power-to-gas technology can be used along with biogas facilities which require the heat of the P2G electrolysis process. The CO₂ emission of biogas plants could also be used in the methanation process of P2G.

Also, the high cost of such an operation eliminates the competitiveness of this technology with fossil fuel technologies in the current situation, and in the absence of government subsidies and tax reliefs, this technology may be discarded. However, despite losses and high construction and operation costs, converting electricity to gas in the future may be cost effective because of increasing taxes on carbon emission as well as the incremental trend of fossil fuel cost.

1.3.3 Peer-to-Peer Technologies (P2P)

Peer-to-peer technology refers to the action of trading energy between the advanced customers which are capable of generation and distribution of energy with next-door neighbors or a neighborhood, technically called “prosumers.” There are studies about the economic benefits of this technology. Generally, cost-saving features could be divided into three parts which are explained below.

1.3.3.1 Energy Expenses

Peer to peer can effectively help the customers with the energy price. Two scenarios are already analyzed in this issue. The first one is when the feed-in tariff of power-to-grid injection is lower than the retail price of electricity. In this case, the prosumers can trade the energy with customers via peer-to-peer technology with a price in the range more than fixed tariffs and less than the energy retail rate, creating benefits for prosumers and customers. In order for this business to survive, it is important to set the right tariffs. If tariffs are too close to or equal to the retail price, there may be no profit margin for prosumers and the business will be eventually out of order.

This could happen when the price of energy produced and transmitted to the energy system is low due to the efficiency rate and scale economies. However, the second scenario designed for this situation could be useful for prosumers. Price fluctuations in the energy system under the time of use strategy can lead consumers to consider the economically constant rate of energy purchases from distributed generation resources and provide some of the energy they need in this way. This will be profitable for distributed energy generators.

1.3.3.2 Network Costs

Local energy exchanges can eliminate imbalances between production and consumption, one of the consequences of which is a reduction in the energy flow of the line and thus a reduction in transmission and distribution network losses. In addition, the connection points of local distribution networks with the main energy network can assure consumers that their energy needs will continue to be met during local blackouts or generation shortages.

Of course, this will be done with much less energy flow than before. All of the mentioned advantages highlight the importance of setting fair tariffs based on better estimates of network losses. However, it should be noted that not all network losses can be eliminated by using local networks equipped with peer-to-peer technology, as there may still be losses due to illegal grid connections in the network.

1.3.3.3 Grid Services

Due to the increasing trend of distributed generation facilities in energy systems, new challenges in flexibility issues will appear and as a result different flexibility services can be offered to the transmission system (TSO) and distribution system operators (DSO) which will eventually result in a new market for the service providers. Frequency regulation and power balancing in the transmission system and two-way power flows and several voltage problems in the distribution system are the services that are expected to be available.

Because of the efficient, green, distributed energy resource implementations in large scale and conventional fossil fuel power station shutdowns, there will be a need for an optimized and more flexible transmission and distribution grid of which the outcome will be the increased complexity and management issues. But it is clear that eventually, the maintenance and operation costs of the grid will be decreased significantly and there will be great opportunities for new markets.

1.3.3.4 Mobile Convertible Resources

Mobile convertible resources of an energy system, which here means the same as electric vehicles (EVs), can be used as clean energy sources in different situations under certain circumstances. One of the conditions that must be provided for the use of electric vehicles as mobile resources in the energy network is that there should be a complete connection between different parts of the network and all of its actors, from car owners to network operators, which could get done by developed information and communications infrastructure.

Flexibility is not an option but a necessity which means electric vehicle network should be capable of optimized response to other renewable power resource fluctuations in the energy system causing troubles with the energy production and demand balance without having a negative effect on transportation needs. With approximately 85% efficiency of energy conversion in EVs, it is not a case to leave it unattended.

To understand the differences which EV network can make in an energy system, it is good to take a look at a comparison between a typical fossil fuel car and an electric one. In this comparison, gasoline and an electric model of Hyundai Kona 2020 is used as the test case driven in the District of Columbia. The results are in Table 1.9.

One of the initial advantages an EV can have is its green operation. With nine times smaller amount of GHG emissions, this could prevent so many environmental costs. But what is important in this section is its ability to store energy in order to inject into the grid when it is necessary.

If this process is properly controlled and all the infrastructure required to run V2G is provided, the capacity of an electric vehicle battery can be used for applications such as peak load reduction, active and reactive power injection in the required

Table 1.9 Comparison of an EV and typical gasoline vehicle

Vehicle	Annual fossil fuel use (Gal)	Annual electricity use (KWh)	Annual fuel/ electric cost (\$)	Annual operating cost (\$)	Cost per mile (\$)	Annual GHG emissions (Kgs CO ₂)
2020 Hyundai Kona Electric EV	0	1744	226	2094	0.34	568
2020 Hyundai Kona AWD Gasoline	218	0	627	2573	0.42	5223

buses, and network frequency control. Each of these applications will help the system to operate optimally. Peak load reduction service can reduce the need for generation in peak hours, decreasing the overall cost of generation in power plants. In a study in New York, it was estimated that if only 10% of EV owners participate in the peak load reduction project, it will save about 383 MWs for the grid.

The most important issue in implementing the EV storage scenario in the energy system is the owner costs of the vehicle. While charging and discharging, the battery life span can dramatically decrease, causing additional costs of changing or repairing battery. It should be considered that the electricity price and eventually the benefits of vehicle owners should be more than the costs which the vehicle may face. This needs a comprehensive study on the cost estimation of EV penetration in the grid.

1.4 Creation of Energy Hubs

An energy hub is a tool for connecting different types of energy carriers with consumers. The inputs and outputs of an energy hub can consist of different types of energy. Energy inlets such as electricity and natural gas may be delivered to customers in the form of heat, light, or electricity at the outlet. In an energy hub, the connection between energy suppliers and consumers can be one way (from generation to consumption) or two way.

Each energy hub has defined sectors which are connections and storages. For some carriers, connections should be direct in order to transport the energy in its initial form to the consumer without changing any quality specifications of it. For others, the conversion is needed. Most of the converting processes in which some of them are storage methods are usually used in energy hubs like P2G, pump storage, and fuel cells. Like any controllable system, energy hubs are divided into four classes of input/output forms. Single input-single output (SISO), single input-multi-output (SIMO), multi-input-single output (MISO), and multi-input-multi-output (MIMO) are the classes in which energy hub systems are categorized as in Fig. 1.14 [17].

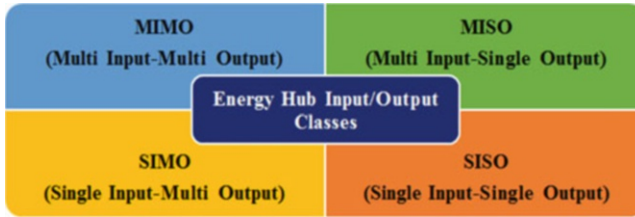


Fig. 1.14 Energy hub input/output classes

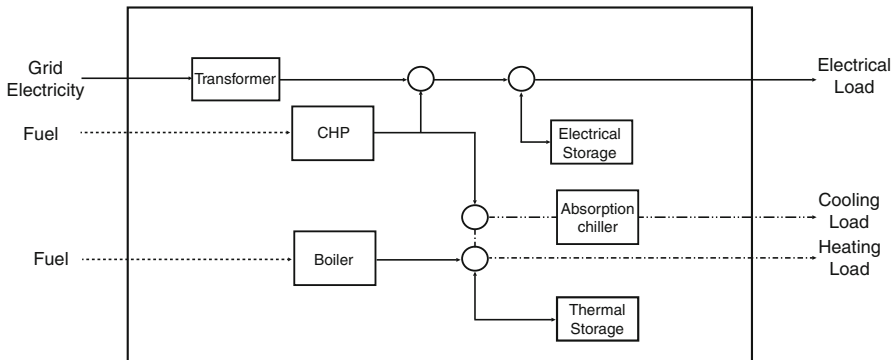


Fig. 1.15 Schematic representation of a common structure of the energy hub [18]

Aggregating different energy carriers in order to create a comprehensive energy system that is capable of meeting the different needs of customers is the first step in economic savings. Prevention of huge investments in expanding infrastructure and improving efficiency is one of the benefits of energy hubs. In this section, the optimal operation of hubs along with the impact of different specifications on the cost-saving trends of multi-carrier energy systems is discussed.

1.4.1 Optimal Operation

Optimal operation of an energy hub (Fig. 1.15) is a short-term analyzing issue in which economic dispatch and unit commitment of previously implemented distributed generators are found out [19]. In the discussion of energy hubs, since the installation costs of distributed power plants have already been paid and the energy hub is to be implemented on them, they are not considered in the optimal operation calculations. The only important factors in these calculations are the costs of fuel, depreciation, and greenhouse gas (GHG) emissions. Even fixed O&M costs (the costs which are set and fixed and will not change normally like operator salary, etc.)

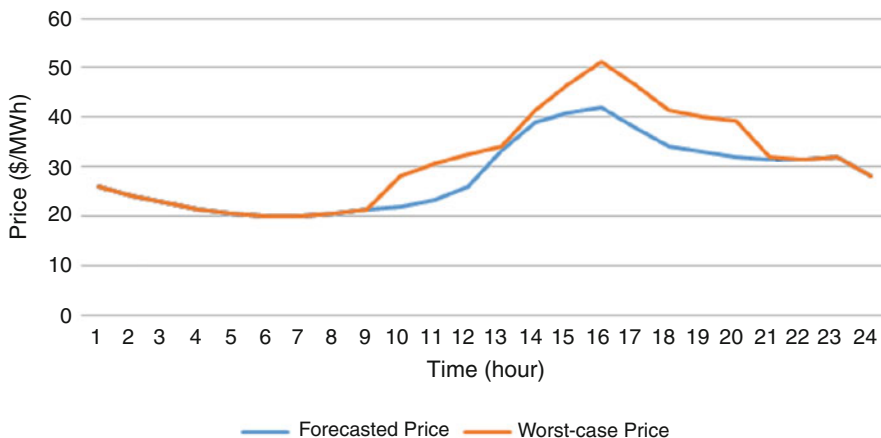


Fig. 1.16 Power market price after implementation of robust optimization method [20]

can be excluded from the objective function of optimization due to ineffectiveness in the calculations.

Due to a study on optimal management of energy hub demands [18], usage of different storage technologies can reduce the operational costs up to 20% in summer and 16% in winter. Implementing CHP and absorbing chillers in the system can provide the heat and cool demands of consumers while keeping the balance of heat production and consumption due to the presence of uncontrollable heat demands. The overall cost reduction percentages will be 34% for summer and 33% for winter. In order to determine the economic benefit of an optimally operated energy hub, it is necessary to consider the mentioned cost savings, in addition to the investment costs of energy hub installations.

In another study on integrated power and gas systems [20], a robust operating model in which the worst case of the system condition in purchasing energy from the market is considered to do robust optimal scheduling is introduced. The model consists of a 6-node gas network integrated with the 6-bus energy system. In this study, the optimal operation of the system is analyzed during the uncertainties of market prices. The results have shown that the CHP power plant which has the most share of energy provided in the mentioned system can satisfy the heat demand of the system equivalent to 40 MWth on average per hour. Besides the CHP and a gas-fired power plant in this model, there is a wind turbine connected to the fifth bus of the energy system which helps the operators to reach the optimal point. Although the optimal daily operation cost of the system has increased by 6%, reaching 2,701,547 \$, the robust operation of the system is obtained, causing the prevention of system failure from price uncertainties in meeting the demand (Figs. 1.16 and 1.17).

However, in a realistic simulation of integration between gas and electricity networks in order to get energy, heat, and cooling outputs in an office in Tehran [21], operational risks of a smart energy hub were controlled with conditional value-at-risk (CVaR) method, which resulted in a slight increase of operational costs by

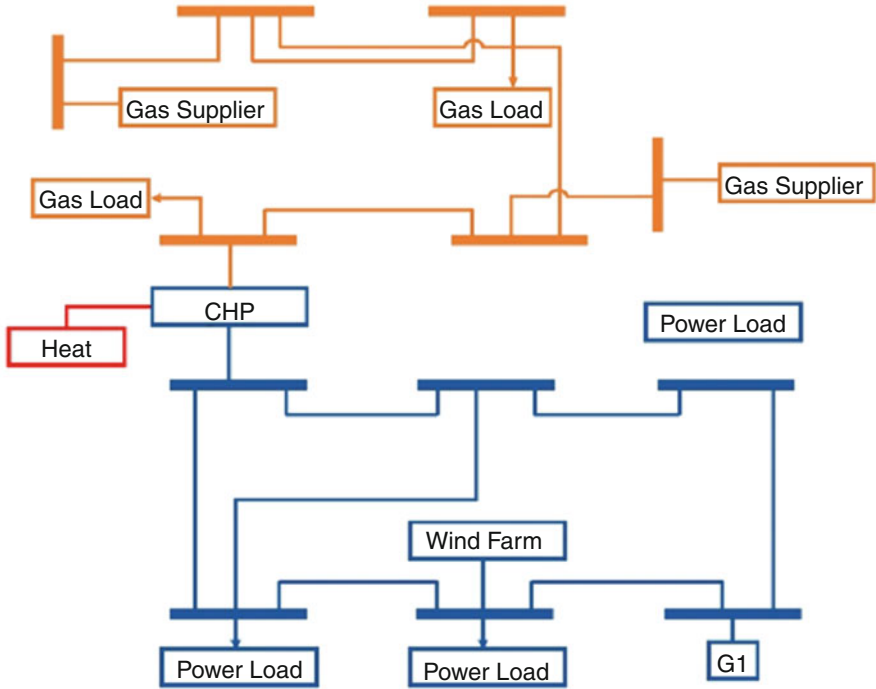


Fig. 1.17 The studied integrated power and gas system for second study [20]

Table 1.10 Simulation results for Tehran case study

Test mode	Base case	CVaR included (optimal)	Without CVaR
Cost (\$)	1228.82	374.26	293.96
Cost saving (%)	–	69.54	76.08
Reduction of electricity (%)	–	126.97	137.57

6.54%. In this study, ten different scenarios were shortlisted from numerous scenarios with assistance of Monte Carlo simulation in the presence of uncertainties in real-time electricity price, gas price, and energy demand in the test case, wherein after calculations the third configuration was detected as the most cost-saving and economic approach. The simulation results for this study are available in Table 1.10.

In [22], a robust optimization is introduced for the day-ahead scheduling of a hydrogen-based energy hub in which the total energy cost of this system is minimized via this method with consideration of uncertainties in electricity prices. Due to the outcomes of this study, the overall cost of energy hub has decreased by up to 7.8% while the robustness of the system against price uncertainties has increased by up to 30%. Detailed approaches are being introduced for energy hubs to decrease their overall cost while considering uncertainties.

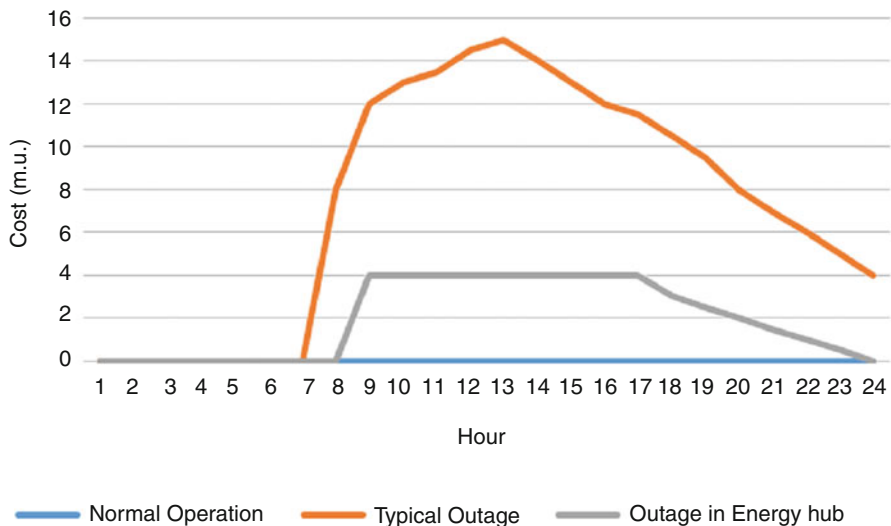


Fig. 1.18 Cost evaluation of different situations (per m.u.) [23]

1.4.2 Flexibility and Reliability

Flexibility in energy systems refers to the concept that expresses the system’s ability to balance energy production with its consumption in the event of any imbalance at any level. Flexibility is usually expressed in the form of available electric power to create ascending and descending ramps in the system power flow. In an energy hub, flexibility includes a wide range of energy applications including heat, transportation, storage, and direct consumption.

Reliability in an energy system also demonstrates the system’s ability to provide sufficient power, implement demand response programs, and provide sufficient capacity in the system to meet customer needs. To gain reliability in a system, some necessities need to be considered. Incentives and motivating policies, accurate forecasts of demand (99.998% of customer demand must be forecasted in order to meet the standards), active energy markets managing energy price signals, reliable infrastructure for transmission and distribution, secure operating, and being able to recover system state while imbalances appear in the system are just some of the specifications needed to state the system reliable.

Outages in the energy system can cost a lot in different consuming groups. Also if the outage is not controlled by any means, it can cause cascade failures which might end up to blackout. Due to a study [23], a model predictive control can reduce the impact of outages in an energy hub significantly. Due to this study, as a result of implementing the mentioned control on the system, outage costs have dropped by about 73% at peak times in comparison with the normal outage costs (Fig. 1.18). The interesting point in this comparison is that the cost of blackouts in the predictive control method does not exceed a certain amount. In addition, other results of this

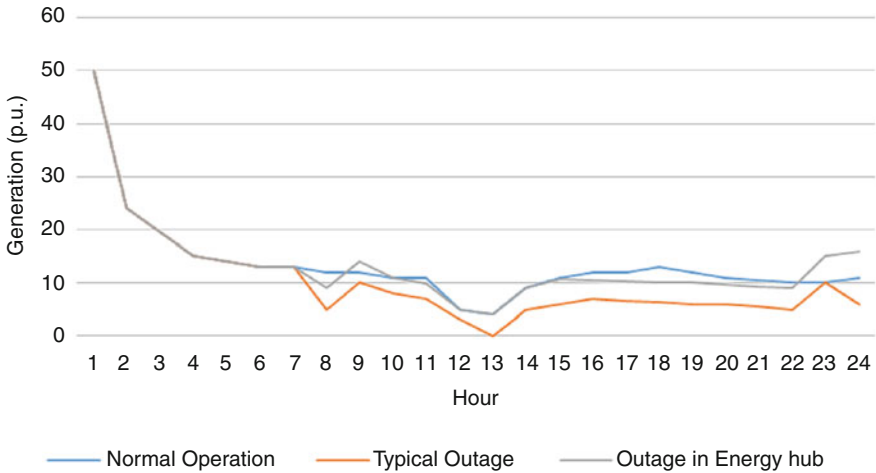


Fig. 1.19 Generation levels in different situations (per p.u.) [23]

study show that by implementing the same control method, the amount of energy production in power plants and other generators of the studied distribution network does not change much compared to normal (Fig. 1.19). However, in normal black-outs, the level of generator output drops and intensifies the blackout, resulting in the system's inability to recover faster after a disturbance.

The implementation of different forms of energy with the ability to transform them into each other provides a wide range of flexibility and reliability simultaneously. Conversion of energies in an energy hub can eliminate the risk of local or wide-area outages while maintaining the demand response solutions like peak demand reduction. Because of the higher reliability and lower need for the expansion of facilities related to a specific energy form and also incentives set by governments, the price of energy can get reduced significantly, providing higher opportunities for the energy trading schemes to be executed in the system.

1.4.3 Resiliency and Stability

Resiliency in an energy hub is the ability to maintain reasonable energy demand while anomalies affect the system. The higher speed of recovery in post-fault time interval while having alternative ways to respond to the energy demand of consumers is one of the resilience system's specifications. There are plenty of things like price fluctuations, shortage of energy source supplies, temporary failures in the grid, and predicted anomalies in which an energy hub can be resilient against them. Lower energy intensity which will eventually end up to lower demands and lower imports of energy, variety of electrical energy supplies which can ensure the capacity of the system for demand response, estimation of load losses while specifying energy

capacity margins to maintain the reliability of the system, and persistent infrastructure to obtain the highest reliability ratio of the grid are the elements which will be needed to consider a system resilient.

For an energy hub with different fuels and technologies supplying its power flow, different scenarios should be considered and various market options should be noted in order to gain resiliency. For example, if a multi-carrier energy hub loses its natural gas supply, grid management should consider immediately importing necessary fuel to eliminate the shortage of operating expensive power plants to meet the demand. However, it is important to notice that resiliency can reduce emission costs while preventing any unwanted costs of general blackouts or local outages. In a study done by the UK Energy Research Centre (UK ERC) [24], the approximate savings in costs of the system will be about £33 billion while there will be about £35 billion savings in emission costs.

1.5 Environmental Issues

In an energy system with different carriers, one of the most important issues is the environmental impacts of different fuels and technologies. While different conventional and renewable energies are used to meet the demand, there are several positive and negative points about the operation of the system. First of all, as renewables are taking place to generate the majority of customer energy needs, there will be lower environmental adverse impacts compared with the time when traditional energy systems were operating.

Biomass and landfill stations can produce electricity with a lower amount of greenhouse gas emissions in comparison with fossil fuels. Wind turbines are improved and they are no more a threat to birds and bats flying around. Solar energy harvesters are also accounted for as clean energy, with a probable slight impact on water resources of dry ecosystems which are used for cooling and service affairs. Hydropower plants are also a clean energy source but they may have some negative impact on fish lives and their population, migration, and essential oxygen levels; with improved systems, these impacts have been minimized. “Clean coal” technology is now being implemented on coal power plants in order to increase the efficiency and remove the harmful particles from their emissions.

Besides the most important factor in environmental issues of energy systems which are air emissions, there are some other issues like greenhouse gases, cooling, land use, and waste disposal. To understand the environmental aspects of an energy system, it is necessary to consider both monetary and nonmonetary impacts of this process. These numbers and definitions will also differ from a kind of fuel to another, from a technology to another, and from a set of regulations to another [25]. All of these actions are a sign of a positive effect of giving attention to the environmental challenges which are also considered in the “Paris Agreement” Article 6, part 4. In order to analyze multi-carrier energy systems from the environmental viewpoint, there is a need for short-term and midterm/long-term detailed studies.

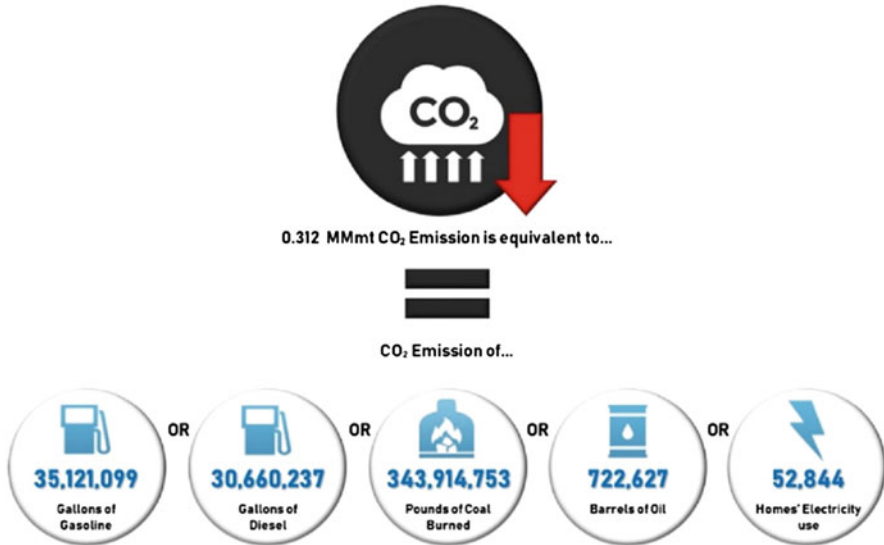


Fig. 1.20 Emission equation calculation, data driven from epa.gov

1.5.1 Imminent Effects

To know the importance of eco-friendly technologies used in multi-carrier energy systems, we should consider that due to studies that are done on this subject, the average amount of monthly emission reduction for energy use is about 26,010.1 metric tons per billion Btu. It makes the annual amount to be something about 0.312 MMmt/BBtu. As it is shown in Fig. 1.20, this amount of emission reduction is significant and will create many more opportunities to develop the energy system toward green energy.

The UK has plans to shut down its coal-fired power plants and had already shut down two of them in April 2020, with a plan to convert the old coal mines to geothermal power plants. On the other side, Sweden is trying to use hydrogen as its main fuel for heat sources in steel-melting facilities, which will decrease fossil fuel consumption significantly, causing less pollution. Tidal turbines were installed in China in order to harvest tidal energy. Austria is planning to shut its last coal-fired power plant down due to their renewable energy plans. The Indian community is showing attention to clean transportation and the sale of electric and hybrid cars has raised over there during the second quarter of 2020. These and changes like this can positively affect the environment, preserving what is necessary for future generations.

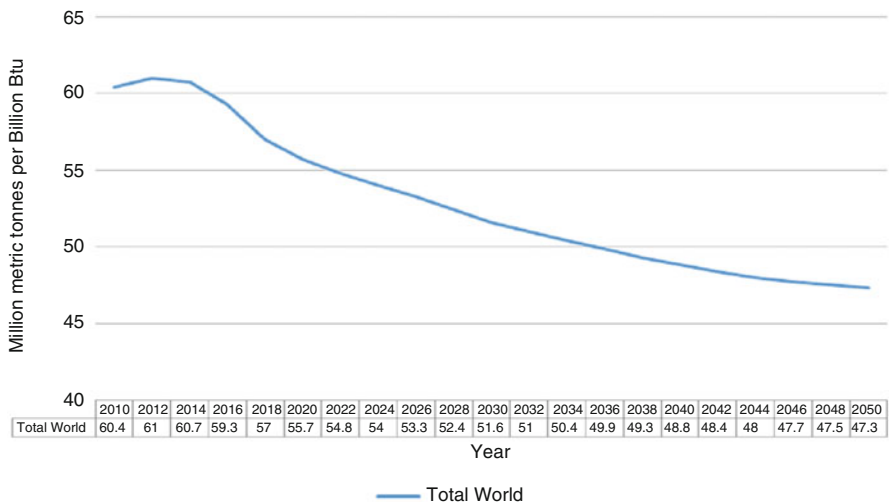


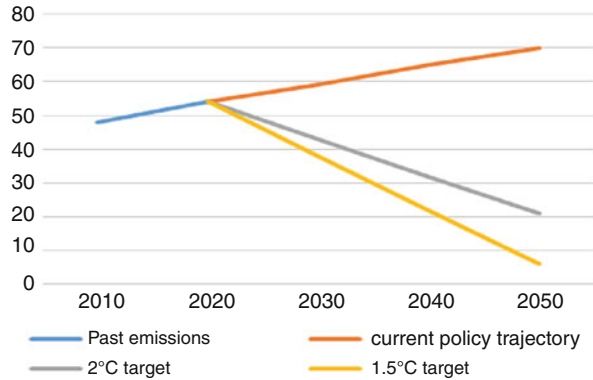
Fig. 1.21 Carbon dioxide intensity of energy use, data driven from eia.gov

1.5.2 Midterm and Long-Term Achievements

During the process of sustainable development in many countries, different road maps were created and outlooks were predicted and published. All of these outlooks share one main purpose, which is decreasing the greenhouse gas and polluting emissions until a specific deadline. Long-term effects of applying such plans for obtaining green energy will vary by region but what is obvious is that due to the predictions of the Paris Agreement, if the effective trend of decarbonizing industrial and commercial sections plus the energy utilities continue, the result will be very promising. Due to PA, by implementing the regulations and policies in the energy and industry section, the emissions could stop at a constant level, while applying harsh rules and strict provisions will result in more than 50% decrease in emissions [26].

The US energy information agency has predicted the average amount of carbon emissions for the world in the energy section which shows that after 2017, all of the predicted values are descending. The CO₂ emission values in 2017 will decrease from 57.6 MMmt/BBtu to 47.3 MMmt/BBtu in 2050 (Fig. 1.21). Many factors can be responsible to determine the slope of this diagram like economic growth, fuel costs, and unpredicted global incidents. One good example is the coronavirus pandemic that appeared in the last quarter of 2019. As per official reports, CO₂ production has decreased by 8% per month in 2020, which will result in a faster downward trend of the overall emission diagram. However, it is estimated that the diagram will regain its normal trend in the upcoming years, by increasing the emission 4% more, resulting in an overall 4% emission reduction in 2021.

Fig. 1.22 Paris Agreement emission reduction targets



It is good to mention that one of the main concerns about the future of the earth is its temperature. By the increasing trend of greenhouse gases in the following years, this number has been increased to a dangerous threshold of 4–5°. This number must be below 2° in order to prevent unwanted damages to the cities and enormous costs of sea-level risings, food crop destruction, etc. A study done by the Stockholm Resilience Center shows that even setting a threshold on 2° may not be enough as, from one point onwards, the situation may get worse than before. Global warming can trigger a process in which nature can intensify global warming itself, causing the earth to be a “hothouse.” Due to this issue, some approaches are pointing to the 1.5° of temperature rising besides developing emission reduction technologies to reduce the greenhouse gas impact more (Fig. 1.22).

1.6 Demand Response Solutions

Generally, demand response refers to any change of customers and end users’ energy consumption data in response to the price changes which could differ from time to time. These programs can have cost-saving effects if they are implemented in an energy system. They are usually divided into two categories, time-based and incentive-based programs [27]. Different subsections of each group are available in Fig. 1.23.

Time of use program refers to a pricing system in which three different prices are calculated for the consumption of mostly residential customers due to the time of energy use. Those prices are called peak, off-peak, and average. Due to the implementation of advanced metering technologies in smart grids, the consumption data could be available remotely which makes the pricings accurate. Critical peak price is also a system in which there are different prices during the peak times of grid energy consumption in some days in a year. Real-time pricing refers to a method that defines the price of energy for each hour of the day (prices for minutes and seconds can be

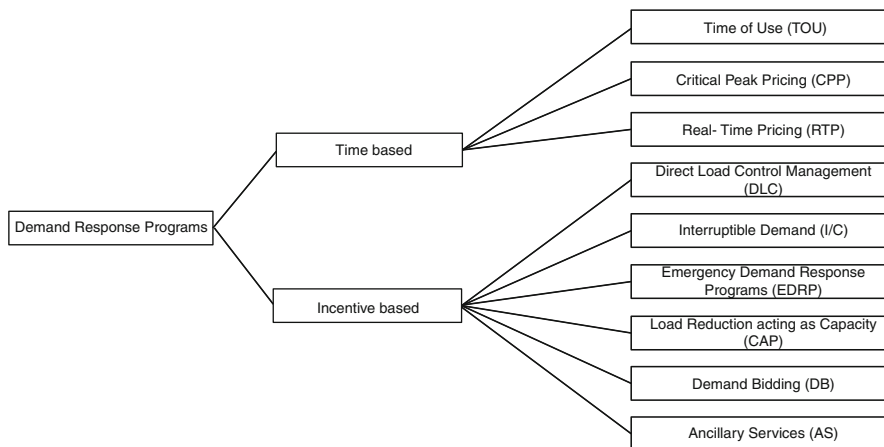


Fig. 1.23 Demand response programs

available for smart grid infrastructure). RTP is strictly dependent on the energy market.

In a study done by Electric Reliability Council of Texas (ERCOT) on its restructured energy market [28], it is shown that a new approach of aggregated demand response (AGG DR) was initiated in the energy market in which CPP was implemented in their pricing system. With their 12,000 participants in the AGG DR program of which 800 were industrial consumers, they had about 600 MW demand reduction in their four summer coincident peak time intervals which were about 15 min in 4 months of June till September. This study also shows the importance of incentives paid to parties in order to increase their participation in the program wherein eventually they are planning to increase the price cap up to 3000\$ per MWh. Although there was not so much change in consumption patterns of participants during the initial price spikes according to results, there were low but noticeable changes in the spikes that occurred in 2007. Concerning different issues like incentives, transmission line costs, and distributed energy generators, AGG DR is accounted as a useful hybrid approach with CPP or even in some cases RTP, in order to control the demand.

Direct load control management is a way to control energy consumption in special occasions (like summer days) or peak times. In this program, incentives will be paid to customers who can reduce their consumption in those days. Interruptible demand refers to a plan to control the peak value of grid consumption by making the customers reduce their usage for a specific amount of time (30 min to 1 h). Participation in this program is only permitted for a fixed range of consumers and failure in reduction is usually faced with penalties. The emergency demand response program (EDRP) is also an incentive-based demand response method in which customers choose to change their consumption patterns when system reliability is at stake. There are incentives for participants in EDRP but no penalties for refusals.

Load reduction in some consumers up to 100 KW for example, in order to increase the capacity of the grid on critical occasions, is also an incentive-based program that has no fines for loads that have not participated. In demand bidding, large-scale customers suggest the price for taking part in the load reduction program. Ancillary services provide the same opportunity as demand bidding for a vast range of customers with one condition that they should participate in the program within a short amount of time (in minutes usually) when it is needed.

These programs have their specific effects on multi-carrier energy systems but what is same for all of them is that they are implemented to achieve economic results from the operating costs of the grid in which the participation of customers has a great impact on defining the reduction of consumption and controlling the system which ends up in reduced operational costs. In the below subsections, differences each of the programs can create in the overall operating costs of the system are analyzed and shown due to a study [29].

1.6.1 Time-Based Demand Response Programs

Time-based demand response programs have a significant effect on decreasing the operating costs of energy systems. Due to studies, among different methods, CPP can smoothly shave the load peak while changing the off-peak pattern slightly. This approach has the least financial savings among other methods. The time of use program can adjust the demand diagram smoothly for 24 h, not as smooth as CPP obviously. RTP is also a bit successful in decreasing the demand during the peak time and valley filling during the off-peak with the lowest operational cost among the others. However, cost reduction alone is not the most important factor in deciding which program to implement. The ratio between consumption and cost reduction is needed to be analyzed in order to handle the accurate efficiency state to find the best solution. Here, TOU has the best performance compared to RTP and CPP. The comparison diagrams between the programs and the base approach are available in Figs. 1.24 and 1.25.

1.6.2 Incentive-Based Demand Response Programs

Unlike the time-based demand response programs, some of the incentive-based programs are presumed to have the best results among the other demand response programs in optimizing the operational costs. EDRP has the most reduction in demand, almost 70% for the peak time value. Interruptible load controlling is also a suitable program to meet the cost reduction goals in energy hubs. Compared to these two methods, DLC and CAP methods do not show the necessary efficiency to

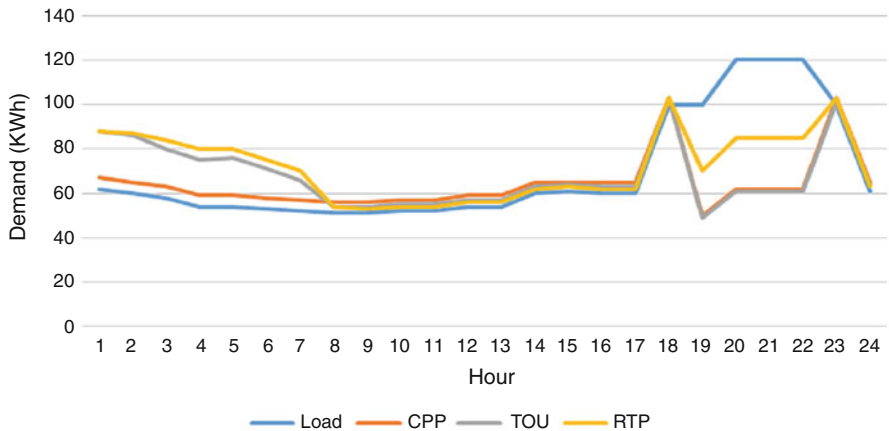


Fig. 1.24 Demand diagram per hour with/without time-based DR programs [29]

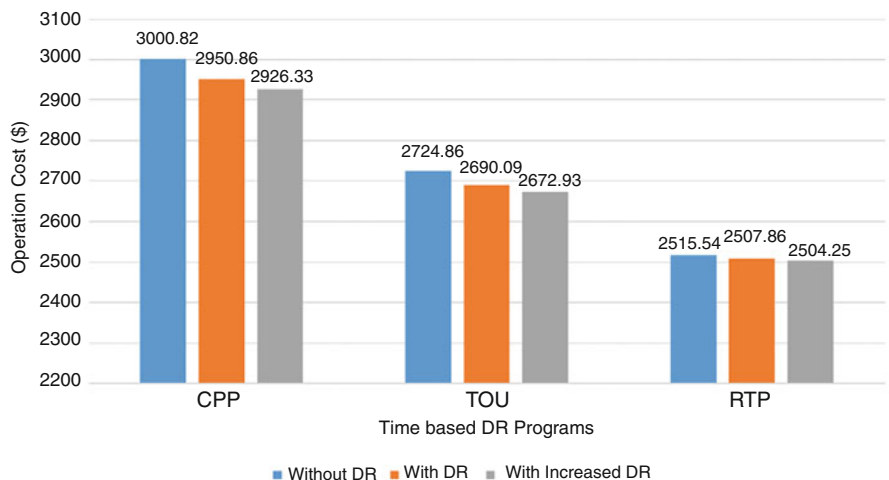


Fig. 1.25 Operation cost comparison between base and demand response-included systems [29]

control the consumption in the necessary times and the program may fail in case of need. Their demand diagram is somehow the same as the baseload diagram and because of that they should be implemented in the system if social options and technical infrastructure permit. The comparison diagrams between the programs and the base approach are available in Figs. 1.26 and 1.27.

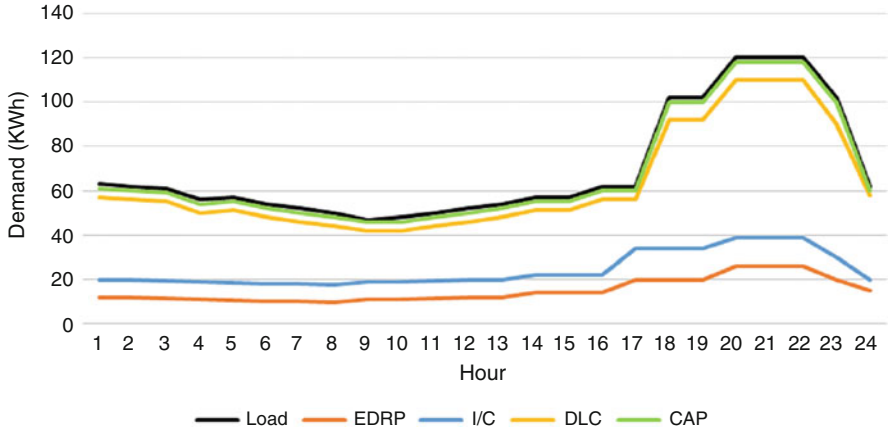


Fig. 1.26 Demand diagram per hour with/without incentive-based DR programs [29]

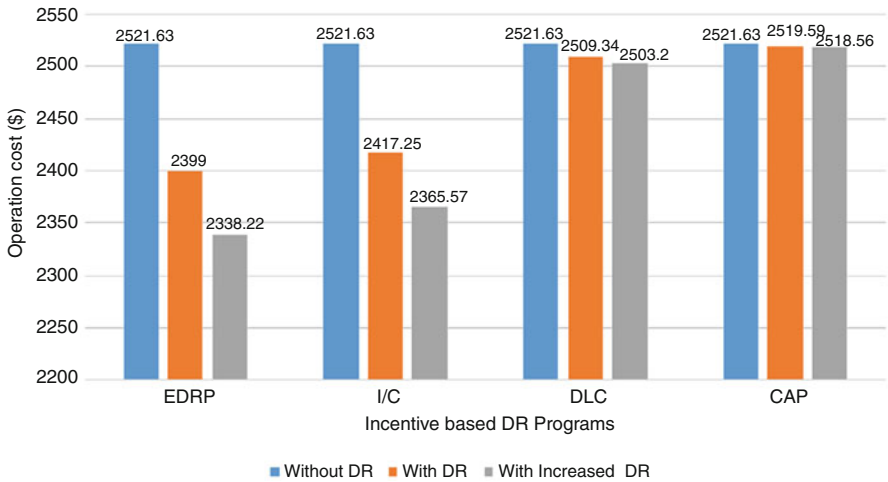


Fig. 1.27 Operation cost comparison between base and demand response-included systems [29]

1.7 Conclusion

After discussing new energy types and technologies and analyzing the possibility of replacing them with traditional coal and other fossil fuel power plants, the possibility of implementing energy conversion projects and finally creating an energy hub, consideration of reliability and resiliency constraints in the system, execution of demand response programs, and economical comparison of the environmental effects of multi-carrier energy systems with the traditional energy systems in this

chapter, it can be seen that the implementation of energy systems with several carriers can reduce the cost of design and construction, operation and maintenance, optimization, and environmental impacts as well as adjust rational and reasonable energy prices for consumers. The importance of this is due to the fact that over time, fossil energy resources will be depleted, and if they are used continuously, serious climate change may occur on Earth, making the condition impossible to return to the previous point. Given these circumstances, as well as the appearance of innovative loads like EVs in the future, systems must be designed to reduce energy costs in addition to meeting these needs.

References

1. (EIA) USEIA (2018) Electric Power Annual. 2018, 239
2. Shell International and The Development Research Center, Ishwaran M, King W, Haigh M, Lee T, Nie S (2017) Roadmap for Natural Gas Market Liberalisation and Regulatory Reform. In: Shell Centre, The Development Research Center (DRC) of the State Council of the People's Republic of China (eds) China's Gas Development Strategies. Advances in Oil and Gas Exploration & Production. Springer, Cham. https://doi.org/10.1007/978-3-319-59734-8_14
3. (EIA) USEIA (2020) Cost and Performance Characteristics of New Generating Technologies, Center, Bipartisan Policy. Annual Energy Outlook 2020. United States Energy Information Agency (EIA)
4. Rao K (2019) Wind energy for power generation: meeting the challenge of practical implementation. Springer Nature Switzerland AG
5. Secretariat I (2012) Renewable energy technologies: cost analysis series, Wind Power. IRENA, Abu Dhabi
6. I. Geothermal Power: Technology Brief (2017) International renewable energy agency. IRENA, Abu Dhabi
7. IRENA (2012) Renewable energy technologies: cost analysis series. Biomass for Power Generation. p. 60
8. EIA U (2008) Electric power annual 2008. DOE/EIA-0348
9. Dielen G (2012) "Renewable energy technologies-cost analysis series: hydropower". International Renewable Energy Agency
10. Mohammadi-Ivatloo B, Jabari F (2018) Operation, planning, and analysis of energy storage systems in smart energy hubs. Springer International Publishing AG, part of Springer Nature
11. Nazari-Heris M, Mohammadi-Ivatloo B, Gharehpetian GB, Shahidehpour M (2018) Robust short-term scheduling of integrated heat and power microgrids. IEEE Syst J 13:3295–3303
12. Gondal IA (2019) Offshore renewable energy resources and their potential in a green hydrogen supply chain through power-to-gas. Sustain Energy Fuels 3:1468–1489
13. Mirzaei MA, Nazari-Heris M, Mohammadi-Ivatloo B, Zare K, Marzband M, Anvari-Moghaddam A (2020) A novel hybrid framework for co-optimization of power and natural gas networks integrated with emerging technologies. IEEE Syst J
14. Imani M, Ghoreishi SF, Allaire D, Braga-Neto UM (2019) MFBO-SSM multi-fidelity Bayesian optimization for fast inference in state-space models. Proceedings of the AAAI Conference on Artificial Intelligence, 7858–7865
15. de Boer HS, Grond L, Moll H, Benders R (2014) The application of power-to-gas, pumped hydro storage and compressed air energy storage in an electricity system at different wind power penetration levels. Energy 72:360–370
16. Zohuri B, McDaniel P (2017) Combined cycle driven efficiency for next generation nuclear power plants: an innovative design approach. Springer, New York

17. Ezzati SM, Shourkaei HM, Faghihi F, Mozafari SB, Soleymani S (2019) Optimum energy hub economic dispatch using chance constrained optimization. 2019 International Power System Conference (PSC): IEEE, 209–215
18. Mohammadi M, Noorollahi Y, Mohammadi-ivatloo B, Hosseinzadeh M, Yousefi H, Khorasani ST (2018) Optimal management of energy hubs and smart energy hubs – a review. *Renew Sust Energ Rev* 89:33–50
19. Salehimalah M, Akbarimajd A, Valipour K, Dejamkhooy A (2018) Generalized modeling and optimal management of energy hub based electricity, heat and cooling demands. *Energy* 159:669–685
20. Mirzaei MA, Nazari-Heris M, Mohammadi-Ivatloo B, Zare K, Marzband M, Pourmousavi SA (2020) Robust Flexible Unit Commitment in Network-Constrained Multicarrier Energy Systems. *IEEE Systems Journal*, 1–10
21. Roustai M, Rayati M, Sheikhi A, Ranjbar A (2018) A scenario-based optimization of Smart Energy Hub operation in a stochastic environment using conditional-value-at-risk. *Sustain Cities Soc* 39:309–316
22. Mansour-Saatloo A, Agabalaye-Rahvar M, Mirzaei MA, Mohammadi-Ivatloo B, Zare K (2020) Robust scheduling of hydrogen based smart micro energy hub with integrated demand response. *J Clean Prod* 122041
23. Almassalkhi M, Hiskens I (2011) Cascade mitigation in energy hub networks. 2011 50th IEEE Conference on Decision and Control and European Control Conference: IEEE 2011, 2181–2188
24. Skea J, Ekins P, Winskel M (2011) *Energy 2050: making the transition to a secure low carbon energy system*. Routledge, London
25. Teske S (2019) *Achieving the Paris climate agreement goals: global and regional 100% renewable energy scenarios with non-energy GHG pathways for+ 1.5 C and+ 2 C*. Springer Nature Springer
26. Wuebbles D, Fahey D, Hibbard K (2017) *US Global Change Research Program: Climate Science Special Report*.
27. Aalami H, Moghaddam MP, Yousefi G (2010) Demand response modeling considering interruptible/curtailable loads and capacity market programs. *Appl Energy* 87:243–250
28. Zarnikau J, Hallett I (2008) Aggregate industrial energy consumer response to wholesale prices in the restructured Texas electricity market. *Energy Econ* 30:1798–1808
29. Pazouki S, Ardalan S, Haghifan M-R (2015) Demand response programs in optimal operation of multi-carrier energy networks. *Indian J Sci Technol* 8:1–7

Further Reading

1. Mohammadi-Ivatloo B, Nazari-Heris M (2019) *Robust optimal planning and operation of electrical energy systems*. Springer Nature Switzerland AG
2. Zhang X, Shahidehpour M, Alabdulwahab A, Abusorrah A (2015) Optimal expansion planning of energy hub with multiple energy infrastructures. *IEEE Transac Smart Grid* 6:2302–2311
3. Sadeghi H, Rashidinejad M, Moeini-Aghtaie M, Abdollahi A (2019) The energy hub: an extensive survey on the state-of-the-art. *Appl Therm Eng* 161:114071
4. Wang A, Liu J, Wang W (2018) Flexibility-based improved model of multi-energy hubs using linear weighted sum algorithm. *J Renewable Sustainable Energy* 10:015901
5. Kamyab F, Bahrami S (2016) Efficient operation of energy hubs in time-of-use and dynamic pricing electricity markets. *Energy* 106:343–355
6. White CD, Zhang KM (2011) Using vehicle-to-grid technology for frequency regulation and peak-load reduction. *J Power Sources* 196:3972–3980
7. Kiaee M, Cruden A, Sharkh S (2015) Estimation of cost savings from participation of electric vehicles in vehicle to grid (V2G) schemes. *J Modern Power Syst Clean Energy* 3:249–258

8. Mazza A, Bompard E, Chicco G (2018) Applications of power to gas technologies in emerging electrical systems. *Renew Sust Energy Rev* 92:794–806
9. Götz M, Lefebvre J, Mörs F, Koch AM, Graf F, Bajohr S et al (2016) Renewable power-to-gas: a technological and economic review. *Renew Energy* 85:1371–1390
10. Vega LA (2010) Economics of ocean thermal energy conversion (OTEC): an update. Offshore Technology Conference
11. VanBrakle JD (2011) Manomet: time to turn up the heat on woody biomass. *J For* 109:244
12. Administration USEI (2017) Distributed generation and combined heat & power system characteristics and costs in the buildings sector. In: Energy USDoE, editor. U.S. Energy Information Administration (EIA): Independent Statistics & Analysis, p. 146
13. IRENA I (2018) Renewable power generation costs in 2017. Report, International Renewable Energy Agency, Abu Dhabi
14. Sheikhi A, Mozafari B, Ranjbar AM (2011) CHP optimized selection methodology for a multi-carrier energy system. 2011 IEEE Trondheim PowerTech: IEEE 1–7
15. Hydropower (2004) Setting a Course for Our Energy Future United States. <https://www.nrel.gov/docs/fy04osti/34916.pdf>
16. Liu T, Zhang D, Wang S, Wu T (2019) Standardized modelling and economic optimization of multi-carrier energy systems considering energy storage and demand response. *Energy Convers Manage* 182:126–142
17. Green O, Studies G (2012) OECD green growth studies. Director 104. <https://doi.org/10.1787/9789264115118-en>
18. Amir V, Azimian M, Razavizadeh AS (2019) Reliability constrained optimal design of multicarrier microgrid. *Int Transac Electr Energy Syst* 29:e12131
19. Sheikhi A, Ranjbar AM, Oraee H, Moshari A (2011) Optimal operation and size for an energy hub with CCHP. *Energy Power Eng* 3:641
20. Beigvand SD, Abdi H, La Scala M (2017) A general model for energy hub economic dispatch. *Appl Energy* 190:1090–1111
21. Roustaei M, Niknam T, Salari S, Chabok H, Sheikh M, Kavousi-Fard A et al (2020) A scenario-based approach for the design of smart energy and water hub. *Energy* 195:116931
22. Papadimitriou C, Anastasiadis A, Psomopoulos C, Vokas G (2019) Demand response schemes in energy hubs: a comparison study. *Energy Procedia* 157:939–944
23. Sarlak G, Moghimi SM (2016) Energy management optimizing in energy HUB with regard to pollution and storage effects. *Phys Sci Int J* 11:1–10
24. Gholizadeh N, Gharehpetian GB, Abedi M, Nafisi H, Marzband M (2019) An innovative energy management framework for cooperative operation management of electricity and natural gas demands. *Energy Convers Manag* 200:112069
25. Komarnicki P, Lombardi P, Styczynski Z (2017) Electric energy storage systems: flexibility options for smart grids. Springer, Berlin, Heidelberg
26. Brown MA, York D, Kushler M (2007) Reduced emissions and lower costs: combining renewable energy and energy efficiency into a sustainable energy portfolio standard. *Electr J* 20:62–72
27. Widl E, Jacobs T, Schwabeneder D, Nicolas S, Basciotti D, Henein S et al (2018) Studying the potential of multi-carrier energy distribution grids: a holistic approach. *Energy* 153:519–529
28. Daryani N, Tohidi S (2019) Economic dispatch of multi-carrier energy systems considering intermittent resources. *Energy Environ* 30:341–362
29. Sheikhi A, Ranjbar A, Oraee H (2012) Financial analysis and optimal size and operation for a multicarrier energy system. *Energ Buildings* 48:71–78
30. Swisher J, Jannuzzi G, Redlinger R (1997) Integrated resource planning
31. Seifi H, Sepasian MS (2011) Load forecasting. *Electric power system planning: issues, algorithms and solutions*. Springer, Berlin, Heidelberg, pp 45–67
32. Seifi H, Sepasian MS (2011) Some economic principles. *electric power system planning: issues, algorithms and solutions*. Springer, Berlin, Heidelberg, pp 31–44

Chapter 2

Introduction and Literature Review of the Operation of Multi-carrier Energy Networks



Mehrdad Ghahramani, Milad Sadat-Mohammadi, Morteza Nazari-Heris,
Somayah Asadi, and Behnam Mohammadi-Ivatloo

2.1 Introduction

Energy supply has been one of the most important issues facing mankind in recent decades [1]. All of the various fields of this issue, such as consumption by various demands, switching between various resources, and providing from different energy systems, are influential in human life [2]. Also, the ever-increasing population of the world and the growing need for energy and reducing fossil fuels along with environmental pollution have caused many problems for the international community. Energy directly affects all aspects of a country, such as politics, internal security, economy, and environment; consequently, energy policy in different countries seeks to provide sustainable energy supply [3]. In recent decades, most of the energy production has been provided through thermal power plants using fossil fuels, in which due to low productivity and high losses, most of the produced energy is wasted [4]. Also, the produced energy is transferred through long transmission lines from the place of production to the place of consumption and delivered to consumers by sophisticated distribution systems. Utilizing thermal power plants due

M. Ghahramani

Faculty of Electrical and Computer Engineering, University of Tabriz, Tabriz, Iran
e-mail: m.ghahramani94@ms.tabrizu.ac.ir

M. Sadat-Mohammadi · M. Nazari-Heris (✉) · S. Asadi

Department of Architectural Engineering, Pennsylvania State University, State College, PA,
USA

e-mail: miladsm@psu.edu; mun369@psu.edu; sxa51@psu.edu

B. Mohammadi-Ivatloo

Faculty of Electrical and Computer Engineering, University of Tabriz, Tabriz, Iran

Department of Energy Technology, Aalborg University, Aalborg, Denmark

e-mail: mohammadi@ieee.org

to the lack of fossil fuels and environmental pollution, along with the high investment cost of energy transmission and distribution, logically makes no sense. One of the proposed models to solve these problems and achieve a sustainable energy model is the use of multi-carrier energy systems (MCESs) where several different energy carriers interact optimally with each other and are responsible for providing optimal energy. MCES has various environmental, economic, and technical benefits such as reducing energy costs, increasing reliability, and improving the performance of the system [5].

2.2 Operation of Multi-carrier Energy Systems with Different Objectives

In general, issues related to multi-carrier energy systems fall into several categories, including the optimization objectives, energy flow constraints of multiple energy carriers, uncertainty-handling methods in multi-carrier energy systems, etc. The energy flow analysis has been investigated in recent publications by a narrative focus on power, heat, and gas flow in networks. In [6], a power flow model has been proposed based on a linear scheme while this problem is also solved for the integration of electrical and heating networks in [7]. The authors of [8] have proposed a power flow model for the combination of gas, power, and heat network. The results of this study show that the power flow of multi-carrier systems cannot be decoupled, and these carrier infrastructure are completely dependent. The researchers of [9] have utilized a goal attainment scheme for an optimal power flow problem where the presence of several interconnected multi-carrier energy systems has been considered.

As mentioned, the other type of issues which the operator of multi-carrier systems faces are optimization problems. In addition, in studies on optimization of integrated multi-carrier systems the presence of other challenges has also been studied. For instance, environmental and emission problems; regulation in power network infrastructure; flexibility, reliability, and sustainability of supply [10]; quality of supplied power [11]; complicity of connections; power protection; and penetration of distributed and renewable energy resources have been considered in optimal operation of such systems that a number of these studies are listed below. In [12], the optimal operation of a smart multi-carrier system has been conducted where DR programs are utilized for balancing supply and demand. The infrastructure of a multi-carrier system including optimal sizing and design of it has been studied in [13] as a multi-objective problem where one of the objectives is the optimal operation of such a system. The researchers of [14] are seeking an optimization model that maximizes the profit of a multi-carrier energy system. An optimal operation scheme has been utilized in [15] which takes into account the constraints of real-time and dynamic pricing. In [16], the affiliation of carriers at both load and supply side has been considered for studying about the adequacy of a multi-carrier energy system. The

authors of [17] proposed an optimal operation model where DR programs and renewable energy resources are taken into account. In [18], the penetration of electric vehicles has been considered in the optimal operation of a multi-carrier energy system. The reliability of a multi-carrier energy system has been studied through the optimal operation of such systems in [19, 20]. The combination of heat and electrical carriers has been studied as an economic dispatch problem using a genetic algorithm [21] while this problem has been solved by whale optimization algorithm [22]. The penetration of renewable energy sources in the operation of a multi-carrier energy system has been studied in [23]. The authors of [24] introduced a residential multi-carrier heat and power energy system where electric vehicles have been utilized. In [25] a hierarchical model has been presented for energy management of a multi-carrier energy system where control layers including monitoring, optimizing, and implementation have been considered in optimal operation. A new algorithm based on a teaching-learning scheme has been conducted on the operation of multi-carrier energy systems in [26]. In [27], the authors have studied both of the optimization problem and power flow problem for a multi-carrier energy system using TVAC-GSA method.

To summarize the objectives studied in the operation of multi-carrier energy systems, Table 2.1 is given that concentrates on the type of interconnection in multi-carrier energy networks, the main objective, and novelties of each study.

2.3 Various Energy Carriers in Multi-carrier Energy

In recent decades, most of the studies just focused on the utilization of one energy carrier for supplying the required demand. The major part of these studies focused on providing and challenges of electrical power supply [47, 48]. In addition, there are a lot of studies where the authors have noticed other energy carriers such as natural gas network [49, 50], and heating system [51, 52] networks. But recently, the integration between various kinds of energy carriers has been taken into consideration.

2.3.1 Gas and Electricity Resources

A huge part of the produced energy by power plants comes from fossil fuels such as natural gas, coal, and oil. Recently, due to the increasing presence of gas generators, microturbines, and power-to-gas storage systems, natural gas is increasingly playing a role in providing electricity [53]. In the United States, the integration of gas in producing electrical energy has increased by about 12% from 2005 to 2016. Also, worldwide, the use of gas to generate electricity has risen from 15% in 2000 to 50% in 2014 [54]. A simplified schematic of power and gas systems is demonstrated in Fig. 2.1. In recent years, comprehensive studies have been conducted on the integration of electrical and gas energy. A security-constrained model has been

Table 2.1 Summary of objectives in the area of multi-carrier system operations

Reference	Type of interconnection	Main objective	Novelties	Solution method	Publication date
[28]	Power and water	Minimizing daily power production cost of hydrothermal plants	Using a new optimization method to obtain optimal operation cost	Real-coded genetic algorithm	2017
[29]	Power and gas	Analysis of cost-benefit for power-to-gas units	Optimization of hydrogen storage technology and methanation capacity	MATLAB optimization toolbox	2020
[30]	Power and gas	Analyzing the penetration of renewable energy sources and power-to-gas systems	Proposing a detailed model of P2G plants	–	2020
[31]	Power, gas, and heat	Optimal operation concerning wind power uncertainty with economy and safety analysis	Applying conditional value-at-risk for the uncertainty of wind power as well as proposing a linearization model	GAMS optimization solvers-CPLEX	2020
[32]	Power, gas, and heat	Maximizing social welfare of each energy system considering interconnectivity constraints	Proposing an equilibrium model for gaming process of each network operator in the market	GAMS optimization solvers-IPOPT	2020
[33]	Power and heat	Minimizing heat and power production cost of CHP plants	Proposing a novel optimization method to obtain optimal operation cost	Harmony search method	2019
[34]	Power and heat	Minimizing the cost of heat and power demand-supply using CHP plants	Applying a new approach called stochastic fractal search algorithm	Stochastic fractal search algorithm	2020
[35]	Power and heat	Maximization of the savings and minimization of the risk associated with power price as well as environmental issues	Proposing a bi-objective function and a stochastic operation model of power and heat systems	Internet of Things (IoT) software platforms	2020
[2]	Gas, power, heat, and water	Optimal operation of multi-carrier energy systems considering energy storage facilities	Studying interconnection among gas, power, heat, and water energy carriers	GAMS optimization solvers-DICOPT	2020

[36]	Power and heat	Optimal operation of integrated heat and power network with small-scale fuel cell	Considering thermal energy storage and fuel cell and application of a quasi-static method for coupling the dynamic components	MATLAB	2020
[37]	Power and water	Management of electrical energy for a water desalination plant	Considering hybrid renewable energy resources including photovoltaic cells and wind turbine connected to batteries	MATLAB-Simulink	2020
[38]	Power and water	Modeling, designing, and optimizing a joint water and energy supply network for an area	Considering hybrid solar-wind renewable sources for power and heat supply	GAMS optimization solvers-CPLEX	2020
[39]	Power and water	Minimizing power supply cost of the hydrothermal system	Introducing a novel approach for attaining optimal operation cost	Harmony search	2018
[40]	power and heat	Maximization of the system cost-savings	Maximizing annual savings of the system based on a probabilistic method	Genetic algorithm	2020
[41]	Power and water	Optimal power flow of integrated hydrothermal and wind turbines	Proposing a sine cosine algorithm for obtaining the optimal setpoints of the problem	Sine cosine algorithm	2020
[42]	Power and gas	Optimal operation of power and gas systems with integration of wind power	Dealing with the uncertainty of wind power using a robust model	Decomposition method	2020
[43]	Power and gas	The optimal energy flow of power and gas networks	Employing information gap decision theory for dealing with wind power output and using a linearization method	MATLAB platform	2020
[44]	Gas, power, heat, and water	Operation of multi-carrier networks considering uncertain parameters	Applying information-gap decision theory to model the power load uncertainty	GAMS optimization solvers	2020

(continued)

Table 2.1 (continued)

Reference	Type of interconnection	Main objective	Novelties	Solution method	Publication date
[45]	Power and gas	The optimal energy flow of integrated power and gas systems	Studying demand response and compressed air energy storage as well as wind power uncertainty	GAMS optimization solvers-CPLEX and MATLAB YALMIP toolbox	2020
[46]	Power and gas	Minimizing cost and emission	Considering power-to-gas technology and demand response programs	GAMS optimization solvers	2020

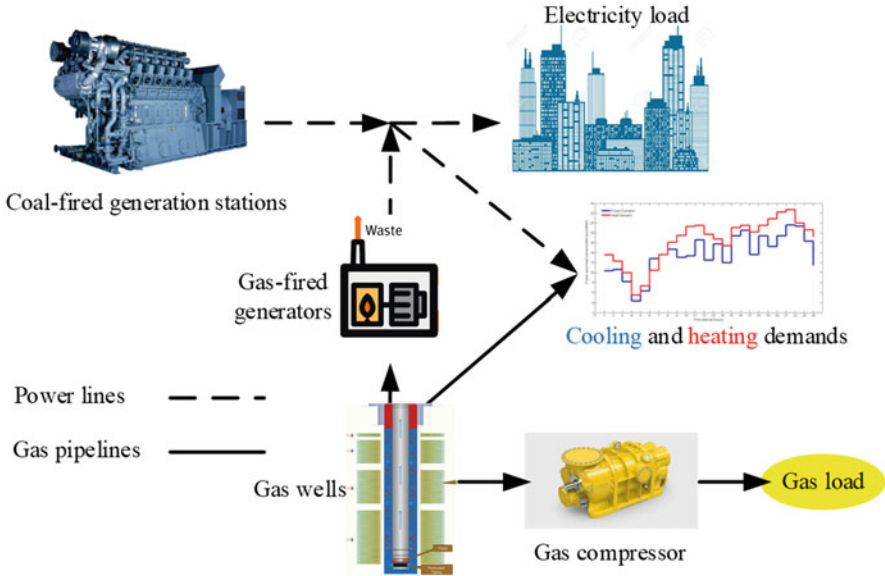


Fig. 2.1 Integrated power and gas systems

presented for integration of power and gas networks in [55], and all of the constraints of both of the networks including transmission and pipelines have been taken into account. A coordinated model for optimal operation of integrated power and gas networks is presented in [56], in which the uncertainty of wind generation was considered. In addition, a DR program is utilized for adjusting gas and power demands. The authors of [57] utilized the Newton–Raphson method for the power flow problem of an integrated gas and power network. A robust operation method is utilized in [58] to investigate the role of considering the integration of gas and power systems in adjusting demand. The researchers of [59] introduced a bi-level model for optimal energy scheduling of integrated gas and electricity networks, where the objectives are minimizing operational costs and maximizing the profit of the owner. The authors of [60] presented another bi-level model for IGEN dealing with constraints of both of the energy carriers.

In [61], a different model of previous bi-level schemes has been presented in order to study the energy management of an IGEN that investigates optimal operation and expansion planning of such networks in the lower and upper levels, respectively. In [62], the researchers have presented a competing model for two objectives of the energy management problem of IGENs, where the objective function of the problem is to minimize costs and pollution at the same time.

In [63], the authors proposed a robust operation model for IGENs, where a bi-level scheme is utilized where the constraints of gas-fueled plants and power-to-gas sites are considered. Stochastic optimal scheduling is proposed in [64], in order to determine the optimal operation point of gas-fueled plants and power-to-gas

technologies. A multi-objective scheme with competing objectives is proposed in [65] where the objectives are decreasing emission and operation costs of IEGNs. The authors of [66] proposed a unit commitment model for an IEGN, which considered the possible losses of power plants and the outages of system lines based on security-constrained schemes.

In [67] an energy management framework of IEGNs is presented for determining optimal performance points of system carriers where the master problem is the generation of the power network, and the subproblem is a mixed-integer linear programming method for the natural gas system.

An IEGS operation model is proposed in [68], where the case study is European gas and power network for studying the possible outages of the gas system. In [69] the researchers have proposed a multi-objective model for solving optimal scheduling problems of IEGS with lower operating costs. This reference utilized a genetic algorithm for determining an economic emission dispatch optimally.

2.3.2 Electricity and Heat Resources

Recently, new technologies have been used in the energy supply of commercial buildings, and large industrial and residential units. One of the most important forms of energy required in these units is heat, which is provided by local units. CHP units, which are shown in Fig. 2.2, play a key role in efficiently providing this energy so that the supply of electric and heat load by these units has increased the efficiency by 90% and has led to a reduction in the cost of providing electricity and heat energy [70]. The combination of electrical and heat systems (IEHS) has been studied in

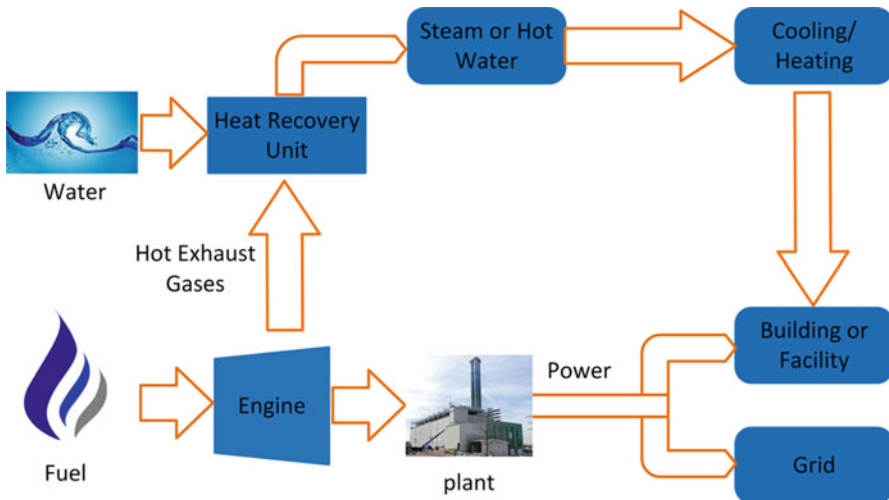


Fig. 2.2 The basic of CHP plants

several studies and the results show the improvement of efficiency in providing the required thermal and electrical loads. In [71], a unit commitment scheme has been presented for IEHS where the constraints of CHP units and heating system are considered. In addition, the authors of this study presented a heat storage system in order to handle the uncertainties of wind turbines which have improved the flexibility of the system. The researchers of [72] have analyzed the energy scheduling of an IEHS where the uncertainties of wind turbines and energy prices are taken into account. In [73, 74], the authors have presented a multi-objective model for the management of an IEHS to minimize the emission and the system operation cost. In [75] a bi-level power flow scheme has been introduced for IEHS where the objective is maximizing the profit of system and CHP profits. The researchers of [76] introduced a deterministic model for scheduling an IEHS while the uncertainties of price, wind, and demand in energy scheduling of such a system have been considered. In [77], the combination of heat and power systems is done by a micro-CHP in order to supply the need for heat and power of a multi-apartment housing. The researchers of [78, 79] have studied various aspects of the IEHS's presence in distribution networks. In distribution networks, IEHS can exchange power with the upstream network while providing the required energy of local demands. This exchange can help the operator to decrease the purchasing power from the upstream grid in high-price hours. A stochastic model is presented in [80] where a distributed energy aggregator and the effect of CHP and PV system have been studied for reaching an optimal bidding strategy. In [81], an optimal multi-objective scheme is studied for decreasing the emission and operation costs of primary energy input. In this reference, the presented system is studied in two modes of islanded and grid connected in order to achieve the best sizes of technologies.

2.3.3 Water and Electricity Resources

Clean and potable water is one of the most basic human needs in industry, agriculture, and daily life around the world [82]. A significant portion of the world's population suffers from a lack of access to clean water [83]. In the future, this issue will be more problematic due to the growth rate of the world's population and the expansion of growing industries [84]. One way to supply the required water of human life is to use the process of desalination of seawaters and oceans. Given that more than 95% of the water on Earth is saltwater, desalination will provide huge amounts of freshwater. Numerous items, including electricity prices, the volume of salt that dissolved in the water unit, and the capacity of the technology, affect the cost of desalination of water and the supply of freshwater [85]. Numerous methods have been studied for the process of desalination of water, including membrane structures and thermal technologies [86–88]. The issue that necessitates the integration of the power with water carriers is the high consumption of electrical energy by desalination technologies. High energy consumption in the desalination process requires an

adequate local supply of electricity. In addition to the connection of electricity and water carriers in the field of desalination of brackish water, the relationship between these two carriers through pumped hydro storage systems has been considered for the past years, so that more than 95% of energy storage systems are pumped hydro storage systems. Hydro storage technologies give the network operator the ability to quickly enter the network in the event of a power outage and prevent network frequency drops. The presence of this technology improves the performance of the power systems and increases the flexibility of the system operator. The integration of electrical and water carriers through desalination technologies and hydro pumped storage systems has received much attention.

2.4 Uncertainty-Handling Methods in Operation of Multi-carrier Energy Systems

There are various interspersions for the content of risk according to the context in which it is used. Mostly, we define it as a possibility of an unintended situation occurring, which is mainly due to the uncertainty in the process of decision-making. This situation can be an undesirable environmental, technical, or economic event. In the process of risk management, four important questions should be answered including the happening events, the method of measuring risk, the output, and the preventive proceedings [89].

There are various schemes for modeling the uncertainties [90], including fuzzy schemes [91], scenario-based schemes [92], IGDT-based schemes [93], and robust optimization [94]. In the scenario-based schemes, different models have been utilized for addressing the uncertainties of the problem including variance [95], short-fall probability [96], stochastic dominance [97], value-at-risk (VaR) [98], and conditional value-at-risk (CVaR) [99].

Various studies have examined the uncertainty of different parameters in integrated energy carriers. The uncertainty of load fluctuations is studied in [100], and the indeterminacy of market prices which depend on the peak and nonpeak hours, and different seasons of the year are taken into consideration in [101]. The uncertainty of these parameters complicates the predetermined network planning and creates challenges for the system operator. A stochastic programming model is presented in [102] where the fluctuations of load, price, and wind have been considered in optimal risk management of an integrated energy carrier system. The authors of [103] have introduced a Monte Carlo model for the optimal operation of an integrated energy carrier system where DR programs have been studied. In [104] a stochastic management model has been utilized for uncertainty modeling of an integrated energy carrier system where the thermal energy and DR are considered. A robust model for optimization of an integrated energy carrier system is used for uncertainty modeling in [105]. In [106, 107] a CVaR measure is utilized to address optimal energy management of an integrated energy system in the presence of

uncertainties. A scenario-based optimization scheme has been developed in [108], where a CHP-based microgrid helped an integrated energy carrier system in handling the uncertainties of load and energy price. A developed gravitational search algorithm (GSA) based on the time-varying acceleration coefficient (TVAC) has been utilized for an economic dispatch problem of integrated energy carriers in [109]. An integrated energy carrier system has been scheduled based on fuzzy model conceptions in [110]. A Monte Carlo model for a combination of a multi-energy carrier system and a storage device is presented in [111, 112] where DR schemes are considered. In this reference, the ability of the multi-carrier system in adjusting the uncertainties of market prices is considered. In order to decrease the consequences of load and price uncertainties on a multi-carrier energy system, the authors of [113] have introduced a model predictive control. In addition, the presence of storage technologies and renewable devices is taken into account.

The presence of various technologies and their effects on decreasing uncertainties and improving the performance of multi-carrier energy systems have been studied in different studies. Uncertainty modeling of multi-carrier energy systems utilizes CHP [114, 115], boiler units [116], storage technologies [117], and renewable energy sources [118] to ensure sustainable power supply. Finally, to summarize the application of well-known uncertainty-handling methodologies for the operation of multi-carrier energy systems, Table 2.2 is given.

2.5 Conclusions

The operation of multi-carrier energy networks considering the integration between power and gas, heat and power, water, and power energy carriers is investigated in this study. Firstly, the objective of operation models proposed for multi-carrier energy systems is discussed that shows the main models considered for such systems including the energy flow models and the objectives proposed for the operation of multi-carrier systems. Also, the integration between energy carriers was investigated which shows the main focus of the studies of integration between power and gas carriers, power and heat carriers, and water and power carriers. Finally, the uncertainty-handling methodologies proposed for the operation of multi-carrier energy systems were studied that showed risk analysis, and robust models have been discussed in a high portion of studies in the area of uncertain operation of multi-carrier energy systems.

Table 2.2 Implementation of various uncertainty-handling methods for optimal operation of multi-carrier energy networks

Reference	Uncertainty-handling approach	Uncertain parameter(s)	Publication date
[119]	Probabilistic programming	The power output of renewable energy resource	2020
[120]	Robust optimization	Power, gas, and heat loads, power price, and electric vehicles	2020
[121]	Robust optimization	Renewable energy and power price	2020
[122]	Interval prediction-based robust optimization	Power market price	2020
[123]	Information-gap decision theory	Load, wind, and photovoltaic power	2019
[124]	Information-gap decision theory	Power market price and wind power	2019
[125]	Robust optimization	Power and heat demands, power price, and solar irradiation	2020
[126]	Information-gap decision theory	Power consumption of electric vehicles	2019
[127]	Information-gap decision theory	Power market price	2019
[128]	Stochastic programming	Power load, wind power, and power price	2019
[129]	Fuzzy set method	Energy loads, wind power, and power market price	2020
[130]	Hybrid robust optimization and stochastic programming	Power and gas loads	2019
[131]	Stochastic programming	Renewable power output, traveling time of electric vehicles, energy prices, and power/heat demands	2020
[132]	Scenario-based stochastic programming and conditional value-at-risk	Wind power and loads	2019
[133]	Robust optimization	Power market price	2019
[134]	Stochastic programming	Loads, renewable power output, and power market	2017

References

1. Ghahramani M, Nazari-Heris M, Zare K, Mohammadi-Ivatloo B (2019) Energy and reserve management of a smart distribution system by incorporating responsive-loads/battery/wind turbines considering uncertain parameters. *Energy* 183:205–219
2. Nazari-Heris M, Mohammadi-Ivatloo B, Asadi S (2020) Optimal operation of multi-carrier energy networks with gas, power, heating, and water energy sources considering different energy storage technologies. *J Energy Storage* 31:101574
3. Mirzaei MA, Heris MN, Zare K, Mohammadi-Ivatloo B, Marzband M, Asadi S et al (2020) Evaluating the impact of multi-carrier energy storage systems in optimal operation of integrated electricity, gas and district heating networks. *Appl Therm Eng* 176:115413

4. Ghahramani M, Zare K, Mohammadi IB (2018) Optimal energy procurement of smart large consumers incorporating parking lot, renewable energy sources and demand response program. *Int J Smart Electr Eng* 7(04):145–154
5. Ghahramani M, Nojavan S, Zare K, Mohammadi-Ivatloo B (2018) c. Elsevier, pp 139–159
6. Gharebaghi S, Safdarian A, Lehtonen M (2019) A linear model for AC power flow analysis in distribution networks. *IEEE Syst J* 13(4):4303–4312
7. Liu X, Wu J, Jenkins N, Bagdanavicius A (2016) Combined analysis of electricity and heat networks. *Appl Energy* 162:1238–1250
8. Shabanpour-Haghighi A, Seifi AR (2015) An integrated steady-state operation assessment of electrical, natural gas, and district heating networks. *IEEE Trans Power Syst* 31(5):3636–3647
9. La Scala M, Vaccaro A, Zobaa A (2014) A goal programming methodology for multiobjective optimization of distributed energy hubs operation. *Appl Therm Eng* 71(2):658–666
10. Yan M, Zhang N, Ai X, Shahidepour M, Kang C, Wen J (2018) Robust two-stage regional-district scheduling of multi-carrier energy systems with a large penetration of wind power. *IEEE Transactions on Sustainable Energy* 10(3):1227–1239
11. Nazerian, E, Gharebaghi S, Safdarian, A (2017) Optimal distribution network reconfiguration considering power quality issues, 2017 Smart Grid Conference (SGC), Tehran, pp. 1–6
12. Sheikhi A, Bahrami S, Ranjbar AM (2015) An autonomous demand response program for electricity and natural gas networks in smart energy hubs. *Energy* 89:490–499
13. Evins R (2015) Multi-level optimization of building design, energy system sizing and operation. *Energy* 90:1775–1789
14. Moghaddam IG, Saniei M, Mashhour E (2016) A comprehensive model for self-scheduling an energy hub to supply cooling, heating and electrical demands of a building. *Energy* 94:157–170
15. Tesfa B, Mishra R, Zhang C, Gu F, Ball A (2013) Combustion and performance characteristics of CI (compression ignition) engine running with biodiesel. *Energy* 51:101–115
16. Wolff MS, Teitelbaum SL, McGovern K, Pinney SM, Windham GC, Galvez M et al (2015) Environmental phenols and pubertal development in girls. *Environ Int* 84:174–180
17. Brahman F, Honarmand M, Jadid S (2015) Optimal electrical and thermal energy management of a residential energy hub, integrating demand response and energy storage system. *Energ Buildings* 90:65–75
18. Rastegar M, Fotuhi-Firuzabad M (2015) Load management in a residential energy hub with renewable distributed energy resources. *Energ Buildings* 107:234–242
19. Shariatkhalah M-H, Haghifam M-R, Parsa-Moghaddam M, Siano P (2015) Modeling the reliability of multi-carrier energy systems considering dynamic behavior of thermal loads. *Energ Buildings* 103:375–383
20. Koeppl G, Andersson G (2009) Reliability modeling of multi-carrier energy systems. *Energy* 34(3):235–244
21. Haghrah A, Nazari-Heris M, Mohammadi-Ivatloo B (2016) Solving combined heat and power economic dispatch problem using real coded genetic algorithm with improved Mühlenbein mutation. *Appl Therm Eng* 99:465–475
22. Nazari-Heris M, Mehdinejad M, Mohammadi-Ivatloo B, Babamalek-Gharehpetian G (2019) Combined heat and power economic dispatch problem solution by implementation of whale optimization method. *Neural Comput Appl* 31(2):421–436
23. Sepponen M, Heimonen I (2016) Business concepts for districts' Energy hub systems with maximised share of renewable energy. *Energ Buildings* 124:273–280
24. Rastegar M, Fotuhi-Firuzabad M, Lehtonen M (2015) Home load management in a residential energy hub. *Electr Power Syst Res* 119:322–328
25. Xu X, Jia H, Wang D, David CY, Chiang H-D (2015) Hierarchical energy management system for multi-source multi-product microgrids. *Renew Energy* 78:621–630
26. Shabanpour-Haghighi A, Seifi AR (2016) Effects of district heating networks on optimal energy flow of multi-carrier systems. *Renew Sust Energ Rev* 59:379–387

27. Beigvand SD, Abdi H, La Scala M (2016) Optimal operation of multicarrier energy systems using time varying acceleration coefficient gravitational search algorithm. *Energy* 114:253–265
28. Nazari-Heris M, Mohammadi-Ivatloo B, Haghrah A (2017) Optimal short-term generation scheduling of hydrothermal systems by implementation of real-coded genetic algorithm based on improved Mühlenbein mutation. *Energy* 128:77–85
29. Gorre J, Ruoss F, Karjunen H, Schaffert J, Tynjälä T (2020) Cost benefits of optimizing hydrogen storage and methanation capacities for power-to-gas plants in dynamic operation. *Appl Energy* 257:113967
30. Belderbos A, Valkaert T, Bruninx K, Delarue E, D'haeseleer W (2020) Facilitating renewables and power-to-gas via integrated electrical power-gas system scheduling. *Appl Energy* 275:115082
31. Chen X, Wang C, Wu Q, Dong X, Yang M, He S et al (2020) Optimal operation of integrated energy system considering dynamic heat-gas characteristics and uncertain wind power. *Energy* 117270
32. Xi Y, Zeng Q, Chen Z, Lund H, Conejo AJ (2020) A market equilibrium model for electricity, gas and district heating operations. *Energy* 117934
33. Nazari-Heris M, Mohammadi-Ivatloo B, Asadi S, Geem ZW (2019) Large-scale combined heat and power economic dispatch using a novel multi-player harmony search method. *Appl Therm Eng* 154:493–504
34. Alomoush MI (2020) Optimal combined heat and power economic dispatch using stochastic fractal search algorithm. *J Modern Power Syst Clean Energy* 8(2):276–286
35. Olympios AV, Le Brun N, Acha S, Shah N, Markides CN (2020) Stochastic real-time operation control of a combined heat and power (CHP) system under uncertainty. *Energy Convers Manag* 216:112916
36. Bird TJ, Jain N (2020) Dynamic modeling and validation of a micro-combined heat and power system with integrated thermal energy storage. *Appl Energy* 271:114955
37. Charrouf O, Betka A, Abdeddaim S, Ghamri A (2020) Artificial Neural Network power manager for hybrid PV-wind desalination system. *Math Comput Simul* 167:443–460
38. Mehrjerdi H (2020) Modeling and integration of water desalination units in thermal unit commitment considering energy and water storage. *Desalination* 483:114411
39. Nazari-Heris M, Babaei AF, Mohammadi-Ivatloo B, Asadi S (2018) Improved harmony search algorithm for the solution of non-linear non-convex short-term hydrothermal scheduling. *Energy* 151:226–237
40. Ersoz I, Colak U (2016) Combined cooling, heat and power planning under uncertainty. *Energy*, 109:1016–1025
41. Dasgupta K, Roy PK, Mukherjee V (2020) Power flow based hydro-thermal-wind scheduling of hybrid power system using sine cosine algorithm. *Electr Power Syst Res* 178:106018
42. Zhang Y, Huang Z, Zheng F, Zhou R, Le J, An X (2020) Cooperative optimization scheduling of the electricity-gas coupled system considering wind power uncertainty via a decomposition-coordination framework. *Energy* 194:116827
43. Fan J, Tong X, Zhao J (2020) Multi-period optimal energy flow for electricity-gas integrated systems considering gas inertia and wind power uncertainties. *Int J Electr Power Energy Syst* 123:106263
44. Nazari-Heris M, Mohammadi-Ivatloo B, Asadi S (2020) Optimal operation of multi-carrier energy networks considering uncertain parameters and thermal energy storage. *Sustainability* 12(12):5158
45. Li Y, Wang J, Han Y, Zhao Q, Fang X, Cao Z (2020) Robust and opportunistic scheduling of district integrated natural gas and power system with high wind power penetration considering demand flexibility and compressed air energy storage. *J Clean Prod* 256:120456
46. Nazari-Heris M, Mirzaei MA, Mohammadi-Ivatloo B, Marzband M, Asadi S (2020) Economic-environmental effect of power to gas technology in coupled electricity and gas systems with price-responsive shiftable loads. *J Clean Prod* 244:118769

47. Ghahramani M, Heris MN, Zare K, Ivatloo BM (2017) Incorporation of demand response programs and wind turbines in optimal scheduling of smart distribution networks: A case study. Conference Incorporation of demand response programs and wind turbines in optimal scheduling of smart distribution networks: A case study. In 2017 Conference on Electrical Power Distribution Networks Conference (EPDC), IEEE, p. 25–32
48. Ghahramani M, Nazari-Heris M, Zare K, Mohammadi-Ivatloo B (2020) Optimal energy and reserve management of the electric vehicles aggregator in electrical energy networks considering distributed energy sources and demand side management *Electric Vehicles in Energy Systems*: Springer, Switzerland; p. 211–31
49. Midthun KT, Bjorndal M, Tomasgard A (2009) Modeling optimal economic dispatch and system effects in natural gas networks. *Energy J* 30(4):155–180
50. Chebouba A, Yalaoui F, Smati A, Amodeo L, Younsi K, Tairi A (2009) Optimization of natural gas pipeline transportation using ant colony optimization. *Comput Oper Res* 36(6):1916–1923
51. Sartor K, Quoilin S, Dewallef P (2014) Simulation and optimization of a CHP biomass plant and district heating network. *Appl Energy* 130:474–483
52. Sandou G, Oлару S (2009) Particle swarm optimization based NMPC: An application to district heating networks, *Nonlinear Model Predictive Control*. Springer, Switzerland pp 551–559
53. Mohammadi M, Noorollahi Y, Mohammadi-Ivatloo B, Yousefi H (2017) Energy hub: from a model to a concept – a review. *Renew Sust Energy Rev* 80:1512–1527
54. Lee B, Lee H, Kang S, Lim H (2019) Stochastic techno-economic analysis of power-to-gas technology for synthetic natural gas production based on renewable H₂ cost and CO₂ tax credit. *J Energy Storage* 24:100791
55. Alabdulwahab A, Abusorrah A, Zhang X, Shahidehpour M (2015) Coordination of interdependent natural gas and electricity infrastructures for firming the variability of wind energy in stochastic day-ahead scheduling. *IEEE Transac Sustainable Energy* 6(2):606–615
56. Erdener BC, Pambour KA, Lavin RB, Dengiz B (2014) An integrated simulation model for analysing electricity and gas systems. *Int J Electr Power Energy Syst* 61:410–420
57. Bai L, Li F, Cui H, Jiang T, Sun H, Zhu J (2016) Interval optimization based operating strategy for gas-electricity integrated energy systems considering demand response and wind uncertainty. *Appl Energy* 167:270–279
58. Zeng Q, Fang J, Li J, Chen Z (2016) Steady-state analysis of the integrated natural gas and electric power system with bi-directional energy conversion. *Appl Energy* 184:1483–1492
59. He C, Liu T, Wu L, Shahidehpour M (2017) Robust coordination of interdependent electricity and natural gas systems in day-ahead scheduling for facilitating volatile renewable generations via power-to-gas technology. *J Modern Power Syst Clean Energy* 5(3):375–388
60. Cui H, Li F, Hu Q, Bai L, Fang X (2016) Day-ahead coordinated operation of utility-scale electricity and natural gas networks considering demand response based virtual power plants. *Appl Energy* 176:183–195
61. Li G, Zhang R, Jiang T, Chen H, Bai L, Li X (2017) Security-constrained bi-level economic dispatch model for integrated natural gas and electricity systems considering wind power and power-to-gas process. *Appl Energy* 194:696–704
62. Zeng Q, Zhang B, Fang J, Chen Z (2017) A bi-level programming for multistage co-expansion planning of the integrated gas and electricity system. *Appl Energy* 200:192–203
63. Gu C, Tang C, Xiang Y, Xie D (2019) Power-to-gas management using robust optimisation in integrated energy systems. *Appl Energy* 236:681–689
64. Shu K, Ai X, Fang J, Yao W, Chen Z, He H et al (2019) Real-time subsidy based robust scheduling of the integrated power and gas system. *Appl Energy* 236:1158–1167
65. Li Y, Liu W, Shahidehpour M, Wen F, Wang K, Huang Y (2018) Optimal operation strategy for integrated natural gas generating unit and power-to-gas conversion facilities. *IEEE Transac Sustainable Energy* 9(4):1870–1879

66. He L, Lu Z, Zhang J, Geng L, Zhao H, Li X (2018) Low-carbon economic dispatch for electricity and natural gas systems considering carbon capture systems and power-to-gas. *Appl Energy* 224:357–370
67. Zhang X, Che L, Shahidehpour M, Alabdulwahab A, Abusorrah A (2016) Electricity-natural gas operation planning with hourly demand response for deployment of flexible ramp. *IEEE Trans Sustainable Energy* 7(3):996–1004
68. He C, Wu L, Liu T, Shahidehpour M (2016) Robust co-optimization scheduling of electricity and natural gas systems via ADMM. *IEEE Trans Sustainable Energy* 8(2):658–670
69. Deane J, Ciaráin MÓ, Gallachóir BÓ (2017) An integrated gas and electricity model of the EU energy system to examine supply interruptions. *Appl Energy* 193:479–490
70. Cheng L, Liu C, Huang R, Li H. An optimal operating strategy for CCHP in multi-energy carrier system. Conference An optimal operating strategy for CCHP in multi-energy carrier system. *IEEE*, p. 1–5
71. Nazari-Heris M, Mohammadi-Ivatloo B, Gharehpetian GB, Shahidehpour M (2018) Robust short-term scheduling of integrated heat and power microgrids. *IEEE Syst J* 13(3):3295–3303
72. Di Somma M, Caliano M, Graditi G, Pinnarelli A, Menniti D, Sorrentino N et al (2020) Designing of cost-effective and low-carbon multi-energy nanogrids for residential applications. *Inventions* 5(1):7
73. Kalogirou SA (2005) Seawater desalination using renewable energy sources. *Prog Energy Combust Sci* 31(3):242–281
74. Fiorenza G, Sharma V, Braccio G (2003) Techno-economic evaluation of a solar powered water desalination plant. *Energy Convers Manag* 44(14):2217–2240
75. Tabrizi FF, Sharak AZ (2010) Experimental study of an integrated basin solar still with a sandy heat reservoir. *Desalination* 253(1–3):195–199
76. Dore MH (2005) Forecasting the economic costs of desalination technology. *Desalination* 172(3):207–214
77. Xiao G, Wang X, Ni M, Wang F, Zhu W, Luo Z et al (2013) A review on solar stills for brine desalination. *Appl Energy* 103:642–652
78. Li Z, Wu W, Wang J, Zhang B, Zheng T (2015) Transmission-constrained unit commitment considering combined electricity and district heating networks. *IEEE Trans Sustainable Energy* 7(2):480–492
79. Najafi A, Falaghi H, Contreras J, Ramezani M (2016) Medium-term energy hub management subject to electricity price and wind uncertainty. *Appl Energy* 168:418–433
80. ali Shaabani Y, Seifi AR, Kouhanjani MJ (2017) Stochastic multi-objective optimization of combined heat and power economic/emission dispatch. *Energy* 141:1892–1904
81. Alipour M, Zare K, Seyedi H (2018) A multi-follower bilevel stochastic programming approach for energy management of combined heat and power micro-grids. *Energy* 149:135–146
82. Lu S, Gu W, Zhou J, Zhang X, Wu C (2018) Coordinated dispatch of multi-energy system with district heating network: modeling and solution strategy. *Energy* 152:358–370
83. Alipour M, Mohammadi-Ivatloo B, Zare K (2015) Stochastic scheduling of renewable and CHP-based microgrids. *IEEE Transac Ind Inf* 11(5):1049–1058
84. Caliano M, Bianco N, Graditi G, Mongibello L (2016) Economic optimization of a residential micro-CHP system considering different operation strategies. *Appl Therm Eng* 101:592–600
85. Majidi M, Zare K (2018) Integration of smart energy hubs in distribution networks under uncertainties and demand response concept. *IEEE Trans Power Syst* 34(1):566–574
86. Mirzapour-Kamanaj A, Majidi M, Zare K, Kazemzadeh R (2020) Optimal strategic coordination of distribution networks and interconnected energy hubs: a linear multi-follower bi-level optimization model. *Int J Electr Power Energy Syst* 119:105925
87. Mongibello L, Bianco N, Caliano M, Graditi G (2016) Comparison between two different operation strategies for a heat-driven residential natural gas-fired CHP system: heat dumping vs load partialization. *Appl Energy* 184:55–67

88. Di Somma M, Graditi G, Siano P (2018) Optimal bidding strategy for a DER aggregator in the day-ahead market in the presence of demand flexibility. *IEEE Trans Ind Electron* 66(2):1509–1519
89. Koonce AM, Apostolakis G, Cook B (2008) Bulk power risk analysis: Ranking infrastructure elements according to their risk significance. *Int J Electr Power Energy Syst* 30(3):169–183
90. Soroudi A, Amraee T (2013) Decision making under uncertainty in energy systems: State of the art. *Renew Sust Energy Rev* 28:376–384
91. Soroudi A (2012) Possibilistic-scenario model for DG impact assessment on distribution networks in an uncertain environment. *IEEE Trans Power Syst* 27(3):1283–1293
92. Soroudi A, Afrasiab M (2012) Binary PSO-based dynamic multi-objective model for distributed generation planning under uncertainty. *IET Renew Power Gener* 6(2):67–78
93. Soroudi A, Ehsan M (2012) IGDT based robust decision making tool for DNOs in load procurement under severe uncertainty. *IEEE Trans Smart Grid* 4(2):886–895
94. Ghahramani M, Nazari-Heris M, Zare K, Mohammadi-Ivatloo B (2018) Energy management of electric vehicles parking in a power distribution network using robust optimization method. *J Energy Manage Technol* 2(3):22–30
95. Conejo AJ, Carrión M (2010) Morales JM. Springer, Decision making under uncertainty in electricity markets
96. Albrecht P (1993) Shortfall returns and shortfall risk. Institut für Versicherungswissenschaft
97. Whitmore GA, Findlay MC (1978) Stochastic dominance: an approach to decision-making under risk. Lexington Books
98. Hassan R, De Neufville R, McKinnon D. Value-at-risk analysis for real options in complex engineered systems. Conference Value-at-risk analysis for real options in complex engineered systems, vol. 4. IEEE, p. 3697–704
99. Rockafellar RT, Uryasev S (2000) Optimization of conditional value-at-risk. *United States of America J Risk* 2:21–42
100. Nojavan S, Majidi M, Zare K (2017) Performance improvement of a battery/PV/fuel cell/grid hybrid energy system considering load uncertainty modeling using IGDT. *Energy Convers Manage* 147:29–39
101. Nojavan S, Zare K, Feyzi MR (2013) Optimal bidding strategy of generation station in power market using information gap decision theory (IGDT). *Electr Power Syst Res* 96:56–63
102. Pazouki S, Haghifam M-R (2016) Optimal planning and scheduling of energy hub in presence of wind, storage and demand response under uncertainty. *Int J Electr Power Energy Syst* 80:219–239
103. Pazouki S, Haghifam M-R, Moser A (2014) Uncertainty modeling in optimal operation of energy hub in presence of wind, storage and demand response. *Int J Electr Power Energy Syst* 61:335–345
104. Vahid-Pakdel M, Nojavan S, Mohammadi-Ivatloo B, Zare K (2017) Stochastic optimization of energy hub operation with consideration of thermal energy market and demand response energy. *Convers Manage* 145:117–128
105. Parisio A, Del Vecchio C, Vaccaro A (2012) A robust optimization approach to energy hub management. *Int J Electr Power Energy Syst* 42(1):98–104
106. Tavakoli M, Shokridehaki F, Akorede MF, Marzband M, Vechiu I, Pouresmaeil E (2018) CVaR-based energy management scheme for optimal resilience and operational cost in commercial building microgrids. *Int J Electr Power Energy Syst* 100:1–9
107. Gazijahani FS, Ravadanegh SN, Salehi J (2018) Stochastic multi-objective model for optimal energy exchange optimization of networked microgrids with presence of renewable generation under risk-based strategies. *ISA Trans* 73:100–111
108. Nazari-Heris M, Abapour S, Mohammadi-Ivatloo B (2017) Optimal economic dispatch of FC-CHP based heat and power micro-grids. *Appl Therm Eng* 114:756–769
109. Beigvand SD, Abdi H, La Scala M (2017) A general model for energy hub economic dispatch. *Appl Energy* 190:1090–1111

110. Perera ATD, Nik VM, Mauree D, Scartezzini J-L (2017) Electrical hubs: An effective way to integrate non-dispatchable renewable energy sources with minimum impact to the grid. *Appl Energy* 190:232–248
111. Kienzle F, Ahcin P, Andersson G (2011) Valuing investments in multi-energy conversion, storage, and demand-side management systems under uncertainty. *IEEE Transac Sustainable Energy* 2(2):194–202
112. Kienzle F, Andersson G. Location-dependent valuation of energy hubs with storage in multi-carrier energy systems. Conference Location-dependent valuation of energy hubs with storage in multi-carrier energy systems. IEEE, p. 1–6
113. Arnold M, Andersson G. Model predictive control of energy storage including uncertain forecasts. Conference Model predictive control of energy storage including uncertain forecasts, vol. 23. Citeseer, p. 24–9
114. Nojavan S, Majidi M, Najafi-Ghalelou A, Zare K. Supply side management in renewable energy hubs. Operation, planning, and analysis of energy storage systems in smart energy hubs: Springer; 2018. p. 163–87
115. Majidi M, Nojavan S, Zare K (2018) Multi-objective optimization framework for electricity and natural gas energy hubs under hydrogen storage system and demand response program, Operation, planning, and analysis of energy storage systems in smart energy hubs. Springer, pp 425–446
116. Majidi M, Nojavan S, Esfetanaj NN, Najafi-Ghalelou A, Zare K (2017) A multi-objective model for optimal operation of a battery/PV/fuel cell/grid hybrid energy system using weighted sum technique and fuzzy satisfying approach considering responsible load management. *Sol Energy* 144:79–89
117. Majidi M, Nojavan S, Zare K (2017) Optimal stochastic short-term thermal and electrical operation of fuel cell/photovoltaic/battery/grid hybrid energy system in the presence of demand response program. *Energy Convers Manag* 144:132–142
118. Nazari-Heris M, Madadi S, Mohammadi-Ivatloo B (2018) Optimal management of hydrothermal-based micro-grids employing robust optimization method, Classical and recent aspects of power system optimization. Elsevier, pp 407–420
119. Shahidehpour M, Zhou Y, Wei Z, Sun G, Chen S (2020) Multistage robust look-ahead unit commitment with probabilistic forecasting in multi-carrier energy systems. *IEEE Transac Sustainable Energy*
120. Zafarani H, Taher SA, Shahidehpour M (2020) Robust operation of a multicarrier energy system considering EVs and CHP units. *Energy* 192:116703
121. Lu X, Liu Z, Ma L, Wang L, Zhou K, Yang S (2020) A robust optimization approach for coordinated operation of multiple energy hubs. *Energy* 197:117171
122. Zhu X, Zeng B, Dong H, Liu J (2020) An interval-prediction based robust optimization approach for energy-hub operation scheduling considering flexible ramping products. *Energy* 194:116821
123. Rahmani S, Amjady N (2019) Optimal operation strategy for multi-carrier energy systems including various energy converters by multi-objective information gap decision theory and enhanced directed search domain method. *Energy Convers Manag* 198:111804
124. Najafi A, Marzband M, Mohamadi-Ivatloo B, Contreras J, Pourakbari-Kasmaei M, Lehtonen M et al (2019) Uncertainty-based models for optimal management of energy hubs considering demand response. *Energies* 12(8):1413
125. Amir V, Azimian M (2020) Dynamic multi-carrier microgrid deployment under uncertainty. *Appl Energy* 260:114293
126. Moghaddas-Tafreshi SM, Jafari M, Mohseni S, Kelly S (2019) Optimal operation of an energy hub considering the uncertainty associated with the power consumption of plug-in hybrid electric vehicles using information gap decision theory. *Int J Electr Power Energy Syst* 112:92–108

127. Majidi M, Nojavan S, Zare K (2019) Optimization framework based on information gap decision theory for optimal operation of multi-energy systems, *Robust Optimal Planning and Operation of Electrical Energy Systems*. Springer, pp 35–59
128. Yuan Z, He S, Alizadeh AA, Nojavan S, Jernsittiparsert K (2020) Probabilistic scheduling of power-to-gas storage system in renewable energy hub integrated with demand response program. *J Energy Storage* 29:101393
129. Mohammadi M, Noorollahi Y, Mohammadi-ivatloo B (2020) Fuzzy-based scheduling of wind integrated multi-energy systems under multiple uncertainties. *Sustainable Energy Technol Assess* 37:100602
130. Sanjani K, Vahabzad N, Nazari-Heris M, Mohammadi-Ivatloo B (2019) A robust-stochastic approach for energy transaction in energy hub under uncertainty, *Robust Optimal Planning and Operation of Electrical Energy Systems*. Springer, pp 219–232
131. Kazemdehdashti A, Mohammadi M, Seifi A, Rastegar M (2020) Stochastic energy management in multi-carrier residential energy systems. *Energy* 117790
132. Jadidbonab M, Babaei E, Mohammadi-ivatloo B (2019) CVaR-constrained scheduling strategy for smart multi carrier energy hub considering demand response and compressed air energy storage. *Energy* 174:1238–1250
133. Najafi-Ghalelou A, Nojavan S, Zare K, Mohammadi-Ivatloo B (2019) Robust scheduling of thermal, cooling and electrical hub energy system under market price uncertainty. *Appl Therm Eng* 149:862–880
134. Amir V, Jadid S, Ehsan M (2017) Probabilistic optimal power dispatch in multi-carrier networked microgrids under uncertainties. *Energies* 10(11):1770

Chapter 3

An Optimal Operation Model for Multi-carrier Energy Grids



Mohammad Saadatmandi, Seyed Mehdi Hakimi, and Pegah Bahrevar

3.1 Introduction

In recent decades, electricity consumption in the world has been increasing significantly due to the development of technology, while electricity-generating companies faced many problems to meet the needs of consumers due to traditional and consequent dependence on fossil fuels, losses in distribution lines, and need for high initial investment for the establishment of power generation units. Accordingly, in order to solve problems over the years, as well as to reduce dependence on fossil fuels, which are considered as limited resources, electricity companies have been using renewable energy resources (i.e., solar panels and wind turbines), small production units, small-scale energy resources (SSERs), storage systems, and optimization of energy management programs on their agenda, but in this direction these companies faced new challenges with some technical issues such as power quality, reliability, optimal energy management, and especially maximum use of the available production resources [1].

To optimize energy management in a power grid with various producing sectors, engineers and researchers designed a grid with telecommunication infrastructure and the ability to connect us to equipment, including producing equipment and consumer goods, which was introduced as the smart grid [2, 3]. However, a small area in the grid that included several energy carriers and small producing sectors, including renewable energy resources such as solar and wind panels and other resources such as storage and controllable loads, is named microgrid [4]. The main idea of this microgrid is to solve grid problems such as providing improvements in traditional power supply and system performance problems.

M. Saadatmandi · S. M. Hakimi (✉) · P. Bahrevar
Department of Electrical Engineering and Renewable Energy Research Center, Damavand Branch, Islamic Azad University, Damavand, Iran
e-mail: sm_hakimi@damavandiau.ac.ir; p.bahrevar@damavandiau.ac.ir

Considering the intelligent structure of this type of grid and the ability to modify and optimize grid's performance using automated management systems, experts believe that these grids will significantly increase the control and performance of systems; in recent years, this operation has also been approved [5]. In fact, microgrids due to their electrical and communication infrastructure, including software and hardware for monitoring and managing production, instantaneous control, charge-level determination, instantly determining the state of charge of equipment, and their energy consumption, significantly lead to reduced energy consumption and cost as well as an increased grid reliability [6].

Meanwhile, microgrids, which include several sources of energy production, are known as multi-carrier energy microgrids. The main challenge of exploiting such grids is the optimal use of various energy resources and energy equipment. During these years, lots of research has been done on the operation and scheduling of various energy carrier infrastructure, which has led to some limitations in their operation. However, the high penetration of SSERs with a significant reduction in gasoline consumption has increased the enthusiasm of consumers and electricity companies to use multi-energy grids [7]; accordingly, in scientific forums integrated multi-carrier energy systems have been discussed in terms of capabilities and increased productivity, some of which are briefly mentioned in [8, 9].

The concept of energy hub system has been introduced to define multi-carrier systems [10]. The EH system includes a variety of energy carriers such as converters and storages to meet the demand [11]; this system model has been studied according to the problems of operation [12] and planning [13, 14].

Currently, the optimal performance of various energy carriers is done automatically and autonomously, while most of the existing energy infrastructure are worn out and have high losses. On the other hand, congestion on transmission lines and increased demand were motivating factors for researchers to turn to research to find solutions to ensure and improve the future of energy management systems. The research results show that the effective use of the available MCMG infrastructure is considered as an energy hub system and a reliable solution. This means that instead of examining and inspecting different carriers in energy systems separately, different energy infrastructure should examine and operate these energy carriers simultaneously [15].

Energy optimization has made great strides after defining the concept of energy hub [16]. This issue has been solved with optimization methods [17]. One of the used methods is decentralized multi-agent method for economic dispatch (ED), which is presented by Kai and colleagues [18, 19].

Optimal operation of several microgrids has been investigated by Nikmehr and his colleagues in [20]. In this reference, while the uncertainty of distributed energy resources (DER) is considered, the problem of economic dispatch of MGs is also examined from different perspectives, so in this chapter, extensive problems are shown [21]. In ref. [22], the optimization of microgrids has been studied by considering the demand response mechanism and flexible loads that can be connected to the grid.

In order to reduce the cost of operation in reference [23], an economic dispatch method has been studied for optimal operation and in accordance with the instantaneous energy optimization method [24]. The purpose of the reference [25] is the issue of ED in the multifunctional operation problem, which not only considers the cost of performance, but also extends it to the presence of electric vehicles. Similarly, Zah et al. have optimized a multi-objective problem, in which the battery life of the model is defined as an objective function [26].

The economic dispatch optimization problem in literature has been categorized into different models as well as solvers [27, 28]; for example, in [20, 27] the particle swarm optimization (PSO) algorithm, tabu search (TS), genetic algorithm (GA) [11, 29], ant colony [30], and game theory are methods that are used in optimal dispatching problem. Optimal management of existing resources to meet demands is one of the main problems in the operation of MGs [31]. To achieve this aim, smart grid infrastructure in order to distribute energy among small resources with the lowest price is regarded in [32] and power balances between generation and loads via existing infrastructure and responsive equipment are performed in [33–37].

The loads can be divided into two categories: (1) static and (2) flexible. Flexible loads can be transferred to other hours of the day and night. Due to the influence of various resources in future smart grids, the concept of demand-side management DSM covers a wide range of loads [22]. The DSM program only includes loads that can be controlled directly (controllable) or transferred to off-peak hours. Flexible loads that can be moved to other hours have been discussed in previous studies: [23, 24] and [30, 38]. Washing machines and dryers, dishwashers, vacuum cleaners, etc. are examples of flexible loads [10].

In ref. [39], an innovative method for solving economic dispatch of CHP has been proposed. Easy execution, better convergence, and ability to check multiple constraints in complex search spaces are the superiority of the proposed algorithm compared to the recent and provided methods. The issue of energy planning for CHP based on the uncertainty of loads in MGs, wind speed, and power market is defined in reference [40]. In this paper, the responses to random programming have been implemented in order to make the successful participation of CHP systems with MGs in the electricity market, but the final energy tariff for the species has not been modeled for different loads. A more complex model of the previous article has been used according to the epsilon bond method with the fuel cell unit in addition to the hydrogen tank [41].

In ref. [42], in order to reduce air pollution caused by gas emissions as well as reduce costs, Jiang Lu and his colleagues have developed a multi-objective optimization model with combination of power and heat systems (CHP) provided for microgrid. During this research, a microgrid with several energy carriers, including CHP unit, wind turbine, photovoltaic system, fuel cell, electric boiler, and electric and heat storage, has been considered. During this research, minimizing economic and environmental costs has been considered as two simultaneous objectives.

In ref. [43], a mathematical function is presented to schedule the units in the grid and the optimal power flow. In this paper, researchers have used mixed-integer linear programming to implement their intended model. The researchers aim to minimize

operating costs as well as make optimal use of energy storage equipment, renewable energy resources, and CHP system in microgrids. The results of this study showed that the simultaneous use of energy storage systems and CHP system in a microgrid will greatly reduce operating costs.

Optimal energy management for microgrids connected to the main grid, which includes several energy carriers, including renewable energy resources, combined heat and power systems (CHP), and energy storage systems, has been studied in [44]. The researchers' aim in this paper was to reduce the cost of exploiting the microgrid. Finally, the results of using random data to realize the amount of energy stored in storages and renewable energy resources to manage real-time microgrid management indicate a reduction in operating costs of a microgrid.

An IREMS has been proposed in [8, 45] for smart homes. Main purpose of this system was to minimize costs while the most energy demand was limited to different elements like operation of residential loads and solar/wind resources. Therewith, a storage solution has been proposed to minimize the loss of power produced by solar/wind resources.

Reference [46] presents sizing and siting of different equipment in microgrids containing renewable energy systems. Reference [47] presents new techniques for demand-side management in order to deal with operative uncertainties within the outline of an energy hub. In [48] a novel method is offered to calculate the influence of energy storage on the operation of a microgrid.

Accordingly, the most important contribution of this research can be considered as follows:

1. Proposing a novel energy management system to meet electric and heat loads so that it is proportionate to the tariff of multi-carrier energy in the microgrid
2. Evaluating the simultaneous operation of multi-carrier energy in microgrid and its impact on the final cost of consumers
3. Expanding a new formulation for smart appliances such as washing machines and dryers' loads and combined heat and power system

According to the proposed goal, the structure intended for this chapter will be as follows: The structure of the desired microgrid will be introduced, and then the economic model will be introduced for various parts of this microgrid, i.e., suppliers, reservoirs, and loads. Moreover, for the optimal operation of the microgrid an objective function is represented which shows the microgrid's profit. Also, in order to optimize this objective function, PSO algorithm has been used and at the end of the chapter the results of the proposed model have been examined.

3.2 Suggested Microgrid Structure

The microgrids studied in this chapter include controllable/uncontrollable loads and generators of less than 500 kW and storages; microgrids can be connected to the national grid or operated independently, i.e., as an island. The structure of the studied

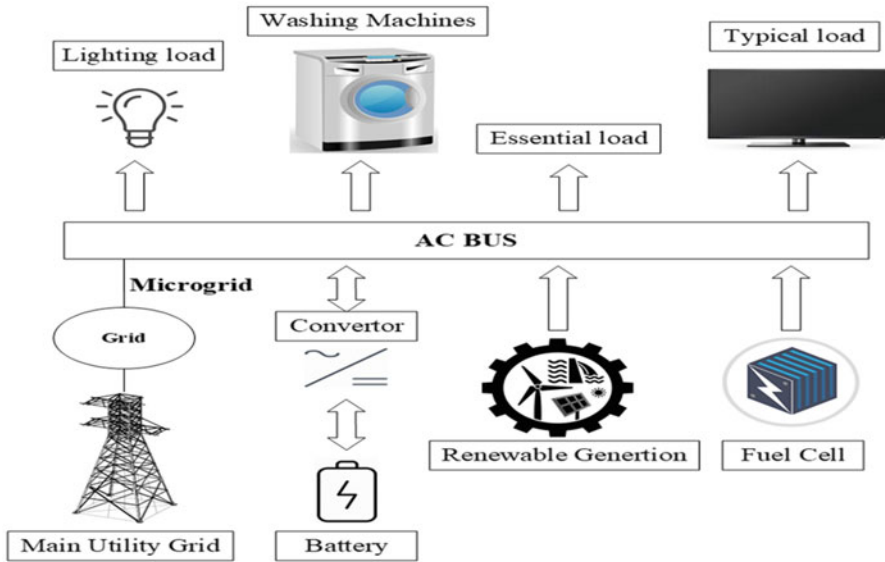


Fig. 3.1 Suggested microgrid structure

microgrid is shown in Fig. 3.1. The grid includes wind turbines, photovoltaic systems, fuel cell systems, storage devices (i.e., batteries), and loads located on an AC bus. At the junction of the generators to the buses, a number of electronic power converters have been used, which in this study are assumed to have zero losses. The studied microgrid has the ability to exchange energy with the global grid and can also be used as an island. In fact, what is presented in this dissertation is a smart energy management system for the optimal use of this microgrid in the market environment.

In this research, the microgrid manager is responsible for management and uses the optimization methods of planning to formulate the microgrid operation in the next 24 h. One of the parameters of optimal management in this program is to determine the amount of energy exchange with the distribution grid (buying or selling energy) at different hours of the next day. Therefore, predicting the energy price of the distribution grid and the rate of renewable energy generation is extremely important for greater profitability of the microgrid, because these parameters are very fundamental for deciding how to interact with the distribution grid. Accordingly, the microgrid manager decides to behave as a load in a certain hour and buy energy from distribution grid or sell to the grid, because the energy generated and transferred to the grid by the microgrid is not high. In this chapter it is assumed that all the energy transferred to the grid is purchased according to a guaranteed contract between the microgrid and the distribution grid, and this has no effect on the market price. In the proposed model, first the purchasing price of energy from the microgrid is equal to the purchasing price of renewable generators in Iran, and then it is assumed that the microgrid has a guaranteed contract with the distribution grid to

buy all the energy generated, so the purchasing price is less than the selling price to the grid. Simultaneously by determining how to interact with the distribution grid, the decision about the number of generators of local units is made by the microgrid manager. The profit or microgrid's loss depends directly on the microgrid manager, so optimal planning is very important for interacting with the distribution grid.

3.3 Considered Grid

In this section, the suppliers, storage devices, and types of loads available in the microgrid (energy carriers) and used in a smart home are modeled, respectively.

3.3.1 Suppliers

In this chapter's model, power generation resources include solar energy systems (PV photovoltaics), wind turbines, and fuel cell systems.

3.3.2 Wind Production Unit

The output power of wind turbines in any location depends on the speed, height of the hub, and speed-power diagram of different models of wind turbines. Therefore, to obtain the wind speed at the hub height Eq. (3.1) is used [49]:

$$V = V_1 \left(\frac{h}{h_1} \right)^b \quad (3.1)$$

In Eq. (3.1) h and h_1 are the height of the hub and the height of the wind speed reading, respectively, and V and V_1 are the wind speed at the height of the hub and the speed of the wind reading at the height h_1 , respectively. In fact, using this equation and having the wind speed in that area, the wind speed at the hub height can be calculated to generate electricity. In this regard, parameter b relies on the environmental conditions shown in Table 3.1 for different environments.

After calculating the wind speed, the wind turbine's output power can be obtained through Eq. (3.2) [51]:

Table 3.1 Index b for various conditions [50]

Friction factor (x)	Specification of the Earth type
0.06	Unstable air on the surface of open water
0.10	Natural air on the surface of open water
0.16	Natural air on the flat open beach
0.11	Unstable air on the flat open beach
0.27	Stable air on the surface of open water
0.27	Unstable air on the residential districts
0.34	Natural air on the residential districts
0.40	Stable air on the beach's surface
0.60	Stable air on the residential districts

$$P_{wt} = \begin{cases} 0 & V < V_{ci} \\ P_r(A + B \times V + C \times V^2) & V_{ci} < V < V_r \\ P_r & V_r < V < V_{co} \\ 0 & V > V_{co} \end{cases} \quad (3.2)$$

In this regard, P_r represents the nominal power of the turbine; V_{ci} and V_{co} , respectively, are the low and high cutoff speeds; and V_1 is the speed related to the nominal power of the turbine. Also, A , B , and C are coefficients that are calculated from the following equations [51]:

$$A = \frac{1}{(V_{ci} - V_r)^2} \left\{ V_{ci}(V_{ci} + V_r) - 4V_{ci}V_r \left[\frac{V_{ci} + V_r}{2V_r} \right]^3 \right\} \quad (3.3)$$

$$B = \frac{1}{(V_{ci} - V_r)^2} \left\{ 4(V_{ci} + V_r) \left[\frac{V_{ci} + V_r}{2V_r} \right]^3 - (3V_{ci} + V_r) \right\} \quad (3.4)$$

$$C = \frac{1}{(V_{ci} - V_r)^2} \left\{ 2 - 4 \left[\frac{V_{ci} + V_r}{2V_r} \right]^3 \right\} \quad (3.5)$$

3.3.2.1 Wind Generation Cost

The price per Kwh of energy produced by wind turbines depends on parameters such as initial investment costs, operating costs, maintenance, amount of electrical energy produced per year, turbine life span, and interest rates. In wind units, the cost of fuel is zero, but the cost of the initial investment (turbine, grid connection, and construction work) is high which is about 80% of wind unit's investment, and the operating and maintenance costs will be low [49].

The initial investment cost is calculated using Eq. (3.6). Then, to calculate the annual payment fee, you can add the maintenance cost of the system (m) to it, so we have

$$A' = A + OM_{wt} \quad (3.6)$$

The energy produced in the whole year (E) for one wind unit is calculated from Eq. (3.7):

$$E = P \times CF \times 8700 \quad (3.7)$$

In Eq. (3.7), P is the nominal capacity (kW), and CF is the capacity factor. Considering Eq. (3.7), the specific cost of generating electricity in this system is calculated through the equation below:

$$C = \frac{A'}{E} \quad (3.8)$$

According to Eqs. (3.7) and (3.8), the production cost of wind unit will be modeled as Eq. (3.9):

$$C_{wt} = \frac{A'_{wt}}{P_{wt} \times CF_{wt} \times 8700} \quad (3.9)$$

In this regard, P_w is the nominal installed capacity of wind in terms of kilowatts, CF_w is the capacity factor, and A'_w is calculated using Eq. (3.6).

3.3.3 Solar Production Unit

Using the available sunlight intensity on the inclined plane, environmental temperature, and constructive data for solar panel as inputs, output power P_{PV} of a solar unit can be calculated as in Eq. (3.10):

$$P_{PV} = N_{PV} \eta_g A_m G_t \quad (3.10)$$

in which N_{PV} is the number of solar arrays, η_g is the efficiency of the solar unit, A_m is the area of each solar array in terms of m^2 , and G_t is the intensity of sunlight on the surface of the solar array in terms of W/m^2 .

The instantaneous efficiency of the solar unit can be calculated according to Eq. (3.11):

$$\eta_g = \eta_r \eta_{pt} [1 - \beta_t (T_c - T_r)] \quad (3.11)$$

where η_r is the PV reference efficiency, β_t is the thermal coefficient, T_c is the cell temperature, and T_r and PV reference temperature are both in Celsius. In Eq. (3.11), η_{pt} is the efficiency of the power adjustment equipment, and since we have omitted to review and consider it in this dissertation, we assume its range to be 100%.

T_c can be calculated from Eq. (3.12):

$$T_c = T_a + G_t \frac{\text{NOCT} - 20}{800} \quad (3.12)$$

where T_a is the ambient temperature per Celsius and NOCT is the nominal operating temperature of the solar cell.

3.3.3.1 Cost of Photovoltaic Solar Power Plant Production

In general, based on mentioned points, the cost of production of solar units can be divided into two parts: the cost of initial investment and the cost of operation and maintenance (a fixed cost per year). Accordingly, the cost function can be provided for these photovoltaic systems according to the following equation:

$$A'_{PV} = A_{PV} + \text{OM}_{PV} \quad (3.13)$$

In this regard, A is the initial investment cost and is calculated by Eq. (3.14). OM_{PV} is also a cost of operation and maintenance that is considered a fixed annual amount. If the EPV is the approximate total annual energy production for solar cells, the cost per kilowatt hour of energy produced by these units is calculated using the following equation:

$$C_{PV} = \frac{A'_{PV}}{E_{PV}} = \frac{A_{PV} + \text{OM}_{PV}}{P_{PV} \text{CF}_{PV} \times 8700} \quad (3.14)$$

In this regard, P_{PV} is the nominal installed capacity of the solar panels and CF_{PV} is the capacity factor, which is determined by the annual operation of the panels.

3.3.4 Fuel Cell

According to [52], the power output and cost of the fuel cell system in the proposed grid can be modeled as follows:

$$P_{fc} = H_u \times \eta_{fc} \times 37.8 \quad (3.15)$$

In Eq. (3.15), η_{fc} is the fuel cell efficiency and it is equal to 37.8 and H_u is the amount of using hydrogen in kg.

The costs of the fuel cell system are also modeled as follows:

$$NPC_{fc} = NPCI(N_{fc}.CC_{fc}.RC_{fc}.OM_{fc}.L_{fc}.ir.R) \quad (3.16)$$

In this regard, the parameters are defined in Nomenclature.

We know that 1 year is 365 days, and the main purpose of the dissertation is 24-h exploitation, so we divide the final net cost by 365 to get the net cost in 1 day:

$$d = \left(\frac{NPC}{365 * 20} \right) \quad (3.17)$$

3.3.4.1 Fuel Cell Capacity Limit

1. The output of each capacity must not exceed their design capacity:

$$0 \leq P_{fc}(t) \leq P_{fcMax} \quad (3.18)$$

In this regard, P_{fcMax} is the maximum power of the fuel cell.

2. Heating constraint:

$$P_{Thermal}(t) = P_{space}(t) + P_{water}(t) \quad (3.19)$$

in which $P_{water}(t)$ is hot water power and $P_{space}(t)$ is house heating power.

3.3.5 Storage Systems (Battery Modeling)

Batteries are usually considered as a constant voltage source. The life span of a battery is directly related to various parameters such as the amount of charge and discharge of the battery, so it is possible to model the operation of a storage system in the grid as follows [53]:

$$C_{wc} = \frac{C_{wc.bat}}{\sqrt{\eta_{bat}} \cdot Q_{lifetime} \cdot N_{bat}} \quad (3.20)$$

In this regard, C_{wc} is the cost of erosion of the battery in terms of \$/Kwh, $C_{wc.bat}$ is the cost of replacement of the battery bank in terms of \$, N_{bat} is the number of

batteries in the battery bank, Q_{lifetime} is calculated by Eq. (3.21), and η_{bat} is also the battery charge efficiency factor (discharge efficiency is considered to be 100%):

$$Q_{\text{lifetime}} = \text{CFD.DOD} \frac{q_{\text{max}} \cdot V_{\text{bat.nom}}}{1000} \quad (3.21)$$

This equation is a laboratory relationship for determining the battery life, in which the CTF represents the number of defective cycles, DOD is the percentage of discharge depth, q_{max} is the maximum battery capacity in terms of Ah, and $V_{\text{bat.nom}}$ is the nominal battery voltage [54]. Also, another cost for batteries is the cost of repairs and maintenance, which is a fixed cost. Therefore, the total cost of the battery bank is modeled as in Eq. (3.22):

$$C_{\text{bat}} = C_{\text{bat.wc}} + C_{\text{bat.om}} \quad (3.22)$$

In this case, C_{bat} is the total cost of the battery, $C_{\text{bat.wc}}$ is the cost of erosion of the battery, and $C_{\text{bat.om}}$ is the maintenance cost. There will be limitations on the operation of the battery bank in a small grid, which are modeled as follows:

Battery charge status at the specific time [55]:

$$\text{SOC}(t + \Delta t) = \text{Soc}(t) + \eta_{\text{bat}} \left[\frac{P_{\text{bat}}(t)}{U_{\text{bus}}} \right] \Delta t \quad (3.23)$$

In this regard, $P_{\text{bat}}(t)$ is the power charged or discharged by the battery bank (positive charge and negative discharge), U_{bus} is the bus voltage to which the battery bank is connected, and Δt is the hourly time interval for which an hour is allotted in this research.

The battery charge status is between the maximum and minimum nominal capacity [54]:

$$\text{SOC}_{\text{min}} \leq \text{SOC} \leq \text{SOC}_{\text{max}} \quad (3.24)$$

SOC_{Min} and SOC_{Max} are usually linked by Eq. (3.25):

$$\text{SOC}_{\text{min}} = (1 - \text{DOD}) \cdot \text{SOC}_{\text{max}} \quad (3.25)$$

3.3.6 Consumers

The proposed microgrid in this chapter has two types of consumers: (1) uncontrollable loads and (2) controllable loads.

3.3.6.1 Washing Machines and Dryers

One of the most expensive household loads is machines such as washing machines and dishwashers. These devices have a high consumption in a short period of time (1–2 h). Accordingly, by presenting the demand response program for this type of equipment and transferring their consumption time to another time, the load curve can be adjusted according to the small grid products.

According to the algorithm defined in each time interval, the difference between the domestic production of the loads is calculated; if this amount is higher than the load required by the washing machines, all these loads are provided; otherwise the excess amount is transferred to the next time interval. The amount of power that is transferred to the next time interval in each interval is calculated through Eq. (3.26):

$$P_{\text{wash.after}_i} = P_{\text{wash}_i} - (P_{\text{wt},i} \text{ OR } P_{\text{pv},i} \text{ OR } P_{\text{fc},i}) - P_{\text{load.total},i} \quad (3.26)$$

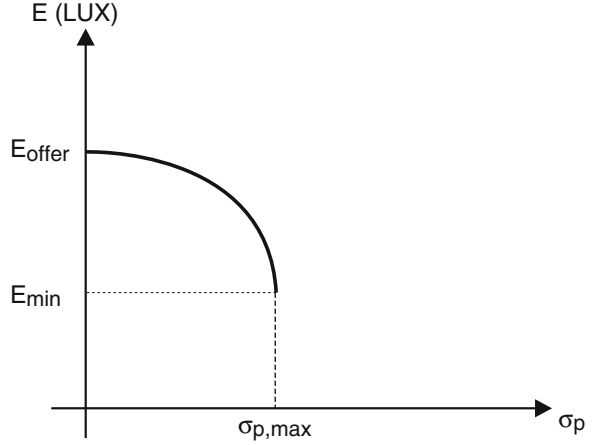
In this regard, $P_{\text{wash.after}_i}$ demonstrates the power transferred to the next time period, P_{wash_i} the requested power of the washing machines in the time interval i , $P_{\text{wt},i}$ the wind turbine power production in the time interval i , $P_{\text{pv},i}$ the solar production power in time intervals, and i and $P_{\text{fc},i}$ the power output of the fuel cell. Also, $P_{\text{load.total},i}$ indicates the amount of power requested by other loads. In order to encourage consumers in this way, in exchange for transferring these devices to another time, a percentage of the electricity price of the distribution grid (α_{wash}) in that period is considered as encouragement for the consumer.

3.3.6.2 Lighting Loads

Another major consumer of electricity is light loads. These loads are the largest consumers of electrical energy, creating a peak in the electric load curve. Therefore, by controlling the brightness and power consumption of these loads, it is possible to save on electricity consumption.

To perform this method, an intelligent LMS lighting control system is needed, which is used in smart homes. Of course, to have a smart control system in a building, the building must not be a smart one. In other words, from the set of electrical and mechanical installations, only the lighting part can be intelligently controlled. With the implementation of this system, various capabilities are created, one of the most important of which is to adjust the value of light shining from the lamps in commensurate to the natural light of the environment and energy price. To adjust the brightness of different lamps, we need electronic ballasts. For example, for incandescent and halogen lamps, the light flux of these lamps is proportional to the voltage applied to both ends, so as the voltage applied to the two ends of the lamp decreases, and the light flux emitted from the lamp also decreases. AC/AC converters have been used to adjust the brightness of this group of lamps. Such circuits are also called dimers. In these circuits, power electronics are used to transform the

Fig. 3.2 Characteristic control of lighting intensity according to the price of electrical distribution grid



voltage wave applied to the two ends of the lamp. This reduces the effective voltage across the lamp head and reduces the light emitted from the lamp. In fluorescent and compact fluorescent lamps (low consumption), electronic ballasts must be used to adjust the light intensity of the lamp. Because the fluorescent flux emitted by fluorescent lamps is affected by the mercury vapor pressure inside the lamp, in this case the ballasts, voltage, current, and frequency characteristics change so that the fluorescent flux increases or decreases. However, because the human sensitivity curve is altered by changes in logarithmic light, it is possible to change the light of the bulb in the form of logarithmic changes to make the residents feel better.

In order to change the consumption of light loads with the energy price, a curve in the form of Fig. 3.2 for the intensity of light and the price of electric energy can be considered. In this curve, the horizontal axis represents the predicted deviation of the predicted minimum price, which is calculated according to Eq. (3.27), and the vertical axis shows the allowable light intensity range (according to the lighting table) for the desired location. Due to this feature, the changes in light intensity and the price of electricity are considered as a low concurrent contribution so that in low price changes, the light intensity decreases slightly, but in higher price changes, light intensity decreases more. Given the specified two points, $(0, E_{offer})$ and $(\sigma_{p, \max}, E_{min})$, and the fact that the slope of the tangent line at the point, $(0, E_{offer})$, is equal to zero, the equation of this contribution will be as Eq. (3.28):

$$\sigma_{p,i} = \rho_{grid,i} - \rho_{grid, \min} \quad (3.27)$$

$$E = -\frac{E_{offer} - E_{min}}{\sigma_{p, \max}^2} (\sigma_p^2 + E_{offer}) \quad (3.28)$$

In Eq. (3.27) $\sigma_{p,i}$ indicates the price deviation from the minimum price in the time interval i , $\rho_{grid,i}$ the grid price in the range i , and $\rho_{grid, \min}$ the minimum predicted price in the next 24 h. In Eq. (3.28), E_{offer} is the recommended brightness intensity

Table 3.2 Room lighting loss coefficient

Cleanness of the room	Good	Medium	Weak
LLF	0.75	0.70	0.65

for the desired location, E_{\min} indicates the minimum brightness intensity, and $\sigma_{p. \max}$ is the maximum predicted price deviation from the predicted minimum price. In Eq. (3.28), the amount of light intensity obtained is equal to the total amount of illumination obtained from the lamps and the ambient natural light shown in Eq. (3.29):

$$E = E_{\text{lamp}} + DF \times E_{\text{day}} \quad (3.29)$$

In Eq. (3.29), E_{day} is related to the intensity of light in a given space due to daylight. The daylight factor is usually used to indicate the effect of light on the indoor environment. This coefficient is expressed as the ratio of the intensity of light on a given internal surface and at the same time the intensity of light in the external environment on a horizontal surface in an unobstructed place. Equation (3.30) shows this coefficient, in which case E_i indicates the light intensity of the indoor environment due to daylight and E_0 indicates the light intensity of the outdoor environment:

$$DF = \frac{E_i}{E_0} \times 100 \quad (3.30)$$

Now, using Eqs. (3.28) and (3.31), the light flux required for the lamp can be calculated:

$$\varphi = \frac{E_{\text{lamp}} \cdot L \cdot W}{CU \cdot LLF} \quad (3.31)$$

In this regard, φ is the luminous flux; L and W are the length and width of the room, respectively; CU is the coefficient of interest that is obtained from the lighting tables; and LLF is the coefficient of light loss that is obtained according to Table 3.2.

Another quantity that is considered for lamps is the coefficient of the luminous efficiency of the lamp, which shows the ratio of the luminous flux to the electrical power of the lamp. Therefore, according to the light efficiency factor of the lamp and Eqs. (3.28) and (3.31), the electrical power of the lamp can be obtained:

$$P_{\text{light}} = [E - E_{\text{day}}] \frac{L \cdot W}{CU \cdot LLF \cdot \eta} \quad (3.32)$$

In this regard, η also represents the luminous efficiency coefficient of the lamp.

3.4 Objective Function

The main purpose of this study is to maximize profits, provided that all operating constraints are met. Through the defined function, the level of participation of generators, storage devices, and energy exchange with the distribution grid is determined with the aim of increasing the profit of the microgrid. However, due to the nature of the renewable units, it is not possible to consider the status of these generators (on/off) and their instantaneous production is continuously injected into the grid; in this regard, the time interval is 24 h a day.

As it is clear from Eq. (3.33), this objective function has two parts, income and cost, which are listed below in the form of a collection of small grid income and expenses.

Small grid income:

- Selling power to the regional distribution grid
- Selling power to the uncontrollable loads
- Selling power to the typical loads
- Selling power to the washing and dryer's machines
- Selling power for lighting

Small grid costs:

- The cost of purchasing energy from the distribution grid
- Solar unit production cost
- Price of wind's generators
- Production cost of fuel cell unit
- Price of stored energy in the battery
- Pay penalty for typical loads if they are cut
- Pay money as bonus, due to the time movement of loads of household washing appliances

Considering what is mentioned above, the microgrid administrator should provide a plan for the operation of the microgrid, which aims to increase the microgrid's profit. According to the set of incomes and costs, there is a need for a range of information such as load forecasting, solar and wind forecast, fuel cell electric and thermal power generation, upstream energy price forecasting, temperature forecasting, lighting level forecasting, and technical specifications of small production unit grids including the cost of selling energy to loads, the amount of fines for cutting regular loads, and the amount of rewards for transporting loads from house appliances. According to the mentioned expenses and incomes, the amount of expenses and incomes are modeled as follows:

$$\begin{aligned}
\text{OF} = \sum_{t=1}^{24} \{ & [P_{\text{grid}}(t) \times \rho_{\text{grid}}(t) + P_{\text{Load.e}}(t) \times \rho_{\text{Load.e}}(t) + P_{\text{normal}}(t) \times \rho_{\text{normal}} \\
& + P_{\text{wash}}(t) \times \rho_{\text{wash}}(t) + P_{\text{light}}(t) \times \rho_{\text{light}}] - [C_{\text{fc}}(t) + C_{\text{PV}}(t) \\
& + C_{\text{w}}(t) + C_{\text{bat}}(P_{\text{bat}}(t)) + C_{\text{shed}}(P_{\text{normal.curtail}}(t)) + \text{penalty}_{\text{wash}}(t)] \} \quad (3.33)
\end{aligned}$$

This objective function indicates incomes minus grid costs for the next 24 h.

In this regard, the first phrase is the incomes from the selling of power to the grid or purchasing from the grid, respectively (positive indicates selling and negative indicates purchasing); other phrases represent income from the selling of power to different loads. In the second phrase, first the costs of solar, wind, and fuel cell production are given, then the cost of energy storage in the battery, the amount of fine due to disconnection of normal loads, and finally the incentive due to transfer of loads of household washing appliances to other time intervals. Therefore, for optimal operation of this microgrid, the OF objective function must be maximized according to its constraints. Also, in this chapter, PSO algorithm has been used to optimize the operation of the desired microgrid.

3.4.1 Power Balance

The most important precondition for solving the optimization problem is to meet the balance between production, purchase, or sale to the grid and consumption for a period of 1 h, which is equal to the moment of Eq. (3.34):

$$\begin{aligned}
& [P_{\text{load.e}}(t) + P_{\text{normal}}(t) + P_{\text{wash}}(t) + P_{\text{light}}(t) + P_{\text{grid}}(t)] \\
& = [P_{\text{bat}}(t) + P_{\text{wt}}(t) + P_{\text{pv}}(t) + P_{\text{fc}}(t)] \quad (3.34)
\end{aligned}$$

In this regard, the positive/negative sign of $P_{\text{bat}}(t)$ indicates the battery charge/discharge mode.

3.4.2 Limitation in Energy Exchange with Distribution Grid

Due to the technical constraints such as capacity of transmission grid, capacity of transformers and breakers, and other related instruments, it is essential to consider a maximum amount for the maximum exchanging power between microgrid and upstream distribution grid that is shown in Eq. (3.35):

$$\left| P_{\text{grid}}(t) \leq P_{\text{grid}}^{\max} \right| \quad (3.35)$$

In this regard, P_{grid} is the exchange power with the upstream distribution grid and P_{grid}^{\max} is the maximum power that can be exchanged with the grid.

3.5 Specification of the Intended Microgrid

3.5.1 Solar and Wind Units

In this simulation, the capacity of the solar unit is 250 kW and the capacity of the wind unit is assumed to be 100 kW for two turbines. This solar unit consists of 250 W modules whose specifications are according to Table 3.3 [56, 57].

3.5.2 Specifications of Fuel Cell Units

Features of the CHP system and fuel cell technology used in the chapter are presented as Table 3.4.

Table 3.3 Technical specifications [56, 57]

Description	Specification
<i>(a) PV module</i>	
Model	SUNTECH
Maximum power	250 W
Optimum operating voltage	31.1 V
Module efficiency	16.6%
<i>(b) Wind turbine</i>	
Model	Aeolos-H
Max power (wind only)	50 KW
Rated speed	10 m/s
Cut-in speed	<6.7 mph (3 m/s)

Table 3.4 Main specification of 150 kW technology [58]

Capital cost (\$/kW)	Maintenance cost (\$/Kwh)	Electrical efficiency (η_{ge})	Heating efficiency (η_{gh})
1100	0.015	44%	46%
900	0.015	39%	43%
700	0.015	35%	40%

3.5.3 Battery Bank

In this microgrid, a battery bank is used to store energy. The battery bank includes Surrelta 4KS25P batteries, which are described in Table 3.5 [59]. In order to have a reservation in the operation of the microgrid, the lowest battery charge level is 80 kWh.

3.5.4 Energy Exchange Between Microgrid and Distribution Grid

In this chapter, the exchange with the upstream distribution grid is bidirectional and the installed transformer has a capacity of 300 KW with 90% efficiency:

$$P_{\text{grid}}^{\text{max}} = 300 \times 0.9 = 270 \text{ KW}$$

It is assumed that the price of the upstream distribution grid is constant. For this purpose, the electricity tariffs of Iran's electricity network have been used in accordance with [60], according to which for the residential customers with a power of more than 30 kW and less than 30 kW, the energy price is according to Table 3.6. Also, the purchasing price of energy from the microgrid has been considered based on the purchasing of energy from renewable generations in off-peak load and peak load in accordance with Iranian tariffs. It should be noted that due to the difference in exchange rates between the Iranian currency and the US dollar, the final profit has been converted into US dollars by a specific factor.

Table 3.5 Battery specifications of battery banks [59]

Type	Nominal capacity (Ah)	Nominal voltage (V)	Round trip efficiency (%)	Q_{lifetime} (kWh)	Energy (kWh)	DOD (%)	N_{Bat}	$C_{\text{rep. bat}}$ (\$)
Surrelta 4KS25P	1900	4	80	10,569	7.6	90	40	900

Table 3.6 The tariff of energy exchange between microgrid and distribution grid [60]

Time	7–19	19–23	23–7
Energy tariff for more than 30 kW (kWh/\$)	0.034	0.068	0.017
Energy tariff for less than 30 kW (kWh/\$)	0.044	0.088	0.022

3.5.5 Initial Conditions of Microgrid

In this simulation, the initial conditions (time before the first time period) for the battery charge level are equal to the minimum value and for the solar unit it is assumed that it was on before the first time period.

3.6 Outputs of the Program, Review, and Analysis of Scenarios

According to the information provided in the previous section, in this section, the output of various designs and scenarios for the simulated microgrid are given and the obtained results have been analyzed.

3.6.1 Simulation of the First Scenario

In this scenario, there is no demand response program. The results of the scheduling, including the production of solar, wind, and fuel units; power stored in the battery; and the amount of energy exchange with the global electricity grid over the next 24 h, are presented in Fig. 3.3. In this scenario, the microgrid’s profit will be \$785,694.1.

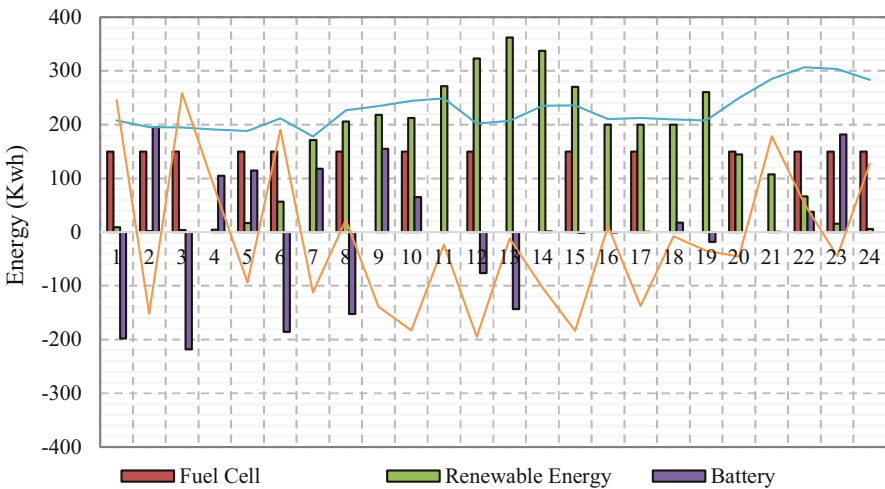


Fig. 3.3 Energy balance in the whole microgrid in the first design

As it is shown in Fig. 3.3 at a time when renewable energy production is higher than the demand of consumers, the microgrid acts as a supplier for the distribution grid and sells energy to it. On the other hand, when the amount of renewable production does not meet the demands of customers, the fuel cell and battery system will enter the circuit and respond to part of the required load of the microgrid, which will reduce the purchase of power from the global grid, and in some cases, the excess production capacity is injected into the national grid, which in turn increases the profitability of the grid.

3.6.2 Simulation of the Second Scenario

3.6.2.1 Loads of Household Washing Appliances

As mentioned in the previous sections, in the proposed microgrid model, the time of consumption of washing appliances' loads is coordinated with wind and solar production, and for the transfer of consumption time, the reward is paid to the consumers. Figure 3.4 shows the time of consumption of these loads after and before the implementation of the control program. As shown in Fig. 3.4, only 12 and 13 loads have been transferred, and the reason for this is that the control program has not found it cost effective to transfer other loads due to the amount of incentives paid.

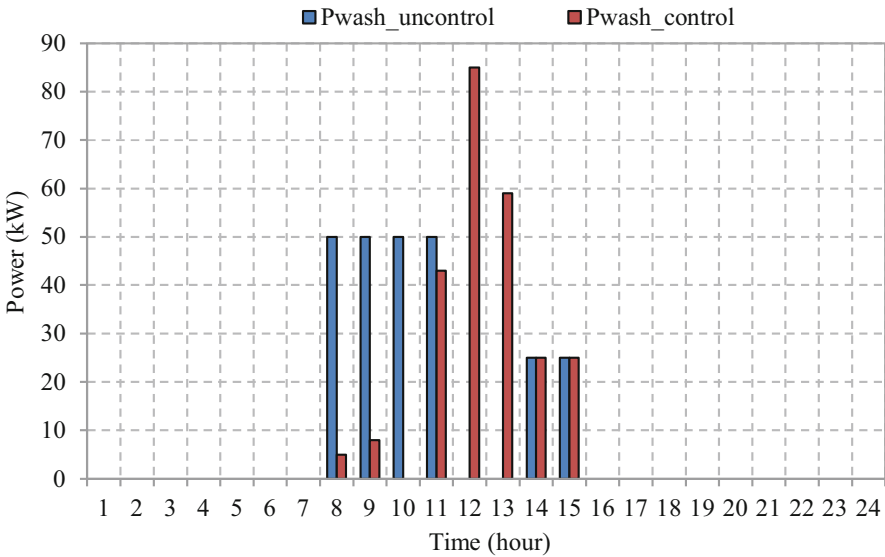


Fig. 3.4 Power consumption diagram of household appliance's loads with the implementation of the control program

3.6.2.2 Lighting Loads

In order to control the light loads, the brightness of these loads and consequently their energy consumption are calculated through the equations of the Sect. 3.3.6.2 and matched to the energy price of the global electricity grid. Figure 3.4 shows the power consumption diagram of these loads after and before the implementation of the control program. According to Fig. 3.5 it has been shown that by implementing this control program, there is a coordination between the consumption of lighting loads and the price of the energy market, so that, for example, during peak hours, their consumption has been reduced. Also, in this control method, it is suggested to reduce the brightness level of the lights in the midnight hours, when the amount of traffic is very low, and the result of simulating this proposal is shown from 1 to 5 in Fig. 3.5.

3.6.2.3 Optimization of Production in Microgrid According to the Second Scenario

After implementing the demand response program and the control program for washing appliances and lighting loads, the cost of the proposed microgrid will be significantly reduced, and as a result, the profitability of the grid will increase and will reach \$930,708.8. The flowchart of this plan and the production curve of the microgrid and energy exchanges with the power grid are shown in Figs. 3.6 and 3.7.

Comparing the second scenario with the first scenario, it can be concluded that the amount of microgrid production has decreased. In this chapter’s microgrid model,

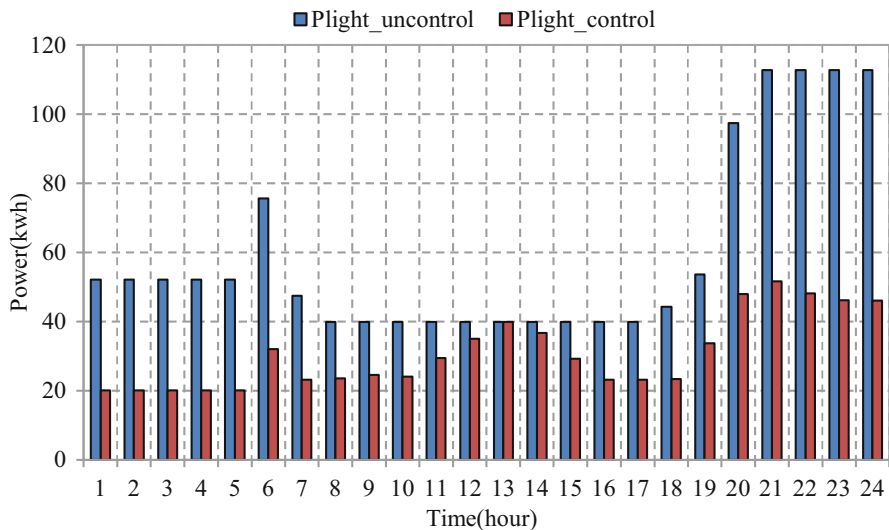


Fig. 3.5 Energy consumption diagram of lighting loads by applying the control program

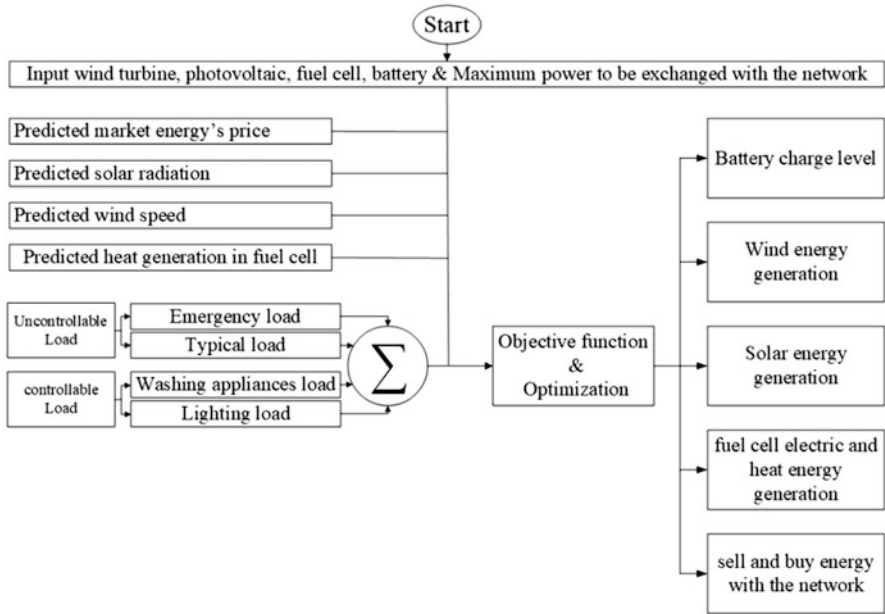


Fig. 3.6 Energy balance in the whole microgrid in the second design [52]

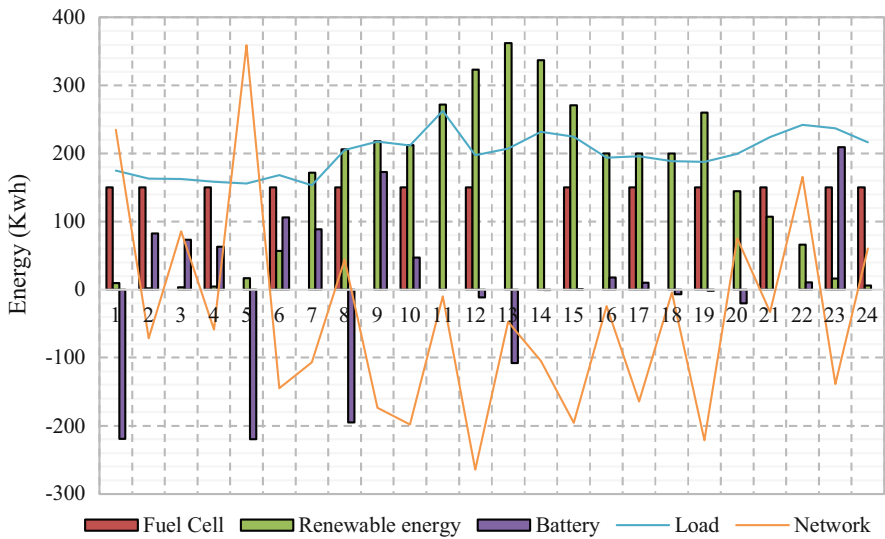


Fig. 3.7 Energy balance in the whole microgrid in the second design

which aims to increase profits, it would be better if controllable loads be sensitive to the prices of the global electricity grid. Because in this way, if the network's price is high, the amount of power consumption will be reduced, and as a result, the income of the microgrid will increase, and if the price of the network is low, the cost of the microgrid will decrease; both of these will result in increasing network profitability.

Also, due to the fact that according to the policy of electricity networks the purchasing rate of power for the electricity network is higher than the selling rate (due to reducing dependence on traditional power generation systems), accordingly, demand response programs in the microgrid to further profitability means selling electricity to the global grid and responding to network loads by purchasing from the traditional power grid; therefore, to address such a problem and to create load-bearing structures and demand response programs by microgrids, existing free energy markets should be infrastructural.

3.7 Conclusion

In order to make the best use of the mentioned microgrid, different scenarios were simulated and then checked; the following are the results of this research:

Implementing control programs in a way that can cover changes in unmanageable energy resources or changes in energy market prices can reduce costs or increase the profitability of microgrid utilization. Implementing load control programs can reduce the probability of loss of microgrid utilization.

In structures where the microgrid has no load and the purpose is only to increase profitability, it makes improve if controllable loads be sensitive to prices. But in structures where the loads are owned by the microgrid itself and the purpose is to reduce costs, controllability of loads will often be appropriate with changes in energy resources.

Virtual energy storage is available in electric water heaters as well as refrigerators, taking into account the level of comfort of consumers and the allowable temperature range.

Some house loads, like washing and dryer's loads, need a lot of power in a short time. Therefore, it is possible to reduce operating costs and increase the profitability of the microgrid by transferring their consumption time to periods when the rate of renewable energy production is high or the cost of purchasing energy from the distribution grid is low. Lighting loads are one of the major consumers of electrical energy. Therefore, as the results of this study have showed, using the proposed method of this study in order to sensitize these loads to price changes in the permitted lighting range can significantly increase the profitability of microgrid utilization and reduce the cost of electricity consumption.

3.8 Suggestions

It is recommended that the various components of the microgrid, i.e., the wind and solar generator, battery, as well as multiple loads, be placed on different buses to check the voltage and transmission limitations in the microgrid structure during operation.

One of the new loads that have received a lot of attention today is electric cars. It is suggested that one or two parking lots be provided in the microgrid structure for charging these vehicles and that the uncertainty in their operation be modeled.

It is suggested that other optimization methods (similar to the bird community algorithm) be used to optimize the operation of the microgrid.

Acknowledgments Special thanks is given to the department of research and technology of the Islamic Azad University, Damavand Branch, for their valuable support throughout all the phases of this research.

Nomenclature

Abbreviation

CHP	Combined heat and power
DER	Distributed energy resources
DSM	Demand-side management
ED	Economic dispatch
EH	Energy hub system
IREMS	Intelligent residential energy management system
MCE	Multi-carrier energy
MCMG	Multi-carrier microgrid
SEMS	Smart energy management system
SSER	Small-scale energy resources

Indexes

N	Number of solar panels
t	Time

Variables

$P_{\text{grid}}(t)$	Power exchanged between microgrid and network [kW] [kW]
$\rho_{\text{grid}}(t)$	Predicted electrical power price in grid [\$/kW] [\$/kW]
$P_{\text{load. e}}(t)$	Sold power for uncontrollable loads [kW] [kW]
$P_{\text{normal}}(t)$	Sold power for typical loads [kW] [kW]
$P_{\text{wash}}(t)$	Sold power for washing and drying loads [kW] [kW]
$P_{\text{light}}(t)$	Sold power for lighting [kW] [kW]
P_{wt}	Power of wind unit
P_{pv}	Power of solar unit
P_{fc}	Power of fuel cell
η_{g}	Efficiency of solar unit

CC_{fc}	Initial investment cost of a fuel cell [\$/kW]
OM_{fc}	Repairing and maintaining cost of a fuel cell [\$/kW]
RC_{fc}	Replacement costs of fuel cell equipment [\$/kW]
L_{fc}	Fuel cell's life span

Constants

$\rho_{load, e}(t)$	Price of power sold for uncontrollable loads [\$/kW] [\$/kW]
$\rho_{normal}(t)$	Price of power sold for typical loads [\$/kW] [\$/kW]
$\rho_{wash}(t)$	Price of power sold for washing and drying machines [\$/kW] [\$/kW]
$\rho_{light}(t)$	Price of power sold for lighting [\$/kW] [\$/kW]
C_{PV}	Solar unit generation costs
C_{fc}	The cost of producing a unit of fuel cell
C_w	Wind unit generation costs
C_{bat}	Charge and discharge energy costs
C_{shed}	The amount of refund for cut typical loads
penalty _{wash} (t)	The courage to shift the washing loads

References

1. Saito N, Niimura T, Koyanagi K and Yokoyama R (2009) Trade-off analysis of autonomous microgrid sizing with PV, diesel, and battery storage. *2009 IEEE Power & Energy Society General Meeting, Calgary, AB*, pp. 1–6
2. Ipakchi A, Albuyeh F (2009) Grid of the future. *IEEE Power Energy Mag* 7(2):52–62
3. (2010) The smart grid. *U.S. Department of Energy*, vol. 99, p. 48
4. Jiayi H, Chuanwen J, Rong X (2008) A review on distributed energy resources and MicroGrid. *Renew Sust Energ Rev, Elsevier* 12(9):2472–2483
5. B S (2016) Development of a self-healing strategy for future smart microgrids. *EEE Trans Smart Grid* 8(2):868–880
6. Conti S, Rizzo SA (2014) Probability of adequacy evaluation considering power output correlation of renewable generators in smart grids. *Int J Electr Power Energy Syst* 61:145–151
7. Krause T, Andersson G, Frohlich K, Vaccaro A (2011) Multiple-energy carriers: modeling of production, delivery and consumption. *Proc IEEE* 99(1):15–27
8. Geidl M, Koeppl G, Favre-Perrod P, Klockl B, Andersson G, Frohlich K (2007) Energy hubs for the future. *IEEE Power Energy Mag* 5:24–30
9. Liu C, Shahidehpour M, Wang J (2011) Coordinated scheduling of electricity and natural gas infrastructures with a transient model for natural gas flow. *Chaos* 21(2)
10. Geidl M, Andersson G (2007) Optimal power flow of multiple energy carriers. *IEEE Trans Power Syst* 22(1):145–155
11. Sheikhi A, Ranjbar AM, Oraee H (2012) Financial analysis and optimal size and operation for a multicarrier energy system. *Energy Build* 48:71–78
12. Moeini-Aghaie M, Abbaspour A, Fotuhi-Firuzabad M, Hajipour E (2014) A decomposed solution to multiple-energy carriers optimal power flow. *IEEE Trans Power Syst* 29(2):707–716
13. Geidl M (2007) Integrated modeling and optimization of multi-carrier energy systems. *Ph.D. dissertation*, vol. ETH Diss, p. 17141
14. Geidl M, Andersson G (2007) Optimal coupling of energy infrastructures. Conference: IEEE Lausanne Powertech Processing:1398–1403
15. Florea GG, Dobrescu R, Rohat OI (2013) From bridge to control hub—the power smart grid evolution. *2nd International Conference on Systems and Computer Science*, pp. 26–27

16. Shahidehpour M (2011) Our aging power systems Infrastructure and life extension issues. *IEEE Power Energy Magazine*, pp. 22–76
17. Cai N, Nga NTT, Mitra J (2012) Economic dispatch in microgrids using multi-agent system. *North American Power Symposium (NAPS)*, p. 1–5
18. Xu Y, Liu W (2011) Stable multi-agent-based load shedding algorithm for power systems. *IEEE Trans Power Syst* 26(4):2006–2014
19. Abido MA (2006) Multi objective evolutionary algorithm for electric power dispatch problem. *IEEE Trans Evol Comput* 10(3):315–329
20. Nikmehr N, Ravadanegh SN (2015) Optimal power dispatch of multi-microgrids at future smart distribution grids. *IEEE Trans Smart Grid* 5(1):1949–3053
21. Hernandez-Aramburo CA, Green TC, Mugniot N (2005) Fuel consumption minimization of a microgrid. *IEEE Trans Ind Appl* 41(3):673–681
22. Jin M, Feng W, Liu P, Marnay C, Spanos C (2017) MOD-DR: microgrid optimal dispatch with demand response. *Appl Energy* 187:758–776
23. De Brabandere K, Vanthournout K, Driesen J, Deconinck G, Belmans R (2007) Control of microgrids. *IEEE Power Engineering Society General Meeting*:1–7
24. Qingjun S, Guangchao G, Quanyuan J (2012) Real-time energy dispatch of standalone microgrid. *Processing China Soc Electric Engineering (CSEE)*, p. 26–35
25. Zakariazadeh A, Jadid S, Siano P (2014) Multi-objective scheduling of electric vehicles in smart distribution system. *Energy Convers Manag* 79:43–53
26. Zhao B, Zhang X, Chen J, Wang C, Guo L (2013) Operation optimization of standalone microgrids considering lifetime characteristics of battery energy storage system. *IEEE Trans Sustainable Energy* 4(4):934–943
27. Yuyang M, Jinling L, Guodong Z (2012) Improved multi-objective particle optimization algorithm based scheduling optimization of grid-connected microgrid. *Electr Power Sci Eng* 28(7):15–20
28. Deng D, Li G (2015) Research on economic operation of grid-connected DC microgrid. *International Conference on Renewable Power Generation*
29. Kinjyo Y (2012) Optimal operation of smart grid with fuel cell in isolated islands. *J Int Council Elect Eng* 2(4):423–429
30. Xin A, Minyong C, Zhili L (2009) Based on chaos ant colony algorithm for the micro grid environmental and economy operation. *Univ N China Electr Power* 36(5):2–6
31. Koutsopoulos I, Tassiulas L (2011) Challenges in demand load control for the smart grid. *IEEE Netw* 25(5):16–21
32. Chen C, Duan S, Cai T, Liu B, Hu B (2011) Smart energy management system for optimal micro grid economic operation. *IET Renewable Power Gener* 5(3):258–267
33. Guerrero J, Chandorkar M, Lee T, Loh P (2013) Advanced control architectures for intelligent microgrids—part I: centralized and hierarchical control. *IEEE Trans Ind Electron* 60(4):1254–1262
34. Guerrero JM, Loh PC, Lee T, Chandorkar M (2013) Advanced control architectures for intelligent microgrids—part II: power quality, energy storage, and AC/DC microgrids. *IEEE Trans Ind Electron* 60(4):1263–1270
35. Moradi-Dalvand M, Nazari-Heris M, Mohammadi-ivatloo B, Galavani S, Rabiee A (2020) A two-stage mathematical programming approach for the solution of combined heat and power economic dispatch. *IEEE Syst J* 14(2):2873–2881
36. Nazari-Heris M, Mohammadi-Ivatloo B, Asadi S, Geem ZW (2019) Large-scale combined heat and power economic dispatch using a novel multi-player harmony search method. *Appl Therm Eng* 154:493–504
37. Nazari-Heris M, Mehdinejad M, Mohammadi-Ivatloo B, Babamalek-Gharehpetian G (2019) Combined heat and power economic dispatch problem solution by implementation of whale optimization method. *Neural Comput & Applic* 31:421–436
38. Varadarajan M, Swarup KS (2008) Solving multi-objective optimal power flow using differential evolution. *IET Gener Transm Distrib* 2(5):720–730

39. Haghrah A, Nazari-Heris M, Mohammadi-Ivatloo B (2016) Solving combined heat and power economic dispatch problem using real coded genetic algorithm with improved Mühlhenbein mutation. *Appl Therm Eng* 99:465–475
40. Alipour M, Mohammadi-Ivatloo B, Zare K (2015) Stochastic scheduling of renewable and CHP-based microgrids. *IEEE Trans Ind Inf* 11(5):1049–1058
41. Nazari-Heris M, Abapour S, Mohammadi-Ivatloo B (2017) Optimal economic dispatch of FC-CHP based heat and power micro grid. *Appl Therm Eng* 114:756–769
42. Liangce H, Zhingang L, Pan L, Hao Z, Xueping L, Jiangfeng Z (2019) Optimal economic and emission dispatch of a micro grid with a combined heat and power system. *Appl Energy* 12 (4):604
43. Yordanos KS, Jianhua Z, Dehua Z (2020) Optimal energy management strategy in microgrid with mixed energy resources and energy storage system. *IET Cyber Phys Syst Theor Appl* 5 (1):80–84
44. Guanglin Z, Yu C, Yongsheng C, Demin L, Lin W (2017) Optimal energy management for microgrids with combined heat and power (CHP) generation, energy storages and renewable energy sources. *Appl Energy* 10(9):1288
45. Arun SL, Selvan MP (2018) Intelligent residential energy management system for dynamic demand response in smart buildings. *IEEE Syst J* 12(2):1329–1340
46. Hakimi SM, Hasankhani A, Shafie-khah M, Catalao JPS (2019) Optimal sizing and siting of smart microgrid components under high renewables penetration considering demand response. *IET Renewable Power Gener* 13:1809–1822
47. Roofegari nejad R, Hakimi SM, Moghaddas Tafreshi SM (2016) Smart virtual energy storage control strategy to cope with uncertainties and increase renewable energy penetration. *J Energy Storage* 6:80–94
48. HassanzadehFard H, Moghaddas-Tafreshi SM, Hakimi SM (2011) Effect of Energy Storage Systems on Optimal Sizing of Islanded Micro grid Considering Interruptible Loads. *3rd International Youth Conference on Energetics (IYCE)*
49. Chang TP (2010) Estimation of wind energy potential using different probability density functions. *Appl Energy. from Elsevier* 88(5):1848–1856
50. Akpinar EK, Akpinar S (2008) Estimation of wind energy potential using finite mixture distribution models. *Energy Convers Manag* 50(4):877–884
51. Zaibi M, Champenois G, Roboam X (2016) Smart power management of a hybrid photovoltaic/wind stand-alone system coupling battery storage and hydraulic network. *Math Comput Simul* 146(5):210–228
52. Poormoayed N, Saadatmandi M, Hakimi SM, Khaki B (2018) Intelligent residential energy management system in smart building considering fuel cell and PHEVs. *Int J Energy Smart Grid* 3(1):26–39
53. Atia R, Yamada N (2016) Sizing and analysis of renewable energy and battery Systems in Residential Microgrids. *IEEE Trans Smart Grid* 7(2):1204–1213
54. Pokharel GB, Lie BK, Fleten TT (2008) Management of price uncertainty in short-term generation planning. *IET Gener Transm Distrib* 2(4):491–504
55. Hakimi SM, Saadatmandi M, Shafie-khah M, Catalão J (2019) Smart household management systems with renewable generation to increase the operation profit of a microgrid. *IET Smart Grid* 2(4):522–528
56. "Solar Panel," [Online]. <http://www.solardesigntool.com/components/module-panel-solar/Sanyo/955/HIT-H250E01/specification-data-sheet>
57. "Wind Turbine," [Online]. <https://en.wind-turbine-models.com/turbines/1856-aeolos-aeolos-h-50kw>
58. Sheikhi A, Mozafari B, Ranjbar AM (2011) CHP optimized selection methodology for a multi-carrier energy system. *IEEE Trondheim PowerTech*
59. "Battery Bank," [Online]. <https://www.homerenergy.com/products/pro/version-history.html>
60. "Energy tariff," [Online]. <http://tariff.moe.gov.ir>

Chapter 4

Energy Markets of Multi-carrier Energy Networks



Seyed Mahdi Kazemi-Razi and Hamed Nafisi

4.1 Introduction

Electricity is a commodity capable of being traded through long-term and short-term trading. An electricity market is a mechanism enabling long-term trades by contracts, which are considered as private bilateral transactions between counterparties. The short-term trades allow purchase through bids and sales through the offers, generally in the form of financial or obligation swaps [1, 2]. The multi-carrier energy network (MCEN) power is managed by MCEN operator (MCENO) which is a unit to optimize the MCEN operation economically (tries to maximize MCEN revenue through its power management). Moreover, it must take into account the technical constraints of MCEN performance. To this end, it can participate in different markets to purchase/sell energy for providing energy consumption of MCEN consumers and maximize its revenue by optimized energy purchased/sold in these markets. As a result, MCENO is one of the actors participating in the markets, which determines the amount of energy that wants to be purchased/sold in any market according to received price signals [1]. Also, the market actor can be each of the producers (such as generators or distributed energy resources) and consumers (such as electrical loads or electrical heat pumps), which participates in different markets to purchase/sell energy or provides the ancillary services. The market players can also be divided into the following groups [3]:

S. M. Kazemi-Razi · H. Nafisi (✉)
Department of Electrical Engineering, Amirkabir University of Technology (Tehran Polytechnic), Tehran, Iran
e-mail: s.m.kazemi@aut.ac.ir; nafisi@aut.ac.ir

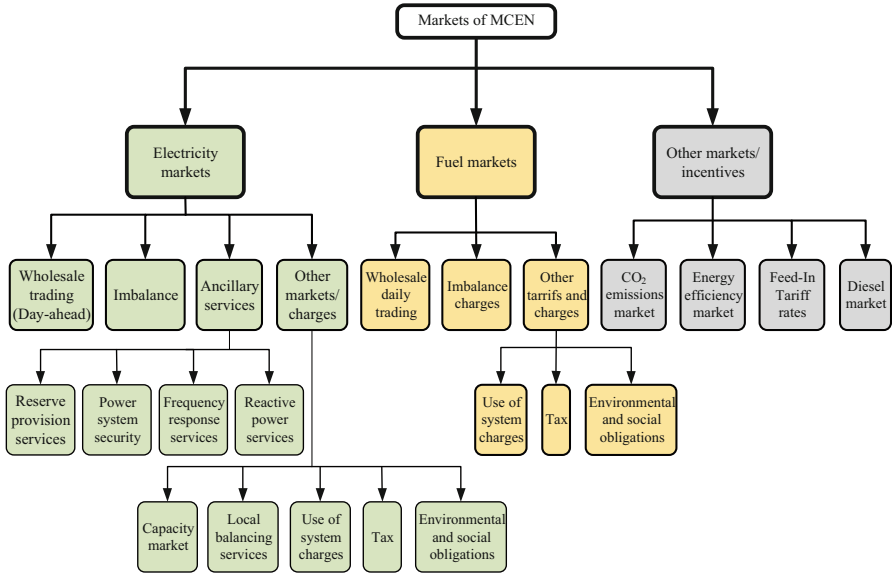


Fig. 4.1 Different markets that MCEN can participate

1. System operator
2. Actors under the supervision of the system operator including generation companies (GENCOs), transmission companies (TRANSCO), distribution companies (DISCOs), retailer companies, aggregators (such as MCENOs), brokers, and consumers

The system operator is a unit that controls the markets' operation and their contracts.

Since the MCEN includes multi-carrier energy vectors (e.g., electricity, fuel, heat), MCENO needs to participate in electricity markets. Besides, it must participate in a fuel market to purchase it for substituting fuel with electricity. In most MCEN, gas is the typical fuel for substituting and there are appliances to consume gas as an input. Also, MCENO must consider the grid charges due to using the power system (transmission and distribution system) facilities. Figure 4.1 shows all different markets where MCENO can participate in supplying energy consumption and maximizing the MCEN revenue.

These markets are divided into three categories which are entitled electricity markets, fuel markets, and other markets/charges. Each of these markets includes subsections that are described in more detail in the next sections. The electricity markets and fuel markets provide electricity and gas to MCEN that are required to supply MCEN consumers. But the last (named other markets/incentives) includes some charges which affect MCEN operation. These charges often are set by supervisory bodies (e.g., government) for the implementation of specific policies such as less damage to the environment. The MCENO participation in the electricity and gas

market is modeled in [4–8]. Reference [9] models the MCENO participation in the electricity market, but does not consider the gas market. Participation in reserve provision services is investigated in [5, 6, 9]. In addition, the balancing services resulting from scheduling of plug-in electric vehicle aggregator are reviewed in ref. [10]. The reserve provision includes three types of primary reserve, secondary reserve, and tertiary reserve, which are modeled in ref. [11]. Reserve participation by MCENO helps the system operator to balance the energy in the power system. Use of system charges and tax are modeled in ref. [6, 12] by considering them on the purchase price of electricity. The authors in ref. [13, 14] pay attention to the low-carbon systems. One of the heat-generating equipment that reduce CO₂ emissions is electric heat pump (EHP), which models have been proposed to integrate the EHPs into the power system [5]. Many references are presented for clearing the market price by considering the bids/offers of aggregators. For example, a joint energy and reserve market clearing model is presented that minimizes the payment cost while maximizing voltage stability.

It is noted that these markets have a determined time step (typically, it is an hour, half an hour such as the UK, or a quarter of an hour depending on the country/region) and operation calculations are processed based on this time step.

It should be noted that the current MCENs are classified as follows [15]:

1. Integrated electricity and gas sources (some of their advantages compared to networks with only electricity carrier are quick response to uncertainties, less harmful gas emissions, and cost saving as a result of more flexibility)
2. Integrated electricity and water sources (their advantages include less harmful gas emissions by using the renewable energy for water desalination, compared to thermal desalination and economic, social, and ecological development, in addition to hydro storage technology response to power shortage, which is effective in increasing network resiliency and stability)
3. Integrated electricity, gas, and water sources (their advantages include reduced CO₂ emissions in the water desalination process with renewable electricity, improved operation cost, reduced pollutant gas emissions, improved resiliency and efficiency, lower fuel cost, quick response to probabilities resulting from more flexibility, producing usable water by desalination systems, as well as producing electricity by hydroelectric generation units)

Due to the fact that MCENs include electrothermal equipment (e.g., combined heat and power (CHP)), boiler, hydropower plant, power-to-gas technology, heat storage, as well as gas storage, they have more flexibility for optimized performance in the market, compared to networks with only electricity carrier.

1. The presence of storage equipment can lead to energy storage at low-energy-price moments and consumption of stored energy at high-energy-price moments. Therefore, the ability to shift the time of energy consumption and also respond to energy shortage/surplus creates optimized performance (lower cost and increased flexibility) for the MCEN.

2. Electrothermal equipment allows the MCENO to be able to supply loads with energy carrier at a lower price by comparing the prices of different carriers. As a result, the energy carrier/appliance substitution helps the optimized performance.

There are studies that investigate the impact of different equipment on MCEN performance and cost [12, 16] (reference [16] investigates the power management of MCENs with power, gas, water, and heating carriers alongside the storages such as pumped hydro energy storage, gas storage, and thermal energy storage). Reference [17] analyzes the impact of using storage equipment on the cost of MCEN performance.

4.2 Electricity Markets

Electricity as a commodity is traded between producers and consumers via determined contracts through the wholesale trading market. These contracts are concluded and at the time of energy delivery determined in the contract the consumer receives the energy. Given the need to balance the electricity production and consumption moment by moment, the purchase/sell contracts can only be concluded up until the significant time (gate closure) which is determined by the system operator and the actors that participated in the market must declare the amount of electricity they want to generate/consume according to their contracts. Therefore, the system operator specifies which contracts can be implemented without causing problems in the system performance technically and energy balance. After this time, the electricity can only be traded through a balancing market to compensate for the shortage/surplus of energy (imbalance market) [2]. Producers and consumers determine the entire energy generated and consumed in the system by concluding the contracts in the wholesale trading market. However, the expected balance of generation and consumption may be lost due to the producers and load uncertainties (such as solar and wind generations) and the occurrence of unforeseen outages (such as damage to generators and lines and other facilities of transmission system). At this state, the producer or consumer needs to trade its energy shortage/surplus in the imbalance market.

Moreover, the violators must pay penalties associated with the deviation from their contracted generation/consumption through a pre-planned process [2]. It is notable that in addition to the imbalance market, the system operator can procure other balancing services to provide the balance of generation and consumption in the system. These services are explained in Sect. 4.3 in detail. The energy balancing is necessary for providing the security and quality of power supply and this can increase the system reliability. The system operator determines the relevant price of balancing services. Because MCENs integrate with power supply resources, they can participate in the mentioned markets as a load and purchase the energy, when their power generation is less than their load. But, at the hours when the amount of generation is more than their load, MCENs can sell their energy surplus in the

markets as a producer. In case of a violation from the contract amount, MCENO must pay the penalty and is required to compensate its shortage/surplus in the imbalance market [18].

Wholesale markets are divided into several categories, which are described in detail in Sects. 4.2.1–4.2.3. Day-ahead markets are commonly used in the MCEN power management, which are described in Sect. 4.2.4.

4.2.1 Bilateral Trading Markets

In this type of market, producers and customers enter into contracts directly without the intervention of a third party. These types of contracts are made in one of the following three ways [2]:

1. Long-term contracts
2. Trading over the counter
3. Electronic trading

In this type of market, the producer accepts purchase bids in which the bid price is greater than/equal to the cost of generating energy by its generators and the consumer accepts offers of sale at a lower than/equal to its acceptable price.

4.2.2 Electricity Pools

In this type of market, producers offer their sales including price and amount of energy, which are arranged upwards based on their price. Consumers bid their purchases (including price and amount of energy), which are also arranged downwards, resulting in a curve as shown in Fig. 4.2. From the intersection of these two

Fig. 4.2 Stacks of offers and bids in the electricity pools

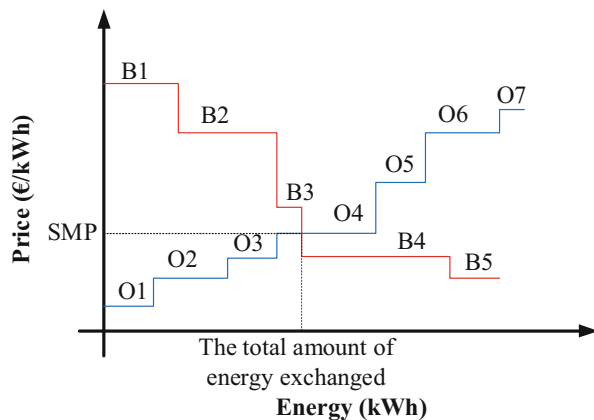


Table 4.1 The status of purchases/sales in a pool market

	Identifier	Price (€/kWh)	The amount of energy (kWh)	Status
Offers	O1	21	50	☑
	O2	22.36	100	☑
	O3	24	70	☑
	O4	25.2	150	☑ (Some of its energy is supplied)
	O5	27.5	50	-
	O6	30.47	85	-
	O7	31.1	40	-
Bids	B1	32	65	☑
	B2	30	130	☑
	B3	26	30	☑
	B4	24	200	-
	B5	23	50	-

curves, the market settlement price (i.e., system marginal price (SMP)) is obtained. Producers with an offer of less than or equal to SMP, as well as consumers with a bid of more than or equal to SMP, are accepted in this market.

For example, consider the sale offers and purchase bids offered in this market for a specific period (during 14:00–15:00 on June 1, 2020), which are listed in Table 4.1 and also shown in Fig. 4.2 [2].

Here, SMP is equal to 25.2 (€/kWh). As can be seen, only the producers O1, O2, O3, and O4, with an offer price of less than or equal to 25.2, are accepted in this market. Also, the consumers B1, B2, and B3, which have a bid price more than 25.2, are accepted.

4.2.3 Hybrid Model

This market is a combination of the characteristics of the previous two markets, and any actor who does not want to have a bilateral contract participates in the pool market. Participation in the pool market is not mandatory here [3].

4.2.4 Day-Ahead Market

Most of the energy consumption is provided through contracts in the day-ahead market. These contracts are concluded between producer and consumer for energy delivery in the next 24 h and the producer must provide the contracted energy at a scheduled time. The cost of delivered energy is paid to the producer through a planned process by the consumer [2]. The connection diagram of the actors in this market is shown in Fig. 4.3.

According to the contract concluded by the producer and consumer in the past, at the time of energy delivery, a scheduled amount of energy must be transmitted from producer to consumer. As Fig. 4.3 shows, this energy reaches the consumer by the transmission system. The transmission system operates under the supervision of the system operator. Now, according to the contract, a certain cost is directly paid from the consumer to the producer for energy production, which is shown in blue. Also, due to the use of the transmission system, both parties of the contract should pay the system operator the use-of-system cost (USC), which is shown in green. This process is the same for each of the 1 to n contracts (Fig. 4.3) [2]. Two examples of

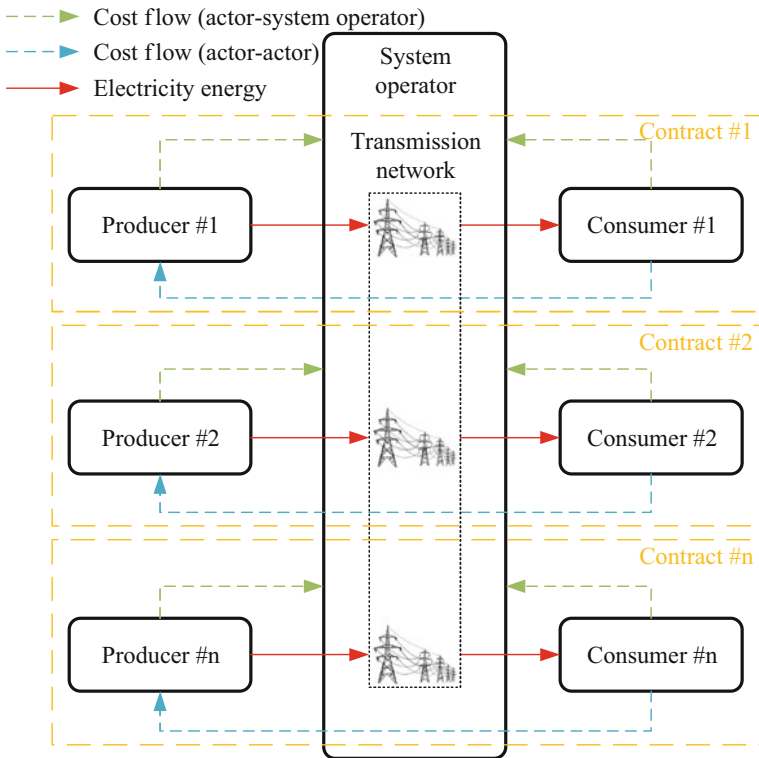


Fig. 4.3 The connection diagram of the actors in the day-ahead market

these markets, used in the UK, are detailed in [12]. The most important feature of this market is that the price is known before the time of energy delivery. As a result, the prices are suitable and reliable for wholesale electricity (proper to schedule the amount of purchase/sale of energy based on price signals).

Integration of power generation, with any kind, to MCEN such as CHP, photo-voltaic (PV), and wind turbine (WT) increases the operational cost of MCENO. The MCENO compares the cost of power generation by these sources with the purchase price of energy from the day-ahead market, and based on that, it is decided whether to buy or produce the needed energy. Also, if the selling price of energy is high enough, MCENO may decide to produce the energy as a generator and sell it in this market. As a result, MCEN can enter into a contract with other actors.

4.2.5 Imbalance Market

A part of the energy balance, as described in Sect. 4.2, is provided by the imbalance market. In this way, the actors bid/offer in the imbalance market. In some references, the imbalance market is named balancing mechanism [12] or spot market [2]. This is a managed market because the bids/offers are chosen by a third party (system operator), not bilaterally. The reason this market is named spot market is that it determines the price of energy imbalance. Another part of the energy balance provision is implemented by ancillary services, which are explained in Sect. 4.3 in detail. The diagram of the position of different actors in this market is in the form of Fig. 4.4.

Fig. 4.4 Different actors in the imbalance market

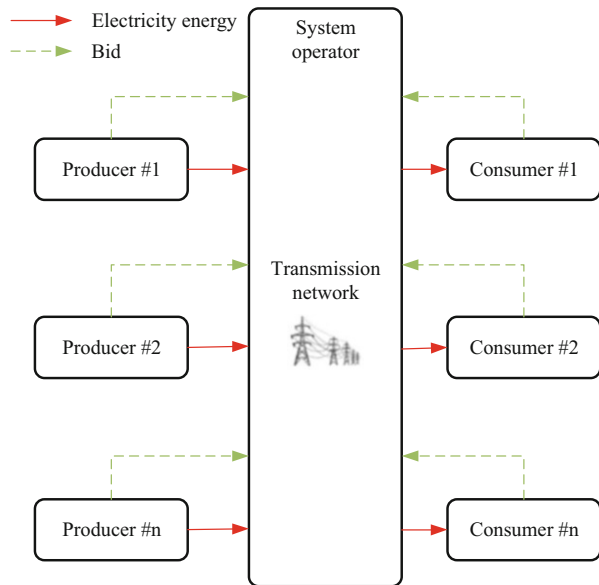
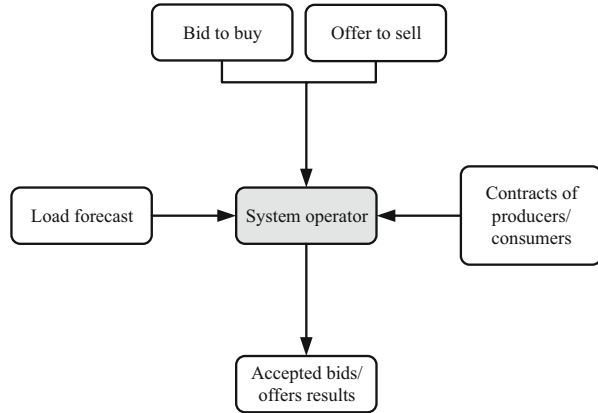


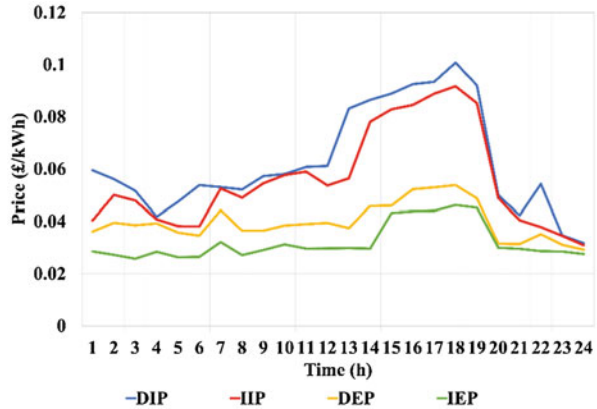
Fig. 4.5 The system operator in the imbalance market



The imbalance market allows all actors to submit their offers for selling the energy to the system (which is shown in Fig. 4.4 in green) and bids to purchase energy from the system (which is shown in Fig. 4.4 in green), with the prices that the actors choose. According to the actor's contracts and power system load forecasting, the system operator agrees to bid/offer in such a way to balance electricity on the transmission system. The accepted bids/offers of actors are reported on balancing mechanism reporting services (e.g., in the UK, Elexon reports the bids/offers [19]). The red lines in Fig. 4.3 show the path of electricity flow if the system operator accepts the bid/offer of that actor. It is noteworthy that only actors that have a shortage/surplus in their production/consumption participate in this market. The system operator chooses these bids/offers based on the announced prices so that the energy of the entire system is balanced [1]. The system operator uses this market as a tool to balance the production with consumption and minimize the system stress caused by imbalance after the gate closure [20]. The input and output data of the system operator in this market are shown in Fig. 4.5.

Therefore, the system operator can ensure the stability of the power system. In the first stage, for each imbalance market participant (IMP), the value of its contract is compared to its metered volume to determine its imbalance. Then, each of the IMPs has to buy or sell energy to cover their imbalance. Energy is purchased/sold at the system purchase/sale price. These prices are set based on the main pricing method or reserve pricing method. The main pricing method reflects the cost of balancing the system (i.e., the cost of bids/offers accepted in the imbalance market and adjustments made for the imbalance market). The reserve pricing method reflects the market price of electricity for that time step. If the system is short of generation (generation < consumption), system buy price is calculated according to the main pricing method and system sell price is calculated based on the reserve pricing method. But if the system is long (generation > consumption), the system sell price is calculated based on the main pricing method and system buy price is calculated according to the reserve pricing method. As a result, the actors who have participated in the

Fig. 4.6 The day-ahead and imbalance market prices, on a weekday winter day, for 2014 [1]



imbalance market will pay the increments. Also, those who have helped to increase the balance of the system will not be penalized.

Each bid/offer is accompanied by an offer/bid, respectively, to ensure that each of the accepted bids/offers can be canceled if required. The system operator prefers more time between gate closure and delivering energy to have more opportunities for balance calculations. In contrast, the producers and consumers prefer the gate closure to be closer to energy delivery to reduce their pricing risk in the imbalance market [2]. The bids/offers can be accepted at any time between the gate closure and the end of the time step. In addition to using for energy balancing directly, the imbalance market can be used for other reasons as follows:

1. Ensuring the capacity of actors to provide operating reserve or negative reserve
2. Frequency reserve provision to set the frequency in the standard range
3. Short-term operating reserve provision (fast reserve) to reduce rapidly the stresses caused by imbalances

The most bids/offers accepted in the imbalance market can be implemented in 2 min or less [12]. The bids/offers presented by participated actors in this market create an average marginal imbalance market bid and average marginal imbalance market offer, which determines the buy/sell energy price in the imbalance market at each time step of day. The average buy/sell energy price of this market alongside the day-ahead market price is shown for a weekday winter day in Fig. 4.6 (extracted from Elexon and *Office of Gas and Electricity Markets* (Ofgem) in the UK [19, 21]).

The day-ahead import price, day-ahead export price, imbalance import price, as well as imbalance export price are shown by DIP, DEP, IIP, and IEP in Fig. 4.6, respectively. As can be seen, there is a peak in prices in the evening (17:00–20:00). As a result, the MCEN shifts the energy consumption to the off-peak hours (02:00–06:00) to increase its revenue using energy storage systems. Given that the imbalance market price is not known before the time of energy delivery, in the presentation of system power management algorithms, the price of previous years that show the general pattern of price is used. Then, due to a large number of

samples, using the scenario reduction algorithms [22], the desired number of samples is obtained. Another way to consider the price of this market is to use probabilistic models to predict the price [1]. MCENs are also forced to participate in these markets in the event of equipment failure or overproduction. As a result, the MCENO should try to determine a more appropriate bid/offer according to the conditions of the system.

In this market, the bid value is usually lower than the marginal price and the offer value is higher than the marginal cost [2], according to Eqs. (4.1)–(4.4):

$$A_i^{\text{offer}} = A_i + \alpha \quad \forall i \quad (4.1)$$

$$\alpha \geq 0 \quad (4.2)$$

$$B_i^{\text{bid}} = B_i + \beta \quad \forall i \quad (4.3)$$

$$\beta \geq 0 \quad (4.4)$$

where A_i and A_i^{offer} are the marginal cost and offer of producer i , respectively. Also, B_i is the marginal price of electricity from the point of view of consumer i . The purchase bid of consumer i submitted to the imbalance market is B_i^{bid} . α and β are positive fixed values that are determined by the producer and the consumer, respectively.

As a result, MCENO needs to accurately estimate the load of MCEN consumers. Because if there is an error in the predicted value and the actual value of the load, MCENO is forced to participate in the imbalance market and as a result its income decreases. As mentioned in the previous sections, MCENO needs to make a better purchase/sale price based on market forecasted price, in order to participate more optimally in the imbalance market. When MCENO needs to sell energy in the market, given that power generation with MCEN resources (e.g., CHP) is costly, the value of Pr^{MCEN} , which is the MCEN profit, in Eq. (4.5) must be positive in order for the energy sale to be beneficial:

$$\text{Pr}^{\text{MCEN}} = \rho^{\text{market}} \times P_i - \text{cost}^{\text{MCEN}}(P_i) \quad (4.5)$$

where P_i is the generated power of MCEN in a considered time step. ρ^{market} and $\text{cost}^{\text{MCEN}}(P_i)$ are the market price and cost of MCEN for generating the power P_i , respectively. Deriving from Eq. (4.5) results in Eqs. (4.6) and (4.7):

$$\frac{d \text{Pr}^{\text{MCEN}}}{dP_i} = \rho^{\text{market}} - \frac{d \text{cost}^{\text{MCEN}}(P_i)}{dP_i} = 0 \quad (4.6)$$

$$\frac{d \text{cost}^{\text{MCEN}}(P_i)}{dP_i} = \rho^{\text{market}} \quad (4.7)$$

In other words, the sale price of energy in the market should be equal to the marginal cost of MCEN, which was also obtained in Eqs. (4.1) and (4.2) [2].

Because MCEN has a high storage capacity, as a hybrid participant who is both productive and consumable, MCENO may decide to buy electricity during the hours when the market price is low and store it in its storage facilities. Then, in the hours when the price of energy sales is high, it sells energy back in the market. This increases MCENO revenue. MCENO, of course, must also consider the cost of storing energy in the storage process and make a decision accordingly. In addition, the feeder between the MCEN and the upstream network also has a limited capacity, and the voltage and current constraints within the MCEN create some limitations. Also, storing energy in the storage and then delivering it have a definite efficiency. As a result, Eq. (4.8) must be considered:

$$\begin{aligned} -P_{\text{purchase}} \times \rho^{\text{purchase}} - \text{cost}^{\text{storage}}(P_{\text{purchase}}) + P_{\text{purchase}} \times \eta^{\text{storage}} \times \rho^{\text{sell}} \\ \geq \pi^{\text{threshold}} \end{aligned} \quad (4.8)$$

where P_{purchase} , ρ^{purchase} , $\text{cost}^{\text{storage}}(P_{\text{purchase}})$, η^{storage} , ρ^{sell} , and $\pi^{\text{threshold}}$ are the power purchased from market, purchase price of the market, cost of storing energy in the storage, storage efficiency, sale price of energy to the market, and accepted value between revenue and cost of MCEN, respectively.

4.3 Electricity Ancillary Services

These services are presented to balance the energy (separately from the imbalance market) and solve the other issues. Ancillary services can sometimes be mandatory (e.g., the conditions of connection to the system) and sometimes be commercial (providing the services to increase revenue). The system operator lists commercial ancillary services. The use of ancillary services occurs when one of the following two conditions exists [12]:

1. If the result of service cannot be obtained using the imbalance market (for example, if the response time needs to be faster than what the imbalance market can provide, or if there is a demand for reactive power)
2. When the system operator believes that maintaining energy balance can be more economical through some of the services (such as reserve services to avoid price risk of the imbalance market)

Some of the most ancillary services are described through Sects. 4.3.1–4.3.4 [23].

4.3.1 Black Start

There may be a general or partial shutdown in the transmission system. In these events, it is needed to make sure that there is contingency equipment in the system so

that the power supply can be restored at the appropriate time. The black start is a system recovery service from a shutdown. This service is provided from the power plant, which can start the main blocks of generation on-site without depending on the external generations. During a black start event, the service provider must start up its main generators and energize the parts of the transmission system and the distribution network. It must support a sufficient amount of load to control the unstable system. The generator providing the black start service may be needed to provide the start-up supplies for other plants to develop system recovery. Not all plants need to be able to provide black start service.

4.3.1.1 Technical Requirements

1. Ability to start up the generator (at least one unit of the plant) from the shutdown state without using the external power supplies and be able to energize a part of the system within 2 h
2. Ability to quickly accept loading of demand blocks, in a range of 35–50 MW, as well as control the frequency and voltage levels in a standard range (the standard range of frequency is 47.5–52 Hz) during the block loading process
3. Capability to supply at least three consecutive black starts to be able to eliminate possible tripping during recovery
4. Backup fuel supplies, ideally in the range of 3–7 days
5. Necessary equipment to ensure that all generation units can be turned off to stay in a state of readiness for a subsequent start-up
6. Ability to maintain the high service availability on both the main and auxiliary generating plant (the required availability is 90%)
7. The reactive capability to charge the transmission system and distribution network according to the standard (in the 400 kV or 275 kV, at least 100 Mvar is needed)

4.3.1.2 Participation

Participants can provide other ancillary services, as long as the implementation of additional services has no impact on black start delivery. Each actor can participate in this service with the technical requirements, which is an annual service.

4.3.1.3 Service Payments

1. Availability payment: for being available to provide this service (£/MW/h)
2. Exercise price: an agreed amount paid for this service test (£/MWh)

4.3.2 Enhanced Frequency Response (EFR)

It is a service to provide frequency response in 1 s or less. This service tries to maintain system frequency closer to 50 Hz. An example of a frequency violation curve for July 8, 2012, is shown in Fig. 4.7, which attempts to keep the frequency close to 50 using frequency response services.

1. Low-frequency static: a static service, which is triggered at 49.6 Hz with a minimum power 1 MW and must be able to deliver the entire output within 1 s
2. Dynamic low-high: a dynamic service, which delivers the equivalent volumes of primary, secondary, and high-frequency response

4.3.2.1 Technical Requirements

1. Low-frequency static: The trigger level is 49.6 Hz with full response within 1 s and the duration is 30 min.
2. Dynamic low-high: There must be equal-volume delivery of the primary, secondary, and high response. In addition, this service needs the technical requirements of FFR service.

4.3.2.2 Participation

Having the conditions in technical requirements (Sect. 4.3.2.1), the actor must submit its request to the system operator for providing the service.

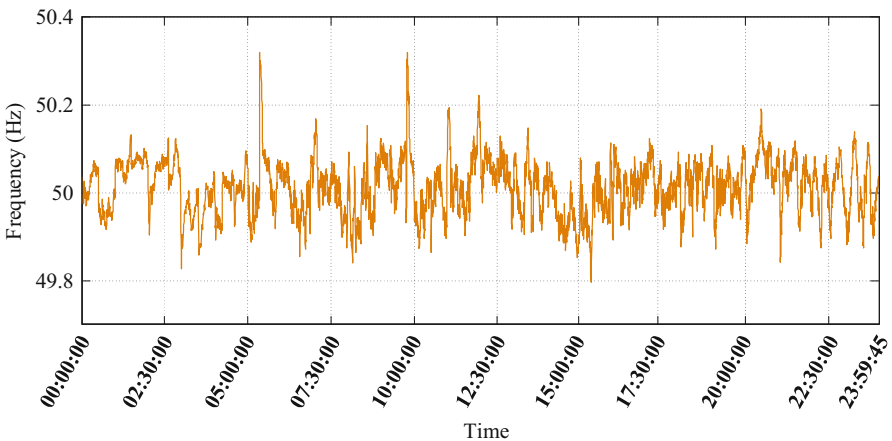


Fig. 4.7 The frequency violation curve on July 8, 2020, in the UK [19]

4.3.2.3 Service Payments

The availability payment is paid monthly. Each unavailability needs to be reported to the system operator.

4.3.3 Enhanced Reactive Power Service (ERPS)

It is a service to provide voltage support, which exceeds the minimum technical requirement. This service is appropriate for generators which can provide or absorb the reactive power. Also, this service can be provided alongside other services. Wherever there is a plant or device that can generate/absorb reactive power, it can provide this service, whether it is a synchronized plant or anywhere else that can generate/absorb reactive power.

4.3.3.1 Technical Requirements

When this service is provided by a generator, as a condition of its application to the transmission system, the ability of reactive power must exceed the minimum technical requirement of obligatory reactive power service (ORPS). The service provision needs to be consistent with the commercial service agreement. The generators are generally instructed to provide a determined Mvar, which must be provided within 2 min. The duration of the contracts is 6 months. To participate in this service, the generator must be accepted in pre-defined tests and then the contract will be concluded.

4.3.3.2 Participation

It is announced via tenders, which is held every 6 months. The actor must then take the predetermined tests.

4.3.3.3 Service Payments

1. Availability price (£/Mvar/h)
2. Synchronized capability price (£/Mvar/h)
3. Utilization price (£/Mvarh)

4.3.4 Fast Reserve

Fast delivery of active power in fast reserve service is implemented by increasing generation and reducing consumption. This service is used to manage frequency violations, which may occur suddenly. Sometimes changes in production or demand are unpredictable. The generators, storages, and aggregated demand-side responses are among those which can provide this service. Moreover, providers can participate in other services at the same time. The fast reserve is required at all hours. However, there is a greater need for it during the daytime (usually between 06:00 and 23:00). The use of these units in this service changes depending on the system conditions, demand profile, and plants. However, providers are utilized for 5 min, ten times a day. Providers are expected to be able to provide a reserve for 15 min.

When providing a service reserve, it should be noted that there are the following constraints for the reserve service provider [2]:

$$\text{Power}_i + \text{Reserve}_i \leq P_i^{\max} \quad \forall i \quad (4.9)$$

$$\text{Power}_i \geq P_i^{\min} \quad \forall i \quad (4.10)$$

$$\text{Reserve}_i \geq R_i^{\min} \quad \forall i \quad (4.11)$$

$$\text{Reserve}_i \leq R_i^{\max} \quad \forall i \quad (4.12)$$

$$R_i^{\max} < P_i^{\max} - P_i^{\min} \quad \forall i \quad (4.13)$$

where Power_i , Reserve_i , P_i^{\min} , and P_i^{\max} are the power, reserve, minimum power, and maximum power of service provider i , respectively. Also, R_i^{\min}/R_i^{\max} indicate the minimum/maximum amount of reserve of service provider i .

4.3.4.1 Technical Requirements

The necessary technical requirements in fast reserve service are as follows:

1. The power delivery must be completed within 2 min from dispatch instruction.
2. The minimum value of the delivery rate must be 25 MW/min.
3. Reserve energy must be available for at least 15 min.
4. Must be able to deliver a minimum of 25 MW.

4.3.4.2 Participation

If the provider meets the conditions declared in technical requirements, it could be accepted in a pre-qualification assessment. The tender of this service is held on a monthly competitive basis and the providers can request for 1 month or multiple months. Then the suppliers participating in the tender are selected based on the fact that they have created a lower cost compared to the others.

4.3.4.3 Service Payments

There are three types of payment fees for this service.

1. Availability price (£/h): It is for hours when a provider makes a fast reserve available.
2. Nomination price (£/h): It is for being called upon to provide the service.
3. Utilization (£/MWh): It is paid for delivered energy.

In addition to the presented services, there are also other services that the actors can provide. The details of the requirements and different prices of these services are explained in [23]. These services include:

1. Firm frequency response (FFR)
2. Short-term operating reserve (STOR)
3. Balancing market start-up
4. Demand-side response
5. Demand turnup
6. Intertrips
7. Mandatory response services
8. Obligatory reactive power service
9. Super SEL
10. System operator to system operator
11. Transmission constraint management

Therefore, the stated ancillary services can be divided into four categories, according to Fig. 4.8, which are reserve provision, power system security, frequency response, and reactive power. MCEN first notifies the system operator of each of the services it wants to provide, along with its offer price, which is indicated in Fig. 4.8 with the phrase MCEN offer price for service provision. By reviewing the requirements of that service for the actor, the system operator allows the actor to participate in the tender of that service if the actor meets those requirements. Actors who provide the equivalent amount of service at the lowest cost are selected. MCEN then provides the service within the period specified in the contract and receives its revenue from the system operator for the service provision specified in Fig. 4.8 with the phrase MCEN revenue from service provision. The operator must manage the MCEN power in such a way that it is able to provide the services contracted in the desired period.

4.4 Other Electricity Markets and Charges

In addition to mentioned markets in Sects. 4.2.4 and 4.2.5, as well as energy-balancing services in Sect. 4.3, there are other markets/services which are designated to improve the MCEN operation and also the entire power system. Notably, some of

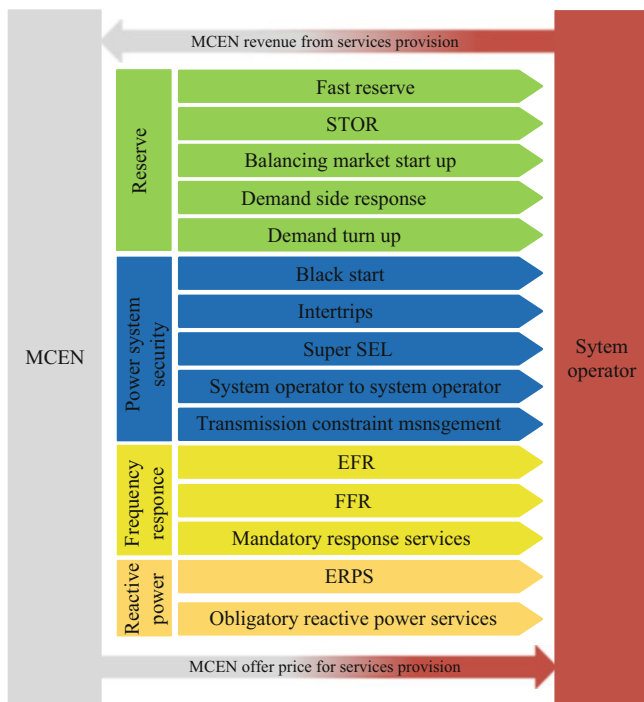


Fig. 4.8 A variety of ancillary services provided by MCEN

these markets will be complete and implemented in the next years. One of these markets/services is the capacity market which is created to ensure generation adequacy. Due to the significant load peak growth (from electric vehicles and electric heat pumps), the other services entitled local balancing services must be designed to limit the imbalances in MCEN power management.

Because the producers and consumers use the transmission system and distribution networks for delivering and receiving the energy, it is needed to pay the USC for the maintenance and expansion of these markets. These usage rates are generally regulated and announced to users each year [1]. For example, in the UK, the contributions of generators and end users to transmission system costs are, respectively, 27% and 73%, while all distribution network costs are supplied by end users [12].

4.4.1 Capacity Market

The capacity market procures the capacity, which is needed to be available when there is a capacity call. The actors who do not provide the required capacity during a call must pay the penalty. The actors with overproduction during a call will be paid

for overproduction (only the providers who announce until the contracts are closed or the providers who respond to requests from the system operator). The payments are implemented through a special framework (such as Elexon in the UK [19]). By introducing a new suitable market for repaying fixed costs, day-ahead market prices are expected to be decreased. All the actors can participate in this market, except for the actors who contract for renewable payment obligations or feed-in tariffs, as well as the power plant with carbon capture and storage technology. The actors in this market are classified as follows [12]:

1. The actors as price takers (existing capacity)
2. The actors as price makers (e.g., demand response and new capacity)

The price makers set the price of capacity. Based on the National Grid Company [23], the contribution of demand response in this market is very low and it is needed to encourage them to increase their contribution. One of these incentives is to consider a lower penalty for failing to deliver energy. The providers of capacity receive an availability fee to be available, as well as a utilization fee [23].

4.4.2 Local Balancing Services

Demand for electricity is continuously growing (especially with the advent of electric heating and electric vehicles) and can create imbalance stress for the power system. As a result, it is necessary to provide these added loads in such a way that special attention is paid to the price. Some of the services can be provided by the distribution network operator (DNO) on nearby feeders to balance the system locally. The value of these services is very much associated with their conditions. It is also related to the price of factors such as network characteristics (e.g., network type), as well as a lack of capacity in the distribution network. The greater the shortage, the lower the value of the service [12]. By solving the problem of lack of capacity locally, this balancing stress, which had caused concern for the system operator in the system, is solved by DNO. One of the major benefits of this service is less loss compared to other types of energy-balance services. DNOs must notify the system operator of their request for this service.

4.4.3 Use of System Charges

As stated, after concluding the contract between the producer and the consumer, both of them need to use the transmission system and distribution network for receiving the energy by consumers. Also, for participating in other markets/services (such as reserve provision), they must use the transmission system and distribution network. As a result, tariffs need to be paid for the use of these two networks, which will be spent on repairing, expanding, and continuing the operation of these two networks

[1]. Typically, there are several types of charges for using the transmission system and distribution network. Distribution network use-of-system (DNUoS) charges, which are paid by consumers, are levied by DNOs. Also, transmission system use-of-system (TSUoS) charges, which are paid by consumers and generators, are received by the system operator. The balancing service use-of-system (BSUoS) charges are received by the system operator. BSUoS is paid by generators and consumers to be used for maintaining the system balance.

4.4.3.1 DNUoS Charges

DNUoS charges are determined by DNO and its amount is variable. Also, it may be different for each type of consumer based on their meter types and connection levels. Here, the consumers are classified into two groups, wherein their payments are separate:

1. Non-half-hourly end users are usually charged a flat rate alongside a fixed charge.
2. Half-hourly end users are usually charged according to a time-varying energy tariff (£/kWh), in addition to a fixed charge (£/day), a capacity charge (£/kVA/day), as well as a reactive power charge (£/kvarh).

The consumers try to reduce DNUoS costs by shifting consumption to times with lower energy charge and decreasing the required energy capacity [12].

4.4.3.2 TSUoS Charges

TSUoS charges are paid by non-half-hourly end users according to their consumption in the period 16:00–19:00. For half-hourly end users, TSUoS charges are calculated based on the end-user average consumption on three specified time steps of the year, which are related to maximum consumption time. As a result, half-hourly end users are trying to reduce the TSUoS costs by minimizing the consumption at these three time steps. These three time steps are also used to reduce the peak of the system and the required investment of generation and transmission system. Therefore, the management of these three time steps can be a service to the system operator. The generators are charged according to transmission entry capacity (TEC) [24].

TSUoS charges vary for consumers in different parts of the country for the following reasons:

1. Differences in operating, maintaining, and expanding costs in various areas
2. Distance between production and consumption

4.4.3.3 BSUoS Charges

BSUoS charges vary by costs of balancing the system and are paid by consumers at each time step. The consumers try to reduce the BSUoS cost by shifting the consumption to the time with lower BSUoS charges. The BSUoS shows the flexibility of generation. BSUoS charges depend on the balancing actions that are taken each day [25].

4.4.4 Tax

Taxes are related to consumption, which need to be considered as a payment by actors. The MCENO commonly considers this payment and another use-of-system charges (Sect. 4.4.3) in the energy purchase price from the market. Therefore, the impact of the tax is investigated in power management and investment issues [1, 5]. The tax rates for domestic and commercial loads are 5% and 20%, respectively.

4.4.5 Environmental and Social Obligations

A set of obligations may be applied to consumers by regulatory bodies, which include the following two categories:

1. Environmental obligations
2. Social obligations

The consumers must pay these obligations to the government. The obligations for domestic loads include the following [12]:

1. Energy company obligation (ECO)
2. Renewable obligation certificates (ROCs)
3. Feed-in tariffs (FiT)
4. Warm home discount (WHD)

There is a climate change levy (CCL) for commercial loads. CCL (£/kWh) is a single-stage nondeductible tax with environmental goals that are a part of the climate change program. CCL is applied to industrial and commercial actors for supplying energy. It is applied to natural gas, coal, and coke, as well as liquefied petroleum gas in addition to electricity. There are three supplies, where the CCL is not fully applied [26]:

1. Excluded (such as domestic loads)
2. Exemption (for example, in some forms of transport, export)

3. Reduced rate (such as a 65% reduction for intensive facilities, which sign the climate change agreement (CCA))

The relationship of CCL with other taxes is detailed in [26]. In addition to CCA, there are other programs such as carbon management, where large commercial consumers have to pay costs according to carbon management program if they do not participate in the CCA [27]. Given that retailers determine end-user payments, environmental and social obligations may be shifted to end-user payments based on retailers' decisions.

The contributions of ECO, ROCs, as well as WHD on energy bills are estimated using a parameter named supply market indicator (SMI), which is explained in [21]. CCL costs are usually publicly available for any type of load. In [28], one of their values is stated.

In MCEN power management, these obligations, like the use-of-system charges (Sect. 4.4.3) and tax (Sect. 4.4.4), can be considered in the energy purchase price from the markets.

4.5 Fuel Markets

In this section, the fuel sales market is addressed to supply the fuel required for MCEN equipment. Since most MCENs use gas as fuel for substitution with electricity, in the next section, we will look at the gas sales market and other related services.

4.5.1 Wholesale Daily Trading

In the gas wholesale market, MCEN purchases gas for uses such as input for equipment (e.g., gas boiler (GB) and CHP) to supply its thermal loads. It should be noted that several special fuels can be used in MCENs, but due to the more use of gas in MCENs, in different types of fuels used, this chapter investigates the gas. Gas price is constant throughout the day due to the presence of gas storage in the network [6]. Because of the presence of gas storage (gas stored in pipes), there is no gas balance issue, unlike the electricity network. Therefore, as the energy balance issue has been raised in electricity networks, several services have been created. However, in gas networks, this issue does not need attention. The balance issue in gas networks is discussed in Sect. 4.5.2. There are two types of markets for wholesale trading of gas:

1. Bilateral contracts in which energy delivery will take place at a determined time in the future.
2. The exchanges which provide an on-the-day market: In the exchanges, the contract is concluded the day before the energy delivery day, which is concluded

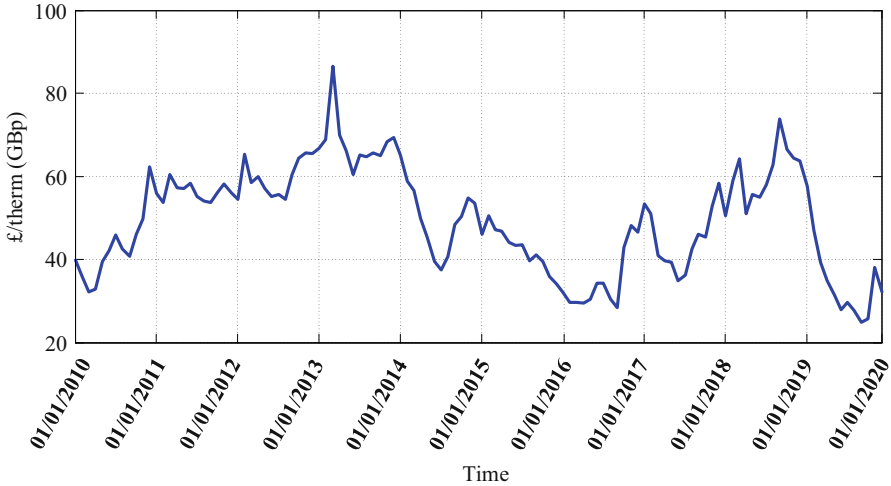


Fig. 4.9 The monthly average price of gas in the UK [29]

for the next day based on the specified and flat price of gas. This model is often used in MCEN power management issue and the gas cost in the next day is calculated according to its fixed and flat price [1, 4, 5].

As mentioned, gas price changes daily. The monthly average price of gas in day-ahead contracts for 2010–2019 is shown in Fig. 4.9.

4.5.2 Imbalance Charges

Imbalance charges are charged if the amount of gas delivered is more or less than the amount of the contract. The system marginal price is used to calculate the imbalance charges. If the actor delivers more gas compared to the contract, it must pay the marginal sell price for this imbalance. But if the actor delivers less gas, it must pay the marginal buy price to the system [12].

As other factors/services are associated with gas imbalance, it is noteworthy that in the gas market, like the electricity market, there is risk management and solutions have been provided for it in [30]. There are also gas storage services sold that allow actors to inject/withdraw gas into/from virtual storage [31].

4.5.3 Use-of-System Charges

In the gas network, there are two networks entitled transmission system and distribution network, which are used to transfer the gas from sellers to consumers. These network charges are detailed in Sects. 4.5.3.1 and 4.5.3.2.

4.5.3.1 Transmission System Charges

Due to the use of the electricity network to transmit electrical power, the system usage charges had to be paid for maintaining, expanding, as well as operating the electricity network (Sect. 4.4.3). Similar to the electricity, the gas transmission system is used to deliver the contracted gas. As a result, the charges set for using the gas transmission system must be paid. The gas transmission system charges include four parts as follows:

1. Commodity charges (£/kWh)
2. Exit capacity (£/kWh/day)
3. Entry capacity (£/kWh/day)
4. Fixed charges (£/day)

Some actors may buy the right to transfer gas using the transmission system, but they may not use it and do not transfer any amount of gas. In these conditions, the entry/exit capacity is applied [12]. Entry capacity gives the daily right for transferring the gas up to the allowed limit. Exit capacity gives the right for absorbing gas from the system up to the considered limit [32]. A more detailed definition, as well as values of these rates, is given in [33]. Gas transmission agents usually purchase the entry/exit capacity. The transmission charges vary according to their location on the system and gas transmission agent, while the commodity charges are usually a flat rate. The fixed charges depend on several factors [34].

4.5.3.2 Distribution Network Charges

Like the distribution network charges mentioned in Sect. 4.4.3, called DNUoS charges, the gas distribution network charges are applied to consumers and vary by the distribution company in each part of the gas distribution network. The components of gas distribution network charges are as follows [12]:

1. System charges (consist of commodity charges and capacity charges)
2. Customer charges (it is a fixed charge that consists of a size-dependent capacity charge)

4.5.4 Tax

Gas consumption, like electricity consumption, adds some tax to costs. This tax is paid by consumers and is important in MCEN power management calculation. The tax rates are 5% and 20% for domestic and commercial gas consumption, respectively [35].

4.5.5 Environmental and Social Obligations

In gas consumption, environmental and social obligations only include ECO and WHD. The commercial gas consumption must also pay the CCL costs. They can reduce these costs by participating in CCA. As a result, the considered rules for climate change levy are almost the same for both electricity and gas networks. As stated in Sect. 4.4.5 for the electricity network, in the gas networks, SMI can also be used to estimate the ECO and WHD impacts on energy bills [33].

4.6 Other Markets/Incentives

In addition to the electricity and gas markets which the MCENO communicates with to meet the needs of its consumers, some other markets/services are set up by regulatory bodies to control the actors' performance and help reduce environmental pollution. They can also be used to implement policies such as reducing the need for new investment. These markets/services are explained through Sects. 4.6.1–4.6.4.

4.6.1 CO₂ Emissions Market

Some generators, such as thermal power plants, produce more CO₂ than renewable sources such as PV and WT. CO₂ emissions market by setting appropriate prices for CO₂ encourages producers to supply energy in ways that bring less CO₂ into the atmosphere. The mechanism of the application of this market for generators is clear. But for demand-side resources (e.g., demand response or small resources such as GB and CHP), the use of this market needs further investigations. It should be noted that CO₂ prices usually affect the offers of generators. One of the impacts of CO₂ prices is a change in the amount of demand response or substitution of equipment/energy vectors. Because by applying these prices, the cost of operation of each type of generator has changed. These prices should be adjusted in general so that the cost of low-carbon resources is lower than that of other generators such as gas power plants. Reducing CO₂ emissions can be achieved by using any of the following [36]:

1. Power sector
2. Buildings
3. Industry
4. Transportation
5. Agriculture
6. Waste and F-gases

The contribution of each of these to CO₂ emissions in 2013 is shown in Fig. 4.10.

Fig. 4.10 The CO₂ emissions by each of its sources [36]

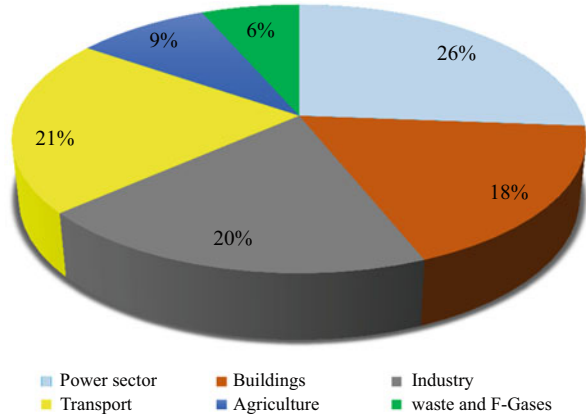


Table 4.2 CO₂ prices in the UK [36]

Year	CO ₂ price (€/t CO ₂)
2008	21.12
2009	7.59
2010	12.54
2011	14.39
2012	8.09
2013	5.17
2014	5.02

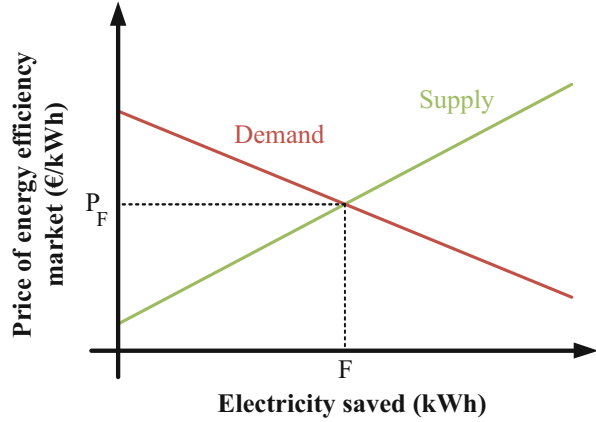
Figure 4.10 shows that the parts related to industry, agriculture, and transportation have the most contribution in CO₂ emissions. Table 4.2 gives CO₂ prices in the UK from 2008 to 2014 in February.

Due to the high penetration of renewable resources in MCEN, its ability to produce low-carbon power is high, which helps to avoid high costs for carbon production.

4.6.2 Energy Efficiency Market

Since the load growth requires the creation of new resources and investment, it is preferable to increase energy efficiency as much as possible first. A similar level of electricity services can be obtained from inefficient energy conversion technologies with higher power consumption or an efficient energy conversion technology with lower power consumption. Therefore, the efficiency of these equipment creates a market entitled energy efficiency market [37]. These markets are still in the design stage and have not been implemented. In addition, these markets can be coupled with other markets, and MCENs are able to participate in them. Also, the energy

Fig. 4.11 The mechanism of energy efficiency market [37]



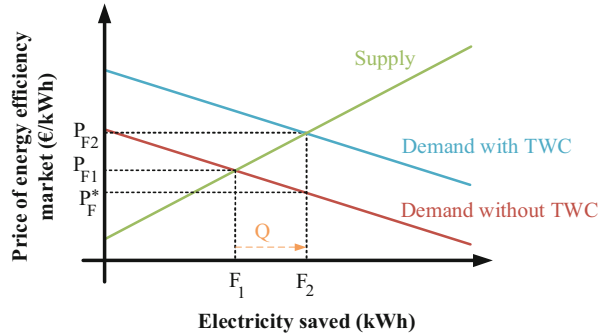
efficiency markets can use price signals to encourage actors to prioritize their energy efficiency. Creating the mechanism of this market can be different in supply and demand sides. On the supply side, it has been suggested that conditions be created for producers with higher energy efficiency to be the main players in the market. But another solution is to enable energy efficiency products and services. On the demand side, it has been suggested that using price signals creates conditions for actors to prioritize energy efficiency or offer new methods for financing energy efficiency [38]. Figure 4.11 shows the mechanism of the type of market that changes the amount of consumption (demand side). In this diagram, each unit on the horizontal axis represents 1 kWh/year that the consumer saves.

The demand curve shows the marginal willingness that the consumer is willing to pay to participate in the market. Also, the supply curve shows the price that energy efficiency producers need to pay to participate in this market. In this case, the cost is based on €/kWh saved and shows the current value of capital, installation, operating, and maintenance cost of energy efficiency market for an additional kWh saved. In this market, consumers purchase a quantity of F_1 from the energy efficiency market at price P_F . There are schemes such as tradable white certificate (TWC) that in the energy efficiency market specify a target in terms of the total saving required in electricity consumption (Q), which is required from the investment in individual electricity saving projects. Using the formulation of this TWC scheme, Q is related to F_2 as in Eq. (4.14), which is shown in Fig. 4.12:

$$F_2 = F_1 + Q \quad (4.14)$$

According to Fig. 4.12, this scheme creates a shift to the right in the demand curve in such a way that there is more demand at a certain price. This is an expected result based on Eq. (4.14). It is noteworthy that the consideration of supply and demand curves can be done in the following two ways [37]:

Fig. 4.12 The effect of a TWC scheme on the energy efficiency market [37]



1. Static baselines which use linear supply and demand curves
2. Dynamic baselines updated based on regulations to consider changes in various factors that affect energy consumption

Reference [37] provides more detailed information on how the TWC is priced, as well as the amount of consumption reduction by the energy efficiency market in different situations.

4.6.3 Feed-In Tariff Rates

Sometimes incentives are paid to produce using specific resources. For example, there are tariffs for electricity generation with renewable sources to produce less carbon. Tariffs are also set to use electricity instead of fuel to generate heat, because electricity is cleaner compared to fuel (Table 4.7). Of course, the goal of incentives is not always to use low-carbon technologies, and other goals (such as the use of small-scale renewables) may be considered. The Ofgem announces the feed-in tariff (FIT) rates that are set by the *Department for Business, Energy and Industrial Strategy* (BEIS) [39]. The FIT rates are shown in Tables 4.3–4.6, from January 1, 2019, to March 31, 2019. Also, Table 4.7 shows the renewable heat incentives (RHIs) for heat generated by EHP, which uses electricity as input. It is observed that the FIT rates are different for each size, which shows the effect of economies of scale.

4.6.4 Diesel Market

The diesel price change is based on the global oil price. Table 4.8 gives the diesel price in European countries, excluding tax and duty, for the three consecutive years 2018, 2019, and 2020, in May. The diesel price increased in 2019 compared to 2018, and in 2020 it has decreased in most countries. For example, in the UK, the diesel price is 35.1 p/l in 2020.

Table 4.3 The FIT rates set for PV [39]

Total capacity of PV (kW)	Tariff (p/kWh)
0–10	3.49
10–50	3.71
50–250	1.55

Table 4.4 The FIT rates set for large PV [39]

Total capacity of PV (kW)	Tariff (p/kWh)
250–1000	1.36
1000–5000	0.15

Table 4.5 The FIT rates set for CHP [39]

Total capacity of CHP (kW)	Tariff (p/kWh)
0–2	14.84

Table 4.6 The FIT rates set for WT [39]

Total capacity of WT (kW)	Tariff (p/kWh)
0–50	8.42
50–100	4.98
100–1500	1.58
1500–5000	0.48

Table 4.7 The renewable heat incentives (RHI) set for EHP [12]

Type of EHP (–)	Incentive (p/kWh)
Domestic (ASHP)	7.3
Domestic (GSHP)	18.8
Commercial (ASHP)	2.5
Commercial (GSHP)	2.6

In addition, the diesel price in the UK over the years has been compared in Fig. 4.13. Figure 4.13 shows that the current price of diesel is almost equal to its average price in previous years. Diesel consumption also includes tax and duty, the amounts of which can be obtained from [28, 35]. MCENOs can supply input fuel for equipment such as diesel generators at these prices.

Table 4.8 European diesel price excluding tax and duty, at mid-May [28]

Country	Year		
	2018	2019	2020
Austria	53.1	54.1	36.1
Belgium	52.4	53.8	32.8
Denmark	61.0	61.5	40.0
Finland	55.8	59.3	42.7
France	52.0	54.0	31.7
Germany	51.9	53.1	36.5
Greece	60.6	62.0	41.3
Ireland	50.6	51.7	36.6
Italy	52.8	54.2	36.1
Luxembourg	54.1	55.4	34.0
Netherlands	55.0	55.4	42.1
Portugal	55.1	55.8	36.9
Spain	55.6	57.0	38.8
Sweden	68.1	67.7	50.2
UK	49.0	54.8	35.1
Bulgaria	50.8	53.5	30.7
Croatia	55.0	58.4	38.0
Cyprus	55.3	56.4	37.0
Czech Republic	50.8	52.8	33.4
Estonia	50.6	54.1	40.9
Hungary	53.9	56.3	37.6
Latvia	50.7	56.0	28.3
Lithuania	53.5	54.4	31.7
Malta	46.6	49.2	54.6
Poland	53.7	54.8	35.4
Romania	55.9	56.2	38.4
Slovakia	54.4	57.2	39.6
Slovenia	48.0	50.3	24.3

4.7 Conclusions

In this chapter, the markets/services where MCENs can participate, as well as the charges they face are presented. It includes three categories of markets/services/charges related to electricity, gas, and other charges/incentives. As mentioned, the MCENO objective is to maximize revenue. As a result, MCENO can maximize its revenue by optimally participating in various energy markets while meeting the energy demand of MCEN consumers and avoiding the constraints. Because MCEN equipment requires electricity and gas to operate, MCENO must purchase energy from these two markets. Also, if the power generation of the MCEN's internal resources increases compared to the amount of load, MCENO will sell the surplus electricity in the market and increase its revenue. Given the probabilities of load and

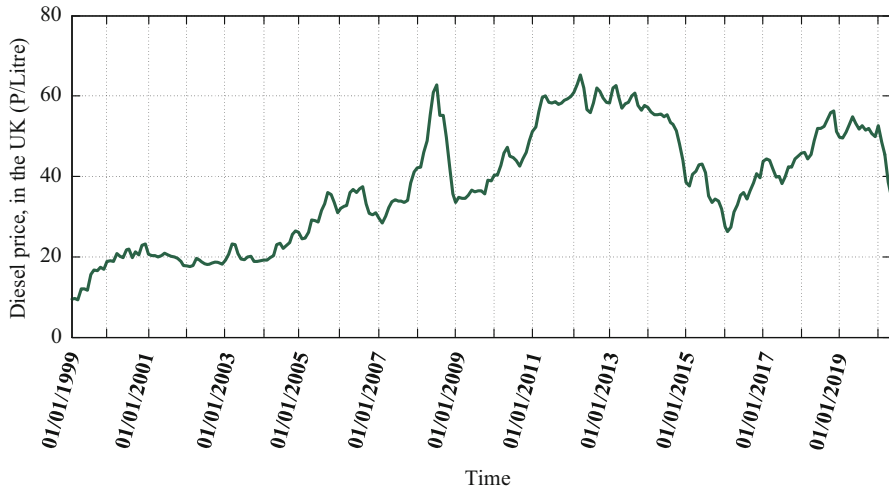


Fig. 4.13 Diesel price in the UK [28]

energy resources of MCEN and the successive variations in the direction of imbalance, MCENO can use the imbalance market. To maintain the security and power quality of the network, the system operator must consider services (e.g., EFR, FFR, fast reserve, STOR, as well as ERPS in Sect. 4.3) to keep the frequency and voltage levels within the standard range. As a result, if the equipment inside the MCEN has the necessary conditions for these services, MCENO can provide these services and increase its revenues. Because MCEN uses the transmission system and distribution network of electricity and gas to purchase/sell energy and provide services, they have to pay USC charges (DNUoS, TSUoS, as well as BSUoS in Sect. 4.4.3). They should also consider the taxes and obligations (Sects. 4.4.4 and 4.4.5) set by regulatory bodies for attending these networks. Due to the importance of reducing environmental pollution, MCENO should consider low-carbon performance (Sects. 4.6.1 and 4.6.3). Also, because of the extensive presence of renewable sources such as PV and WT, it is suitable in MCENs to pay attention to low-carbon performance. It is concluded that MCENO should pay attention to the following steps:

1. Know the technical specifications of MCEN's interior equipment accurately and know how much power and how much of each service MCEN can produce in total at any given time.
2. Predict the electrical and thermal load consumption in MCEN with high accuracy.
3. Decide which services it can participate in depending on MCEN conditions to maximize revenue.
4. Predict market prices.
5. Use the appropriate power management algorithm to determine the optimal purchase/sale value and the appropriate offer prices for energy sales and service delivery.

Therefore, MCENO's revenue is maximized by participating in available markets. It should be noted that USC charges, taxes, and different obligations must be considered by MCENO and as mentioned before they can be considered in the energy purchase price. Due to the instantaneous amount of USC charges, MCEN power management shifts the use of the transmission system and distribution network to the times with lower USC charges. Another result is that due to the nonuniformity of electricity prices during the day and the existence of peak prices in the evening, it is necessary to use energy storage to shift purchasing energy from peak hours to off-peak hours. The most important results of this chapter, which are used by MCEN, can be listed as follows:

1. Maximizing the revenue by selling energy in the market and transferring energy purchase to times with lower prices
2. Using the imbalance market due to the uncertainties of loads and renewable energy resources
3. Performance with low carbon production
4. Providing ancillary services due to the high flexibility of MCENs
5. Transferring system usage time to hours with lower USC charges

References

1. Kazemi-Razi SM (2020) Optimal scheduling of active distribution networks in the context of energy and reserve market. Amirkabir University of Technology (Tehran Polytechnic)
2. Kirschen DS, Strbac G (2018) Fundamentals of power system economics. John Wiley & Sons
3. Shahidehpour M, Yamin H, Li Z (2003) Market operations in electric power systems: forecasting, scheduling, and risk management. John Wiley & Sons
4. Coelho A, Neyestani N, Soares F, Lopes JP (2020) Wind variability mitigation using multi-energy systems. *Int J Electr Power Energy Syst* 118:105755
5. Good N, Mancarella P (2019) Flexibility in multi-energy communities with electrical and thermal storage: a stochastic, robust approach for multi-service demand response. *IEEE Trans Smart Grid* 10:503–513
6. Kazemi-Razi SM, Askarian-Abyaneh H, Nafisi H, Marzband M, Samadian-Zakaria M (2020) Optimization of operation of microgrid by thermal demand response considering enhancement of consumers' thermal comfort. *Iran Electr Ind J Qual Product* 8:68–77
7. Ceseña EAM, Mancarella P (2018) Energy systems integration in smart districts: robust optimisation of multi-energy flows in integrated electricity, heat and gas networks. *IEEE Trans Smart Grid* 10:1122–1131
8. Yazdani-Damavandi M, Neyestani N, Chicco G, Shafie-Khah M, Catalao JPS (2017) Aggregation of Distributed Energy Resources Under the Concept of Multienergy Players in Local Energy Systems. *IEEE Trans. Sustain. Energy* 8:1679–1693
9. Saint-Pierre A, Mancarella P (2016) Active distribution system management: A dual-horizon scheduling framework for DSO/TSO interface under uncertainty. *IEEE Trans. Smart Grid* 8:2186–2197
10. Vayá MG, Andersson G (2015) Self scheduling of plug-in electric vehicle aggregator to provide balancing services for wind power. *IEEE Trans Sustain Energy* 7:886–899
11. Pavić I, Capuder T, Kuzle I (2017) A comprehensive approach for maximizing flexibility benefits of electric vehicles. *IEEE Syst J* 12:2882–2893
12. Good N P (2015) Techno-economic assessment of flexible demand. The University of Manchester (United Kingdom)

13. Chen X, Lv J, McElroy MB, Han X, Nielsen CP, Wen J (2018) Power system capacity expansion under higher penetration of renewables considering flexibility constraints and low carbon policies. *IEEE Trans Power Syst* 33:6240–6253
14. Clegg S, Mancarella P (2015) Integrated electrical and gas network flexibility assessment in low-carbon multi-energy systems. *IEEE Trans Sustain Energy* 7:718–731
15. Nazari-heris M, Jabari F, Mohammadi-ivatloo B, Asadi S, Habibnezhad M (2020) An updated review on multi-carrier energy systems with electricity, gas, and water energy sources. *J Clean Prod*:123136
16. Nazari-Heris M, Mohammadi-Ivatloo B, Asadi S (2020) Optimal operation of multi-carrier energy networks with gas, power, heating, and water energy sources considering different energy storage technologies. *J Energy Storage* 31:101574
17. Mirzaei MA, Nazari-Heris M, Zare K, Mohammadi-Ivatloo B, Marzband M, Asadi S, Anvari-Moghaddam A (2020) Evaluating the impact of multi-carrier energy storage systems in optimal operation of integrated electricity, gas and district heating networks. *Appl Therm Eng*:115413
18. Kazemi-Razi S M, Mirsalim M, Askarian-Abyaneh H, Nafisi H, Marzband M (2018) Maximization of wind energy utilization and flicker propagation mitigation using SC and STATCOM in 2018 Smart Grid Conference (SGC) 1–6
19. Elexon (2020) Bids and offers. <https://www.bmreports.com/bmrs/?q=help/about-us>
20. Elexon (2020) Imbalance market data.. <https://www.bmreports.com/bmrs/?q=balancing/>
21. Ofgem (2020) Ofgem reports.. <https://www.ofgem.gov.uk/electricity>
22. Heitsch H, Römisch W (2003) Scenario reduction algorithms in stochastic programming. *Comput Optim Appl* 24:187–206
23. NationalgridESO (2020) Balancing services.. <https://www.nationalgrideso.com/industry-information/balancing-services>
24. NationalgridESO (2020) Transmission network use of system (TNUoS) charges.. <https://www.nationalgrideso.com/charging/transmission-network-use-system-tnuos-charges>
25. NationalgridESO (2020) Balancing Services Use of System (BSUoS) charges.. <https://www.nationalgrideso.com/charging/balancing-services-use-system-bsuos-charges>
26. HMRC (2020) Climate change levy (CCL).. <https://www.gov.uk/hmrc-internal-manuals/vat-fuel-and-power/vfup5000>
27. DECC (2020) Carbon management in DECC.. <https://www.gov.uk/guidance/making-the-department-of-energy-climate-change-sustainable>
28. DECC (2020) Quarterly energy prices.. <https://www.gov.uk/search/all?keywords=Quarterly+energy+prices&order=relevance>
29. Ofgem (2020) Wholesale market indicators.. <https://www.ofgem.gov.uk/data-portal/wholesale-market-indicators>
30. Endex I (2020) Risk management.. <https://www.theice.com/clearing/risk-management>
31. Endex I (2020) ICE endex auctions & gas storage services.. <https://www.theice.com/endex/auctions>
32. Ofgem (2020) Entry and exit capacity.. <https://www.ofgem.gov.uk/gas/transmission-networks/entry-and-exit-capacity>
33. Networks G (2020) Regulatory affairs overview.. <https://www.gasnetworks.ie/corporate/gas-regulation/gni-regulatory-affairs/>
34. Endex I (2020) Pricing data & analytics.. <https://www.theice.com/market-data/pricing-and-analytics>
35. HMRC (2020) Fuel and power (VAT Notice 701/19).. <https://www.gov.uk/guidance/vat-on-fuel-and-power-notice-70119>
36. Change C on C (2014) Meeting Carbon Budgets—2014 Progress Report to Parliament
37. Sorrell S, Harrison D, Radov D, Klevnas P, Foss A (2009) White certificate schemes: economic analysis and interactions with the EU ETS. *Energy Policy* 37:29–42
38. DECC (2020) Building a market for energy efficiency: call for evidence
39. Ofgem (2020) Feed-In Tariff (FIT) rates.. <https://www.ofgem.gov.uk/environmental-programmes/fit/fit-tariff-rates>

Chapter 5

Optimal Operation of Multi-carrier Energy Networks Considering Demand Response Programs



Mehrdad Setayesh Nazar and Alireza Heidari

5.1 Introduction

The smart energy hub (SEH) concept is widely used in power system literature based on the fact that the smart grid (SG) infrastructure utilizes multi-carrier distributed energy resources (DERs) that are controlled in a decentralized manner [1]. The SEH can generate, store, and convert electrical, heating, and cooling energy and utilizes a different form of energy conversion technologies [2].

The main facilities of SEHs are combined cool, heat, and power (CCHP), boilers, absorption chiller (ACH), compression chiller (CCH), electrical storage system (ESS), cooling energy storage system (CSS), and thermal energy storage system (TSS) [1]. Further, the demand response programs (DRPs), plug-in hybrid electric vehicles (PHEVs), and intermittent electricity generation facilities such as wind turbines (WTs) and photovoltaic arrays (PVAs) can be utilized in a smart distribution system. These energy resources have stochastic behavior and the integration of these resources into the smart distribution system may complicate the operational paradigms [3].

An active multi-carrier energy distribution system (AEDS) may utilize SEH facilities, WT, PVA, and PHEV parking lots as DERs and supply its electrical, heating, and cooling loads through the multi-carrier energy transmission networks.

M. Setayesh Nazar (✉)
Faculty of Electrical Engineering, Shahid Beheshti University, Tehran, Iran
e-mail: m_setayesh@sbu.ac.ir

A. Heidari
School of Electrical Engineering and Telecommunication, University of New South Wales,
Sydney, NSW, Australia
e-mail: Alireza.heidari@unsw.edu.au

The optimal day-ahead operational planning (ODAOP) consists of the commitment of distributed energy resource facilities considering uncertainties of variables, security criteria, economic evaluations, and environmental aspects.

The ODAOP problem has been explored over recent years and multiple types of research were carried out to assess different aspects of this complicated problem.

Reference [1] introduced a two-level optimization framework for DA scheduling of distribution system that transacted electricity with energy hubs. The energy hubs proposed their contribution bids and the distribution system explored the optimality of submitted bids. The algorithm adopted linear optimization process and the 33-bus IEEE test system was utilized to assess the method. The operational costs of the system were reduced by 82% with respect to the base case. Reference [2] introduced an energy flow model to determine the capacity of energy-generating units. The TSS and CSS were modeled and the environmental, energetic, and economic variables were presented in the formulation. The particle swarm optimization (PSO) algorithm was utilized and the cost of system, environmental emission, and energy consumption were reduced by 11.2%, 25.9%, and 12.2%, respectively. Reference [3] proposed the optimal scheduling of energy centers, gas network, and electric system. Emission, voltage deviations, energy loss, operation costs, and pressure deviation of natural gas were considered and the analytic hierarchy process was utilized. The proposed method reduced the operating costs and energy consumptions by 21.77% and 39.12%, respectively. Reference [4] introduced the optimal scheduling of intelligent park MicroGrid (MG) in China and the genetic algorithm was utilized to optimize the problem. The proposed method reduced operation costs by 1.68%. Reference [5] proposed a stochastic optimization algorithm for energy hub DA scheduling that utilized conditional value-at-risk method. The risk mitigation method was used and operation cost was reduced by 1.37%. Reference [6] presented an energy hub model for optimal scheduling of DERs and mixed-integer linear programming (MILP) approach was utilized to minimize the operation costs. The results showed that the optimization algorithm reduced the operation costs by about 23%. Reference [7] introduced an iterative two-stage framework for optimization of interactions of the electric distribution system and SEHs. The stochastic optimization process was utilized to model the uncertainties of the wind electricity generations. Reference [8] proposed a mixed-integer nonlinear programming (MINLP) approach to scheduling of CCHP-based systems. The energy and cost-saving ratios were utilized to model the problem and the results compared the conventional systems with the CCHP-based systems. Reference [9] described the integrated model of CCHP-based energy hub wherein the emission pollution and operation costs were minimized. The algorithm successfully reduced emission pollution and operation costs by 2.3% and 4%, respectively. Reference [10] utilized an MINLP algorithm to schedule an energy hub. The efficiencies of electrical system for a cold day and hot day were improved by 59% and 47%, respectively. Further, the efficiencies of the heating load system for a cold day and hot day were improved by 15% and 29%, respectively. Reference [11] introduced an energy consumption model for a decentralized energy system that reduces energy consumption and peak load. The algorithm reduced the emission pollutant by about 46% that utilized DERs for

energy generation. Reference [12] utilized a two-stage framework that carried out the stochastic optimization for scheduling of energy and reserve. The method considered intermittent electricity generation and heating loads. The DRP procedure was utilized to minimize the operation costs and the results showed that the method reduced the system costs by about 15%. Reference [13] explored the effectiveness of DRP alternatives for modifying the heating and electrical loads. The model minimized the procurement costs; meanwhile, it maximized the system's profits. The consumption cost of the multi-carrier energy system was reduced and the peak load of energy carriers was modified. Reference [14] introduced a framework for energy management of multi-energy hubs and the model considered power quality, regulation costs, and voltage deviation variables in the goal programming. Reference [15] presented an algorithm for minimizing operation costs and emission pollution of energy hubs and modeled the PHEVs, DRPs, and ESSs as control variables. The procedure considered the revenue of energy sold to the upward network and the process increased the energy hub revenue by about 105% with respect to the base case. Reference [16] introduced a two-stage optimization algorithm for the DA and RT operation horizons. The optimization process was performed for electrical and thermal systems and results showed that the algorithm successfully reduced the system costs. Reference [17] proposed a multi-objective optimization process that considered the emission pollution, energy consumption, and system costs. The introduced method reduced operation costs by 24%. Reference [18] modeled an energy hub that utilized CCHP facilities and DRP alternatives. The operation costs of the energy hub and distribution system were reduced by 14% and 10%, respectively. Reference [19] introduced the responsive load model applications in a multi-carrier energy system and the procedure modeled different alternatives for responsive loads. The case study was carried out for a home and its costs were reduced by 4%. Reference [20] introduced a six-level optimization algorithm for optimal operation of a distribution system in DA and RT horizons considering risk-averse strategy. The DRP alternatives were utilized by the system. The 123-bus IEEE test system was utilized to assess the proposed method and the results showed that the revenue of the system was increased by 324% risk-averse conditions with respect to the base case. Reference [21] utilized an information-gap decision theory to model the stochastic behavior of the electricity and natural gas networks. The model minimized total costs of operation and encountered the uncertainties of electrical load, wind electricity generation, and gas load demands. Reference [22] presented a hydrogen-based smart micro-energy hub model that considered demand response alternatives and fuel cell-based hydrogen storage systems. The proposed model minimized the DA operational costs using the robust optimization process. Reference [23] introduced a two-stage unit commitment process for optimal operation of gas and electricity networks considering DRPs. The optimization procedure utilized ϵ -constraint technique to find the best solutions. Reference [24] proposed a two-stage stochastic network-constrained unit commitment for coordinated power and gas networks considering air energy storage and wind turbines. The effect of the participation of gas-fueled power plant in the energy and reserve markets has been investigated. Reference [25] introduced a value-at-risk-based stochastic model to

determine the optimal DA scheduling of energy hubs. The model considered the power-to-gas storage and compressed air energy storage systems. The model utilized the load shifting procedure for multiple electrical loads and reduced the operational costs by 4.5%.

The described references do not consider the locational marginal price (LMP) optimization on their operational scheduling optimization. Further, the introduced algorithm simultaneously optimizes DA and RT energy transactions in different multi-carrier energy resources.

5.2 Problem Modeling and Formulation

The AEDS operator (AEDSO) transacts energy with the upward electricity market and supplies the electrical, heating, and cooling load of downward customers. The AEDSO can sell active and reactive power to the upward electricity market. Further, it can transact electricity with PHEV parking lots. As shown in Fig. 5.1, the AEDS is equipped with the CCHPs, PVAs, SWTs, gas-fueled distributed generation (DGs),

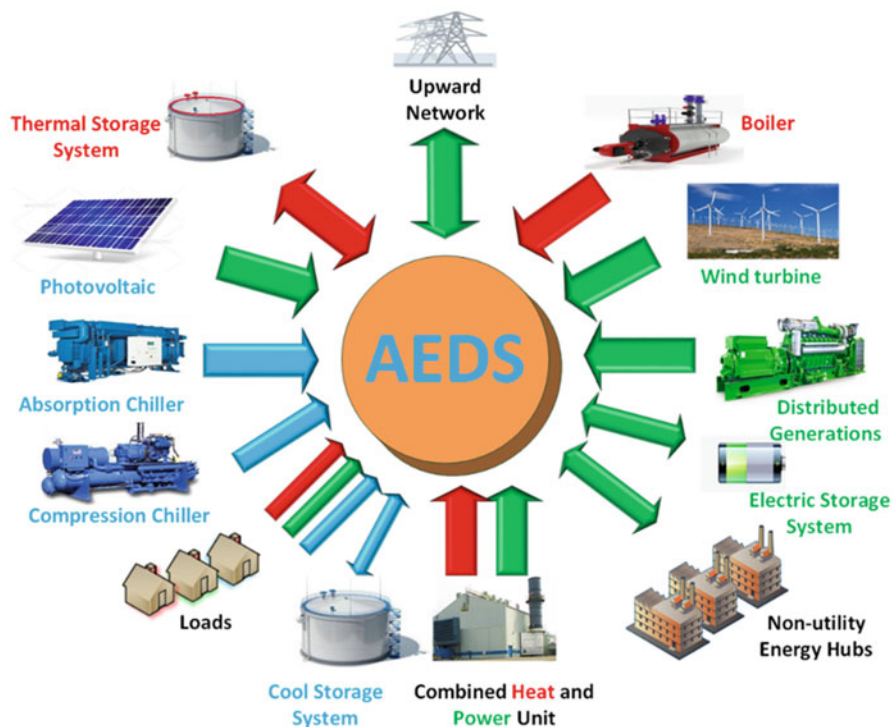


Fig. 5.1 The schematic diagram of AEDS energy interactions

TSSs, CSSs, and ESSs. The customers may have different energy generation, storage, and conversion facilities that can be modeled as energy hubs [26–28].

The AEDSO utilizes the DRP alternatives that consist of direct load control (DLC), time of use (TOU), and involuntary load shedding (ILS) alternatives and it schedules the distributed energy resources to maximize its revenues. The energy hub of customer that is named as the nonutility energy hub (NUEH) can sell its surplus active and reactive electrical energy to the upward system and participate in DRPs in DA and RT markets.

The optimization process of AEDSO has two-time horizons: DA market and RT market. Thus, the objective functions of ODAOP can be decomposed into DA and RT market horizons.

For the DA horizon, the AEDSO should optimize the scheduling of its distributed energy resources in DA horizon considering the uncertainties. The uncertainties of the problem in DA horizon are upward electricity market price, multi-carrier energy demands, intermittent DERs, PHEV contribution scenarios, and NUEH commitment strategies.

The AEDSO distributed energy resources are CCHPs, TSSs, CSSs, intermittent power generations (IPGs), and ESSs. Further, the PHEVs, NUEHs, and DRPs can be utilized as energy resources.

Thus, the objective function of optimal scheduling of system resource problem for the DA horizon can be proposed as Eq. (5.1):

$$\text{Min } \mathcal{A} = \sum_{\text{NWMS}} \text{prob.} \left(\begin{array}{l} W_1 (C_{\text{AEDSO}}^{\text{DA}} \cdot \psi_{\text{AEDSO}}^{\text{DA}} + \sum_{\text{NPHEVS}} \text{prob.} \cdot C_{\text{PHEV}}^{\text{DA}} \cdot \psi_{\text{PHEV}}^{\text{DA}}) \\ + C_{\text{Purchase}}^{\text{DA}} + \sum_{\text{NDRPS}} \text{prob.} \cdot C_{\text{DRP}}^{\text{DA}} + \\ \sum_{\text{NIPGS}} \text{prob.} \cdot C_{\text{IPG}}^{\text{DA}} + \sum_{\text{NNUEHS}} \text{prob.} \cdot C_{\text{NUEH}}^{\text{DA}} \\ - \text{revenue}^{\text{DA}}) + W_2 (\sum \text{LMP}) \end{array} \right) \quad (5.1)$$

The objective function is decomposed into eight groups: (1) the commitment costs of DERs that consist of CCHPs, PVAs, SWTs, gas-fueled DGs, TSSs, CSSs, and ESSs; (2) the energy purchased from the PHEVs costs; (3) the energy purchased from wholesale market costs; (4) the DRP costs; (5) the IPG costs; (6) the energy purchased from NUEH costs; (7) the revenue of AEDSO; and (8) the sum of LMPs.

The AEDSO can sell active, reactive, and spinning reserve to the upward wholesale market. Thus, the revenue of AEDSO can be written as Eq. (5.2):

$$\text{revenue}^{\text{DA}} = \sum_{\text{NWMS}} \text{prob.} \left(\sum \alpha_{\text{active}}^{\text{DA}} \cdot P_{\text{active}}^{\text{DA_upward}} + \sum \beta_{\text{active}}^{\text{DA}} \cdot Q_{\text{active}}^{\text{DA_upward}} \right. \\ \left. + \sum \gamma_{\text{spinning}}^{\text{DA}} \cdot R_{\text{spinning}}^{\text{DA_upward}} \right) \quad (5.2)$$

The revenue of AEDSO consists of three terms: (1) the revenue of active energy, (2) the revenue of reactive energy, and (3) the revenue of spinning reserve.

Equation (5.1) has the following groups of constraints of which some are not presented due to the lack of space:

1. The maximum discharge and charge constraints of ESS, TSS, and CSS [29].
2. The maximum discharge and charge constraints of PHEVs [1].
3. The energy storage facilities cannot discharge and charge at the same time constraints [29].
4. The DRP constraints [1].
5. The AEDS device loading constraints, electrical load flow constraints, and mass balance equations.

For the RT horizon, the AEDSO should minimize the deviations of its scheduling from the optimal values of DA horizon. Thus, the objective function of optimal scheduling of system resource problem for the RT horizon can be proposed as Eq. (5.3):

$$\text{Min } \mathfrak{M} = W_1(\Delta C_{\text{AEDSO}}^{\text{RT}} + \Delta C_{\text{PHEV}}^{\text{RT}} + \Delta C_{\text{Purchase}}^{\text{RT}} + \Delta C_{\text{DRP}}^{\text{RT}} + \Delta C_{\text{IPG}}^{\text{RT}} + \Delta C_{\text{NUEH}}^{\text{RT}} - \Delta \text{revenue}^{\text{RT}}) + W_1\left(\sum \text{LMP}\right) \quad (5.3)$$

The objective function is decomposed into eight groups: (1) the mismatch values of commitment costs of DERs; (2) the mismatch values of energy purchased from the PHEV costs; (3) the mismatch values of energy purchased from wholesale market costs; (4) the mismatch values of DRP costs; (5) the mismatch values of IPG costs; (6) the mismatch values of energy purchased from NUEH costs; (7) the mismatch values of revenue of AEDSO; and (8) the sum of LMPs.

The mismatch values of revenue of AEDSO in RT horizon can be written as Eq. (5.4):

$$\Delta \text{revenue}^{\text{RT}} = \left(\sum \alpha_{\text{active}}^{\text{RT}} \cdot \Delta P_{\text{active}}^{\text{RT-upward}} + \sum \beta_{\text{active}}^{\text{RT}} \cdot \Delta Q_{\text{active}}^{\text{RT-upward}} \right) \quad (5.4)$$

The revenue of AEDSO in RT horizon consists of two terms: (1) the mismatch values of revenue of active energy and (2) the mismatch values of revenue of reactive energy.

Equation (5.3) has the same constraints as in Eq. (5.1) in the RT scheduling horizon.

5.3 Solution Algorithm

For the optimization algorithm, the following assumptions are considered:

1. The alternating current (AC) load flow is linearized [1].

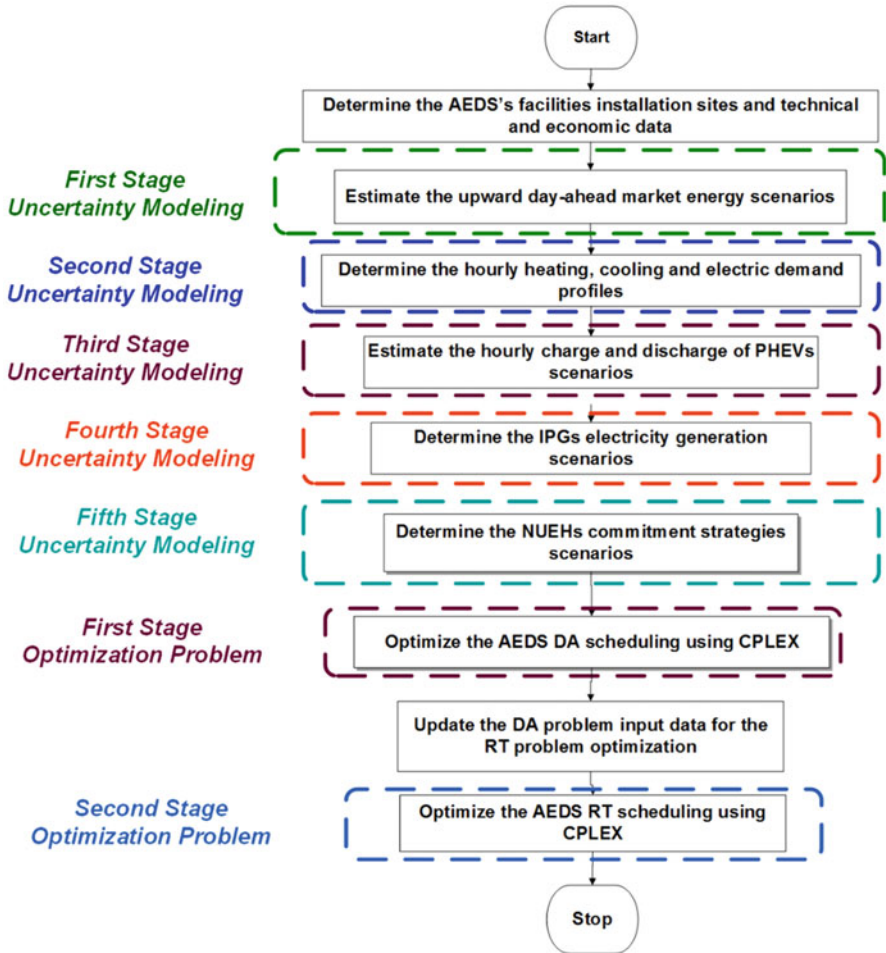


Fig. 5.2 Flowchart of the proposed algorithm

2. Scenario generation and reduction procedures are performed for modeling of uncertainties using the proposed procedure in [1].
3. All of the bids/offers of the distribution system are accepted by the wholesale market operator.
4. The DA load and price forecasting procedures are performed using the introduced method in [30].
5. The LMPs are calculated based on the introduced models of References [31–33].

The linear optimization of the two-staged problem was carried out using the CPLEX solver of GAMS. The flowchart of the algorithm is presented in Fig. 5.2.

5.4 Simulation Results

An industrial district 125-bus test system was used to assess the proposed algorithm. The NUEHs are presented in Fig. 5.3. Tables 5.1 and 5.2 present the optimization input data for the 125-bus system and NUEHs, respectively. The 125-bus industrial district system consists of multiple NUEHs, parking LOTs (PLOTs), CCHs, ACHs, CHPs, DGs, TSSs, CSSs, ESSs, and IPGs.

Figure 5.4 presents the wholesale electricity market price for three reduced scenarios. Figure 5.5 shows the hourly cooling, heating, and electrical load of the NUEHs for one of the reduced scenarios. Figure 5.6 presents the PVA and SWT electricity generation for energy hub for one of the reduced scenarios. Multiple scenario generation and reduction procedures were carried out.

The two-staged optimization procedure was carried out for DA and RT operational horizons. Figure 5.7 presents the estimated stacked column PLOT electricity generation/consumption for DA horizon. The estimated net transacted energy of PLOTs for DA was about 1233.40 kWh and its mean value was about 2.447 kWh. The estimated maximum values of DA PLOTs' charge and discharge were 20.7895 kWh and 11.1845 kWh, respectively. The optimization procedure updated the input data using the described process and the estimated PLOT electricity generation/consumption for RT horizon was determined.

Figure 5.8 shows the estimated stacked column PLOT electricity generation/consumption for RT horizon. The estimated net transacted energy of PLOTs for RT was about 1326.69 kWh and its mean value was about 2.632 kWh. The estimated maximum values of RT PLOTs' charge and discharge were 23.5473 kWh and 10.8208 kWh, respectively.

Figure 5.9 depicts the estimated CCH and ACH cooling energy generation, CSS cooling energy charge and discharge, and cooling energy loss for DA horizon. The aggregated cooling energy generations of CCHs and ACHs in DA horizon were about 81.111 MWh and 23.371 MWh, respectively. Further, the mean values of cooling energy generations of CCHs and ACHs in DA horizon were about 3.379 MWh and 0.973 MWh, respectively.

Figure 5.10 shows the estimated CCH and ACH cooling energy generation, CSS cooling energy charge and discharge, and cooling energy loss for RT horizon. The aggregated cooling energy generations of CCHs and ACHs in RT horizon were about 59.843 MWh and 18.112 MWh, respectively. Further, the mean values of cooling energy generation of CCHs and ACHs in RT horizon were about 2.493 MWh and 0.754 MWh, respectively.

Figure 5.11 presents the estimated stacked column NUEH electricity generation/consumption for DA horizon. The estimated net transacted energy of NUEHs for DA was about 24.229 MWh and its mean value was about 72.11 kWh. The estimated maximum values of DA NUEHs' electricity consumptions/generations were 2357.33 kWh and 2538.12 kWh, respectively.

Figure 5.12 depicts the estimated stacked column of NUEH electricity generation/consumption for RT horizon. The estimated net transacted energy of NUEHs for RT

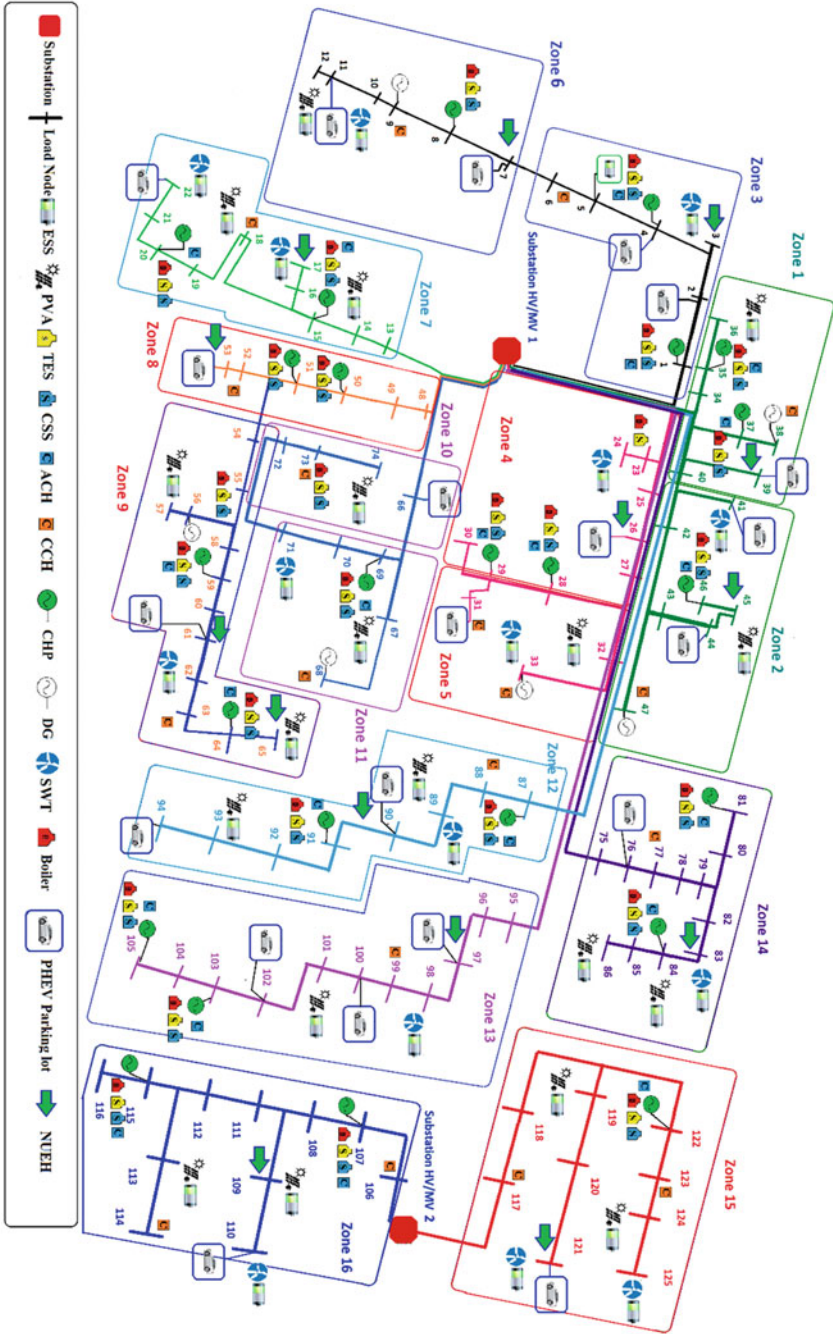


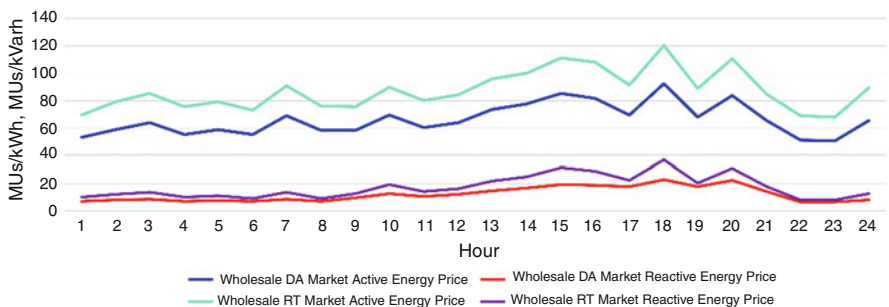
Fig. 5.3 The 125-bus industrial district distribution system

Table 5.1 The optimization input data for the 125-bus system

Distribution system parameters	Value
Number of solar irradiation scenarios	5000
Number of SWT power generation scenarios	5000
Number of upward market price scenarios	150
Number of PHEV contribution scenarios	5000
Number of DRP commitment scenarios	3000
Number of solar irradiation reduced scenarios	20
Number of SWT power generation reduced scenarios	20
Number of upward market price reduced scenarios	3
Number of PHEV contribution reduced scenarios	20
Number of DRP commitment reduced scenarios	20

Table 5.2 The optimization input data for the NUEHs

NUEH parameters	Value
Number of solar irradiation scenarios	5000
Number of SWT power generation scenarios	5000
Number of proposed DSO TOU price and DLC fee scenarios	15
Number of PHEV contribution scenarios	1000
Number of solar irradiation reduced scenarios	5
Number of SWT power generation reduced scenarios	5
Number of TOU price and DLC fee reduced scenarios	3
Number of PHEV contribution reduced scenarios	4

**Fig. 5.4** The wholesale electricity market price for three reduced scenarios

was about 20.206 MWh and its mean value was about 60.13 kWh. The estimated maximum values of RT NUEHs' electricity consumptions/generations were 1497.23 kWh and 1381.83 kWh, respectively.

Figure 5.13 shows the estimated NUEH electricity generation/consumption, IPG electricity generation, CHP and DG electricity generation, and import/export of electricity for the DA horizon. The aggregated electricity generation of IPGs and CHPs and DGs were about 117.848 MWh and 123.432 MWh, respectively.

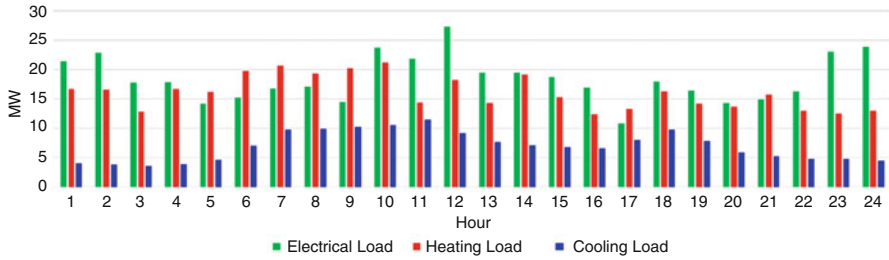


Fig. 5.5 Hourly cooling, heating, and electrical load of the energy hubs

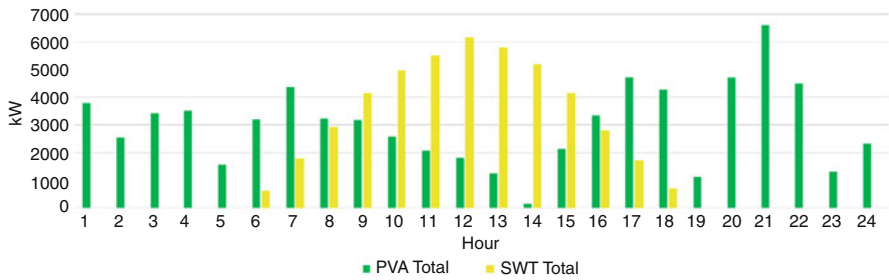


Fig. 5.6 The PVA and SWT electricity generation for energy hub for one of the reduced scenarios

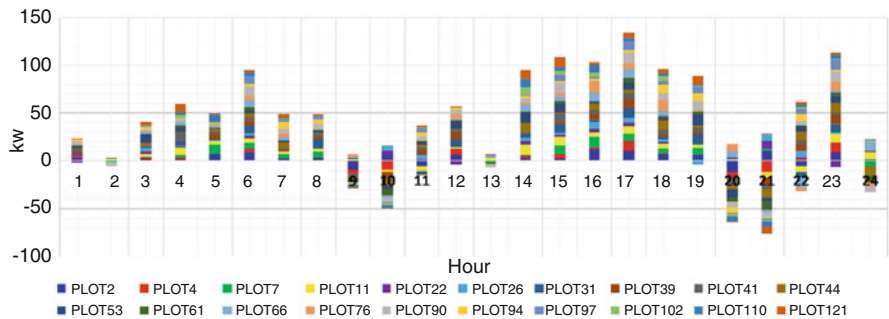


Fig. 5.7 The stacked column of PLOT electricity generation/consumption for DA horizon

The net transacted energy of the system with the upward market was about 228.447 MWh for the DA horizon.

Figure 5.14 presents the estimated NUEH electricity generation/consumption, IPG electricity generation, CHP and DG electricity generation, and import/export of electricity for RT horizon. The aggregated electricity generation of IPGs and CHPs and DGs were about 140.132 MWh and 136.187 MWh, respectively.

The net transacted energy of the system with the upward market was about 189.349 MWh for the RT horizon.

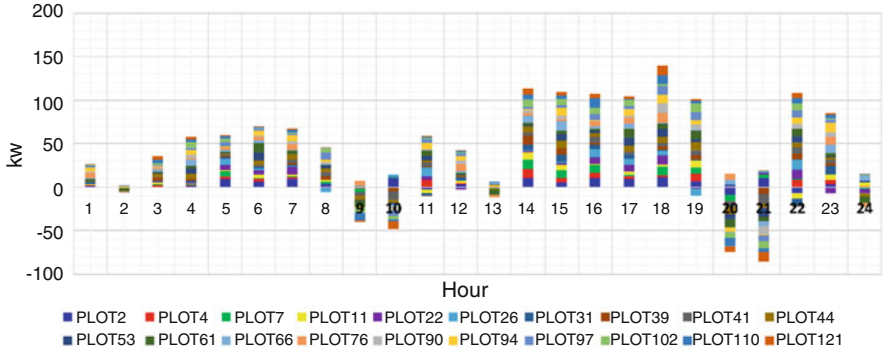


Fig. 5.8 The stacked column of PLOT electricity generation/consumption for RT horizon

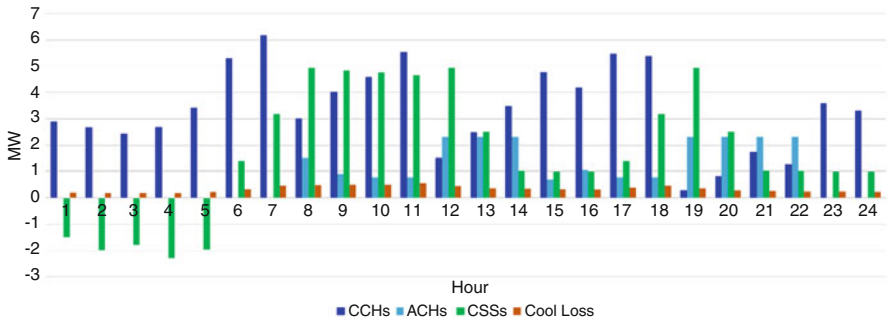


Fig. 5.9 The estimated CCH and ACH cooling energy generation, CSS cooling energy charge and discharge, and cooling energy loss for DA horizon

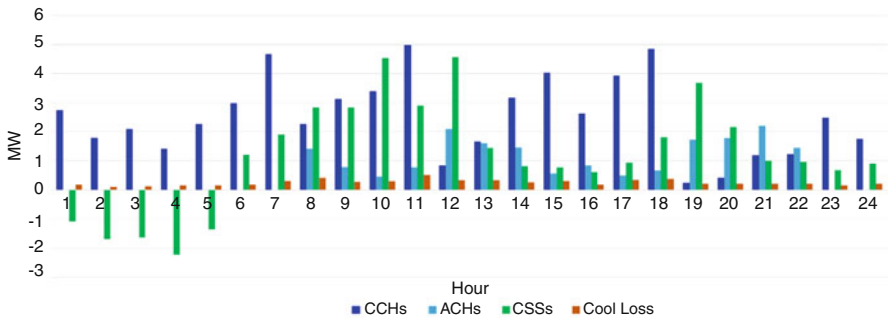


Fig. 5.10 The estimated CCH and ACH cooling energy generation, CSS cooling energy charge and discharge, and cooling energy loss for RT horizon

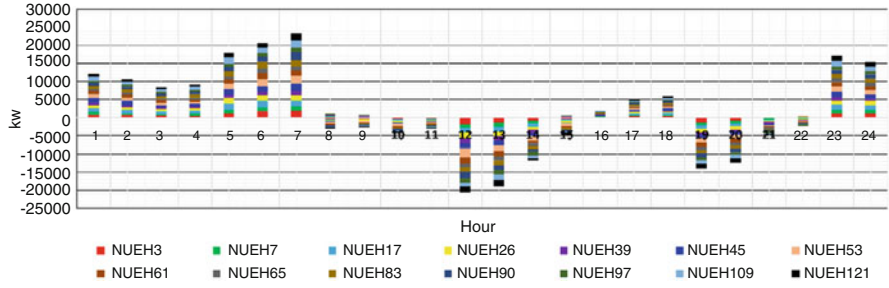


Fig. 5.11 The estimated stacked column of NUEH electricity generation/consumption for DA horizon

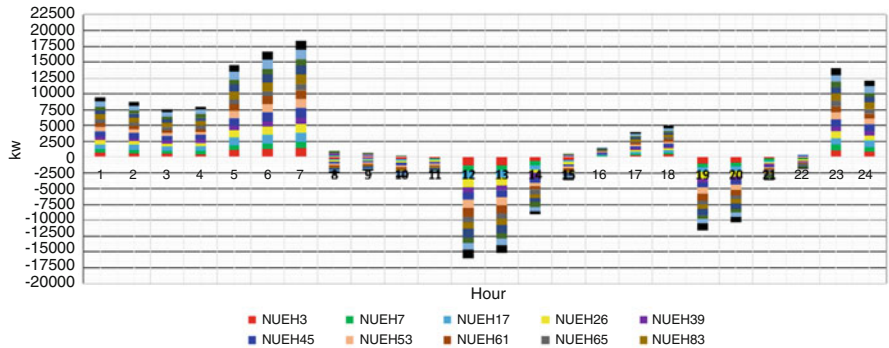


Fig. 5.12 The estimated stacked column of NUEH electricity generation/consumption for RT horizon

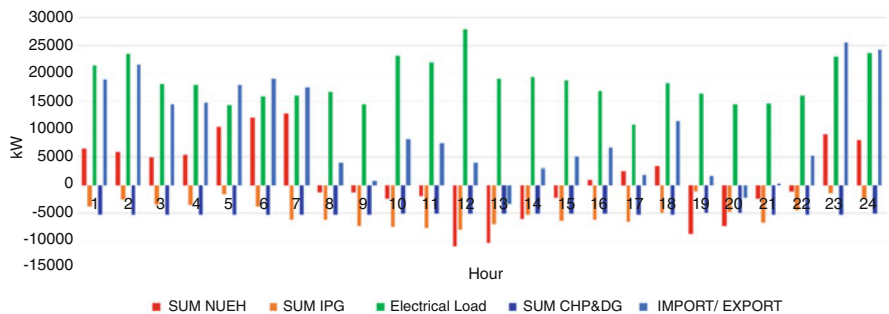


Fig. 5.13 The estimated NUEH electricity generation/consumption, IPG electricity generation, CHP and DG electricity generation, and import/export of electricity for DA horizon

Figure 5.15 depicts the estimated CHP and boiler heating energy generation, TSS heating energy charge and discharge, and heating energy loss for DA horizon.

The aggregated heating energy generation of CHPs and boilers in DA horizon were about 178.358 MWh and 183.102 MWh, respectively. Further, the mean values

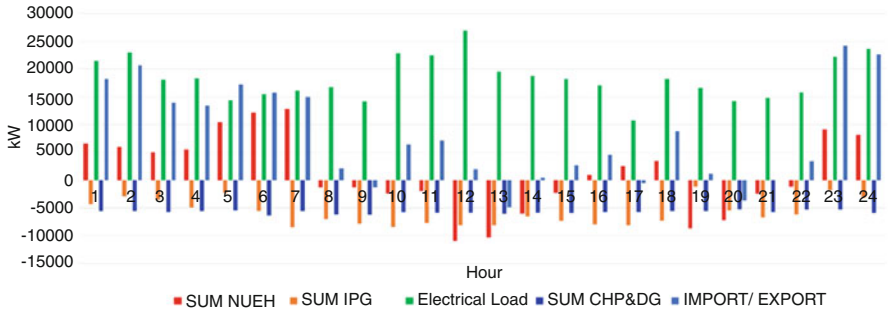


Fig. 5.14 The estimated NUEH electricity generation/consumption, IPG electricity generation, CHP and DG electricity generation, and import/export of electricity for RT horizon

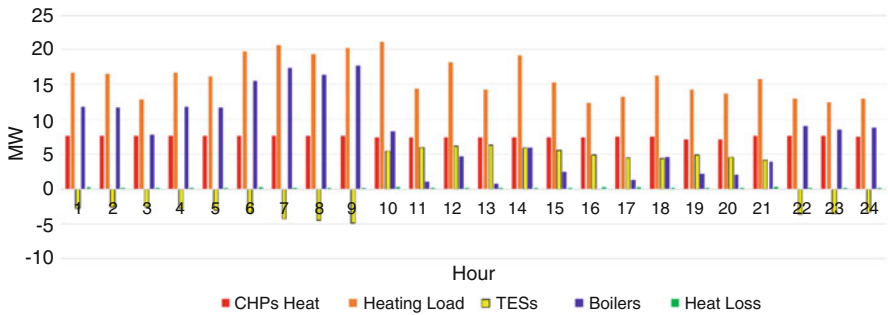


Fig. 5.15 The estimated CHP and boiler heating energy generation, TSS heating energy charge and discharge, and heating energy loss for DA horizon

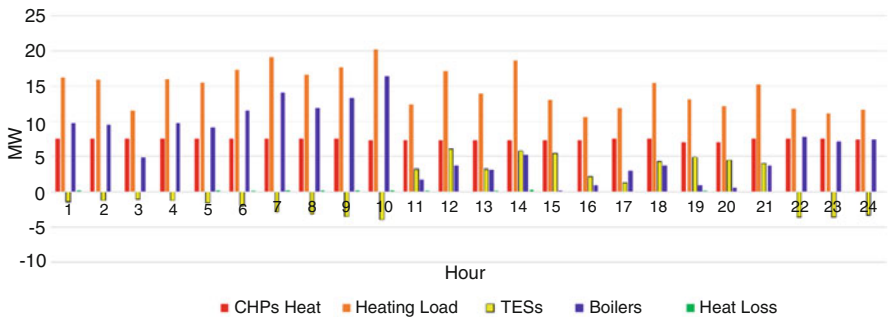


Fig. 5.16 The estimated CHP and boiler heating energy generation, TSS heating energy charge and discharge, and heating energy loss for RT horizon

of heating energy generation of CHPs and boilers in DA horizon were about 7.431 MWh and 7.629 MWh, respectively.

Figure 5.16 shows the estimated CHP and boiler heating energy generation, TSS heating energy charge and discharge, and heating energy loss for RT horizon.

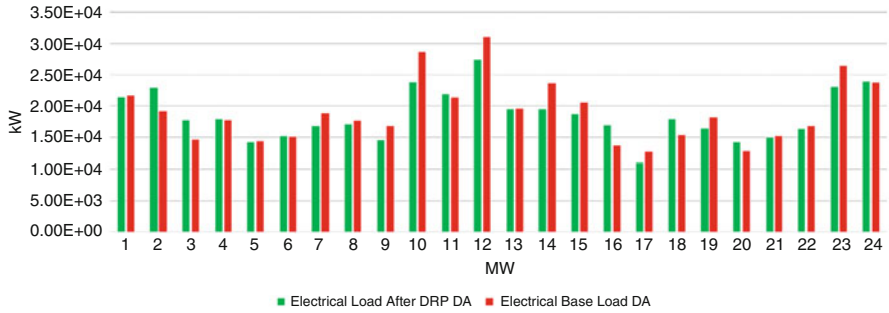


Fig. 5.17 The estimated electrical load after DRP and the base electrical load for DA horizon

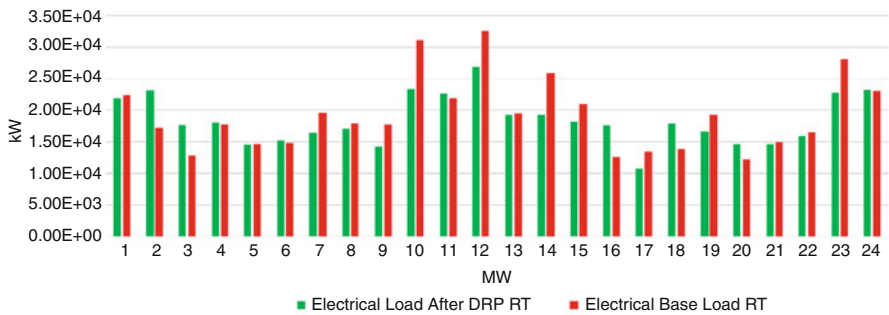


Fig. 5.18 The estimated electrical load after DRP and the base electrical load for RT horizon

The aggregated heating energy generation of CHPs and boilers in RT horizon were about 178.698 MWh and 183.732 MWh, respectively. Further, the mean values of heating energy generation of CHPs and boilers in RT horizon were about 7.659 MWh and 7.425 MWh, respectively.

Figure 5.17 presents the estimated electrical load after DRP and the base electrical load for DA horizon. The aggregated electrical energy consumptions before and after DRP implementation in DA horizon were about 443 MWh and 455 MWh, respectively. Further, the mean values of electrical energy consumptions before and after DRP implementation in DA horizon were about 18.52 MWh and 19.01 MWh, respectively.

Figure 5.18 shows the estimated electrical load after DRP and the base electrical load for RT horizon. The aggregated electrical energy consumptions before and after DRP implementation in RT horizon were about 461 MWh and 442 MWh, respectively. Further, the mean values of electrical energy consumptions before and after DRP implementation in RT horizon were about 19.21 MWh and 18.40 MWh, respectively.

Figure 5.19 depicts the estimated cost/benefit of NUEHs and distribution system for DA horizon. The estimated aggregated revenues of NUEHs for purchasing of active and reactive power to the distribution system in DA horizon were about

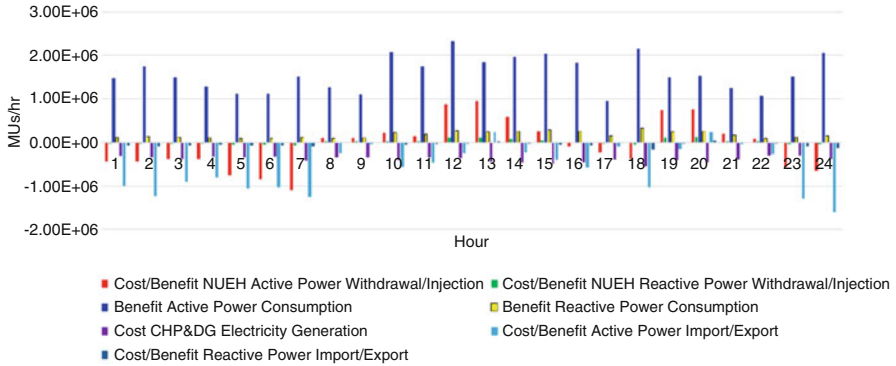


Fig. 5.19 The estimated cost/benefit of NUEHs and distribution system for DA horizon

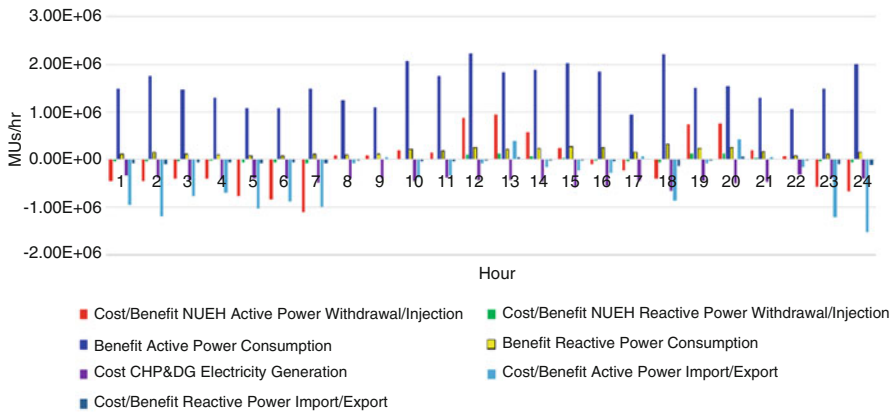


Fig. 5.20 The estimated cost/benefit of NUEHs and distribution system for RT horizon

1.37 MMU and 0.116 MMU, respectively. The aggregated revenues of AEDSO for purchasing of active and reactive power to its customers in DA horizon were about 37.8 MMU and 4.15 MMU, respectively. The aggregated cost of electricity generation of CHPs and DGs was about 9.37 MMUs. Finally, the aggregated costs of active and reactive energy purchased from DA upward market were about 14.1 MMU and 1.28 MMU, respectively.

Figure 5.20 shows the estimated cost/benefit of NUEHs and distribution system for RT horizon. The aggregated revenues of NUEHs for purchasing of active and reactive power to the distribution system in RT horizon were about 1.3664 MMU and 0.11559 MMU, respectively. The aggregated revenues of AEDSO for purchasing of active and reactive power to its customers in RT horizon were about 37.73 MMU and 4.1492 MMU, respectively. The aggregated cost of electricity generation of CHPs and DGs was about 10.29 MMUs. Finally, the aggregated costs of active and reactive energy purchased from RT upward market were about 10.76 MMU and 0.9037 MMU, respectively.

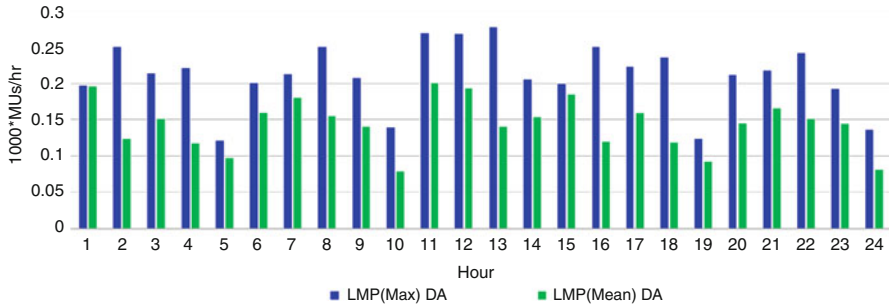


Fig. 5.21 The estimated maximum and mean values of LMPs for DA horizon

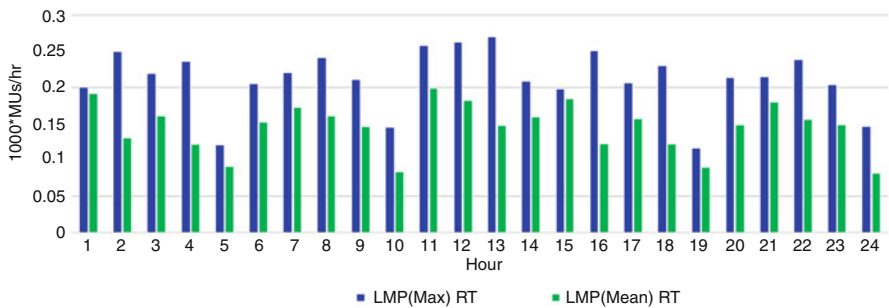


Fig. 5.22 The estimated maximum and mean values of LMPs for RT horizon

Figure 5.21 presents the estimated maximum and mean values of LMPs for DA horizon. The maximum values of LMP_{max} and LMP_{mean} were about 276.8 MU/h and 200.94 MU/h, respectively. Further, the average values of LMP_{max} and LMP_{mean} were about 210.7 MU/h and 143.61 MU/h, respectively

Figure 5.22 shows the estimated maximum and mean values of LMPs for RT horizon. The maximum values of LMP_{max} and LMP_{mean} were about 269.08 MU/h and 198.32 MU/h, respectively. The average values of LMP_{max} and LMP_{mean} were about 210.26 MU/h and 144.71 MU/h, respectively

The proposed algorithm successfully reduced the maximum values of LMP_{max} and LMP_{mean} .

5.5 Conclusion

This chapter presented an optimal operational scheduling algorithm for active distribution system that utilized multiple-energy resources to supply the electrical, cooling, and heating loads. The nonutility energy hubs transacted with the system and participated in the demand response programs. Further, the absorption chillers, compression chillers, boilers, thermal and cooling energy storages, electrical storage

systems, plug-in hybrid vehicle parking lots, and intermittent energy generation facilities were considered in the model and optimization process. The introduced algorithm optimized the multi-carrier energy system operational scheduling in day-ahead and real-time horizons.

The costs of operation and energy purchased from active and reactive upward markets were considered in the optimization process. Further, the locational marginal prices of system buses were formulated in the introduced optimization procedure. The objective functions and constraints were linearized and the CPLEX solver was utilized to optimize the problem.

An industrial district multiple-energy carrier system was used to assess the introduced method. The optimization process was carried out and the operational scheduling of system in day-head and real-time horizons was determined. The optimization algorithm successfully minimized the operational costs and locational marginal prices of the system and encountered the nonutility energy hub contributions in the operational scheduling of multi-carrier energy system. The optimization procedure successfully reduced the locational marginal prices by about 2.78%.

Nomenclature

Abbreviations

AC	Alternating current
AEDS	Active multi-carrier energy distribution system
AEDSO	AEDS operator
ACH	Absorption chiller
CCH	Compression chiller
CCHP	Combined cool, heat, and power
CSS	Cooling energy storage system
DA	Day-ahead
DER	Distributed energy resource
DLC	Direct load control
DRP	Demand response program
ESS	Electrical storage system
ILS	Involuntary load shedding
LMP	Locational marginal price
MG	Microgrid
MILP	Mixed-integer linear programming
MINLP	Mixed-integer nonlinear programming
NUEH	Nonutility energy hub
ODAOP	Optimal day-ahead operational planning
PHEV	Plug-in hybrid electric vehicle
PLOT	Parking LOT
PSO	Particle swarm optimization
PVA	Photovoltaic arrays
SEH	Smart energy hub
SG	Smart grid
TSS	Thermal energy storage system
TOU	Time of use
WT	Wind turbine

Variables

C_{AEDSO}^{DA}	The day-ahead cost of operation of AEDSO
C_{PHEV}^{DA}	The day-ahead cost of operation of PHEV
$C_{Purchase}^{DA}$	The day-ahead cost of electricity purchased from upward market
C_{DRP}^{DA}	The day-ahead cost of DRP
C_{IPG}^{DA}	The day-ahead cost of IPG
C_{NUEH}^{DA}	The day-ahead cost of electricity purchased from NUEHs
ψ	The binary decision variable of resource commitment
revenue ^{DA}	The revenue of active and reactive sold to the DA upward market
Prob	Probability of scenario
W	Weighting factor
α_{active}^{DA}	The price of active energy sold to DA electricity market
β_{active}^{DA}	The price of reactive energy sold to DA electricity market
NWMS	Number of wholesale market price scenarios
ΔC_{AEDSO}^{RT}	The mismatch of real-time cost of operation of AEDSO
ΔC_{PHEV}^{RT}	The mismatch of real-time cost of operation of PHEV
$\Delta C_{Purchase}^{RT}$	The mismatch of real-time cost of electricity purchased from upward market
ΔC_{DRP}^{RT}	The mismatch of real-time cost of DRP
ΔC_{IPG}^{RT}	The mismatch of real-time cost of IPG
ΔC_{NUEH}^{RT}	The mismatch of real-time cost of electricity purchased from NUEHs
$\Delta revenue^{RT}$	The mismatch of revenue of active and reactive sold to the RT upward market

References

1. Bostan A, Setayesh Nazar M, Shafie-khah M, Catalão JPS (2020) Optimal scheduling of distribution systems considering multiple downward energy hubs and demand response programs. *Energy* 190:116349
2. Wang J, Zhai Z, Jing Y, Zhang C (2010) Particle swarm optimization for redundant building cooling heating and power system. *Appl Therm Eng* 87:3668–3679
3. Lin W, Jin X, Mu Y, Jia H, Xub X, Yu X, Zhao B (2018) A two-stage multi-objective scheduling method for integrated community energy system. *Appl Energy* 216:428–441
4. Wang Y, Huang Y, Wang Y, Zeng M, Li F, Wang Y, Zhang Y (2018) Energy management of smart micro-grid with response loads and distributed generation considering demand response. *J Clean Prod* 197:1069–1083
5. Dolatabadi A, Mohammadi-Ivatloo B (2017) Stochastic risk-constrained scheduling of smart energy hub in the presence of wind power and demand response. *Appl Therm Eng* 123:40–49
6. Ma T, Wu J, Hao L (2017) Energy flow modeling and optimal operation analysis of the micro energy grid based on energy hub. *Energy Convers Manag* 133:292–306
7. Davatgaran V, Saniei M, Mortazavi S (2019) Smart distribution system management considering electrical and thermal demand response of energy hubs. *Energy* 169:38–49
8. Wu J, Wang J, Li S (2012) Multi-objective optimal operation strategy study of micro-CCHP system. *Energy* 48:472–483
9. Saberi K, Pashaee-Didani H, Nourollahi R, Zare K, Nojavan S (2019) Optimal performance of CCHP based microgrid considering environmental issue in the presence of real time demand response. *Sustain Cities Soc* 45:596–606
10. Gerami Moghaddam I, Saniei M, Mashhour E (2016) A comprehensive model for self-scheduling an energy hub to supply cooling, heating and electrical demands of a building. *Energy* 94:157–170

11. Orehounig K, Evins R, Dorer V (2015) Integration of decentralized energy systems in neighbourhoods using the energy hub approach. *Appl Energy* 154:277–289
12. Shams M, Shahabi M, Khodayar M (2018) Stochastic day-ahead scheduling of multiple energy carrier microgrids with demand response. *Energy* 155:326–338
13. Sheikhi A, Bahrami S, Ranjbar A (2015) An autonomous demand response program for electricity and natural gas networks in smart energy hubs. *Energy* 89:490–499
14. La Scala M, Vaccaro A, Zobaa A (2014) A goal programming methodology for multiobjective optimization of distributed energy hubs operation. *Appl Therm Eng* 71:658–665
15. Brahman F, Honarmand M, Jadid S (2015) Optimal electrical and thermal energy management of a residential energy hub, integrating demand response and energy storage system. *Energ Buildings* 90:65–75
16. Ramírez-Elizondo LM, Paap GC (2015) Scheduling and control framework for distribution-level systems containing multiple energy carrier systems: theoretical approach and illustrative example. *Int J Electr Power Energy Syst* 66:194–215
17. Fang F, Wang Q, Shi Y (2011) A novel optimal operational strategy for the CCHP system based on two operating modes. *IEEE Trans Power Syst* 27:1032–1041
18. Rastegar M, Fotuhi-Firuzabad M, Lehtonen M (2015) Home load management in a residential energy hub. *Electr Power Syst Res* 119:322–328
19. Maleh M, Akbarimajid A, Valipour K, Dejamkhooy A (2018) Generalized modeling and optimal management of energy hub based electricity, heat and cooling demands. *Energy* 159:669–685
20. Bostan A, Setayesh Nazar M, Shafie-khah M, Catalão JPS (2020) An integrated optimization framework for combined heat and power units, distributed generation and plug-in electric vehicles. *Energy* 202:117789
21. Mirzaei MA, Nazari-Heris M, Mohammadi-Ivatloo B, Zare K, Marzband M, Anvari-Moghaddam A (2020) A novel hybrid framework for co-optimization of power and natural gas networks integrated with emerging technologies. *IEEE Syst J*:1–11
22. Saatloo AM, Agabalaye-Rahvar M, Mirzaei MA, Mohammadi-Ivatloo B, Abapour M, Zare K (2020) Robust scheduling of hydrogen based smart micro energy hub with integrated demand response. *J Clean Prod* 267:122041
23. Nazari-Heris M, Mirzaei MA, Mohammadi-Ivatloo B, Marzband M, Asadi S (2020) Economic-environmental effect of power to gas technology in coupled electricity and gas systems with price-responsive shiftable loads. *J Clean Prod* 244:118769
24. Mirzaei A, Sadeghi Yazdankhah A, Mohammadi-Ivatloo A, Marzband M, Shafie-khah M, Catalao JPS (2019) Stochastic network-constrained co-optimization of energy and reserve products in renewable energy integrated power and gas networks with energy storage system. *J Clean Prod* 223:747–758
25. Mirzaei MA, Zare Oskouei M, Mohammadi-Ivatloo B, Loni A, Zare, Marzband M, ; Shafiee M (2020) Integrated energy hub system based on power-to-gas and compressed air energy storage technologies in the presence of multiple shiftable load. *IET Gener Transm Distrib*, 14: 2510–2519
26. Nazari-Heris M, Mohammadi-Ivatloo B, Asadi S (2020) Optimal operation of multi-carrier energy networks with gas, power, heating, and water energy sources considering different energy storage technologies. *J Energy Storage* 31:101574
27. Nazari-Heris M, Mohammadi-Ivatloo B, Asadi S (2020) Optimal operation of multi-carrier energy networks considering uncertain parameters and thermal energy storage. *Sustainability* 12:5158
28. Mirzaei MA, Nazari-Heris M, , Mohammadi-Ivatloo B, Zare K, Marzband M, Anvari-Moghaddam (2019) Hourly price-based demand response for optimal scheduling of integrated gas and power networks considering compressed air energy storage. *Demand response applications in smart grid*. Springer: 55–74

29. Varasteh F, Setayesh Nazar M, Heidari A, Shafie-khah M, Catalão JPS (2019) Distributed energy resource and network expansion planning of a CCHP based active microgrid considering demand response programs. *Energy* 172:79–105
30. Setayesh Nazar M, Eslami Fard A, Heidari A, Shafie-khah M, Catalão JPS (2018) Hybrid model using three-stage algorithm for simultaneous load and price forecasting. *Electr Power Syst Res* 165:214–228
31. Salarkheili S, Setayesh Nazar M (2017) Capacity withholding assessment in the presence of integrated generation and transmission maintenance scheduling. *IET Gener Transm Distrib* 11:3903–3911
32. Salarkheili S, Setayesh Nazar M (2016) Capacity withholding analysis in transmission-constrained electricity markets. *IET Gener Transm Distrib* 10:487–495
33. Salarkheili S, Setayesh Nazar M (2015) New indices of capacity withholding in power markets. *Int Trans Electr Energy Syst* 25:180–196

Chapter 6

Optimal Scheduling of Hybrid Energy Storage Technologies in the Multi-carrier Energy Networks



Morteza Zare Oskouei, Hadi Nahani, Behnam Mohammadi-Ivatloo, and Mehdi Abapour

6.1 Introduction

Recently, the use of electricity, natural gas, and district heat networks in the form of multi-carrier energy networks has attracted more attention to deal with some concerns regarding environmental issues [1]. The interdependent energy conversion facilities in multi-carrier energy networks prepare the flexible operation [2] and boost the supply reliability [3] and efficiency of the multiple energy systems [4]. In order for optimum exploitation of interconnected energy networks, the utilization of up-to-date energy storage technologies like power-to-gas (P2G) storage, compressed air energy storage (CAES) unit, and power-to-heat (P2H) storage has grown in worldwide [5]. The energy storage systems play an indispensable role in the sustainable transformation of multiple energy networks by storing and generating environmental energy. However, the decentralized and distributed deployment of energy storage systems into multi-carrier energy networks poses crucial challenges for decision makers to economically and safely use storage technologies. Over recent years, various day-ahead scheduling processes have been introduced to utilize the energy storage technologies in optimal coordination with multi-carrier energy networks.

Authors of ref. [6] have presented an energy management framework for integrated electricity and natural gas networks with respect to the cost-benefit

M. Zare Oskouei (✉) · H. Nahani · M. Abapour
Faculty of Electrical and Computer Engineering, University of Tabriz, Tabriz, Iran
e-mail: morteza_zare@ieee.org; h.nahani@tabrizu.ac.ir; abapour@tabrizu.ac.ir

B. Mohammadi-Ivatloo
Faculty of Electrical and Computer Engineering, University of Tabriz, Tabriz, Iran
Department of Energy Technology, Aalborg University, Aalborg, Denmark
e-mail: bmohammadi@tabrizu.ac.ir

optimization problem. The strategy considered the interactions of the P2G storage for optimal scheduling and improving the performance of the integrated energy systems. The adaptation of coordination between thermal energy storage and natural gas storage to maintain steady energy generation in various layers of energy systems under different dynamic characteristics has been investigated in ref. [7]. In ref. [8], the CAES unit and energy conversion facilities have been simultaneously used in the framework of multi-carrier energy systems to reduce the total operational cost of the integrated system by relying on distributed generation. Authors of [9] have presented a two-stage unit commitment scheduling method that considered electricity and natural gas networks, CAES unit, and different energy centers. Three important indices have been considered to characterize the total operating cost of the integrated energy system, carbon emission, and pressure of pipelines in the gas network. In [10], an efficient energy system has been developed consisting of P2G storage to examine the optimal scheduling of energy systems and achieve optimal exergy and heat recovery. Simulation results showed that the proposed method increased energy efficiency by up to 56%. Authors of ref. [11] have evaluated the performance of the P2G technology to demonstrate its feasibility and applicability for reducing the curtailment of wind. The main goal of this study was to maximize the use of wind farms in the presence of multi-carrier energy networks as well as to minimize undesirable load shedding during contingency situations. Furthermore, authors of ref. [12] have presented a risk-constrained strategy for the CAES unit to participate in the electricity market with regard to the uncertainty of the electricity market price.

In terms of economic analysis of energy storage technologies, several studies have been accomplished to investigate the barriers and facilitators in achieving the intended economic goals [13–15]. Authors of [16] have introduced a developed deterministic strategy to achieve sustainable exploitation of regional integrated energy systems. The principal goal of [16] is to decrease the total operating cost of the regional energy system by optimal scheduling of energy storage systems. The simulation results indicated that the total operating cost of the regional integrated energy system was reduced by 8.45% by using the proposed scheduling strategy. In ref. [17], an optimal coordinated operation scheme of various energy storage systems and conversion facilities has been introduced to reach the overall optimum solution for multi-carrier energy systems. In ref. [18], a comprehensive analysis from the perspective of energy and exergy has been done to determine the key requirements for modeling integrated cooling/heating/power systems in the presence of the CAES unit. The presented strategy was implemented in a large-scale integrated energy system to study the various aspects of the energy management algorithm. Authors of ref. [19] have provided optimal energy management strategy in net-zero energy district systems for interconnected distributed energy storage that have been solved by Pareto-optimal solutions. The main concern of the mentioned study is to cover the various energy demands in a reliable manner as well as minimize the total annualized cost. In ref. [20], the energy flow analysis of the P2G storage has been presented based on the scenario-based stochastic model. The optimal capacity and operation scheduling of P2G storage have been investigated to minimize the operational cost of the multi-carrier energy system.

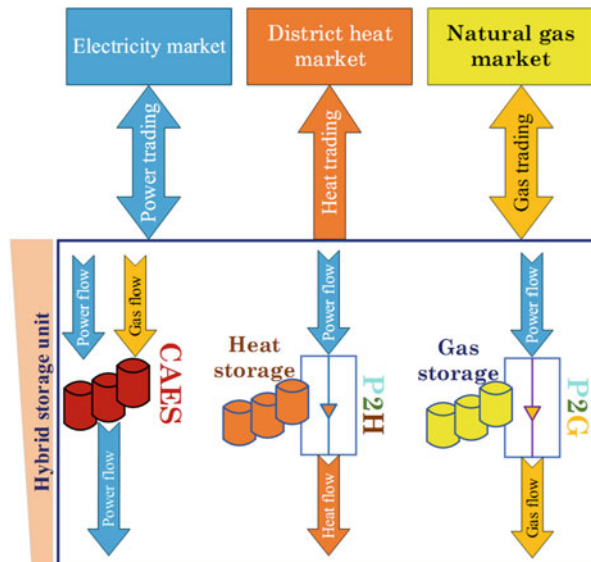
This chapter aims to analyze the economic participation mechanism of a hybrid storage unit in the framework of multi-carrier energy networks using an optimal energy management strategy. The proposed optimization problem is deployed from the perspective of the hybrid energy storage unit owner, and the main goal is to maximize the profit of the hybrid energy storage unit through maximum participation in the various layers of the day-ahead energy markets. In this regard, the hybrid storage unit is composed of three well-known technologies of energy storage systems, including P2G storage, CAES unit, and P2H storage.

The remainder of this chapter can be organized as follows: Section 6.2 presents an explanation of each energy storage technology and mathematical formulation. Illustrative examples and result discussions are presented in Sect. 6.3. Finally, the concluded remarks are in Sect. 6.4.

6.2 Mathematical Formulation and Structure of Hybrid Storage Unit

The technical explanations and mathematical formulation of the optimal offering strategy for the economic participation of the hybrid energy storage unit in the multi-carrier energy networks have been presented in the following subsections. The hybrid energy storage unit for this study consists of three significant components which are P2G storage, CAES unit, and P2H storage. The overview of the hybrid energy storage unit is demonstrated in Fig. 6.1.

Fig. 6.1 Schematic of hybrid storage unit operation



6.2.1 Objective Function

This chapter presents a mechanism for the optimal participation of the hybrid energy storage unit in pool electricity, gas, and district heat markets. It is assumed that the hybrid energy storage unit submits its offers to the various energy markets during the day-ahead market. The profit function for the participation of hybrid energy storage unit in multiple energy markets can be formulated as follows:

$$\begin{aligned} & \max_V : \\ & \sum_{t \in \text{NT}} \left(\lambda_t^e E_t^{\text{DA}} + \lambda_t^g G_t^{\text{DA}} + \lambda_t^h H_t^{\text{DA}} - \sum_{i \in \text{NI}} [\text{VE}(P_{i,t}^D + P_{i,t}^S) + \text{VC}(P_{i,t}^C + P_{i,t}^S)] \right) \end{aligned} \quad (6.1)$$

In (6.1), the profit of the hybrid energy storage unit is maximized with regard to the specified set of decision variable $V = \{E_t^{\text{DA}}, G_t^{\text{DA}}, H_t^{\text{DA}}\}$. The objective function, given in (6.1), is composed of four mathematical expressions. The first three terms represent the revenue obtained or the cost incurred from trading energy with the day-ahead energy markets. The last term demonstrates the variable maintenance and operation costs of the CAES unit in various modes (i.e., charging, discharging, and simple cycle modes). It is worth noting that E_t^{DA} , G_t^{DA} , and H_t^{DA} may take positive or negative value in each time interval. Positive values express the delivered energy to the energy markets and negative values represent the purchased energy from the energy markets.

Equations (6.2)–(6.4) indicate the energy limits of the hybrid unit to guarantee that the various energy storage technologies' offers in the energy markets do not exceed the energy limit of the system:

$$E_t^{\text{DA}} = \sum_{i \in \text{NI}} (P_{i,t}^S + P_{i,t}^D) - \sum_{l \in \text{NL}} \sum_{m \in \text{NM}} \sum_{i \in \text{NI}} (P_{l,t} + P_{m,t} + P_{i,t}^C), \quad \forall t \in \text{NT} \quad (6.2)$$

$$H_t^{\text{DA}} = \sum_{m \in \text{NM}} (\text{HP}_{m,t} + H_{m,t}^D), \quad \forall t \in \text{NT} \quad (6.3)$$

$$G_t^{\text{DA}} = \sum_{l \in \text{NL}} (G_{l,t}^D + \text{GP}_{l,t}) - \sum_{i \in \text{NI}} \text{GI}_{i,t}, \quad \forall t \in \text{NT} \quad (6.4)$$

6.2.2 CAES Unit

In recent years, CAES units have become one of the most widely used electrical energy storage systems. The reason for this widespread acceptance is that the CAES units allow energy system operators to use electricity and gas networks

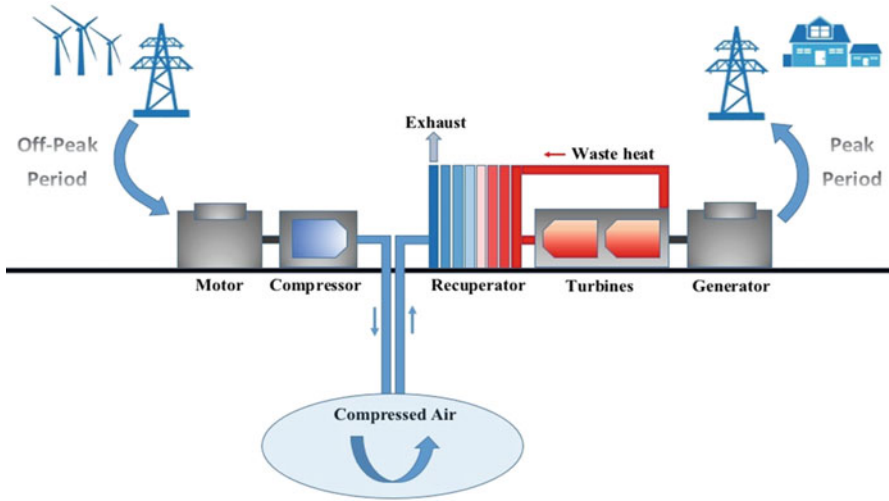


Fig. 6.2 Operation mechanism of the CAES unit

simultaneously. In the context of this storage, the energy system operator can store electrical energy and/or gas energy in the form of high-pressure compressed air in an underground cavern or container as a reservoir during the valley and off-peak periods. On the other hand, the stored compressed air can be converted to electricity by means of an expander as well as a turbine generator during peak demand periods [21]. Figure 6.2 shows the schematic of a CAES unit. According to this figure, the compression and expansion processes are performed in two separate stages to increase the efficiency of the system compared to conventional gas turbine systems. Air reservoirs are divided into two operation modes based on the thermodynamic conditions [22]: (1) sliding-pressure operation with a constant volume such as underground rock caverns, salt caverns, and aquifers and (2) constant-pressure operation such as pumped hydro compressed air storage and underwater pressure vessels. Currently, much research has focused on the advanced adiabatic compressed air energy storage (AA-CAES), liquid air energy storage (LAES), supercritical compressed air energy storage (SC-CAES), and small-scale CAES unit to improve energy efficiency, achieve energy sustainability, and reduce greenhouse gas emissions.

The mathematical model of operation of the CAES unit can be expressed by (6.5)–(6.12). Based on (6.5), the energy level of the CAES unit at time t is a function of the energy levels at time $t - 1$ and the amount of charging or discharging rates at time t . Equation (6.6) guarantees that the performance of the CAES unit's reservoir does not exceed the allowable capacity. Equation (6.7) indicates that the capacity of the CAES reservoir at the initial and final scheduling intervals must be equal. Inequalities (6.8)–(6.10) limit the lower and upper rates of charging, discharging, and simple cycle modes of the CAES unit. According to (6.11) the CAES unit should be utilized in one of the three available modes, i.e., charging, discharging, and

simple cycle. Finally, (6.12) shows the amount of injected natural gas into the CAES unit in simple cycle and discharging modes:

$$A_{i,t} = A_{i,t-1} + \eta_i^C P_{i,t}^C - \frac{P_{i,t}^D}{\eta_i^D}, \quad \forall t \in \text{NT}, i \in \text{NI} \quad (6.5)$$

$$A_i^{\text{Min}} \leq A_{i,t} \leq A_i^{\text{Max}}, \quad \forall t \in \text{NT}, i \in \text{NI} \quad (6.6)$$

$$A_{i,0} = A_{i,\text{NT}}, \quad \forall i \in \text{NI} \quad (6.7)$$

$$P_i^{C,\text{Min}} I_{i,t}^C \leq P_{i,t}^C \leq P_i^{C,\text{Max}} I_{i,t}^C, \quad \forall t \in \text{NT}, i \in \text{NI} \quad (6.8)$$

$$P_i^{D,\text{Min}} I_{i,t}^D \leq P_{i,t}^D \leq P_i^{D,\text{Max}} I_{i,t}^D, \quad \forall t \in \text{NT}, i \in \text{NI} \quad (6.9)$$

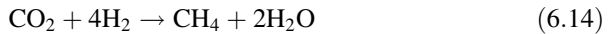
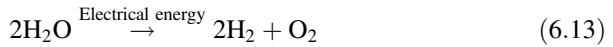
$$P_i^{S,\text{Min}} I_{i,t}^S \leq P_{i,t}^S \leq P_i^{S,\text{Max}} I_{i,t}^S, \quad \forall t \in \text{NT}, i \in \text{NI} \quad (6.10)$$

$$I_{i,t}^C + I_{i,t}^D + I_{i,t}^S \leq 1, \quad \forall t \in \text{NT}, i \in \text{NI} \quad (6.11)$$

$$\text{GI}_{i,t} = \frac{P_{i,t}^D}{\eta_i^D} + \frac{P_{i,t}^S}{\eta_i^S}, \quad \forall t \in \text{NT}, i \in \text{NI} \quad (6.12)$$

6.2.3 P2G Storage

P2G storage is a long-term chemical storage that can convert electrical energy into gaseous energy carriers such as hydrogen, methane, or synthetic natural gas (SNG). In this type of storage, the hydrogen is produced directly via water electrolysis and then it may be converted into methane or synthetic natural gas using a methanation reaction. Alkaline, proton exchange membrane (PEM), and solid oxide electrolysis cell (SOEC) are the most common technologies to perform the process of water electrolysis [23]. The performed chemical reaction in this storage can be described by the following equations:



The produced hydrogen can be used as fuel for hydrogen energy vehicles (mobility) or industrial raw materials. In addition, according to the methanation Eq. (6.14), the existing hydrogen can be reacted with carbon dioxide (CO_2) to produce methane (CH_4). The generated methane can be stored by geological reservoirs, gas cylinders, or natural gas pipelines for further use. The equivalent mathematical model of the P2G storage is presented in the following.

The level of gas reservoir in the P2G storage at each time interval is expressed by Eq. (6.15). In Eqs. (6.16) and (6.17) the energy constraint of the P2G storage is stated. Inequalities (6.18) and (6.19) ensure that the amounts of charging and discharging of P2G storage do not exceed their allowable ranges. Based on (6.20), generated natural gas by the P2G storage can be stored in the reservoir or traded in the gas market. Finally, the rate of input power into the P2G storage is limited as presented in (6.21):

$$A_{l,t} = A_{l,t-1} + G_{l,t}^C - G_{l,t}^D, \quad \forall t \in \text{NT}, l \in \text{NL} \quad (6.15)$$

$$A_l^{\text{Min}} \leq A_{l,t} \leq A_l^{\text{Max}}, \quad \forall t \in \text{NT}, l \in \text{NL} \quad (6.16)$$

$$A_{l,0} = A_{l,\text{NT}}, \quad \forall l \in \text{NL} \quad (6.17)$$

$$0 \leq G_{l,t}^C \leq G_l^{C,\text{Max}}, \quad \forall t \in \text{NT}, l \in \text{NL} \quad (6.18)$$

$$0 \leq G_{l,t}^D \leq G_l^{D,\text{Max}}, \quad \forall t \in \text{NT}, l \in \text{NL} \quad (6.19)$$

$$G_{l,t}^C + GP_{l,t} = \eta_l P_{l,t}, \quad \forall t \in \text{NT}, l \in \text{NL} \quad (6.20)$$

$$0 \leq P_{l,t} \leq P_l^{\text{Max}}, \quad \forall t \in \text{NT}, l \in \text{NL} \quad (6.21)$$

6.2.4 P2H Storage

P2H technology refers to converting electrical energy into heat energy through various thermal reactions. P2H systems can be operated in centralized and decentralized modes [24]. In the centralized system approach, the existing infrastructure such as large-scale electric boilers and heat pumps are located far away from various consumers. In these systems, the generated heat energy is transmitted to consumers through district networks [25]. On the contrary, the decentralized systems are designed on the small scale and placed very close to the consumption location [26]. In both centralized and decentralized heating systems, thermal energy storage systems play an important role in storing heat energy.

Similar to the P2G storage, the equivalent mathematical model of the P2H storage can be described by Eqs. (6.22)–(6.28). The heat reservoir balance and reservoir capacity limit are specified by Eqs. (6.22) and (6.23). Also, Eq. (6.24) states that the level of the heat reservoir at the first and last intervals must be equal. The maximum rates of charged and discharged heat by the P2H storage are specified by Eqs. (6.25) and (6.26). According to Eq. (6.27) the produced heat by the P2H system can be delivered to the district heat market or charged in the heat reservoir. Moreover, based on Eq. (6.28), the injected power into the P2H storage should be lower than the permissible capacity:

$$A_{m,t} = (1 - \eta_m)A_{m,t-1} + H_{m,t}^C - H_{m,t}^D - \beta_{\text{loss}}\text{SU}_{m,t} + \beta_{\text{gain}}\text{SD}_{m,t}, \quad (6.22)$$

$$\forall t \in \text{NT}, m \in \text{NM}$$

$$A_m^{\text{Min}} \leq A_{m,t} \leq A_m^{\text{Max}}, \quad \forall t \in \text{NT}, m \in \text{NM} \quad (6.23)$$

$$A_{m,0} = A_{m,\text{NT}}, \quad \forall m \in \text{NM} \quad (6.24)$$

$$0 \leq H_{m,t}^C \leq H_m^{C,\text{Max}}, \quad \forall t \in \text{NT}, m \in \text{NM} \quad (6.25)$$

$$0 \leq H_{m,t}^D \leq H_m^{D,\text{Max}}, \quad \forall t \in \text{NT}, m \in \text{NM} \quad (6.26)$$

$$H_{m,t}^C + \text{HP}_{m,t} = \text{cop}_m P_{m,t}, \quad \forall t \in \text{NT}, m \in \text{NM} \quad (6.27)$$

$$0 \leq P_{m,t} \leq P_m^{\text{Max}}, \quad \forall t \in \text{NT}, m \in \text{NM} \quad (6.28)$$

6.3 Simulation Results

In this section, the presented structure is used for the operation scheduling of a hybrid energy storage unit in coordination with various layers of energy markets. The proposed model is mixed-integer programming (MIP) and solved using CPLEX solver in GAMS [27].

6.3.1 Input Data

To evaluate the proposed structure, the considered hybrid energy storage unit includes a CAES unit, a P2G storage, and a P2H storage to participate in the day-ahead electricity, natural gas, and district heat markets. The specifications of the hybrid energy storage unit are given in Table 6.1. The prices of the electricity, natural gas, and district heat energy markets are depicted in Fig. 6.3 [28]. It should be noted that in order to perform the simulation, the units of the electricity, gas, and heat markets were presented in an equivalent framework.

Table 6.1 Characteristics of the hybrid storage unit

Parameter	Value	Parameter	Value
$A_i^{\text{Min}}, A_i^{\text{Max}}$ (MWh)	50, 350	VE, VC (\$/MWh)	0.87
$P_i^{(\cdot),\text{Min}}, P_i^{(\cdot),\text{Max}}$ (MW)	5, 50	η_l, η_m	0.75, 0.4
$\eta_i^C, \eta_i^D, \eta_i^S$	0.9, 0.9, 0.4	cop_m	1.5
$A_l^{\text{Min}}, A_l^{\text{Max}}$ (MWh)	50, 180	$A_m^{\text{Min}}, A_m^{\text{Max}}$ (MWh)	0, 60
$G_l^{C,\text{Max}}, G_l^{D,\text{Max}}$ (MW)	40, 40	$H_m^{C,\text{Max}}, H_m^{D,\text{Max}}$ (MW)	20, 20
P_l^{Max} (MW)	50	P_m^{Max} (MW)	20

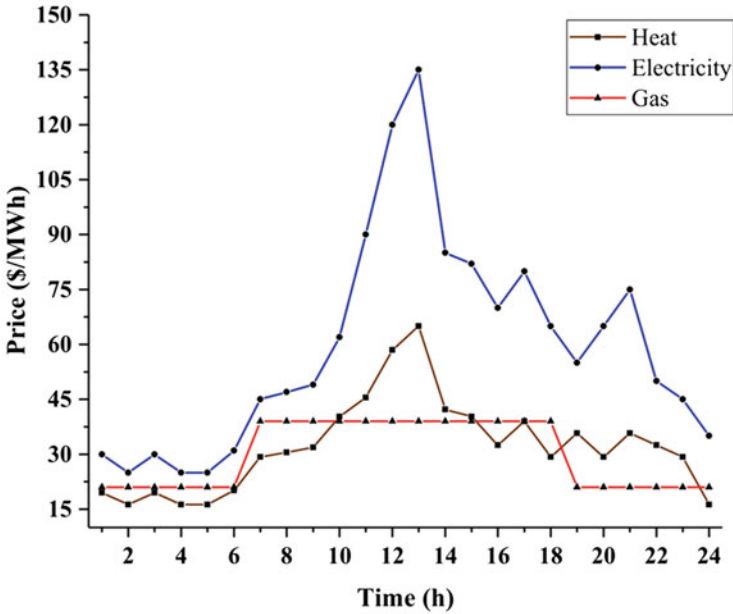


Fig. 6.3 Predicted hourly prices of electricity, gas, and heat

6.3.2 Results

The hourly optimal trading of the hybrid energy storage unit in the day-ahead electricity, gas, and district heat markets is shown in Fig. 6.4. Due to the high price of electrical power, most transactions had taken place in the electricity market. According to this figure, the absolute value of traded energy in the electricity market is equal to 873.47 MW. On the other hand, this amount for the gas and heat markets is equal to 722.5 MW and 99.68 MW, respectively. In addition, the total profit of the hybrid storage unit is equal to \$10,499.79.

Figures 6.5–6.7 show the hourly optimal scheduling of the CAES unit, P2G storage, and P2H storage. As it is shown in Fig. 6.5, the hybrid storage unit owner purchases electrical power and natural gas from the day-ahead electricity and gas markets to utilize the capabilities of the CAES storage in times when the gas and electricity prices are low. On the contrary, when the electricity and natural gas markets prices are high, this facility is used in discharging mode. Moreover, to gain more profits through activity between various layers of energy networks, the CAES system is exploited in the simple cycle mode from 19 to 21. According to Figs. 6.6 and 6.7, when the gas and heat markets are in high-price periods, the hybrid storage unit owner uses the ability of P2G and P2H facilities to increase its profit. The energy level of reservoirs in each energy storage technology is shown in Fig. 6.8.

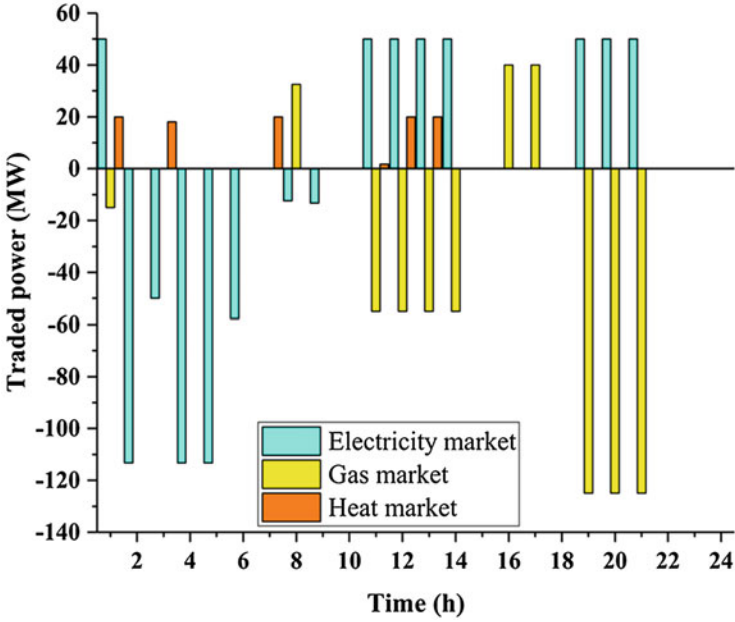


Fig. 6.4 Optimal bilateral dispatches in the day-ahead energy markets

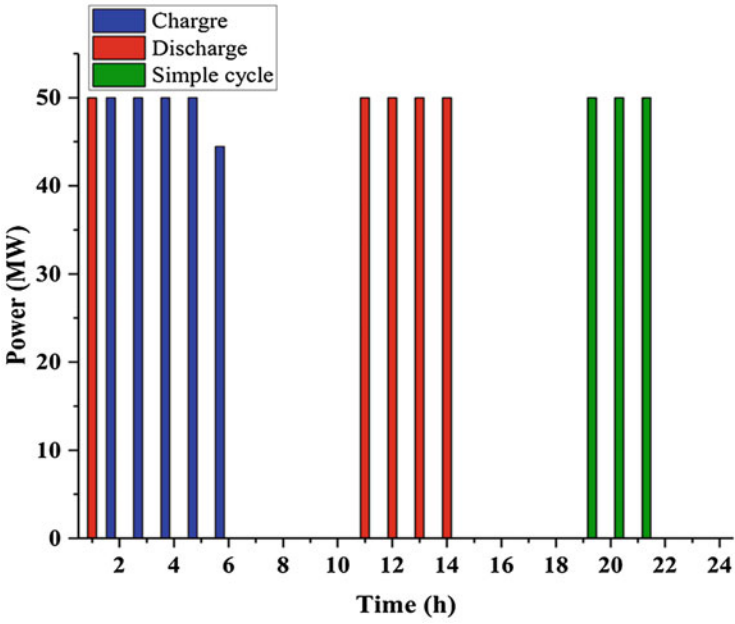


Fig. 6.5 Hourly optimal scheduling of CAES unit

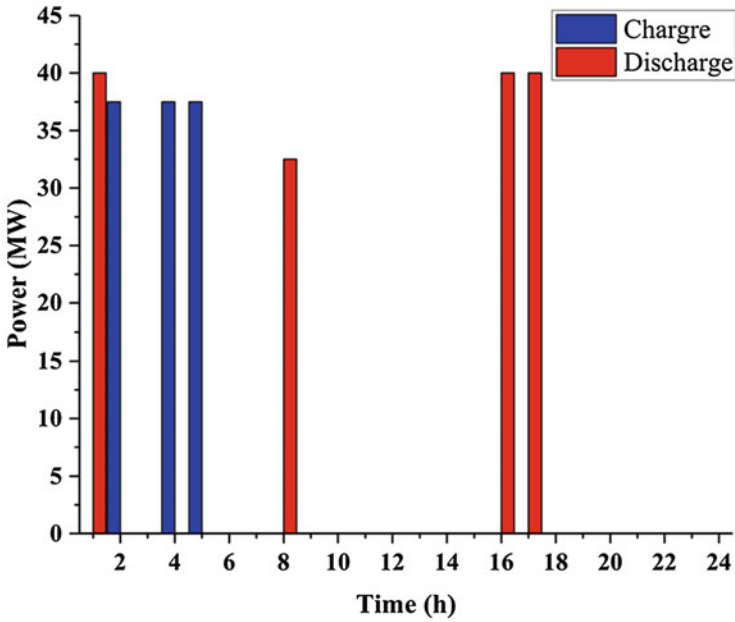


Fig. 6.6 Hourly optimal scheduling of P2G storage

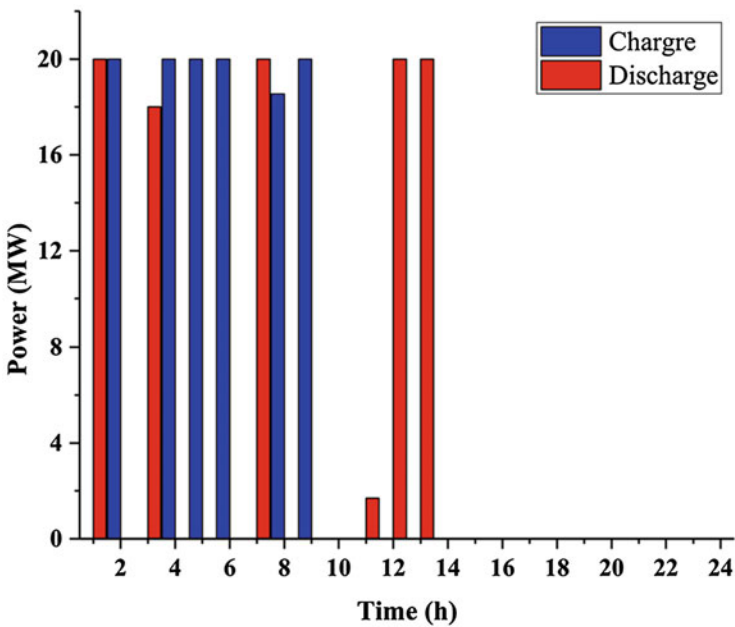


Fig. 6.7 Hourly optimal scheduling of P2H storage

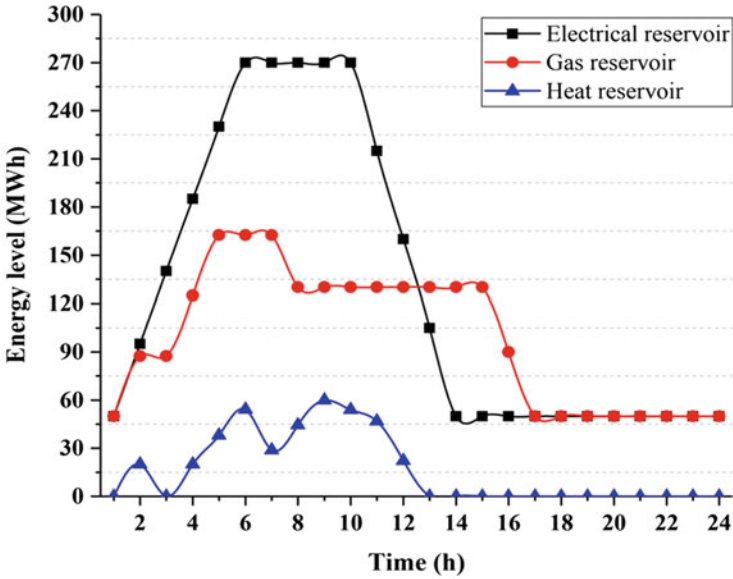


Fig. 6.8 The reservoir energy for each storage technology

Table 6.2 The effect of various units on hybrid storage unit’s profit

Case no.	Available storage units	Total profit (\$)	Profit changes (%)
Base case	CAES + P2G + P2H	10,499.791	–
C1	CAES+P2G	9274.722	–11.66
C2	CAES+P2H	9022.291	–14.07
C3	P2G + P2H	2702.569	–74.26

It should be noted that the presented results are related to the situation that the CAES unit, P2G storage, and P2H storage have been used simultaneously to make more profit in multi-carrier energy markets. In Table 6.2, the total profit of the hybrid storage unit in different operation modes is compared with the initial mode (i.e., the integrated participation of all three units). As can be seen, the highest profit margins are related to the situation in which all three storage units are operated simultaneously. In the meantime, the role of the CAES unit is undeniable.

6.4 Conclusions

This chapter solved a self-scheduling problem for short-term scheduling of the hybrid energy storage unit in joint day-ahead electricity, gas, and district heat markets. The proposed approach is evaluated using a realistic case study from the hybrid storage unit owner’s perspective in which the profit of the CAES unit, P2G

storage, and P2H storage operation is maximized. The introduced scheme enables the hybrid storage unit owner to adjust its activity procedure to maximize the hybrid system's profit in the multi-carrier energy networks. According to the simulation results, the hybrid storage unit's profit is increased up to \$10,499.791 with the simultaneous use of the CAES unit, P2G storage, and P2H storage.

Nomenclature

Indices (sets)

i (NI)	CAES unit
l (NL)	P2G storage
m (NM)	P2H storage
t (NT)	Scheduling time interval

Parameters

$A_{(\cdot)}^{\text{Min}}, A_{(\cdot)}^{\text{Max}}$	Minimum and maximum energy limit
$G_l^{C,\text{Max}}, G_l^{D,\text{Max}}$	Maximum stored/supplied natural gas by P2G storage
$H_m^{C,\text{Max}}, H_m^{D,\text{Max}}$	Maximum stored/supplied heat by P2H storage
$P_i^{C,\text{Min}}, P_i^{C,\text{Max}}$	Min/max charge capacity of the CAES unit
$P_i^{D,\text{Min}}, P_i^{D,\text{Max}}$	Min/max discharge capacity of the CAES unit
$P_i^{S,\text{Min}}, P_i^{S,\text{Max}}$	Min/max capacity of CAES unit in simple cycle mode
P_l^{Max}	Maximum allowable power consumption by P2G storage
P_m^{Max}	Maximum allowable power consumption by P2H storage
VC, VE	Operating/maintenance costs of compressor and expander
$\lambda_r^e, \lambda_i^g, \lambda_t^h$	Day-ahead wholesale electricity, gas, and heat prices
cop_m	Coefficient of P2H storage performance
$\eta_{(\cdot)}^C, \eta_{(\cdot)}^D$	Charge/discharge efficiency of various facilities

Variables

$A_{(\cdot), t}$	The energy level of various storage technologies
E_t^{DA}	Bidding/offering capacity of the day-ahead electricity market
G_t^{DA}	Bidding/offering capacity of the day-ahead gas market
$G_{l,t}^C, G_{l,t}^D$	Stored/supplied natural gas in charge/discharge modes by P2G storage
$GI_{i,t}$	Consumed natural gas by the CAES unit
$GP_{l,t}$	Produced natural gas by P2G storage
H_t^{DA}	Bidding/offering capacity of the day-ahead heat market
$H_{m,t}^C, H_{m,t}^D$	Stored/supplied heat in charge/discharge modes by P2H storage
$HP_{m,t}$	Produced heat by P2H storage
$P_{i,t}^C, P_{i,t}^D$	Stored/supplied power in charge/discharge modes by CAES unit
$P_{i,t}^S$	Generated power in simple cycle mode by CAES unit
$P_{l,t}$	Consumed power by P2G storage
$P_{m,t}$	Consumed power by P2H storage
$I_{i,t}^C, I_{i,t}^D, I_{i,t}^S$	Binary variables to show on/off status of facilities

References

1. Ma T, Wu J, Hao L (2017) Energy flow modeling and optimal operation analysis of the micro energy grid based on energy hub. *Energy Convers Manag* 133:292–306
2. Nazari-Heris M, Mirzaei MA, Mohammadi-Ivatloo B et al (2020) Economic-environmental effect of power to gas technology in coupled electricity and gas systems with price-responsive shiftable loads. *J Clean Prod* 244:118769
3. Mohammadi M, Noorollahi Y, Mohammadi-Ivatloo B et al (2017) Energy hub: from a model to a concept—a review. *Renew Sust Energ Rev* 80:1512–1527
4. Asl DK, Hamed A, Seifi AR (2020) Planning, operation and flexibility contribution of multi-carrier energy storage systems in integrated energy systems. *IET Renewable Power Gener* 14 (3):408–416
5. Mirzaei MA, Oskouei MZ, Mohammadi-ivatloo B et al (2020) An Integrated Energy Hub System based on Power-to-Gas and Compressed Air Energy Storage Technologies in presence of Multiple Shiftable Loads. *IET Gener Transm Distrib* 14(13)
6. Gorre J, Ruoss F, Karjunen H et al (2020) Cost benefits of optimizing hydrogen storage and methanation capacities for power-to-gas plants in dynamic operation. *Appl Energy* 257:113967
7. Rashid K, Mohammadi K, Powell K (2020) Dynamic simulation and techno-economic analysis of a concentrated solar power (CSP) plant hybridized with both thermal energy storage and natural gas. *J Clean Prod* 248:119193
8. Jadidbonab M, Babaei E, Mohammadi-ivatloo B (2019) CVaR-constrained scheduling strategy for smart multi carrier energy hub considering demand response and compressed air energy storage. *Energy* 174:1238–1250
9. Mirzaei MA, Yazdankhah AS, Mohammadi-Ivatloo B et al (2019) Stochastic network-constrained co-optimization of energy and reserve products in renewable energy integrated power and gas networks with energy storage system. *J Clean Prod* 223:747–758
10. Ajiwibowo MW, Darmawan A, Aziz M (2019) A conceptual chemical looping combustion power system design in a power-to-gas energy storage scenario. *Int J Hydrog Energy* 44 (19):9636–9642
11. Gholizadeh N, Vahid-Pakdel MJ, Mohammadi-ivatloo B (2019) Enhancement of demand supply's security using power to gas technology in networked energy hubs. *Int J Electr Power Energy Syst* 109:83–94
12. Shafiee S, Zareipour H, Knight AM et al (2017) Risk-constrained bidding and offering strategy for a merchant compressed air energy storage plant. *IEEE Trans Power Syst* 32(2):946–957
13. Xu D, Wu Q, Zhou B et al (2019) Distributed multi-energy operation of coupled electricity, heating and natural gas networks. *IEEE Trans Sustainable Energy*. 1-1
14. Chen Y, Wei W, Liu F et al (2017) A multi-lateral trading model for coupled gas-heat-power energy networks. *Appl Energy* 200:180–191
15. Mei J, Wang X, Kirtley JL (2020) Optimal scheduling of real multi-carrier energy storage system with hydrogen-based vehicle applications. *IET Renewable Power Gener* 14(3):381–388
16. Mirzaei MA, Nazari-Heris M, Mohammadi-Ivatloo B et al (2020) A novel hybrid framework for co-optimization of power and natural gas networks integrated with emerging technologies. *IEEE Syst J*:1–11
17. Liu X, Yan Z, Wu J (2019) Optimal coordinated operation of a multi-energy community considering interactions between energy storage and conversion devices. *Appl Energy* 248:256–273
18. Mohammadi A, Ahmadi MH, Bidi M et al (2017) Exergy analysis of a combined cooling, heating and power system integrated with wind turbine and compressed air energy storage system. *Energy Convers Manag* 131:69–78
19. Sameti M, Haghghat F (2018) Integration of distributed energy storage into net-zero energy district systems: optimum design and operation. *Energy* 153:575–591
20. Wang X, Bie Z, Liu F et al (2020) Bi-level planning for integrated electricity and natural gas systems with wind power and natural gas storage. *Int J Electr Power Energy Syst* 118:105738

21. Lund H, Salgi G (2009) The role of compressed air energy storage (CAES) in future sustainable energy systems. *Energy Convers Manag* 50(5):1172–1179
22. Budt M, Wolf D, Span R et al (2016) A review on compressed air energy storage: basic principles, past milestones and recent developments. *Appl Energy* 170:250–268
23. Eveloy V, Gebreegziabher T (2019) Excess electricity and power-to-gas storage potential in the future renewable-based power generation sector in the United Arab Emirates. *Energy* 166:426–450
24. Abdon A, Zhang X, Parra D et al (2017) Techno-economic and environmental assessment of stationary electricity storage technologies for different time scales. *Energy* 139:1173–1187
25. Michels H, Pitz-Paal R (2007) Cascaded latent heat storage for parabolic trough solar power plants. *Sol Energy* 81(6):829–837
26. Laing D, Steinmann W-D, Tamme R et al (2006) Solid media thermal storage for parabolic trough power plants. *Sol Energy* 80(10):1283–1289
27. Generalized Algebraic Modeling Systems (GAMS). April 2011. <http://www.gams.com>
28. MIBEL (Iberian market, [Online]. <http://www.erse.pt/eng/Paginas/ERSE.aspx>

Chapter 7

A Decomposition-Based Efficient Method for Short-Term Operation Scheduling of Hydrothermal Problem with Valve-Point Loading Effects



Elnaz Davoodi and Behnam Mohammadi-Ivatloo

7.1 Introduction

Any country or state does not contain large reserves of the coal or the nuclear fuels. In order to decrease pollution of the environment, the generation of thermal plants should be cut down as much as possible. Thus, a combination of hydro and thermal power generation is essential. The economic dispatch of a thermal generation system is usually much simpler than the economic dispatch of a hydrothermal system. Due to the natural differences in the watersheds, man-made storage and discharge parts are applied to control the water flows. On the other hand, in virtue of the other natural or man-made restrictions imposed on the operation of hydroelectric structures, all hydro plants look different. The arrangement of water release is necessary for the coordination of the operation of hydroelectric plants. In accordance with the scheduling range, the hydro system process can be split up into a long-term and a short-term scheduling problem. The long-term hydro scheduling problem entails a long-term forecast of water availability and the arrangement of reservoir water discharge over a long period of time that relies on the capacity of the reservoirs. Usual long-time scheduling includes 1 week to 1 year or a number of years, in which hydro structures with a capacity of sustained water over numerous seasons usually require climatological and statistics study. Short-range hydro scheduling describes a lapse of 1 day to 1 week. It means the minimum cost is attained by the hour-by-hour scheduling of the total generations on hydrothermal systems. The run of river hydro plants can provide the whole lot or a part of the base load and the peak of remaining load is fulfilled by a suitable mixture of thermal plants and reservoir-type hydro plants. Choosing the most cost-effective operating state of a hydro-thermal

E. Davoodi · B. Mohammadi-Ivatloo (✉)

Faculty of Electrical and Computer Engineering, University of Tabriz, Tabriz, Iran

e-mail: e.davoodi@tabrizu.ac.ir; bmohammadi@tabrizu.ac.ir

plant should be determined in a proper way. The optimal scheduling problem in hydrothermal systems can be regarded as optimizing the total fuel cost of thermal plants considering the constraint of hydro production over a pre-specified time interval [1]. It should be mentioned that in the deregulated energy systems, the objective function of hydrothermal scheduling would be minimizing total profit instead of minimizing the cost [2]. This chapter studies the classic version of the hydrothermal scheduling that considers cost minimization objective function. A number of the mathematical optimization methods like dynamic programming [3], decomposition techniques [4, 5], Lagrangian relaxation [6, 7], linear programming [8, 9], nonlinear programming [10], and net flow programming [11] are suggested for the solution of SHGS problem. In addition, in recent years, a great deal of artificial intelligence algorithms, such as genetic algorithm (GA) [12, 13], differential evolution [14], harmony search algorithm [15], particle swarm optimization (PSO) [16, 17], cuckoo search algorithm [18, 19], and gravitational search algorithm [20] are applied for solving SHGS problem. The heuristic optimization approaches are created to be effective in handling the problems without any limitation on the shape or kind of the optimization curve. On the other hand, these stochastic methods do not always assure to finding the global solution; in general, they give a reasonable solution, which is suboptimal. Furthermore, premature convergence is also the main shortcoming of these methods. A review of solving the SHGS problem by different approaches is presented in [33]. The classical Benders decomposition (generalized Benders decomposition (GBD)) [21], Dantzig-Wolfe decomposition [22], and optimality condition decomposition (OCD) [23] are among the most important methods to handle the numerous large structured optimization problems. These methods decompose the problems by relaxing the constraints or fixing the variables. However, the frame of the problem has a great impact on the success of such approaches. In some cases, these procedures are resourceful and they are not competitive with other methods. However, the simple elegance but robust performance of these approaches enables many researchers to not only utilize those methods, but also aim at improving the efficiency of the methods and develop their applicability.

Thanks to the innate mathematical form of SHGS problems containing complicated variables, in this chapter a dependable Benders decomposition based on distinct Benders cut framework is proposed. The presented method is inspired by Amjady et al.'s work [5] for addressing a short range of cost-effective generation scheduling of cascaded hydrothermal arrangements regarding numerous equality and inequality constraints of thermal and also hydroelectric plants. The modified Benders decomposition method enhances the deficiencies of the GBD approach and decreases the duality gap between the upper and lower bounds. Moreover, the proposed strong cuts are a very efficient technique for some large problems that require decomposition principles.

The remnant of this chapter is prepared as follows: First, the formulation of a hydrothermal generation system is represented. In the second section, the framework of the proposed Benders decomposition algorithm and its utilization in the SHGS problem are expounded. Then the performance of the proposed approach on a system including four hydro plants and one thermal generation is investigated, and

the results of other methods and different solvers are compared with the outputs of the proposed BD. Eventually, the chapter concludes in the last section.

7.2 Problem Description

The prime purpose of the optimal scheduling of power plant production is generally decreasing the full amount of generation cost while meeting all the equality and inequality constraints. However, since the marginal costs of the hydro plants are not notable, the SHGD problem basically deals with optimizing the fuel cost of thermal plants by considering the generating constraints, energy balance condition, and available water at the time stated as well. Most importantly, besides determination of the thermal and hydro plant power generation during a short-term scheduling horizon, the SHGD problem finds out the start-up and shutdown arrangement of thermal plants. On the contrary, thorough operating costs should be decreased so much so that customer demand is fulfilled with proper levels of security. Figure 7.1 shows a simple hydrothermal system referred to as the fundamental system which comprises one hydro and one thermal plant supplying power to load connected at the center of plants.

7.2.1 Objective Function

The fuel cost functions of the hydrothermal power units usually are in a quadratic form as follows:

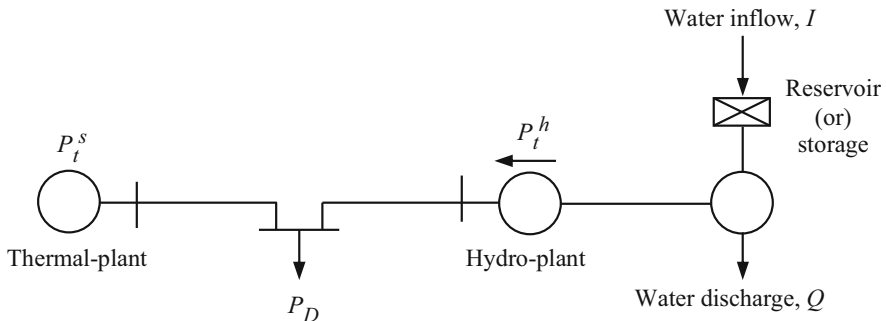


Fig. 7.1 Fundamental hydrothermal system

$$\min F_{\text{cost}} = \sum_{t=1}^T \sum_{i=1}^{N_s} c_i + b_i P_{i,t}^s + a_i (P_{i,t}^s)^2 \quad (7.1)$$

Equation (7.1) shows the production cost of the SHGD problem that just relies on the thermal plant variables, because hydroelectric plants do not have a significant cost in the power production step. In a real turbine generator system, separate nozzle groups in a valve system control the steam inflowing the turbine. Best efficiency of this system can be obtained when operating (presumably) at maximum output. So, valves are opened in sequence when increasing the output to obtain the maximum possible efficiency for a given output. The final outcome is a rippled efficiency curve which is known as valve-point effects, and this case can be added to fuel cost function in the form of a sinusoidal component as follows:

$$\min F_{\text{cost}} = \sum_{t=1}^T \sum_{i=1}^{N_s} \times \left[c_i + b_i P_{i,t}^s + a_i (P_{i,t}^s)^2 + |d_i \cdot \sin(e_i \cdot (P_{i,\min}^s - P_{i,t}^s))| \right] \quad (7.2)$$

7.2.2 Constraints

A number of equality and inequality constraints associated with the thermal and hydro plants must be fulfilled while objective cost function is minimized:

A. Equality constraints

- Real power balance constraint: Finally, the entire hydro and thermal plants must produce the power in a way that the demand is to be met exactly for a scheduled period. Equation (7.3) represents this concept:

$$\sum_{i=1}^{N_s} P_{i,t}^s + \sum_{j=1}^{N_h} P_{j,t}^h - P_{D,t} = 0, \quad t = 1, 2, \dots, T \quad (7.3)$$

Water release rate and reservoir water head are the fundamental variables in the hydroelectric generation, which can be stated as follows:

$$P_{j,t}^h = h_{1j} \cdot (V_{j,t})^2 + h_{2j} \cdot (Q_{j,t})^2 + h_{3j} \cdot V_{j,t} \cdot Q_{j,t} + h_{4j} \cdot V_{j,t} + h_{5j} \cdot Q_{j,t} + h_{6j}, \\ j = 1, 2, \dots, N_h, \quad t = 1, 2, \dots, T \quad (7.4)$$

- Hydraulic continuity constraints: The storage reservoir volume relies on the previous reservoir capacity, water discharge, and inflow rate in the determined interval along with water discharge and spillage of the upstream units with the delay time between reservoir i and its upstream in the specified horizon as follows:

$$V_{j,t} = V_{j,t-1} + I_{j,t} - Q_{j,t} - S_{j,t} + \sum_{k=1}^{N_{uj}} (Q_{k,t-\tau_{kj}} + S_{k,t-\tau_{kj}}), \quad (7.5)$$

$$j = 1, \dots, N_h, t = 1, \dots, T$$

- Initial and final reservoir storage capacity limits:

$$V_{j,0} = V_j^{\text{begin}}, \quad V_{j,T} = V_j^{\text{end}}, \quad j = 1, \dots, N_h \quad (7.6)$$

B. Inequality constraints

- Generation limit constraints: The decision variable bounds are described as constraints (7.7)–(7.10):

$$P_{i,\min}^s \leq P_{i,t}^s \leq P_{i,\max}^s, \quad i = 1, \dots, N_s \quad (7.7)$$

$$P_{j,\min}^h \leq P_{j,t}^h \leq P_{j,\max}^h, \quad j = 1, \dots, N_h \quad (7.8)$$

- Hydroelectric plant discharge limits:

$$Q_{j,\min} \leq Q_{j,t} \leq Q_{j,\max}, \quad j = 1, \dots, N_h \quad (7.9)$$

- Reservoir storage capacity limits:

$$V_{j,\min} \leq V_{j,t} \leq V_{j,\max}, \quad j = 1, \dots, N_h \quad (7.10)$$

7.3 Proposed Solution Methodology

7.3.1 Benders Decomposition

Benders decomposition is one of the classical solution approaches in [mathematical programming](#) that let us to solve the large optimization problems with complicating variables in a decomposed way at the cost of iteration. In 1972, Geoffrin [22] generalized the approach proposed by Benders for developing the structure of the method to the class of optimization problems. Indeed, Benders splits problems into

two parts, and thereby simplifies the solution process by (repeatedly) solving (a) a relaxed form of the original problem denominated as the master problem, and (b) the other one is denominated the subproblem so that it can be decomposed by blocks in subproblems, or it achieves such a flexible structure that it is much simpler than dealing with the initial problem. If the first-stage results are infeasible so that convergence is not achieved, then additional constraint or constraints are produced and added to the master problem, which is then resolved till no cuts can be produced. The generated cut is denominated as an “optimality cut” if obtained results of handling the master problem are a part of a complete feasible solution, or is called a “feasibility cut” if the fixing of the master problem partial solution leads to an infeasible subproblem. It is noteworthy that a subproblem is a specific case of the original problem that is further restricted to the original problem and so gives upper bound of the objective function. On the other hand, since the master problem estimates the primary problem, the obtained result of this problem gives a lower bound of the main problem. As iterations rise, the master problem and subproblems exchange the obtained information and render the solution more and more accurately. This process continues until the gap between the dual and primal bounds is closed.

The Benders cut of the suggested decomposition is a bit different version of the standard GBD method. In the current study, sturdy Benders cuts are utilized in the master problem, which eliminates the weaknesses of the Benders framework and helps to find the exact solutions. However, all techniques based on GBD comprise the main three steps below:

- Step 1.** To solve the subproblems and obtain the Lagrange multipliers
- Step 2.** To solve the master problem and generate Benders cuts
- Step 3.** To precisely decide how much output should be scheduled from plants that have been committed

7.3.1.1 Subproblem

Given the cost function of the composite thermal plant in a quadratic form, the subproblem can be expressed as in Eq. (7.11) or (7.12):

$$Z_s = \min \left\{ \sum_{t=1}^T \left(\sum_{i=1}^{N_s} b_i P_{i,t}^s + a_i (P_{i,t}^s)^2 \right) \right\} \quad (7.11)$$

On the other hand, by superimposing the valve-point loading effects as a sinusoidal term onto the fuel cost, the subproblem is changed as follows:

$$Z_s = \min \left\{ \sum_{t=1}^T \left(\sum_{i=1}^{N_s} b_i P_{i,t}^s + a_i (P_{i,t}^s)^2 + |d_i \cdot \sin(e_i \cdot (P_{i,\min}^s - P_{i,t}^s))| \right) \right\} \quad (7.12)$$

Notice that the real power balance (7.3) and the maximum active power output of thermal units (7.7) are considered as the subproblem's constraints. In addition, in this problem, dispatch decision variables of $P_{j,t}^h$ are assumed to be fixed at the values obtained from solving the master problem. In this step by fixing a set of complicating variables, their dual values can be attained once the solution of the subproblems and then the optimal dual variables of the subproblem are used to construct Benders cut added to the master problem which is solved again. Benders cut helps to improve the problem-solving process. Accordingly, considering the fixed value for variable $P_{j,t}^h$ for a scheduled horizon, the supplementary constraint that should be considered to the subproblem would be

$$P_{j,t}^h = \bar{P}_{j,t}^h : \lambda_{P_{j,t}^h} \quad (7.13)$$

where $\bar{P}_{j,t}^h$ is the preceding value of $P_{j,t}^h$ achieved from the master problem and $\lambda_{P_{j,t}^h}$ is the dual value associated with this additional constraint. This dual value provides a linear approximation of the change rate of the subproblem costs which is produced by the unitary change of $P_{j,t}^h$.

7.3.1.2 Master Problem

The master problem minimizes fixed terms of the cost curve whereas it must satisfy the total constraints of the hydroelectric power plants as follows:

$$Z_m = \min \left\{ \sum_{t=1}^T \left(\sum_{i=1}^{N_s} (c_i) + \alpha_t \right) \right\} \quad (7.14)$$

The objective function (7.14) is subject to hydraulic continuity (7.5), initial and ultimate reservoir storage capacity restrictions (7.6), upper and lower limits of active power outputs on hydraulic units (7.8), hydroelectric plant discharge bounds (7.9), reservoir storage capacity restrictions (7.10), and also Benders cut. The solution of the master problem supplies α_t and $P_{j,t}^h$. The upper limits of the Benders cuts are determined by α_t as follows:

$$\alpha_t \geq Z_{s,t} + \sum_{j \in N_h} \lambda_{p_t^h} \cdot (P_{j,t}^h - \bar{P}_{j,t}^h) \quad (7.15)$$

$\bar{P}_{j,t}^h$ is the fixed value connected to the variable which is calculated in the previous iteration in the master problem. $\lambda_{p_t^h}$ is the dual variable corresponding to the constraints (7.13) of the subproblem. Note that the conduct of the master problem above relies upon the iterative development of α_t and if α_t can yield a convex envelope, the master problem would suitably duplicate the original problem; hence this method can meet the solution of the main problem. In addition, since the master problem is a relaxed framework of the original problem, it provides the lower bound of the problem. Under certain conditions, the computational efficiency of the traditional Benders decomposition is not acceptable, and this method may fail to converge or cannot obtain the accurate results. To overwhelm this drawback, different tactics for improving Benders decomposition have been employed [24, 25]. Magnanti and Wong [26] proposed a new methodology for enhancing the GBD algorithm when it is faced with the mixed-integer problems. This strategy is based on generating well-organized Benders or Pareto-optimal cuts. This technique helps to speed up the convergence of the algorithm as well as a theory for differentiating “good” model formulations of a problem. On the other hand, due to the great efficiency of the proposed technique, it can handle a broad set of optimization algorithms such as Dantzig-Wolfe decomposition and cutting plane methods. But when Benders subproblem is difficult, Magnanti-Wong does not allow quick suboptimal solutions. Furthermore, generating the cuts requires to solve the subproblem firstly and this issue is problematic for mixed-integer programs with the convex hull formulation that need one Benders cut. Although Magnanti-Wong algorithm is proposed to solve the master problem and subproblem to produce a unique Benders cut, a main drawback of this algorithm is that one cannot always straightforwardly find a Benders master problem core point. Hence, Papadakos in [27] presents some models that subproblem does not have to be solved to generate Benders cuts and this technique helps in the master problem that would be closer one step to find the best point. Additionally, since in many cases of problems finding a core point for Benders master problems is very difficult, this reference raises the different Magnanti-Wong points to create Pareto-optimal cuts for a specific type of problems. The other type of Benders cut is entitled maximum feasible subsystem (MFS) that results in the development of the efficiency of original GBD for some types of problems. This strategy generates additional Benders cuts in every iteration and hence the number of the optimality cuts increases. In this way, this acceleration technique leads to a considerable reduction of CPU time. However, the obtained results of the proposed strategy by Saharidis and Ierapetritou are not very different when the number of the feasibility cuts is not high during the iterations. Furthermore, computational complexity might gratuitously be stepped up owing to the devoting time for solving the extra problems for the generation of MFS cuts.

A new way to generate cuts and use two sets of subproblems which are proposed in the current study solves a short-term hydrothermal generation scheduling problem via an algorithm-based BD.

The master problem makes use of integer programming method for solving a part of objective function including integer variables while subproblems utilize nonlinear programming solution method to shape the continuous part of the objective function related to the constraints. In addition, in case of infeasible first-set subproblem, the equivalent second subproblem set is regarded. Owing to violation of constraints, the first-set subproblems become infeasible; for this reason, the penalty terms are applied for penalizing these violated constraints in the second-set subproblems. Next, strong Benders cuts are generated to bring down the CPU time. The strong Benders cuts are originated from Pareto-optimal cuts considering that strong cut can take over from other cuts among the earlier iterations. The following presents the mathematical details of the suggested Benders cut generation.

7.3.1.3 Benders Cut Generation

If an hourly first-set subproblem becomes practicable, the subsequent Benders cut would count up to the master problem in the next generations:

$$\alpha_{t,g} \geq Z_{s,t,g} + \sum_{j \in N_h} \lambda_{p_{t,g}^h} \cdot \left(P_{j,t,g}^h - \bar{P}_{j,t,g}^h \right) \quad (7.16)$$

where

$$\begin{aligned} & Z_{s,t,g} + \sum_{j \in N_h} \lambda_{p_{t,g}^h} \\ & \quad \cdot \left(P_{j,t,g}^h - \bar{P}_{j,t,g}^h \right) \\ & = \text{Max} \left[Z_{s,t} + \sum_{j \in N_h} \lambda_{p_t^h} \cdot \left(P_{j,t}^h - \bar{P}_{j,t}^h \right) \right]_t \\ & = 1, \dots, \text{current time-1} \end{aligned} \quad (7.17)$$

To put in another way, the subscript g indicates iteration with the maximum value of $Z_{s,t} + \sum_{j \in N_h} \lambda_{p_t^h} \cdot \left(P_{j,t}^h - \bar{P}_{j,t}^h \right)$ among all earlier iterations. It is noticeable that the “Max” operator in (7.17) does not contain the latest iteration.

7.4 Benders Decomposition-Based Method for SHGS Problem

The procedural steps have been depicted in this section for applying the proposed approach to the problem described above. In the SHGS problem, the real power outputs of the thermal units are used as decision variables to form the objective function of the problem. To implement the proposed BD method to deal with the variable-head hydrothermal scheduling problem, the detailed stepwise producer is as follows:

Step 0: Initialization: *Input the necessary data and load the initial parameters:*

At this point, the data is introduced for handling the SHGS problem and the other required parameters such as iteration ($\text{iter} = 0$), upper bound ($\text{UB} = +\infty$), and lower bound ($\text{LB} = -\infty$) are initialized.

Update the iteration counter, $\text{iter} = \text{iter} + 1$.

Solve the master problem not including the Benders cuts:

Indeed, the main result of this stage is obtaining the value of $P_{j,t}^h$ that is acquired by solving the objective function $Z_{m,t}$ (Eq. (7.14)) accompanied with constraints (7.4–7.6) and (7.8–7.10).

Step 1: Subproblem solution: *Solve the subproblem (7.12).*

When the master problem computed the primary variables, the obtained solution must be taken as a constraint explicitly in subproblem. Accordingly, the objective function (7.12) is subject to restrictions (7.3), (7.7), and (7.13) and is solved and the values of $Z_{s,t}$ and $\lambda_{p_{t,m}^h}$ are procured.

Step 2: Convergence verification. *Update upper and lower bounds:*

$$\text{UB} = Z_m + \sum_{t=1}^T Z_{s,t} - \sum_{t=1}^T \alpha_t \text{ and } \text{LB} = Z_m. \text{ UB contains the cost function of}$$

the SHGS without considering the Benders cuts, and LB includes a part of the cost function with the strong cuts.

If the convergence standard does not hold, continue to step 3; otherwise, stop. The convergence criterion relies on the existing gap between the updating of upper and lower bounds. If the duality gap is smaller than the specified tolerance $\left(\frac{|\text{UB}-\text{LB}|}{\text{UB}} \leq \varepsilon\right)$, stop and display the optimal solution; otherwise, go to the next step.

Step 3: Master problem solution: *Update the iteration counter, $\text{iter} = \text{iter} + 1$.*

Solve the master problem (7.14)–(7.17): The master problem with feasibility cuts is solved for gaining $P_{j,t}^h$. In this step, the strong generated cuts force the master problem to fulfill the associated constraints. Once the solution of this problem is specified, the algorithm continues in Step 1.

The authors deduced from analyzing several scenarios that whenever the fix-cost puts into the master problem instead of the subproblem, the presented

decomposition indicates faster convergence, hence this type of decomposition is opted for obtaining the output results in all of the scenarios.

7.5 Computational Results

Test system: The presented Benders decomposition sketch is investigated on the system counting an equivalent thermal unit and a multi-chain cascade of four hydro units. It should be noted that firstly, it is supposed that the problem involves only solving the dispatch problem, and the unit commitment problem has not been regarded, and secondly, the cost functions of several committed thermal units are embodied by a compound fuel cost function [28]. The hydraulic test system according to Fig. 7.6 is as follows: (I) a multi-chain cascade flow network in which all the plants are sited on one stream; (II) river transport delay between consecutive reservoirs has been considered; (III) owing to the small capacity of reservoirs, the head of reservoirs is variable; (IV) natural inflow rates and load demand are considered variable during the scheduling period; (V) total scheduling period is assumed to be 1 day and it is split up into 24 one-hour sessions ($T = 24$); (VI) all the spillages are assumed zero; and in addition, (VII) the valve-point loading effects of the thermal plants are also regarded. Moreover, in cascade hydroelectric systems, the hydro plants are located on the same streams and plant relies on the immediate upstream plant. The upstream plant inputs discharge to the immediate downstream plant. It should be stated that a thermal unit is representative of the equivalent thermal plant that possibly comprises numerous units. So, the presented characteristic is for a virtual equivalent thermal unit. The non-smooth operating cost of thermal power station is given by $a_i = 0.002$, $b_i = 19.2$, $c_i = 5000$, $e_i = 5000$, and $h_i = 0.085$ which are presented in Eq. (7.2). The minimum and maximum generation bounds of the thermal plants are 500 MW and 2500 MW, respectively. The details about hydropower plant production coefficients, load demands, reservoir restrictions, generation restrictions, and reservoir inflows of the test system are provided in Tables 7.4–7.7, respectively, in Appendix. The proposed Benders method implements the Generalized Algebraic Modeling System (GAMS) software package [29] to handle the hydrothermal scheduling problem. The solver of the subproblem is SNOPT-NLP and CONOPT-DNLP solver is considered for solving the master problem.

The obtained results by the proposed approach are given in Table 7.1, and different methods such as MDNLPSO [17], MAPSO [31], RCGA-AFSA [32], and also CONOPT and SNOPT solvers that are two well-known DNLP optimization solvers in GAMS software, used for solving complex NLP and DNLP problems, are applied for comparing the results. In addition, the obtained CPU times of multifarious methods are displayed in Table 7.1 and are compared with each other. Figure 7.2 illustrates the procedure of decreasing the gap between UB and LB with incrementing the iteration number. In other words, how to optimize the total cost of thermal plants and hydroelectric power plants can be inferred from the figure.

Table 7.1 Comparison of the scheduling results provided by different algorithms for the test case

Method	Cost (\$)	CPU time (s)
MDNLPSO [17]	923,961	119
DE [30]	928,662.84	8.70
MAPSO [31]	924,636.88	–
DRQEA [30]	925,485.21	7.50
TLBO [31]	924,550.78	–
RCGA-AFSA [32]	927,899.872	13
CONOPT	941,205.70	6.00
SNOPT	946,026.66	1.74
Proposed BD	888,690.13	7.45

After the sixth iteration, required powers are distributed optimally in the specified time stages among the plants and the gap tends to be zero. Thermal and hydropower plants divide the hourly demand between themselves in a way that results in the lowest cost; besides, those plants satisfy demand. Hence, for each time span, the corresponding power balance equation is obtained. For instance, in the third time period, the load level is 1360 MW, and the outputs are $P_{\text{hydro1}} = 99.5$ MW, $P_{\text{hydro2}} = 87.13$ MW, $P_{\text{hydro3}} = 57.66$ MW, $P_{\text{hydro4}} = 199.72$ MW, and $P_{\text{thermal}} = 915.98$ MW. The obtained optimum powers have put in their specific limits and also meet the third interval demand. These results have been indicated precisely in Table 7.2. In addition, the arrangement and the constraints of the hydro unit system such as reservoir storage capacity restriction, water transport delay among cascaded reservoirs, and availability of water influence on the output of a certain hydro unit over a determined time interval are completely fulfilled. Finally, other detailed outputs (water discharge and storage volume during 24 h) of the hydro units have been presented in Table 7.3. According to this table, the output characteristics of the hydro plants have not exceeded their limits and have followed the defined (7.3)–(7.6).

Statistical outcomes of the simulations and extra technical data of the hydrothermal coordination problem can be observed in Figs. 7.3–7.5. The power generated and load demand by the hydro and thermal plants have been drawn in Figs. 7.2 and 7.3 and Figs. 7.4 and 7.5 display the hourly capacity of the reservoirs and the release of hydro plants, respectively.

According to Table 7.1, the average convergence time of the suggested method to the optimum is 7.45 s, and the optimal cost is \$888,690.13. By comparison with the other methodologies and solvers, it is clear that the proposed approach produces comparable final outcomes with regard to minimum cost and execution time. It should be noted that improvement of 3.88% of optimal cost in comparison with the best cost achieved until now (\$924,550.78) was obtained in reasonable computing CPU time, while satisfying all the problem constraints, indicating the superiority and reliability of the proposed approach in handling the real SHGS problems.

Table 7.2 Generation schedule of hydro and thermal generators

Hour	Hydro plant				Thermal plant	Total
	Generation (MW)				Generation (MW)	Generation (MW)
	Plant 1	Plant 2	Plant 3	Plant 4		
1	95.85	73.65	58.04	200.09	942.37	1370
2	97.4	84.88	57.03	209.36	941.33	1390
3	99.5	87.13	57.66	199.72	915.98	1360
4	95.34	82.37	50.89	156.79	904.61	1290
5	95.73	84.11	57.96	202.85	849.40	1290
6	95.64	84.02	58.98	210.46	960.9	1410
7	94.4	79.56	62.46	215.12	1198.47	1650
8	91.55	73.94	61.50	207.00	1566.02	2000
9	94.5	79.45	64.43	246.11	1755.51	2240
10	95.42	81.78	62.81	255.54	1824.46	2320
11	100.94	77.67	59.39	260.13	1731.88	2230
12	99.45	80.84	59.23	281.34	1789.14	2310
13	95.63	77.78	62.60	282.65	1711.34	2230
14	104.49	75.98	60.30	296.17	1663.06	2200
15	98.13	79.82	58.85	295.38	1597.82	2130
16	107.94	90.76	59.38	323.53	1488.39	2070
17	106.22	84.95	59.18	322.80	1556.85	2130
18	104.03	75.87	57.89	301.72	1600.50	2140
19	105.14	82.39	56.15	325.36	1670.96	2240
20	105.58	77.09	53.17	308.10	1736.05	2280
21	55.00	65.71	57.74	276.67	1784.87	2240
22	103.60	72.33	57.49	310.85	1575.73	2120
23	94.29	62.58	58.00	295.51	1339.61	1850
24	102.94	75.9	56.47	303.55	1051.14	1590

7.6 Conclusions

This chapter has addressed short-term hydrothermal scheduling problem based on an improved Benders decomposition method. The major contribution in this study consists of proposing strong Benders cuts to ameliorate the computational characteristic of the general BD method for solving the SHGS problem. The provided decomposition framework is simple, clean, and effective, even for dominant real power system problems. The practicability and efficiency of the proposed approach are confirmed by an electric energy system that comprises several hydro and thermal plants with valve point effect for 24-h time horizon, and the outcomes are reported. The optimal cost of the considered case study achieved by proposed BD is \$888,690.13, which can save \$35,860.65 daily compared to the best reported results. This considerable reduction in generation cost provides the superior quality solution with great accuracy and prime convergence properties. Moreover, the obtained results illustrate a reasonable computation time in comparison with the other

Table 7.3 Hourly discharge and storage volume of hydro plants

Hour	Hydro plants				Hydro plants			
	Discharge ($\times 10^4 \text{ m}^3$)				Storage volume ($\times 10^4 \text{ m}^3$)			
	Plant 1	Plant 2	Plant 3	Plant 4	Plant 1	Plant 2	Plant 3	Plant 4
1								
2	5.00	6.00	26.26	13.00	105.00	82.00	151.84	109.80
3	5.00	6.00	25.29	13.00	109.00	84.00	134.75	99.20
4	14.62	15.00	10.00	17.80	102.38	78.00	133.75	83.00
5	5.00	6.00	24.49	13.00	104.38	81.00	122.26	70.00
6	13.79	15.00	10.00	16.77	96.59	74.00	135.88	79.49
7	13.96	15.00	12.38	18.70	89.63	66.00	147.50	86.07
8	5.00	6.00	25.85	13.00	92.63	66.00	144.43	83.07
9	5.00	6.00	10.00	13.00	96.63	67.00	165.39	94.56
10	5.00	6.00	26.67	13.00	101.63	69.00	159.73	91.56
11	5.00	6.00	25.93	13.00	107.63	72.00	145.8	90.95
12	14.80	15.00	11.79	19.89	104.83	66.00	146.01	96.92
13	5.00	6.00	10.00	13.00	109.83	68.00	149.01	93.92
14	5.00	6.00	26.04	13.00	115.83	70.00	147.77	107.58
15	14.87	13.95	12.96	16.49	112.96	65.05	157.81	117.02
16	5.00	6.00	25.94	13.00	118.96	68.05	145.87	115.82
17	5.00	6.00	25.77	13.00	123.96	70.05	142.97	112.82
18	12.96	6.00	12.69	13.00	120.00	71.05	151.23	125.86
19	5.00	6.00	25.53	13.00	123.00	71.05	138.71	125.81
20	5.00	6.00	10.00	13.00	125.00	72.05	148.67	138.75
21	15.00	13.49	10.00	18.86	116.00	66.56	150.67	145.66
22	5.00	6.00	10.00	13.00	118.00	69.56	153.67	145.35
23	15.00	12.56	10.00	24.88	111.00	66.00	166.67	146.00
24	5.00	6.00	10.00	13.00	115.00	68.00	176.16	143.00

methods for this application. Therefore, considering all the results of the case study with the SHGS problem, it can lead to the conclusion that the proposed approach, using new Benders cuts, outperforms previous algorithms and demonstrates excellent performance in dealing with practical hydrothermal scheduling.

Nomenclature

Indices

- i Thermal plant index
- j Hydro plant index
- k Upstream hydro unit (directly above the j th hydroelectric plant) index
- t Time period (hour) index

Variables

- $P_{i,t}^s$ Power production of the i th thermal unit at period t (MW)
- $P_{j,t}^h$ Power production of the j th hydro unit at period t (MW)

Fig. 7.2 Lower and upper bound evolution of the proposed BD method

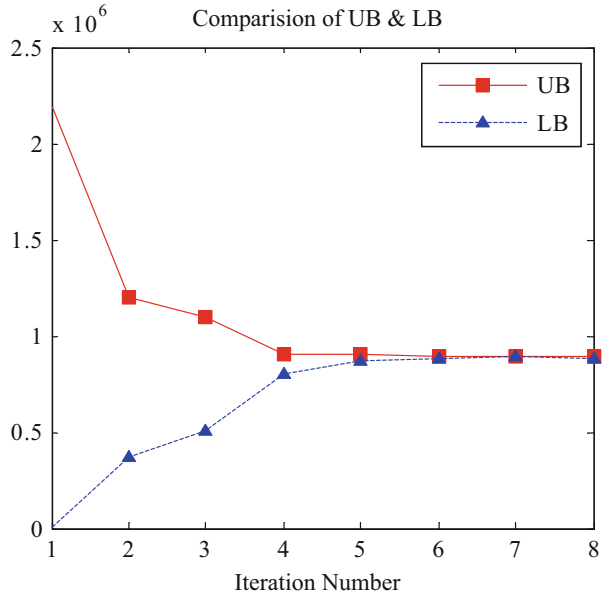
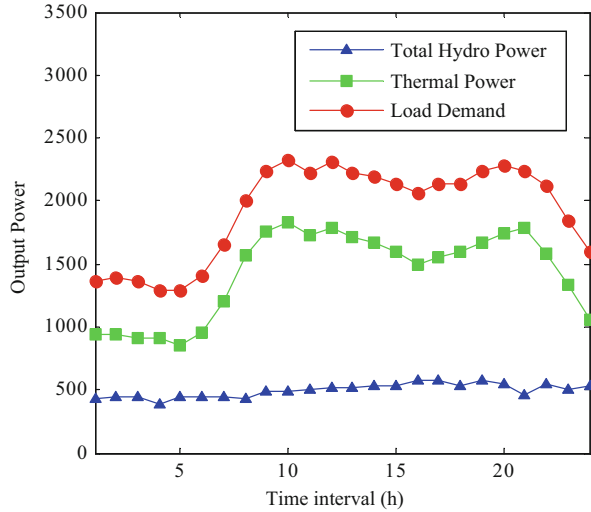


Fig. 7.3 Hydro production, thermal production, and load demand for the test case



- $Q_{j,t}$ Water release rate of the j th reservoir at period t (m^3)
- $V_{j,t}$ Storage reservoir capacity of the j th reservoir at period t (m^3)
- $I_{j,t}$ Nature inflow rate of the j th reservoir at period t (m^3)
- $S_{j,t}$ Spillage of the j th reservoir at period t (m^3)

Fig. 7.4 Reservoir storage volumes for the test case

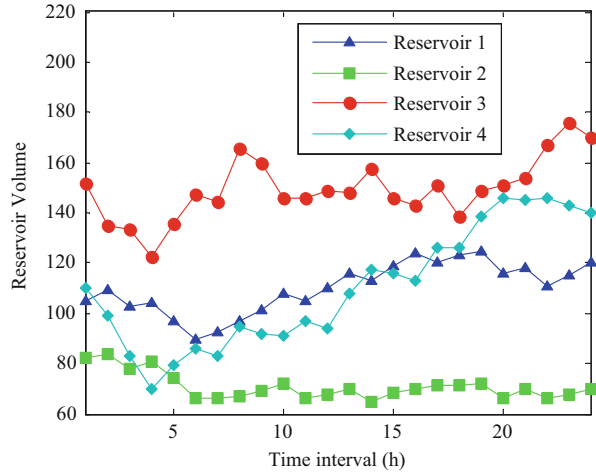
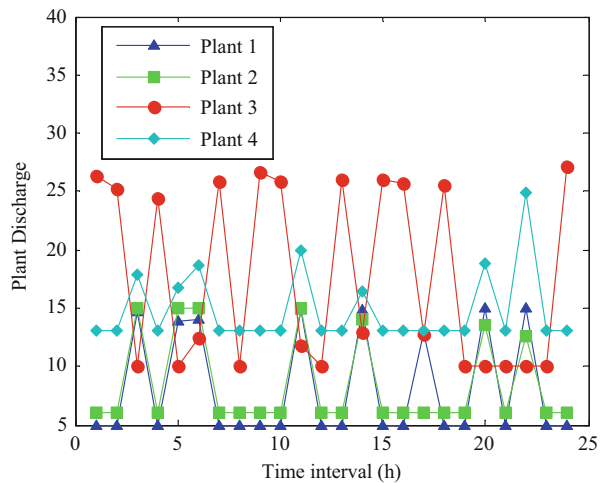


Fig. 7.5 Hourly hydro plant discharge



Constants

- a_i, b_i, c_i Quadratic production coefficients of the cost function of unit i
- d_i, e_i Valve loading coefficients of the i th thermal unit
- $P_{D, t}$ Load demand at period t
- $h_{1j}, h_{2j}, h_{3j}, h_{4j}, h_{5j}, h_{6j}$ Power production coefficients related to hydro plant j
- $P_{i, \min}^s, P_{i, \max}^s$ Minimum and maximum limits of the active power production related to thermal unit i
- $P_{j, \min}^h, P_{j, \max}^h$ Minimum and maximum limits of the active power production related to hydro plant j
- $Q_{j, \min}, Q_{j, \max}$ Minimum and maximum limits of the water release rate related to hydroelectric plant j
- $V_{j, \min}, V_{j, \max}$ Minimum and maximum limits of the storage volume of the reservoir j
- N_s Number of thermal generating units

N_h	Number of hydroelectric plants
N_{ij}	Number of upstream units directly above the j th hydroelectric plant
T	The whole time periods over scheduling horizon
τ_{kj}	Water transport delay from reservoir k to j
V_j^{begin}	Initial storage reservoir capacity of the j th reservoir
V_j^{end}	Ultimate storage reservoir capacity of the j th reservoir

Appendix

Figure 7.6 illustrates the hydraulic configuration of the test system. Table 7.4 presents the power generation coefficients of hydro units and the hourly load demand has been indicated in Table 7.5. The technical properties of the hydro units are shown in Table 7.6. The water inflow of the reservoirs has been displayed in Table 7.7 and finally Table 7.8 shows the time delay between the reservoirs and the number of upstream reservoirs.

Fig 7.6 Hydraulic system test network

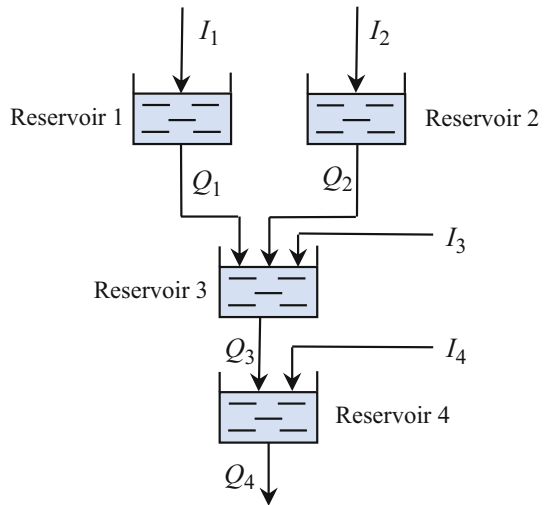


Table 7.4 Hydro power generation coefficients

Plant	h_1	h_2	h_3	h_4	h_5	h_6
1	-0.0042	-0.42	0.030	0.90	10.0	-50
2	-0.0040	-0.30	0.015	1.14	9.5	-70
3	-0.0016	-0.30	0.014	0.55	5.5	-40
4	-0.0030	-0.31	0.027	1.44	14.0	-90

Table 7.5 Load demand for 24 h

Hour	$P_D(\text{MW})$	Hour	$P_D(\text{MW})$	Hour	$P_D(\text{MW})$	Hour	$P_D(\text{MW})$
1	1370	7	1650	13	2230	19	2240
2	1390	8	2000	14	2200	20	2280
3	1360	9	2240	15	2130	21	2240
4	1290	10	2320	16	2070	22	2120
5	1290	11	2230	17	2130	23	1850
6	1410	12	2310	18	2140	24	1590

Table 7.6 Hydropower plant reservoir storage capacity limits, reservoir initial and end conditions, plant discharge limits ($\times 10^4 \text{ m}^3$), and plant generation limits (MW)

Plant	$V_{j, \min}$	$V_{j, \max}$	V_j^{begin}	V_j^{end}	$Q_{j, \min}$	$Q_{j, \max}$	$P_{j, \min}^h$	$P_{j, \max}^h$
1	80	150	100	120	5	15	0	500
2	60	120	80	70	6	15	0	500
3	100	240	170	170	10	30	0	500
4	70	160	120	140	6	20	0	500

Table 7.7 Hydropower plant reservoir inflows ($\times 10^4 \text{ m}^3$)

Hour	Reservoir				Hour	Reservoir				Hour	Reservoir			
	1	2	3	4		1	2	3	4		1	2	3	4
1	10	8	8.1	2.8	9	10	8	1	0	17	9	7	2	0
2	9	8	8.2	2.4	10	11	9	1	0	18	8	6	2	0
3	8	9	4	1.6	11	12	9	1	0	19	7	7	1	0
4	7	9	2	0	12	10	8	2	0	20	6	8	1	0
5	6	8	3	0	13	11	8	4	0	21	7	9	2	0
6	7	7	4	0	14	12	9	3	0	22	8	9	2	0
7	8	6	3	0	15	11	9	3	0	23	9	8	1	0
8	9	7	2	0	16	10	8	2	0	24	10	8	0	0

Table 7.8 Time delay between the reservoirs and number of upstream reservoirs

Reservoir	1	2	3	4
N_u	0	0	2	1
τ_k	2	3	4	0

References

1. Nazari-Heris M, Mohammadi-Ivatloo B, Asadi S (2018) Robust stochastic optimal short-term generation scheduling of hydrothermal systems in deregulated environment. *J Energy Syst* 2 (4):168–179
2. Ruzic S, Rajakovic N, Vuckovic A (1996) A flexible approach to short-term hydro-thermal coordination. I. Problem formulation and general solution procedure. *IEEE Trans Power Syst* 11 (3):1564–1571
3. Wood AJ, Wollenberg BF (2012) Power generation, operation, and control. John Wiley & Sons
4. Yan H, Luh PB, Guan X, Rogan PM (1993) Scheduling of hydrothermal power systems. *IEEE Trans Power Syst* 8(3):1358–1365
5. Amjady N, Ansari MR (2013) Hydrothermal unit commitment with AC constraints by a new solution method based on benders decomposition. *Energy Convers Manag* 65:57–65
6. Guan X, Luh PB, Yen H, Rogan P (1994) Optimization-based scheduling of hydrothermal power systems with pumped-storage units. *IEEE Trans Power Syst* 9(2):1023–1031
7. Guan X, Luh PB, Zhang L (1995) Nonlinear approximation method in Lagrangian relaxation-based algorithms for hydrothermal scheduling. *IEEE Trans Power Syst* 10(2):772–778
8. Shawwash ZK, Siu TK, and Russel S (1999) The BC Hydro short term hydro scheduling optimization model in Power Industry Computer Applications. PICA'99. Proceedings of the 21st 1999 IEEE International Conference 183–189
9. Gil E, Araya J (2016) Short-term hydrothermal generation scheduling using a parallelized stochastic mixed-integer linear programming algorithm. *Energy Procedia* 87:77–84
10. Hoseynpour O, Mohammadi-Ivatloo B, Nazari-Heris M, Asadi S (2017) Application of dynamic non-linear programming technique to non-convex short-term hydrothermal scheduling problem. *Energies* 10(9):1440
11. Franco P, Carvalho M, Soares S (1994) A network flow model for short-term hydro-dominated hydrothermal scheduling problems. *IEEE Trans Power Syst* 9(2):1016–1022
12. Nazari-Heris M, Mohammadi-Ivatloo B, Haghrah A (2017) Optimal short-term generation scheduling of hydrothermal systems by implementation of real-coded genetic algorithm based on improved Mühlenbein mutation. *Energy* 128:77–85
13. Haghrah A, Mohammadi-ivatloo B, Seyedmonir S (2014) Real coded genetic algorithm approach with random transfer vectors-based mutation for short-term hydrothermal scheduling. *IET Gener Transm Distrib* 9(1):75–89
14. Zhang J, Lin S, Qiu W (2015) A modified chaotic differential evolution algorithm for short-term optimal hydrothermal scheduling. *Int J Electr Power Energy Syst* 65:159–168
15. Nazari-Heris M, Fakhim Babaei A, Mohammadi-Ivatloo B, Asadi S (2018) Improved harmony search algorithm for the solution of non-linear non-convex short-term hydrothermal scheduling. *Energy* 151:226–237
16. Wu Y, Wu Y, Liu X (2019) Couple-based particle swarm optimization for short-term hydrothermal scheduling. *Appl Soft Comput* 74:440–450
17. Rasoulzadeh-Akhijahani A, Mohammadi-Ivatloo B (2015) Short-term hydrothermal generation scheduling by a modified dynamic neighborhood learning based particle swarm optimization. *Int J Electr Power Energy Syst* 67:350–367
18. Nguyen TT, Vo DN (2019) The application of an effective cuckoo search algorithm for optimal scheduling of hydrothermal system considering transmission constraints. *Neural Comput & Applic* 31(8):4231–4252
19. Nguyen TT, Vo DN (2016) An efficient cuckoo bird inspired meta-heuristic algorithm for short-term combined economic emission hydrothermal scheduling. *Ain Shams Eng J* 14(1):18–28
20. Gouthamkumar N, Sharma V, Naresh R (2015) Disruption based gravitational search algorithm for short term hydrothermal scheduling. *Expert Syst Appl* 42(20):7000–7011
21. Geoffrion AM (1972) Generalized benders decomposition. *J Optim Theory Appl* 10 (4):237–260

22. Dantzig GB, Wolfe P (1960) Decomposition principle for linear programs. *Oper Res* 8 (1):101–111
23. Rabiee A, Mohammadi-Ivatloo B, Moradi-Dalvand M (2013) Fast dynamic economic power dispatch problems solution via optimality condition decomposition. *IEEE Trans Power Syst* 29 (2):982–983
24. Fischetti M, Salvagnin D, Zanette A (2010) A note on the selection of Benders' cuts. *Math Program* 124(1):175–182
25. Saharidis GK, Minoux M, Ierapetritou MG (2010) Accelerating benders method using covering cut bundle generation. *Int Trans Oper Res* 17(2):221–237
26. Magnanti TL, Wong RT (1981) Accelerating Benders decomposition: algorithmic enhancement and model selection criteria. *Oper Res* 29(3):464–484
27. Papadakos N (2008) Practical enhancements to the Magnanti–Wong method. *Oper Res Lett* 36 (4):444–449
28. Kumar S, Naresh R (2007) Efficient real coded genetic algorithm to solve the non-convex hydrothermal scheduling problem. *Int J Electr Power Energy Syst* 29(10):738–747
29. Generalized algebraic modeling systems (GAMS). <http://www.gams.com>
30. Wang Y, Zhou J, Mo L, Zhang R, Zhang Y (2012) Short-term hydrothermal generation scheduling using differential real-coded quantum-inspired evolutionary algorithm. *Energy* 44 (1):657–671
31. Roy PK (2014) Teaching learning based optimization for short-term hydrothermal scheduling problem considering valve point effect and prohibited discharge constraint. *Int J Electr Power Energy Syst* 53:10–19
32. Fang N, Zhou J, Zhang R, Liu Y, Zhang Y (2014) A hybrid of real coded genetic algorithm and artificial fish swarm algorithm for short-term optimal hydrothermal scheduling. *Int J Electr Power Energy Syst* 62:617–629
33. Nazari-Heris M, Mohammadi-Ivatloo B, Gharehpetian GB (2017) Short-term scheduling of hydro-based power plants considering application of heuristic algorithms: a comprehensive review. *Renew Sust Energy Rev* 74:116–129

Chapter 8

Optimal Scheduling of Electricity-Gas Networks Considering Gas Storage and Power-to-Gas Technology



Amir Talebi and Ahmad Sadeghi-Yazdankhah

8.1 Introduction

Owing to growing concerns about the energy crisis in the world, deployment of wind energy in power grids has increased. By the end of 2019, the total capacity of all wind plants installed in the world was 651 GW which has increased by 10% compared to 2018 [1]. Alongside the benefits of wind energy, its intermittent and uncertain characteristic causes the operation of power grids more complex. On the contrary, gas-fired power units (GFPU) can cope with wind intermittency since they have high flexibility. With the installation of GFPU in power grid, the interdependency of electricity and gas networks must be considered in the scheduling of two networks.

The interdependency of electricity and gas networks has been investigated in various studies. The effect of gas network on the security-constrained scheduling of generation units has been addressed in ref. [2–4]. In reference [5], using piecewise linear approximation, the optimal power and gas flow problem has been structured as mixed-integer linear programming. Alternating direction method of multiplier algorithm has been suggested in ref. [6] to decrease the computational complexity of gas and power system optimization. In [7] it has been demonstrated that pressure drops or gas outages decrease the reliability of power grid because GFPU go to off-line mode. In reference [8] augmented relaxation approach has been applied to optimize electricity and gas network operation. The authors in ref. [9] have shown that the reliability of electricity and gas networks can be affected by each other. Day-ahead scheduling of gas and power systems has been addressed in ref. [10]. In this paper, nonconvex gas flow constraints are relaxed to convex constraints by second-order cone programming. References [11–18] have addressed the interdependency

A. Talebi (✉) · A. Sadeghi-Yazdankhah
Department of Electrical Engineering, Sahand University of Technology, Tabriz, Iran
e-mail: sadeghi@sut.ac.ir

between electricity and gas networks with uncertainties. Reference [11] has used the information-gap decision theory method to incorporate the uncertainty of electricity price in the coordination of electricity and gas systems. References [12, 13] have incorporated wind uncertainty, load forecast error, and random outage of power units/lines in the stochastic scheduling of electricity and gas networks. Optimal scheduling of electricity and gas networks has been addressed in references [14, 15]. In ref. [14] wind uncertainty has been incorporated in a distributionally robust optimal scheduling model. Uncertainties of loads and wind have been considered in the optimal scheduling of electricity-gas networks in ref. [15]. A two-stage robust approach has been proposed in ref. [16] for the coordination of electricity and gas networks with wind uncertainty. The impact of gas delivery uncertainty and gas price variability on the scheduling of power units has been investigated in ref. [17]. The authors in reference [18] have introduced an interval method to optimize the operation of electricity and gas networks under wind uncertainty. However, gas transmission constraints may restrict gas supply to GFPU and influence their operation in power grid. This issue becomes more apparent during high-demand hours. Gas storage can alleviate the impact of gas delivery restrictions on the operation of GFPU by storing/releasing gas in low/high-demand hours. References [19, 20] have shown that power production of GFPU is increased by using gas storage. The effect of gas storage in the robust scheduling of electricity and gas systems has been evaluated in ref. [21].

Recently, by introducing power to gas (PtG) as a promising technology, the interdependency between power grid and gas network has gotten deeper. PtG increases the interdependency of electricity and gas networks by converting extra wind energy to synthetic natural gas, thereby preventing wind energy curtailment. Two processes are carried out in PtG [22]:

1. Electrolysis (to convert wind energy into hydrogen)
2. Methanization (to convert hydrogen into methane)

The produced natural gas can be used by gas consumers in gas network or stored by gas storage for later use. The economic benefits of using PtG in the operation of electricity and gas networks have been evaluated in [23]. Reference [24] has presented a robust model that incorporates PtG technology and uncertainties of wind/electrical load in the co-optimization of electricity and gas networks. The authors in [25] have provided a probabilistic energy flow model for power network and gas system integrated with PtG technology. In reference [26] it has been shown that PtG can be useful in reducing emissions and costs. The authors have introduced the IGDT stochastic method in [27], which evaluates the effect of PtG and demand response on the optimization of two systems.

This chapter introduces a stochastic model to achieve optimal scheduling of electricity and gas networks with the integration of gas storage and PtG technology. This chapter creates the following contributions:

- The influence of gas transmission restrictions on the operation of GFPU in power grid is investigated.
- Gas storage is used to improve the operation of electricity and gas networks, which reduces the impact of gas transmission restrictions on power grid.
- PtG technology is applied to accommodate all wind energy, which converts curtailed wind energy to natural gas.

The remainder of this chapter is as follows: Sect. 8.2 provides the problem formulation of the proposed stochastic model. Simulation results on a test system are shown in Sect. 8.3, and Sect. 8.4 provides the conclusions of this study.

8.2 Problem Formulation

The purpose of the proposed model is to achieve an optimal solution in operation of electricity and gas systems taking into account corresponding constraints. Wind uncertainty is addressed through stochastic optimization. In this optimization method, uncertain parameters are represented by scenarios and their probabilities. Formulation of the stochastic model is provided in the following:

8.2.1 Objective Function

Operation costs (startup/shutdown and production) of non-GFPUs, production cost of gas wells, operation cost of gas storage, and costs of wind curtailment and load shedding are considered as the system costs in this study. The objective function (8.1), which includes these costs, is as follows:

$$\min \sum_s Pb_s \left[\sum_t \left(\sum_{i \notin GF} (STU_{i,t,s}^{NGF} + SHD_{i,t,s}^{NGF} + FC_{i,t,s}(P_{i,t,s})) \right. \right. \\ \left. \left. \sum_{spl} \zeta_{gas} V_{spl,t,s} + \sum_{gt} \zeta_{gt} GS_{gt,t,s}^{dch} \right. \right. \\ \left. \left. \sum_w \zeta^{crit} \cdot (Pe_{w,t,s}^f - Pe_{w,t,s}) + \sum_d \zeta^{shed} \cdot Pd_{d,t,s}^{sh} \right) \right] \quad (8.1)$$

Operational constraints of this optimization model are as follows:

8.2.2 Electricity System Constraints

The production capacity of each power unit is bounded by (8.2):

$$P_i^{\min} r_{i,t,s} \leq P_{i,t,s} \leq P_i^{\max} r_{i,t,s} \quad (8.2)$$

For successive periods, each power unit can increase/decrease its output to a certain value, which is called a ramp-up/down limit. These limitations are presented by (8.3) and (8.4):

$$P_{i,t,s} - P_{i,t-1,s} \leq \text{URM}_i \quad (8.3)$$

$$P_{i,t-1,s} - P_{i,t,s} \leq \text{DRM}_i \quad (8.4)$$

Startup and shutdown costs of non-GFPUs are presented by (8.5) and (8.6):

$$\text{STU}_{i,t,s}^{\text{NGF}} = \text{stu}_i^{\text{ng}}(r_{i,t,s} - r_{i,t-1,s}) \quad i \notin \text{GF} \quad (8.5)$$

$$\text{SHD}_{i,t,s}^{\text{NGF}} = \text{shd}_i^{\text{ng}}(r_{i,t-1,s} - r_{i,t,s}) \quad i \notin \text{GF} \quad (8.6)$$

Gas consumption of GFPUs during startup/shutdown is determined by (8.7) and (8.8):

$$\text{SUP}_{i,t,s}^{\text{GP}} = \text{stg}_i^g(r_{i,t,s} - r_{i,t-1,s}) \quad i \in \text{GF} \quad (8.7)$$

$$\text{SDN}_{i,t,s}^{\text{GP}} = \text{shg}_i^g(r_{i,t-1,s} - r_{i,t,s}) \quad i \in \text{GF} \quad (8.8)$$

Minimum up/down time of power units is stated in (8.9) and (8.10):

$$(L_{i,t-1,s}^{\text{up}} - T_i^{\text{up}})(r_{i,t-1,s} - r_{i,t,s}) \geq 0 \quad (8.9)$$

$$(L_{i,t-1,s}^{\text{down}} - T_i^{\text{down}})(r_{i,t,s} - r_{i,t-1,s}) \geq 0 \quad (8.10)$$

The amount of power transmitted from one bus to another bus at each hour is determined by (8.11) and is bounded by (8.12). Also, the power balance must be satisfied in each bus which is formulated in Eq. (8.13):

$$\text{flw}_{mn,t,s} = \frac{\theta_{m,t,s} - \theta_{n,t,s}}{X_{mn}} \quad (8.11)$$

$$-\text{flw}_{mn}^{\max} \leq \text{flw}_{mn,t,s} \leq \text{flw}_{mn}^{\max} \quad (8.12)$$

$$\sum_{i \in \text{GMM}} P_{i,t,s} + \sum_{w \in \text{WMB}} P e_{w,t,s} - \sum_{q \in \text{PGM}} P t_{q,t,s}^{pgs} - \sum_{d \in \text{DM}} P d_{d,t} + \sum_{d \in \text{DM}} P d_{d,t,s}^{sh} = \sum_{n \in \text{BM}} f l w_{mn,t,s} \quad (8.13)$$

The limitations of load shedding and wind output are specified through (8.14) and (8.15):

$$0 \leq P e_{w,t,s} \leq P e_{w,t,s}^f \quad (8.14)$$

$$0 \leq P d_{d,t,s}^{sh} \leq P d_{d,t} \quad (8.15)$$

8.2.3 Gas Network Constraints

In the gas network, pipelines have a key role and it can be said that they are the most important part of the gas network. Gas pipelines are responsible for transporting fuel from wells to gas loads (such as GFPU and residential consumers). Gas flow in pipelines depends on pressure difference between two nodes, type of gas, and pipeline characteristic (diameter, length, and roughness). Gas flow in pipeline is modeled through Eq. (8.16), in which Γ represents gas flow direction:

$$g f w_{g_m g_n,t,s} = \Gamma(P s_{g_m,t,s}, P s_{g_n,t,s}) \cdot J_{g_m g_n} \sqrt{\left| (P s_{g_m,t,s})^2 - (P s_{g_n,t,s})^2 \right|} \quad (8.16)$$

$$\Gamma(P s_{g_m,t,s}, P s_{g_n,t,s}) = \begin{cases} 1 & P s_{g_m,t,s} \geq P s_{g_n,t,s} \\ -1 & P s_{g_m,t,s} < P s_{g_n,t,s} \end{cases} \quad (8.17)$$

Capacity of gas wells and pressure of nodes are bounded by (8.18) and (8.19):

$$V_{spl}^{\min} \leq V_{spl,t,s} \leq V_{spl}^{\max} \quad (8.18)$$

$$P s_{g_m}^{\min} \leq P s_{g_m,t,s} \leq P s_{g_m}^{\max} \quad (8.19)$$

Similar to the power balance in the electricity grid, the gas balance must be satisfied in each gas node which is modeled by Eq. (8.20):

$$\sum_{spl \in \text{SPN}} V_{spl,t,s} + \sum_{gt \in \text{GSN}} \left(\text{GS}_{gt,t,s}^{dch} - \text{GS}_{gt,t,s}^{ch} \right) - \sum_{i \in \text{GUN}} Gg_{i,t,s} - \sum_{gl \in \text{RGN}} Gd_{gl,t} + \sum_{q \in \text{PGN}} Ht_{q,t,s}^{pgs} = \sum_{g_n \in \text{RN}} gfw_{g_n g_n,t,s} \quad (8.20)$$

The interdependency between the two networks is created by GFPU and PtG. The amount of gas consumption/production of GFPU/PtG is determined by (8.21) and (8.22):

$$Gg_{i,t,s} = (Fg_{i,t,s}^{\text{GP}} + \text{SUP}_{i,t,s}^{\text{GP}} + \text{SDN}_{i,t,s}^{\text{GP}}) / \text{HHV} \quad i \in \text{GF} \quad (8.21)$$

$$Ht_{q,t,s}^{pgs} = \phi \cdot Pt_{q,t,s}^{pgs} \cdot \eta_q^{pgs} / \text{HHV} \quad (8.22)$$

8.2.4 Gas Storage Constraints

When gas consumption in the gas network is low/high, gas storage acts as load/supplier. Technical limitations in the operation of gas storage are given in (8.23)–(8.26). Constraints (8.23)–(8.25) are related to charge/discharge and capacity of storage. The quantity of gas in the storage at time t and scenario s is determined by (8.26):

$$0 \leq \text{GS}_{gt,t,s}^{ch} \leq \text{GS}_{gt}^{ch, \max} \quad (8.23)$$

$$0 \leq \text{GS}_{gt,t,s}^{dch} \leq \text{GS}_{gt}^{dch, \max} \quad (8.24)$$

$$\text{GT}_{gt}^{\min} \leq \text{GT}_{gt,t,s} \leq \text{GT}_{gt}^{\max} \quad (8.25)$$

$$\text{GT}_{gt,t,s} = \text{GT}_{gt,t-1,s} + \eta_{gt}^{ch} \text{GS}_{gt,t,s}^{ch} - \frac{\text{GS}_{gt,t,s}^{dch}}{\eta_{gt}^{dch}} \quad (8.26)$$

8.3 Simulation Results

In this section, simulation results of applying the proposed framework on a case study (6-bus power system with the 6-node gas network [13]) are presented. This test system is depicted in Fig. 8.1. Power system has six buses, three loads, two GFPU, one non-GFPU, and seven power lines. Gas network has six nodes, two residential consumers, five pipelines, and two wells. The electricity system and gas network are coupled through two GFPU and one PtG unit. GFPU are placed in nodes 1 and 3 of

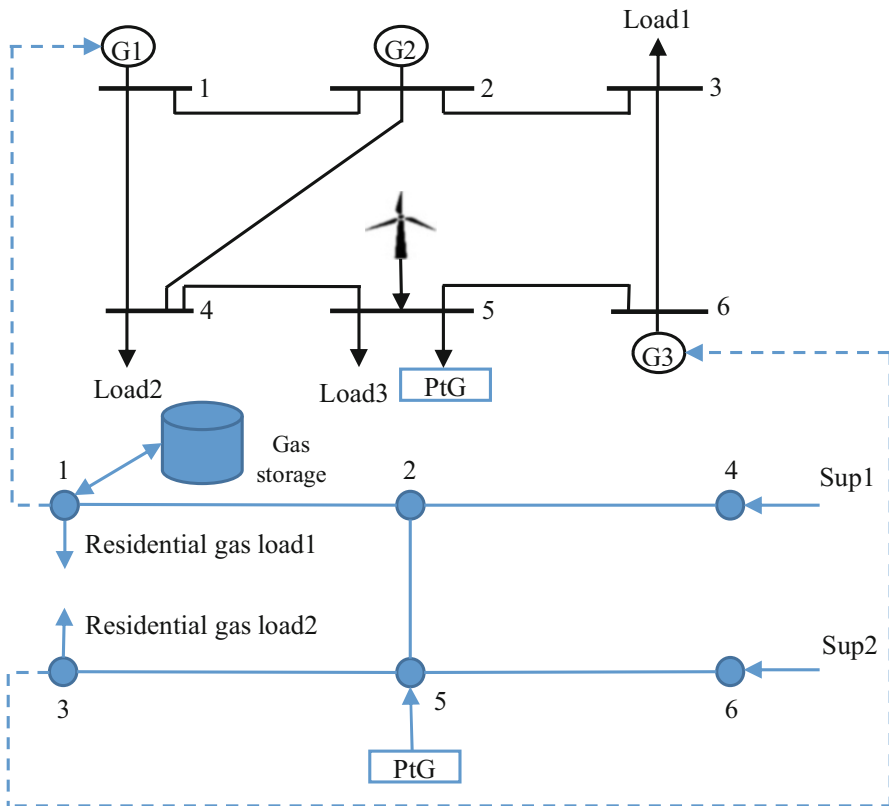


Fig. 8.1 Test system

Table 8.1 Technical data of units

Unit	Ramp (MW/h)	Pmax	Pmin	Min up (h)	Min down (h)	Int. status (h)	α (MBtu/MW ² h)	β (MBtu/MWh)	γ (MBtu/h)
G1	55	220	100	4	4	4	0.0004	13.5	176.9
G2	50	100	10	2	3	-3	0.001	32.6	129.9
G3	20	20	10	1	1	-1	0.005	17.7	137.4

the gas system and buses 1 and 6 of the electricity system. Also, the PtG unit is placed in node 5 of the gas network and bus 5 of the electricity system. GAMS/DICOPT solver is used for solving this model [28]. The data of power units, power lines, electrical loads, gas wells, gas transmission system, residential gas loads, and gas storage are provided in Tables 8.1–8.8. The costs of load shedding and wind spillage are 100\$/MW and 1000\$/MW.

The following cases will be analyzed in the scheduling of electricity and gas networks.

Table 8.2 Parameters of power lines

Line	From bus	To bus	X	Capacity (MW)
1	1	2	0.17	200
2	1	4	0.258	100
3	2	3	0.197	100
4	2	4	0.14	100
5	3	6	0.37	100
6	4	5	0.37	100
7	5	6	0.018	100

Table 8.3 Data of electricity loads

Time (h)	Load (MW)	Time (h)	Load (MW)	Time (h)	Load (MW)	Time (h)	Load (MW)
1	175.1	7	173.3	13	242.1	19	245.9
2	165.1	8	190.4	14	243.6	20	237.3
3	158.6	9	205.5	15	248.8	21	237.3
4	154.7	10	217.2	16	255.7	22	227.1
5	155	11	228.6	17	256	23	201.5
6	160.4	12	236.1	18	246.7	24	196.7

Table 8.4 Parameters of wells

Well	Node	Min (kcf/h)	Max (kcf/h)	Cost (\$/kcf)
1	4	1500	5000	1
2	6	2000	6000	1

Table 8.5 Parameters of pipelines

Pipeline	From node	To node	J (kcf/Psig)
1	1	2	50.6
2	2	4	50.1
3	2	5	37.5
4	3	5	43.5
5	5	6	45.3

Table 8.6 Node pressure data

Node	Min (Psig)	Max (Psig)
1	105	120
2	120	135
3	125	140
4	130	155
5	140	155
6	150	175

Table 8.7 Gas storage data

Node	Min capacity (kcf)	Max capacity (kcf)	Max charge (kcf/h)	Max discharge (kcf/h)	Cost (\$/kcfh)
1	500	3000	500	500	0.5

Table 8.8 Data of residential gas loads

Time (h)	Load (kcf)	Time (h)	Load (kcf)	Time (h)	Load (kcf)	Time (h)	Load (kcf)
1	3000.7	7	3127.6	13	3363	19	3665.6
2	2937.5	8	3396.6	14	3194.7	20	3800
3	2922.9	9	3463.9	15	3228.4	21	3732.8
4	2939.8	10	3553.5	16	3295.7	22	3665.6
5	2998	11	3430.2	17	3396.6	23	3396.6
6	3160.7	12	3430.2	18	3497.5	24	3094.02

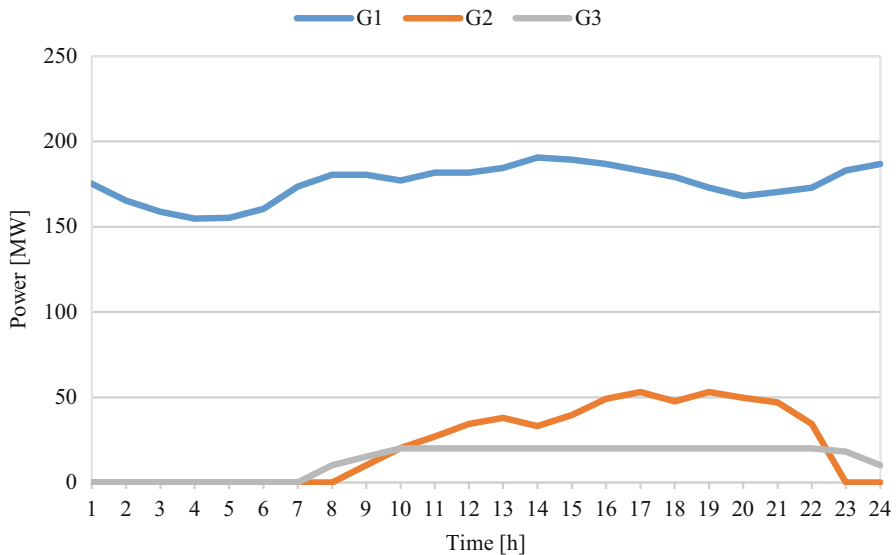


Fig. 8.2 Hourly scheduling of power units

8.3.1 Case 1: Deterministic Scheduling

Hourly dispatch of power units in 24 h is presented in Fig. 8.2. Power unit 1 has the smallest fuel coefficient between power units in this system. So, it is dispatched in all hours. In high-demand hours production of the power unit 1 is impacted by the gas transmission system; therefore, power units 2 and 3 are dispatched to meet the electrical load. The daily cost of the system is \$16,6581.1. It is worth mentioning

that the total production of power units 1 and 2, without gas transmission limitations, is 4552.5 MW and 265.1 MW, respectively. However these values are changed to 4211 MW (unit 1) and 535.1 MW (unit 2), taking into account the limitations of gas transmission system.

8.3.2 Case 2: Incorporating Gas Storage in Case 1

Gas storage by storing/releasing gas in low/high-demand hours reduces the effect of gas network on the operation of GFPU. As shown in Fig. 8.3 (comparison between this case and previous case), production of the power unit 1 (cheapest unit) has been increased in high-demand hours. In contrast, production of the power unit 2 (expensive unit) has been decreased. Table 8.9 gives a summary of these results. According to this table, it can be seen that the total production of power unit 1 has increased by 186.9 MW and the total production of power unit 2 has decreased by 193.8 MW. The daily cost of the system is \$164,202.3.

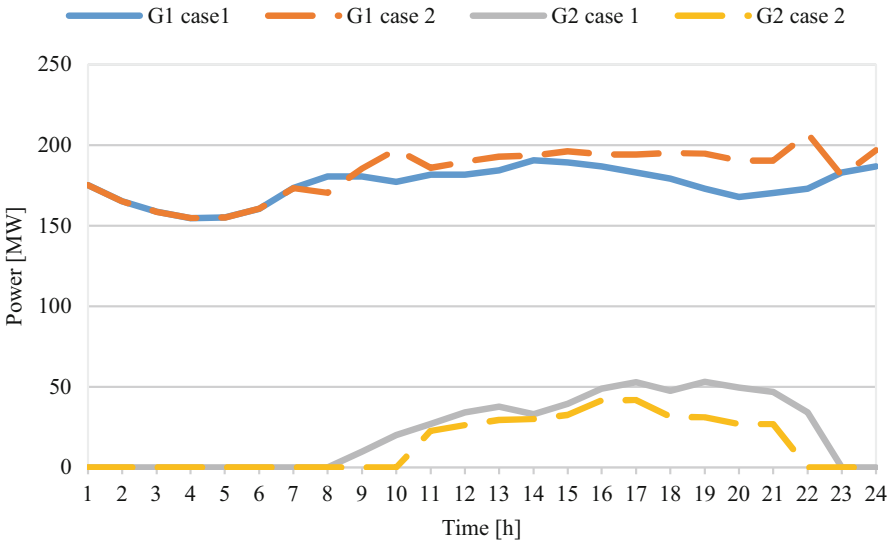


Fig. 8.3 Hourly scheduling of units 1 and 2 in cases 1–2

Table 8.9 Comparison of the total production of units 1 and 2 in cases 1–2

Case	Total production of unit 1 (MW)	Total production of unit 2 (MW)
1	4211	535.1
2	4397.9	341.3

8.3.3 Case 3: Incorporating PtG Unit in Case 2

Figure 8.4 shows the role of the PtG unit in raising the integration of wind energy in electricity and gas networks. As illustrated in this figure, without PtG unit, 360.4 MW of wind energy is curtailed in $t = 1$ to $t = 8$. However with the integration of PtG unit into the model, all curtailed wind energy is converted to natural gas. The produced gas is transferred to the gas system and consumed by gas loads. The total gas production of two gas wells, without the use of PtG unit, is 127,441 kcf. However, using PtG unit, this value is decreased to 126,267.1 kcf. According to this, the daily cost of the system is decreased to \$127,576.8, compared to case 2.

8.3.4 Case 4: Stochastic Scheduling of Case 3

In case 4, wind uncertainty is considered in the scheduling of electricity and gas networks. The normal distribution function with standard deviation of 10% is applied to show the wind forecast error. Wind scenarios are generated by the Monte Carlo method (1000 scenarios with equal probability) [26]. Then, by applying fast backward method in the SCENRED tool, the number of scenarios is decreased to 5 [29]. The daily cost of the system in each scenario is shown in Table 8.10. As represented in this table, in scenarios 3 and 4, the daily cost of the network is more than case 3. This is due to a wind forecast error. Also, power production of power

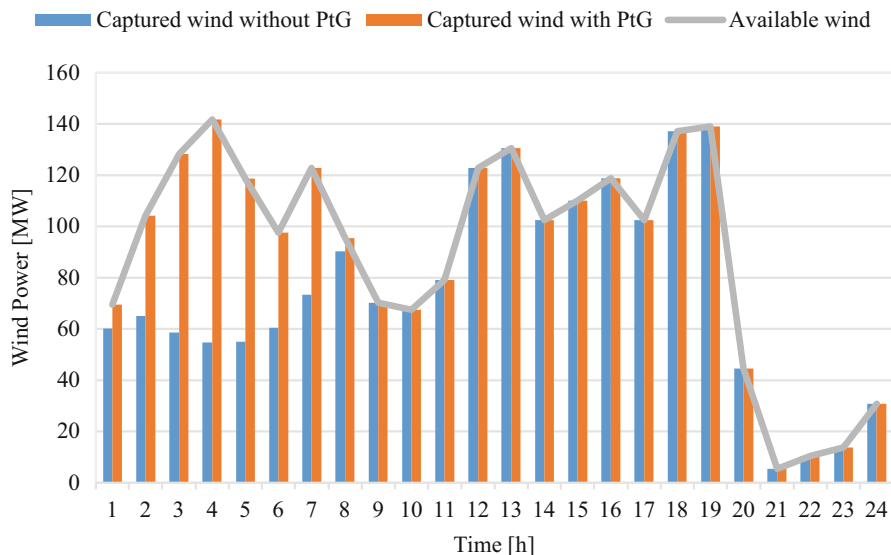


Fig. 8.4 Captured wind power with/without PtG

Table 8.10 Daily cost in each scenario

Scenario	S1	S2	S3	S4	S5
Daily cost	125,477.9	126,981.7	127,829.9	129,315.7	126,369.4

unit 1 and gas production of gas wells in each scenario are presented in Tables 8.11 and 8.12.

8.4 Conclusions

This chapter has presented an approach for scheduling of electricity and gas networks taking into account PtG technology and gas storage. A stochastic programming method has been applied to address the uncertainty pertaining to wind energy. The suggested model determines the cost-effective scheduling of two networks within 24 h while meeting the operational limitations of the two systems. Four different case studies are considered and the corresponding results discussed. Simulation results indicate that gas pipelines limit the transportation of gas to GFPU. So, to meet the electrical loads, expensive units are committed to compensating for the deficiency of generation. In addition, gas storage can relieve the impact of pipelines in the operation of GFPU and lead to lower daily costs. Moreover, PtG unit not only absorbs the excess amount of wind energy (which is wasted in the power system) but also acts as a supplement for gas suppliers. In this way, the daily cost of the network is further reduced.

Nomenclature

Indices

g_m, g_n	Gas nodes
m, n	Electricity system buses
d, gl	Electrical and gas loads
spl, q, t, gt, i, w	Gas supplier, PtG, time, gas storage, power unit, and wind farm
s	Scenario

Sets

GF	Gas-fuel units
SPN, GSN	Gas wells and storages
PGN	Set of PtGs in gas network
DM, RGN	Set of electrical and gas loads
BM, RN	Set of buses and gas nodes
GMM, WMB, BM	Set of power units, wind farm, and buses
PGM	Set of PtGs in electricity system

Table 8.11 Hourly generation of power unit 1 in each scenario

Hour	Scenario					Hour	Scenario				
	1	2	3	4	5		1	2	3	4	5
1	115	115	115	115	115	13	100	107.5	113.2	122.6	103.4
2	100	100	100	100	100	14	129.6	138.1	142.5	149.9	134.8
3	100	100	100	100	100	15	126.2	135.2	140.1	148.1	131.7
4	100	100	100	100	100	16	123.6	133.3	138.5	147.1	129.5
5	100	100	100	100	100	17	141.9	150.3	154.8	162.2	147.1
6	100	100	100	100	100	18	100	105.3	111.3	121.1	100.9
7	100	100	100	100	100	19	112.8	106.4	108.7	121.6	105.1
8	100	100	100	103	100	20	167.8	161.4	163.7	176.6	160.1
9	127.4	133.2	136.3	141.3	130.9	21	201.3	201.7	201.9	202.3	201.5
10	141.9	147.5	150.5	155.3	145.3	22	205.5	196.4	196.9	207.6	196.1
11	140.4	146.9	150.4	156.1	144.4	23	185.6	186.8	187.4	188.4	186.3
12	100	109.5	114.9	123.7	105.6	24	162.4	165	166.3	168.5	164

Table 8.12 Gas production of gas wells in each scenario

Hour	Scenario				
	1	2	3	4	5
1	4635.5	4654.4	4664.5	4681.1	4647.1
2	4319.3	4347.6	4362.7	4529.1	4336.6
3	4201.3	4236.1	4254.8	4285.4	4222.7
4	4147.2	4185.7	4206.3	4240.1	4170.8
5	4263.1	4295.2	4312.4	4340.6	4282.7
6	4494.4	4520.8	4535.1	4558.3	4510.6
7	4411.2	4444.5	4462.3	4491.6	4431.6
8	4837.2	4863.1	4876.9	4929.6	4853.1
9	5320.9	5397.2	5438.1	5505	5367.6
10	5603.4	5677	5716.3	5780.9	5648.5
11	5460.3	5546.4	5592.5	5668.1	5513.1
12	4921.6	5049.5	5120.8	5237.9	4997.9
13	4845.7	4956.2	5032.1	5156.5	4901.4
14	5081.1	5192.4	5251.9	5349.7	5149.3
15	5069.3	5189.1	5253.2	5358.4	5142.7
16	5101.6	5230.7	5299.8	5413.2	5180.7
17	5909.6	5557.5	5617.2	5715.2	5514.4
18	5393.4	5061.1	5140.7	5413.1	5345.6
19	5257.4	5732.1	5630.7	5935.9	5203.4
20	6674.4	6589.8	6668.4	6674.4	6571.1
21	6640.9	6640.9	6640.9	6640.9	6640.9
22	6126.3	6607.2	6607.2	6126.3	6607.2
23	5991.8	5991.8	5991.8	5991.8	5991.8
24	5416.2	5711.1	5840.5	5840.5	5840.5

Parameters

- URM_{*i*}, DRM_{*i*} Ramp-up/down of unit *i*
- T_i^{up}, T_i^{dwn} Minimum up/down time of unit *i*
- stu_i^{ng}, shd_i^{ng} Startup/shutdown cost of non-GFPU
- $Pd_{d,t}, Gd_{gl,t}, Pe_{w,t,s}^f$ Predicted value of electrical and gas loads and wind energy
- p_i^{max}, p_i^{min} Max/min value of unit *i*
- stg_i^g, shg_i^g Startup/shutdown gas usage of GFPU
- flw_{mn}^{max}, X_{mn} Capacity and reactance of power line
- $J_{g_m g_n}$ Pipeline constant
- $V_{i,spl}^{max}, V_{i,spl}^{min}$ Max/min value of gas well
- ζ_{gas}, ζ_{gt} Production/operation cost of gas well/storage
- P_s^{max}, P_s^{min} Max/min value of pressure
- $\zeta_{g_m}^{shed}$ Wind curtailment/load shedding cost
- $\zeta^{crit}, \zeta^{shed}$ Wind curtailment/load shedding cost
- $GS_{gt}^{ch,max}, GS_{gt}^{dch,max}$ Limitation of charge/discharge of storage
- Pb_s Probability of scenario *s*
- $GT_{gt}^{max}, GT_{gt}^{min}$ Max/min value of storage
- $\eta_{gt}^{ch}, \eta_{gt}^{dch}$ Coefficients of gas storage

Variables

$r_{i, t, s}$	Commitment variable
$P_{q,t,s}^{pgs}, H_{q,t,s}^{pgs}$	Power consumption/gas production of PtG
$gfw_{gm,gn,t,s}, flw_{mn,t,s}$	Gas/power flow in pipeline/power line
$GT_{gt, t, s}$	Amount of gas in storage
$P_{i, t, s}, V_{spl, t, s}$	Power/gas production of power unit/gas well
$STU_{i,t,s}^{NGF}, SHD_{i,t,s}^{NGF}$	Startup/shutdown cost of non-GFPU at hour t
$L_{i,t,s}^{up}, L_{i,t,s}^{dwn}$	Up/down time of power unit i
$P_{gm,t,s}^s$	Pressure of node
$Gg_{i, t, s}$	Gas usage of GFPU at time t
$GS_{gt,t,s}^{ch}, GS_{gt,t,s}^{dch}$	Gas storage charge/discharge at hour t
$SUP_{i,t,s}^{GP}, SDN_{i,t,s}^{GP}$	Startup/shutdown gas of GFPU
$Pe_{w, t, s}$	Power production of wind farm at hour t
$Pd_{d,t,s}^{sh}$	Electrical load shedding at hour t
$\theta_{m, t, s}$	Voltage angle of bus m

References

1. Global Status of Wind Power. (2019). <https://gwec.net/global-wind-report-2019/>
2. Shahidehpour M, Fu Y, Wiedman T (2005) Impact of natural gas infrastructure on electric power systems. Proc IEEE 93(5):1042–1056
3. Li T, Eremia M, Shahidehpour M (2008) Interdependency of natural gas network and power system security. IEEE Trans Power Syst 23(4):1817–1824
4. Liu C, Shahidehpour M, Fu Y, Li Z (2009) Security-constrained unit commitment with natural gas transmission constraints. IEEE Trans Power Syst 24(3):1523–1536
5. Yang L, Zhao X, Li X, Feng X, Yan W (2019) An MILP-based optimal power and gas flow in electricity-gas coupled networks. Energy Procedia 158:6399–6404
6. Wen Y, Qu X, Li W, Liu X, Ye X (2017) Synergistic operation of electricity and natural gas networks via ADMM. IEEE Trans Smart Grid 9(5):4555–4565
7. Fedora PA. Reliability review of North American gas/electric system interdependency. In: 37th Annual Hawaii International Conference on System Sciences, 2004. Proceedings of the, 2004. IEEE, p 10 pp.
8. Biskas P, Kanelakis N, Papamathaiou A, Alexandridis I (2016) Coupled optimization of electricity and natural gas systems using augmented Lagrangian and an alternating minimization method. Int J Electr Power Energy Syst 80:202–218
9. Correa-Posada CM, Sanchez-Martin P, Lumbreras S (2017) Security-constrained model for integrated power and natural-gas system. J Mod Power Syst Clean Energy 5(3):326–336
10. Xu Y, Zhao F, Lai LL, Wang Y. Integrated electricity and natural gas system for day-ahead scheduling. In: 2019 IEEE International Conference on Systems, Man and Cybernetics (SMC), 2019. IEEE, pp 2242–2247
11. Sohrabi F, Jabari F, Mohammadi-Ivatloo B, Soroudi A (2019) Coordination of interdependent natural gas and electricity systems based on information gap decision theory. IET Gener Transm Distrib 13(15):3362–3369
12. Alabdulwahab A, Abusorrah A, Zhang X, Shahidehpour M (2015) Coordination of interdependent natural gas and electricity infrastructures for firming the variability of wind energy in stochastic day-ahead scheduling. IEEE Trans Sustainable Energy 6(2):606–615
13. Alabdulwahab A, Abusorrah A, Zhang X, Shahidehpour M (2017) Stochastic security-constrained scheduling of coordinated electricity and natural gas infrastructures. IEEE Syst J 11(3):1674–1683

14. Zhang Y, Le J, Zheng F, Zhang Y, Liu K (2019) Two-stage distributionally robust coordinated scheduling for gas-electricity integrated energy system considering wind power uncertainty and reserve capacity configuration. *Renew Energy* 135:122–135
15. He C, Wu L, Liu T, Wei W, Wang C (2018) Co-optimization scheduling of interdependent power and gas systems with electricity and gas uncertainties. *Energy* 159:1003–1015
16. Yang J, Zhang N, Kang C, Xia Q (2018) Effect of natural gas flow dynamics in robust generation scheduling under wind uncertainty. *IEEE Trans Power Syst* 33(2):2087–2097
17. Zhao B, Conejo AJ, Sioshansi R (2017) Unit commitment under gas-supply uncertainty and gas-price variability. *IEEE Trans Power Syst* 32(3):2394–2405
18. Bai L, Li F, Cui H, Jiang T, Sun H, Zhu J (2016) Interval optimization based operating strategy for gas-electricity integrated energy systems considering demand response and wind uncertainty. *Appl Energy* 167:270–279
19. Talebi A, Sadeghi-Yazdankhah A, Mirzaei MA, Mohammadi-Ivatloo B. Co-optimization of Electricity and Natural Gas Networks Considering AC Constraints and Natural Gas Storage. In: 2018 Smart Grid Conference (SGC), 2018. IEEE, pp 1–6
20. Zhang X, Che L, Shahidehpour M. Impact of natural gas system on short-term scheduling with volatile renewable energy. In: Power & Energy Society General Meeting, 2015 IEEE, 2015. IEEE, pp 1–5
21. He Y, Shahidehpour M, Li Z, Guo C, Zhu B (2017) Robust constrained operation of integrated electricity-natural gas system considering distributed natural gas storage. *IEEE Transactions on Sustainable Energy* 9(3):1061–1071
22. Guoqiang S, Shuang C, Zhinong W, Sheng C (2017) Multi-period integrated natural gas and electric power system probabilistic optimal power flow incorporating power-to-gas units. *J Mod Power Syst Clean Energy* 5(3):412–423
23. Yu X, Zhu G, Wang S, Ding Y. Economic Impact of Power to Gas in Integrated Electricity and Gas System with High Wind Penetration. In: 2018 IEEE Innovative Smart Grid Technologies-Asia (ISGT Asia), 2018. IEEE, pp 640–645
24. He C, Wu L, Liu T, Shahidehpour M (2017) Robust co-optimization scheduling of electricity and natural gas systems via ADMM. *IEEE Trans Sustainable Energy* 8(2):658–670
25. Chen S, Wei Z, Sun G, Cheung KW, Sun Y (2016) Multi-linear probabilistic energy flow analysis of integrated electrical and natural-gas systems. *IEEE Trans Power Syst* 32(3):1970–1979
26. Nazari-Heris M, Mirzaei MA, Mohammadi-Ivatloo B, Marzband M, Asadi S (2020) Economic-environmental effect of power to gas technology in coupled electricity and gas systems with price-responsive shiftable loads. *J Clean Prod* 244:118769
27. Mirzaei MA, Nazari-Heris M, Mohammadi-Ivatloo B, Zare K, Marzband M, Anvari-Moghaddam A (2020) A novel hybrid framework for co-optimization of power and natural gas networks integrated with emerging technologies. *IEEE Systems Journal* 14(3):3598–3608
28. DICOPT manual – GAMS <https://www.gams.com/latest/docs/gams.pdf>
29. GAMS/SCENRED <https://www.gams.com/latest/docs/gams.pdf>

Chapter 9

Uncertainty Modeling in Operation of Multi-carrier Energy Networks



Manijeh Alipour, Mehdi Jalali, Mehdi Abapour, and Sajjad Tohidi

9.1 Introduction

The progress in the technological innovations of distributed generation in the last decades has led to establishment of the smart grid. This development serves as an aegis for distributed energy resources comprising energy storage, wind, and combined heat and power units in response to reliability, emission, efficiency, and economic enhancement of future energy requirement (biofuel, heat, electricity, hydrogen, cooling, etc. [1]). The energy resource incorporation to the distribution network may not only be helpful for customers in terms of participating in the energy management and energy production in order to lessen their costs; it will be fruitful in peak time intervals to diminish the generators' starting costs and to foil transmission line expansion costs. The smart grid concept, which is portrayed in [2], presents a picture to realize the aims of optimal operation of the energy resources.

Recently, integrated energy systems are considered as “microgrid [3]” and “energy hub [4].” An energy hub (EH) is defined as a multi-carrier energy system consisting of multiple energy conversion, storage, and/or network technologies. An EH is characterized by some degree of local control and exists on various spatial scales, from the level of a single building to a larger geographic region. Combined with energy storage, conversions between various energy carriers in an EH facilitate greater flexibility in the energy supply [5]. Multi-carrier energy systems (MESs) provide various types of energy to customers like the natural gas, electricity, cool, and heat. The interdependency among natural gas, heating, and power systems is rising due to the extensive growth of electrically powered heating facilities and cogeneration systems. The EH performs as a transitional agent amid consumers and

M. Alipour (✉) · M. Jalali · M. Abapour · S. Tohidi
Faculty of Electrical and Computer Engineering, University of Tabriz, Tabriz, Iran
e-mail: alipour@tabrizu.ac.ir; mehdi.jalali@tabrizu.ac.ir; abapour@tabrizu.ac.ir;
stohidi@tabrizu.ac.ir

suppliers. Therefore, multi-energy incorporation is a prevailing tendency and the EH is supposed to perform a pivotal role in allotting energy sources more effectively. In addition, energy hubs are especially beneficial for enabling the integration of intermittent renewable energy resources like solar and wind. Regarding the characteristics of combined cooling, heating, and power (CCHP)-based MESs, various operation strategies are established to improve the environmental and economic benefits [6]. Moreover, uncertainties deriving from renewable energy sources and energy demand are challenging the operation of MESs and could threaten the system efficacy.

The literature contains several studies on the scheduling of energy hubs and microgrids considering the uncertainty sources. A few works are described here briefly. The optimal probabilistic scheduling of EHs is addressed in [7]. Load and price uncertainties as the most ambiguous parameters are modeled using a $2m + 1$ point estimation method. In order to evaluate the coordinated operation of MESs a robust optimization is presented in [8]. The main objective of established model is to minimize the overall cost of the MES, by employing natural gas structure dynamics and power system uncertainties. A management structure for the smart island comprising water hub and smart energy and microgrid is provided in ref. [8]. The main aim of the model in ref. [8] is to minimize the total operation and investment costs in addition to the environmental pollutant costs. Due to the uncertainties in the proposed management framework, scenario-based approach is presented to model the uncertainty factors. An optimal load dispatch model is proposed in ref. [9] for a community energy hub. The aim of ref. [9] is to lessen the total cost of community energy hub, comprising CO₂ emission cost and operation cost. The uncertainties associated with electric vehicles are developed utilizing the Monte Carlo simulation, and also a robust optimization method is implemented to handle the power market's price uncertainty.

The interval optimization [10, 11] minimizes the overall cost interval rather than the worst-case scenarios' cost in the robust optimization. Moreover, it operates mathematically better than stochastic optimization. An interval optimization-based scheduling framework for gas- and electricity-embedded energy systems is presented in ref. [12] considering wind uncertainty.

This chapter mainly focuses on the CCHP-based MES scheduling under various uncertainties. The interval optimization is presented in the chapter to tackle energy hub uncertainties. The EH uncertainties include wind power and electricity demand that are described as interval numbers. In addition, the stochastic optimization and interval optimization methods are being conducted for evaluation.

9.2 Arithmetic and Pessimistic Preference Order Relation of Interval Numbers

An interval number characterizes the domain of a random variable. It takes its left and right boundaries, where the right limit of the interval number represents the greatest possible quantity of a random variable, and the left limit represents the lowest possible quantity. Further, interval numbers could be symbolized by their width and mean value. Bear in mind that \tilde{C} and \tilde{D} are two interval cost quantities in a minimization problem. The interval numbers' expanded addition, scalar multiplication, and subtraction are described in the following [13]:

$$\tilde{C} = [c^L, c^R] = \{c : c^L \leq c \leq c^R\} \quad (9.1)$$

$$\tilde{C} = \langle m(\tilde{C}), w(\tilde{C}) \rangle = \{b | m(\tilde{C}) - w(\tilde{C}) \leq c \leq m(\tilde{C}) + w(\tilde{C})\} \quad (9.2)$$

$$m(\tilde{C}) = (c^L + c^R)/2 \quad (9.3)$$

$$w(\tilde{C}) = (c^R - c^L)/2 \quad (9.4)$$

$$\lambda \tilde{C} = \lambda [c^L, c^R] = \begin{cases} [\lambda c^L, \lambda c^R] & \text{if } \lambda \geq 0 \\ [\lambda c^R, \lambda c^L] & \text{if } \lambda < 0 \end{cases} \quad (9.5)$$

$$\tilde{C} + \tilde{D} = [c^L + d^L, c^R + d^R] \quad (9.6)$$

$$\tilde{C} - \tilde{D} = [c^L - d^R, c^R - d^L] \quad (9.7)$$

$$m(\tilde{C} + \tilde{D}) = m(\tilde{C}) + m(\tilde{D}) \quad (9.8)$$

$$m(\tilde{C} - \tilde{D}) = m(\tilde{C}) - m(\tilde{D}) \quad (9.9)$$

$$w(\tilde{C} + \tilde{D}) = w(\tilde{C} - \tilde{D}) = w(\tilde{C}) + w(\tilde{D}) \quad (9.10)$$

A predilection ordering procedure for interval numbers is suggested in [14], from a pessimistic operator's viewpoint. In this respect, fuzzy function, the predilection level between \tilde{C} and \tilde{D} , is delineated for a decision maker's tendency on \tilde{C} over \tilde{D} (9.11). In addition, a pessimism degree, i.e., ξ , has been assigned in the range [0, 1] to describe the decision maker's risk acceptance. Then, the EH's pessimism degree would be compared with fuzzy value to decide which interval is desirable: If $P_C(\tilde{C}) < \xi$, \tilde{C} is superior to \tilde{D} ; if $P_D(\tilde{C}) > \xi$, \tilde{D} is preferable than \tilde{C} :

$$P_{D'}(\tilde{C}) = \begin{cases} 1 & \text{if } m(\tilde{C}) = m(\tilde{D}) \\ \frac{c^R - c^R}{w(\tilde{B}) - w(\tilde{D})} & \text{if } m(\tilde{C}) \leq m(\tilde{D}) \leq c^R - w(\tilde{D}) \\ 0 & \text{otherwise} \end{cases} \quad (9.11)$$

Model (9.12) introduces the creation of interval optimization. The interval numbers' tendency to order from a pessimistic operator's viewpoint could be streamlined [15]. So, $\tilde{C} \succ \tilde{D}$ is in conformity with (9.13). Put it another way, Eq. (9.13) is a satisfactory and crucial requirement for evaluating that \tilde{D} is preferred to \tilde{C} . The interval optimization can be converted to (9.14):

$$\begin{aligned} \min \tilde{U} &= f(x, \tilde{y}) \\ h(x, \tilde{y}) &= 0 \\ g(x, \tilde{y}) &\geq 0 \end{aligned} \quad (9.12)$$

$$m(\tilde{C}) + (1 - \xi) \times w(\tilde{C}) \succ m(\tilde{D}) + (1 - \xi) \times w(\tilde{D}) \quad (9.13)$$

$$\begin{aligned} \min m(\tilde{U}) &+ (1 - \xi) \times w(\tilde{U}) \\ \tilde{H} &= h(x, \tilde{y}) \\ \tilde{G} &= g(x, \tilde{y}) \end{aligned} \quad (9.14)$$

$$m(\tilde{H}) + (1 - \xi) \times w(\tilde{H}) = 0$$

$$m(\tilde{G}) + (1 - \xi) \times w(\tilde{G}) \geq 0$$

$$m(\tilde{C}) = (c^L + c^R)/2 \quad (9.15)$$

$$m(\tilde{C}) = (c^R + c^L)/2 \quad (9.16)$$

9.3 Energy Hub Description

The EH configuration is a usual hybrid design of several energy sources as illustrated in Fig. 9.1. Regarding the disparity of the production of energy flow, the structure can be split into three function components. The first component is the trigeneration unit that includes an absorption chiller, a waste heat recovery device, and a microturbine. The second component is the electricity unit that is composed of batteries, photovoltaics, and power grid. Ultimately, the heating unit as the third unit is a ground source heat pump. The inputs of the EH are gas, solar, and

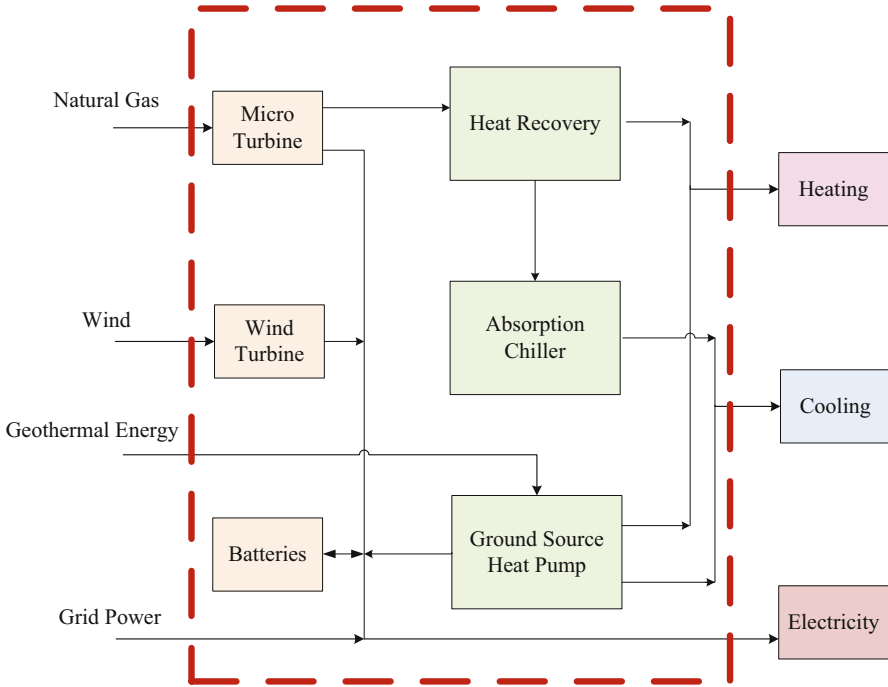


Fig. 9.1 Structure of the CCHP-based energy hub

geothermal energies, and electrical energy from the grid. Moreover, the outputs are electrical, cooling, and thermal energies which will satisfy the electric, cooling, and heat demands.

9.4 Optimal Scheduling of Energy Hub

The chapter aims to achieve the optimal schedules of EH by considering uncertainties in the real-world situation. The interval-based optimization is implemented to model the uncertainties related to the hub’s wind power generation and energy hub’s load.

9.4.1 Objective Function

The hub’s objective function could be written as (9.17):

$$\min \left\{ \sum_{t=1}^{N_T} \left(P_{\text{Buy},t}^{\text{grid}} - P_{\text{Sale},t}^{\text{grid}} \right) \cdot c^{\text{grid}} + c^{\text{fuel}} \cdot G_t^{\text{MT}} + \left(c_{\text{cur}}^D P_{\text{cur},t}^D + c_{\text{cur}}^w P_{\text{cur},t}^w \right) \right. \\ \left. + \left(c^{\text{MT}} \cdot P_t^{\text{MT}} + c^{\text{HP}} \cdot Q_t^{\text{HP}} \right) + c^{\text{Bat}} \cdot E_t^{\text{Bat}} + p^{\text{em}} \cdot \left(\eta^{\text{grid}} P_t^{\text{grid}} + \eta^{\text{MT}} G_t^{\text{MT}} \right) \right\}. \quad (9.17)$$

The first term of objective function denotes the net purchased cost from upper grid. The second and third terms state the fuel cost, and interrupted electrical load and curtailed wind generation costs, respectively. The microturbines and heat pumps' maintenance costs are presented in the fourth term. Besides, the batteries' depreciation cost and the carbon emission influenced by power exchange with the upper grid and microturbine output power are represented in the fifth and the last terms, respectively.

9.4.2 Constraints

In this section equal and unequal constraints of components and proposed system are presented.

9.4.2.1 Microturbine

Integrating heat recovery causes recycling of thermal energy which is used to supply thermal loads besides absorption chiller. In (9.18)–(9.19), the conversion relation among the electricity, heat, and natural gas is presented:

$$G_t^{\text{MT}} = \frac{P_t^{\text{MT}}}{\eta_t^{\text{GMT}} h^v} \quad (9.18)$$

$$Q_t^{\text{MT}} = G_t^{\text{MT}} h^v (1 - \eta_t^{\text{GMT}} - c^{\text{TL}}) \quad (9.19)$$

where parameters η_t^{GMT} , h^v , and c^{TL} are generation efficiency, heat value of 1 m³ natural gas, and coefficient of thermal loss, respectively. In order to model the performance of microturbine in different loading conditions, the fitted value of generation efficiency is formulated as follows:

$$\eta_t^{\text{GMT}} = \alpha + \beta \left(\frac{P_t^{\text{MT}}}{C_t^{\text{MT}}} \right) + \gamma \left(\frac{P_t^{\text{MT}}}{C_t^{\text{MT}}} \right)^2 + \varsigma \left(\frac{P_t^{\text{MT}}}{C_t^{\text{MT}}} \right)^3 \quad (9.20)$$

parameters α , β , γ , and ς are constant coefficients, and C_t^{MT} denotes maximum power output of microturbine. The trigeneration unit's generated heating and cooling capacity can be determined based on microturbines' heat output as follows:

$$Q_t^{\text{MT}} = \frac{1}{\eta^{\text{HR}}} \left(Q_{\text{heating},t}^{\text{HR}} + Q_{\text{cooling},t}^{\text{HR}} \right) \quad (9.21)$$

$$Q_t^{\text{AC}} = Q_{\text{cooling},t}^{\text{HR}} \cdot \omega^{\text{AC}} \quad (9.22)$$

It is noteworthy that devices should be operated considering capacity limits. The pertaining constraints are as follows:

$$P_{\min}^{\text{MT}} \leq P_t^{\text{MT}} \leq P_{\max}^{\text{MT}} \quad (9.23)$$

$$Q_{\min}^{\text{AC}} \leq Q_t^{\text{AC}} \leq Q_{\max}^{\text{AC}} \quad (9.24)$$

9.4.2.2 Energy Storage Unit

The current energy storage charging state can be written as

$$E_t = E_{t-1}(1 - \delta) + \Delta T \left(x_t^{\text{ch}} \frac{P_t^{\text{ch}} \eta^{\text{ch}}}{C^{\text{B}}} - x_t^{\text{dis}} \frac{P_t^{\text{dis}}}{\eta^{\text{dis}} C^{\text{B}}} \right) \quad (9.25)$$

Cycle of charging and discharging and state of charge should be limited due to material properties and excessive price. By introducing x_t^{ch} and x_t^{dis} as binary variables of charging and discharging, i.e., $x_t^{\text{ch}}, x_t^{\text{dis}} \in \{0, 1\}$, the charging and discharging process can be written as follows:

$$x_t^{\text{ch}} + x_t^{\text{dis}} \leq 1 \quad (9.26)$$

$$P_{\min}^{\text{ch}} \times x_t^{\text{ch}} \leq P_t^{\text{ch}} \leq P_{\max}^{\text{ch}} \times x_t^{\text{ch}} \quad (9.27)$$

$$0 \leq P_t^{\text{dis}} \leq P_{\max}^{\text{dis}} \times x_t^{\text{dis}} \quad (9.28)$$

$$\sum_{t=1}^t |x_t^{\text{ch}} - x_{t-1}^{\text{ch}}| \leq N^{\text{ch}} \quad (9.29)$$

$$\sum_{t=1}^t |x_t^{\text{dis}} - x_{t-1}^{\text{dis}}| \leq N^{\text{dis}} \quad (9.30)$$

$$E_{\min} \leq E_t \leq E_{\max} \quad (9.31)$$

Due to the grid limitation, the exchanged electricity with the grid in peak and valley hours should be limited as follows:

$$P_{\min}^{\text{G}} \leq P_t^{\text{G}} \leq P_{\max}^{\text{G}} \quad (9.32)$$

9.4.2.3 Heating Unit

The efficiency of ground source heat pump is formulated in (9.33) to model different values of heat pump, regarding the state of cooling and heating:

$$\eta^{\text{HP}} = \frac{Q_t^{\text{HP}}}{P_t^{\text{HP}}} \quad (9.33)$$

9.4.2.4 Energy Balance Constraints

The constraints corresponding to the equality of supply and demand in terms of electricity, heating, and cooling can be stated as follows:

$$P_t^W - P_{t,\text{cur}}^W + P_t^{\text{MT}} + P_t^G + P_t^{\text{dis}} = P_t^D - P_{t,\text{cur}}^D + P_t^{\text{HP}} + P_t^{\text{ch}} \quad (9.34)$$

$$Q_t^{\text{HR}} + Q_t^{\text{HP}} = Q_{\text{heating},t}^D \quad (9.35)$$

$$Q_t^{\text{AC}} + Q_t^{\text{HP}} = Q_{\text{cooling},t}^D \quad (9.36)$$

9.5 Interval Optimization Model of Hub in the Day-Ahead Stage

To handle the uncertainties, the grid exchange, interrupted electrical load, and curtailed wind power are allowed to alter surrounded by a restricted range. The objective function value considering the interval optimization, involving the interval variables, can be written as

$$\begin{aligned} \min \left\{ \sum_{t=1}^{N_T} \left([m(\mathbf{P}_t^{\text{grid}}) + (1 - \xi_{\text{of}})w(\mathbf{P}_t^{\text{grid}})] .c^{\text{grid}} + c^{\text{fuel}} .G_t^{\text{MT}} \right. \right. \\ \left. \left. + \left(c_{\text{cur}}^D [m(\tilde{\mathbf{P}}_{\text{cur},t}^D) + (1 - \xi_{\text{of}})w(\tilde{\mathbf{P}}_{\text{cur},t}^D)] + c_{\text{cur}}^W [m(\tilde{\mathbf{P}}_{\text{cur},t}^W) + (1 - \xi_{\text{of}})w(\tilde{\mathbf{P}}_{\text{cur},t}^W)] \right) \right. \right. \\ \left. \left. + (c^{\text{MT}} .P_t^{\text{MT}} + c^{\text{HP}} .Q_t^{\text{HP}}) + c^{\text{Bat}} .E_t^{\text{Bat}} + p^{\text{em}} .(\eta^{\text{grid}} [m(\mathbf{P}_t^{\text{grid}}) + (1 - \xi_{\text{of}})w(\mathbf{P}_t^{\text{grid}})] + \eta^{\text{MT}} G_t^{\text{MT}}) \right\} \quad (9.37) \end{aligned}$$

The constraints in Sect. 9.4 will be adjusted to incorporate the uncertainty of electrical load and wind power in terms of interval numbers. Therefore, the interval-based EH operation can be resolved regarding the procedure outlined in Sect. 9.2.

9.6 Simulation Studies

The proposed interval-based scheduling is applied on the energy hub configuration which is a usual hybrid design of several energy sources as illustrated in Fig. 9.1. The interval and stochastic simulations are conducted to compare two methods. The system data are adopted from [16] and the CNY is converted to USD. The gas price and the carbon emission tax are 0.6 \$m³ and 0.87 \$kg, respectively. The grid power price is set to 0.16 \$kWh. The system parameters are presented in Table 9.1. Moreover, the cooling and heat demands of the hub in a typical day of summer are demonstrated in Fig. 9.2 [17].

Up to 20% of the electrical load is supposed to be curtailable in emergencies. The penalty factors for interrupted electrical load and curtailed wind power are supposed to be 1 \$/kWh and 0.5 \$/kWh [18]. In order to assess the model, two case studies, i.e., the interval-based and stochastic-based optimization models, are designed.

Table 9.1 System data

Parameter	Value	Parameter	Value
c^{TL}	0.26	η^{MT}	1.96 kg/m ³
η^{HP}	4.09	η^{grid}	0.872 kg/kWh
η^{ch}/η^{dis}	0.95/0.96	c^{Bat}	0.014 \$/kW
c^{MT}	0.011 \$/kW	η_t^{GMT}	0.3
c^{HP}	0.0011	δ	0.04
h^v	9.7 kW h/m ³	ω^{AC}	1.1

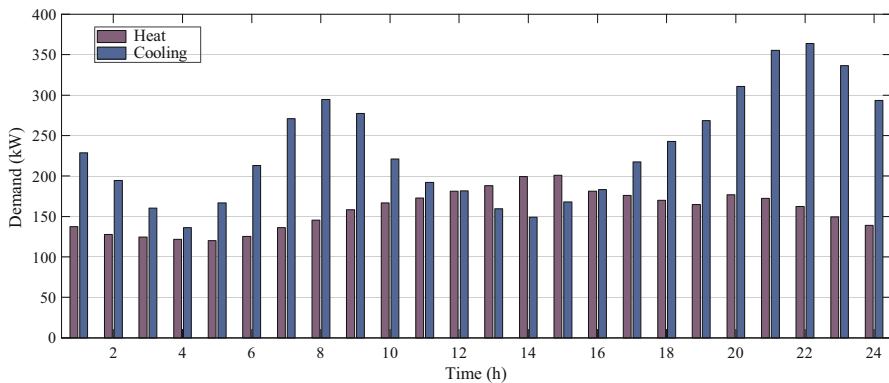


Fig. 9.2 The cooling and heat demands of the hub

9.6.1 Case Study 1: Interval-Based Scheduling of CCHP Systems

The interval optimization method is employed as an uncertainty modeling approach. The pessimism degree of hub’s total cost is set to be 0.3. Further, the pessimism degree for the DG’s output is assumed to be 0 to prevent the contravention of the constraints. The ARIMA model is utilized to forecast the wind generation and load intervals [19, 20]. The wind power and electrical demand intervals are presented in Fig. 9.3. As it was mentioned, the grid power exchange, the unserved load, and the curtailed wind power are assumed to be flexible in a specific range to handle the wind power and load uncertainties.

The power production of units as well as the energy exchanges with the grid are depicted in Fig. 9.4. According to Fig. 9.5, the hub will sell in 12:00–16:00. In 12:00–16:00 the wind generation is in a high level and the electrical load is in low level. Therefore, the hub will sell the energy to the grid and charge the battery. Moreover, it will buy electrical energy in 1:00–11:00 since the wind generation is in low level. The lower level of exchanged energy with the grid is zero to minimize the cost interval. The curtailed load interval is illustrated in Fig. 9.5. Regarding Fig. 9.5, there is no curtailed load in 12:00–16:00 which is in the same direction of the results of energy production in the hub. It should be mentioned that indicating the simulation outputs, the wind generation curtailment is determined to be zero and not shown in Fig. 9.4. Table 9.2 represents the sensitivity analysis of the pessimism degree for the cost. By increasing the pessimism degree, the EH is apt to more uncertainty level to lessen the cost midpoint. The model will turn out to be a worst-case optimization, once the pessimism degree of the cost is set to zero. These outputs can provide notification of the cost intervals for the hub’s decision maker to select optimal preferred pessimism degree of cost values.

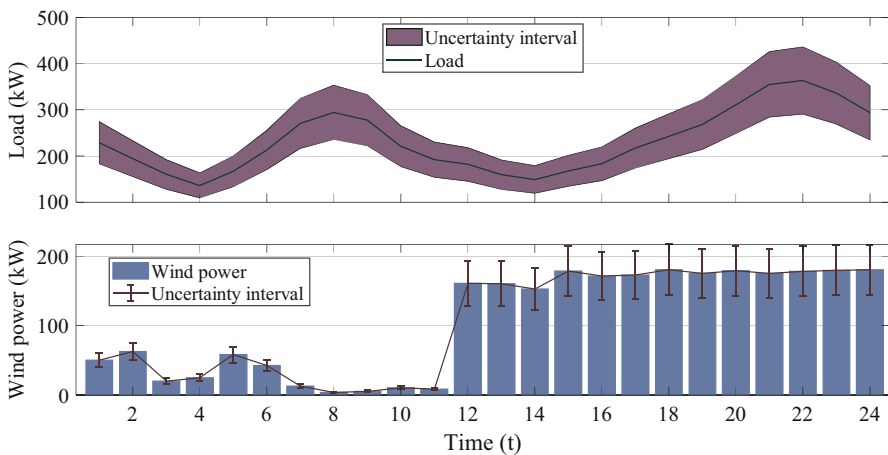


Fig. 9.3 Wind power and electrical load intervals

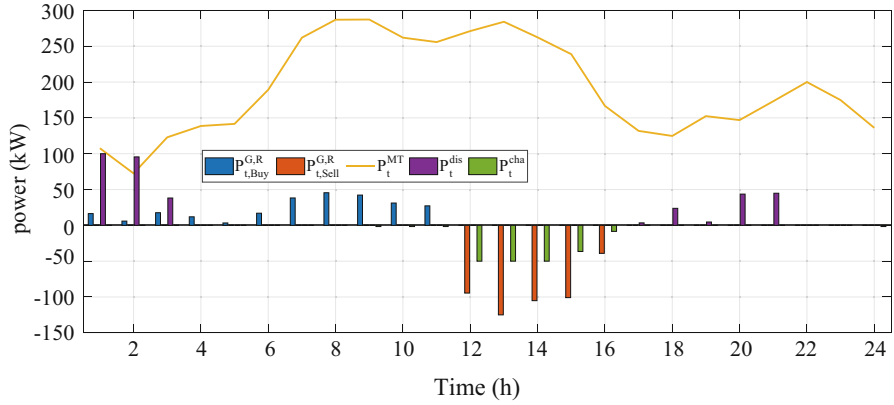


Fig. 9.4 The generated power results for the interval optimization

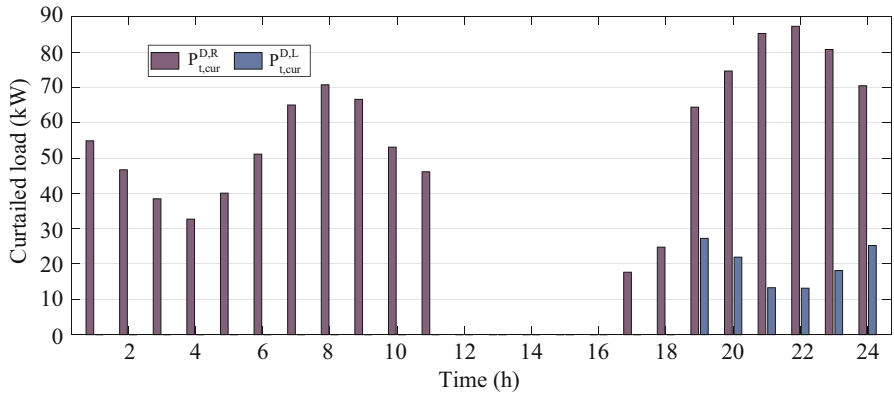


Fig. 9.5 The curtailed electrical load results for the interval optimization

Table 9.2 The energy hub’s degree of pessimism effects for cost

Pessimism degree ξ_f	Cost interval (\$)	Cost midpoint (\$)
0	(27,791.1, 30,785.7)	29,288.4
0.2	(27,770.2, 30,791.2)	29,280.7
0.4	(27,763.4, 30,796.5)	29,279.9
0.6	(27,750.3, 30,802.9)	29,276.6
0.8	(27,719.5, 30,820.2)	29,269.8
1	(27,675.1, 30,825.1)	29,250.1

Table 9.3 Simulation result comparison

Uncertain parameter interval	Cost for interval optimization (\$)	Cost for stochastic optimization (\$)
10	29,275.4	29,274.7
20	29,278.6	29,276.5
30	29,282.2	29,280.1

9.6.2 Case Study 2: Stochastic-Based Scheduling of CCHP Systems

For the stochastic optimization, the scenario generation and reduction procedures [19, 20] are implemented to acquire the scenario set including 20 wind power and 20 electrical load scenarios. The total costs of EH operation for the interval and stochastic optimization methods are provided in Table 9.3. The pessimism degree of hub's total cost is set to 0.5. Regarding Table 9.3, it can be noticed that by considering a certain interval for uncertain parameters, the operation cost for the stochastic optimization is less than interval optimization's cost. This observation is due to the stochastic optimization endeavor to minimize the expected operation costs for the scenario sets. Although the computing time complexity of stochastic optimization can be significantly reduced by using the scenario reduction procedure, the rare extreme occurrences will be omitted. As a conclusion, the reliability of stochastic optimization is undesirable in the real-world scheduling.

9.7 Conclusions

This chapter introduces an interval-based optimization model for the scheduling of CCHP-based EHs. The authors employ interval optimization for considering electrical load and wind power uncertainties. The interval optimization only requires the upper and lower bounds of uncertain parameter prediction to resolve the hub's scheduling problem. According to the simulation results, the cost interval increases by increasing the pessimism degree. The results of interval optimization can assist the EH's decision maker to decide on the optimal preferred values for the pessimism degree. In addition, the stochastic optimization is carried out for comparison. Regarding the comparison results, interval optimization is an appropriate and practicable method to handle uncertain parameters without knowing the probability distribution supposition. In addition, the proposed interval optimization offers both reliability and economy advantages, in comparison with the stochastic optimization method.

References

1. Gu W, Wu Z, Bo R, Liu W, Zhou G, Chen W, Wu Z (2014) Modeling, planning and optimal energy management of combined cooling, heating and power microgrid: a review. *Int J Electr Power Energy Syst* 54:26–37
2. Moradijoo M, Moghaddam MP, Haghifam MR, Alishahi E (2013) A multi-objective optimization problem for allocating parking lots in a distribution network. *Int J Electr Power Energy Syst* 46:115–122
3. Jalali M, Zare K, Seyedi H, Alipour M, Wang F (2019) Distributed model for robust real-time operation of distribution systems and microgrids. *Electr Power Syst Res* 177:105985
4. Frik R, Favre-Perrod P (2004) Proposal for a multifunctional energy bus and its interlink with generation and consumption. High voltage Laboratory, ETH, Zurich
5. Alipour M, Zare K, Seyedi H (2018) Joint electricity and heat optimal power flow of energy hubs. In operation, planning, and analysis of energy storage systems in smart energy hubs. Springer, Cham, pp 391–409
6. Li L, Mu H, Li N, Li M (2015) Analysis of the integrated performance and redundant energy of CCHP systems under different operation strategies. *Energy Buildings* 99:231–242
7. Alipour M, Zare K, Abapour M (2017) MINLP probabilistic scheduling model for demand response programs integrated energy hubs. *IEEE Trans Industr Inform* 14(1):79–88
8. He C, Wu L, Liu T, Shahidehpour M (2016) Robust co-optimization scheduling of electricity and natural gas systems via ADMM. *IEEE Trans Sustainable Energy* 8(2):658–670
9. Lu X, Liu Z, Ma L, Wang L, Zhou K, Feng N (2020) A robust optimization approach for optimal load dispatch of community energy hub. *Appl Energy* 259:114195
10. Liu Y, Jiang C, Shen J, Hu J (2015) Coordination of hydro units with wind power generation using interval optimization. *IEEE Trans Sustainable Energy* 6(2):443–453
11. Huang H, Li F, Mishra Y (2015) Modeling dynamic demand response using Monte Carlo simulation and interval mathematics for boundary estimation. *IEEE Trans Smart Grid* 6(6):2704–2713
12. Bai L, Li F, Cui H, Jiang T, Sun H, Zhu J (2016) Interval optimization based operating strategy for gas-electricity integrated energy systems considering demand response and wind uncertainty. *Appl Energy* 167:270–279
13. Moore RE, Kearfott R B, & Cloud MJ (2009) Introduction to interval analysis. Society for Industrial and Applied Mathematics
14. Sengupta A, Pal TK (2000) On comparing interval numbers. *Eur J Oper Res* 127(1):28–43
15. Zhang Y, Le J, Zheng F, Zhang Y, Liu K (2019) Two-stage distributionally robust coordinated scheduling for gas-electricity integrated energy system considering wind power uncertainty and reserve capacity configuration. *Renew Energy* 135:122–135
16. Wang L, Li Q, Sun M, Wang G (2016) Robust optimisation scheduling of CCHP systems with multi-energy based on minimax regret criterion. *IET Gener Transm Distrib* 10(9):2194–2201
17. Ma T, Wu J, Hao L (2017) Energy flow modeling and optimal operation analysis of the micro energy grid based on energy hub. *Energy Convers Manag* 133:292–306
18. Zhang Y, Huang Z, Zheng F, Zhou R, An X, Li Y (2020) Interval optimization based coordination scheduling of gas–electricity coupled system considering wind power uncertainty, dynamic process of natural gas flow and demand response management. *Energy Rep* 6:216–227
19. Alipour M, Zare K, Mohammadi-Ivatloo B (2016) Optimal risk-constrained participation of industrial cogeneration systems in the day-ahead energy markets. *Renew Sust Energy Rev* 60:421–432
20. Alipour M, Zare K, Seyedi H, Jalali M (2019) Real-time price-based demand response model for combined heat and power systems. *Energy* 168:1119–1127

Chapter 10

Optimal Planning and Design of Multi-carrier Energy Networks



Hamid HassanzadehFard, Arezoo Hasankhani, and Seyed Mehdi Hakimi

10.1 Introduction

Nowadays, considering the serious fossil fuel lacks and environmental issues, efficient and optimal planning of different resources has become one of the critical subjects. The conventional power system, gas, and thermal network are mostly managed and planned separately, which is not useful considering the efficient and economical operation of the overall system. The energy hub has been developed as a novel idea for optimization of multi-energy systems' flexibility and efficiency [1].

The most important advantage of energy hub is the efficient use of distributed generation (DG) units in rural and remote applications to overcome the need for installing new lines and environmental issues. According to the World Bank, more than 2 billion persons live in rural regions which are located far from the utility network [2]. The mentioned regions are the main potential market of energy hub implementing renewable energy resources in order to satisfy their demands.

References [3, 4] present the profits of microgrid (MG), such as efficiency and reliability enhancement, system loss reduction, voltage sag improvement, and so on. It is recognized that application of combined cooling, heating, and power

H. HassanzadehFard

Department of Electrical Engineering, Miyaneh Branch, Islamic Azad University, Miyaneh, Iran

e-mail: hamid.hassanzadehfard@m-iau.ac.ir

A. Hasankhani

Department of Computer and Electrical Engineering and Computer Science, Florida Atlantic University, Boca Raton, FL, USA

e-mail: ahasankhani2019@fau.edu

S. M. Hakimi (✉)

Department of Electrical Engineering and Renewable Energy Research Center, Damavand Branch, Islamic Azad University, Damavand, Iran

e-mail: sm_hakimi@damavandiau.ac.ir

(CCHP) has positive effects on energy saving. However, CCHP is not a suitable option when either there is little need for heat or cooling loads are more than heating loads. This study considers the extension of cogeneration with heat-driven cooling, i.e., trigeneration, which may offer a good possibility for application of CCHP in abovementioned circumstances and may lead to a better application of energy hub system.

10.1.1 Literature Review

10.1.1.1 Microgrid Optimization

The allocation of DG units in MG systems is one of the most important approaches to provide the efficient operation and planning of microgrid. Furthermore, gas network and electricity network have been simultaneously studied in some researches. Different studies have followed this trend to find the optimal planning, while various loads have been considered.

Reference [5] proposes a novel method of the day-ahead scheduling problem for a general microgrid system. Reference [6] presents an innovative optimization model for planning the plug-in hybrid electric vehicle equipment in a microgrid. Reference [7] determines the optimum power that is produced via the renewable energy resources in a microgrid in order to minimize the overall cos. In Ref. [8], authors present modeling and optimization of a municipal microgrid located in a city area. This microgrid consists of large residential complexes, hospitals, and universities. Furthermore, HOMER software is used to optimize the size of microgrid modules. Reference [9] investigates different scenarios for the design of a multi-energy system. The objective is to define the optimal sizes of the components. In Reference [10], a novel method considering several stakeholders is presented to improve a framework for community microgrids. The proposed two-stage optimization policy produces chances for several stakeholders to finance the design of microgrids.

Reference [11] investigates different scenarios for energy management systems via hierarchical genetic algorithm to maximize the revenue produced by the energy exchange with the grid. In Ref. [12], a demand response algorithm based on economic linear programming is established to minimize the operating cost of a combined heat and power microgrid system. Reference [13] presents a new professional fuzzy system-based smart meta-heuristic technique for sizing and energy management. The proposed energy management operation is facilitated to set the membership functions and rules of the fuzzy logic expert system. Reference [14] discusses the energy management in the presence of renewable energy systems in virtual power plants. In Ref. [15], the optimal energy planning of MG is done considering the integration of renewable energy systems instead of fossil fuel-based power plants.

Reference [16] presents planning of stand-alone [microgrids](#) for rural and urban uses. This study provides a detailed evaluation between the different cost modules.

The purposes of Ref. [17] are offering a complete analysis on novel organizations of AC and DC microgrid, and then defining the size and optimum strategy with hybrid renewable energy resources in a MG to increase the reliability and decrease microgrid costs. Reference [18] presents a new two-stage microgrid scheduling procedure to select optimum sitting and sizing of microgrid components. Reference [19] presents a three-layer multi-agent system considering the energy storage system and power-heat load demand-side management based on the real condition of China to determine the problems of microgrid energy management. The PSO algorithm is very effective in the optimal planning of different renewable energy systems in MGs [20–21].

Reference [22] analyzes a novel technique for planning of microgrid, while renewable energy penetration is considered high. Moreover, an innovative planning algorithm for smart electrical appliances is proposed. Reference [23] studies an energy interchange scheme between smart buildings including renewable energy resources, and thermal and electrical loads. Reference [24] presents sizing and sitting of different equipment in MGs containing renewable energy systems. Reference [25] proposes a new methodology to evaluate the effect of energy storages on the optimum capacity of DG units and cost of an off-grid microgrid. A novel energy management methodology for renewable resource operation in the smart MG is proposed [26] in order to address the operation of MG in the electricity market. Reference [27] proposes a stochastic mixed-integer programming methodology to determine the optimal sizes of various DGs, considering both economic benefits and resilience performance. A novel hybrid optimization method based on differential evolution and chaos theory is proposed in ref. [28] for the optimum operation of a microgrid, including renewable and nonrenewable energy resources.

10.1.1.2 Energy Hub Optimization

Many studies have attempted to determine the optimal design and optimum operation strategy of the energy hub system. Energy hub is usually analyzed and modeled as a multi-carrier system.

Reference [29] proposed a multi-follower bi-level optimization method to find the optimum interaction between distribution network and energy hubs in order to reduce the total operation cost. An optimal operation model is developed in ref. [1] to manage the multiple energy hubs considering electricity and thermal loads in order to reduce the total cost of energy hubs. In ref. [30], a particle swarm optimization (PSO) algorithm is used for optimization of an energy hub system, which aims to improve the overall energy expense and reduce the pollution. Reference [31] develops an optimal load dispatch methodology for a community energy hub to minimize the operation and emission cost of the system. A hybrid interval stochastic framework is proposed in ref. [32] for optimum operation of energy hub system considering electrical and thermal demand response program and thermal energy market in order to minimize the operation cost. Reference [33] investigates the energy production of energy hubs in Canadian community to reduce the emissions

of greenhouse gas and energy cost. A systematic methodology is proposed in ref. [34] to optimally design the hybrid energy hub systems for sustainable building expansion.

10.1.2 Motivation and Contributions

Innovations of the present work can be listed as follows:

1. Developing optimal planning in order to supply simultaneously thermal loads and electrical loads in energy hub, while two types of thermal loads including space heating and home heat water are considered
2. Considering reliability indices for optimal planning of the components in the energy hub
3. Implementing the urban waste of the energy hub for generating the required thermal energy

In this chapter, a new methodology is proposed for optimal planning of an energy hub including electrical, heating, and cooling loads using PSO algorithm. Also, the reliability parameters of the system are considered. In this work, three scenarios are considered for supplying the electrical loads of energy hub: (a) total generated power of energy hub can satisfy demands; (b) total generated power of energy hub is more than demand; and (c) total generated power of energy hub cannot meet demand.

The remaining parts of this chapter are categorized as follows. Section 10.2 introduces the energy hub concept. Then, system optimal planning is presented in Sect. 10.3. System cost and objective function are modeled in Sect. 10.4. The numerical simulation and obtained results are presented in Sect. 10.5. Finally, conclusion is presented in Sect. 10.6.

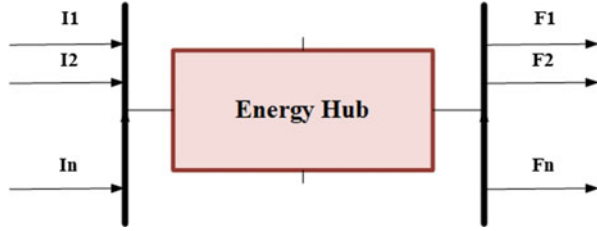
The proposed methodology is applied on Ganje site located in north-west of Iran. Two scenarios are assessed in this chapter. Firstly, the waste is used to supply the cooling and heating loads of energy hub, while the waste is not used in the second scenario.

10.2 Energy Hub Concept

Energy hub concept was firstly presented in 2007 [35], which is used to introduce an integrated methodology for interaction between different energy carriers. Energy hub is considered as a unit where different energy carriers can be altered, stored, and distributed. The inputs of the system including natural gas, electricity, and produced power of DG units are optimized in energy hub system to satisfy the electrical, thermal, and cooling loads.

Different types of components exist in energy hub such as energy conversion devices, energy transmission, and energy storage devices. The energy conversion

Fig. 10.1 Input-output model for energy hub [31]



devices are used to realize the coupling and conversion among different types of distributed energy resources. The energy transmission devices including gas network pipelines, heat network pipelines, and so on are used for transferring the input energy to the output side without energy conversion [31]. The energy storage devices include electrical and thermal storages. Figure 10.1 depicts the input-output model for the mentioned system.

Energy hub defines the conversion correlation between input carriers and outputs in a multi-carrier system. This correlation can be defined as a matrix:

$$\begin{bmatrix} F_1 \\ F_2 \\ \vdots \\ F_n \end{bmatrix} = \begin{bmatrix} C_{11} & C_{12} & \dots & C_{1m} \\ C_{21} & C_{22} & \dots & C_{2m} \\ \vdots & \vdots & \ddots & \vdots \\ C_{n1} & C_{n2} & \dots & C_{nm} \end{bmatrix} \begin{bmatrix} I_1 \\ I_2 \\ \vdots \\ I_m \end{bmatrix} \quad (10.1)$$

where C is the coupling matrix and each component of this matrix introduces the energy efficiency, I denotes the input energy carriers, and F determines the output energy flows. The components of energy hub are modeled as follows.

10.2.1 Wind Turbine

The produced power of a turbine is obtained according to its speed-power curve as depicted in Fig. 10.2.

The produced power of the wind turbine is obtained by the following formula [36]:

$$\begin{cases} 0 & V < V_{c_in}, V > V_{c_off} \\ P_{WG_max} \times \left(\frac{(V - V_{c_in})}{(V_r - V_{c_in})} \right)^3 & V_{c_in} \leq V < V_r \\ P_{WT_max} \times \frac{P_f - P_r}{V_{c_off} - V_r} \times (V - V_r) & V_r \leq V \leq V_{c_off} \end{cases} \quad (10.2)$$

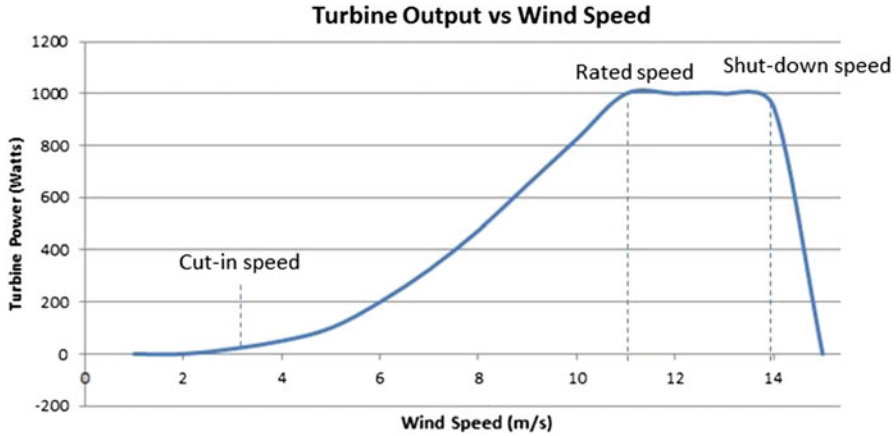


Fig. 10.2 Produced power of a turbine vs. wind speed

where $V_{c_in} [\frac{m}{s}]$ is cut-in wind speed; $V_{c_off} [\frac{m}{s}]$ is cutout wind speed; $V [\frac{m}{s}]$ is wind speed; $V_r [\frac{m}{s}]$ is rated wind speed; $P_{WT_max} [kW]$ is maximum power of wind turbine; and $P_f [kW]$ is power of wind turbine in cutout wind speed.

The rated capacity of the wind turbine is considered equal to 7.5 kW. Capital cost, replacement cost, and maintenance cost of the turbine are equal to 19,400\$, 15,000\$, and \$75/year, respectively. Lifetime of a wind turbine is considered equal to 20 years [36].

10.2.2 Fuel Cell

Fuel cell (FC) combines oxygen with hydrogen to generate electricity. The heating value of hydrogen and its density are equal to $3.4 [\frac{kWh}{m^3}]$ and $0.09 [\frac{kg}{m^3}]$, respectively. Accordingly, the quantity of energy produced by 1 kg hydrogen can be defined as

$$\frac{3.4 (\frac{kWh}{m^3})}{0.09 (\frac{kg}{m^3})} = 37.8 (\frac{kWh}{kg}) \tag{10.3}$$

So, the produced energy of FC (kWh) is determined by hydrogen requirement (kg) $\times \eta_{fc} \times 37.8$, while η_{fc} is the efficacy of the FC.

The lifetime of the FC and its efficacy are considered equal to 5 years and 50%, respectively [36]. The capital cost, replacement costs, and operational cost are considered as 3000\$, 2500\$, and \$0.02/h for a 1 kW system, respectively.

10.2.3 Electrolyzer

An electrolyzer is an electrochemical system, which converts water and electricity to oxygen and hydrogen. The capital, replacement, and maintenance costs of the electrolyzer are considered equal to 2000\$, 1500\$, and \$20/year, respectively [36]. The produced hydrogen can be stored and used in fuel cell units. The amount of required energy to generate 1 kg hydrogen is calculated as follows (efficiency of electrolyzer is considered equal to 90%):

$$E_{elz} \left(\frac{\text{kWh}}{\text{kg}} \right) = \frac{3.4 \left(\frac{\text{kWh}}{\text{m}^3} \right)}{0.09 \left(\frac{\text{kg}}{\text{m}^3} \right)} \times 100 = 41.97 \quad (10.4)$$

The amount of hydrogen generated at each hour is obtained by dividing the surplus power of wind turbine to 41.97:

$$\text{Hydrogen produced (kg)} = \frac{1 \times P_{wg-el}(\text{kWh})}{41.97 \left(\frac{\text{kWh}}{\text{kg}} \right)} \quad (10.5)$$

10.2.4 Other Components

The other components of studied energy hub include anaerobic reactors, hydrogen tank, power converter, and absorption chiller, which are described as follows.

The anaerobic process is a natural process that occurs in the lack of oxygen. In the mentioned energy hub, the urban waste is collected every day and utilized in the anaerobic reactor to generate methane.

There are different techniques to store hydrogen in storage tank for later use. Capital cost, replacement cost, and operational cost of a tank with 1 kg capacity are considered equal to 1300\$, 1200\$, and \$15/year, respectively. In addition, the lifetime of a hydrogen tank is taken to be 20 years [36].

In this chapter, the power electronic circuit, known as the inverter, is implemented to convert DC into AC. In the mentioned energy hub, the output power of the following sources is considered as the DC input to the inverter:

1. DC-generated power of the fuel cell units
2. DC-generated power of the variable speed wind turbines

The life span of a power converter is taken as 15 years with an efficacy of 90% [36]. The capital and replacement costs of a 1 kW system are considered as 800\$ and 750\$, respectively.

The absorption chiller with the efficacy of 80% is considered to supply the cooling demand in the energy hub. Absorption chillers are widely implemented in refrigeration using low-grade heat.

10.3 Energy Hub Optimal Planning

As it is mentioned in previous section, different components are considered in the studied energy hub. The energy hub contains FCs, wind turbines, electrolyzers, hydrogen and thermal storage tanks, absorption chiller, reformer, and anaerobic reactor.

The main objective of this work is determining the optimal planning for each component in order to minimize the total energy hub costs. We consider three different conditions for energy hub:

1. The energy resources in energy hub can supply both electrical and thermal demand.
2. The produced energy by resources in energy hub is lower than total demand.
3. The produced energy by resources in energy hub is higher than total demand.

The considered reliability index in this study is equivalent load factor (ELF), which can be obtained as follows [37–38]:

$$\text{ELF} = \frac{1}{N} \sum_{i=1}^N \frac{Q_i(t)}{D_i(t)} \quad (10.6)$$

where $Q_i(t)$ is the interrupted loads at each hour and $D_i(t)$ denotes the electrical loads at each hour.

When the total generated energy in energy hub cannot provide the required demand of the system, 10% electrical demand can be interrupted as the ELF reliability is less than 0.01. In this study, the penalty is considered for interrupting the loads, which is equal to 0.482\$/kWh.

Figure 10.3 illustrates the studied energy hub system.

The following scenarios are considered for supplying cooling and heating demands in energy hub.

1. Heat produced by FC is supplying thermal loads.
2. Generated natural gas by the urban waste is supplying thermal loads in energy hub.
3. Purchased methane is supplying thermal loads in energy hub.

In fact, at first we use the heat produced by FC for supplying heating and cooling loads in energy hub; then if it is not enough, the produced methane by waste will be implemented for supplying cooling and heating demands in energy hub. Finally, if

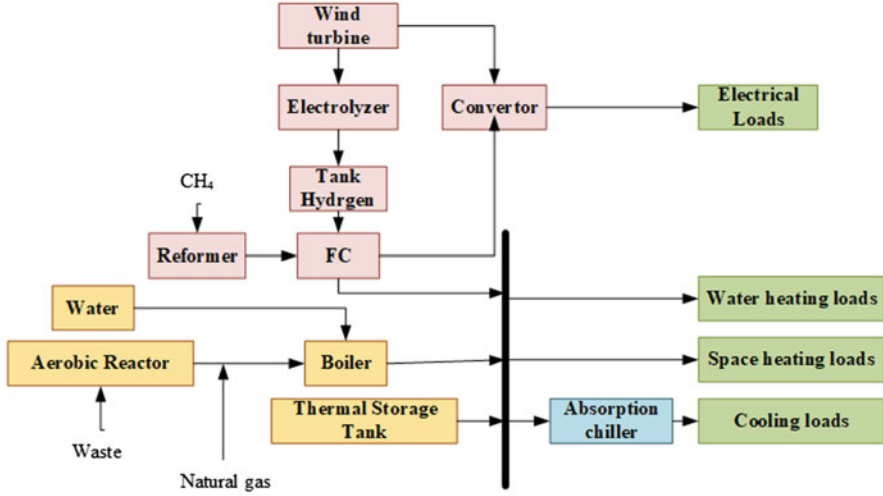


Fig. 10.3 A schematic of studied energy hub

the total produced heat in energy hub cannot meet demands, the purchased natural gas will be used.

We suppose that produced waste in the energy hub is about 20 kg at each hour. In this study, we suppose that the heat produced by FC is equal to 1.04 of its generated electricity. The density of methane is equal to $0.55 \text{ (kg/m}^3\text{)}$, so 27.642 kWh of energy will be added to waste each time.

Figure 10.4 shows the planning algorithm for providing the thermal demand in energy hub.

The following three approaches are considered in planning algorithm in order to provide the thermal demand in the system.

First condition: Heat supplied by FC is more than the thermal demands in the studied energy hub, which is formulated as follows:

$$P_{FC}(t) \times 1.04 > P_{\text{Heat}}(t) + P_{\text{water}}(t) + \frac{P_{\text{Cooling}}(t)}{0.8} \quad (10.7)$$

$$E_{\text{storage}}(t+1) = E_{\text{storage}}(t)$$

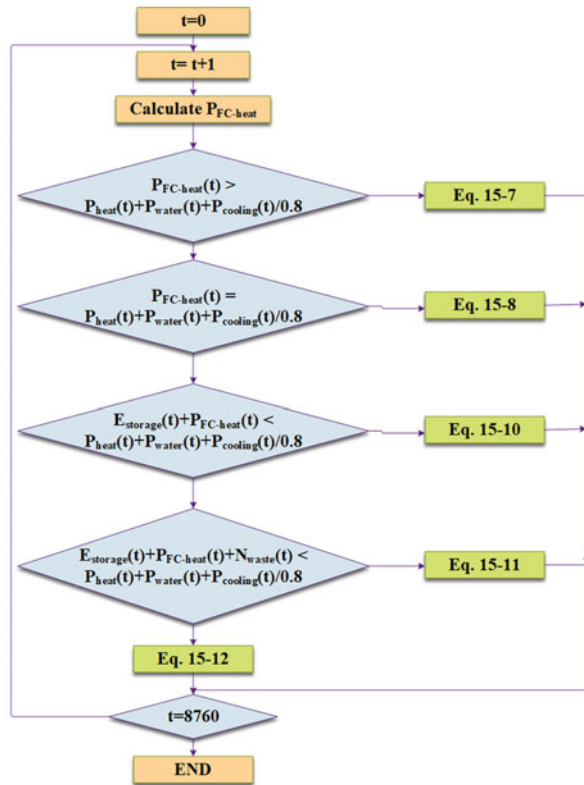
$$+ \left(P_{FC}(t) \times 1.04 - P_{\text{Heat}}(t) - P_{\text{water}}(t) - \frac{P_{\text{Cooling}}(t)}{0.8} \right) P_{FC-\text{Heat}}(t)$$

$$= P_{\text{Heat}}(t) + P_{\text{water}}(t) + \frac{P_{\text{Cooling}}(t)}{0.8}$$

$$N_G(t) = 0$$

$$N_{\text{waste}}(t+1) = N_{\text{waste}}(t) + 27.642$$

Fig. 10.4 A flowchart of proposed planning algorithm for supplying all heating and cooling demands in the studied energy hub



where $P_{FC}(t)$ is the produced electricity of FC, and $P_{Cooling}(t)$ is the cooling demand of the system. $P_{Heat}(t)$ denotes space heating demand, and $P_{water}(t)$ is water heating demand. $P_{FC-Heat}(t)$ shows the produced heat of FC, $N_{gas}(t)$ determines the bought methane, and $N_{waste}(t)$ specifies the produced energy of waste at each hour. $E_{storage}(t)$ is the stored energy in battery storages at each hour.

In this condition, the surplus produced heat of fuel cell is stored in the thermal storage and the produced thermal energy of waste is stored.

Second condition: The generated heat of FC is equivalent to thermal demand in energy hub, which is formulated as follows:

$$P_{FC}(t) \times 1.04 = P_{Heat}(t) + P_{water}(t) + \frac{P_{Cooling}(t)}{0.8} \quad (10.8)$$

$$E_{storage}(t+1) = E_{storage}(t)$$

$$N_G(t) = 0$$

$$N_{waste}(t+1) = N_{waste}(t) + 27.642$$

$$P_{\text{FC-Heat}}(t) = P_{\text{Heat}}(t) + P_{\text{water}}(t) + \frac{P_{\text{Cooling}}(t)}{0.8}$$

Third condition: The heat produced by FC cannot satisfy thermal demand in energy hub, which is formulated as follows:

$$P_{\text{FC}}(t) \times 1.04 < P_{\text{Heat}}(t) + P_{\text{water}}(t) + \frac{P_{\text{Cooling}}(t)}{0.8} \quad (10.9)$$

If the heat produced by FC cannot supply all thermal loads, the following cases are considered:

- The available heat in thermal storage can supply the remaining thermal demands in energy hub, so

$$P_{\text{FC-Heat}}(t) = P_{\text{FC}}(t) \times 1.04 \quad (10.10)$$

$$E_{\text{storage}}(t+1) = E_{\text{storage}}(t) - \left(P_{\text{water}}(t) + P_{\text{Heat}}(t) + \frac{P_{\text{Cooling}}(t)}{0.8} - P_{\text{FC}}(t) \times 1.04 \right)$$

$$N_{\text{waste}}(t+1) = N_{\text{waste}}(t) + 27.642$$

$$N_G(t) = 0$$

- The total available heat in thermal storage with heat generated by FC cannot provide the thermal demand in energy hub, so two approaches can be considered. Firstly, the total generated heat in energy hub can provide the heating and cooling demands of the system, which is formulated as follows:

$$P_{\text{FC-Heat}}(t) = P_{\text{FC}}(t) \times 1.04 \quad (10.11)$$

$$E_{\text{storage}}(t+1) = 0$$

$$N_{\text{waste}}(t+1) = N_{\text{waste}}(t) - (P_{\text{water}}(t) + P_{\text{Heat}}(t) + \frac{P_{\text{Cooling}}(t)}{0.8} - P_{\text{FC}}(t) \times 1.04 - E_{\text{storage}}(t)) + 27.642$$

$$N_G(t) = 0$$

Secondly, total generated heat in energy hub cannot provide the cooling and heating demand of energy hub. Then, the remaining demand is provided by the purchased natural gas:

$$P_{\text{FC-Heat}}(t) = P_{\text{FC}}(t) \times 1.04 \quad (10.12)$$

$$E_{\text{storage}}(t+1) = 0$$

$$N_{\text{waste}}(t+1) = 27.642$$

$$N_G(t) = (P_{\text{water}}(t) + P_{\text{Heat}}(t) + \frac{P_{\text{Cooling}}(t)}{0.8} - P_{\text{FC-Heat}}(t) - N_{\text{waste}}(t) - E_{\text{storage}}(t))/1.083$$

10.4 Modeling Cost of Energy Hub

Net present value (NPV) is introduced by computing the costs and benefits for each period of a finance. In this study, the NPV is chosen to calculate the total cost of each component including installation (CC), replacement (RC), and operating (OMC) costs.

10.4.1 Net Present Value

The NPV of each component can be calculated as follows:

$$\text{NPV} = N \times \left(\text{CC} + \text{RC} \times K + \text{OMC} \times \frac{1}{\text{CRF}(ir, R)} \right) \quad (10.13)$$

$$\text{CRF}(ir, R) = \frac{ir(1+ir)^R}{(1+ir)^R - 1} \quad (10.14)$$

$$K = \sum_{n=1}^Y \frac{1}{(1+ir)^{L \times n}} \quad (10.15)$$

$$Y = \left[\frac{R}{L} \right] - 1 \text{ if } R \text{ is dividable to } L \quad (10.16)$$

$$Y = \left[\frac{R}{L} \right] \text{ is } R \text{ is not dividable to } L \quad (10.17)$$

N is the optimum amount of each element. L is the lifetime of each DG unit, ir is the interest rate, and R is the project lifetime.

10.4.2 The Objective Function

In this section, an efficient objective function is proposed according to the economic consideration in order to optimally manage our proposed energy hub to provide the electricity, thermal, and cooling demands.

The main purpose of this study is determining the optimum design of energy hub in order to minimize the following objective function:

$$\begin{aligned} \text{OF} = & \text{NPC}_{\text{WT}} + \text{NPC}_{\text{El}} + \text{NPC}_{\text{Tank}} + \text{NPC}_{\text{FC}} + \text{NPC}_R + \\ & \text{NPC}_{\text{Conv}} + \text{NPC}_{\text{Gas}} + \text{NPC}_{\text{TS}} + \text{NPC}_{\text{Chil}} + \text{NPC}_{\text{Pi}} \end{aligned} \quad (10.18)$$

where NPC_{Pi} is the total cost of penalty for interruption of the electrical demand, and NPC_{Gas} shows the total cost of consumed natural gas in energy hub. NPC_{Pi} and NPC_{Gas} can be obtained by the following formula:

$$\text{NPC}_{\text{Pi}} = \sum_{t=1}^{8760} Q_i(t) \times C_{\text{Penalty}} / \text{CRF}(ir, R) \quad (10.19)$$

$$\text{NPC}_{\text{Gas}} = \frac{C_{\text{Gas}} \times N_G}{\text{CRF}(ir, R)} \quad (10.20)$$

where C_{Penalty} and C_{Gas} show the penalty factor for load interruptions and cost of purchased gas, respectively.

10.5 Simulation Results and Discussion

In this chapter, MATLAB software is used to develop a complex optimization model [39] and to investigate the optimization of DG units in order to minimize the energy economics and environmental impacts in the proposed energy hub system. Furthermore, PSO algorithm is implemented as the optimization methodology to solve the optimization problem. In this section, the presented optimal planning is tested in a sample residential sector. The studied energy hub includes four types of loads: electricity, home water heating, space heating, and cooling demand. Hence, different thermal loads and electrical demand should be supplied in the studied system, which highlights the need for developing energy hub. The annual load profiles of the abovementioned loads are illustrated in Figs. 10.5–10.8. As it can be seen in Fig. 10.5, residential loads fluctuate between 150 and 500 kW.

The water heating load profile is shown in Fig. 10.6. From this figure, it can be seen that the water heating load decreases between 4000 and 6800, which is related to hot seasons. Furthermore, the heating demand decreases to almost zero throughout this period. However, space cooling load increases over this period.

According to Fig. 10.6, the water heater demand is required throughout a year. However, this type of demand is less during hot seasons.

In hot seasons, the space heating demand is equal to zero (Fig. 10.7). In addition, space cooling demand is not seen during cold seasons (Fig. 10.8). In this study, the annual wind speed and load curve data are determined based on the Ganje site. The annual wind speed is illustrated in Fig. 10.9.

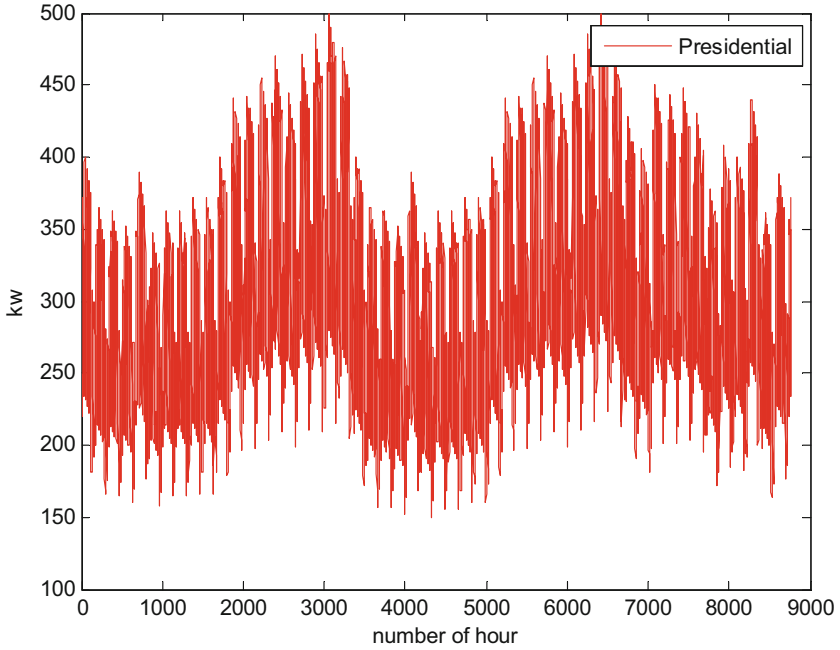


Fig. 10.5 Residential electrical load curve

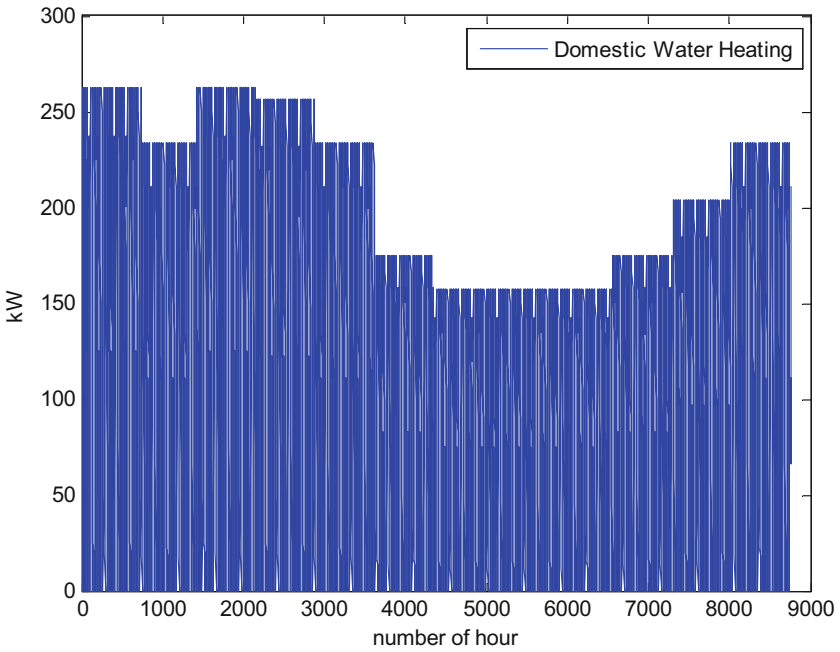


Fig. 10.6 Domestic water heating load profile

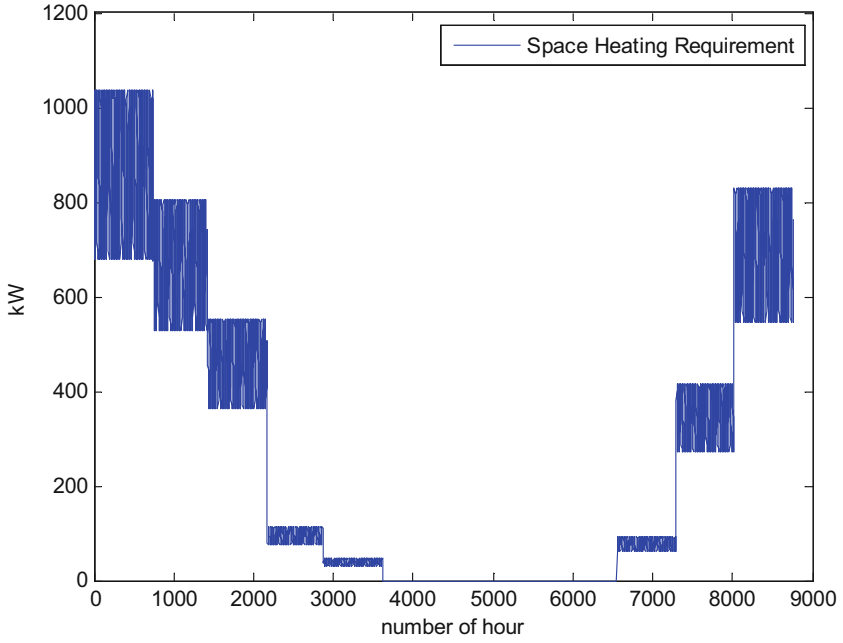


Fig. 10.7 Space heating load profile

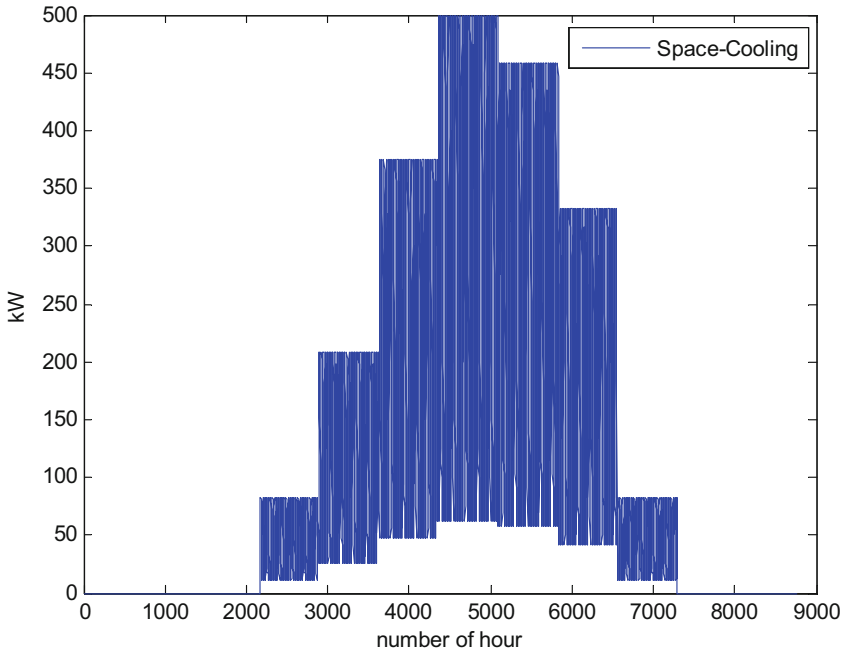


Fig. 10.8 Space cooling load profile

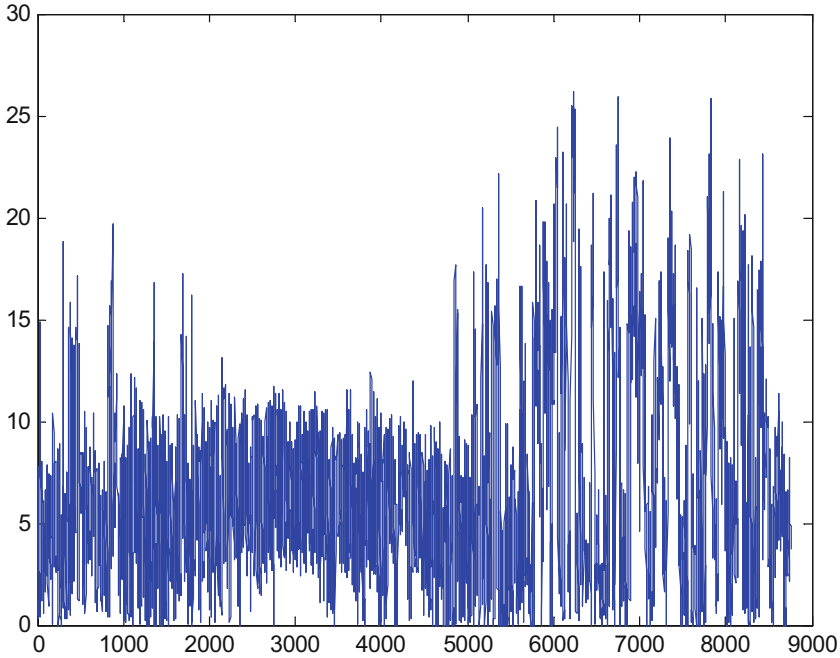


Fig. 10.9 Annual wind speed in Ganje site

Table 10.1 Installation cost of all used components (\$)

Wind turbine	Electrolyzer	Hydrogen tank	Fuel cell	Converter
19,400 (7.5 kW)	2000	1300	3000	800

The installation cost of each component is also considered in the simulation procedure as the input data, which are depicted in Table 10.1.

The generated power of wind turbine can be obtained by Eq. (10.2) according to the wind speed curve. Two scenarios are considered to provide the cooling and heating demands:

1. Waste is utilized to supply the thermal demands of energy hub.
2. Waste is not used to supply thermal loads in energy hub.

10.5.1 *Generated Heat of Waste Is Utilized to Provide the Cooling and Heating Demands*

In this section we consider that waste is utilized to generate heat for thermal demands. Table 10.2 depicts the optimum capacity of each component after utilizing the optimal planning on the studied energy hub.

Table 10.2 Optimum capacity of each component in the energy hub (kW)

Wind turbine	Electrolyzer	Hydrogen tank	Fuel cell	Energy hub cost
572	2007	4915	491	27.5778

Table 10.3 The amount of interrupted loads

Interrupted loads (kWh)	Penalty	ELF
$1.2146 * 10^3$	$5.7479 * 10^3$	$2.9596 * 10^{(-4)}$

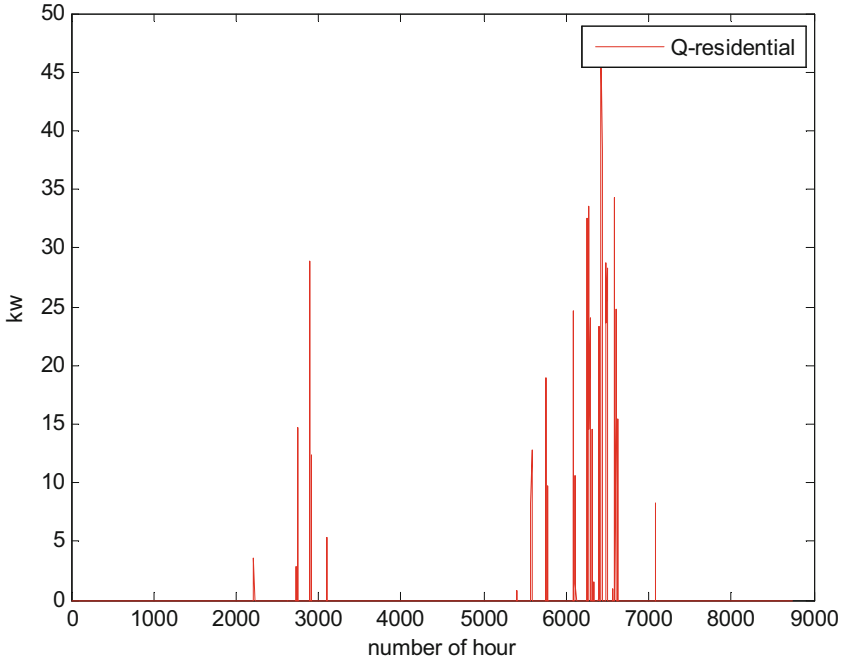


Fig. 10.10 The annual amount of interrupted loads

The total consumed natural gas is equivalent to 2.5738 M^3 . Table 10.3 shows the quantity of interrupted loads.

It can be seen from Table 10.3 that the ELF is at its permissible limit which is less than 0.01. Figure 10.10 depicts the hourly amount of interrupted loads. As it can be seen in this figure, the most interruption occurs between 6000 and 6600, which is caused by less production throughout this period. In other words, if the produced power of renewable energy systems cannot meet loads, interrupting some loads is inevitable. However, there is no interruption between 3100 and 5000, which verifies the high production of renewable energy systems over this period.

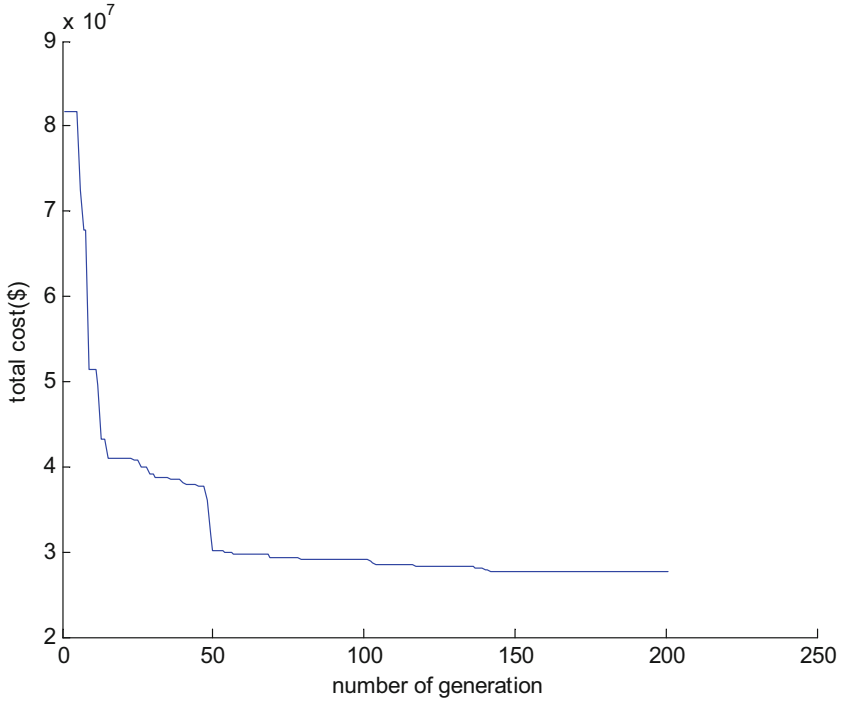


Fig. 10.11 Convergence of the objective function in terms of iterations

Figure 10.11 illustrates the convergence of objective function in terms of iterations. As it can be seen in this figure, total cost minimizes over iterations, which almost converges at 140th iteration. In this study, PSO algorithm is used to minimize objective function, and its efficiency is verified in previous works. Moreover, Fig. 10.12 shows the load profile and transferred power from converters to load. As it can be seen from this figure, total demand is precisely supplied with transferred power from converter. Furthermore, Fig. 10.13 shows the produced power of wind turbine at each hour, transferred power from wind units to electrolyzer, and power that the wind turbine transfers to the converters. In addition, Fig. 10.14 shows hourly produced power of FC. As it can be seen in this figure, produced power mostly fluctuates between 350 kW and 500 kW.

Figure 10.15 shows the hydrogen stored in the hydrogen storage during a year. We can see from this figure that high amount of hydrogen is stored throughout a year, which highlights the importance of hydrogen storage.

As shown in Fig. 10.15, peak load happens at time = 6500. At this time, the total produced power of energy hub cannot satisfy demand. Therefore, the demand of energy hub is interrupted according to the reliability index constraint. The reason is that the total energy generated in energy hub cannot provide demand in the studied system. Figure 10.16 depicts the produced heat of FC. Moreover, Fig. 10.17 shows

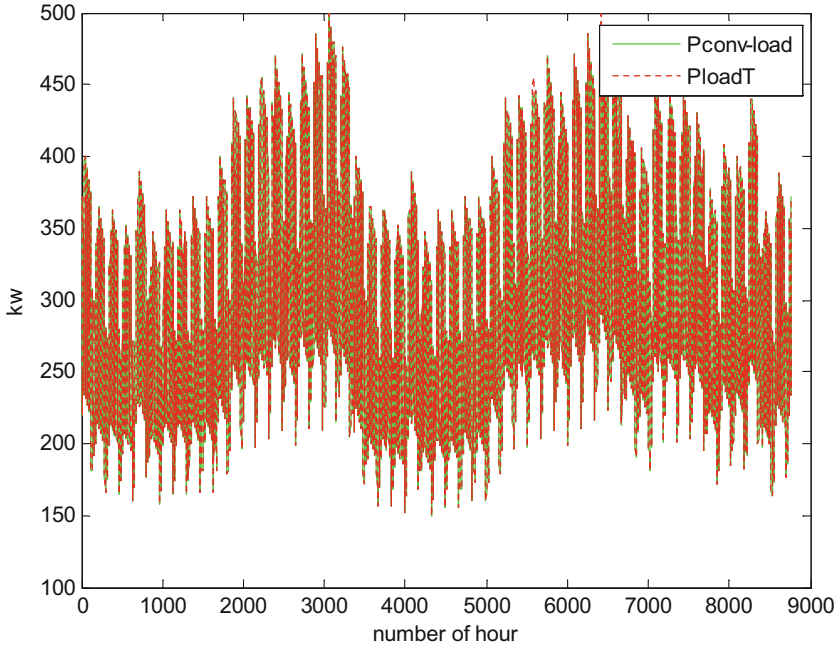


Fig. 10.12 Required power of load in area and transferred power from converters to load

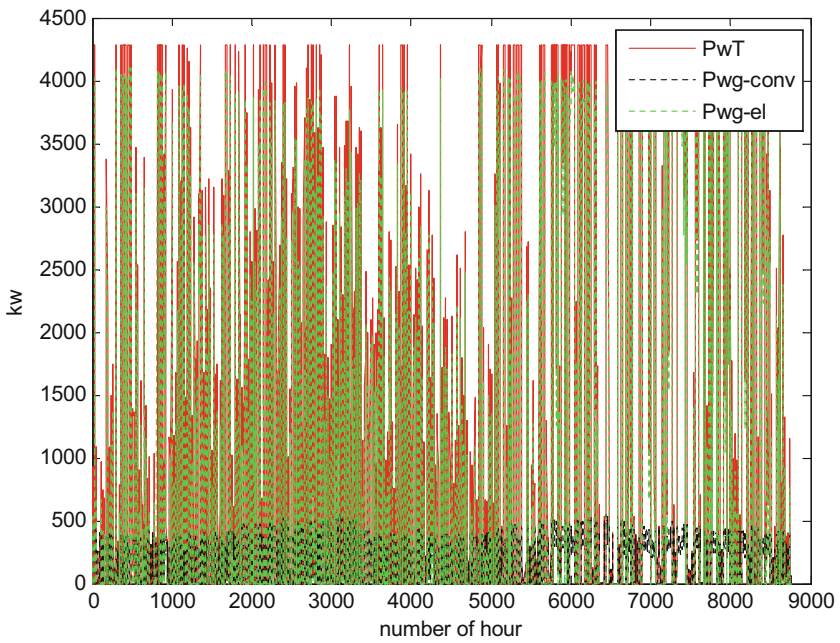


Fig. 10.13 The hourly produced power of wind turbines, transferred power from wind turbines to electrolyzer, and power that wind turbine gives to the converters

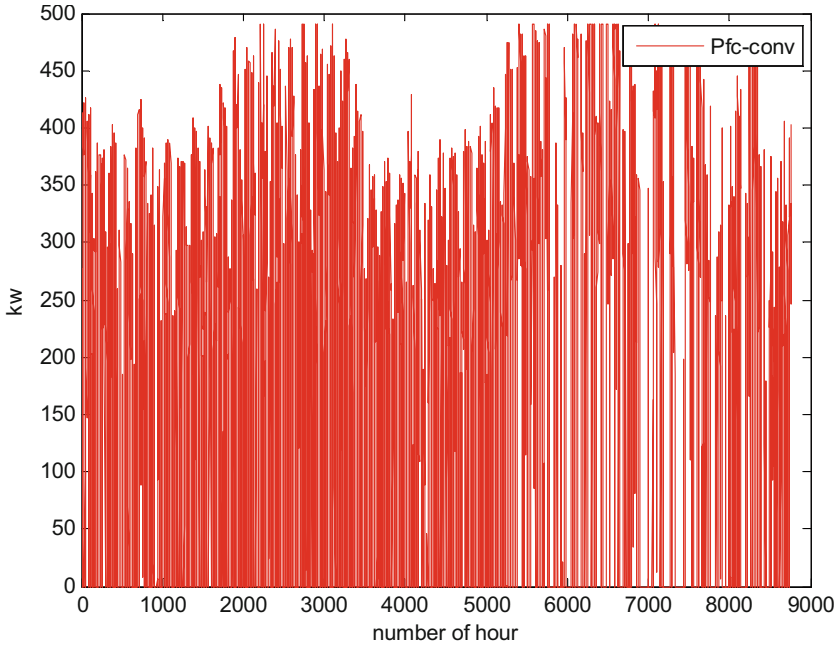


Fig. 10.14 The power generated by fuel cell

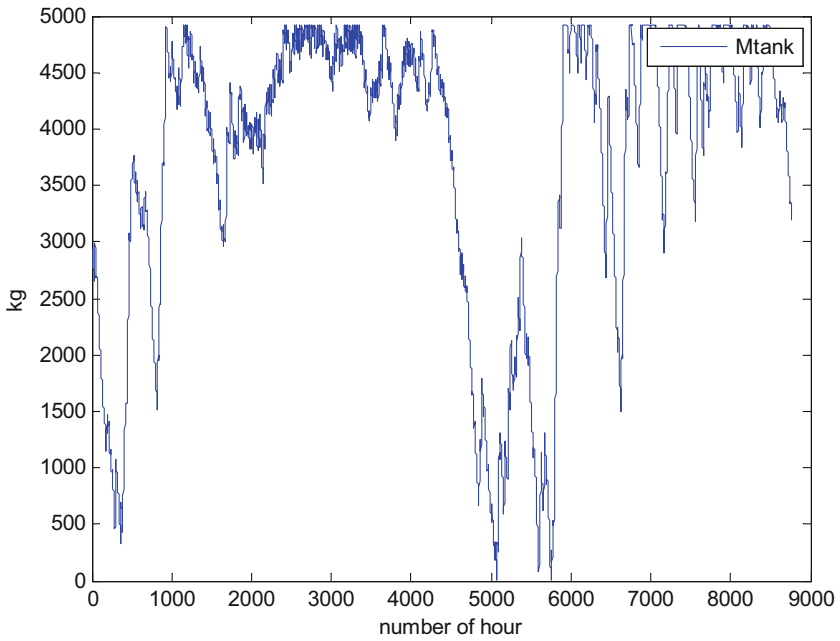


Fig. 10.15 The stored hydrogen in hydrogen storage at each hour

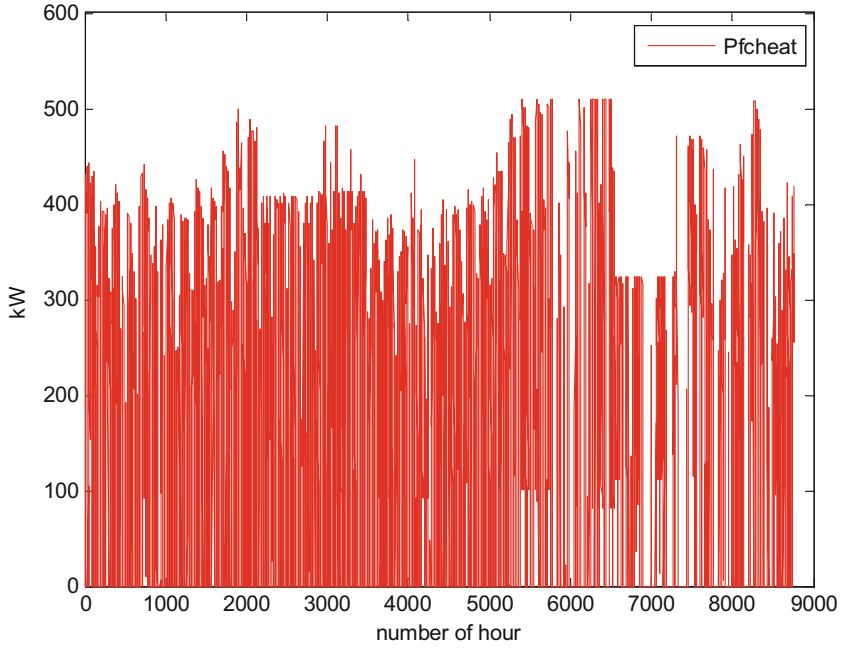


Fig. 10.16 Heat generated by fuel cell at each hour

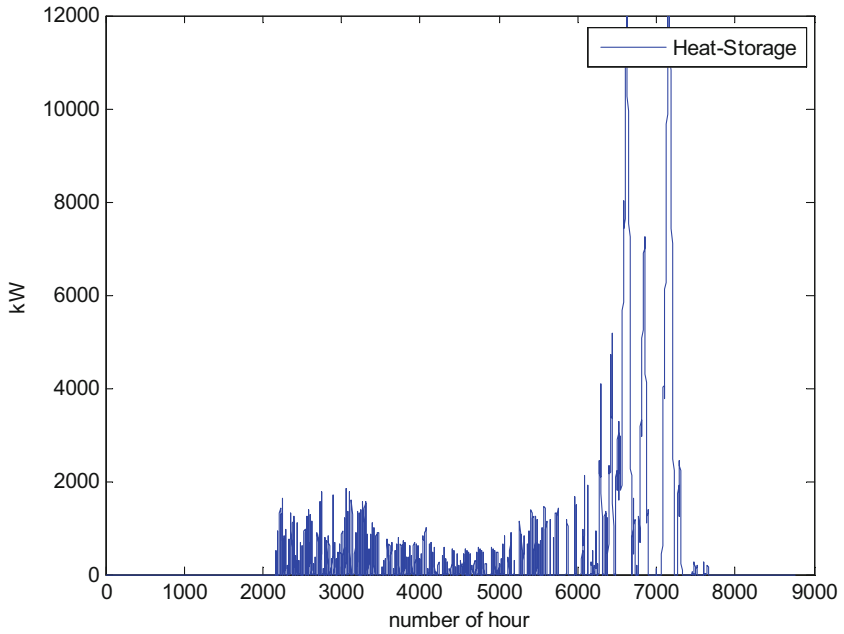


Fig. 10.17 The stored heat in thermal storage

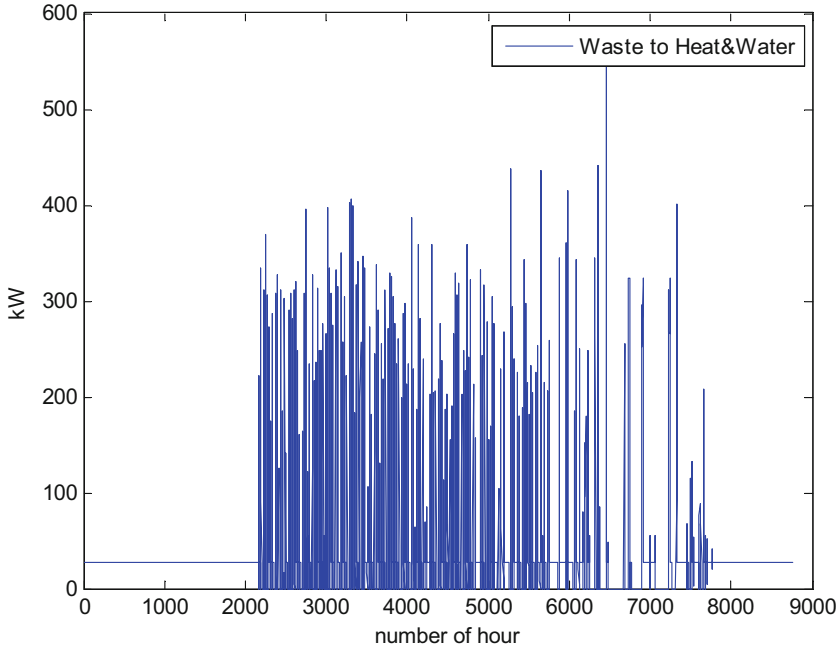


Fig. 10.18 The produced heat of waste

the variations of energy stored in thermal storage. From this figure, it can be seen that the thermal energy is mostly stored between 2200 and 3500 due to high thermal energy production over this period. Furthermore, Fig. 10.18 depicts the produced heat of waste to supply the thermal demand, which increases between 2200 and 5800 due to lower thermal energy production over this period. In fact, FC cannot meet thermal loads over this period, so thermal loads are supplied with waste. Finally, the amount of consumed gas at each hour is shown in Fig. 10.19, which decreases from initial consumption of 1180 m^3 to the amount of 380 m^3 at time = 2200. It is also seen from this figure that the natural gas consumption is equal to zero from time = 6500 to time = 6700. Furthermore, it can be concluded from Fig. 10.19 that at the times between 500 and 700 the amount of consumed gas is more than other times.

10.6 Conclusion

In this study, a novel planning methodology is proposed to determine the optimal operation of all components in energy hub. The studied energy hub includes wind turbine, FC, and electrolyzer, while producing heat from waste is also considered as an option for supplying thermal loads. In this study, two scenarios were analyzed, which include supplying thermal loads with or without considering thermal energy

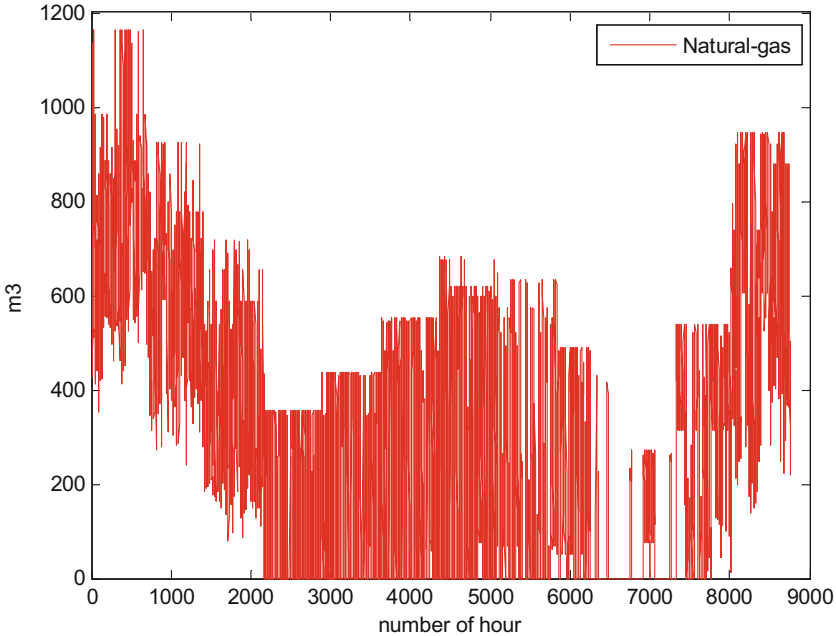


Fig. 10.19 The amount of consumed gas (m^3) at each hour

produced by waste. It was shown that if the waste is not used, the total purchased gas will be increased. In the studied energy hub, four types of loads including electrical loads, space heating loads, water heating loads, and space cooling loads were considered. Since FCs are considered as a backup for wind turbines, the studied energy hub shows high reliability.

Besides, the surplus produced hydrogen of electrolyzer and reformer is utilized to charge the hydrogen tank, which causes increasing of reliability and satisfying of the demand. The output power of renewable energy resources is mainly dependent on environmental conditions. Therefore, these types of DG units cannot completely supply the demand. Applying energy storage devices solves this problem considerably. In the studied energy hub, hydrogen storage is implemented to supply the demand. It was verified that the proposed energy hub scheme and optimal planning are appropriate for Ganje due to some reasons. Firstly, a high amount of agricultural waste is available. Secondly, the wind speed is appropriate for installing wind turbine and supplying electrical loads. Finally, high costs of gas transmissions and its negative environmental impacts can be solved using energy hub. In addition, the simulation results depict that the thermal storage is mostly storing the thermal energy between 2200 and 3500 h due to high thermal energy production by FC units over this period. Furthermore, the natural gas consumption is equal to zero from 6500 to 6700 h. Hence, during this period, the generated energy of FC units and the stored energy in the thermal storage can satisfy the total thermal demand of the energy hub, and our proposed planning methodology operates successfully in meeting all thermal demand.

Nomenclature

List of Symbols

C	Coupling matrix
I	Input energy carriers
F	The output energy flows
V_{c_in}	Cut-in wind speed
V_{c_off}	Cutout wind speed
V	Wind speed
V_r	Rated wind speed
P_{WT_max}	Maximum power of wind turbine
P_f	Power of wind turbine in cutout wind speed
η_{fc}	Efficacy of fuel cell
E_{elz}	Amount of required energy to generate 1 kg hydrogen
$Q_i(t)$	Interrupted loads at each hour
$D_i(t)$	Electrical loads at each hour
$P_{FC}(t)$	Produced electricity of fuel cell
$P_{Cooling}(t)$	Cooling demand of energy hub
$P_{Heat}(t)$	Space heating demand of energy hub
$P_{water}(t)$	Water heating demand of energy hub
$P_{FC - Heat}(t)$	Produced heat of fuel cell units
$N_G(t)$	Purchased methane from gas network
$N_{waste}(t)$	Produced energy of waste
$E_{storage}(t)$	Stored energy in battery storages
L	Lifetime of DG unit
N_{DG}	Optimal number of DG units
Ir	Interest rate
R	Project lifetime
NPC_{Pi}	Total cost of penalty for interruption of electrical demand
NPC_{Gas}	Total cost of consumed natural gas in energy hub
$C_{Penalty}$	Penalty factor for load interruptions
C_{Gas}	Cost of purchased gas

Abbreviation

DG	Distributed generation
MG	Microgrid
CCHP	Combined cooling, heating, and power
PSO	Particle swarm optimization
FC	Fuel cell
ELF	Equivalent load factor
NPV	Net present value
CC	Installation cost
RC	Replacement cost
OMC	Operating costs
CRF	Capital rate factor
NPC	Net present cost

References

1. Lu X, Liu Z, Ma L, Wang L, Zhou K, Yang S (2020) A robust optimization approach for coordinated operation of multiple energy hubs. *Energy* 197:117171
2. Patel MR (1999) *Wind and solar power systems*. CRC Press, USA
3. Lasseter RH (2002) Microgrids. *IEEE Power Eng Soc Transm Distrib Conf*:305–308
4. Chris M, Giri V (2006) Microgrids in the evolving electricity generation and delivery infrastructure. *IEEE Power Eng Soc Gen Meet*:18–22
5. Moretti L, Martelli E, Manzolini G (2020) An efficient robust optimization model for the unit commitment and dispatch of multi-energy systems and microgrids. *Appl Energy* 261:113859
6. Mortaz E, Vinel A, Dvorkin Y (2019) An optimization model for siting and sizing of vehicle-to-grid facilities in a microgrid. *Appl Energy* 242:1649–1660
7. Dulau LI, Bica D (2019) Optimization of generation cost in a microgrid considering load demand. *Procedia Manuf* 32:390–396
8. Raji AK, Luta DN (2019) Modeling and optimization of a community microgrid components. *Energy Procedia* 156:406–411
9. Mariani RR, Chea Wae SO, Mazzoni S, Romagnoli A (2020) Comparison of optimization frameworks for the design of a multi-energy microgrid. *Appl Energy* 257:113982
10. Meena NK, Yang J, Zacharis E (2019) Optimisation framework for the design and operation of open-market urban and remote community microgrids. *Appl Energy* 252:113399
11. Leonori S, Paschero M, Mascioli F, Rizzi A (2020) Optimization strategies for microgrid energy management systems by genetic algorithms. *Appl Soft Comput* 86:105903
12. Zheng Y, Jenkins B, Kornbluth K, Traeholt C (2018) Optimization of a biomass-integrated renewable energy microgrid with demand side management under uncertainty. *Appl Energy* 230:836–844
13. El-Bidairi K, Nguyen H, Jayasinghe SDG, Mahmoud T, Penesis I (2018) A hybrid energy management and battery size optimization for standalone microgrids: a case study for Flinders Island, Australia. *Energy Convers Manag* 175:192–212
14. Hasankhani A, Gharehpetian GB (2016) Virtual power plant management in presence of renewable energy resources, In 2016 24th Iranian Conference on Electrical Engineering (ICEE), 665–669
15. Hasankhani A, Vahidi B, Riahy GH (2014) Replacing diesel generator with wind turbine & li-ion battery in virtual power plant. *Sci Int* 26(2):583
16. Phurailatpam C, Rajpurohit B, Wang L (2018) Planning and optimization of autonomous DC microgrids for rural and urban applications in India. *Renew Sust Energy Rev* 82(1):194–204
17. Ghiasi M (2019) Detailed study, multi-objective optimization, and design of an AC-DC smart microgrid with hybrid renewable energy resources. *Energy* 169:496–507
18. Gao J, Chen J, Cai Y, Zeng S, Peng K (2020) A two-stage microgrid cost optimization considering distribution network loss and voltage deviation. *Energy Rep* 6:263–267
19. Li C, Jia X, Zhou Y, Li X (2020) A microgrids energy management model based on multi-agent system using adaptive weight and chaotic search particle swarm optimization considering demand response. *J Clean Prod* 262:121247
20. HassanzadehFard H, Jalilian A (2016) A novel objective function for optimal DG allocation in distribution systems using meta-heuristic algorithms. *Int J Green Energy* 13(15):1624–1634
21. HassanzadehFard H, Jalilian A (2018) Optimal sizing and siting of renewable energy resources in distribution systems considering time varying electrical/heating/cooling loads using PSO algorithm. *Int J Green Energy* 15(2):113–128
22. Hakimi SM, Hasankhani A, Shafie-khah M, Catalao JPS (2020) Demand response method for smart microgrids considering high renewable energies penetration. *Sustainable Energy Grids Networks* 21:100325
23. Hakimi SM, Hasankhani A (2020) Intelligent energy management in off-grid smart buildings with energy interaction. *J Clean Prod* 244:118906

24. Hakimi SM, Hasankhani A, Shafie-khah M, Catalao JPS (2019) Optimal sizing and siting of smart microgrid components under high renewables penetration considering demand response. *IET Renewable Power Gener* 13:1809–1822
25. HassanzadehFard H, Moghaddas-Tafreshi S. M, Hakimi S. M (2011) Effect of Energy Storage Systems on Optimal Sizing of Islanded Micro-grid Considering Interruptible Loads. 3rd International Youth Conference on Energetics, Leiria, Portugal
26. Hakimi SM, Bagheritabar H, Hasankhani A, Shafie-khah M, Lotfi M, & Catalão JP (2019) Planning of Smart Microgrids with High Renewable Penetration Considering Electricity Market Conditions. In 2019 IEEE International Conference on Environment and Electrical Engineering and 2019 IEEE Industrial and Commercial Power Systems Europe (EEEIC/I&CPS Europe) (pp. 1-5). IEEE
27. Wu D, Ma X, Huang S, Fu T, Balducci P (2020) Stochastic optimal sizing of distributed energy resources for a cost-effective and resilient microgrid. *Energy* 198:117284
28. Mandal S, Mandal KK (2020) Optimal energy Management of Microgrids under Environmental Constraints Using Chaos Enhanced Differential Evolution. *Renew Energy Focus* 34:129–141
29. Kamanaj AM, Majidi M, Zare K, Kazemzadeh R (2020) Optimal strategic coordination of distribution networks and interconnected energy hubs: a linear multi-follower bi-level optimization model. *Int J Electr Power Energy Syst* 119:105925
30. Zhang H, Cao Q, Gao H, Wang P, Zhang W, Yousefi N (2020) Optimum design of a multi-form energy hub by applying particle swarm optimization. *J Clean Prod* 260:121079
31. Lu X, Liu Z, Ma L, Wang L, Zhou K, Feng N (2020) A robust optimization approach for optimal load dispatch of community energy hub. *Appl Energy* 259:114195
32. Jamalzadeh F, Mirzahosseini AH, Faghihi F, Panahi M (2020) Optimal operation of energy hub system using hybrid stochastic-interval optimization approach. *Sustain Cities Soc* 54:101998
33. Ghorab M (2019) Energy hubs optimization for smart energy network system to minimize economic and environmental impact at Canadian community. *Appl Therm Eng* 151:214–230
34. Xu S, Yan C, Jin C (2019) Design optimization of hybrid renewable energy systems for sustainable building development based on energy-hub. *Energy Procedia* 158:1015–1020
35. Geidl M, Koepfel G, Favre-Perrod P, Kloeckl B, Andersson G, Froehlich K (2007) Energy hubs for the future. *IEEE Power Energy Mag* 5(1):24–30. <https://doi.org/10.1109/mpae.2007.264850>
36. Khan MJ, Iqbal MT (2005) Pre-feasibility study of stand-alone hybrid energy systems for applications in Newfoundland. *Renew Energy* 30(6):835–854
37. Hakimi SM, Moghaddas-Tafreshi SM, HassanzadehFard H (2011) Optimal sizing of reliable hybrid renewable energy system considered various load types. *J Renewable Sustainable Energy* 3:062701
38. HassanzadehFard H, Bahreyni AA, Dashti R, Shayanfar HA (2015) Evaluation of reliability parameters in micro-grid. *Iran J Electr Electron Eng* 11(2):127–136
39. Zarringhalami M, Hakimi S. M, Javadi M (2010) Optimal regulation of STATCOM controllers and PSS parameters using hybrid particle swarm optimization. 14th International Conference on Harmonics and Quality of Power-ICHQP. IEEE, Bergamo, Italy

Chapter 11

Risk-Constrained Generation and Network Expansion Planning of Multi-carrier Energy Systems



Mehrdad Setayesh Nazar and Alireza Heidari

11.1 Introduction

The distributed energy resource (DER) commitment strategies have changed the operational and planning exercises and increased the interdependency of multi-energy carrier systems [1]. The traditional methods of expansion planning of electric distribution system have widely changed because the electrical DERs are injecting electricity into the main grid and some of the electrical system users are prosumers.

The multi-carrier energy supplier (MCES) supplies the energy of downward customers and active microgrids (AMGs) and transacts energy with the upward market. The AMG may participate in the upward utility demand response programs (DRPs).

The optimal generation and network expansion planning (OGNEP) problem is a complex multidimensional problem that consists of analyzing economic, environmental, and technical aspects. Over recent years, different methods of OGNEP have been studied and various aspects of the problem are explored.

Reference [1] proposed an algorithm for multi-energy DER expansion planning. The bi-level optimization algorithm was used to minimize the aggregated costs and maximize reliability. The method was applied to a building complex and assessed the impact of different energy supply configurations on the costs. The algorithm reduced the aggregated costs of the system by about 54.7%. Reference [2] proposed the district energy system planning method that models emission, input exergy, and

M. Setayesh Nazar (✉)

Faculty of Electrical Engineering, Shahid Beheshti University, Tehran, Iran

e-mail: m_setayesh@sbu.ac.ir

A. Heidari

School of Electrical Engineering and Telecommunication, University of New South Wales, Sydney, NSW, Australia

e-mail: Alireza.heidari@unsw.edu.au

input energy as decision variables. The optimal solution reduced the values of input variables by about 6%, 24%, and 14.7%, respectively. Reference [3] utilized the mixed-integer linear programming (MILP) optimization algorithm to optimize the planning of combined heat and power (CHP)-based units. Reference [4] presented an optimal planning method for the heating system that minimized total aggregated investment and running costs. The algorithm results revealed that the system costs and emissions reduced by 25% and 5%, respectively. Reference [5] proposed a linear optimization procedure for the planning of electrical and district heating systems that minimized the costs. Reference [6] introduced a multi-indicator of system performance for the CHP-based system planning. The heating system was planned based on the minimization of system costs. Reference [7] introduced a planning procedure for the electric and heating energy subsystems that utilized the heuristic optimization algorithm to minimize costs and voltage deviations. Two case studies assessed the proposed algorithm. Reference [8] proposed the optimal topology and facility characteristics of an energy system that minimized the system's costs using mixed-integer programming. Reference [9] utilized the MILP algorithm to determine the district heating planning topology that the method minimized emissions and maximized savings. The cost of the test system was reduced by 30%. Reference [10] utilized the dynamic optimization procedure for the planning of a heating system, the process maximized the revenue of the system, and the environmental and economic constraints were modeled.

Reference [11] introduced the mixed-integer nonlinear programming (MINLP) model for planning of heating system that considered the renewable DERs and the detailed model of facilities. The algorithm reduced the system's costs by about 15%. Reference [12] planned the heating system to minimize the aggregated costs. The method was assessed for a real system and the costs reduced by 33%. Reference [13] considered the uncertainties of stochastic variables in the planning of the electrical system and utilized a heuristic optimization procedure. Reference [14] proposed a planning procedure for a hybrid energy system that consisted electrical, gas, hydrogen storage, and district heating systems. The method used a multilevel optimization method that utilized genetic algorithm (GA) for optimizing the planning problem and MILP process for scheduling of system resources. Reference [15] introduced a MILP model of planning that minimized the cost of system and emissions. Reference [16] utilized the linear programming for determining the optimal characteristics of real system facilities and the algorithm minimized the emissions and system costs. Reference [17] proposed a two-level optimization process that modeled the uncertainties of DERs. The model was optimized using a column and constraint generation algorithm. Reference [18] utilized a heuristic optimization algorithm for the planning of energy system and considered the risk-averse strategy of planning. A risk index was used to evaluate the planning alternatives using Monte Carlo simulation process. Reference [19] presented a framework for considering the impact of coordinated bidding of participants on the planning problem. A multistage optimization process was proposed. Reference [20] addressed a hierarchical framework for integrated planning of electrical and district heating networks that considered the electricity transactions with AMGs. A three-stage optimization process was

proposed that determined the expansion planning decision variables, AMG transactions, and system’s contingency. Reference [21] presented an optimization algorithm for hybrid electric and thermal energy systems that considered the seasonal difference of electrical loads of system. The proposed algorithm allocated the energy storage facilities to perform demand-side management alternatives. Reference [22] addressed a constrained unit-commitment optimization framework for multi-carrier energy systems that minimized the operation costs. The proposed method reduced the operation costs by 20%.

The introduced references did not consider the impact of marginal pricing on the multi-energy carriers’ expansion planning problem. This book chapter is about the expansion planning of multi-carrier energy system algorithm that considers the locational pricing impact on the planning exercise.

11.2 Problem Modeling and Formulation

As shown in Fig. 11.1, the MCESO operator (MCESO) utilizes boilers, CHP units, thermal energy storages (TESs), and electrical storage systems (ESSs).



Fig. 11.1 The diagram of MCESO energy interactions

The OGNEP problem has four sources of uncertainty: the customers' energy consumption (CEC), electricity market price, AMG bidding scenarios and power transactions with MCES, and intermittent power generation (IPG).

Thus, the uncertainties of OGNEP can be modeled as a four-level stochastic problem. At the first stage, the CEC scenarios (CECSs) are generated. At the second stage, the electricity market scenarios are generated. At the third stage, the AMG bidding and power transaction with MCES are calculated. Finally, the IPG scenarios (IPGSs) are determined.

The AMGs can change the value of locational marginal prices (LMPs) by increasing their bidding price [23–25]. The MCESO should consider the LMP values in its expansion planning exercises based on the fact that the higher values of LMPs may increase the planning costs.

The optimal OGNEP should maximize the MCES revenues and minimize the aggregated system costs. Thus, the objective function of OGNEP can be proposed as in Eq. (11.1):

$$\begin{aligned} \text{Min } \mathbb{Z} = & \sum_{N\text{Year}} \sum_{NWMS} \text{prob.} \sum_{NCECS} \text{prob.} \left(W_1 (C_{MCES} \cdot \phi_{MCES} + \sum_{NAMGS} \text{prob.} \cdot C_{AMGs} \cdot \phi_{AMGs}) \right. \\ & \left. + C_{\text{Purchase}} + \sum_{NIPGS} \text{prob.} \cdot C_{IPG} + ENSC \right. \\ & \left. - \text{revenue} \right) + W_2 \sum_{NB} (LMP - -LMP) \\ & + \beta \left(\zeta - \frac{1}{1-\alpha} \sum_{NWMS} \text{prob.} \sum_{NCECS} \text{prob.} \cdot \eta \right) \end{aligned} \quad (11.1)$$

The objective function components are (1) the aggregated costs of MCES facilities, (2) the costs of AMG contributions, (3) the energy purchased costs, (4) the IPG costs, (5) the energy sold benefits, and (6) the conditional value-at-risk multiplied by the factor β .

Equation (11.1) is constrained by multiple economic and technical constraints that are categorized into the following groups [1]:

1. Budget constraint
2. Device loading constraints
3. Charge and discharge of energy storage constraints
4. Demand response program constraints
5. Electrical load flow constraints
6. Mass balance equation constraints

11.3 Solution Algorithm

The model is a non-convex MINLP problem. Figure 11.2 shows the optimization process that utilizes a four-stage uncertainty modeling. The confidence level is $\alpha = 0.95$.

For optimization procedure, the hybrid elitist non-dominated sorting GA (HNSGA-II) is used and adaptive genetic algorithm (AGA) and non-dominated sorting genetic algorithm (NSGA) results are compared. The NSGA-II creates a parent population and GA operators are used to create a child population. The solutions of the last accepted front are sorted and a set of points are selected based on their fitness value [26]. The HNSGA-II uses a weighted objective of Chebyshev metric that converts multiple objective functions to a single objective function. The proposed HNSGA-II can be presented as follows:

1. Create a random parent population that its fitness equals to non-dominated level.
2. Binary selection, recombination, and mutation operators create child population.
3. The combined population is formed and parent and child population solutions are compared.
4. The values of objective functions are logged.
5. The following weight factor is assigned as in Eq. (11.2):

$$\text{Weight ObF}_i = \frac{(\text{ObF}_i^{\text{Max}} - \text{ObF}_i) / (\text{ObF}_i^{\text{Max}} - \text{ObF}_i^{\text{Min}})}{\sum_i (\text{ObF}_i^{\text{Max}} - \text{ObF}_i) / (\text{ObF}_i^{\text{Max}} - \text{ObF}_i^{\text{Min}})} \tag{11.2}$$

ObF = Objective functions of Eq. (11.1).

6. A search around the existing solution is performed for optimizing the objective function. The weights produce a Pareto-optimal solution for convex regions. If non-convex regions, there are no weight factors, Chebyshev metric must be used, and non-domination check must be performed to ensure elitism [26].
7. A clustering technique is used to reduce the size of the optimal set [27].

To assess the performance of proposed algorithms the inverted generational distance (IGD) [27] is used. It is presented as in Eq. (11.3):

$$\text{IGD} = \frac{\sqrt{\sum_{i=1}^n \text{dis}_i^2}}{n} \tag{11.3}$$

where n is the number of true PF components, and dis is the Euclidean distance between the calculated and the nearest set member of non-dominated solutions [27].

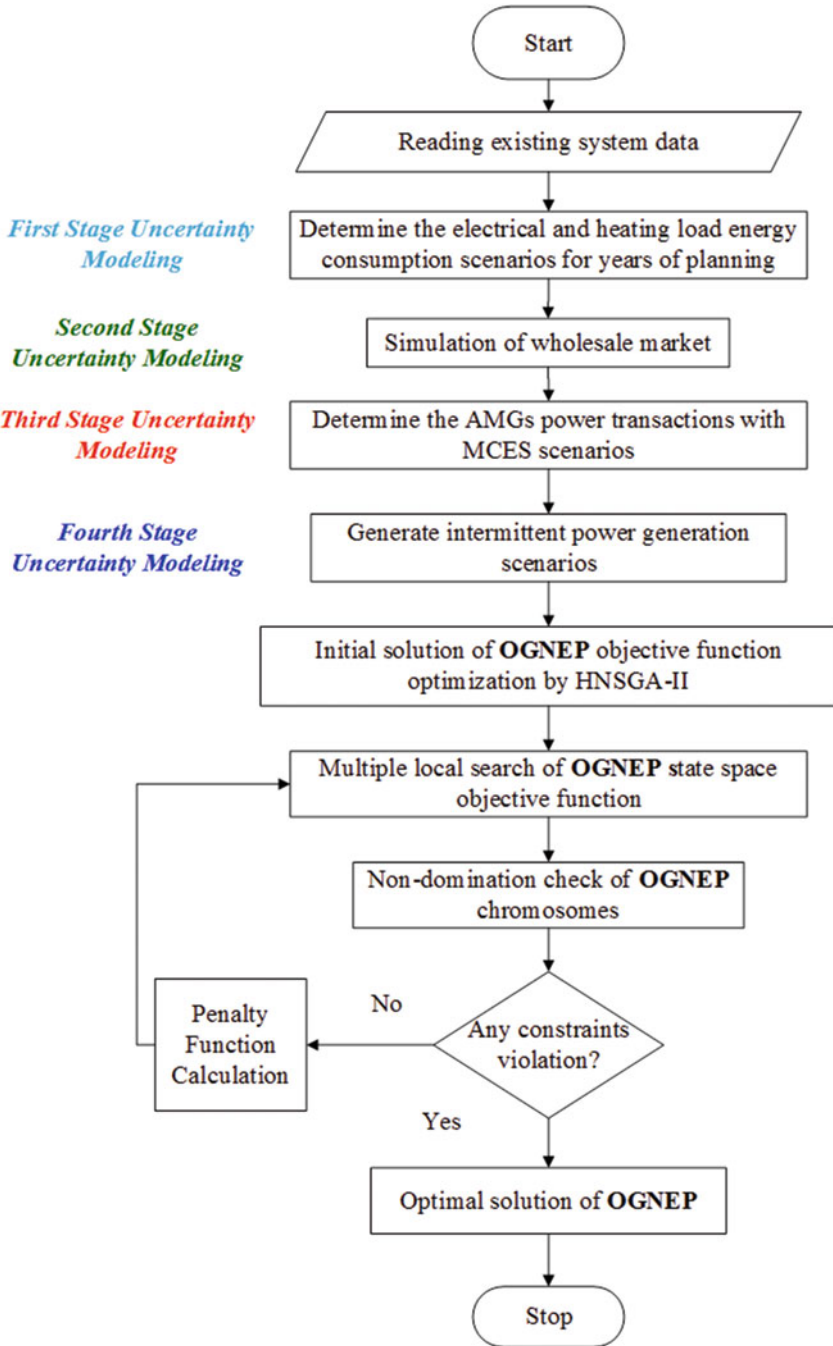


Fig. 11.2 Flowchart of proposed OGNEP algorithm

11.4 Simulation Results

A 14-bus system was used for case study and Fig. 11.3 shows the system topology. Tables 11.1–11.6 present system data. This network was a part of an industrial park district energy.

Multiple scenario generation and reduction procedures were performed for determining system uncertainties. Tables 11.1 and 11.2 present the CHP and district heating network parameters, respectively. Tables 11.3 and 11.4 show the district heating facility parameters and electrical network device parameters, respectively. Table 11.5 shows the distributed generation facility parameters.

Figure 11.4 presents one of the reduced scenarios of the electricity generation of wind turbine and solar photovoltaic of MCES.

Four reduced scenarios of AMG electricity transaction are considered that can be decomposed into the following types:

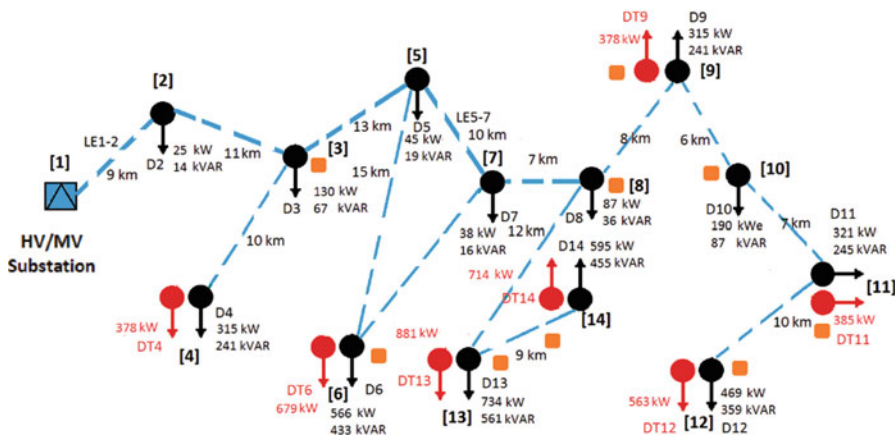


Fig. 11.3 Optimal topology of MCES for the final year of the planning horizon and different scenarios

Table 11.1 The CHP characteristics

CHP capacity (kW)	Investment cost (billion MUs)	$a + bp + cp^2$ (MU/h)			Yearly maintenance cost
		a	b	c	
1060	935	6.2864	29.1	1.1256	85,195
1131	1180	6.9821	31.2	1.0566	0.2498
1415	1381	8.2467	33.3	1.0542	0.2361
1820	1792	9.8780	32.8	0.9861	0.2312
2433	2399	12.1865	32.5	0.9953	0.2334
3041	3020	14.6500	31.8	0.9930	0.2366
3888	3200	18.7012	31.5	1.0246	0.2240
5327	4690	24.6373	31.2	1.0298	0.2186

Table 11.2 The district heating network parameters





Pipe type	Investment costs (MU/m)	Yearly maintenance cost (MU/m)
	850	95
	730	82
	680	73
	560	62

Table 11.3 The district heating facility parameters

Boiler capacity (kW)	Investment costs (MMUs)	Yearly maintenance costs (1000*Mus)	TES capacity (kWh)	Investment costs (MMUs)
400	1256	982	1500	9800
500	1698	1246	2000	12,980
600	2350	1678	2500	14,500
700	2980	1992	4000	16,900
800	3245	2250	5000	23,250
900	3892	2680	5500	25,700
1000	4600	2850	6000	27,600

Type 1: The bidding price of AMG and their electricity transactions with the MCESO were at their maximum value.

Type 2: The variables of the first type multiplied by 75%.

Type 3: The variables of the first type multiplied by 50%.

Type 4: The variables of the first type multiplied by 25%.

Further, six scenarios were considered:

Scenario 1: The optimal EDN and DHN expansion planning were separately performed for $\beta = 0$. In this procedure, the heating system weight factors for the planning of the electrical system were assumed to be zero for the entire planning horizon.

Scenario 2: The OGNEP was performed and only DERs of the system were allocated for $\beta = 0$.

Scenario 3: The OGNEP was performed and DERs of the system were allocated. The first type of scenario of AMG electricity transactions was considered for $\beta = 1$.

Scenario 4: The OGNEP was performed and DERs of the system were allocated. The second type of scenario of AMG electricity transactions was considered for $\beta = 0.67$.

Scenario 5: The OGNEP was performed and DERs of the system were allocated. The third type of scenario of AMG electricity transactions was considered for $\beta = 0.33$.

Scenario 6: The OGNEP was performed and DERs of the system were allocated. The first type of scenario of AMG electricity transactions was considered for $\beta = 0$.

Table 11.4 The electrical network device parameters







Primary network			Switching device					
Type	Investment cost (MU/m)	$R(\Omega/m)$	$X(\Omega/m)$	Type	Investment cost (MU/m)	$R(\Omega/m)$	$X(\Omega/m)$	Maintenance cost (1000*MU/s)
	245,739	0.127	0.101		8650	0.138	1.356	285
	211,437	0.159	0.104		6975	0.159	1.871	320
	189,678	0.196	0.107		5950	0.175	2.326	365

Table 11.5 The distributed generation facility parameters

DG capacity (kW)	Investment cost (1000*MMUs)	$a + bp + cp^2$ (MU/h)			Yearly maintenance cost
		<i>a</i>	<i>b</i>	<i>c</i>	
330	2.26	39.7	1.0852	0.2887	132,941.176
625	4.04	37.8	1.09	0.2503	237,647.058
749	4.75	36.7	1.1042	0.2484	279,411.764
850	5.26	35.4	1.055	0.2438	309,411.765
1130	6.6	33.8	1.0566	0.2361	388,235.294
1415	7.76	33.5	1.1012	0.2413	465,470.588

Table 11.6 The optimal location and capacity of MCES facilities

Scenario 1							
#Bus	CHP (kW)	#Bus	Boiler (kW)	#Bus	TES (kW)		
6	1131	4	400	4	1500		
9	540	6	700	9	1500		
12	1131	9	400	11	1500		
13	1060	11	400	13	2500		
14	848	12	600	14	2500		
		13	900				
		14	800				
Scenario 2							
#Bus	CHP (kW)	#Bus	Boiler (kW)	#Bus	TES (kW)		
6	1131	4	400	4	1500		
12	1131	6	700	9	1500		
13	1060	9	400	11	1500		
14	1415	11	400	13	2500		
		12	600				
		13	900				
		14	800				
Scenario 3						AMGs	
#Bus	CHP (kW)	#Bus	Boiler (kW)	#Bus	TES (kW)	#Bus	DG (kW)
6	1415	4	400	4	1500	3	625
12	1131	6	700	9	1500	8	540
13	1060	9	400	11	1500	10	540
14	1415	11	400	13	2500		
		12	600				
		13	900				
		14	800				
Scenario 4						AMGs	
#Bus	CHP (kW)	#Bus	Boiler (kW)	#Bus	TES (kW)	#Bus	DG (kW)
6	1415	4	400	4	1500	3	633
12	1131	6	700	9	1500	10	633
13	1060	9	400	11	1500		

(continued)

Table 11.6 (continued)

14	1415	11	400	13	2500		
		12	600				
		13	900				
		14	800				
Scenario 5						AMGs	
#Bus	CHP (kW)	#Bus	Boiler (kW)	#Bus	TES (kW)	#Bus	DG (kW)
6	1415	4	400	4	1500	3	540
12	1131	6	700	9	2000	8	435
13	1060	9	400	11	1500	10	330
14	1415	11	400	13	2500		
#Bus	DG (kW)	12	600				
3	625	13	900				
		14	800				
Scenario 6						AMGs	
#Bus	CHP (kW)	#Bus	Boiler (kW)	#Bus	TES (kW)	#Bus	DG (kW)
6	1415	4	400	4	1500	8	435
12	1131	6	700	9	2000	10	330
13	1060	9	400	11	1500		
14	1415	11	400	13	2500		
		12	600				
		13	900				
		14	800				

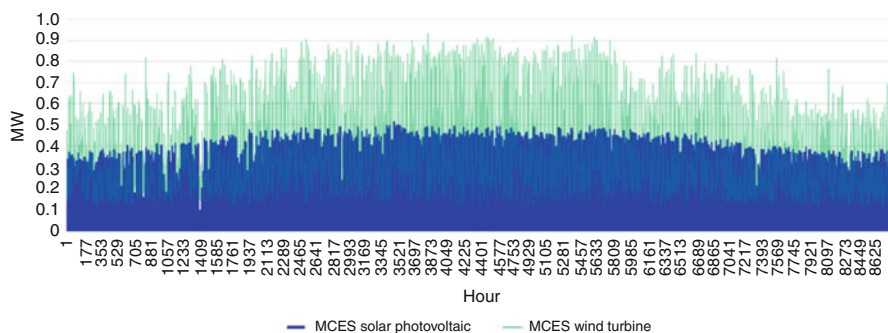


Fig. 11.4 The electricity generation of wind turbine and solar photovoltaic of MCES

Figure 11.5 presents the optimal topology of MCES. Further, Table 11.6 presents the optimal location and capacity of MCES facilities. As shown in Fig. 11.5 and Table 11.6, the OGNEP allocated more system DER for the third scenario. Further, the OGNEP costs were highly increased when the risk-averse strategy of planning was selected.

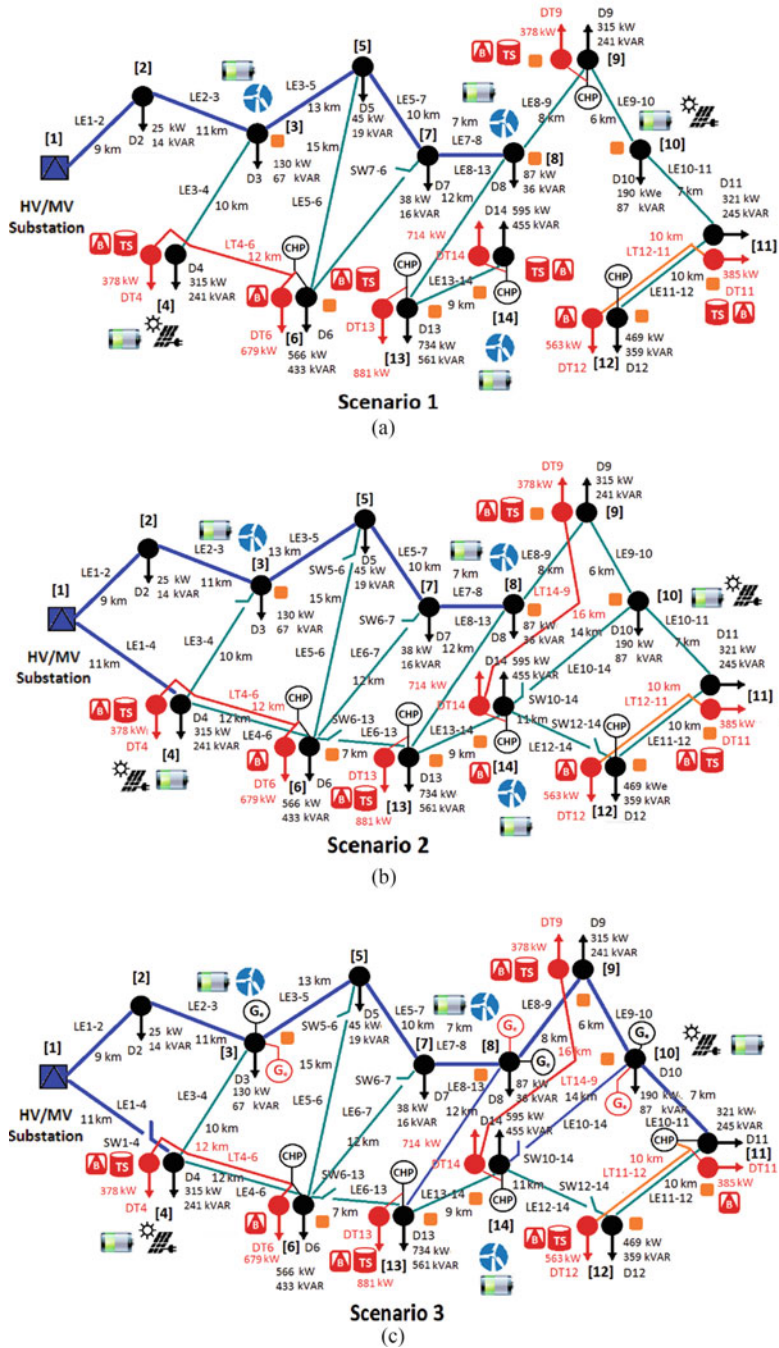
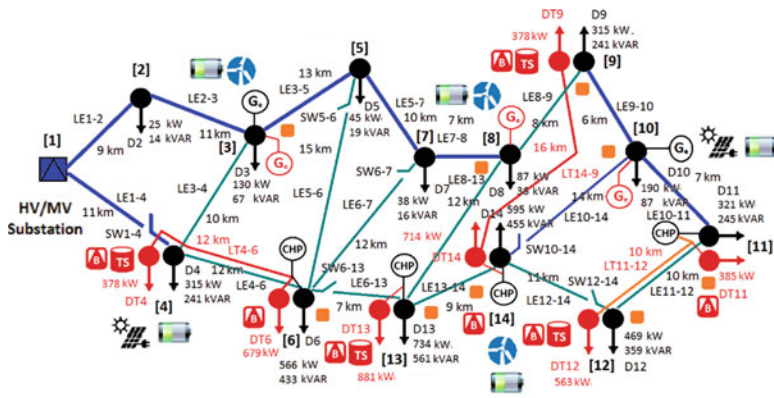
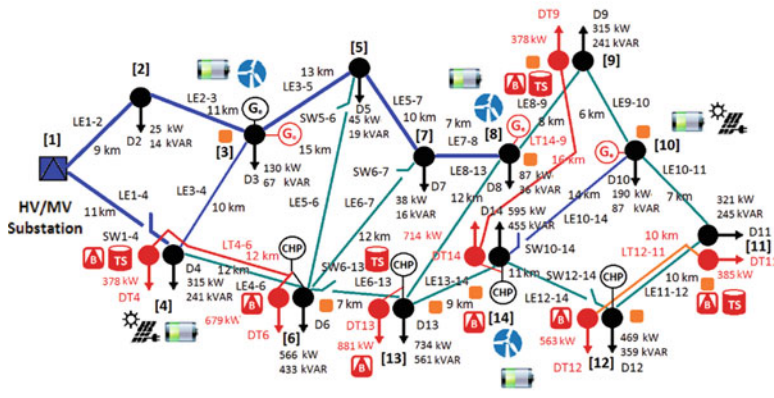


Fig. 11.5 Optimal topology of MCES



Scenario 4
(d)



Scenario 5
(e)

Fig. 11.5 (continued)

Figure 11.6 presents the IGD index for objective functions of AGA, NSGA, and HNSGA-II algorithms versus the number of generations. As shown in Fig. 11.6, the HNSGA-II was much more efficient than other optimization algorithms for reducing the IGD index.

Figure 11.7 presents the Pareto front of the second, third, and fourth objective functions of OGNEP versus the fifth objective function. The final solutions obtained by HNSGA-II had better spread and convergence than those by NSGA and AGA.

Figure 11.8 presents the maximum and average values of LMPs of MCES for the sixth scenario and the final planning year. As shown in Fig. 11.8, the OGNEP reduced the maximum and average values of LMPs for the sixth scenario. Figure 11.9 presents the heat dispatch of heating facilities for the peak day of the sixth scenario and the final planning year.

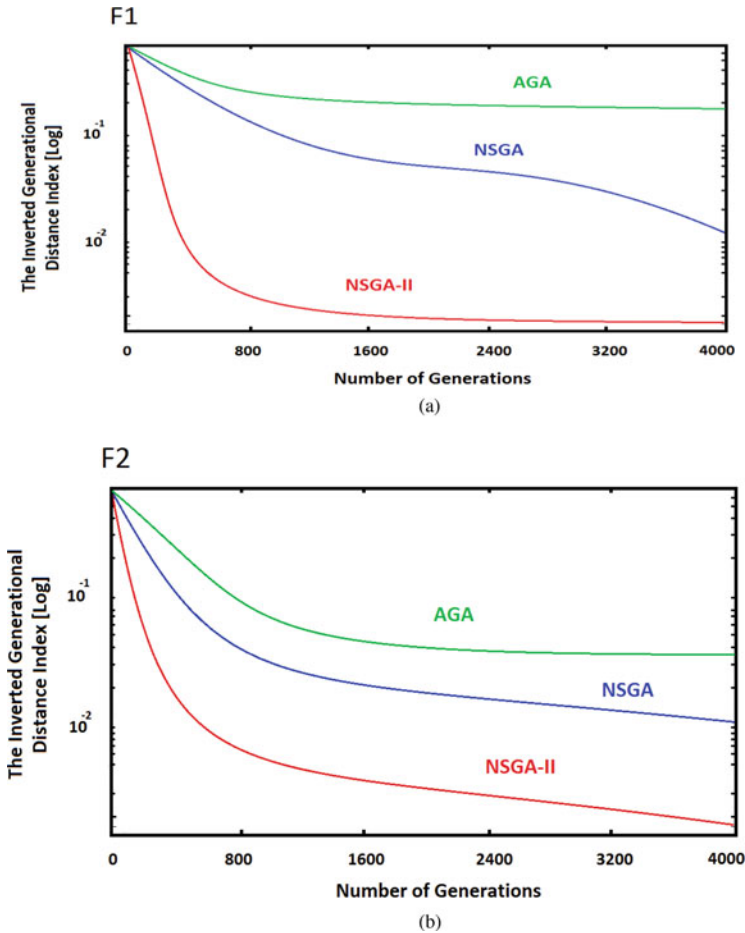


Fig. 11.6 The IGD index for objective functions of AGA, NSGA, and HNSGA-II algorithms

Figure 11.10 depicts the total system costs for different planning scenarios. The proposed HNSGA-II algorithm successfully found the optimal values of the MINLP objective functions

11.5 Conclusion

This chapter introduced the risk-averse optimal expansion planning algorithm for multi-carrier energy supplier system that utilized distributed energy resources to supply the electrical and heating loads. The multi-carrier energy system transacted electricity with the downward active microgrids and the optimization process

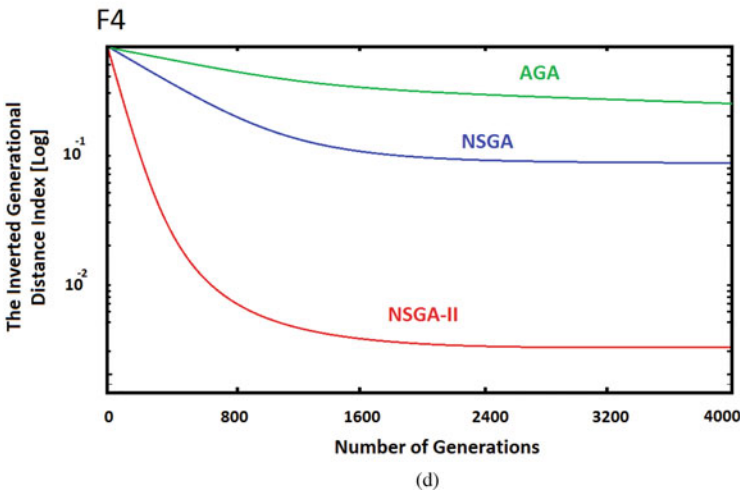
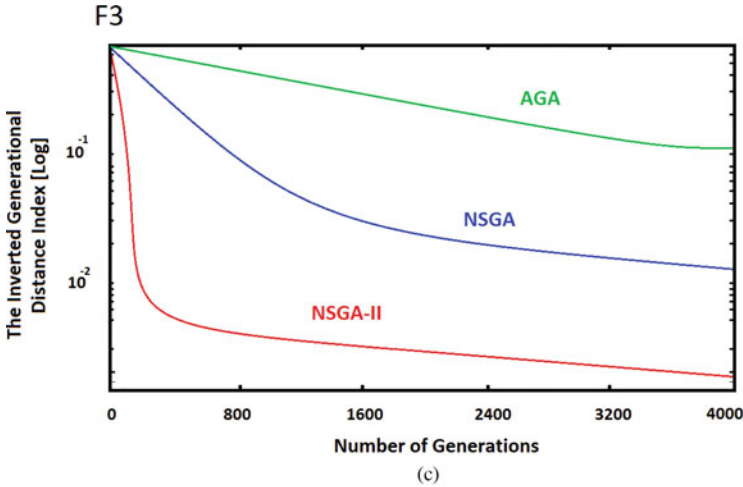


Fig. 11.6 (continued)

optimized the contribution of microgrids in the expansion planning horizon. The costs consisted of investment, operation, and energy purchased from active microgrids. Further, the energy-not-supplied costs and the locational marginal prices of system buses were formulated in the introduced model. The algorithm was optimized using different optimization processes and their results were compared. The hybrid elitist non-dominated sorting genetic algorithm, adaptive genetic algorithm, and non-dominated sorting genetic algorithm were used to optimize the formulated problem.

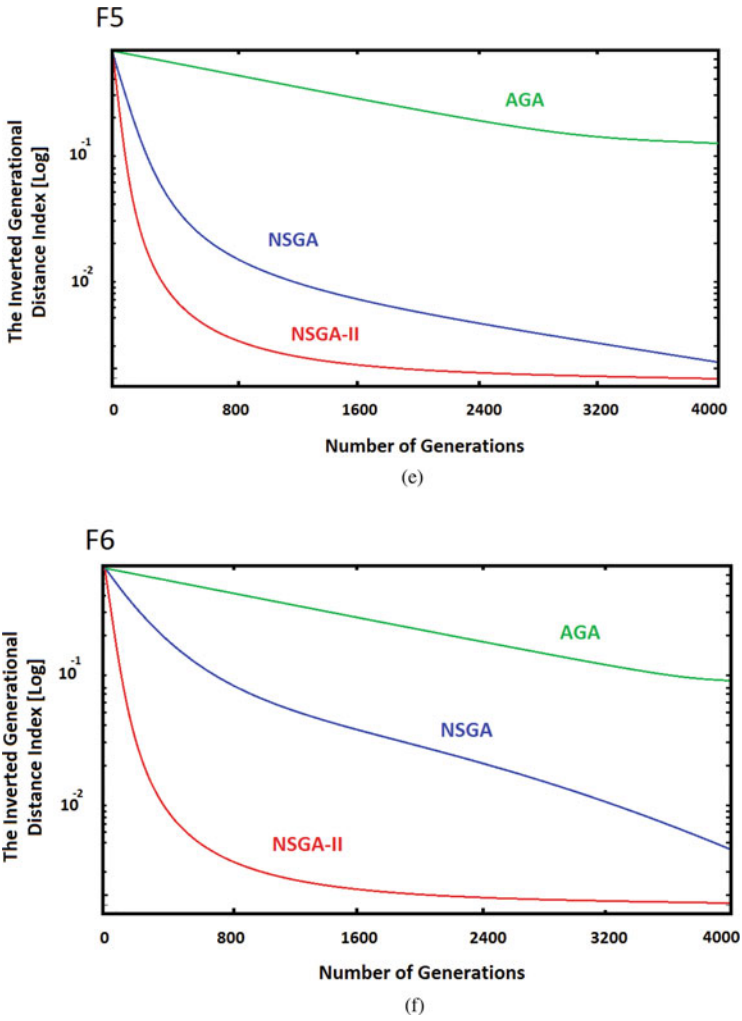
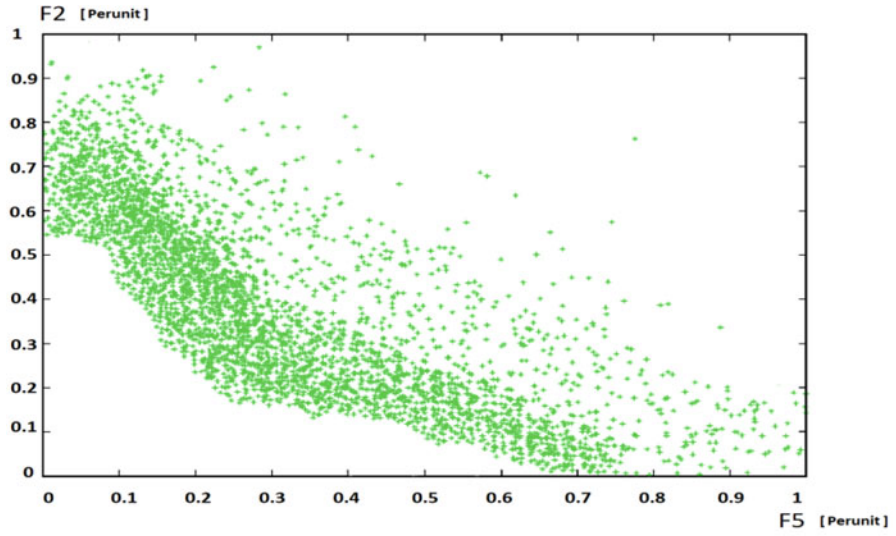
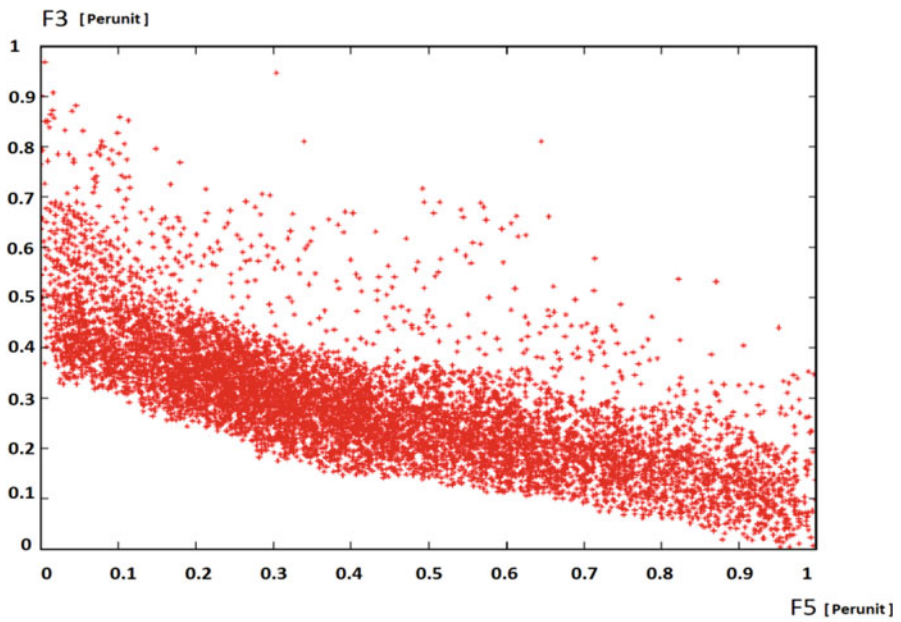


Fig. 11.6 (continued)



(a)



(b)

Fig. 11.7 The Pareto front of the second, third, and fourth objective functions of OGNEP versus the fifth objective function

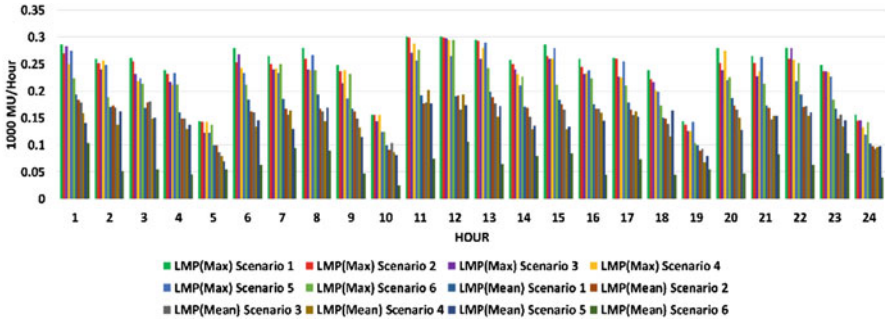


Fig. 11.8 The maximum and average values of LMPs of MCES for the sixth scenario and the final planning year

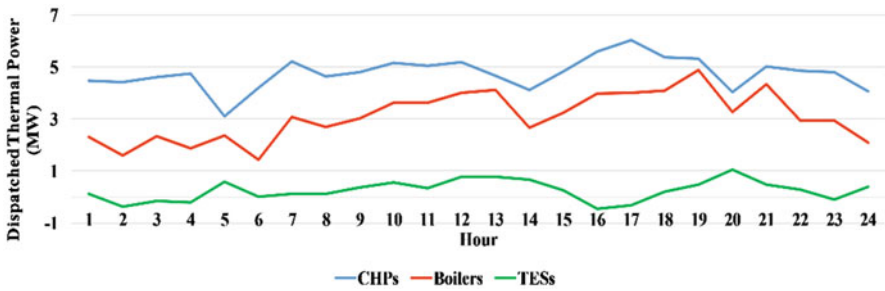


Fig. 11.9 The heat dispatch of heating facilities for the peak day of the sixth scenario and the final planning year

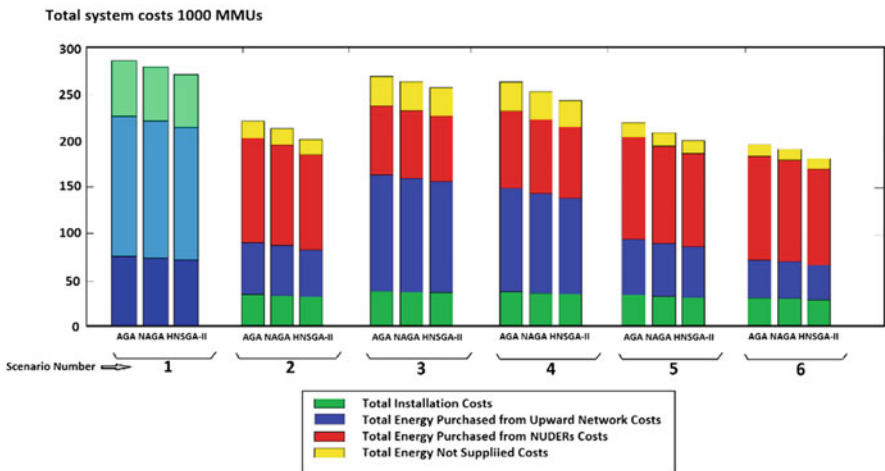


Fig. 11.10 The system costs for different scenarios of OGNEP and optimization procedures

An industrial district multiple-energy carrier system was used to assess the introduced method, the optimization process was carried out, and the expansion planning outputs were determined. The optimization algorithm successfully minimized the total investment, operational costs, and locational marginal prices of the system. The process encountered the active microgrid contributions in the planning of the multi-carrier energy system.

Nomenclature

Abbreviations

AGA	Adaptive genetic algorithm
AMG	Active microgrids
CEC	Customers’ energy consumption
CECSs	CEC scenarios
CHP	Combined heat and power
ESS	Electrical storage systems
DER	Distributed energy resource
DRP	Demand response program
GA	Genetic algorithm
HNSGA-II	Hybrid elitist non-dominated sorting GA
IGD	Inverted generational distance
IPG	Intermittent power generation
IPGSs	IPG scenarios
LMP	Locational marginal price
MCES	Multi-carrier energy supplier
MCESO	MCES operator
MILP	Mixed-integer linear programming
MINLP	Mixed-integer nonlinear programming
NSGA	Non-dominated sorting genetic algorithm
OGNEP	Optimal generation and network expansion planning
PF	Pareto front
TES	Thermal energy storages

Variables

C_{MCES}	The investment and operational costs of MCES facilities
C_{AMGs}	The costs of AMG contributions
$C_{Purchase}$	The electricity purchased from upward market costs
C_{IPG}	The costs of IPGs
ENSC	Energy-not-supplied cost
revenue	The revenue of energy sold
ϕ_{MCES}	Binary decision variable of MCES facility installation
ϕ_{AMGs}	Binary decision variable of AMG commitment
α	Confidence level
β	Weighting parameter
ζ, η	Auxiliary variables used to compute the CVaR
NYear	Number of planning horizon
NWMS	Wholesale market scenarios
NCECS	Customers’ energy consumption scenarios
NIPGS	Intermittent power generation scenarios

References

1. Varasteh F, Setayesh Nazar M, Heidari A, Shafie-khah M, Catalão JPS (2019) Distributed energy resource and network expansion planning of a CCHP based active microgrid considering demand response programs. *Energy* 172:79–105
2. Hou J, Xu P, Lu X, Pang Z, Chu Y, Huang G (2018) Implementation of expansion planning in existing district energy system: a case study in China. *Appl Energy* 211:269–281
3. Moradi S, Ghaffarpour R, Ranjbar AM, Mozaffari B (2017) Optimal integrated sizing and planning of hubs with midsize/large CHP units considering reliability of supply. *Energy Convers Manag* 148:974–992
4. Aringhieri R, Malucelli F (2003) Optimal operations management and network planning of a district system with a combined heat and power plant. *Ann Oper Res* 120:173–199
5. Mehleri ED, Sarimveis H, Markatos NC, Papageorgiou LG (2013) Optimal design and operation of distributed energy systems: application to Greek residential sector. *Renew Energy* 51:331–342
6. Franco A, Versace M (2017) Optimum sizing and operational strategy of CHP plant for district heating based on the use of composite indicators. *Energy* 124:258–271
7. Abbasi AR, a Seifi AR (2014) Energy expansion planning by considering electrical and thermal expansion simultaneously. *Energy Convers Manag* 83:9–18
8. Soderman J, Petterson F (2006) Structural and operational optimization of distributed energy systems. *Appl Therm Eng* 26:1400–1408
9. Delangle A, Romain S, Lambert C, Shah N, Acha S, Markides CN (2017) Modelling and optimising the marginal expansion of an existing district heating network. *Energy* 140:209–223
10. Mojica JL, Petersen D, Hansen B, Powell KM, Hedengren JD (2017) Optimal combined long-term facility design and short-term operational strategy for CHP capacity investments. *Energy* 118:97–115
11. Mertz T, Serra S, Henon A, Reneaume JM (2016) A MINLP optimization of the configuration and the design of a district heating network: academic study cases. *Energy* 117:450–464
12. Bordin C, Gordini A, Vigo D (2016) An optimization approach for district heating. *Eur J Oper Res* 252:296–307
13. Rastgou A, Moshtagh J (2018) Improved harmony search algorithm for electrical distribution network expansion planning in the presence of distributed generators. *Energy* 151:178–202
14. Lia B, Rochea R, Paire D, Miraoui A (2018) Optimal sizing of distributed generation in gas/electricity/heat supply networks. *Energy* 151:675–688
15. Wang H, Zhang H, Gu C, Lid F (2017) Optimal design and operation of CHPs and energy hub with multi objectives for a local energy system. *Energy Procedia* 142:1615–1621
16. Weber C, Shah N (2011) Optimization based design of a district energy system for an eco-town in the United Kingdom. *Energy* 36:1292–1308
17. Wu M, Kou L, Hou X, Ji Y, Xu B, Gao H (2019) A bi-level robust planning model for active distribution networks considering uncertainties of renewable energies. *Int J Electr Power Energy Syst* 105:814–822
18. Samper M, Vargas A (2013) Investment decisions in distribution networks under uncertainty with distributed generation - part I: model formulation. *IEEE Trans Power Syst* 28:2341–2351
19. Qaeini S, Setayesh Nazar M, Yousefian M, Heidari A, Shafie-khah MR, Catalão JPS (2019) Optimal expansion planning of active distribution system considering coordinated bidding of downward active microgrids and demand response providers. *IET Renewable Power Gener* 13:1291–1303
20. Qaeini S, Setayesh Nazar M, Varasteh F, Shafie-khah MR, Catalão JPS (2020) Combined heat and power units and network expansion planning considering distributed energy resources and demand response programs. *Energy Convers Manag* 211:112776
21. Yan Z, Zhang Z, Liang R, Jin W (2020) An allocative method of hybrid electrical and thermal energy storage capacity for load shifting based on seasonal difference in district energy planning. *Energy* 207:118139

22. Mirzaei MA, Nazari Heris M, Zare K, Mohammadi-Ivatloo B, Marzband M, Asadi S, Anvari-Moghaddam A (2020) Evaluating the impact of multi-carrier energy storage systems in optimal operation of integrated electricity, gas and district heating networks. *Appl Thermal Energy* 176:115413
23. Salarkheili S, Setayesh Nazar M (2017) Capacity withholding assessment in the presence of integrated generation and transmission maintenance scheduling. *IET Gener Transm Distrib* 11:3903–3911
24. Salarkheili S, Setayesh Nazar M (2016) Capacity withholding analysis in transmission-constrained electricity markets. *IET Gener Transm Distrib* 10:487–495
25. Salarkheili S, Setayesh Nazar M (2015) New indices of capacity withholding in power markets. *Int Trans Electr Energy Syst* 25:180–196
26. Sarkar R, Mohammadian M, Yao X (2003) *Evolutionary optimization*. Kluwer Academic Press
27. Zitzler E, Thiele L, Laumanns L, Fonseca CM, Fonseca VGD (2003) Performance assessment of multiobjective optimizers: an analysis and review. *IEEE Trans Evol Comput* 7:117–132

Chapter 12

Uncertainty Modeling in Operation of Multi-carrier Energy Networks



Mohammad Salehimalah, Adel Akbarimajd, Khalil Valipour,
and Abdolmajid Dejamkhooy

12.1 Introduction

As you know, the concept of energy hub (EH) refers to the simultaneous and integrated planning and management of different energy infrastructure in order to meet the demand on the consumer side. Input energy carriers can be supplied by using the bilateral contracts in the EH, through the upstream networks or energy production equipment. Then, by optimal management, the input energies are delivered to the outputs by the generation, transmission, distribution, conversion, and storage devices in the EH, to meet various demands in consumer side such as electricity, heating, and cooling.

In the last decade, the penetration of the concept of EH has increased as a viable solution to supply various energy demands in an affordable, adequate, and secure way for consumers and sustainable energy development, too. Therefore, we have been facing an increasing expansion of research in modeling the short-term, medium-term, and long-term planning of multi-carrier energy systems in recent years. From this aspect, we discuss about short-term planning (operation) of EH in this chapter.

The optimal operation problem in EH is actually determining the optimal operating point of energy generation, conversion, and storage devices by considering the flexibility and dynamics of EH, in order to supply different loads with the lowest cost.

Input data in optimization problems can be certain or uncertain. In certain optimization problems, it is assumed that the inputs of the problem have known values. Therefore, the output decision variables will be valid for a period of time. But

M. Salehimalah (✉) · A. Akbarimajd · K. Valipour · A. Dejamkhooy
Department of Electrical and Computer Engineering, Faculty of Technical and Engineering,
University of Mohaghegh Ardabili, Ardabil, Iran
e-mail: Akbarimajd@uma.ac.ir; majiddejam@uma.ac.ir

if the descriptive input data of a system are uncertain, then the prediction of the performance ahead is definitely uncertain.

In fact, uncertainty is originated from the difference between the input data to the problem and the actual data that exists. It happens due to various reasons such as inaccessibility of accurate data when solving the problem (that leads to prediction error), incorrect data measurement (that leads to measurement error), and approximations and simplification of data in the implementation process (that leads to implementation error). Like many engineering problems, optimal operation of EH is uncertain. For various reasons multi-carrier energy systems in the concept of EH are faced with uncertainty too. These reasons include the random nature of renewable energy sources connected to the EH, errors in forecasting the price of energy carriers, changes in the proposed price of upstream networks and energy market rules, forecasting of the electrical vehicle owners' behaviors, consumer demand prediction errors, measurement and reporting of errors, and implementation and simplifications errors. Therefore, the optimal operation of the EH requires exact modeling, and accurate and close-to-reality modeling will be possible by considering the uncertainties in these systems. Because in real-world problems, a sudden change in one data imposes a lot of cost on the system and makes the solution impossible and inefficient. So, managers and decision makers have to decide while they are facing various uncertainties.

Therefore, to reduce the challenge for EH owners and decision makers, it is necessary to consider these uncertainties in order to determine the correct strategy for optimal operation and also to increase the usefulness of these systems. Different methods are introduced to model the uncertainty; each has different advantages and disadvantages, including computational accuracy, computational load, and response speed. Therefore, in this chapter, we intend to review the historical data of these parameters and their modeling methods comprehensively.

Accordingly, in this study, in addition to considering the types of uncertainties and their modeling methods in the optimal operation of EHs, we will review the researches which are done in this field. Finally, we intend to help reader to find appropriate idea for modeling and optimization in this field that leads to more close-to-real decision and avoiding more extra costs by addressing the research gaps in previous research and studies.

The parts of this chapter are as follows.

In the second and third sections, we represent the types of uncertainty and their modeling methods in this field, respectively. In the fourth section, we review previous articles and researches in this regard. Finally, in the fifth section, we announce research gap and propose suggestions for future research.

12.2 Types of Uncertainty

Uncertainty is the difference between the known (or predicted) data and their actual values [1]. The possibility to achieve certain information is approximately zero. Also, the smallest change of input information can change the optimality significantly. Various variables in modeling an issue can have a random behavior along with exact unpredictable changes of their own. Each of these variables, which should be considered as uncertain data in an issue, affects the results. Thus, by appropriate modeling of these uncertain data, their effect on the results' exactness, accuracy, and optimality will be more visible. These uncertain variables have various sources and different reasons, and they are related to the parameters of different parts. Considering these issues can classify different types of uncertainties.

At the sequel, review of uncertainty in different articles and different classifications is pointed briefly.

In 1989, Ho considered two types of uncertainties. The first type was an environmental uncertainty that is originated from the environment (such as the rate of customer demand or the price of electricity market), and the second type was the system uncertainty that is related to the structure and equipment of system (such as the equipment's forced outage rate because of their failure).

In [2], uncertainty is divided into two categories, including parametric uncertainty that is originated from lack of knowledge about the amounts of model parameters, and structural uncertainty that is originated from uncertainty of model equation. Authors in [3] divided the types of uncertainty into six categories based on their sources.

1. Inherent randomness that random uncertainty is presented in essence and nature and one can consider it easily in probabilistic models.
2. Measurement error that leads to uncertainty in the measured quantity amount: If several measurements are done, this error can be estimated by statistical methods and easily captured in the related probabilistic models.
3. Systematic errors in the results of the measurements that originate from human errors due to difficulty or ignoring.
4. Natural variation that originates from natural system changes in different times and places and consistently is uncertain towards various natural conditions.
5. Model uncertainty that is originated from the nature of the system and insufficient knowledge about its processes, the outline of functions, and the number of parameters.
6. Subjective judgment uncertainty due to interpretation, especially when the data are few and have an error.

In refs. [4, 5], different types of uncertainties are divided into five categories:

1. Knowledge or epistemic uncertainty is because of lack or limitation of knowledge in planning and decision-making about the system. The subcategories of this type of uncertainty include the following items:

Context and framing uncertainty: This is because of decision makers and planners' understanding or knowledge about the content of planning and assessment and setting boundary conditions of realities and uncertainties and it is more available in conceptual models.

Model uncertainty: Due to features of models, knowledge uncertainty can be created that is divided into other subcategories (model uncertainty) by itself:

Model input and output data: Input data can be divided into two internal system data (model system data), and different features of system parameters. Output data (external driving forces) describe the uncertainties in system environment that can be based on lack of knowledge or changes of data.

Data uncertainty can possibly originate from measurement errors including used instrumentations, quality and calibration frequency of instrumentations, data reading, user error, sampling method, or data recovery. The uncertainty of exact and fixed parameters (as an example, ϵ or π) is that the exact amount of these parameters can be ignored in analyses. This uncertainty is the intentional or unintentional faulty knowledge of parameters. Parameters can be divided into two categories: priority chosen parameters that will be fixed in the beginning of the study and calibrated parameters that are unknown at the beginning of modeling and should be determined through calibration:

Model structure uncertainty that is because of misunderstanding or interpretation of real system processes, such as economic and physical processes, and also because of the simplification of complex dynamical system for a model presentation from the theory point of view

Model technical uncertainties that are created by software and hardware errors

Model output uncertainty, from the collection of other uncertainties (data, parameters, structure, and so on)

Besides the above categories, we can recognize one more category:

The uncertainty of models with different time and place criteria can also be one subcategory of this category.

2. Linguistic uncertainty, which is originated from the stated information by a human that is based on natural language: This type of uncertainty includes three subcategories:
 - Vagueness uncertainty is originated from scientific and natural limitations of language in the correct presentation of some parameters.
 - Ambiguity, in the words that have several meanings and their exact meaning, is not evident.
 - Under specificity that is not in definition or development of some information or concepts or sufficient cognition will be achieved.
3. Variability/aleatory/random/stochastic uncertainty, originated from natural mutability (that in our idea includes time and place changes of phenomena and is not reducible), human behavioral pattern changes, changes in technology and organizations.

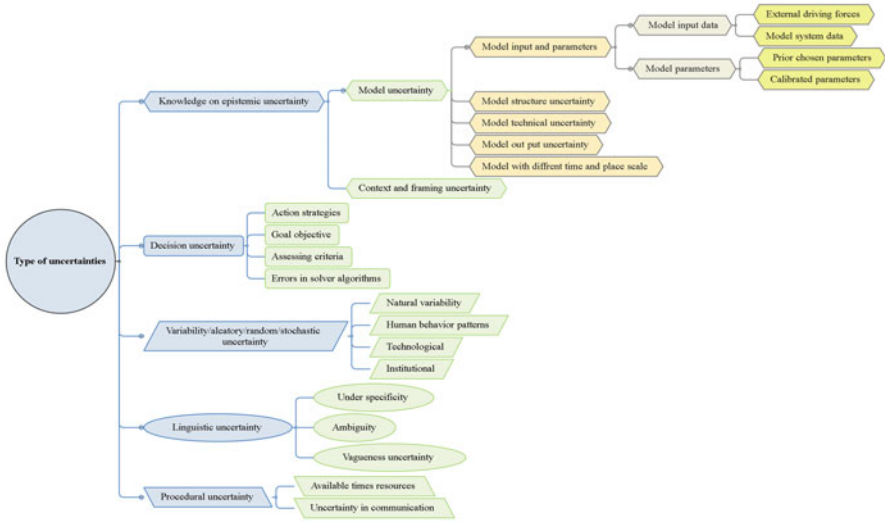


Fig. 12.1 Type of uncertainties

4. Decision uncertainty that is because of ambiguity in definitions, amounts, and comparison of goals or function indices. This uncertainty includes incapability in the prediction of other organizations’ decisions in the future, and incapability in predicting a set of goals in future, and each rational index. Of course, we believe that we can consider the error in the algorithm-solving model as a part of the decision-making uncertainty.
5. Procedural uncertainty that is originated from the available time and sources: It means that extra time and sources (unplanned) are required to achieve new data or information. Also, uncertainty is essential in the relation between results and models that can lead to delay in an attempt, choice of amounts in limited range, and dangerous management decisions. This type of uncertainty depends on the method of information presentation and its correct understanding.

According to the mentioned sources and to sum up the discussion about different types of uncertainty, in Fig. 12.1, we present uncertainty types and their subcategories.

Understanding of this diversity in uncertainty sources and distinguishing among them specify the rate of effectiveness, and the improvement of modeling performance and decision-making. However, functionally preparation of decision-making models and management of systems are remarkably related to the approach of modeling and its appropriateness to the type of uncertainty.

12.3 Existing Methods for Uncertainty Modeling

Uncertain data modeling leads to accurate, optimal, and close-to-real response. These uncertainties are modeled by different methods (Fig. 12.2). Although these methods are different in modeling and explanation of uncertain parameters, all of them try to reduce the undesirable effects arising from ignoring the uncertain parameters. In the following, we introduce several methods of uncertainty modeling.

Considering uncertainties at the planning and management stage of systems is more critical and crucial in multiple energy systems and EHs, due to the number of different devices and energy carriers used in them. Thus, we are interested in reviewing the existing methods for modeling and considering uncertainties in such systems. Although these methods have differences in the modeling and inclusion of uncertain parameters, their common purpose is reducing of the adverse effects of uncertainties' ignorance.

In the following, we introduce some uncertainty modeling methods. These methods have been introduced and categorized in different fields and different publications. Our purpose in this section is to summarize and review these methods as well as address papers that deal with multiple-energy systems and EHs, using existing methods for considering uncertainties. The categorization of these methods is summarized in ref. [4, 6–8]. We have summed up all of them in Fig. 12.2 and we have also added branches to this tree and updated it. We will detail them in the following subsections.

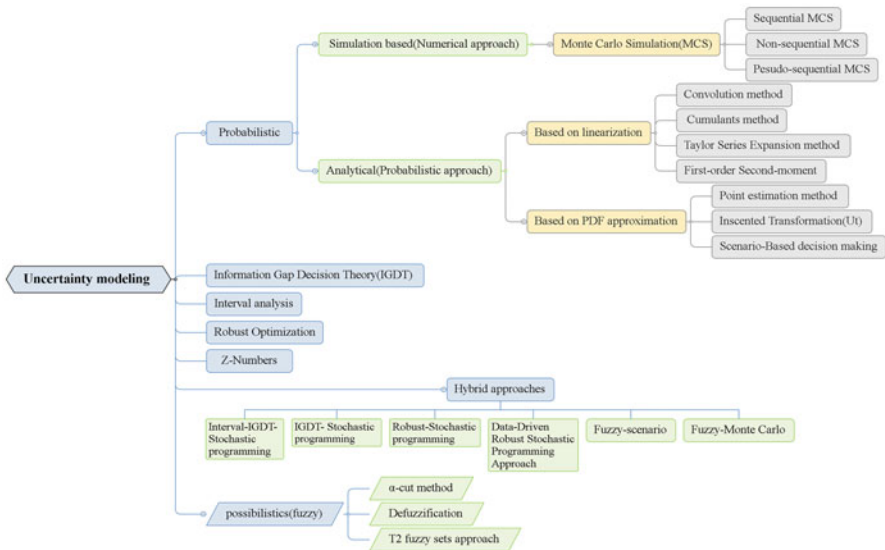


Fig. 12.2 Type of uncertainty modeling methods

12.3.1 Probabilistic Methods

Nowadays, many probabilistic techniques are applied to modeling uncertainty parameters in engineering system problems. Often when we have sufficient historical data in uncertain situation, or when the probability density functions (PDFs) of input parameters are available, the probabilistic methods are used. These approaches usually use PDF for describing uncertainty parameters, because some uncertain input parameters follow the PDF, such as normal or log-normal distribution for load demand, beta distribution for solar radiation, and Weibull distribution for wind speed variations, to describe uncertainties. Then the aim of this approach is to provide PDF of output variable, and in order to obtain it several methods are suggested in some literature for the probabilistic approach. The most frequently used techniques for uncertainty modeling use the idea of probability methods. We can classify these techniques into two categories: simulation-based approaches and analytical ones.

12.3.1.1 Simulation-Based Probabilistic Analysis

Monte Carlo Simulation (MCS)

MCS is one of the most usual stochastic techniques. It is suitable for modeling of uncertainty parameters and is a broad practical numerical method. The reason is that MCS does not depend on a system size and it can be used when we have highly nonlinear systems or are faced with a complicated system with many uncertain variables [9]. This method is flexible, simple to be implemented, and applicable for convex and non-convex problems and all types of the distribution function. However, a large number of required simulations to get accurate solutions and thus high computational burden are some of the disadvantages of the MCS technique. In the implementation of MCS as an iterative method, usually the following steps in the flowchart of Fig. 12.3 are required [7, 10, 11]:

It is noteworthy that by evaluating the PDF for the model output, the mean value, standard deviation, and other specifications of the output PDF can be extracted.

Three types of MCS methods which are used for probabilistic uncertainty analysis of engineering systems are sequential MCS, pseudo-sequential MCS, and nonsequential MCS [7]. The sequential Monte Carlo (SMC) techniques are a set of simulation-based approaches that obtain an easy and pleasant method to compute the posterior distribution. The SMC is simple to run, very flexible, and applicable in a typical adjustment. The nonsequential MCS provides comparable precision to sequential MCS with less computational burden [12]. A system state is a combination of all component states; likewise each component state can be determined by sampling the probability of the component appearing in that state, so nonsequential MCS is sometimes called “state sampling approach” [7]. In pseudo-sequential MCS, pseudorandom samples of model inputs are generated according to the PDFs

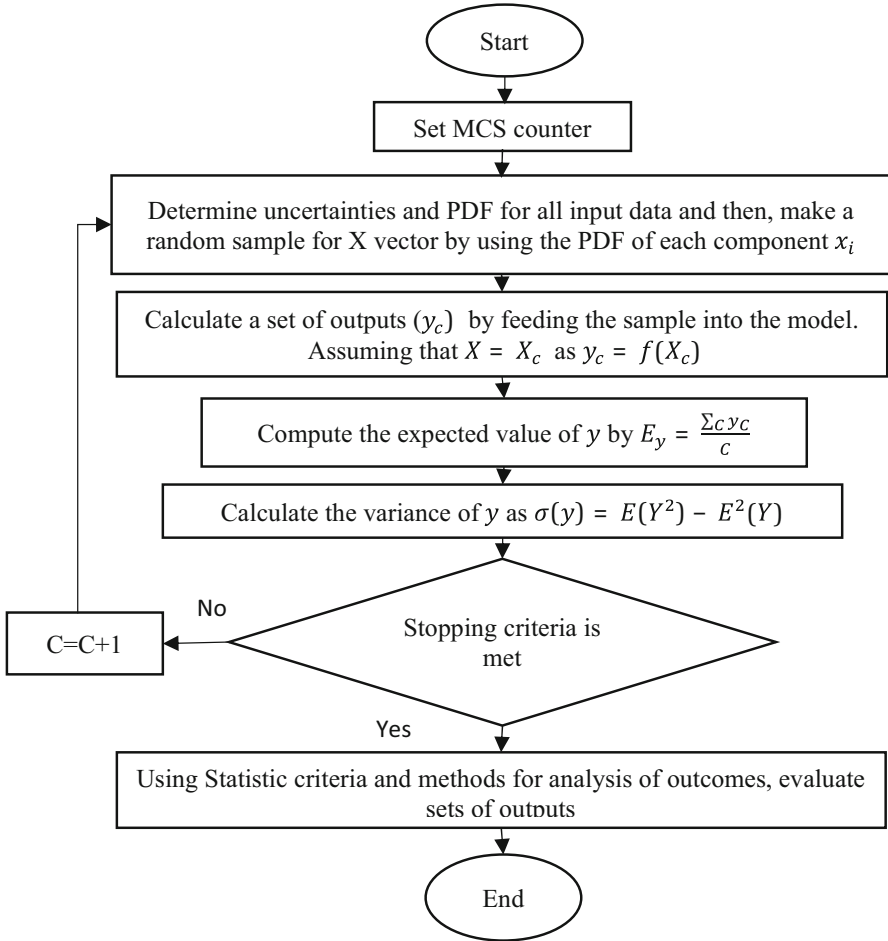


Fig. 12.3 A general flowchart of MCS method

specified for each input. In general, Monte Carlo technique needs a large number of random values. So it is necessary to develop pseudo-sequential Monte Carlo simulation to be faster than former Monte Carlo [13]. Also, there are some techniques such as Latin hypercube sampling (LHS) [14], sample-splitting approach [15], and fission and roulette method [16] that are used to reduce the computational burden of MCS. High efficiency in the face of non-differential and non-convex problems, support of all PDF types, nonrequirement for accurate recognition transfer function to calculate, and convenience of implementation are some of the advantages of MCS method. However, in contrast, heavy computation burden usually because of iteration and a large number of simulations by increasing the degrees of freedom of the solution space can be some of the disadvantages of MCS.

12.3.1.2 Analytical Approaches Based on Probabilistic Analysis

The analytical methods are usually explained by mathematical expressions, approximation, and simplifications, and have more complex algorithms [17]. These methods express system's input and output in terms of mathematical expressions. The analytical approaches can be classified into two different categories, including the methods based on (1) linearization and (2) PDF approximation.

Linearization-Based Methods

The first analytical methods are based on linearization and Taylor series expansion, and their objective is to create output PDF from input PDF. They try to linearize the nonlinear transformation function. In these methods, mathematical operations such as convolution, calculating the coefficients of expansions, and other mathematic processes are applied to calculate PDFs of output parameters from the PDFs of input parameters. Some of these methods such as convolution, cumulants and moments, first-order second moment, Gram–Charlier series, Edgeworth expansion, Taylor series, and Cornish–Fisher expansion are in this category.

Convolution method: The main drawbacks of this technique are heavy computation burden and a long time to determine the output PDFs. In order to solve this problem Allan et al. [18] have used the discrete Fourier transform (DFT) for reducing the computation load. Later, the concept of cumulant method is introduced to improve this condition.

Cumulant method: This method uses lightweight calculations to determine the PDF for a linear combination of different stochastic variables instead of convolution.

However, the drawback of the cumulant-based algorithm is the inaccuracy related to limitation due to using of the cumulants. By using the moments or cumulants of the distribution we can calculate the expansion coefficients. Three different approximation expansions are represented below [7]:

1. Gram–Charlier series: This lets many PDFs to be shown as a series composed of a standard normal distribution and its derivatives [7, 19].
2. Edgeworth expansion: This is used when a stochastic variable is normalized [7, 20, 21].
3. Cornish–Fisher expansion: This expansion is based on the cumulants of the variable and the quantiles of the standard normal probability distribution. This method is used to approximate the inverse function of the CDF (variable's quantile) [7, 22].

Taylor series: It is used for approximating a function by using a finite number of terms of its Taylor series.

First-order second method (FOSM): This method is used to determine stochastic moments of a linearized function with random input variables, based on a first-order Taylor series approximation and the first and second moments of the input variables.

In order to obtain output parameters' mean value and standard deviation by this technique we just need the mean value and the standard deviations of the input parameters and not the detailed PDFs [7, 23, 24].

All of these mentioned methods in this category are reliable on linearization (by variant difficulty and errors), while the increasing of error is estimated by using a suitable linear function. These hardness and inexactitude in linearization trend cause the introduction of other types of methods, which do not need the linearization process. Therefore, new methods based on PDF approximation have been introduced that we review in the following [7, 25].

PDF Approximation-Based Methods

The analytical method's goal is to prepare the appropriate samples of input variables, which can keep adequate data about the PDF of input variables. Indeed, a PDF approximation is easier than an approximation of a nonlinear transformation function [8]. Second group of analytical approaches is based on PDFs of input parameter approximation by using the suitable samples. Approximate-based techniques prepare a brief explanation of the statistical attributes of output stochastic variables. Scenario-based decision-making method, point estimation method (PEM), and unscented transformation (UT) method are in this group, which are clarified in the following.

Point Estimation Method (PEM)

This method acts based on the concept of moments of uncertain input parameters. In a problem with n uncertain parameters, the significant steps are as follows [6, 26]:

Step 1: Set $E(Y) = 0$, $E(Y^2) = 0$ and $k = 1$.

Step 2: Specify the locations and probabilities of concentrations, $\vartheta_{k,i}$ and $P_{k,i}$, respectively, as follows:

$$\vartheta_{k,i} = \frac{1M_3(z_k)}{2\sigma_{z_k}^3} + (-1)^{i+1} \sqrt{n + \frac{1}{2} \left(\frac{M_3(z_k)}{\sigma_{z_k}^3} \right)^2} \tag{12.1}$$

$$P_{k,i} = (-1)^i \frac{\vartheta_{k,3-i}}{2n \sqrt{n + \frac{1}{2} \left(\frac{M_3(z_k)}{\sigma_{z_k}^3} \right)^2}} \tag{12.2}$$

Notice that $M_3(z_k)$ is the third moment of parameter z_k .

Step 3: Estimate the concentration points $z_{k,i}$, as given below:

$$Z_{k,i} = \mu_{z_k} + \vartheta_{k,i} \times \sigma_{z_i}, i = 1, 2 \tag{12.3}$$

μ_{z_k} and σ_{z_i} are the mean and the standard deviation of $z_{k,i}$, respectively.

Step 4: Calculate the f for both $z_{k,i}$, as

$$Z = [z_1, z_2, \dots, z_{k,i}, \dots, z_n], i = 1, 2 \quad (12.4)$$

Step 5: Calculate $E(Y)$ and $E(Y^2)$ using

$$E(Y) = E(Y) + \sum_{i=1}^2 P_{K,i} f(z_1, z_2, \dots, z_{k,i}, \dots, z_n) \quad (12.5)$$

$$E(Y^2) = E(Y^2) + \sum_{i=1}^2 P_{K,i} f^2(z_1, z_2, \dots, z_{k,i}, \dots, z_n) \quad (12.6)$$

Step 6: Set $k = k + 1$ if $k < n$ and then go to step 2; otherwise continue.

Step 7: Calculate the mean and the standard deviation as

$$\mu_Y = E(Y) \quad (12.7)$$

$$\sigma_Y = \sqrt{E(Y^2) - E^2(Y)} \quad (12.8)$$

By concentration we mean the first few central moments of a stochastic variable on i points for each variable and this method is focused on the statistical information presented by this concentration [7].

PEM method is simple and easy to implement. It is a non-iterative and computationally efficient technique so it does not pose any difficulty in convergence problem. However, this method has some disadvantages as follows [7, 27]:

- It provides more reliable answers for non-skewed PDFs.
- It just gives the mean and standard deviation of the uncertain outputs.
- There is not any data about the shape of the output's PDF.
- It can be applied for problem just when we have its PDF.
- If the number of random variables is large, the accuracy would become low.
- Basic method of 2PEM cannot consider the correlation between random variables.

Nevertheless, the modified version of 2PEM applies to problems with spatial correlation among multiple uncertain input parameters. However, PEM does not give information about the precise shape of the output variable's PDF and presents the mean value and standard deviation of PDF. Similar to other probabilistic approaches, PEM also requires PDF of uncertain parameters and gives a better performance for non-skewed PDFs.

More information on these methods is available in ref. [28]. It is significant that probabilistic approaches can run in appropriate condition with enough historical data

about uncertain parameters to make PDF of these variables. When such historical data do not exist, the possibilistic uncertainty modeling approach may be useful [8].

Unscented Transformation (UT) Method

In order to prevail over the weaknesses of traditional probabilistic techniques such as linearization process used in these methods, unscented transformation (UT) method was expanded. This method is a reliable method for computation of the statistics of an output stochastic variable under a set of nonlinear transformation and is known as a reliable technique in the evaluation of stochastic problems with/without correlated uncertain variables. Indeed, approximating a probability distribution is easier than an arbitrary nonlinear function [8, 17, 29]. Compared with the MCS method, UT approach has a higher accuracy level and is quicker. In summary, some of the essential properties of the UT technique are efficient computation, being highly functional, being easy to implement, acceptable precision without reduction by increasing the number of random variables, and capability of handling correlated variables. The UT method is easy to run, time efficient, and reliable to obtain the uncertain variable output by a set of nonlinear transformations, and it is highly functional in order to solve problems with correlation among multiple uncertain input parameters, but it must be mentioned that this method is only applicable in problems wherein their PDFs of input variable exist, and it is also noticeable that more uncertain variable needs more time for running the program. In order to study all steps and mathematical formulation of UT method and for more details, interested readers are referred to [8, 30]. An advisable trade-off must be regarded between the lack of information and reducing of the computational burden [8].

Scenario-Based Decision-Making

It is evident that, because of the uncountable occurrences of uncertain parameters, investigation of all of the realizations of them is not impossible. Instead, we are interested in considering them as much as possible. Indeed, the realization space is divided into countable finite parts (scenarios) with a determined heaviness (probability). Therefore, one of the ways to consider these parameters could be converting them into several limited and countable discrete scenarios with associated probabilities. This process was the beginning of the formation of the scenario-based method. By scenario we mean a likely realization of an uncertain set of parameters that are generated by using the PDF of each uncertain parameter. Z_s is the set of scenarios. The expected value of output variable, y , is calculated as follows [6]:

$$y = \sum_{s \in \Omega_j} \pi_s \times f(Z_s) \quad (12.9)$$

where $\sum_{s \in \Omega_j} \pi_s = 1$ and π_s are the probability of s^{th} scenario. For selecting a small set, Ω_J , with the cardinality of N_{Ω_s} , from the original set, Ω_j , we should select a small set of scenarios when the number of scenarios is large [6, 31].

The scenario-based decision-making method is an approximate method that is easy to run and computationally efficient, and needs the statistical information of input parameters to convert the continuous space of uncertain ambiance into limited number of discrete scenarios with related probability. For more details of scenario-based decision-making method and scenario reduction techniques, readers can refer to ref. [32, 33].

A comprehensive two-stage multi-objective decision-making model in the optimal operation problem of EH to minimize both energy costs and related level of risk is presented in [34] which obtains the ability to make decisions under uncertainty by creating a trade-off between cost and reliability of the system. A scenario-based approach is applied to the model of uncertainties in electricity demand, electricity price, and wind power generation by consideration of normal PDF, Rayleigh PDF, and Weibull PDF, respectively. Authors in [35] have evaluated the effect of RES on multi-energy system planning by an optimization model under uncertainties. They have modeled various uncertainty parameters by the usage of related distributions, such as binominal distribution for solar and wind power generation, normal distribution for demand, and Bernoulli distribution function for unavailability of generation units. Modeling of the uncertainties of demand, wind, and solar generation power, in isolated microgrid, is proposed in ref. [36] in order to investigate real-time dispatching problem and unit commitment in it. For this purpose, different scenarios by consideration of the probability of each state have been presented by usage of the discrete statistical distribution. An optimal operational model of multi-carrier energy system, in the presence of the electrical demand, heat demand, and natural gas demand; electrical and thermal energy market prices; and wind farm output power as uncertainty parameters, has been provided by using scenario-based stochastic method in [37] taking into account thermal demand response program (TDRP) and electrical demand response program (EDRP). The Monte Carlo simulation (MCS) has been applied to generate scenarios by using normal PDF for demands and prices and Weibull PDF for wind speed. A scenario-based approach has been used in [33] for modeling of uncertainties in the solar and wind output generation. Other researches that have provided model uncertainties by using probabilistic approaches are presented in Table 12.2 in more detail.

12.3.2 Possibilistic Method

There are a bunch of variables with access to their PDF not being possible due to the lack of proper and accurate historical information, and therefore they could not be modeled with probabilistic methods. These variables are called possibilistic variables and fuzzy representation is used to model the conventional spatial variables.

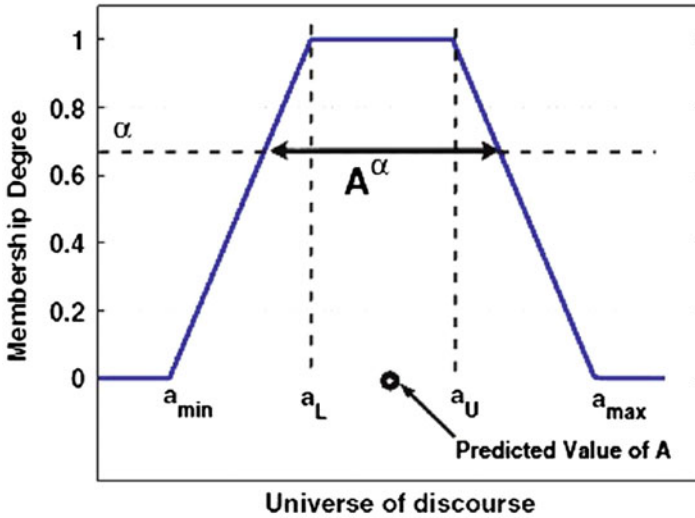


Fig. 12.4 A sample for membership function and α -cut [28]

In engineering and especially in power systems, any external factor may influence the power system's parameters, so they are not closed systems. **On the other hand**, picking out the suitable PDF for uncertain variables is not simple and it is not feasible in most conditions especially when the existing data is insufficient or imprecise. So, using classical probability theory in the power systems meets some problems. In such cases it is suggested to use the possibility theory and fuzzy logic could be the best alternative [7, 28].

12.3.2.1 Fuzzy Type 1

The idea of possibilistic logic or fuzzy logic was first proposed by Lotfi Zadeh, which suggested that the membership value to a set is the key to decision-making when faced with uncertainty [38].

Assume that $y = f(x_1, x_2, \dots, x_n)$ where:

- X : Is a vector containing uncertain input parameter of the system such as wind's speed/hourly electricity price
- f : Is the system model for the specific uncertainty such as hub's scheduling in all the year/in the electricity market
- y : Is the output variable such as the optimum ordering of hub's element to having minimum cost investment or maximum profit

Type of membership function employed to formulate the specific uncertain parameter depends on expert's opinion and trapezoidal membership function is a common one (Fig. 12.4).

The most substantial subject beyond the shape of the membership function (MF) is finding the MF for output (y) with the known MF for input (x). To find this, two steps should be done:

1. α -Cut Method

If we know the possibility distributions of the uncertain input variable, the output's one can be determined by using α -cut method. (In some literature such as [38] “ α -cut” is named as “ λ -cut” method.)

For a given input variable \tilde{X} the α -cut of X is defined as

$$A^\alpha = \left\{ x \in U \mid \pi_{\tilde{x}}(x) \geq \alpha, 0 \leq \alpha \leq 1 \right\} \quad (12.10)$$

$$A^\alpha = [\underline{A}^\alpha, \overline{A}^\alpha] \quad (12.11)$$

\overline{A}^α and \underline{A}^α are upper and lower limits of A^α , respectively, that can be found with optimization methods [7].

2. Defuzzification

This step is used to convert the fuzzy number to crisp one. Based on [38] there are seven methods for defuzzification, but the most common method which is introduced in [6–8] is “centroid method” that is also called “center of area or center of gravity”:

$$X^* = \frac{\int \pi_{\tilde{x}}(x) x dx}{\int \pi_{\tilde{x}}(x) dx} \quad (12.12)$$

12.3.2.2 Fuzzy Type 2 (T2) Set Approach

Determining the exact degree of membership for a fuzzy set is difficult. Fuzzy systems have a limited ability to reduce the effects of uncertainty in fuzzy rules due to their membership functions with precise membership degrees. In real world we are faced with many sources of uncertainty even when we are using the fuzzy logic.

For example the meanings of the words that are used with different people are different; for instance when a man says “He is tall” he means over than 2 m but when a woman says “He is tall” she means more than 170 cm mostly. Furthermore, the knowledge gained through experts is uncertain because in many cases experts do not agree with each other. Add to that the error of measurements that are done in gathering process of the primary data in fuzzy systems, etc. These all have the uncertainty concept and uncertainty in fuzzy modeling, which doubles the fuzziness and makes the new definition and that is fuzzy-fuzzy modeling or fuzzy type 2. Type 1 has a 2-dimensional MF but type 2 has 3-D ones (you can see this in Fig. 12.5).

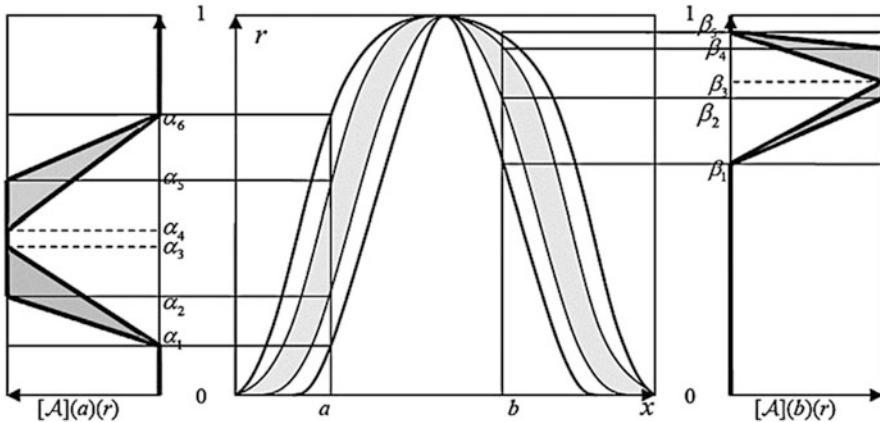


Fig. 12.5 The concept of an interval-valued type 2 fuzzy set [39]

Type 2 fuzzy systems are always used in a hybrid format with robust [40] or stochastic methods [41] and it is similar to Z-numbers (will be mentioned below) to some extent, but it is not able to show the level of reliability in the form of sentences, despite its wide usages in decision-making, such as solving fuzzy relation equations, survey processing, prediction of time series, function estimation, time-varying channel equalization, and control mobile robots. It is not used in the field of energy hub system uncertainty modeling because of this lack of reliability.

12.3.3 Hybrid Approaches

In the EHs there are different devices and agents that it is desirable to model the uncertainty associated with each of them. In this regard, it is worth to remember the following:

Although the power output from the transformer is often regarded as stable, there are two specific influential factors that introduce instability into its operation. These factors are the fluctuations of the grid power [42], and the mechanical degradation/failure/repair of transformer hardware [43].

The grid power is represented by a distribution function [42] and the mechanical degradation/failure/repair process is represented by a Markov model [44]. To model the dynamic behavior of loads, many multistate probabilistic models have been proposed ranging from a single load-aggregated representation up to more complex individual load modeling [45].

Due to privacy issues, gathering the operational data of each EV (electrical vehicle) might not be so easy and the model parameter’s estimation relies on expert judgments and knowledge of driver behavior so the possibilistic distribution is chosen to model the uncertainties in EV power.

Table 12.1 Uncertainties in the multi-energy systems

Component	Parameter	Source of uncertainty	Type of information available	Uncertainty representation
Solar generator	Solar irradiation	Irradiation variability	Historical data	Probabilistic (e.g., beta)
	Operation parameters	Incomplete knowledge	Experts' judgments, users' experiences	Possibilistic
Wind turbine	Wind speed	Speed variability	Historical data	Probabilistic (e.g., Weibull)
	Operation parameters	Incomplete knowledge	Experts' judgments, users' experiences	Possibilistic
PHEV aggregation	Power output owners' behavior pattern	Incomplete knowledge, subjective decisions	Experts' judgments, users' experiences	Possibilistic
Market prices	Energy prices	Variability of price	Historical data	Probabilistic (e.g., normal and Log-normal distribution)
Hub components	Input power from grid	Power fluctuations	Historical data	Probabilistic
	Random failure of equipment	Mechanical degradation/ failure date	Historical data	Probabilistic [e.g., gamma (AC, EHP) and Weibull (CHP, B)]
Demands	Load value	Consumption variability	Historical data	Probabilistic (e.g., normal)
	Customer's behavior on carrier-based demand response programs			

Most of the time, historical solar irradiation data and wind speed data are sufficient and accessible. So, both of them use probabilistic distribution such as beta distribution in solar field [46, 47] and Weibull distribution for wind speed uncertainty [48, 49].

On the contrary, the operation parameters of the renewable generators (e.g., cut-in speed of wind turbine, ambient temperature of solar panel) may be modeled by possibilistic distributions, because renewable generators are end users and it depends on them [48, 49]. Even if these data are available, the detailed factory data sheet information is not provided by their manufacturer due to commercial reasons [50]. The reader can see the summary of these uncertainties in Table 12.1.

In the hub systems with the existence of many devices, and where different kinds of uncertainties are possible, the decision maker is sometimes faced with a

multivariate objective function that probabilistic and possibilistic methods cannot solely model their uncertainties and these approaches should be combined to model uncertainties in them.

Assume $y = f(X, Z)$, and that X and Z are the vector of uncertain input parameters. X has a possibilistic nature such as electricity price, Z is such an electrical load that its PDF is available, and y is the output variable.

To model the uncertainties in such systems, we need to use a hybrid approach that covers probabilistic and possibilistic uncertainties simultaneously.

1. Possibilistic Monte Carlo approach

The mixed possibilistic Monte Carlo approach has the following steps [28]:

Step 1: For each $z_i \in Z$, generate a value using its PDF, Z_i^e .

Step 2: Calculate $(\bar{y}^\alpha)^e$ and $(\underline{y}^\alpha)^e$ as follows:

$$(\bar{y}^\alpha)^e = \min f(Z^e, X^\alpha) \tag{12.13}$$

$$(\underline{y}^\alpha)^e = \max f(Z^e, X^\alpha) \tag{12.14}$$

$$X^\alpha = (\underline{X}^\alpha, \bar{X}^\alpha) \tag{12.15}$$

To gain the statistical data for estimating the output’s PDF or its expected value these steps are repeated several times.

2. Possibilistic scenario-based approach

Below steps are done for this method [51]:

Step 1: Generate the scenario set describing the behavior of Z , Ω_f .

Step 2: Reduce the original scenario set and make a small set, Ω_s .

Step 3: Calculate (\bar{y}^α) and (\underline{y}^α) as follows:

$$(\bar{y}^\alpha) = \min \sum_{s \in \Omega_s} \pi_s \times f(Z_s, X^\alpha)$$

$$(\underline{y}^\alpha) = \max \sum_{s \in \Omega_s} \pi_s \times f(Z_s, X^\alpha) \tag{12.16}$$

$$X^\alpha = (\underline{X}^\alpha, \bar{X}^\alpha) \tag{12.17}$$

Step 4: Defuzzify y .

Despite the accuracy and reality of hybrid approach, it is not used to model the uncertainties in EH because of its complexity.

12.3.4 Z-Numbers

As we said before the data in EHs are often imperfect because of their unreliability and nature. The aspects of the defective information are uncertainty and imprecision. Uncertainty characterizes the degree of truth, and imprecision characterizes the content of the data.

Fuzzy set theory and Z-number, introduced by Zadeh (2011), can be used to deal with these factors in the modeling of such systems especially for multi-criteria decision-making (MCDM) [51].

A Z-number is an ordered pair of fuzzy numbers denoted as $Z = (A, B)$ where the first component, A , represents the fuzzy value of the uncertain variable, X , and the second parameter, B , shows the reliability of A and both are described in natural language [52]. Compared with the classical fuzzy number, Z-number has more ability to describe the knowledge of human and the results have less security risk level and can describe both restraint and reliability. This concept represents the reliability of input data that can be used in many areas such as decision-making, forecasting, risk assessment, economics, and engineering.

Since the EH is directly faced with the uncertainties of the input data, the use of Z-numbers for more realistic EH models is inevitable and by developing and improving the arithmetic of Z-numbers its applications in EH models can contribute significantly to realization of these models [4].

For example, let us consider the prediction of the energy market. As it is known this parameter depends on the number of factors. If we say “Electricity price will be something higher in this year” it is considered as a more possible event with the reliability of 100%. This event can be expressed more exactly as “Electricity price will be something higher in this year, very likely.” So the event can be described by a Z-number in the form of $Z = (A, B)$ in the second condition, where X is a price of the energy (includes gas, electricity, and so on) market, A is the constraint which is “something higher,” and B is the reliability of A which is “very likely.”

12.3.5 Robust Optimization (RO)

Before proceeding with a robust optimization method and related papers, we first give a brief definition of a robust model and a robust response. A robust model is a model that represents the space in which, for all scenarios that determine the input data, it is always in an open or near-accessible position. The robust answer is also the answer that is relevant or acceptable in all scenarios that are determined for the input data.

Resilient optimization: In robust optimization, probabilities are uncertain, and uncertain parameters are estimated through discrete scenarios or interval boundaries. In a discrete state, for each parameter, based on past experiences and studies and feasibility studies, several different numbers are proposed; each of them is referred to

as “scenario.” In the continuous state, each deterministic parameter is determined with a specified interval.

In a “robust” approach, the ultimate goal is to minimize the worst cost or regret. It means that, in this method, the problem is optimized in the worst case, and the answer to the optimization problem is feasible for all scenarios. Indeed, in the robust optimization, the best answer is chosen from the answers that are justifiable for all scenarios. It can be said that robust theory of optimization is a risk-averse approach to dealing with optimization problems under uncertainty.

In other words, the principle of robust optimization is “immunizing a solution against adverse realizations of uncertain parameters within a given uncertainty set” [11].

One of the applications of this method is solving the optimization problems with inadequate information about the nature of the uncertain parameters and the impossibility of extracting PDFs [53]. The concept of robust optimization was first proposed in 1973 by Soyster [54], who developed a pessimistic robust programming approach for dealing with certain linear programming problems. A few years later, Ben-Tal, Nemirovski, and EL-Ghaoui (1998–2000) developed Soyster’s method to deal with uncertain linear programming problems with various convex uncertainties which was an essential step in the development of this theory.

Afterwards, Bertsimas and Sim (2004) in [55] and Inuiguchi and Sakawa (1998) introduced the “soft worst case approach” in robust optimization. A more flexible version of a pessimistic robust approach tries to minimize the worst value of the objective function, but it does not seek to satisfy all constraints in the worst possible case.

In ref. [56, 57], a robust optimization method was used to optimize the short-term energy efficiency of EH to minimize the cost of energy where the uncertainty of equipment output efficiency deviation from their nominal values exists. In [58], the uncertainty of demand and price of electricity and gas in the planning of the hybrid energy system was considered to be based on a robust optimization method and is modeled for a commercial building. A two-stage day-ahead robust model was suggested to consider wind speed variations for a multi-energy system (MES) in two modified networks, namely 6-bus networks with three nodes of gas and 118 buses of IEEE network with 10 nodes of gas, which increases the flexibility of power systems in the presence of variable wind power [59]. The robust scheduling of multi-carrier energy hub system (MCHES) under market price uncertainty has been modeled in ref. [60], by applying robust optimization approach (ROA).

According to these papers, it can be concluded that a robust optimization method as a conservative approach can reduce the adverse effects of uncertain parameters to some extent although it will not always have an optimal solution.

The formulation of a robust optimization method may take several forms. For more information about the details of various robust optimization methods and its various forms, the reader can refer to papers such as [6, 7, 54, 55, 61, 62].

More details about these researches are provided in Sect. 12.4.

12.3.6 Information-Gap Decision Theory Method

This method was first proposed by Yakov Ben-Haim [1]. It does not need PDF or membership function. It determines the differences (errors) between parameter values and their estimated ones. In other words this method measures the deviation of errors, but not the probability of outcomes, regarding the lack of information in the decision-making process.

The IGDT approach is proposed for evaluating and modeling unknown random variables, and in this method, the uncertain values are approximated via variation intervals. Also, IGDT-based model does not require any probabilistic estimation of uncertain parameters. Thus, it is not sensitive to the random variable forecast [62].

In the following, the mathematical description of this method is expressed in the form of a brief optimization problem [6, 7, 102]:

$$f = \min_x (f(X, \gamma)) \quad (12.18)$$

$$H_i(X, \gamma) \leq 0, \forall i \in \Omega_{\text{Ineq}} \quad (12.19)$$

$$G_j(X, \gamma) = 0, \forall j \in \Omega_{\text{Eq}} \quad (12.20)$$

$$\gamma \in \Gamma \quad (12.21)$$

In the above equations, γ is the vector of input uncertain parameters, Γ is the set of uncertainties that describes the behavior of γ , and X is the set of decision-making variables in the problem. In general, the objective function of $f(X, \gamma)$ depends on both uncertain parameters γ and the decision-making variable X . The mathematical expression of uncertainty set is expressed as follows:

$$\forall \gamma \in \Gamma(-\gamma, \zeta) = \left[\gamma : \left| \frac{\gamma - (-\gamma)}{-\gamma} \right| \leq \zeta \right] \quad (12.22)$$

in which $-\gamma$ is the predicted value for the uncertain input parameter. ζ is the maximum possible deviation of actual value of the uncertain parameter from its predicted value, which is also called the uncertainty radius, which is usually uncertain for the decision maker.

Assuming that in Eqs. (12.18)–(12.21) there is no deviation from the uncertain parameter of its predicted value, the base case model is defined as

$$f_b = \min_x (f(X, \bar{\gamma})) \quad (12.23)$$

$$H_i(X, \bar{\gamma}) \leq 0, \forall i \in \Omega_{\text{Ineq}} \quad (12.24)$$

$$G_j(X, \bar{\gamma}) = 0, \forall j \in \Omega_{\text{Eq}} \quad (12.25)$$

The output obtained from Eqs. (12.23)–(12.25) gives the base value of the objective function. In other words, the value of the objective function is assumed to be obtained by assuming that the uncertainty parameter is the same as its predicted (or estimated) value. If the actual value of the uncertain parameter varies with its predicted value, decision makers are faced with two different strategies as below.

12.3.6.1 Risk-Averse Strategy

The risk-averse strategy is usually adopted by conservative decision makers. In this strategy, the real realization of the uncertain parameter leads to an increase in the objective function from its base value, and the parameter uncertainty harms the objective function of the problem. The decision maker in this strategy intends to make robust decisions about the probable risks of predicting uncertain input parameters.

Therefore, this strategy tends to determine the optimal value of the decision variables in such a way that the maximum possible uncertainty radius for uncertain parameters is obtained for a certain value of the increase in the objective function. In other words, the objective function is robust against the possibility of error in prediction of the uncertain input parameter.

The mathematical formulation describing this strategy is as follows [1, 7, 27]:

$$\max_x (\hat{\zeta}) \quad (12.26)$$

$$H_i(X, \gamma) \leq 0, \forall i \in \Omega_{\text{Ineq}} \quad (12.27)$$

$$G_j(X, \gamma) = 0, \forall j \in \Omega_{\text{Eq}} \quad (12.28)$$

$$\left\{ \begin{array}{l} \hat{\zeta} = \max_{\zeta} \zeta \\ \max_{\gamma} f(X, \gamma) \leq \Lambda_C \\ \Lambda_C = f_b(X, \gamma) \times (1 + \beta), \gamma \in \Gamma \end{array} \right\} \quad (12.29)$$

$$\left| \frac{\gamma - -\gamma}{-\gamma} \right| \leq \zeta \quad (12.30)$$

$$0 \leq \beta \leq 1 \quad (12.31)$$

In these equations, ζ is the maximum radius of the uncertainty (positive parameter) that is determined in such a way that, for the change of the uncertain parameter γ , the value of the objective function does not exceed the permissible range. Λ_C is the critical value of the objective function (or the maximum allowable in increasing of the objective function's value from its base value), in which the objective function must be secured against it. It usually is determined by the decision maker as tolerable threshold of objective function and is a function of the base value of the objective function. Λ_C is defined as β percent of increase in value of base objective function (f_b). Indeed, β is the positive parameter determined by the decision maker, which indicates the degree of acceptable tolerance in the increasing of objective function's value from the base objective function (f_b) due to possible undesirable uncertainties.

In this strategy, the decision maker will be sure about the value of the objective function for the uncertain parameter variations within the range of determined uncertainty radius and it is not more than the practical limit for determining the uncertainty radius of the uncertain parameter.

12.3.6.2 Risk-Seeker Strategy

The uncertainty of the uncertainty parameter does not always lead to a worsening of the objective function of the problem. In this strategy, the actual realization of the uncertain parameter does not adversely affect the value of the objective function. Meanwhile, the actual value of the uncertain parameter reduces the objective function from its base value.

In this strategy, the decision makers try to make robust decisions against possible errors in predicting uncertain input parameters and seek to achieve an objective function with a value lower than the base value, due to the positive changes of the uncertain parameter. In other words, the decision maker decides for the worst prediction.

In this approach, the decision variables are adjusted so that the minimum uncertainty radius occurs in the prediction of uncertain parameters. The mathematical formulation for describing this strategy is as follows [103]:

$$\min_x (\widehat{\zeta}) \quad (12.32)$$

$$H_i(X, \gamma) \leq 0, \forall i \in \Omega_{\text{Ineq}} \quad (12.33)$$

$$G_j(X, \gamma) = 0, \forall j \in \Omega_{\text{Eq}} \quad (12.34)$$

$$\left\{ \begin{array}{l} \widehat{\zeta} = \min_{\zeta} \zeta \\ f(X, \gamma) \leq \Lambda_O \\ \Lambda_O = f_b(X, \gamma) + \zeta_O |f_b(X, \gamma)|, \gamma \in \Gamma \end{array} \right\} \quad (12.35)$$

In these equations, ζ is the minimum radius of the uncertainty (positive parameter). Λ_O is the value of the opportunity that the objective function should be less than it. ζ_O is determined by the decision maker and is a positive parameter. This parameter determines the greediness degree in a decrease over the base objective function (f_b) due to possible uncertainties.

An information-gap decision theory (IGDT) is proposed to suggest a robust optimization model for optimal management of the EH in the optimal short-time management of EH under the uncertainty in electrical load [76]. In [91], risk-based robust energy management for intelligent building in the existence of the uncertainty in electricity's market price (real time) was modeled by using IGDT with the goal to minimize the operational cost by limit-risk programming. This method was also suggested as a risk management tool to control the adverse effects of uncertainties in wind power, and electrical and thermal loads in a comprehensive risk-based model, with the economic objective to managing an EH as a mixed-integer linear programming (MILP) problem [68]. These papers show the effectiveness of the IGDT method in uncertainty modeling.

More details about the researches which model uncertainty by using IGDT approach in EH concept are also provided in Table 12.2.

12.3.7 Analysis Interval

Interval method is usually used when the interval of variations of uncertain input parameters is available. We suppose that the values of uncertain parameters are chosen from a known interval. It is similar to the probabilistic modeling with a uniform PDF. Thus, this method uses the upper and lower bounds for each uncertain input parameter and it can show uncertainty with them by an interval. By defining the range of input variables the upper and lower bounds of output variables will be

Table 12.2 Summary of studies in the field of uncertainty modeling applications in the operation of energy hub

References	Uncertainty parameters	Type of modeling method	Objective function	Solver	Case study/hub components	Hub input/output ports	Problem	Horizon time	Description and remarks	Publish year
[36]	The variations of prices of all input and output energy carriers	Probabilistic MCS	Max [the daily profits from operation]	–	In four cases/CHP, TES	NG/ED, HD	An optimal model of operation	12 months (daily)	It is assumed that loads for which demand-side management (DSM) schemes for thermal demands are established can be shifted within given constraints	2011
[58]	Wind and solar generation, load	Probabilistic MCS	Min [overall operation costs]	Snopt through the Tomlab interface in MATLAB (R2008b)	Two energy hubs connected to the supply grid/CHP, F, TES, EES	EN,NG/ED, HD	Day-ahead scheduling	24 h	A model predictive control (MPC) strategy applied for keeping the outcomes of predict uncertainties at acceptable levels	2011
[56, 57]	The deviation of the equipment efficiencies from their nominal values	Robust optimization	Min [total energy cost]	CPLEX/GAMS	Nine cases—commercial EH in Canada/CHP, T, F, HPP, FC, TES, HS	EN,NG/ED, HD, hydrogen	MILP—operational of EH	24 h	–	2012

(continued)

Table 12.2 (continued)

References	Uncertainty parameters	Type of modeling method	Objective function	Solver	Case study/hub components	Hub input/output ports	Problem	Horizon time	Description and remarks	Publish year
[63]	Wind power generation	Probabilistic PEM	Min (the electrical and gas costs)	MATLAB	Eleven EHs interconnected in experimental system via 14 electrical buses and 20 nodes of gas/CHP, T, F, WT	EN, NG, W, DH/ED, HD	Probabilistic economic dispatch problem of MECs	24 h	A heuristic optimization method known as MAGA is applied to economic dispatch solving. Wind speed modeled by Weibull PDF. 50 iterations	2013
[34]	Wind, electricity demand and prices	Probabilistic scenario; two stage	Min (cost of energy buying and risk rate)	DICOPT/GAMS	WT, F, CHP, EES	EN, NG/ED, HD	MILP—optimal operation	24 h	In order to risk measure and control the pernicious effects of the uncertainties, CVaR is used. Normal PDF for modeling the demand and price and Rayleigh for modeling of wind uncertainties are used	2014
[64]	Electrical load, wind, RTP market	Probabilistic MCS	Min (operational cost, reliability, and greenhouse gas emission costs)	CPLEX/GAMS	Nine cases—commercial EH/T, CHP, B, WT, TES, EES	EN, NG, WN, W/ED, HD, water	MILP—optimal operation	24 h	Reduce scenario number by using SCENRED and backward/forward EDR	2014

[65]	PHEV charging pattern	Probabilistic PEM	Max ((charge of PHEVs by wind power) + min (costs of input energies and customers' easement)	-	EH power output as the modified IEEE test system with 34-bus/CHP, T, B, WT	EN, NG, W/ED, HD	LP—optimal operation and management	1 day	In order to evaluate the final optimal solution fuzzy min-max approach is applied. MOPSO technique is used to look for the Pareto	2014
[66]	Electricity RTP price and weather (temperature, humidity, wind speed, and solar irradiation) forecast	Probabilistic MCS	Min (costs of energy consumption, total energy, and supply of peak load) by considering greenhouse important parameters, specially, inside temperature and moisture, CO ₂ , and amount of lighting within admissible level	CPLEX/GAMS	Agricultural hub in four cases, greenhouse including fogging system, two-fire heater, electrical cooler, fan, lamp	EN, NG/NG, HD, CD	MILP—optimal operation and management	24 h	Normal PDF is employed to moisture, temperature, and RTP quantity modeling. Weibull and uniform distribution applied to solar and wind output power modeling	2014
[67]	Output power of the rooftop solar panels	Probabilistic PEM	Min (customer's costs)		Residential energy hub—CHP, PHEV, TES, solar panels	EN, NG/ED, HD	Optimal operation and management	24 h	A framework of home energy management (HEM)	2015
[68]	Electric and heat loads, wind power generation	IGDT	Min (total fee of energy buying)	CPLEX/GAMS	CHP, F, EV, WT	EN, NG/ED, HD	MILP—optimal operation of EH	24 h	EV employed as EES	2015

(continued)

Table 12.2 (continued)

References	Uncertainty parameters	Type of modeling method	Objective function	Solver	Case study/hub components	Hub input/output ports	Problem	Horizon time	Description and remarks	Publish year
[69]	Customer's behavior of on carrier-based demand response (CBDR) program participation	Probabilistic scenario	-	CPLEX/ GAMS	Smart multi-energy system	EN, NG, W/hot water	Operation scheduling	24 h	Action of consumers to choose the type of energy to cover their loads presented as uncertainty. The normal PDF is used for CBDR uncertainty modeling	2015
[70]	Electricity price	Probabilistic MCS	Max (operation profit)	-	A multi-carrier energy system in two cases without and with CHP/CHP, T, TES	EN, NG/ED, HD	Operation scheduling	1 day	In this study, three different tariffs were considered for the electricity while fixing of prices was assigned to the local natural gas prices and heat. The normal PDF is used for price uncertainty modeling	2015

[71]	Demands, energy cost prices, electrical generation by renewable sources	Probabilistic MCS and affine arithmetic-based methodology	Min (hourly energy cost, loss of load probability) and max (the renewable power exploitation)	A two-stage solution algorithm	T, CHP, F, WT	EN, NG/ED, HD	Operation scheduling	24 h	MCS is used to compare with proposed technique	2015
[72]	PEV's owners' transmission template in parking lot (PL), wind	Probabilistic scenario	Max (gain of electrical power, NG, reserve, and thermal by interplay in macro-MES and MED, gain of micro-MES by PL interplay and by partaking as reserve)	-	Three cases including micro-MES, micro-MES + PL, micro-MES + reserve market partaking	EN, NG, electrical reserve from PL/ED, HD, electrical reserve	Operation	24 h	Community of EVs in PL is applied as a big EES	2015
[73]	Wind power, vehicle-to-grid (V2G) programs	Probabilistic	Min (charging cost)	-	IEEE 34-node test system /T, WT, CHP, F	EN, NG, W, V2G discharge/ED, HD	Operation strategy	1 year	Computation method of SAIDI and EENS as reliability indices were described	2016
[74]	Solar	Probabilistic PEM	Min (energy fee of customer)	GAMS	Residential energy hub in three cases/CHP, PHEV, solar panels, TES	EN, NG/ED, HD	Operation scheduling	24 h	A framework of home energy management (HEM)	2016
[33]	Wind and solar output generation	Probabilistic scenario	Max [gain of multi-energy players (MEP) by energy interchange in the market of energy and its native energy system]	CPLEX/GAMS	CHP, B, TES, PV, WT	EN, NG/ED, HD	MILP	24 h	In order to model wind power fluctuations Weibull PDF by RWM was applied. Also, K-means clustering was used to reduce scenarios	2017

(continued)

Table 12.2 (continued)

References	Uncertainty parameters	Type of modeling method	Objective function	Solver	Case study/hub components	Hub input/output ports	Problem	Horizon time	Description and remarks	Publish year
[75]	Electricity load and price	Probabilistic PEM (2 m + IPEM)	Min (fee of electricity and NG + start/shutdown cost of F and CHP as a total expense of demand covering)	SBB/CONOPT under GAMS	Three structures: 1-CHP, F, T, TES, EES/2-CHP, F, T, FC, HPP/3-3 CHP nits, 2 F units, T, 2 TES units, 2 EES units	EN, NG/ED, HD, and in addition hydrogen demand in case 2	MINLP—operation scheduling	24 h	TDRP + EDRP	2017
[76]	Electrical load demand	(IGDT)	Min [(cost of equipment operation and energy buying – energy selling income) as an operational expense]	–	CHP, EHP, AC, EH, EES, B	EN, NG/ED, HD, CD	Optimal short-term planning of EH	24 h	–	2017
[37]	Electricity, heat, and gas demands; market price of electricity and heat; wind speed	Probabilistic MCS	Min (expenses of input energy, scheduling, and equipment as an operational cost)	CPLEX/GAMS	In four cases: By taking into account fixed/variable tariff of thermal and TDRP/CHP, WT, B, TES, EES	EN, NG, DH/ED, HD, NG	MILP—optimal operation of smart network's MCES	24 h	TDRP+EDRP/normal PDF for demand and price models /Weibull PDF for wind power	2017
[77]	Wind speed, electricity, and heat loads and their forecasting	Probabilistic MCS	Min (purchased/sold electrical power from/to grid + start/shutdown	CPLEX/GAMS	2 CHP units, 2 B units, WT, EES, TES, AC	EN, NG, W/ED, HD, CD	MILP—wind and SEH unified operational planning	24 h	TDRP + EDRP/ C-Var to measure and evaluate risk/normal or	2017

	in the problem of SEH		cost of devices + B and CHP operational expense + the expense of unserved demands by using the value of lost load (VOLL)] as SEH (operational costs)	CPLEX/ GAMS	S.E. hub/CCHP, AC, B	EN, NG/ED, HD, CD	MILP—optimal operation	24 h	Gaussian PDF was used to demand model/ Rayleigh PDF for wind power model/GAMS/SCENRED to scenario reduction	2018
[78]	Electrical load and its RTP, NG price	Probabilistic MCS	Min (fee of energy and emission penalty as a weighted function)	CPLEX/ GAMS	By 2 EHs, via little and big flexibility/CHP, B, CERG, and WARG	EN, NG/ED, HD, CD	LP—optimal operation	Daily	The CVaR to operational risk control of an SEH	2018
[79]	Uncertainty-accommodating flexibility	Interval optimization	Min (expense of day-ahead energy buying + expense of residual energy required from real time)	The “inprog” function of MATLAB		EN, NG/ED, HD, CD			-	2018
[80]	Wind and solar generation, electrical load variation, and price fluctuations	A distributionally robust chance constrained programming (CCP) reformulation method based on Chebyshev's inequality	Min (daily fee for energy buying (electrical and gas) from the grid + RESO penalty due to not supplying of particular demands and rate of customer's consent)	CPLEX/ GAMS	33-bus IEEE + NGDS with 14 nodes/13 CHPs. In addition, two PV units, one WT, EEs, two gas storages, F and EHP	EN, NG/ED, HD	MILP—a day-ahead optimal operation	Day-ahead	In this work: By reformulation of CCP-based multi-energy residential system (MERS) model, it has become a MISOCP which makes solving easier	2018

(continued)

Table 12.2 (continued)

References	Uncertainty parameters	Type of modeling method	Objective function	Solver	Case study/hub components	Hub input/output ports	Problem	Horizon time	Description and remarks	Publish year
[81]	Electrical price of market	(IGDT)	Min (fee of power buying + operational expense of hub component – benefit of selling electricity to network)	CPLEX/GAMS	Ten intelligent buildings by various behavior of household consume/CHP, B, EES, TES, and smart schedulable appliances	EN, NG/ED, HD	Optimal operation of intelligent building	24 h	Goal = min (risk constrained of operational expense) under uncertainty of market price	2018
[82]	Electrical load and solar power generation	Probabilistic scenario	Min (fee of energy procurement + expense due to converter's start action – extra energy selling income)	The extended mathematical programming (EMP) framework/GAMS	T, F, PV, EES, TES, gas-fired DG, CHP	EN, NG/ED, HD	MILP—day-ahead energy operation of MCEs	Day-ahead, 24 h	Two-stage stochastic MILP	2018
[83]	Electricity price and load, wind, and solar power generation	Hybrid probabilistic MCS/(IGDT)/interval	Min (total fee of energy buying + expense of consumer's inconvenience that their demands are shedding in DSMP)	GAMS	33-bus IEEE with EHs/CHP, EES, B, CAC, WT, PV, T	EN, NG/ED, HD	MINLP—optimal operation in smart EH	24 h	SP to renewable power output/interval and IGDT for electricity price and load uncertainty at the same time/ ϵ -constraint to MO optimization problem-solving/fuzzy for solution's trade-off/electrical demand can participate in DSMPs	2018

[84]	ECDR, RES, and electrical and heat loads	Probabilistic PEM (2 m + IPEM)	-	Newton-Raphson method and Jacobian matrix	14-bus IEEE + 20-node NG + 14-node thermal grid consist of 5 industrial EHs EDRP/Bs, CHPs	EN, NG, DH/ED, HD	Energy flow analysis of MEC	-	Normal PDF with 10% SD to electrical and thermal demand uncertainty mode/Weibull PDF for wind power model/beta PDF for solar output power	2018
[85]	Wind power output	Probabilistic scenario	Min (estimated fee of EHs that are interconnected together through all wind output production scenarios, UCs and DRP fees, coal-fired unit and NG wells' hourly output power, and penalty cost due to discontinuity of wind and demand interruption)	Gurobi 6.5.0 toolbox	By 3 and 17 interconnected EHs on day-ahead planning—in 3 cases: 1—deterministic scheduling of EHs without DR, 2—1 + DR, 3—stochastic scheduling of EH with DR + wind uncertainty/go to remarks	EN, NG/ED, HD	MILP—optimal operation of interconnected EHs	24 h	IDR/LHS for wind power model/backward to reduce scenario/MATLAB 2014 b with YALMIP toolbox to model's code/3 EHs with 2 NG-fired units, coal-fired unit, WT	2018
[86]	Price of market on day-ahead, RTP, wind speed	Probabilistic MCS	Min (NG and electrical purchased fee + electricity exchange with upstream in the online market) and max (maximizes electrical selling bid)	GAMS	Six case studies are considered: two CHP units, EHP, B, WT, EES	EN, NG/ED, HD	MILP—a comprehensive optimal bidding strategy	24 h	-	2018

(continued)

Table 12.2 (continued)

References	Uncertainty parameters	Type of modeling method	Objective function	Solver	Case study/hub components	Hub input/output ports	Problem	Horizon time	Description and remarks	Publish year
[87]	Electricity, heat and cool loads, price of electricity in an electrical market as competitive	Probabilistic scenario	Min (electrical and NG fee)	BONMIN/GAMS	In four cases/ CHP, B, T, AC, EES, air conditioner	EN, NG/ED, HD, CD	Optimal operation	24 h	All of these uncertain parameters have been expressed by using normal PDF	2018
[88]	Wind generation, electrical, and thermal demands	Probabilistic scenario	Min (the expected total cost)	The LINDO solver/GAMS	Two cases in seven conditions/ T, CHP, F, EES, TES, WT	EN, NG, W/ED, HD	MILP—optimal operation	24 h	Normal PDF for demand model/ Weibull PDF wind speed model/price of gas with three tariffs	2018
[89]	Electricity and heat demand, electrical RTP	Probabilistic scenario	Min [fee of power that is bought in day-ahead market + EH's devices' on/off cost (diesel gen, CHP, boiler, heat pump)]	CPLEX/GAMS	CHP, B, T, EHP, diesel-G, EES, TES	EN, NG/ED, HD	MILP—energy management of integrated EHs in MEC based on risk	24 h	Normal PDF and ARIMA are applied for demand and price scenario production, respectively/CVaR to risk control/sensitivity analyses for effective solution/ SCENRED for scenario reduction	2018

[90]	Solar and wind power, electricity, heat loads	Probabilistic scenario	Min [fee of gas and electrical energy from grid + on/off cost of CHP and boilers + diesel generator consumption cost + electrical and heat spinning reserve fee which is planned and presented with responsive demands + operational cost that is predicted within scenarios]	CPLEX/ GAMS	A 10-node microgrid by interconnected EHs via 11 power lines and 5 NG pipelines/CHP, B, diesel-G, WT, PV, EES, TES	EN, NG/ED, HD	MILP—microgrid short-term scheduling to specify the capacity of reserve	24 h	Weibull PDF and beta PDF for wind and solar power models/ Gaussian PDF to load uncertainty model/forward-scenario reduction	2018
[91]	Wind production, electrical price, electricity, and thermal loads	Combined probabilistic MCS/(IGDT)	Min (CHP and boiler production cost + pure fee of energy by considering predicted electrical price + (profit/fee of sold/purchased power) + cost due to CHP's commitment for each scenario and time blocks of planning horizon + punishment term of not-supplied loads	SSB/GAMS	2 CHP units, 2 B units, WT, EES, TES by 34-bus IEEE experiment improved system in hub electrical output port	EN, NG, W/ED, HD	MINLP—operation scheduling	24 h	Rayleigh and normal PDFs for wind power and load scenario production/IGDT for electrical price model/ SCENRED for scenario reduction	2019

(continued)

Table 12.2 (continued)

References	Uncertainty parameters	Type of modeling method	Objective function	Solver	Case study/hub components	Hub input/output ports	Problem	Horizon time	Description and remarks	Publish year
[59]	Wind power	Robust optimization (by nested (C and CG))	Min (on/off cost of NG-fired and electrical units + operational cost) at basis state within worst scenario as a total expense]	Nested (C and CG) generation technique and MATLAB 2014b platform in Gurobi 7.5.1	6-bus electrical + 3-node NG system and 118-bus IEEE + 10-node NG/CHP, TES, EB, EES	EN, NG/ED, HD	MES robust day-ahead planning	24 h	Hourly UC was planned by first-stage problem that was solved in outer loop/ worst condition realization by second-stage problem was solved in inner loop	2019
[92]	Wind production, electricity, and thermal loads	Probabilistic MCS	Min [(CHP, boiler, and CAES operational cost + fee/profit of input/output power from/upstream network + cost of CHP's on/off at every scenario and time blocks of planning + punishment cost due to not-supplied electricity and heat loads by VOLL) that is namely total cost]	CPLEX/GAMS	SMEH/CHP, B, CAES, TES, EHP	EN, NG/ED, HD	MILP—wind and SMEH unified system risk scheduling	24 h	CVaR for risk control/TDRP + EDRP/Rayleigh PDF for wind power model/Gaussian PDF for load model/SCENRED2 for reduction of scenario	2019

[93]	Electrical, heating, and cooling demands, wind speed, and solar irradiances, as well as the price of energy carriers including electricity and natural gas	Probabilistic MCS	Max [total benefit by using revenues minus costs (partaking of DRPs, power produced by REs and NG, cooling energy generated from heat)]	CPLEX/ GAMS	Four case studies: 1—without WT and PV, without DRP; 2—with WT and PV, without DRP; 3—with WT and PV, with 10% of DRP; 4—with WT and PV, 20% DRP + storages/CHP, T, PV, B, AC, WT, TES, EES, CES	EN, NG/ED, HD, CD	MILP—optimal operation of EH	24 h	IDR/normal PDF for load model, Weibull and beta PDFs for wind and solar output model, respectively	2019
[60]	Market price uncertainty	Robust optimization approach	Min [total cost of CO ₂ emission and operational]	GAMS	In three cases: 1—by taking into account TOU/RTP DR/EES, CES, TES, HE, AC, EC, PV, WT, B, GT as a CHP, ST	EN, NG, W, solar/ED, HD, CD	RMILP—robust scheduling of MCHES operation	24 h	EDRP by TOU and RTP	2019
[94]	Electrical and thermal demands and wind speed	Probabilistic MCS	Min [+ load shedding and voltage improvement cost + gas and power network operation cost]	SSB/GAMS	Integrated 14-bus IEEE + 17-node NG in two modes consist of independent operation and integration of gas and power system/CHP, T, B, EES	EN, NG/ED, HD	MINLP—voltage fixity improvement in MSES	–	Rayleigh PDF for wind output model/normal Gaussian PDF for load model/SCENRED2 for scenario reduction	2019

(continued)

Table 12.2 (continued)

References	Uncertainty parameters	Type of modeling method	Objective function	Solver	Case study/hub components	Hub input/output ports	Problem	Horizon time	Description and remarks	Publish year
[95]	Electricity, natural gas, and thermal demand, energy price of market on day-ahead (electrical, gas, and heating), RES power (wind and solar), rate of charge or discharge, energy arrival or departure, capacity of charger of EVs	Probabilistic MCS	Max (hubs profit in the day-ahead market)	GAMS	In nine cases/WT, PV, CHP, EES, B, EVs	EN, NG, DH/ED, HD	MILP	Day-ahead, 24 h	Normal PDF for demand model/ Rayleigh PDF for wind and EV variable model/ beta PDF for solar output model/fast backward/forward for reduction of scenarios	2019
[96]	Power consumption of PHEVs during trips	IGDT	Max (profit of the system)	GAMS	Electrolyzer, HS, FC, B, HES, WT, PV, EES (PHEV)	EN, NG/ED, HD, H2 (FCVs)	MILP—risk-based optimal operation of an energy hub	Daily—24 h	—	2019
[97]	Wind speed and solar irradiances	Probabilistic PEM	Min (gas and power production total cost)	—	The three-hub interconnected system/ CHP, GSHP, F, WT, PV	EN, NG/ED, HD	Operation	24 h	Weibull PDF for wind and beta PDF for solar output modeling	2019

[98]	Wind speed and solar irradiances	Probabilistic MCS (LHS-Nataf)	Probabilistic energy flow	-	123-bus IEEE + 48-node NG/CHP, T, B, P2G, WT, PV	EN, NG/ED, HD	Energy flow	-	Weibull PDF for wind and beta PDF for solar output model	2019
[99]	Behaviors in thermal loads (SIL, SNIL), thermal unplanned hot water demand, uncertain air temperature preference)), unplanned EVs' travel	Probabilistic scenario	Min (required residual energy in order to improve convenience rate + main energy cost)	CPLEX/ GAMS	In four cases/ CCCHP, EES, T	EN, NG/ED, HD	MILP—optimal operation scheduling of smart residential energy hub (SREH)	Day-ahead, 24-h	Shiftable demands are categorized as interruptible and non-interruptible	2020
[100]	Price of electrical and thermal, heat, and electrical loads, wind power	Combined scenario-based/interval	Min (aberration and mean expense of EH)	CPLEX/ GAMS	In two cases with and without DRP/CHP, T, B, EES, HES, WT	EN, NG, DH/ED, HD	MILP—EH optimal operation	Daily, 24-h	Interval technique used for electrical price model/Weibull PDF for wind power model/normal PDF for other uncertainty parameter models/TDRP + EDRP	2020

(continued)

Table 12.2 (continued)

References	Uncertainty parameters	Type of modeling method	Objective function	Solver	Case study/hub components	Hub input/output ports	Problem	Horizon time	Description and remarks	Publish year
[101]	Wind speed and solar irradiances	Probabilistic MCS	Min (cost minimization of an energy hub)	CPLEX/ GAMS	In four case studies/CCHP, PV, WT, CES, EES, HES	EN, NG/ED, HD, CD	MINLP—optimal operation of EH via CES performance	Day-ahead, 24 h	EDRP/Weibull PDF for wind and beta PDF for solar output model/ SCENRED2 for scenario reduction/NG price is fixed	2020
[36]	The variations of prices of all input and output energy carriers	Probabilistic MCS	Max (the daily profits from operation)	–	In four cases/ CHP, TES	NG/ED, HD	An optimal model of operation	12 months (daily)	It is assumed that loads for which demand-side management (DSM) schemes for thermal demands are established can be shifted within given constraints	2011
[58]	Wind and solar generation, load	Probabilistic MCS	Min [overall operation costs]	Snopt through the Tomlab interface in MATLAB (R2008b)	Two energy hubs connected to the supply grid/ CHP, F, TES, EES	EN, NG/ED, HD	Day-ahead scheduling	24 h	A model predictive control (MPC) strategy is used for keeping the consequences of forecast uncertainties at acceptable levels	2011

[56, 57]	The deviation of the equipment efficiencies from their nominal values	Robust optimization	Min [total energy cost]	CPLEX/ GAMS	In nine cases—an energy hub designed in Waterloo, Canada, for the supply of commercial load/CHP, T, F, HPP, FC, TES, HS	EN, NG/ED, HD, hydrogen	MILP—modeling and operation scheduling of an energy hub	24 h	–	2012
[63]	Wind power generation	Probabilistic PEM	Min (the electrical and gas costs)	(Multi-agent genetic algorithm (MAGA)) in MATLAB	The 11-hub test system under study in which there are 14 buses in the electricity network and 20 nodes in the gas network/CHP, T, F, WT	EN, NG, W, DH/ED, HD	Probabilistic economic dispatch problem of MECs	24 h	A heuristic optimization method known as multi-agent genetic algorithm was used to solve an economic dispatch problem. The wind speed predicted utilizing the Weibull fit function in the MATLAB environment. Implementing the proposed method in the MATLAB environment and after 50 iterations, the MAGA has been converged	2013

(continued)

Table 12.2 (continued)

References	Uncertainty parameters	Type of modeling method	Objective function	Solver	Case study/hub components	Hub input/output ports	Problem	Horizon time	Description and remarks	Publish year
[34]	Wind, electricity demand, and prices	Probabilistic scenario; two stage	Min (cost of energy buying and risk rate)	DICOPT/ GAMS	WT, F, CHP, EES	EN, NG/ED, HD	MILP—optimal operation	24 h	The CVaR method is used as a risk measure and it controls the pernicious effects of the uncertainties. The Rayleigh PDF for modeling the variation of wind speed and normal PDF for modeling the demand and price uncertainties are used	2014
[64]	Electrical load, wind, RTP market	Probabilistic MCS	Min (operational cost, reliability, and greenhouse gas emission costs)	CPLEX/ GAMS	Nine different cases (wind, price, and electricity demand certainties and uncertainties)—commercial energy hub/T, CHP, B, WT, TES, EES	EN, NG, WN, W/ED, HD, water	MILP—optimal operation	24 h	The SCENRED tool and backward/forward technique are used to reduce scenario numbers—by considering DR	2014

[65]	PHEV charging pattern	Probabilistic PEM	Max (charge of PHEVs by wind power) + min (costs of input energies and customers' easement)	-	The modified IEEE 34-bus test system as electrical output of hub/CHP, T, B, WT	EN, NG, W/ED, HD	LP—optimal operation and management	1 day	The multi-objective particle swarm optimization (MOPSO) method is employed as a well-organized MO optimization approach to find the Pareto fronts of this optimization. In this chapter, fuzzy min-max method is used for evaluating the final optimal plans and decision-making	2014
[66]	Electricity RTP price and weather (temperature, humidity, wind speed, and solar irradiation) forecast	Probabilistic MCS	Min (costs of energy consumption, total energy, and supply of peak load) by considering greenhouse important parameters, specially, intrans temperature and moisture, CO ₂ , and amount of lighting within admissible level	CPLEX/GAMS	Agricultural hub in four cases, greenhouse including fogging system, two-fire heater, electrical cooler, fan, lamp	EN, NG/NG, HD, CD	MILP—optimal operation and management	24 h	Random values of RTP (hourly Ontario electricity price), temperature, and humidity for each hour are generated using a normal distribution with associated mean and standard deviations for each hour of a day obtained	2014

(continued)

Table 12.2 (continued)

References	Uncertainty parameters	Type of modeling method	Objective function	Solver	Case study/hub components	Hub input/output ports	Problem	Horizon time	Description and remarks	Publish year
[67]	Output power of the rooftop solar panels	Probabilistic PEM	Min (customer's costs)	''	Residential energy hub—CHP, PHEV, TES, solar panels	EN, NG/ED, HD	Optimal operation and management	24 h	from actual data for each season for Ontario, Canada. Also, Weibull and uniform distribution are used for wind speed and solar irradiation, respectively A framework of home energy management (HEM)	2015
[68]	Electric and heat loads, wind power generation	IGDT	Min (the total payments regarding the energy purchase)	CPLEX/GAMS	CHP, F, EV, WT	EN, NG/ED, HD	MILP—optimal operating strategy of the energy hub	24 h	The PEV's have been used as the energy storage device. In order to demonstrate the applicability and strength of the proposed approach four different scenarios are considered as follows: 1—base case	2015

[69]	Customer's behavior of carrier-based demand response (CBDR) program participation	Probabilistic scenario	-	CPLEX/ GAMS	Smart multi-energy system	EN, NG, W/hot water	Operation scheduling	24 h	This uncertainty represents the probabilistic nature of consumers' behavior to select the carriers for supplying their own demand. The normal PDF is used for CBDR uncertainty modeling	2015
[70]	Electricity price	Probabilistic MCS	Max (operation profit)	-	A multi-carrier energy system in two cases without and with CHP/CHP, T, TES	EN, NG/ED, HD	Operation scheduling	1 day	In this study, three different tariffs were considered for the electricity while fixing of prices was assigned to the local natural gas prices and heat. The normal	2015

(continued)

Table 12.2 (continued)

References	Uncertainty parameters	Type of modeling method	Objective function	Solver	Case study/hub components	Hub input/output ports	Problem	Horizon time	Description and remarks	Publish year
[71]	Demands, energy cost prices, electrical generation by renewable sources	Affine arithmetic-based methodology	Min (hourly energy cost, loss of load probability) and max (the renewable power exploitation)	A two-stage solution algorithm	T, CHP, F, WT	EN, NG/ED, HD	Operation scheduling	24 h	PDF is used for price uncertainty modeling To have a term of comparison for the performance evaluation of the proposed methodology, the optimal scheduling problem has been solved by a stochastic programming method based on Monte Carlo simulations	2015
[72]	PEVs' owners' transmission template in parking lot (PL), wind	Probabilistic scenario	Max (electricity, gas, reserve, and heat profits from interaction with macro-MES and MED, micro-MES profit from PL interaction and finally its profit	-	Three cases consist of the following: Case I that is considered to demonstrate micro-MES operational behavior without PL interaction. Case II: the PL is added to the	EN, NG, electrical reserve from PL/ED, HD, electrical reserve	Operation	24 h	In this chapter, aggregation of PEVs' batteries in parking lots (PL) is considered as a bulk electric storage in MES. The energy hub	2015

[73]	Wind power, vehicle-to-grid (V2G) programs	Probabilistic	Min (charging cost)	-	system. Case III compares the behavior of micro-MES operator with and without participating in the reserve market as another source of operational flexibility for micro-MES operator	EN, NG, W, V2G discharge/ED, HD	Operation strategy	1 year	In this chapter, the calculation procedure of two widely used reliability indices, i.e., system average interruption duration index (SAIDI) and expected energy not served (EENS), is explained	2016
[74]	Solar	Probabilistic PEM	Min (the customer's energy cost)	GAMS	Residential energy hub in three cases/ CHP, PHEV, solar panels, TES	EN, NG/ED, HD	Operation scheduling	24 h	A framework of home energy management (HEM)	2016
[33]	Wind and solar output generation	Probabilistic scenario	Max [multi-energy player (MEP) profit resulting from the energy exchange	CPLEX/ GAMS	CHP, B, TES, PV, WT	EN, NG/ED, HD	MILP	24 h	Different realizations of wind power generation are modeled	2017

(continued)

Table 12.2 (continued)

References	Uncertainty parameters	Type of modeling method	Objective function	Solver	Case study/hub components	Hub input/output ports	Problem	Horizon time	Description and remarks	Publish year
[37]	Electricity, heat, and gas demands, market price of electricity and heat, wind speed	Probabilistic MCS	with its local energy system (LES) and the energy market] Min (operation cost consists of imported energy carrier cost in addition to device and program operation cost)	CPLEX/ GAMS	T, CHP, B, WT, TES, EES	EN, NG, DH, wind/ED, HD, NG	MILP—optimal operation	1 day	through a scenario generation process based on the roulette wheel mechanism (RWM) and with Weibull PDF. A scenario reduction technique is considered, using the K-means clustering technique One of the features of this work is adding the thermal demand response program (TDRP) besides the EDRP. For generating the scenarios the normal PDF is used for demands and Weibull PDF is employed for	2017

[75]	Electricity load and price	Probabilistic PEM (2 m + 1 PEM)	Min (total cost of supplying hub demand is composed of the cost of purchased gas and power from the grid + gas furnace and CHP unit's startups-shutdowns)	SBB/CONOPT under GAMS	Three structures: 1—CHP, F, T, TES, EES; 2—CHP, F, T, FC, HPP; 3—3 CHP units, 2 F units, T, 2 TES units, 2 EES units	EN, NG/ED, HD, and in addition hydrogen demand in case 2	MILP—operation scheduling	24 h	The electrical and heat demand response programs have been proposed in order to have optimal hub management	2017
[76]	Electrical load demand	Information-gap decision theory (IGDT)	Min (operating cost related to the installed assets in the energy hub and due to the energy transaction between the utility grid and the energy hub, the cost of purchasing energy and minus the revenue of selling energy from/to the grid)	–	CHP, EHP, AC, EH, EES, B	EN, NG/ED, HD, CD	Optimal short-term energy hub management	24 h	The simulation results showed that the robustness index increased proportionally to the permitted increasing variations of the total operating costs which was expected	2017
[37]	Electricity, heat, and gas demands, market price of	Probabilistic MCS	Min (the operation cost of energy hub consists of imported energy carrier cost in addition to	CPLEX/GAMS	In four cases: Case 1: With constant heat tariff and without TDRP. Case 2: With	EN, NG, DH/ED, HD, NG	MILP—optimal operation of multi-carrier energy system	24 h	In this work, the thermal demand response program (TDRP) is added besides the	2017

(continued)

Table 12.2 (continued)

References	Uncertainty parameters	Type of modeling method	Objective function	Solver	Case study/hub components	Hub input/output ports	Problem	Horizon time	Description and remarks	Publish year
	electricity and heat, wind speed		device and program operation cost)		constant heat tariff and with TDRP. Case 3: With consideration of thermal energy market and without TDRP. Case 4: With consideration of thermal energy market and with TDRP/CHP, WT, B, TES, EES		in smart grid environment		EDRP. For generating the scenarios the normal PDF is used for demands and Weibull PDF is employed for generating wind speed scenarios	
[77]	Wind speed, electricity, and heat loads and their forecasting in the problem of SEH	Probabilistic MCS	Min (SEH operational costs consisting of buying and selling electricity to/from network cost, operation cost of boilers and CHPs, startup and shutdown cost of SEH components + cost of unserved demands by using the value of lost load (VOLL))	CPLEX/GAMS	2 CHP units, 2 B units, WT, EES, TES, AC	EN, NG, W/ED, HD, CD	MILP—the wind-integrated smart energy hub (SEH) operation scheduling problem	24 h	The electrical and thermal loads of the energy hub have been served in the presence of demand response (DR) programs. The CVaR methodology is used to quantify the potential risk of scheduling problem. The normal or Gaussian probability	2017

										density function (PDF) is used to model load forecasting, and Rayleigh PDF is considered to present fluctuation of wind speed. GAMS/SCENRED program is employed to reduce the number of scenarios
[78]	Electrical load and its RTP, NG price	Probabilistic MCS	Min (a weighted sum function consisting of energy bill and penalty for emissions)	CPLEX/GAMS	S.E. hub/CCHP, AC, B	EN, NG/ED, HD, CD	MILP—optimal operation	24 h	The conditional value-at-risk (CVaR) technique is used to control the operational risk of an S.E. hub	2018
[79]	Uncertainty-accommodating flexibility	Interval optimization	Min (the operational cost of the expected scenario and the deviations of the inlet energy flows of the EH where the first line of the objective	The MATLAB “improg” function to calculate the optimization	Two EHs, one with low flexibility and the other with high flexibility, are used to make comparisons in this case study. The	EN, NG/ED, HD, CD	LP—optimal operation	Daily	Uncertainty-accommodating flexibility describes the ability of an EH to serve uncertain and variable loads at its outlet	2018

(continued)

Table 12.2 (continued)

References	Uncertainty parameters	Type of modeling method	Objective function	Solver	Case study/hub components	Hub input/output ports	Problem	Horizon time	Description and remarks	Publish year
[80]	Wind and solar generation, electrical load variation, and price fluctuations	A distributionally robust chance-constrained programming (CCP) reformulation method based	function denotes the day-ahead energy purchase cost of the EH, and the second line denotes the cost of deviations in real time)	CPLEX/GAMS	low-flexibility EH contains only a CERG and B. The high-flexibility EH model contains CHP, B, CERG, and WARG	EN, NG/ED, HD	MILP—a day-ahead optimal operation	Day-ahead	ports without altering the energy flow at its inlet port. The degrees of freedom of uncertainty-accommodating flexibility denotes the number of uncertain and variable loads on outlet ports that an EH can serve while maintaining a constant inlet energy flow Through the proposed reformulation, the CCP-based multi-energy residential system (MERS) model becomes a mixed-integer	2018

	Electrical price of market	on Chebyshev's inequality	term is introduced to punish the RESO if the dispatch of specific loads such as residential heating sources fails to fulfill the satisfaction levels of customers)		the PDS consume natural gas from nodes 2 and 9 from the NGDS, respectively. In addition, two PV units, one WT, EEs, two gas storages, F and EHP			second-order cone programming (MISOCP) model that is less complex and easier to solve than other models in the existing literature. The MERS model is solved by the GAMS/BONMIN solver. The linearized MILP model is solved by the GAMS/CPLEX solver	2018	
[81]	Electrical price of market	(IGDT)	Min (operation cost of CHP, boiler, battery storage system, thermal storage system, cost of purchased power from the upstream grid and minus of profit of selling power to the upstream grid)	CPLEX/GAMS	Sample apartment smart building includes ten smart homes with different living habits/CHP, B, EES, TES, and smart schedulable appliances	EN, NG/ED, HD	Optimal scheduling of apartment smart building	24 h	The main purpose of proposed paper is to minimize risk-constrained operation cost of apartment smart building in the presence of market price uncertainty	2018

(continued)

Table 12.2 (continued)

References	Uncertainty parameters	Type of modeling method	Objective function	Solver	Case study/hub components	Hub input/output ports	Problem	Horizon time	Description and remarks	Publish year
[82]	Electrical load and solar power generation	Probabilistic scenario	Min (the bought energy carrier cost and startup costs of converters, excluding the revenues from selling surplus energy to the grid)	The extended mathematical programming (EMP) framework/GAMS	T, F, PV, EES, TES, and two gas-fired DGs, where one of them is a CHP	EN, NG/ED, HD	MILP—a day-ahead energy operational scheduling of a multi-carrier energy system	Day-ahead, 24 h	A two-stage stochastic mixed-integer linear programming (MILP) framework has been developed for a day-ahead energy scheduling of multi-carrier energy system. Considering the energy price signals, the optimal scheduling problem aims at minimizing the total operational cost of energy hub through the optimization of unit commitment, the output of each unit, and	2018

	Electricity price and load, wind and solar power generation	Hybrid probabilistic MCS/(IGDT)/interval	Min (total cost of purchased energies as well as discom-fort cost of electrical consumers whose loads are curtailed in DSMPs)	GAMS	Hubs in an IEEE 33-bus distribution network under CHP, EES, B, CAC, WT, PV, T	EN, NG/ED, HD	MINLP—optimal operation of smart energy hubs (S.E. hubs)	24 h	Using stochastic programming for modeling the uncertainty of renewable units, interval optimization method, and IGDT are employed to model the uncertainties of price and electrical demand at the same time. In order to solve the multi-objective optimization problem, e-constraint technique is	charging/discharging scheduling of energy storage systems as well as transactions between the energy hub and the main grid	2018
--	---	--	---	------	---	---------------	--	------	---	--	------

(continued)

Table 12.2 (continued)

References	Uncertainty parameters	Type of modeling method	Objective function	Solver	Case study/hub components	Hub input/output ports	Problem	Horizon time	Description and remarks	Publish year
[84]	ECDR, RES, and electrical and heat loads	Probabilistic PEM (2 m + IPEM)	-	The computational time efficiency of the proposed decomposition strategy on solving the deterministic EFMEC of the scenario 1 is compared with the	The MEC test system integrated with the ECDR consumers and RESs consists of 14-bus electrical IEEE, 14-node heating network, and 20-node gas network. In this case, the electrical network consists	EN, NG, DH/ED, HD	Energy flow analysis of an integrated MEC system	-	employed and fuzzy decision-making algorithm is used to select the trade-off solution between average and deviation costs of S.E. hubs. The electricity consumers of energy hubs can participate in DSMPs	2018

	Wind power output	Probabilistic scenario	Min (expected operation cost of interconnected EHs across all wind power scenarios, including the costs of DR program, unit commitments, hourly generation of coal-fired units, hourly production	Solved by the MILP of Gurobi 6.5.0 toolbox	On 3-hub and 17-hub interconnected system in day-ahead scheduling—in 3 cases: 1—deterministic scheduling of EHs without DR, 2—1 + DR, 3—stochastic scheduling	EN, NG/ED, HD	MILP—optimal operation of interconnected EHs	24 h	ECDR and the RES uncertainties are investigated regarding incentives for each energy carrier. The heat and electrical loads are followed from normal PDF with 10% standard deviation (SD). The wind farms are followed from the Weibull PDF. The irradiances are followed from the beta PDF	[85]
--	-------------------	------------------------	---	--	---	---------------	--	------	---	------

(continued)

Table 12.2 (continued)

References	Uncertainty parameters	Type of modeling method	Objective function	Solver	Case study/hub components	Hub input/output ports	Problem	Horizon time	Description and remarks	Publish year
			of natural gas wells, and punishment of wind curtailment and load shedding)		of EH with DR + wind uncertainty/go to remarks				hourly wind power. The backward scenario reduction method is applied. The proposed model is coded in MATLAB 2014b platform with YALMIP toolbox. In three EHS the power transmission system has two natural gas-fired units, one coal-fired unit, one wind farm, and seven transmission lines. Gas transmission system consists of two gas wells, one natural gas storage, and five pipelines.	

										17-Hub system has 24 electric buses, 40 gas nodes, 12 natural gas-fired units, 17 coal-fired units, and 4 wind farms	2018
[86]	Price of market on day-ahead, RTP, wind speed	Probabilistic MCS	Min (the power bought bid + the natural gas cost that is purchased from + power transacted with the grid in the real-time market) and max (maximizes power sell bid)	GAMS	Six case studies are considered. Two CHP units, EHP, B, WT, EES	EN, NG/ED, HD	MILP—a comprehensive optimal bidding strategy	24 h	The proposed bidding strategy in this chapter consists of sell/buy bid in the day-ahead market, since the deviation of power should be compensated in the real-time market by real-time prices	2018	
[87]	Electricity, heat, and cool loads, price of electricity in an electrical market as competitive	Probabilistic scenario	Min (energy costs including electricity and gas)	BONMIN/GAMS	In four cases/ CHP, B, T, AC, EES, air conditioner	EN, NG/ED, HD, CD	An optimal operation of energy hub	24 h	All of these uncertain parameters have been expressed by using normal PDF	2018	
[88]	Wind generation, electrical and thermal demands	Probabilistic scenario	Min (the expected total cost)	The LINDO solver/GAMS	Seven states in two cases were applied/T, CHP, F, EES, TES, WT	EN, NG, W/ED, HD	MILP—optimal operation	24 h	Here, normal PDF was selected to model the loads, and the Weibull PDF was	2018	

(continued)

Table 12.2 (continued)

References	Uncertainty parameters	Type of modeling method	Objective function	Solver	Case study/hub components	Hub input/output ports	Problem	Horizon time	Description and remarks	Publish year
[89]	Electricity and heat demand, electrical RTP	Probabilistic scenario	Min [cost of the procured power from the day-ahead market and the startup and shutdown costs of the units (diesel gen, CHP, boiler, heat pump) in the energy hubs]	CPLEX/ GAMS	CHP, B, T, EHP, diesel-G, EES, TES	EN, NG/ED, HD	MILP—a risk-based framework for energy management of interconnected energy hubs in MEC systems	24 h	applied to represent the output power of a wind generator. The gas price contains three tariffs The normal PDF of the uncertain parameters and auto regressive integrated moving average (ARIMA) models are used to generate scenarios associated with the uncertainty in loads and prices, respectively. Conditional value-at-risk (CVaR) method is used to quantify the risk associated with uncertainties.	2018

[90]	Solar and wind power, electricity, heat loads	Probabilistic scenario	Min [the cost of purchased electricity and natural gas from the main utility, the startup cost of the diesel generators, CHP, and boilers, the fuel cost of diesel generators, as well as the cost for scheduled up-and-down spinning reserve, the cost of up-and-down thermal spinning reserve provided by	CPLEX/ GAMS	A 10-node microgrid. In this microgrid, the electrical and thermal loads are supplied by the energy hubs. The energy hubs are interconnected using 11 distribution lines and five natural gas pipelines. CHP, B, diesel-G, WT, PV, EES, TES	EN, NG/ED, HD	MILP—short-term operation planning of microgrids with multiple-energy carrier networks to determine the scheduled energy and reserve capacity	24 h	Also, sensitivity analyses are conducted to assess the energy procurement scheduling based on the proposed approach. The GAMS/SCENRED program is used to reduce the number of scenarios	2018
------	---	------------------------	---	----------------	---	---------------	---	------	---	------

(continued)

Table 12.2 (continued)

References	Uncertainty parameters	Type of modeling method	Objective function	Solver	Case study/hub components	Hub input/output ports	Problem	Horizon time	Description and remarks	Publish year
[91]	Wind production, electrical price, electricity, and thermal loads	Combined probabilistic MCS/(IGDT)	boilers, the scheduled electrical and thermal reserve provided by responsive loads, the expected operation cost in scenarios]	SSB/GAMS	2 CHP units, 2 B units, WT, EES, TES by modified IEEE 34-node test system in hub electrical output port	EN, NG, W/ED, HD	MINLP—operation scheduling	24 h	The forecast errors of uncertainties related to wind power generation and energy demands are modeled as a scenario, while an IGDT optimization approach is proposed to model electricity price uncertainty. In this chapter, the Rayleigh PDF and the normal distribution are applied to	2019

[59]	Wind power	Robust optimization (by nested (C and CG))	Min [the total cost of MES operation, including power system cost (i.e., startup/shutdown costs and operation costs at base case and worst scenario) and natural gas system cost (e.g., startup/shutdown gas consumption costs for natural gas-fired units at base case and the natural gas consumption cost at worst scenario)]	Nested column and constraint (C and CG) generation method and MATLAB 2014b platform in Gurobi 7.5.1	6-bus system with three natural gas node and a modified IEEE 118 bus with 10-node electricity-natural gas-integrated system. CHP, TES, EB, EES	EN, NG/ED, HD	A robust day-ahead scheduling method for a multi-carrier energy system (MES)	24 h	The first-stage problem which schedules the hourly unit commitment is solved in the outer loop, while the inner loop solves the second-stage problem to realize the worst scenario. Several acceleration	model the variation of wind speed and the electrical and thermal demands, respectively. In this chapter SCENRED tool (fast backward reduction method) is applied
------	------------	--	--	---	--	---------------	--	------	--	--

(continued)

Table 12.2 (continued)

References	Uncertainty parameters	Type of modeling method	Objective function	Solver	Case study/hub components	Hub input/output ports	Problem	Horizon time	Description and remarks	Publish year
[92]	Wind production, electricity, and thermal loads	Probabilistic MCS	Min [total cost (operation costs of the CHP unit, boiler, and CAES system, the cost and benefit of imported and exported electricity from and to local grid and CHP unit startup and shutdown costs in each scenario and time blocks of scheduling problem) + penalty cost (the cost of unserved electrical and thermal demands based on the value of lost load (VOLL))]	CPLEX/ GAMS	SMEH/CHP, B, CAES, TES, EHP	EN, NG/ED, HD	MILP—the risk-constrained scheduling of a wind-integrated smart multi-carrier energy hub (SMEH)	24 h	The CVaR methodology is implemented to model and manage the potential risk of operation cost variation of the SMEH scheduling problem. TDR program besides EDR is applied to reduce the operation cost of the SMEH. Wind turbine generation can be modeled by historical data records of wind speed and Rayleigh PDF is applied to model the variation of wind speed. Demands are modeled by using	2019

[93]	Electrical, heating, and cooling demands, wind speed, and solar irradiances, as well as the price of energy carriers including electricity and natural gas	Probabilistic MCS	Max [the final profit with respect to the difference between income and hub costs (electrical REERs, participation of DRPs, conversion of heat to cooling, conversion of natural gas to electricity)]	CPLEX/GAMS	Four case studies: 1—without WT and PV, without DRP; 2—with WT and PV, without DRP; 3—with WT and PV, with 10% of DRP; 4—with WT and PV, with 20% of DRP, and with energy storage systems. CHP, T, PV, B, AC, WT, TES, EES, CES	EN, NG/ED, HD, CD	MILP—optimal operation of a combined energy system (CES) with the concept of energy hub	24 h	normal Gaussian PDF. Fast backward reduction method (SCENRED2/GAMS) is implemented as scenario reduction algorithm	2019
[60]	Market price uncertainty	Robust optimization approach	Min [the total operation cost and CO2 emission]	GAMS	In three cases: 1—the robust scheduling of the MCHES without considering TOU/RTP rate of DRP. 2—case	EN, NG, W, solar/ED, HD, CD	RMILP—robust scheduling of MCHES operation	24 h	The time-of-use (TOU) and real-time pricing (RTP) rates of DRPs play a vital role in flattening	2019

(continued)

Table 12.2 (continued)

References	Uncertainty parameters	Type of modeling method	Objective function	Solver	Case study/hub components	Hub input/output ports	Problem	Horizon time	Description and remarks	Publish year
[94]	Electrical and thermal demands and wind speed	Probabilistic MCS	Min [the operation costs of the electrical system, natural gas network, and corrective voltage control proceeding cost + load shedding cost]	SSB/GAMS	1 considering TOU rate of DRP. 3—case 1 considering RTP rate of DRP. EES, CES, TES, HE, AC, EC, PV, WT, B, GT as a CHP, ST IEEE 14-bus electrical system and 17-node natural gas system in two modes consist of independent operation and integration of gas and power system/CHP, T, B, EES	EN, NG/ED, HD	MINLP—enhancement of voltage stability in multi-carrier energy systems	-	Load margin is considered as voltage stability index. The Rayleigh PDF and normal Gaussian PDF are used to model the uncertainties in wind speed and demands. The SCENRED2/GAMS (fast backward method) tool has been applied to reduce scenario number	2019

[95]	Electricity, natural gas, and thermal demand, energy price of market on day-ahead (electrical, gas, and heating), RES power (wind and solar), rate of charge or discharge, energy arrival or departure, capacity of charger of EVs	Probabilistic scenario	Max (hub profit in the day-ahead market)	GAMS	In nine cases/WT, PV, CHP, EES, B, EVs	EN, NG, DH/ED, HD	MILP	Day-ahead, 24 h	Monte Carlo simulation (MCS) is used to generate scenario samples considering normal distribution for load and energy price forecasted parameters, and beta and Rayleigh distributions for RES and EV parameters, respectively. The fast backward/forward scenario reduction method is used in this chapter to reduce the scenario number	2019
[96]	Power consumption of PHEVs during trips	IGDT	Max (profit of the system)	GAMS	Electrolyzer, HS, FC, B, HES, WT, PV, EES (PHEV)	EN, NG/ED, HD, H2 (FCVs)	MILP—risk-based optimal operation of an energy hub	Daily, 24 h		2019
[97]	Wind speed and solar irradiances	Probabilistic PEM	Min (the total cost of generation of the electricity and gas)	–	The three-hub interconnected	EN, NG/ED, HD	Operation	24 h	The chance constraints on gas and power flows	2019

(continued)

Table 12.2 (continued)

References	Uncertainty parameters	Type of modeling method	Objective function	Solver	Case study/hub components	Hub input/output ports	Problem	Horizon time	Description and remarks	Publish year
[98]	Wind speed and solar irradiances	Probabilistic MCS (LHS-Nataf)	Probabilistic energy flow	–	Improved IEEE1 23-node system and NGS 48-node system/CHP, T, B, P2G, WT, PV	EN, NG/ED, HD	Energy flow	–	between adjacent hubs are separately applied to the optimization problem. Weibull PDF and beta PDF are applied to wind speed and solar irradiance uncertainty modeling Weibull PDF and beta PDF are used for wind speed and solar irradiance uncertainty modeling	2019
[99]	Behaviors in thermal loads (SIL, SNIL), thermal unplanned hot water demand, uncertain air temperature preference, unplanned EVs' travel	Probabilistic scenario	Min (energy expense and energy deviation which should be defined as comfort level)	CPLEX/GAMS	In four cases/ CCHP, EES, T	EN, NG/ED, HD	MILP—optimal operation scheduling of smart residential energy hub (SREH)	Day-ahead, 24 h	The loads are classified as shiftable and interruptible loads (SIL) and shiftable and non-interruptible loads (SNIL)	2020

[100]	Price of electrical and thermal, heat, and electrical loads, wind power	Combined scenario-based/interval	Min (average and deviation costs of hub energy)	CPLEX/ GAMS	In two cases with and without DRP/CHP, T, B, EES, HES, WT	EN, NG, DH/ED, HD	MILP—optimal operation of an energy hub	Daily, 24 h	The Weibull and normal PDFs are applied to generate scenarios for wind speed and other uncertainties except electricity price that it is modeled by interval optimization. TDRP and EDRP are considered	2020
[101]	Wind speed and solar irradiances	Probabilistic scenario	Min (cost minimization of an energy hub)	CPLEX/ GAMS	In four case studies/CCHP, PV, WT, CES, EES, HES	EN, NG/ED, HD, CD	MINLP—performance of ice storage device in the optimal operation of an energy hub	Day-ahead, 24 h	Price-based demand response (DR) has been considered. The Weibull PDF and beta PDF are used for wind speed and solar irradiance modeling. Monte Carlo simulation is applied to generate 1000 scenarios with the same probabilities randomly.	2020

(continued)

Table 12.2 (continued)

References	Uncertainty parameters	Type of modeling method	Objective function	Solver	Case study/hub components	Hub input/output ports	Problem	Horizon time	Description and remarks	Publish year
									SCENRED2/ GAMS are used to decrease the values of the generated scenarios to 10. The natural gas price is assumed constant	

AC absorption chiller, *B* boiler, *CAC* central air condition, *CAES* compressed air energy storage, *CC* compression chiller, *CCHP* combined cooling, heat, and power, *CD* cooling demand, *CERG* compression electric refrigerator group, *CES* cooling energy storage, *CHP* combined heat and power, *DH* district heat, *Diesel-G* diesel generator, *DT* desalination tank, *EB* electrical boiler, *EES* electrical energy storage, *ED* electrical demand, *EH* electrical heater, *EHP* electrical heat pump, *EN* electrical network, *EV* electric vehicle, *F* furnace, *FC* fuel cell, *FCV* fuel cell vehicle, *FWT* freshwater tank, *GES* gas energy storage, *GFG* gas fire generator, *GSHP* ground-source heat pump, *GT* gas turbine, *HD* heat demand, *HE* heat exchanger, *HES* heat energy storage, *HP* heat pump, *HPP* hydrogen production plant, *HS* hydrogen storage, *H₂* hydrogen, *ND* natural gas demand, *NG* natural gas, *PHEV* plug-in hybrid electric vehicle, *PV* photovoltaic system, *P2G* power-to-gas, *ST* solar thermal, *T* transformer, *W* wind, *WARG* water absorption refrigerator group, *WD* water demand, *WN* water network, *WT* wind turbine

found. It was first proposed by Ramon E. Moore [104, 105]. That is, according to [6, 7], assume a multivariate function in the form of $f = (x_1, \dots, x_n)$ and $lb_i \leq x_i \leq ub_i$ where lb_i and ub_i are the lower and upper bounds for uncertain parameter x_i , respectively. The goal is finding the lower and upper bounds of the objective function f :

$$\begin{aligned} \text{Prob} &= \int_a^d A_1 \frac{1}{\sigma\sqrt{2\pi}} e^{-\frac{(x-\mu)^2}{2\sigma^2}} \\ &= \frac{1}{\sigma\sqrt{2\pi}} \left[\int_z^b \frac{x-a}{b-a} e^{-\frac{(x-\mu)^2}{2\sigma^2}} + \int_b^c e^{-\frac{(x-\mu)^2}{2\sigma^2}} + \int_c^d \frac{x-d}{c-d} e^{-\frac{(x-\mu)^2}{2\sigma^2}} \right] \end{aligned} \quad (12.36)$$

$$G(\text{Prob}) = \mu_{B_2}(\text{Prob}) \quad (12.37)$$

In order to consider the uncertainty of wind in the problem of optimal operation of an interconnected gas-electricity energy system, an interval analysis method has been used in [106] according to DR programs. In [79], an automated and linearized modeling method based on an interval optimization model was suggested to reduce the effect of the uncertainty aggregated in flexibility (which shows the uncertainty of the ability of an EH to provide variable and uncertain loads in the outlet without change in power flow in the input ports) in order for optimal operation of hub energies. The value of two indicators that indicates the flexibility of the EH, named as load-carrying capability and uncertainty-accommodating flexibility, is determined by the degree of freedom of the connection matrices and the area of operation based on the proposed model. The method of functional interval in urban energy system planning with various primary energy sources in [107] has been used to determine suitable alternatives for energy sources in order to model the price of electrical energy under the uncertainty. Considering the lower and upper bounds as a function of useful parameters as functional intervals shows more realistic effect of changes in uncertainty parameters on system performance than the intervals with constant intervals. An interval method is generally used as a hybrid model with other methods for uncertainty modeling.

12.4 Review of Previous Articles

In order to give readers access to more details about researches done in the modeling of uncertainty in hybrid energy system or EH concept and also to know a brief history of them to achieve an idea for more future studies in this field, a summary is

presented in Table 12.2. These details include uncertain parameters, modeling methods, solver, objective function, etc.

This table is designed in 11 columns that are useful for readers. The first column and the last column show the reference number and year of publication of the article, respectively. It is possible to follow the changes in the research process over the years through the last column, and for this reason, we attempt to show the sequence of years in the table. The second column shows the uncertain parameters which are considered in the article. The third column describes how to model these parameters. The objective function of the article is expressed in the fourth column, if mentioned in it. The objective function, together with the constraints presented in the article, forms the basic model of the problem. Although the expression of tools and software was not a necessity, but due to the greater knowledge and readiness of researchers, this information was added in the fifth column. Also, in order to know more about the EH that was studied in these researches and design of tests and comparative research, another information such as type of converter and storage devices, and type of input and output energy carriers in the EH and case studies, is provided in the sixth and seventh columns.

You can see that a change in the base model can lead to the development of the model and thus it is more useful for future work, which will be possible through the fourth, sixth, and seventh columns. The eighth and ninth columns provide information on the type of problem in terms of programming and time horizon, respectively. For example, if there is a problem with the energy flow or MINLP, it is clear from here. In the tenth column, an attempt has been done to provide the extra details for readers such as the considered PDF, methods of generation and reduction of scenarios, and type of demand response program.

In the next section, we will look at how to use this table for future studies. In order for quick access, the historical information of the uncertain parameters and their modeling methods are presented in Table 12.3, which clearly shows the research gap related to the second and third columns of the previous table.

12.5 Conclusion and Discussion

Simultaneous planning and management of transmission, distribution, conversion, storage, and generation of various energy carriers is known as the EH concept. Nowadays, due to the benefits of EHs such as affordable supplying of loads, safe and adequate supply of consumer demand, and using it as a solution in the development of sustainable energy, these systems have received significant attention from researchers and investors. In order to maximize the benefits of the EH, we need to manage and schedule the EH optimally. The prerequisite for optimal EH management is its accurate modeling. So, by considering the uncertain nature of many data in real world (some of which are mentioned in the introduction) accurate and close-to-reality modeling of the EH will also be possible. Although optimal management without modeling the uncertainty parameters helps decision makers to gain an

Table 12.3 Summary of uncertainty modeling applications in energy hub and multi-energy system based on uncertain parameters

	Method	Probabilistic		IGDT	Robust	Possibilistic	Interval	Hybrid
		MCS	Scenario					
Uncertainty parameter								
Wind	Speed (generation profile)	61,80,82,39,91,92,72,97,100,105,106,107,33,108,114, 111	34, 87, 102, 104, 113	73	62	-	70	-
		61,82,97,106, 33,108, 114, 111	101,104	-	-	-	-	-
Tidal	Current speed	-	-	-	-	-	-	-
Price	Electricity	80,82,85,37,91,93,100,106,108	34,101,103	72,95	63	-	107,113	-
		36,93,106,108	-	-	-	-	-	-
	Gas	37,91,108	113	-	-	-	-	-
	Thermal	-	-	-	-	-	-	-
	Water	-	-	-	-	-	-	-
Demand	Electricity	80, 37,92,91,92,72,93,105,106,107,108	34,96,101, 102, 103, 113	71,97,73	-	-	-	-
		37,92,91,92,72, 105,106,107,108	101,102, 103, 112, 113	73	-	-	-	-
	Heat	-	-	-	-	-	-	-
	Cooling	106	101	-	-	-	-	-
	Natural gas	37,91,108	-	-	-	-	-	-
	Water	-	112	-	-	-	-	-
PHEV and EV	Charging pattern (charge/discharge rate)	108	-	-	-	-	-	-
		108,112	-	-	-	-	-	-
	Arrival/departure energy of EVs (power)	-	-	109	-	-	-	-

(continued)

Table 12.3 (continued)

	Method	Probabilistic		IGDT	Robust	Possibilistic	Interval	Hybrid
		MCS	Scenario					
	consumption of EVs during trips)							
	EV's charge capacity	108	-	-	-	-	-	-
	Traffic pattern of PEVs' owners	-	87	-	-	-	-	-
DR participation	CBDR	-	84	-	-	-	-	-
	ECDR	-	-	-	-	-	-	-
Component	Equipment efficiencies	-	-	-	54, 61	-	-	-
	Random outage	-	-	-	-	-	-	-
Weather (temperature and humidity) in agriculture hub		82	-	-	-	-	-	-
	Accommodating flexibility	-	-	-	-	-	77	-

overview of optimization problems, it cannot demonstrate the uncertainty in making real-world strategic decisions.

In this chapter we studied the researches which are carried out in modeling the operational planning of multi-energy systems under the concept of EH in the presence of uncertainty particularly. In the second and third sections, the uncertain parameters and the types of their modeling methods were introduced. Each of these methods attempts to model uncertain input parameters and reduce the adverse effects of their ignorance. Specifically, we investigated the articles on uncertainty modeling of EH with short-term time horizons. Therefore, in order to facilitate the accessibility of researchers to information and important details of each article, the brief information is provided in Table 12.2. In addition, Table 12.3 is designed to provide a better view of the research gap related to columns 2 and 3 of Table 12.2 by a quick access classification.

Here we intend to propose suggestions for future studies using the potential researches that are shown in these tables. As we know, by considering more uncertainty parameters in the model, we can achieve a more realistic model, which will help to reduce the risk in the decision-making strategy and reduce the occurrence of unforeseen unpleasant events. This will make stakeholders, operators, and consumers of energy more interested in using integrated multi-energy systems, thus facilitating the future research. According to Table 12.3 and the second column of Table 12.2, several uncertain parameters can be suggested for future studies. For example, some of these uncertain parameters such as water demand at the hub output, behavior pattern of electric vehicle owners, consumer participation in electrical demand response program (EDRP), and thermal demand response program (TDRP), and temperature and humidity in agricultural EHs have been modeled only once. Some parameters such as the price of water (as an input energy carrier) that is supplied by the upstream network, consumer participation in the cooling demand response program (CDRP), renewable energy, price and amount of some energy carriers which can be sold at the EH output ports including electricity and heat and gas, availability of power generation units, regional heating market, and emergency outage of converter and storage devices have never been modeled. For future work, it is recommended to use these new uncertain parameters along with other parameters.

In Table 12.3 and the third column of Table 12.2, you can see the amount of application of different methods in this field and the potential of using methods for modeling in the future. Probabilistic methods are most commonly used methods in modeling uncertainty parameters. Among the probabilistic methods, simulation-based (Monte Carlo) and analytical (scenario-based) methods have been used the most. This is because these methods, despite their time consumption and computational burden on large issues and large number of scenarios, have easy and quick implementation compared to other methods. Although the response time in the PEM probabilistic method depends on the number of uncertainty parameters of the model, it is the third most widely used method in this field of research due to its appropriate speed and accuracy. Apart from probabilistic methods, the IGDT method was more widely used than other modeling methods. Despite its complexity, this method is

effective and useful for decision makers in extreme uncertainty situations. This is one of the most powerful methods for making decisions that are robust to severe uncertainties. But unlike the robust optimization, it does not need to determine the maximum radius of the uncertainty's interval for uncertainty parameters and is much more flexible. Despite the probabilistic methods such as scenario-based methods and Monte Carlo simulation, IGDT method does not require PDFs of uncertain parameters, and since the output variables are not dependent on scenarios, we encounter with outputs that are efficient and accurate.

In robust method in addition to the difficulty in implementation, especially for nonlinear problems, and an inability of interval approaches in modeling the correlation between intervals, we are facing a costly approach due to its conservatism and taking into account the worse case. In regard of uncertainty in EHS, often due to the availability of different energy carriers and the presence of storage facilities, the worst conditions will cost less than conservatism, and RO (robust optimization) will be less efficient.

Along with the increasing of uncertainty parameters and increasing in the interests of researchers to model such systems more close to real, the application of these methods will become more frequent, especially in a combined manner. In fact, hybrid methods are very effective as a combination of methods to take advantage of all used methods and reduce the disadvantages of them in order to model the parameters. Therefore, by summarizing the discussion of using modeling methods, it is suggested that in order to model uncertainty in the optimal operation of EHS in future work, we should use a combination of methods such as IGDT-SP (stochastic programming), interval-SP, fuzzy-Monte Carlo, fuzzy-scenario-based and DR-SP method, and also possibilistic and fuzzy modeling methods.

Further than recommendation about using these modeling methods together, we propose to consider the other parameters such as operational parameters in solar and wind systems (e.g., cut-in speed of wind turbine and the ambient temperature of solar panel) besides the previous ones in order to have the system's modeling more close to reality. The expansion of the basic model is one of the things that were done according to the needs of future consumers. Therefore, columns 4, 6, and 7 of Table 12.2 can be used for this purpose. This can be done by modifying or developing objective functions, constraints, input energy carriers, and various types of energy in the output, converters, storage, and energy generation resources, as well as some other factors in the model, including reliability indices, pollution emission cost, equipment depreciation cost [108], consumer satisfaction cost, responsibility of loads and voltage control, or loss reduction in the energy transmission networks.

In addition, in each of these cases, different demand response programs can be used, especially the cooling demand response program (CDRP) [108], which has not been used in previous articles.

More than these we suggest using the long-term energy purchase contracts along with the uncertainty in real-time market energy price in the models.

Finally, we hope that by continuing the process of such research and expanding such tables, and by taking into account as many uncertainties as possible in the modeling of such systems, we will move towards sustainable energy development.

References

1. Ben-Haim Y (2006) Info-gap decision theory: decisions under severe uncertainty, 2nd edn. Academic Press, Oxford
2. Edenhofer O, Lessmann K, Kemfert C, Grubb M, Köhler J (2006) Induced technological change: exploring its implication for the economics of atmospheric stabilization. *Energy J*:57–107. <https://doi.org/10.2307/23297057>
3. Uusitalo L, Lehtikoinen A, Helle I, Myrberg K (2015) An overview of methods to evaluate uncertainty of deterministic models in decision support. *Environ Model Softw* 63:24e31
4. Mohammadi M, Noorollahi Y, Mohammadi-Ivatloo B, Yousefi H, Jalilinasabady S (2017) Optimal scheduling of energy hubs in the presence of uncertainty—a review. *J Energy Manage Technol*. <https://doi.org/10.22109/JEMT.2017.49432>
5. Mirakyan A, De Guio R (2015) Modelling and uncertainties in integrated energy planning. *Renew Sust Energ Rev* 46:62–69
6. Soroudi A, Amraee T (2013) Decision making under uncertainty in energy systems: state of the art. *Renew Sust Energ Rev* 28:376–384
7. Aien M, Hajebrahimi A, Fotuhi-Firuzabad M (2016) A comprehensive review on uncertainty modeling techniques in power system studies. *Renew Sust Energ Rev* 57:1077–1089
8. Aien M, Rashidinejad M, Fotuhi-Firuzabad M (2014) On possibilistic and probabilistic uncertainty assessment of power flow problem: a review and a new approach. *Renew Sust Energ Rev* 37:883–895
9. Basil M, Jamieson A (1999) Uncertainty of complex systems by Monte Carlo simulation. *Meas Contr* 32:16–20
10. Dymowa L (2011) Soft computing in economics and finance. Springer. ISRL: 6, pp 41–105
11. Yue X, Pye S, Decarolis J, Li FGN, Rogan F, Gallachoir BO (2018) A review of approaches to uncertainty assessment in energy system optimization models. *Energ Strat Rev* 21:204–217
12. Baudrit C, Dubois D, Guyonnet D (2006) Joint propagation and exploitation of probabilistic and possibilistic information in risk assessment. *IEEE Trans Fuzzy Syst* 14:593–608
13. Jco M, Pereira MVF, Leite da Silva A (1994) Evaluation of reliability worth in composite systems based on pseudo-sequential Monte Carlo simulation. *IEEE Trans Power Syst* 9:1318–1326
14. Yu H, Chung C, Wong K, Lee H, Zhang J (2009) Probabilistic load flow evaluation with hybrid Latin hypercube sampling and Cholesky decomposition. *IEEE Trans Power Syst* 24 (2):661–667
15. Janssen H (2013) Monte-Carlo based uncertainty analysis: sampling efficiency and sampling convergence. *Reliab Eng Syst Saf* 109:123–132
16. Zhaohong B, Xifan W (2002) Studies on variance reduction technique of Monte Carlo simulation in composite system reliability evaluation. *Electr Power Syst Res* 63(1):59–64
17. Julier SJ, Uhlmann JK (2004) Unscented filtering and nonlinear estimation. *Proc IEEE* 92:401–422
18. Allan RN, Leite da Silva AM, Burchett RC (1981) Evaluation methods and accuracy in probabilistic load flow solutions. *IEEE Trans Power Appar Syst*:2539–2546
19. Coroiu F, Bucatariu I, Baloi A (2012) Using the Gram–Charlier expansion in power systems reliability. In: Proceedings of 7th IEEE international symposium on applied computational intelligence and advanced informatics SACI: p. 59–62

20. Schellenberg A, Rosehart W, Aguado J (2005) Cumulant-based probabilistic optimal power flow (P-OPF) with Gaussian and gamma distributions. *IEEE Trans Power Syst* 20:773–781
21. Morrow D, Gan L (1993) Comparison of methods for building a capacity model in generation capacity adequacy studies. *Communications, computers and power in the modern. Environment conference proceedings. IEEE WESCANEX* 93:143–149
22. Stuart A, Ord K (2010) *Kendall's advanced theory of statistics, distribution theory*, 1st edn. Wiley, Chichester, West Sussex
23. Zubo RHA, Mokryani G, Rajamani H-S, Aghaei J, Niknam T, Pillai P (2017) Operation and planning of distribution networks with integration of renewable distributed generators considering uncertainties: A review. *Renewable Sustainable Energy Rev* 72:1177
24. Huang W, Sridhar N (2016) Fatigue failure risk assessment for a maintained stiffener-frame welded structure with multiple site cracks. *Int J Appl Mech* 8:1650024
25. Elishakoff I, van Manen S, Vermeulen PG, Arboez J (1987) First-order second-moment analysis of the buckling of shells with random imperfections. *AIAA J* 25(8):1113–1117
26. Hong HP (1998) An efficient point estimate method for probabilistic analysis. *Reliab Eng Syst Saf* 59(3):261–267
27. Rabiee A, Nikkha S, Soroudi A, Hooshmand E (2017) Information gap decision theory for voltage stability constrained OPF considering the uncertainty of multiple wind farms. *IET Renewable Power Gener* 11(5):585–592. <https://doi.org/10.1049/iet-rpg.2016.0509>
28. Soroudi A, Ehsan M (2011) A possibilistic–probabilistic tool for evaluating the impact of stochastic renewable and controllable power generation on energy losses in distribution networks—a case study. *Renew Sust Energy Rev* 15:794–800
29. Julier S, Uhlmann J, Durrant-Whyte HF (2000) A new method for the nonlinear transformation of means and covariances in filters and estimators. *IEEE Trans Autom Control* 45:477–482
30. Aien M, Fotuhi-Firuzabad M, Aminifar F (2012) Probabilistic load flow in correlated uncertain environment using unscented transformation. *IEEE Trans Power Syst* 27:2233–2241
31. Morales J, Pineda S, Conejo A, Carrion M (2009) Scenario reduction for futures market trading in electricity markets. *IEEE Trans Power Syst* 24(2):878–888
32. Alharbi W, Raahemifar K (2015) Probabilistic coordination of micro-grid energy resources operation considering uncertainties. *Electr Power Syst Res* 128:1–10
33. Damavandi MY, Neyestani N, Chicco G, Shafie-khah M, Catalao JP (2017) Aggregation of distributed energy resources under the concept of multi-energy players in local energy system. *IEEE Trans Sustainable Energy* 8:1679
34. Soroudi A, Mohammadi-Ivatloo B, Rabiee A (2014) Energy hub management with intermittent wind power. In *large scale renewable power generation*. Springer, pp 413–438
35. Arriagada E, López E, López M, Blasco-Gimenez R, Roa C, Poloujadoff M (2015) A probabilistic economic dispatch model and methodology considering renewable energy, demand and generator uncertainties. *Electr Power Syst Res* 121:325332
36. Kienzle F, Ahcin P, Andersson G (2011) Valuing investments in multi-energy conversion, storage, and demand-side management systems under uncertainty. *IEEE Trans Sustainable Energy* 2(2):194–202
37. Vahid-Pakdel MJ, Nojavan S, Mohammadi-ivatloo B, Zare K (2017) Stochastic optimization of energy hub operation with consideration of thermal energy market and demand response. *Energy Convers Manag* 145:117–128. <https://doi.org/10.1016/j.enconman.2017.04.074>
38. Ross TJ (2011) *Fuzzy logic with engineering applications*, 3rd ed. Library of Congress Cataloging-in-Publication Data, WILEY
39. Hu BQ, Wang CY (2014) On type-2 fuzzy relations and interval-valued type-2 fuzzy sets. *Fuzzy Sets Syst* 236:1–32
40. Jin L, Huang G, Cong D, Fan Y (2014) A robust inexact joint-optimal a cut interval type-2 fuzzy boundary linear programming (rij-it2fblp) for energy systems planning under uncertainty. *Int J Electr Power Energy Syst* 56:19–32

41. Jin L, Huang G, Fan Y, Wang L, Wu T (2015) A pseudo-optimal inexact stochastic interval (2 fuzzy sets approach for energy and environmental systems planning under uncertainty: a case study for Xiamen city of China. *Appl Energy* 138:71–90
42. Hegazy YG, Salama MMA, Chikhani AY (2003) Adequacy assessment of distributed generation systems using Monte Carlo simulation. *IEEE Trans Power Syst* 18(1):48–52
43. Ding Y, Wang P, Goel L, Loh PC, Wu Q (2011) Long-term reserve expansion of power systems with high wind power penetration using universal generating function methods. *IEEE Trans Power Syst* 26(2):766–774
44. Massim Y, Zeblah A, Benguediab M, Houraf A, Meziane R (2006) Reliability evaluation of electrical power systems including multi-state considerations. *Electr Eng* 88(2):109–116
45. Veliz FFC, Borges CLT, Rei AM (2010) A comparison of load models for composite reliability evaluation by nonsequential Monte Carlo simulation. *IEEE Trans Power Syst* 25(2):649–656
46. Atwa YM, El-Saadany EF, Salama MMA, Seethapathy R (2010) Optimal renewable resources mix for distribution system energy loss minimization. *IEEE Trans Power Syst* 25(1):360370
47. Conti S, Raiti S (2007) Probabilistic load flow using Monte Carlo techniques for distribution networks with photovoltaic generators. *Sol Energy* 81:1473–1481
48. Billinton R, Gao Y, Karki R (2009) Composite system adequacy assessment incorporating large-scale wind energy conversion systems considering wind speed correlation. *IEEE Trans Power Syst* 24(3):1375–1382
49. Hong YY, Pen KL (2010) Optimal VAR planning considering intermittent wind power using Markov model and quantum evolutionary algorithm. *IEEE Trans Power Delivery* 25(4):2987–2996
50. Rose J, Hiskens IA (2008) Estimating wind turbine parameters and quantifying their effects on dynamic behavior. *Proceedings of Power and Energy Society General Meeting* 1–7
51. Soroudi A (2012) Possibilistic-scenario model for DG impact assessment on distribution networks in an uncertain environment. *IEEE Trans Power Syst* 27(3):1283–1293
52. Kang B, Wei D, Li Y, Deng Y (2012) Decision making using Z-numbers under uncertain environment. *J Comput Inf Syst* 8(7):2807–2814
53. Ben-Tal A, Ghaoui LE, Nemirovski A (2009) *Robust optimization*. Princeton University Press, Princeton
54. Soyster AL (1973) Convex programming with set-inclusive constraints and applications to inexact linear programming. *J Oper Res* 21(2):1154–1157
55. Bertimas D, Sim M (2004) The price of robustness. *J Oper Res* 52(1):35–53
56. Parisio A, Del Vecchio C and Velotto G. (2011) Robust Optimization of Operations in Energy Hub. 50th IEEE Conference on Decision and Control and European Control Conference (CDC-ECC) Orlando, FL, USA, 12–15.
57. Parisio A, Del Vecchio C, Vaccaro A (2012) A robust optimization approach to energy hub management. *Int J Electr Power Energy Syst* 42(1):98–104
58. Akbari K, Nasiri MM, Jolai F, Ghaderi SF (2014) Optimal investment and unit sizing of distributed energy systems under uncertainty: a robust optimization approach. *Energy Buildings* 85:275–286
59. Yan M, Zhang N, Ai X, Shahidehpour M, Kang C, Wen J (2019) Robust two-stage regional-district scheduling of multi-carrier energy systems with a large penetration of wind power. *IEEE Trans Sustain Energy* 10(3). <https://doi.org/10.1109/TSTE.2018.2864296>
60. Najafi-Ghalelou A, Nojavan S, Zare K, Mohammadi-Ivatloo B (2019) Robust scheduling of thermal, cooling and electrical hub energy system under market price uncertainty. *Appl Therm Eng* 149:862–880
61. Labriet M, Nicolas C, Tchung-Ming S, Kanudia A, Loulou R. (2015) Energy decisions in an uncertain climate and technology outlook: how stochastic and robust methodologies can assist policy-makers, informing energy clim. *Policies Using Energy Syst. Model*, Springer International Publishing: pp. 69–91. doi:<https://doi.org/10.1007/978-3-319-16540-04>.

62. Khojasteh M, Jadid S (2015) Decision-making framework for supplying electricity from distributed generation-owning retailers to price-sensitive customers. *Utilities Policy*, 1e12.
63. Moeini-Aghtaie M, Dehghanian P, Fotuhi-Firuzabad M, Abbaspour A (2013) Multiagent genetic algorithm: an online probabilistic view on economic dispatch of energy hubs constrained by wind availability. *IEEE Trans Sustainable Energy* 5(2):699–708
64. Pazouki S, Haghifam M-R, Moser A (2014) Uncertainty modeling in optimal operation of energy hub in presence of wind, storage and demand response. *Int J Electr Power Energy Syst* 61:335–345
65. Moeini-Aghtaie M, Abbaspour A, Fotuhi-Firuzabad M, Dehghanian P (2014) Optimized probabilistic PHEVs demand management in the context of energy hubs. *IEEE Trans Power Delivery* 30:996
66. Bozchalui MC, Cañizares CA, Bhattacharya K (2014) Optimal energy management of greenhouses in smart grids. *IEEE Trans Smart Grid* 6:827
67. Rastegar M, Fotuhi-Firuzabad M, Zareipour H, Moeini-Aghtaie M (2015) A probabilistic energy management scheme for renewable-based residential energy hubs. *IEEE Trans Smart Grid* 8(5):2217
68. Soroudi A and Keane A (2015) Risk averse energy hub management considering plug-in electric vehicles using information gap decision theory. In *Plug In Electric Vehicles in Smart Grids*, pp. 107–127.
69. Neyestani N, Damavandi M, Shafie-khah M, Catalão J, and Chicco G. (2015) Uncertainty characterization of carrier-based demand response in smart multi-energy systems,” in *Power Engineering, Energy and Electrical Drives (POWERENG)*, 2015 IEEE 5th International Conference on, pp. 366–371
70. Zarif M, Khaleghi S, Javidi MH (2015) Assessment of electricity price uncertainty impact on the operation of multi-carrier energy systems. *IET Gener Transm Distrib* 9(16):2586–2592
71. Vaccaro A, Pisani C, Zobaa AF (2015) Affine arithmetic-based methodology for energy hub operation-scheduling in the presence of data uncertainty. *IET Gener Transm Distrib* 9 (13):1544–1552
72. Yazdani-Damavandi M, Moghaddam MP, Haghifam M-R, Shafie-khah M, Catalão JPS (2016) Modeling Operational Behavior of Plug-in Electric Vehicles’ Parking Lot in Multienergy Systems. *IEEE TRANSACTIONS ON SMART GRID*. <https://doi.org/10.1109/TSG.2015.2404892>
73. Moeini-Aghtaie M, Farzin H, Fotuhi-Firuzabad M, Amrollahi R (2016) Generalized analytical approach to assess reliability of renewable-based energy hubs. *IEEE Trans Power Syst* 32:368
74. Rastegar M, Fotuhi-Firuzabad M, Zareipour H, Moeini-Aghtaie M (2016) A probabilistic energy management scheme for renewable-based residential energy hubs. *IEEE Trans Smart Grid* 88:2217
75. Alipour M, Zare K, Abapour M (2017) MINLP probabilistic scheduling model for demand response programs integrated energy hubs. *IEEE Trans Ind Inf* 14:79
76. Javadi MS, Anvari-Moghaddam A, Guerrero JM (2017) Robust energy hub management using information gap decision theory. *IEEE Conf*. <https://doi.org/10.1109/IECON.2017.8216073>
77. Dolatabadi A, Mohammadi-Ivatloo B (2017) Stochastic risk-constrained scheduling of smart energy hub in the presence of wind power and demand response. *Appl Therm Eng* 123:40–49
78. Roustai M, Rayati M, Sheikhi A, Ranjbar AM (2018) A scenario-based optimization of smart energy hub operation in a stochastic environment using conditional-value-at-risk. *Sustain Cities Soc* 39:309–316
79. Wang Y, Cheng J, Zhang N, Kang C (2018) Automatic and linearized modeling of energy hub and its flexibility analysis. 211:705–714
80. Liu W, Zhan J, Chung CY, Li Y (2019) Day-Ahead Optimal Operation for Multi-Energy Residential Systems with Renewables. *IEEE Transactions on Sustainable Energy*. <https://doi.org/10.1109/TSTE.2018.2876387>

81. Najafi-Ghalelou A, Nojavan S, Zare K (2018) Heating and power hub models for robust performance of smart building using information gap decision theory. *Electr Power Energy Syst* 98:23–35
82. Ghasemi A, Banejad M, Rahimiyan M (2018) Integrated energy scheduling under uncertainty in a micro energy grid. *IET Gener. Transm. Distrib* 12(12):2887–2896
83. Majidi M, Zare K (2018) Integration of smart energy hubs in distribution networks under uncertainties and demand response concept. *IEEE Trans Power Syst* 34:566
84. Massrur HR, Niknam T, FotuhiFiruzabad M (2018) Investigation of carrier demand response uncertainty on energy flow of renewable-based integrated electricity-gas-heat systems. *IEEE Trans Ind Inf* 14:5133
85. Zhang Y, He Y, Yan M, Guo C, Ding Y (2018) Linearized stochastic scheduling of interconnected energy hubs considering integrated demand response and wind uncertainty. *Energies* 11:2448. <https://doi.org/10.3390/en11092448>
86. Davatgaran V, Saniei M, Mortazavi SS (2018) Optimal bidding strategy for an energy hub in energy market. *Energy*. <https://doi.org/10.1016/j.energy.2018.01.174>
87. Thang VV, Zhang Y, Ha T, Liu S (2018) Optimal operation of energy hub in competitive electricity market considering uncertainties. *Int J Energy Environ Eng*. <https://doi.org/10.1007/s40095-018-0274-8>
88. Ezzati SM, Faghihi F, Shourkaei HM, Mozafari SB, Soleymani S (2018) Optimum operation of multi-energy carriers in the context of an energy hub considering a wind generator based on linear programming. *J Renewable Sustainable Energy* 10:014702. <https://doi.org/10.1063/1.4991984>
89. Shams MH, Shahabi M, Khodayar ME (2018) Risk-averse optimal operation of multiple-energy carrier systems considering network constraints. *Electr Power Syst Res* 164:1–10. <https://doi.org/10.1016/j.epsr.2018.07.022>
90. Shams MH, Shahabi M, Khodayar ME (2018) Stochastic day-ahead scheduling of multiple energy carrier microgrids with demand response. *Energy*. <https://doi.org/10.1016/j.energy.2018.04.190>
91. Dolatabadi A, Jadidbonab M, Mohammadi-ivatloo B (2019) Short-term Scheduling Strategy for Wind-based Energy Hub: A Hybrid Stochastic/IGDT Approach. *IEEE Transactions on Sustainable Energy*. <https://doi.org/10.1109/TSTE.2017.2788086>.
92. Jadidbonab M, Babaei E, Mohammadi-ivatloo B (2019) CVaR-constrained scheduling strategy for smart multi carrier energy hub considering demand response and compressed air energy storage. *Energy*. <https://doi.org/10.1016/j.energy.2019.02.048>
93. Rikipour D, Barati H (2019) Probabilistic optimization in operation of energy hub with participation of renewable energy resources and demand response. *Energy*. <https://doi.org/10.1016/j.energy.2019.02.021>
94. Jadidbonab M, Vahid-Pakdel MJ, Seyedi H, Behnam M-i (2019) Stochastic assessment and enhancement of voltage stability in multi carrier energy systems considering wind power. *Electr Power Energy Syst* 106:572–584. <https://doi.org/10.1016/j.ijepes.2018.10.028>
95. Dini A, Pirouzi S, Norouzi M, Lehtonen M (2019) Grid-connected energy hubs in the coordinated multi-energy management based on day-ahead market framework. *Energy*. <https://doi.org/10.1016/j.energy.2019.116055>
96. Moghaddas-Tafreshi SM, Jafari M, Mohseni S, Kelly S (2019) Optimal operation of an energy hub considering the uncertainty associated with the power consumption of plug-in hybrid electric vehicles using information gap decision theory. *Electr Power Energy Syst* 112:92–108. <https://doi.org/10.1016/j.ijepes.2019.04.040>
97. Huo D, Gu C, Ma K, Wei W, Xiang Y, Le Blond S (2019) Chance-constrained optimization for multi energy hub systems in a smart city. *IEEE Trans Ind Electron* 66(2). <https://doi.org/10.1109/TIE.2018.2863197>
98. Chen J, Yu Q, Li Q, Lin Z, Li C (2019) Probabilistic energy flow analysis of MCE system considering various coupling units and the uncertainty of distribution generators. *IEEE Access*:7. <https://doi.org/10.1109/ACCESS.2019.2931398>

99. Lu Q, Lü S, Leng Y, Zhang Z (2020) Optimal household energy management based on smart residential energy hub considering uncertain behaviors. *Energy*. <https://doi.org/10.1016/j.energy.2020.117052>
100. Jamalzadeh F, Mirzahosseini AH, Faghihi F, Panahi M (2020) Optimal operation of energy hub system using hybrid stochastic-interval optimization approach. *Sustain Cities Soc* 54:101998. <https://doi.org/10.1016/j.scs.2019.101998>
101. Heidari A, Mortazavi SS, Bansal RC (2020) Stochastic effects of ice storage on improvement of an energy hub optimal operation including demand response and renewable energies. *Appl Energy* 261:114393. <https://doi.org/10.1016/j.apenergy.2019.114393>
102. Kazemi M, Mohammadi-Ivatloo B, Ehsan M (2014) Risk-based bidding of large electric utilities using information gap decision theory considering demand response. *Electr Power Syst Res* 114:86–92
103. Rabiee A, Soroudi A, Keane A (2015) Information gap decision theory based OPF with HVDC connected wind farms. *IEEE Trans Power Syst* 30:6. <https://ieeexplore.ieee.org/document/6985688>
104. Moore R (1966) *Interval analysis*. Prentice-Hall, Englewood Cliff, NJ
105. Moore RE, Kearfott RB, Cloud MJ (2009) *Introduction to interval analysis*, 1st edn. Society for Industrial and Applied Mathematics, Philadelphia, PA
106. Bai L, Li F, Cui H, Jiang T, Sun H, Zhu J (2016) Interval optimization based operating strategy for gas-electricity integrated energy systems considering demand response and wind uncertainty. *Appl Energy* 167:270–279
107. Zhu Y, Huang G, He L, Zhang L (2012) An interval full infinite programming approach for energy systems planning under multiple uncertainties. *Int J Electr Power Energy Syst* 43 (1):375–383
108. Salehimalah M, Akbarimajd A, Valipour K, Dejamkhooy A (2018) Generalized modeling and optimal management of energy hub based electricity, heat and cooling demands. *Energy* 159:669e685. <https://doi.org/10.1016/j.energy.2018.06.122>

Chapter 13

Network Expansion Planning of Multi-carrier Energy Systems



Fazel Mohammadi

13.1 Introduction

The network expansion planning (NEP) including system development and asset management falls into the long-term plans for energy providers. The time frame for expansion planning in energy sectors is in the order of several years. When it comes to future planning for energy sectors, cost plays a major role. In other words, the more accurate the planning the less financial risks associated with asset upgrade and development. In addition to the cost, factors, such as environmental parameters (i.e., emission), reliability, legal and regulatory policies, and socioeconomic impacts, have to be carefully considered since all these factors impose an indirect cost to either the energy provider or the society. Within the past several years, security and physical resilience have also been playing a significant role in expansion planning along with the abovementioned factors [1, 2]. Through the 1980s, sizable power outages within the modern grid were rare, averaging fewer than five on an annual basis. According to a recent report released in 2018 by Eaton, 3526 sizable power outages were reported in the USA, which are largely due to the outdated infrastructure and grid consolidation. This has led to situations in which one small incident is capable of cutting energy to millions of customers. To ensure that energy flow remains constant to a given area, it is necessary to develop sophisticated models and analytical procedures in the expansion/upgrade planning of energy infrastructure. In the past, companies were responsible for future planning only within their fields independently. To put it differently, traditional expansion planning has been mostly in the form of when, where, and what capacity of new resources are needed over future time horizons concerning one type of network, e.g., electric power

F. Mohammadi (✉)

Department of Electrical and Computer Engineering, University of Windsor, Windsor, ON, Canada

e-mail: fazel@uwindsor.ca; fazel.mohammadi@ieee.org

system or natural gas. The integration of electricity, natural gas, and heat sectors has increased significantly in the past decade due to combined cycle thermal power plants. With the increased penetration of gas power plants, coordinated expansion of electricity, natural gas, and heat infrastructure becomes important. In 2019, more than 38% of the total electricity generated in power plants in the USA was from natural gas while the share of coal, nuclear, and renewable was 23%, 20%, and 17%, respectively [3]. In addition, petroleum's share in the electricity generation was less than 2% in 2019. According to a recent report released by the U.S. Energy Information Administration (EIA), natural gas-based combined heat and power (CHP) capacity is expected to experience an annual growth rate of 5% by 2050 [3].

Therefore, electric power generation is becoming highly dependent on the gas network due to the importance of fuel adequacy for gas-fired power generation units. In multi-energy systems, the interconnection among resources should be considered. The optimum investment for multi-energy systems is studied in the literature while considering the demand and constraints at the design stage [4, 5–10]. Additionally, metrics, such as energy efficiency, security, reliability, and emission, are taken into account. A strategic energy plan considering interdependencies among different energy sectors represents a road map for meeting the energy demand while access to affordable and reliable energy is ensured with a minimum cost. Therefore, a clear future planning can potentially contribute to economic development at local and national levels by reducing the uncertainties and making the economic environment more predictable.

In this chapter, a detailed study of integrating electricity, natural gas, and heat systems, in which the main objective is their network expansion together, is provided. This chapter is organized as follows. General information about multi-carrier energy systems is provided in Sect. 13.2. In Sect. 13.3, the formulation of NEP of multi-carrier energy systems is described. The solution method to solve the NEP problem of multi-carrier energy systems is given in Sect. 13.4. Lastly, a brief summary of this chapter is given in Sect. 13.5.

13.2 Multi-carrier Energy Systems

A multi-carrier energy system has four main components including resources, demand, energy conversion, and energy storage. The energy conversion plays a major role in such systems. The primary energy can be converted to useable fuel, heat/cold, or electricity. Each of the secondary forms of energy can also be converted to each other at the distribution level: for instance, fuel to electricity, power to gas (P2G), electricity to heat/cold, and/or fuel to electricity and heat. The main object of multi-carrier energy systems is to optimally convert, store, and distribute different forms of energy to meet the demand in any time frame.

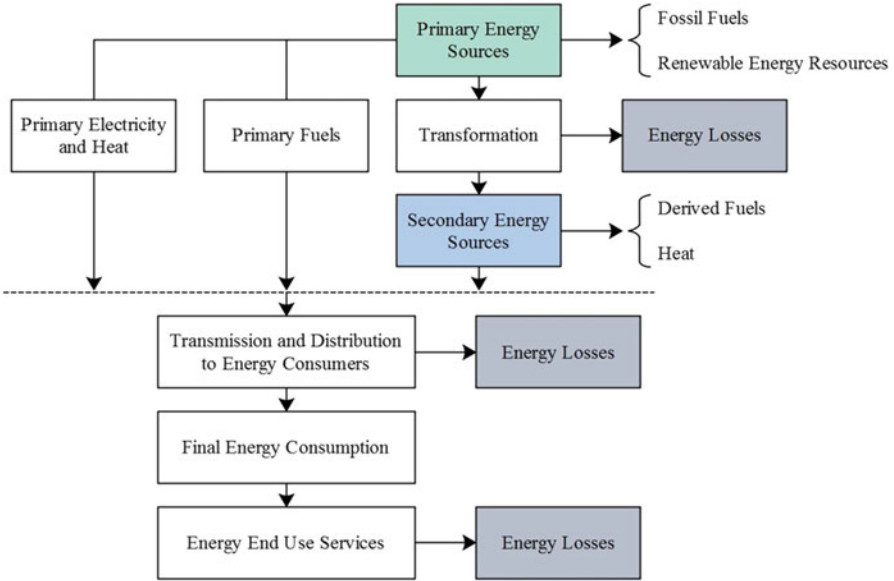


Fig. 13.1 Schematic demonstration of the energy chain from primary energy to energy services

Figure 13.1 shows the schematic of a multi-carrier energy system with two layers discussed above. The gas-fired power plants highly contribute to the interdependencies between two secondary forms of energy, i.e., electricity and natural gas. The gas network is similar to the electric power grids from different perspectives. The natural gas is transported from wellheads to commercial and industrial consumers including power plants through compressors, pipelines, and valves, where the energy conversion is made. Also, the gas can be stored in pipelines, underground, or wells. Using combined heat and power (CHP) systems leads to achieving higher efficiency when the heat and electricity are provided from one single source of fuel (mainly natural gas; however, it can work with a variety of fuels). Furthermore, CHP systems can potentially mitigate negative environmental impacts in urban areas. A generic model of a multi-carrier energy system is illustrated in Fig. 13.2. The CHP unit provides heat and electricity, simultaneously. In addition, the interaction between the electrical and thermal storage systems can be bidirectional. The main benefit of multi-carrier energy systems over traditional energy systems is that the demand can be supplied through multiple carriers leading to a reduced cost of operation. For instance, an electrical load can be supplied by either the electric power grids or the CHP unit.

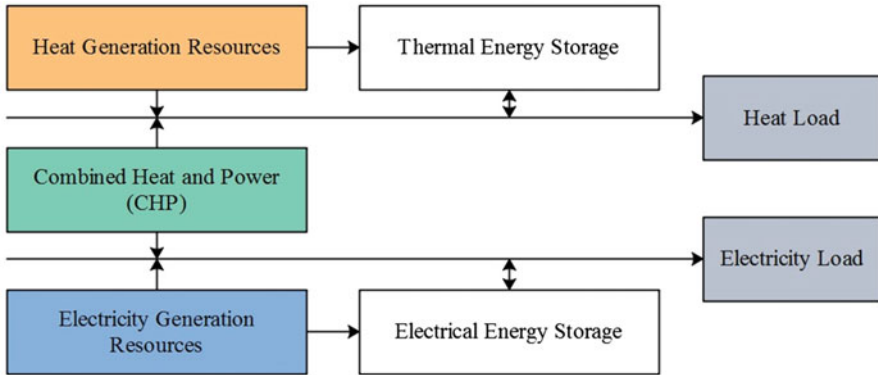


Fig. 13.2 A generic model of the multi-carrier energy systems

13.3 Formulation of Network Expansion Planning of Multi-carrier Energy Systems

For multi-carrier energy systems, NEP is a process, in which the network (transmission lines, cables, pipes, etc.) specifications can properly be determined. As a matter of fact, the network is an infrastructure for transmitting energy in an efficient and reliable manner from generation units (determined in the generation expansion planning phase) to consumers (determined from the load forecasting) via compressor stations and substations, in such a way that (1) consumers' energy demand can be adequately supplied both during normal and contingency conditions, and (2) the minimum costs are incurred.

Hence, NEP for multi-carrier energy systems can be treated as an optimization problem, in which the allocation (both sending and receiving ends), type of new transmission/transportation components, and their required availability times are determined.

Generally, in NEP for multi-carrier energy systems, the main problem is to specify the transmission/transportation paths between compressor stations and substations (both existing and new) and their characteristics. Therefore, the investments as well as operational costs should be minimized while various constraints during normal and contingency conditions are met.

In the simplest form, in NEP for multi-carrier energy systems, the investment costs are mainly due to adding new transmission/transportation paths while the operational costs are related to the costs of energy losses during an element life. In addition, limiting the transfer capability of an element is a major constraint in NEP. An outage of a single element is defined as a contingency and studying the single element outage is referred to as $N - 1$ contingency analysis. Technically, contingency analysis helps to plan the system while considering the outage of every single element and at the same time supplying sufficient energy to the customers when no violation occurs.

13.3.1 Objective Functions

As stated before, the main aim of studying NEP for multi-carrier energy systems is to determine the transmission/transportation paths between compressor stations and substations, both existing and new, as well as their characteristics. For multi-carrier energy systems, the objective functions and constraints are related to the electric power, gas, heat systems, and energy hubs as well as energy purchase costs.

13.3.1.1 Network Expansion Planning: Electric Power Systems

The main aim in the NEP of electric power systems is to minimize the total cost (C_T^E), which is the combination of investment cost (C_{inv}^E), operation cost (C_{op}^E), and repair and maintenance cost (C_{RM}^E), as shown below [11]:

$$C_T^E = \underbrace{C_{N-L} + C_{E-S} + C_{C-S} + C_{U-S} + C_{S-S} + C_{S-L}}_{C_{inv}^E} + \underbrace{C_L}_{C_{op}^E} + C_{RM}^E \quad (13.1)$$

where each of the abovementioned terms is defined as follows:

1. C_{N-L} is the investment cost related to establishing new power transmission lines and is formulated as below:

$$C_{N-L} = \sum_{i \in L_c} C_L(x_i) L_i \quad (13.2)$$

where L_c is the set of candidates, L_i shows the transmission line length of i^{th} candidate, x_i specifies the transmission line type of i^{th} candidate (in terms of voltage level, number of bundles and circuits, etc.), and $C_L(x_i)$ is the investment cost per length for type x_i .

2. C_{E-S} is the investment cost related to the expansion of existing substations so that the operational limits are not violated. This term is formulated as follows:

$$C_{E-S} = \sum_{j \in L_t} C_T(y_j) \quad (13.3)$$

where L_t is the set of transformer candidates, y_j indicates the transformer type of j^{th} candidate (according to the utilities' practices), and $C_T(y_j)$ is the investment cost for type y_j .

3. C_{C-S} is the investment cost related to upgrading a new substation to a higher voltage. This term is formulated as follows:

$$C_{C-S} = \sum_{k \in N_c} C_S(P_{L_k}) \quad (13.4)$$

where N_c is the set of newly upgraded substations and $C_S(P_{L_k})$ is the investment cost for carrying loading P_{L_k} .

4. C_{U-S} is the investment cost related to upgrading an existing substation to a higher voltage while both technical and economic aspects are considered. This term is formulated as below:

$$C_{U-S} = \sum_{l \in N_s} C_U(TP_l) \quad (13.5)$$

where N_s is the set of multi-voltage substations, including existing and new ones; TP_l is the power transmitted through substation l ; and $C_U(TP_l)$ is the investment cost for upgrading substation carrying power loading TP_l .

5. C_{S-S} is the investment cost related to switching substations while no local load is supplied. This term is formulated as follows:

$$C_{S-S} = \sum_{k \in N_w} \left(C_{sw_n}^f + C_{sw}^t(TP_n) \right) \quad (13.6)$$

where N_w is the set of switching substations and normally is selected from the available candidates, $C_{sw_n}^f$ is the cost of n^{th} substation without considering the voltage transformation, and C_{sw}^t is the cost of transformers based on the carrying loading (TP_n) on the substation. It is worth mentioning that $C_{sw_n}^f$ is based on the costs of land, protection devices, etc., in which the voltage is the main factor to determine $C_{sw_n}^f$.

6. C_{S-L} is the investment cost related to splitting a nearby transmission line as input/output to that specific substation. This term is formulated as follows:

$$C_{S-L} = \sum_{k \in N_{sp}} C_{sp_m} \quad (13.7)$$

where N_{sp} is the set of splitting options chosen from the available candidates, and C_{sp_m} is the cost of such splitting (m).

7. C_L is the cost related to active power losses. This term is a function of losses associated with new transformers, new transmission lines, and existing transformers and transmission lines. This term is formulated as follows:

$$C_L = CP_{\text{loss}} \left(\sum_{k \in L_t} R_t(y_j) \left(\frac{P_j}{\cos \varphi} \right)^2 + \sum_{k \in L_e} R_l(x_i) L_i \left(\frac{P_i}{\cos \varphi} \right)^2 + \sum_{k \in L_e} R_k \left(\frac{P_k}{\cos \varphi} \right)^2 \right) \quad (13.8)$$

where CP_{loss} is the cost of per unit losses; $R_t(y_j)$ is the resistance of transformer type y located in position j ; $R_l(x_i)$ is the per unit length resistance of the transmission line type x in position i ; R_k is the resistance of existing transformer and/or transmission line k ; P_j , P_i , and P_k indicate the active power flow of a new transformer j , active power flow of a new transmission line i , and active power flow of an existing transformer and/or transmission line k , respectively; L_e is the set of existing transformers and transmission lines; and $\cos \varphi$ is the average power factor.

In this chapter, C_{RM}^E for power transmission lines is neglected due to the fact that in long-term power system planning, the repair and maintenance cost does not need to be considered.

13.3.1.2 Network Expansion Planning: Gas Systems

The main aim in the NEP of gas systems is to minimize the total cost (C_T^G), which is the combination of investment cost (C_{inv}^G), operation cost (C_{op}^G), and repair and maintenance cost (C_{RM}^G) related to gas networks, including pipelines, compressors, and gas storage units, as shown below [12]:

$$C_T^G = \underbrace{C_p^{\text{inv}} + C_c^{\text{inv}} + C_{gs}^{\text{inv}}}_{C_{\text{inv}}^G} + C_{\text{op}}^G + \underbrace{C_p^{\text{RM}} + C_c^{\text{RM}} + C_{gs}^{\text{RM}}}_{C_{\text{RM}}^G} \quad (13.9)$$

where each of the abovementioned terms is defined as follows:

1. C_p^{inv} is the investment cost related to installing pipelines. This term is formulated as below:

$$C_p^G = \sum_{ij \in \Omega_p} \sum_{k \in K_p} C_{p_k}^{\text{inv}} l_{p_{ij}} x_{p_{ij,k}} \quad (13.10)$$

where Ω_p is the set of candidate branches for adding pipelines, K_p is the set of alternative types of adding pipelines, $C_{p_k}^{\text{inv}}$ indicates the investment cost coefficient of k^{th} pipeline, $l_{p_{ij}}$ is the length of the pipeline between ij branch, and $x_{p_{ij,k}}$ is the binary investment variable for pipelines.

2. C_c^{inv} is the investment cost related to installing compressors. This term is formulated as below:

$$C_c^{\text{inv}} = \sum_{ij \in \Omega_c} \sum_{k \in K_c} C_{c_k}^{\text{inv}} x_{c_{ij,k}} \quad (13.11)$$

where Ω_c is the set of candidates for adding compressors, K_c is the set of alternative types of adding compressors, $C_{c_k}^{\text{inv}}$ indicates the investment cost coefficient of k^{th} compressor, and $x_{c_{ij,k}}$ is the binary investment variable for compressors.

3. C_{gs}^{inv} is the investment cost related to installing gas storage units. This term is formulated as below:

$$C_{gs}^{\text{inv}} = \sum_{j \in \Omega_{gs}} \sum_{k \in K_{gs}} C_{gs_k}^{\text{inv}} x_{gs_{j,k}} \quad (13.12)$$

where Ω_{gs} is the set of candidates for gas storage units, K_{gs} is the set of alternative types of adding gas storage units, $C_{gs_k}^{\text{inv}}$ indicates the investment cost coefficient of k^{th} gas storage unit, and $x_{gs_{j,k}}$ is the binary investment variable for gas storage units.

4. C_{op}^G is the operation cost of gas networks, which should be calculated at each time t stage under each scenario s . This term is formulated as below:

$$C_{op}^G = \sum_{j \in \Omega_{gs}} C_{ogs} \left(f_{j,t,s}^{\text{ig}} + f_{j,t,s}^{\text{og}} \right) \rho_{fp} \quad (13.13)$$

where C_{ogs} indicates the operation cost coefficient of gas storage units; $f_{j,t,s}^{\text{ig}}$ and $f_{j,t,s}^{\text{og}}$ are the gas flow into and out of gas storage units, respectively; and ρ_{fp} is the flow-power conversion coefficient.

5. C_p^{RM} is the repair and maintenance cost related to pipelines. This term is formulated as below:

$$C_p^{\text{RM}} = \sum_{ij \in \Omega_p} \sum_{k \in K_p} C_{p_k}^{\text{RM}} I_{p_{ij}} x_{p_{ij,k}} \quad (13.14)$$

where $C_{p_k}^{\text{RM}}$ indicates the repair and maintenance cost coefficient of k^{th} pipeline.

6. C_c^{RM} is the repair and maintenance cost related to compressors. This term is formulated as below:

$$C_c^{\text{RM}} = \sum_{ij \in \Omega_c} \sum_{k \in K_c} C_{c_k}^{\text{RM}} x_{c_{ij,k}} \quad (13.15)$$

where $C_{p_k}^{\text{RM}}$ shows the repair and maintenance cost coefficient of k^{th} compressor.

7. C_{gs}^{RM} is the repair and maintenance cost related to compressors. This term is formulated as below:

$$C_{gs}^{RM} = \sum_{j \in \Omega_{gs}} \sum_{k \in K_{gs}} C_{gs_k}^{RM} x_{gs_{j,k}}^{RM} \quad (13.16)$$

where $C_{p_k}^{RM}$ refers to the repair and maintenance cost coefficient of k^{th} gas storage unit.

13.3.1.3 Network Expansion Planning: Heat Systems

The main aim in the NEP of heat systems is to minimize the total cost (C_T^H), which is the combination of investment cost (C_{inv}^H), operation cost (C_{op}^H), and repair and maintenance (C_{RM}^H) as shown below [13]:

$$C_T^H = C_{inv}^H + C_{op}^H + C_{RM}^H \quad (13.17)$$

where each of the abovementioned terms is defined as follows:

1. C_{inv}^H is the investment cost related to installing pipelines for the heat systems. This term is formulated as below:

$$C_{inv}^H = \sum_{ij \in \Omega_p} \sum_{k \in K_p} C_{P_k}^{inv} D_{P_{ij}} L_{P_{ij}} x_{P_{ij,k}} + C_B^{inv} \quad (13.18)$$

where Ω_p is the set of candidate branches for adding pipelines, K_p is the set of alternative types of adding pipelines, $C_{P_k}^{inv}$ indicates the investment cost coefficient of k^{th} pipeline depending on the pipe diameter $D_{P_{ij}}$, $L_{P_{ij}}$ is the length of the pipeline between ij branch, $x_{P_{ij,k}}$ is the binary investment variable for pipelines, and C_B^{inv} is the investment cost of the boiler, which depends on its capacity.

2. C_{op}^H is the operation cost related to heat systems that is the summation of cost for generating the requested heat and cost for making the water continuously circulate in the piping networks. This term is formulated as below:

$$C_{op}^H = \sum_{u \in \Omega_S} \sum_{v \in \Omega_R} C_R Q_{u,v} + \sum_{u \in \Omega_S} C_E P_{P_u} \quad (13.19)$$

where Ω_S is the set of candidate sites, Ω_R is the set of candidate resources consumed by the boilers, C_R indicates the unit costs of the resources consumed by the boilers, $Q_{u,v}$ is the resource input in thermal power term for v^{th} resource and u^{th} site, C_E is the unit cost of electricity for making the water circulate in the piping network, and P_{P_u} is the pumping power consumed at the u^{th} site.

In this chapter, C_{RM}^H for heat systems is disregarded.

13.3.1.4 Energy Hub

For energy hubs, the total cost (C_T^{HUB}) is the combination of investment cost ($C_{\text{inv}}^{\text{HUB}}$), operation cost ($C_{\text{op}}^{\text{HUB}}$), and repair and maintenance cost ($C_{\text{RM}}^{\text{HUB}}$), as below [13]:

$$C_T^{\text{HUB}} = C_{\text{inv}}^{\text{HUB}} + C_{\text{op}}^{\text{HUB}} + C_{\text{RM}}^{\text{HUB}} \quad (13.20)$$

where each of the abovementioned terms is defined as follows:

1. $C_{\text{inv}}^{\text{HUB}}$ is the investment cost related to installing energy hubs. This term is formulated as below:

$$C_{\text{inv}}^{\text{HUB}} = \sum_{j \in \Omega_{\text{HUB}}} \sum_{k \in K_{\text{HUB}}} C_{\text{HUB}_k}^{\text{inv}} x_{\text{HUB}_{jk}} \quad (13.21)$$

where Ω_{HUB} is the set of candidate nodes for energy hubs, K_{HUB} is the set of existing nodes connected to energy hubs, $C_{\text{HUB}_k}^{\text{inv}}$ indicates the investment cost coefficient of k^{th} energy hub, and $x_{\text{HUB}_{jk}}$ is the binary investment variable for energy hubs.

2. $C_{\text{op}}^{\text{HUB}}$ is the operation cost related to energy hubs. This term is formulated as below:

$$C_{\text{op}}^{\text{HUB}} = \sum_{j \in K_{\text{HUB}}} \left(C_{o_{\text{P2G}}} p_{j,t,s}^{\text{P2G}} + C_{o_{\text{CHP}}} f_{j,t,s}^{\text{CHP}} \rho_{fp} + C_{o_{\text{GF}}} f_{j,t,s}^{\text{GF}} \rho_{fp} \right) + \sum_{j \in K_{\text{HS}}} C_{o_{\text{HS}}} \left(p_{j,t,s}^{\text{ip}} + p_{j,t,s}^{\text{op}} \right) \quad (13.22)$$

where K_{HS} is the set of candidate nodes for heat systems; $C_{o_{\text{P2G}}}$, $C_{o_{\text{CHP}}}$, $C_{o_{\text{GF}}}$, and $C_{o_{\text{HS}}}$ are the operation cost coefficients P2G, CHP, gas furnace, and heat system, respectively; $p_{j,t,s}^{\text{P2G}}$, $p_{j,t,s}^{\text{ip}}$, and $p_{j,t,s}^{\text{op}}$ are the power flow into P2G from power grids and power flow into and out of thermal storage units, respectively; and $f_{j,t,s}^{\text{CHP}}$ and $f_{j,t,s}^{\text{GF}}$ are the flow into j^{th} CHP and gas furnace at time stage t of scenario s .

3. $C_{\text{HUB}}^{\text{RM}}$ is the repair and maintenance cost related to energy hubs. This term is formulated as below:

$$C_{\text{HUB}}^{\text{RM}} = \sum_{j \in \Omega_{\text{HUB}}} \sum_{k \in K_{\text{HUB}}} C_{\text{HUB}_k}^{\text{RM}} x_{\text{HUB}_k}^{j,k} \quad (13.23)$$

where $C_{\text{HUB}_k}^{\text{RM}}$ refers to the repair and maintenance cost coefficient of k^{th} energy hub.

13.3.1.5 Energy Purchase Cost

The energy purchase cost (C_{EP}) including electricity, gas, and heat purchase for t time stage in s scenario is as follows (N_T is the total number of time stages in a scenario):

$$C_{\text{EP}} = \sum_{t \in N_T} C_{s,t}^E + C_{s,t}^G + C_{s,t}^H \quad (13.24)$$

where each of the abovementioned terms is defined as follows:

1. $C_{s,t}^E$ is the cost of electricity purchased at time stage t of scenario s . This term is formulated as below:

$$C_{s,t}^E = c_{s,t}^E p_{s,t}^E \Delta t \quad (13.25)$$

where $c_{s,t}^E$ is the cost of electricity supply, $p_{s,t}^E$ is the total electricity supply power, and Δt shows the time duration at time stage t of scenario s .

2. $C_{s,t}^G$ is the cost of gas purchased at time stage t of scenario s . This term is formulated as below:

$$C_{s,t}^G = c_{s,t}^G p_{s,t}^G \Delta t \quad (13.26)$$

where $c_{s,t}^G$ is the cost of gas supply and $p_{s,t}^G$ is the total gas supply at time stage t of scenario s .

3. $C_{s,t}^H$ is the cost of heat purchased at time stage t of scenario s . This term is formulated as below:

$$C_{s,t}^H = c_{s,t}^H p_{s,t}^H \Delta t \quad (13.27)$$

where $c_{s,t}^H$ is the cost of heat supply and $p_{s,t}^H$ is the total heat supply at time stage t of scenario s .

13.3.2 Constraints

13.3.2.1 Electric Power Systems

Power Flow Equations

To simplify analysis, for large-scale power systems, one of the reasonable practices is to use DC power flow equations [14, 15]. In addition, power system planners avoid any concern regarding voltage problems and possible convergence issues [16]. However, in the final planning stage, it is necessary to perform AC power flow to achieve an acceptable voltage profile during normal and contingency conditions [17].

The general DC power flow equation for normal condition is as follows [11]:

$$\sum_{j=1}^N B_{ij}(\theta_i - \theta_j) = P_{G_i} - P_{D_i}, \quad \forall i \in n \quad (13.28)$$

where θ_i and θ_j are the voltage-phase angles of bus i and bus j , respectively; B_{ij} is the susceptance of element ij ; P_{G_i} and P_{D_i} are the power generation and demand at bus i , respectively; n indicates the set of system buses; and N denotes the total number of system buses.

Under the contingency condition that is shown by index c , Eq. (13.28) can be written as follows:

$$\sum_{j=1}^N B_{ij}^c(\theta_i^c - \theta_j^c) = P_{G_i}^c - P_{D_i}^c, \quad \forall i \in n \cap m \in C \quad (13.29)$$

where C is the rest of contingencies and m denotes the contingency parameters and variables.

Power Transmission Limits

For the transmission lines and transformers, power transfer should not violate its limits during normal and contingency conditions. Therefore:

$$B_k(\theta_i - \theta_j) \leq \bar{P}_k^N, \quad \forall k \in (L_c + L_t + L_e) \quad (13.30)$$

$$B_k^c(\theta_i^c - \theta_j^c) \leq \bar{P}_k^c, \quad \forall k \in (L_c + L_t + L_e) \cap m \quad (13.31)$$

where \bar{P}_k^N and \bar{P}_k^c are the ratings of k^{th} element during normal and contingency conditions, respectively.

Substation Limits

All existing and new substations have some technical limitations in terms of the number of possible input/output transmission lines and feeders. As a result

$$\sum_{i \in L_c} M_i^j \leq \bar{M}^j, \quad \forall j \in n \quad (13.32)$$

where \bar{M}^j indicates the maximum limit of the number of connecting transmission lines to j^{th} bus, and M_i^j is a binary index to show that there is a connection between transmission lines i and j . If the two buses are not connected to each other, $M_i^j = 0$.

Islanding Conditions

In NEP, no island should appear during normal and contingency conditions. Hence,

$$N_{\text{island}} = 0 \quad (13.33)$$

where N_{island} indicates the number of islands.

13.3.2.2 Gas Systems

The following constraints are related to the expansion of gas systems [12].

Investment and Utilization

The following investment and utilization constraints are related to the expansion of gas networks:

$$\sum_i \sum_{k \in K_p} x_{p_{ij,k}} \leq \bar{X}^p, \quad \forall j \in \Omega_G, i \in ij \in \Omega_p \quad (13.34)$$

where \bar{X}^p is a binary index to show that there is a connection between nodes i and j for k^{th} pipeline. If there is no connection between two nodes, $\bar{X}^p = 0$. Ω_G is a set of newly added gas nodes:

$$\sum_{k \in K_c} x_{c_{ij,k}} \leq \bar{X}^c, \quad \forall ij \in \Omega_c \quad (13.35)$$

where \bar{X}^c is a binary index related to compressors and it can be either 0 or 1:

$$\sum_{k \in K_{gs}} x_{gs\ jk} \leq \bar{X}^{gs}, \quad \forall j \in \Omega_{gs} \quad (13.36)$$

where \bar{X}^{gs} is a binary index related to compressors and the same as \bar{X}^c , it can be either 0 or 1.

Gas Supply Limits

$$0 \leq f_{j,t,s}^S \leq \bar{F}_j^S, \quad \forall j \in \Omega_{GS}, \forall t, \forall s \quad (13.37)$$

where $f_{j,t,s}^S$ is the gas supplied by the gas source node j at time stage t of scenario s , \bar{F}_j^S is the maximum flow limit for gas source node j , and Ω_{GS} is the set of existing source nodes in the gas network.

Pressure Limits

$$\underline{\pi}_j \leq \pi_{j,t,s} \leq \bar{\pi}_j, \quad \forall j \in \Omega_G, \forall t, \forall s \quad (13.38)$$

where $\pi_{j,t,s}$ is the nodal pressure at time stage t of scenario s , and $\underline{\pi}_j$ and $\bar{\pi}_j$ are the minimum and maximum pressure limits, respectively.

Gas Flow Limits

The gas flow balance can be written as follows:

$$\sum_{jk \in JK_{(j)}} f_{jk,t,s} = \sum_{ij \in IJ_{(j)}} f_{ij,t,s} - \underbrace{f_{j,t,s}^L}_{\alpha_{j,t,s}^{*LG} P_{j,t,s}^{LG}} + f_{j,t,s}^S + f_{j,t,s}^{ig} - f_{j,t,s}^{og} \quad (13.39)$$

where $f_{jk,t,s}$ and $f_{ij,t,s}$ are the gas flow through pipeline jk and ij at time stage t of scenario s , respectively; $f_{j,t,s}^L$ indicates the gas load computed by multiplying the gas load rate ($\alpha_{j,t,s}^{*LG}$) by the maximum gas demand of node j ($P_{j,t,s}^{LG}$) at time stage t of scenario s ; and $JK_{(j)}$ and $IJ_{(j)}$ denote the set of feeders whose parent/child is j .

In addition, the Weymouth steady-state gas flow constraints are formulated as follows [18]:

$$\text{sgn}\left(\pi_{i,t,s}^2 - \pi_{j,t,s}^2\right) f_{ij,t,s}^2 = \gamma_{ij}\left(\pi_{i,t,s}^2 - \pi_{j,t,s}^2\right), \quad \forall ij \in \Omega_p, \forall t, \forall s \quad (13.40)$$

$$\text{sgn}\left(\pi_{i,t,s}^2 - \pi_{j,t,s}^2\right) f_{ij,t,s}^2 = \gamma_{ij}\left(\pi_{i,t,s}^2 - \pi_{j,t,s}^2\right) \sum_{k \in K_p} x_{p_{ij,k}}, \quad \forall ij \in \Omega_p, \forall t, \forall s \quad (13.41)$$

If no pipeline is added, the term $\sum_{k \in K_p} x_{p_{ij,k}} = 0$.

To guarantee that a compressor can be added in the pipelines, $\forall ij \in \Omega_c, \forall t, \forall s$, the following constraints should be considered:

$$\begin{cases} \gamma_{ij}\left(\pi_{i,t,s}^2 - \pi_{j,t,s}^2\right) \leq \text{sgn}\left(\pi_{i,t,s}^2 - \pi_{j,t,s}^2\right) f_{ij,t,s}^2 + M \sum_{k \in K_c} x_{c_{ij,k}} \\ \gamma_{ij}\left(\pi_{i,t,s}^2 - \pi_{j,t,s}^2\right) \geq \text{sgn}\left(\pi_{i,t,s}^2 - \pi_{j,t,s}^2\right) f_{ij,t,s}^2 - M \sum_{k \in K_c} x_{c_{ij,k}} \end{cases} \quad (13.42)$$

where γ_{ij} is the transmission coefficient through pipeline ij , and M is the penalty factor.

Equation (13.42) shows that compressors can be added in pipelines that have been built previously. If no compressor is added, Eqs. (13.42) and (13.41) can be equivalent.

Pipeline Operation Limits

For all existing pipelines, the operation limits are as follows:

$$-\bar{F}_{ij}^p \leq f_{ij,t,s} \leq \bar{F}_{ij}^p, \quad \forall ij \in \Omega_p, \forall t, \forall s \quad (13.43)$$

where \bar{F}_{ij}^p is the maximum gas flow through pipeline ij .

For the newly added or candidate pipelines for compressors, the gas flow depends on the maximum flow limits and the investment decision, as follows:

$$-\sum_{k \in K_p} \bar{F}_{p_{ij,k}} x_{p_{ij,k}} \leq f_{ij,t,s} \leq \sum_{k \in K_p} \bar{F}_{p_{ij,k}} x_{p_{ij,k}}, \quad \forall ij \in \Omega_p, \forall t, \forall s \quad (13.44)$$

$$-\bar{F}_{p_{ij,k}} - M \sum_{k \in K_c} x_{c_{ij,k}} \leq f_{ij,t,s} \leq \bar{F}_{p_{ij,k}} + M \sum_{k \in K_c} x_{c_{ij,k}}, \quad \forall ij \in \Omega_c, \forall t, \forall s \quad (13.45)$$

Compressor Operation Limits

For all existing compressors, the operation limits at time stage t of scenario s are as follows:

$$\pi_{j,t,s} = \beta_{ij}^c \pi_{i,t,s} \quad (13.46)$$

$$-\bar{F}_{ij}^c \leq f_{ij,t,s} \leq \bar{F}_{ij}^c \quad (13.47)$$

where β_{ij}^c is a coefficient of the existing compressor, and \bar{F}_{ij}^c denotes maximum flow limit of the compressors.

In addition, for all newly added compressors at time stage t of scenario s , the following constraints should be met:

$$\beta_{ij,k}^c \pi_{i,t,s} - M(1 - x_{cij,k}) \leq \pi_{j,t,s} \leq \beta_{ij,k}^c \pi_{i,t,s} + M(1 - x_{cij,k}) \quad (13.48)$$

$$-\bar{F}_{ij,k}^c - M(1 - x_{cij,k}) \leq f_{ij,t,s} \leq \bar{F}_{ij,k}^c + M(1 - x_{cij,k}) \quad (13.49)$$

The operation limits of the potential compressors to be installed depend on Eqs. (13.48) and (13.49), and are associated with $x_{cij,k}$.

Gas Storage Unit Operation Limits

The operation limits of the gas storage unit at time stage t of scenario s are as follows:

$$\begin{cases} u_{j,t,s}^{sg} + u_{j,t,s}^{rg} \leq 1, \quad \forall t \\ u_{j,t,s}^{rg} = 0 \end{cases} \quad (13.50)$$

$$\begin{cases} 0 \leq f_{j,t,s}^{ig} \leq \sum_{k \in K_{gs}} \bar{F}_k^{gs} x_{gs,jk} u_{j,t,s}^{sg} \\ 0 \leq f_{j,t,s}^{og} \leq \sum_{k \in K_{gs}} \bar{F}_k^{gs} x_{gs,jk} u_{j,t,s}^{rg} \end{cases}, \forall t \quad (13.51)$$

$$S_{j,t,s}^{gs} = \begin{cases} 0 + f_{j,t,s}^{ig} \eta^{ig} \Delta t - \frac{f_{j,t,s}^{og}}{\eta^{og}} \Delta t, & t = 1 \\ S_{j,t-1,s}^{gs} + f_{j,t,s}^{ig} \eta^{ig} \Delta t - \frac{f_{j,t,s}^{og}}{\eta^{og}} \Delta t, & t \geq 2 \end{cases} \quad (13.52)$$

$$0 \leq S_{j,t,s}^{gs} \leq \sum_{k \in K_{gs}} \bar{S}_k^{gs} x_{gs,jk}, \forall t \quad (13.53)$$

where $u_{j,t,s}^{sg}$ and $u_{j,t,s}^{rg}$ are the operation state of storage/release gas for gas storage units, respectively; $S_{j,t,s}^{gs}$ indicates the storage capacity of gas storage units; η^{ig} and

η^{og} are the gas storage and release efficiencies of gas storage units, respectively; and \bar{S}_k^{gs} shows the maximum storage capacity of gas storage unit k .

Equation (13.50) shows that for each gas storage unit, gas storage and release cannot be done at the same time and for the first stage ($t = 1$), it is not allowed to release gas. Equation (13.51) shows that for each gas storage unit, gas storage or release can be done when both $\sum_{k \in K_{gs}} x_{gs\ j,k} = 1$ and $u_{j,t,s}^{rg} = 1$ are satisfied. $S_{j,t,s}^{gs}$ in Eq. (13.52) is associated with the capacity in the former time stage ($S_{j,t-1,s}^{gs}$), flow of gas storage/release in the current time stage ($f_{j,t,s}^{ig}$) and ($f_{j,t,s}^{og}$), gas storage and release efficiencies (η^{ig}) and (η^{og}), and time duration (Δt). Equation (13.53) indicates that for each gas storage unit, its initial capacity ($S_{j,0,s}^{gs}$) should be equal to zero.

13.3.2.3 Heat Systems

The following constraints are related to the expansion of heat systems [13].

Pipeline Constraints

One of the major limitations of heat systems is that pipes can be built in only one direction. As a result, the predefined pipeline layout and one diameter should be considered for each segment [19]. Accordingly,

$$E_{p_{i,j,d}} + E_{p_{j,i,d}} \leq 1 \quad (13.54)$$

$$E_{p_{i,j,d}} \leq d_{i,j} \quad (13.55)$$

$$\sum E_{p_{i,j,d}} \leq 1 \quad (13.56)$$

where $E_{p_{i,j,d}}$ and $E_{p_{j,i,d}}$ denote that pipes of diameter d exist between nodes i and j and vice versa, respectively, and $d_{i,j}$ denotes the diameter of the pipeline between nodes i and j .

Hydraulic Constraints

Three major parameters in heat systems, i.e., flow velocity, heat flow, and allowable pressure drop in the pipelines, strictly depend on the diameter of the pipeline [19]. As a result,

$$Q_{fv_{i,j}} \leq \bar{v}_d + M(1 - E_{p_{i,j,d}}), \forall (i,j), d \quad (13.57)$$

$$4Q_{f_{ij}} \leq \rho_w CP_w Q_{f_{i,j}} \bar{\Delta}t \pi d_d^2 + M(1 - E_{p_{i,j,d}}) \quad (13.58)$$

$$KL_d Q_{f_{i,j}} \leq \bar{\Delta}P_d + M(1 - E_{p_{i,j,d}}) \quad (13.59)$$

where $Q_{f_{i,j}}$ is the water flow velocity between nodes i and j ; \bar{v}_d is the maximum allowable water velocity in a pipe; M has the same definition as before; d_d is the pipe diameter; $Q_{f_{i,j}}$ denotes the heat flow between nodes i and j ; ρ_w and CP_w are the water density at a certain temperature and specific capacity of water, respectively; $\bar{\Delta}t$ is the maximum difference supply-return temperature; KL_d shows the linear coefficient related to the velocity and pressure drop in the pipes; and $\bar{\Delta}P_d$ is the maximum allowable pressure drop in a pipe of diameter d .

Heat Flow Constraints

The heat flow at each node mainly depends on the heat losses and heat consumption at that specific node. In other words,

$$\sum_j (Q_{f_{ij}} - NHL_{ij}) = \sum_j Q_{f_{ji}} - HD_i \quad (13.60)$$

where NHL_{ij} is the network heat losses between nodes i and j , and HD_i denotes the peak demand at node i .

It should be noted that NHL_{ij} can be derived as follows:

$$NHL_{ij} = k\pi(T_{op} - T_{avg})(1 + \chi)d_{i,j} \times 10^{-6} \sum_d E_{p_{i,j,d}} d_d \quad (13.61)$$

where k is the average heat exchange coefficient; T_{op} and T_{avg} are the network operating and average external temperatures, respectively; and χ is the heat loss coefficient of the district heat network.

In addition, the overall pumping power ($P_{i,j,d}$) required to run the network can be calculated as follows:

$$P_{i,j,d} = \frac{\Delta p_{i,j,d} \pi d_d^2 Q_{f_{i,j}} d_{i,j}}{4\eta_p} \quad (13.62)$$

where $\Delta p_{i,j,d}$ is the pressure drop in a pipe between nodes i and j with diameter d , and η_p denotes the network pump efficiency.

13.3.2.4 Energy Hub

For all energy hub nodes, the sum of thermal power inputs and outputs should be equal. Considering the gas flow injecting into the gas furnace/CHP, the thermal power supplied by them can be calculated. It is evident that the gas flow over a particular range can be input into gas furnace/CHP. In addition, P2G and CHP systems in the energy hub should be used to convert the electric power into natural gas and vice versa. As a result, there is an upper power input limit for both P2G and CHP systems [11–13, 19]. The major constraint associated with the energy hubs is as follows:

$$P_H^{GF} + p_H^{CHP} = \underbrace{p_{j,t,s}^{HL}}_{\alpha_{j,t,s}^{*lh} P_{j,t,s}^{Lh}} + p_{j,t,s}^{ip} - p_{j,t,s}^{op} \quad (13.63)$$

where p_H^{GF} , p_H^{CHP} , and $p_{j,t,s}^{HL}$ are the thermal power of gas furnace, CHP, and load, respectively. $p_{j,t,s}^{HL}$ can be calculated by multiplying the maximum power of j^{th} load ($P_{j,t,s}^{Lh}$) by its corresponding rate ($\alpha_{j,t,s}^{*lh}$) at time stage t of scenario s .

Flow limit for gas furnaces is as follows:

$$0 \leq \underbrace{f_{j,t,s}^{GF}}_{\frac{p_H^{GF}}{\rho_H \eta_H^{GF}}} \leq \bar{F}^{GF} \quad (13.64)$$

where \bar{F}^{GF} is the maximum flow limit of gas furnace and η_H^{GF} is the energy conversion efficiency of gas furnace.

Flow limit for CHP units is as follows:

$$0 \leq \underbrace{f_{j,t,s}^{CHP}}_{\frac{p_H^{CHP}}{\rho_H \eta_H^{CHP}}} \leq \bar{F}^{CHP} \quad (13.65)$$

where \bar{F}^{CHP} is the maximum flow limit of CHP unit and η_H^{CHP} is the energy conversion efficiency of CHP unit.

Flow limit for P2G units is as follows:

$$0 \leq \underbrace{p_{j,t,s}^{P2G}}_{\frac{f_{j,t,s}^{P2G} \rho_H}{\eta_H^{P2G}}} \leq \bar{P}^{P2G} \quad (13.66)$$

where \bar{P}^{P2G} , $f_{j,t,s}^{P2G}$, and η^{P2G} are the maximum power input limit, gas output, and efficiency of P2G unit, respectively.

Similar to gas storage units and their operation constraints, shown in Eqs. (13.50)–(13.53), thermal storage units have the following operation limits:

$$\begin{cases} u_{j,t,s}^{sh} + u_{j,t,s}^{rh} \leq 1, \quad \forall t \\ u_{j,t,s}^{rh} = 0 \end{cases} \quad (13.67)$$

$$\begin{cases} 0 \leq p_{j,t,s}^{ip} \leq \sum_{k \in K_{TS}} \bar{P}_k^{TS} x_{ts,jk} u_{j,t,s}^{sh} \\ 0 \leq p_{j,t,s}^{op} \leq \sum_{k \in K_{TS}} \bar{P}_k^{TS} x_{ts,jk} u_{j,t,s}^{rh} \end{cases}, \quad \forall t \quad (13.68)$$

$$S_{j,t,s}^{TS} = \begin{cases} 0 + p_{j,t,s}^{ip} \eta^{sh} \Delta t - \frac{p_{j,t,s}^{op}}{\eta^{rh}} \Delta t, & t = 1 \\ S_{j,t-1,s}^{TS} + p_{j,t,s}^{ip} \eta^{sh} \Delta t - \frac{p_{j,t,s}^{op}}{\eta^{rh}} \Delta t, & t \geq 2 \end{cases} \quad (13.69)$$

$$0 \leq S_{j,t,s}^{TS} \leq \sum_{k \in K_{TS}} \bar{S}_k^{TS} x_{ts,jk}, \quad \forall t \quad (13.70)$$

where $u_{j,t,s}^{sh}$ and $u_{j,t,s}^{rh}$ are the operation state of storage/release heat for thermal storage units, respectively; K_{TS} is the set of alternative types of adding thermal storage units; \bar{P}_k^{TS} is the maximum power flow limit of adding thermal storage units; $x_{ts,jk}$ is the binary investment variable for thermal storage units; $S_{j,t,s}^{TS}$ indicates the storage capacity of thermal storage units; η^{sh} and η^{rh} are the thermal storage and release efficiencies of gas storage units, respectively; and \bar{S}_k^{TS} shows the maximum storage capacity of thermal storage unit k .

13.4 Solution Method

The objective functions presented in Eqs. (13.1), (13.9), (13.17), (13.20), and (13.24) and constraints presented in Eqs. (13.28)–(13.70) comprise a mixed-integer programming (MIP) multistage problem that minimizes the cost of the expansion plan of electric power, gas, and heat systems while satisfying multiple technical and nontechnical constraints. This problem can be solved using MATLAB and/or GAMS software. The solution method can be briefly explained as follows:

Stage 1: Calculating the cost of electric power network expansion using Eq. (13.1)

Stage 2: Calculating the cost of gas network expansion using Eq. (13.9)

Stage 3: Calculating the cost of heat network expansion using Eq. (13.17)

Stage 4: Calculating the cost of energy hub expansion using Eq. (13.20)

Stage 5: Calculating the energy purchase costs using Eq. (13.24)

Stage 6: Determining $\alpha \in [0, 1]$ ($\alpha = 0$: pessimistic decision and $\alpha = 1$: optimistic decision)

Stage 7: Calculating the attribute for most pessimistic scenario (*PS*) using von Neumann-Morgenstern criterion

Stage 8: Calculating the attribute for most optimistic scenario (*OS*) using von Neumann-Morgenstern criterion

Stage 9: Calculating the attribute of each plan using the Hurwicz criterion as follows (A_i denotes the i^{th} attribute):

$$A_i = \alpha PS + (1 - \alpha) OS$$

Stage 10: Prioritizing plans based on the calculated attributes

Stage 11: Selecting the plan with the best A

13.5 Summary

Traditional network expansion planning (NEP) uses independent problems to handle different sources of energy, including electricity, heat, natural gas, and oil. New approaches are developed to deal with the challenges of conventional planning that includes optimization and convergence of energy resources and demand in a shared sense to make the investment and operation as efficient as possible. This chapter is aimed at showing that the key priority for network expansion is a thorough analysis of the integration of electric power, gas, and heat systems. Mathematical models representing multistage optimization problems, along with main equations associated with multi-carrier energy systems, are described. The goal is to reduce all expansion costs of the network subject to technical and nontechnical constraints. Finally, solution methods for solving the multistage NEP of multi-carrier energy systems are discussed.

References

1. Thangavelu SR, Khambadkone AM, Karimi IA (2015) Long-term optimal energy mix planning towards high energy security and low GHG emission. *Appl Energy* 154:959–969
2. Awerbuch S (2006) Portfolio-based electricity generation planning: policy implications for renewables and energy security. *Mitig Adapt Strateg Glob Chang* 11:693–710
3. The British Petroleum Company plc. (2019) BP Annual Energy Outlook. <https://www.bp.com/content/dam/bp/business-sites/en/global/corporate/pdfs/energy-economics/energy-outlook/bp-energy-outlook-2019.pdf>.
4. Zhang X, Shahidehpour M, Alabdulwahab AS, Abusorrah A (2015) Security-constrained co-optimization planning of electricity and natural gas transportation infrastructures. *IEEE Trans Power Syst* 30(6):2984–2993

5. Peters GL (2012) Embedded Natural Gas-Fired Electric Power Generation Infrastructure Analysis: An Analysis of Daily Pipeline Capacity Availability, EnVision Energy Solutions. https://cdn.misoenergy.org/Natural%20Gas-Electric%20Infrastructure%20Interdependency%20Analysis_022212_Final%20Public271159.pdf.
6. Rubio-Barros R, Ojeda-Esteybar D, Añó O, Vargas A (2010) Combined operational planning of natural gas and electric power systems: state of the art. *Natural Gas*, Intech Open, Rijeka, pp 271–288
7. Rubio R, Ojeda-Esteybar D, Añó O, Vargas A (2008) Integrated natural gas and electricity market: a survey of the state of the art in operation planning and market issues, In Proceedings of the IEEE/PES Transmission and Distribution Conference and Exposition: Latin America, Bogota, Colombia, 1–8.
8. Chaudry M, Jenkins N, Qadrdan M, Wu J (2014) Combined gas and electricity network expansion planning. *Appl Energy* 113:1171–1187
9. Barati F, Seifi H, Sepasian MS, Nateghi A, Shafie-khah M, Catalão JPS (2015) Multi-period integrated framework of generation, transmission, and natural gas grid expansion planning for large-scale systems. *IEEE Trans Power Syst* 30(5):2527–2537
10. Qiu J, Dong ZY, Zhao JH, Meng K, Zheng Y, Hill DJ (2015) Low carbon oriented expansion planning of integrated gas and power systems. *IEEE Trans Power Syst* 30(2):1035–1046
11. Seifi H, Sepasian MS (2011) *Electric power system planning: issues, algorithms and solutions*, 1st edn. Springer-Verlag, Berlin Heidelberg, Berlin
12. Wang J, Hu Z, Xie S (2019) Expansion planning model of multi-energy system with the integration of active distribution network. *Appl Energy* 253:113517
13. Vesterlund M, Toffolo A (2017) Design optimization of a district heating network expansion, a case study for the town of Kiruna. *Appl Sci* 7(5):488
14. Mohammadi F, Nazri G-A, Saif M (2020) An improved mixed AC/DC power flow algorithm in hybrid AC/DC grids with MT-HVDC systems. *Appl Sci* 10(1):297
15. Mohammadi F, Nazri G-A, Saif M (2019) A bidirectional power charging control strategy for plug-in hybrid electric vehicles. *Sustainability* 11(16):4317
16. Mohammadi F, Zheng C (2018) Stability Analysis of Electric Power System, In Proceedings of the 4th National Conference on Technology in Electrical and Computer Engineering, Tehran, Iran, 1–8.
17. Shojaei AH, Ghadimi AA, Miveh MR, Mohammadi F, Jurado F (2020) Multi-objective optimal reactive power planning under load demand and wind power generation uncertainties using ϵ -constraint method. *Appl Sci* 10(8):2859
18. Wang C, Wei W, Wang J, Bi T (2019) Convex optimization based adjustable robust dispatch for integrated electric-gas systems considering gas delivery priority. *Appl Energy* 239:70–82
19. Delangle A, Lambert RSC, Shah N, Acha S, Markides CN (2017) Modelling and optimising the marginal expansion of an existing district heating network. *Energy* 140(1):209–223

Index

A

Absorption chillers, 215, 216
Acceleration technique, 166
Active microgrids (AMGs)
 bidding scenarios and power transactions, 238
 DRPs, 235
 electricity transactions, 236, 241, 242
 LMPs, 238
Active multi-carrier energy distribution system (AEDS), 121
Active power losses, 344, 345
Adaptive genetic algorithm (AGA), 239
Advanced adiabatic compressed air energy storage (AA-CAES), 147
AEDS operator (AEDSO), 124
Aggregated demand response (AGG DR), 31
Air reservoirs, 147
Algorithm-based BD, 167
Ambiguity, 260
Anaerobic reactors, 215
Analytical methods, probabilistic techniques
 analytical method's goal, 266
 on linearization, 265
 convolution method, 265
 cumulant method, 265
 FOSM, 265, 266
 methods, 265
 PDFs, 265
 Taylor series, 265
 PDF approximation-based methods
 (see Probability density functions (PDFs))
Ancillary services
 black start, 98, 99

 commercial, 98
 energy balance, 98
 fast reserve service, 102, 103
 frequency response, 100, 101
 imbalance market, 98
 MCEN, 104
 reactive power service, 101
Ant colony, 61
ARIMA model, 204
Artificial intelligence algorithms, 160

B

Balancing service use-of-system (BSUoS)
 charges, 106, 107
Batteries' depreciation cost, 200
Benders cut, 167
Benders decomposition, 160
 Benders cut, 164, 167
 constraints, 164
 flexible structure, 164
 hydraulic test system, 169–170
 master problem, 164–167
 in mathematical programming, 163
 optimality cut, 164
 SHGS problem
 convergence verification, 168
 initialization, 168
 master problem, 168, 169
 subproblem, 168
 thermal units, 168
 subproblems, 164, 165
 system counting, 169
Bilateral trading markets, 91
Bi-level optimization algorithm, 235

- Biomass energy, 6, 7
- Black start
 - service payments, 99
 - start-up supplies, 99
 - system recovery service, 99
 - technical requirements, 99
 - transmission system, 99
- C**
- Capacity market, 104, 105
- Carbon capture and sequestration (CCS)
 - technology, 13
- Carbon emission, 144
- Carrier-based demand response (CBDR), 273, 284, 301, 330
- CCHP-based EHs, 198, 199
- CEC scenarios (CECSs), 238
- CHP-based system planning, 236
- Classical probability theory, 270
- Climate change agreement (CCA), 108, 111
- Climate change levy (CCL), 107, 108, 111
- Coal/nuclear fuels, 159
- CO₂ emissions market, 111, 112
- Column and constraint generation
 - algorithm, 236
- Combination of power and heat systems (CHP), 61
- Combined cooling, heating and power (CCHP), 14
 - application, 209
 - CCHP-based MESs, 196
 - interval-based optimization model, 204, 205
 - stochastic optimization, 206
- Combined cycle plants (CC), 14
- Combined heat and power (CHP), 14
 - capacity, 340
 - characteristics, 241
 - negative environmental impacts, 341
 - power grids, 341
 - single source of fuel, 341
 - units, 236, 237
- Compressed air energy storage (CAES) unit
 - AA-CAES, 147
 - air reservoirs, 147
 - constant-pressure operation, 147
 - cooling/heating/power systems, 144
 - cycle and discharging modes, 148
 - electrical energy storage systems, 146
 - and energy conversion facilities, 144
 - and expansion processes, 147
 - high-pressure compressed air, 147
 - hourly optimal scheduling, 151, 152
 - inequalities, 147
 - LAES, 147
 - maintenance and operation costs, 146
 - operation mechanism, 147
 - risk-constrained strategy, 144
 - SC-CAES, 147
 - sliding-pressure operation, 147
 - small-scale, 147
- Computational efficiency, 166
- Conditional value-at-risk (CVaR) method, 23
- CONOPT-DNLP, 169
- CONOPT method, 169, 170
- Constant-pressure operation, 147
- Context uncertainty, 260
- Convergence verification, 168
- Convolution method, 265
- Cooling demand response program (CDRP), 331, 332
- CO₂ prices, 111, 112
- Cornish–Fisher expansion, 265
- Cost-saving, 1, 19, 24, 30
- Cost-saving characteristics
 - battery bank, 76
 - CHP, 61
 - cost of operation, 61
 - demand-side management, 62
 - dryers, 70
 - economic dispatch (ED), 60, 61
 - EH system, 60
 - electric vehicles, 61
 - electricity consumption, 59
 - energy carrier infrastructure, 60
 - energy exchange, 76
 - energy management, 59, 60, 62
 - energy optimization, 60
 - fuel cell system, 67, 68
 - fuel cell units, 75
 - intelligent structure, 60
 - IREMS, 62
 - lighting loads, 70–72
 - loads, 61
 - MGs, 59, 60, 62–64, 77
 - mixed-integer linear programming, 61
 - objective function
 - distribution grid, 74
 - energy exchange, 74
 - grid, 74
 - microgrid, 73
 - power balance, 74
 - optimal energy management, 62
 - optimal operation, 60
 - optimal performance, 60
 - power generation units, 59

- power grid, 59
 - renewable energy resources, 59
 - scenarios
 - household washing appliances, 78
 - lighting loads, 79
 - microgrid, 79, 81
 - simulation, 77, 78
 - smart grid infrastructure, 61
 - solar and wind units, 75
 - solar/wind resources, 62
 - storage systems, 68, 69
 - suppliers, 64
 - technical issues, 59
 - washing machines, 70
 - wind generation cost, 65, 66
 - wind production unit, 64, 65
 - CPLEX solver, 150
 - Cuckoo search algorithm, 160
 - Cumulant method, 265
 - Curtailed electrical load, 205
 - Customers' energy consumption (CEC), 238
 - α -Cut method, 271
 - Cutting plane methods, 166
- D**
- Dantzig-Wolfe decomposition, 160, 166
 - Day-ahead electricity, 150
 - Day-ahead market, 93, 94
 - Day-ahead scheduling, 179
 - Decision uncertainty, 261
 - Decomposition techniques, 160
 - Defuzzification, 271
 - Demand response programs (DRPs), 235, 328
 - AEDS energy interactions, 124
 - AEDSO, 124
 - CCHP-based systems, 122
 - conditional value-at-risk method, 122
 - cooling energy generations, 128, 132
 - DA horizon, 128, 131, 133, 135, 137
 - distribution system, 135
 - EHS, 122, 123, 125, 128, 131
 - electrical energy consumptions, 135
 - electrical system, 122
 - electricity generation, 123
 - electricity market price, 128, 130
 - energy consumption, 122
 - energy-generating units, 122
 - energy resources, 121
 - gas-fueled power plant, 123
 - heating energy generation, 133
 - heating loads, 123
 - information-gap decision theory, 123
 - linear optimization process, 122
 - multi-carrier energy system, 123
 - NUEHS, 130, 135
 - objective function, 125, 126
 - ODAOP problem, 122
 - 125-bus industrial district distribution system, 129
 - operating costs, 122
 - optimal scheduling, 125
 - optimization procedure, 123, 128
 - optimization process, 123
 - proposed algorithm, 127
 - PVA and SWT electricity generation, 131
 - risk mitigation method, 122
 - RT horizon, 128, 131–137
 - SEH, 121
 - solution algorithm, 126, 127
 - system resource problem, 126
 - 33-bus IEEE test system, 122
 - wind electricity generations, 122
 - Demand response solutions
 - AGG DR program, 31
 - ancillary services, 32
 - direct load control management, 31
 - EDRP, 31
 - energy system, 30
 - implementation, 30
 - incentive-based demand response programs, 32, 33
 - load reduction, 32
 - multi-carrier energy systems, 32
 - pricing system, 30
 - RTP, 31
 - time-based and incentive-based programs, 30
 - time-based demand response programs, 32
 - Deregulated energy systems, 160
 - Diesel market, 114, 115
 - Diesel price, 114–117
 - Differential evolution, 160
 - Distributed energy resources (DERs), 60, 121, 235, 236, 242, 245
 - Distributed generation (DG)
 - units, 209
 - facility, parameters, 241, 244
 - Distribution network operator (DNO), 105
 - Distribution network use-of-system (DNUoS)
 - charges, 106, 110, 118
 - Distribution system operators (DSO), 20
 - District energy system planning method, 235
 - District heating facility, 241, 242
 - District heating network, 143, 241, 242
 - District heat markets, 150
 - Dynamic programming, 160

E

- Economic analysis, 1
- Economic linear programming, 210
- Economics, 1
- Edgeworth expansion, 265
- Electric and heating energy subsystems, 236
- Electric distribution system, 122
- Electric heat pump (EHP), 89
- Electric power generation, 340
- Electric power system, NEP
 - active power losses, 344, 345
 - investment costs, 343, 344
 - islanding conditions, 351
 - multi-voltage substations, 344
 - operation cost, 343
 - power flow equations, 350
 - power transmission limits, 350
 - splitting, 344
 - substation limits, 351
 - total cost, 343
 - voltage transformation, 344
- Electric Reliability Council of Texas (ERCOT), 31
- Electric vehicles (EVs), 20
- Electrical demand response program (EDRP), 269, 331
- Electrical network device, 241, 243
- Electrical storage systems (ESSs), 237
- Electricity, 87, 90, 143, 341
- Electricity-gas networks
 - daily cost, 189, 190
 - day-ahead scheduling, 179
 - electricity loads, 185, 186
 - electricity system, 182–183
 - gas network, 183, 184
 - gas production of gas wells, 190, 192
 - gas storage, 187
 - gas transmission system, 185
 - gas wells, 185, 186
 - hourly generation of power unit, 190, 191
 - hourly scheduling, power units, 187, 188
 - interdependency, 179
 - load shedding, 185
 - node pressure, 186
 - objective function, 181
 - pipelines, 186
 - power lines, 185, 186
 - power units, 185
 - reliability, 179
 - residential gas loads, 185, 187
 - scheduling, 189
 - security-constrained scheduling, 179
 - stochastic scheduling, 180
 - test system, 184, 185
 - wind spillage, 185
 - with wind uncertainty, 180
- Electricity generation, 340
 - solar photovoltaic, 241, 245
 - wind turbine, 241, 245
- Electricity grid, 183
- Electricity markets, 211, 238
 - amount, electricity, 90
 - ancillary services (*see* Ancillary services)
 - bilateral trading, 91
 - capacity market, 104, 105
 - contracts, 87
 - day-ahead market, 93, 94
 - distribution networks, 104
 - EHP, 89
 - electricity pools, 91, 92
 - electricity production, 90
 - energy balance, 90
 - hybrid model, 92
 - imbalance market (*see* Imbalance market)
 - local balancing services, 105
 - MCENs, 88, 90
 - obligations
 - environmental, 107, 108
 - social, 107, 108
 - taxes, 107
 - UoS charges, 105, 106
 - violators, 90
 - wholesale trading market, 90
- Electricity pools, 91, 92
- Electricity price, 275
- Electricity system, 182–183
- Electricity unit, 198
- Electrolyzer, 215
- Electrothermal equipment, 89, 90
- Emergency demand response program (EDRP), 31
- Energy balance condition, 161
- Energy balance constraints, 202
- Energy company obligation (ECO), 108, 111
- Energy conversion devices, 213
- Energy efficiency market, 112–114
- Energy flow analysis, 144
- Energy hubs (EHs)
 - absorption chiller, 215
 - advantage, 209
 - agricultural EHs, 331
 - amount of consumed gas, 230, 231
 - anaerobic reactors, 215
 - annual wind speed in Ganje site, 221, 224
 - benefits, 328
 - carriers, 212

- characterization, 195
- components, 213
- concept, 212
- configuration, 203
- constraints, 357
 - energy balance, 202
 - energy storage unit, 201
 - heating unit, 202
 - microturbines, 200, 201
- convergence of objective function, 226
- cooling and heating demands, 203, 216, 219
- cooling demand, 221
- day-ahead stage, 202
- definition, 195, 198, 199, 213
- DG units, 209
- EH concept, 280, 327, 328
- electricity, 221
- electricity and natural gas, 21
- electrolyzer, 215
- ELF, 216, 225
- energy carriers, 22
- energy conversion devices, 212
- energy resources, 216
- energy storage devices, 213
- energy transmission devices, 213
- engineering problems, 258
- FC, 214, 226, 228, 229
- flexibility, 25, 26
- flexibility in energy supply, 195
- gas furnace, 357
- generated heat of FC, 218
- heat produced by FC, 219
- heat supplied by FC, 217, 218
- home water heating, 221
- hourly amount of interrupted loads, 225
- and hub's wind power generation, 199
- hydrogen stored in hydrogen storage, 226, 228
- hydrogen tank, 215
- IGDT, 280
- IGDT-SP, 332
- inaccessibility of accurate data, 258
- input energy carriers, 257
- input/output classes, 22
- input-output model, 213
- installation cost, 224
- integrated planning and management, 257
- investment cost, 348
- as load-carrying capability, 327
- load profile and transferred power, 226, 227
- MCHES, 276
- as MILP problem, 280
- modeling cost, 220, 221
- and multi-energy system, uncertainty modeling, 329
- objective function, 199, 200, 220, 221
- operation cost, 348
- optimal management, 328
- optimal operation, 22–24, 257, 258
- optimization, 211, 212
- optimum capacity of component, 224, 225
- optimum design, 221
- penetration, 257
- P2G units, 357, 358
- planning algorithm, 217, 218
- power converter, 215
- power electronic circuit, 215
- prevention, 22
- produced energy by resources, 216
- produced heat of waste, 230
- PSO algorithm, 211, 226
- quantity of interrupted loads, 225
- reliability, 25, 26
- reliability index, 216
- repair and maintenance cost, 348, 349
- residential loads fluctuate, 221, 222
- resiliency, 26, 27
- RO method, 276
- scenario-based approach, 269
- scheduling, 196
- solar, 196
- space cooling load profile, 221, 223
- space heating, 221, 223
- stability, 26, 27
- storage devices, 257, 328
- stored heat in thermal storage, 229, 230
- study, 216, 217
- system data, 203
- thermal demand, 217, 218
- transitional agent, 195
- uncertainty, 258
- uncertainty modeling applications, 281
- waste, 217
- water heating load profile, 221, 222
- wind turbine, 213, 214, 226, 227
- Z-numbers, 275
- Energy infrastructure, 339
- Energy management, 195
 - algorithm, 144
 - framework, 143
- Energy markets
 - day-ahead, 145, 146, 152
 - day-ahead market, 146
 - district heat, 150

- Energy markets (*cont.*)
 - multi-carrier, 154
 - and negative values, 146
 - various layers, 150
 - Energy production, 195, 204
 - Energy purchase costs, 238, 349
 - Energy resources, 195
 - Energy sources, 196
 - Energy storage devices, 213
 - Energy storage system
 - electrical, 146
 - optimal scheduling, 144
 - sustainable transformation, 143
 - thermal, 149
 - Energy storage unit, 201
 - Energy supply, 39
 - Energy transmission devices, 213
 - Entire planning horizon, 242
 - Environmental costs, 20
 - Environmental pollutant costs, 196
 - Environmental uncertainty, 259
 - Equality constraints, 162, 163
 - Equivalent load factor (ELF), 216, 225
 - Euclidean distance, 239
- F**
- Fast reserve service
 - frequency violations, 102
 - participation, 102
 - providers, 102
 - service payments, 103
 - technical requirements, 102
 - Feasibility cut, 164
 - Feed-in tariff (FIT) rates, 114, 115
 - Financial risks, 339
 - First-order second method (FOSM), 265, 266
 - Fossil fuel-based power plants, 210
 - Framing uncertainty, 260
 - Frequency response
 - dynamic service, 100
 - frequency violation, 100
 - participation, 100
 - service payments, 101
 - static service, 100
 - technical requirements, 100
 - Fuel cell (FC)
 - DC-generated power, 215
 - and electrolyzer, 230
 - generated energy, 231
 - heat generated, 229
 - heating value, 214
 - heat produced, 216
 - heat supplied, 217
 - lifetime, 214
 - power generated, 226, 228
 - produced heat, 218
 - stored and used, 215
 - system, 67, 68
 - Fuel markets
 - imbalance charges, 109
 - obligations
 - environmental, 111
 - social, 111
 - tax, 110
 - UoS charges, 109, 110
 - wholesale trading, 108, 109
 - Fuzzy set theory, 275
 - Fuzzy systems, 271
- G**
- Game theory, 61
 - GAMS/DICOPT solver, 185
 - Gas delivery uncertainty, 180
 - Gas-fired power generation units, 340
 - Gas-fired power plants, 341
 - Gas-fired power units (GFPU)
 - gas consumption/production, 182, 184
 - gas transmission constraints, 180
 - installation, 179
 - off-line mode, 179
 - operation, 180, 188
 - power production, 180
 - and residential consumers, 183
 - Gas flow, 183
 - Gas furnace, 357
 - Gas network, 144, 183, 184, 341
 - Gas pipelines, 183, 184
 - Gas power plants, 340
 - Gas power units, 7, 9, 11
 - Gas price, 108, 109, 203
 - Gas production, 189
 - Gas storage, 108, 187
 - charge/discharge, 184
 - electricity and gas systems, 180
 - gas delivery restrictions, 180
 - hourly scheduling, 188
 - operation cost, 181
 - and PtG technology, 180
 - storing/releasing gas, 188
 - technical limitations, 184
 - vs. total production of power unit, 188
 - Gas system, NEP
 - compressor operation limits, 354
 - compressors, 345–347

- gas flow limits, 352, 353
 - gas storage unit, 345–347
 - gas storage unit operation limits, 354, 355
 - gas supply limits, 352
 - investment and utilization, 351, 352
 - operation cost, 346
 - pipeline operation limits, 353
 - pipelines, 345, 346
 - pressure limits, 352
 - repair and maintenance cost, 346, 347
 - Gas transmission constraints, 180
 - Gas transmission system, 185
 - Gas turbine systems, 147
 - GBD algorithm, 166
 - Generalized Algebraic Modeling System (GAMS) software, 150, 169, 358
 - Generalized Benders decomposition (GBD), 160
 - Generating constraints, 161
 - Generation limit constraints, 163
 - Genetic algorithm (GA), 61, 160, 236
 - Geothermal energy, 4, 5
 - Gram–Charlier series, 265
 - Gravitational search algorithm (GSA), 49, 160
 - Greenhouse gas emissions, 8
 - Grid consolidation, 339
 - Grid services, 20
- H**
- Harmony search algorithm, 160
 - Heat-driven cooling, 210
 - Heat exchange, 14–16
 - Heating, 195
 - Heating unit, 202
 - Heat pumps, 149, 198
 - Heat system, NEP
 - heat flow constraints, 356
 - hydraulic constraints, 355, 356
 - investment cost, 347
 - operation cost, 347
 - pipeline constraints, 355
 - HOMER software, 210
 - Hybrid elitist non-dominated sorting GA (HNSGA-II), 239
 - Hybrid energy storage technologies
 - CAES unit (*see* Compressed air energy storage (CAES) unit)
 - characteristics, 144, 150
 - day-ahead energy markets, 151, 152
 - decentralized and distributed deployment, 143
 - economic analysis, 144
 - hourly prices of electricity, gas, and heat, 150, 151
 - MIP, 150
 - objective function, 146
 - P2G storage (*see* Power-to-gas (P2G) storage)
 - P2H storage (*see* Power-to-heat (P2H) storage)
 - profit function, 146
 - reservoir energy, 151, 154
 - self-scheduling problem, 154
 - total profit, 154
 - unit operation, 145
 - Hybrid energy systems, 236, 276, 327
 - See also* Uncertainty modeling
 - Hybrid model, 92
 - Hub’s wind power generation, 199
 - Hydraulic continuity, 165
 - Hydraulic continuity constraints, 163
 - Hydraulic test system
 - average convergence time, 170
 - characteristics, 169
 - configuration, 175
 - CONOPT, 169, 170
 - cost functions, 169
 - generation schedule, 170, 171
 - hourly discharge and storage volume, 170, 172
 - hourly hydro plant discharge, 170, 174
 - hydropower plant reservoir inflows, 176
 - hydro production, 170, 173
 - load demand, 170, 173, 175, 176
 - lower and upper bound evolution, 169, 173
 - MAPSO, 169, 170
 - MDNLPSO, 169, 170
 - multi-chain cascade, 169
 - multi-chain cascade flow network, 169
 - non-smooth operating cost, 169
 - power generation coefficients, 175
 - RCGA-AFSA, 169, 170
 - reservoir storage volumes, 170, 174, 176
 - river transport, 169
 - scheduling period, 169
 - SNOPT, 169, 170
 - thermal production, 170, 173
 - time delay, 175, 176
 - upstream plant, 169
 - Hydroelectric plant discharge bounds, 165
 - Hydroelectric plants, 159
 - Hydroelectric power plants, 165
 - Hydrogen, 16
 - Hydrogen energy vehicles (mobility), 148
 - Hydrogen tank, 215

- Hydro power generation coefficients, 175
 - Hydro system process, 159
 - Hydro technologies, 9, 11, 12
 - Hydrothermal generation scheduling
 - Benders decomposition, 160, 163–167
 - cost-effective operating state, 159
 - Dantzig-Wolfe decomposition, 160
 - deregulated energy systems, 160
 - equality constraints, 162, 163
 - fundamental system, 161
 - inequality constraints, 163
 - OCD, 160
 - optimization methods, 160
 - power production, 162
 - short-term scheduling horizon, 161
 - Hydrothermal power units
 - fuel cost functions, 161
- I**
- IGDT stochastic method, 180
 - Imbalance charges, 109
 - Imbalance market
 - actors, 94, 95
 - balancing mechanism, 94
 - bid/offer, 96
 - day-ahead market price, 96
 - energy, 95
 - energy balance, 94, 96
 - IMP, 95
 - MCENO, 97, 98
 - MCENs, 97, 98
 - reserve pricing method, 95
 - sale price, energy, 97, 98
 - spot market, 94
 - storing energy, 98
 - system operator, 95, 96
 - Imbalance market participant (IMP), 95
 - Industrial park district energy, 241
 - Inequality constraints, 163
 - Information-gap decision theory (IGDT), 180
 - base case model, 277
 - base value, objective function, 278
 - description, 277
 - deviation of errors, 277
 - IGDT-SP, 332
 - probabilistic methods, 331
 - risk-averse strategy, 278, 279
 - risk-seeker strategy, 279, 280
 - RO model, 280
 - uncertainty radius, 277
 - uncertainty set, 277
 - vector of input uncertain parameters, 277
 - Inherent randomness, 259
 - Innovative technologies, 12–14
 - Integrated electricity, 89
 - Intelligent building, 280
 - Intermittent power generation (IPG), 238
 - Interval analysis method, 280, 327
 - Interval-based EH operation, 202
 - Interval-based optimization, 199
 - Interval numbers, 197, 198
 - Interval optimization, 196
 - CCHP systems, 204, 205
 - EH, 202
 - Inverted generational distance (IGD)
 - AGA, 247, 248
 - algorithms, 239
 - HNSGA-II, 247, 248
 - NSGA, 247, 248
 - Inverter, 215
 - IPG scenarios (IPGSs), 238
- K**
- Knowledge/epistemic uncertainty, 259
- L**
- Lagrangian relaxation, 160
 - Large-scale electric boilers, 149
 - Latin hypercube sampling (LHS), 264
 - Linear programming, 160
 - Linguistic uncertainty, 260
 - Liquid air energy storage (LAES), 147
 - Load-carrying capability, 327
 - Local balancing services, 105
 - Locational marginal prices (LMPs), 124, 238
 - maximum and average values, 247, 252
 - Long-term hydro scheduling problem, 159
 - Low-grade heat, 216
- M**
- Magnanti–Wong algorithm, 166
 - MAPSO method, 169, 170
 - Marginal costs, 161
 - Master problem, 165–169
 - MATLAB software, 221, 358
 - Maximum feasible subsystem (MFS), 166
 - MCEN operator (MCENO)
 - electricity markets, 88, 89, 98
 - electrothermal equipment, 90
 - energy markets, 116
 - gas market, 88
 - grid charges, 88

- imbalance market, 97, 117
 - load, 97
 - low-carbon performance, 117
 - markets, 87, 88
 - MCEN, 87
 - payment, 107
 - power generation cost, 94
 - reserve participation, 89
- MCES operator (MCESO)
 - energy interactions, 237
 - LMPs, 238
 - utilizes boilers, 237
- MDNLPSO method, 169, 170
- Measurement error, 259, 260
- Methanation, 148
- Microgrids (MGs), 60, 122, 195, 196
 - AC and DC, 211
 - day-ahead scheduling problem, 210
 - design, 210
 - economic linear programming, 210
 - energy management, 210
 - HOMER software, 210
 - off-grid, 211
 - optimization, 210–211
 - planning, 211
 - plug-in hybrid electric vehicle
 - equipment, 210
 - profits, 209
 - proposed energy management operation, 210
 - PSO algorithm, 211
 - renewable energy, 211
 - rural and urban uses, 210
 - scheduling, 211
- Microturbines, 200, 201
- Mixed-integer linear programming (MILP), 122
 - CHP-based units, 236
 - cost of system and emissions, 236
 - district heating planning topology, 236
 - problem, 280
 - scheduling of system resources, 236
- Mixed-integer nonlinear programming (MINLP)
 - approach, 122
 - heating system planning, 236
 - non-convex, 239
- Mixed-integer programming (MIP), 150, 166, 236, 358
- Mobile convertible resources, 20, 21
- Model uncertainty, 259, 260
 - exact and fixed parameters, 260
 - features, 260
 - input data, 260
 - measurement errors, 260
 - output data, 260
 - output uncertainty, 260
 - structure uncertainty, 260
 - technical uncertainties, 260
- Monte Carlo method, 48, 189
- Monte Carlo simulation (MCS), 24, 196, 236
 - fission and roulette method, 264
 - flexible, 263
 - flowchart, 264
 - fuzzy-Monte Carlo, 332
 - implementation, 263, 264
 - LHS, 264
 - nonsequential MCS, 263
 - PDF, 263
 - pseudo-sequential MCs, 263
 - sample-splitting approach, 264
 - scenario-based approach, 269
 - sequential MCS, 263
 - SMC techniques, 263
 - stochastic techniques, 263
 - types, 263
- Multi-carrier energy hub system (MCHES), 293, 321
- Multi-carrier energy networks (MCENs)
 - classification, 89
 - coal and petroleum fuels, 1
 - costs, 1
 - eco-friendly multi-carrier systems, 1
 - economic analysis, 1
 - economics, 1
 - effectiveness, 14
 - electricity generation, 1
 - electricity markets (*see* Electricity markets)
 - electrothermal equipment, 89, 90
 - energy conversion, 14
 - energy conversion facilities, 143
 - energy generation systems, 1
 - environmental issues
 - air emissions, 27
 - biomass and landfill stations, 27
 - “clean coal” technology, 27
 - conventional and renewable energies, 27
 - energy system, 27
 - hydropower plants, 27
 - imminent effects, 28
 - midterm and long-term achievements, 29, 30
 - wind turbines, 27
 - framework, 144, 145
 - gas power units, 7, 9, 11
 - heat exchange, 14–16
 - hybrid energy storage unit, 145

- Multi-carrier energy networks (MCENs) (*cont.*)
- hydro technologies, 9, 11, 12
 - innovations, 14
 - innovative technologies, 12–14
 - markets, 88
 - MCENO (*see* MCEN operator (MCENO))
 - MES, 2
 - natural gas, 1
 - operation (*see* Operation of MCENs)
 - operational cost, 144
 - optimum solution, 144
 - P2G, 16–18
 - renewable energy, 2
 - sustainable transformation, 143
 - wind farms, 144
- Multi-carrier energy supplier (MCES)
- aggregated costs, 238
 - AMGs (*see* Active microgrids (AMGs))
 - bi-level optimization algorithm, 235
 - CHP-based system planning, 236
 - district energy system planning method, 235
 - downward customers, 235
 - LMPs, 247, 252
 - MILP, 236
 - MINLP, 236
 - OGNEP, 235
 - optimal location and capacity, 244, 245
 - optimal topology, 241, 245, 246
 - revenues, 238
 - solar photovoltaic, 241, 245
 - wind turbine, 241, 245
- Multi-carrier energy systems (MCESs), 1
- benefit, 341
 - CCHP (*see* Combined cooling, heating and power (CCHP)-based MESs)
 - demand, 340
 - energy chain, 341
 - energy conversion, 340
 - energy storage, 340
 - ES (*see* Energy hubs (EHs))
 - generic model, 341, 342
 - operation, 196
 - optimal operational model, 269
 - resources, 340
 - ROA, 276
 - types of energy, 195
- Multi-chain cascade flow network, 169
- Multi-energy system (MES), 210, 276
- optimum investment, 340
- Multi-follower bi-level optimization method, 211
- Multi-input-multi-output (MIMO), 21
- Multi-input-single output (MISO), 21
- N**
- Natural gas, 143, 150, 195, 340, 341
- Natural variation, 259
- Net flow programming, 160
- Net present value (NPV), 220, 221
- Network expansion planning (NEP)
- CHP systems (*see* Combined heat and power (CHP))
 - consumers' energy demand, 342
 - EHS, 348–349
 - electric power generation, 340
 - electric power system (*see* Electric power system, NEP)
 - energy infrastructure, 339
 - energy purchase cost, 349
 - environmental parameters, 339
 - gas system (*see* Gas system, NEP)
 - heat system (*see* Heat system, NEP)
 - investment costs, 342
 - metrics, 340
 - optimization problem, 342
 - security and physical resilience, 339
 - single element outage, 342
 - sizable power outages, 339
 - system development and management, 339
 - transmission/transportation components, 342
- Net-zero energy district systems, 144
- Non-convex MINLP problem, 239
- Non-dominated solutions, 239
- Non-dominated sorting genetic algorithm (NSGA), 239
- Non-GFPUs
- startup and shutdown costs, 182
- Nonlinear programming, 160
- Nonsequential MCS, 263
- O**
- Obligatory reactive power service (ORPS), 101
- Ocean thermal energy conversion (OTEC), 14
- Off-grid MG, 211
- Operation of MCENs
- categories, 40
 - electrical power supply, 41
 - electricity and heat resources, 46, 47
 - energy flow analysis, 40
 - energy management, 41
 - energy production, 39
 - energy supply, 39
 - fields of issue, 39
 - gas and electricity resources, 41, 45, 46
 - heat and electrical carriers, 41
 - international community, 39

- objectives, 42, 43
- optimal operation, 40
- optimal power flow, 40
- power flow model, 40
- reliability, 41
- renewable energy sources, 41
- sustainable energy model, 40
- teaching-learning scheme, 41
- thermal power plants, 39
- TVAC-GSA method, 41
- type of issues, 40
- uncertainty-handling methods, 48–50
- water and electricity resources, 47, 48
- Optimal day-ahead operational planning (ODAOP), 122
- Optimal generation and network expansion planning (OGNEP)
 - AMG bidding and power transaction with MCES, 238
 - categorization, 238
 - CECSs, 238
 - DERs, 242, 245
 - electricity market, 238
 - flowchart, 239, 240
 - IPGSs, 238
 - MCES revenues, 238
 - multidimensional problem, 235
 - and objective function, 238, 247, 251
 - system costs, 248, 252
 - uncertainties, 238
- Optimal planning
 - EH (*see* Energy hubs (EHs))
 - innovations, 212
 - MATLAB software, 221
 - MG, 210–211
 - PSO algorithm, 221
- Optimal scheduling
 - electricity-gas networks (*see* Electricity-gas networks)
 - energy storage systems (*see* Hybrid energy storage technologies)
 - gas storage (*see* Gas storage)
 - GFPU (*see* Gas-fired power units (GFPU))
 - PtG (*see* Power-to-gas (PtG) technology)
- Optimality condition decomposition (OCD), 160
- Optimization
 - algorithms, 166
 - AMG transactions, 237
 - bi-level, 235
 - cost-benefit, 143
 - expansion planning decision variables, 237
 - framework, 237
 - GA, 236
 - HNSGA-II, 239
 - IGD, 239
 - MILP, 236
 - objective function, 239
 - and OGNEP, 252
 - system's contingency, 237
- P**
- Parametric uncertainty, 259
- Pareto-optimal cuts, 166, 167
- Particle swarm optimization (PSO), 61, 122, 160, 211, 212, 221, 226
- Peer-to-peer technologies (P2P)
 - energy expenses, 19
 - grid services, 20
 - mobile convertible resources, 20, 21
 - network costs, 19
 - prosumers, 19
- Pessimism degree, 204
- PF components, 239
- Point estimation method (PEM), 266–268
- Possibilistic Monte Carlo approach, 274
- Power balance, 182, 183
- Power converter, 215
- Power electronic circuit, 215
- Power flow equations, 350
- Power plant production, 161
- Power production, 204
- Power systems, 195, 209
- Power to gas (P2G), 16–18
- Power transmission limits, 350
- Power units
 - minimum up/down time, 182
- Power-to-gas (P2G) storage
 - alkaline, 148
 - charging and discharging, 149
 - chemical storage, 148
 - energy constraint, 149
 - energy flow analysis, 144
 - feasibility and applicability, 144
 - gas reservoir, 149
 - hourly optimal scheduling, 151, 153
 - hydrogen, 148
 - integrated energy systems, 144
 - mathematical model, 148
 - methanation, 148
 - and operation scheduling, 144
 - optimal capacity, 144
 - optimal scheduling, 144
 - PEM, 148
 - SOEC, 148

- Power-to-gas (PtG) technology
 - economic benefits, 180
 - electricity and gas networks, 180
 - electrolysis, 180
 - gas consumption/production, 184
 - methanization, 180
 - reducing emissions and costs, 180
 - and uncertainties of wind/electrical load, 180
 - wind power, 189
 - Power-to-heat (P2H) storage
 - centralized and decentralized modes, 149
 - charged and discharged heat, 149
 - hourly optimal scheduling, 151, 153
 - mathematical model, 149
 - reservoir balance, 149
 - reservoir capacity, 149
 - thermal energy storage systems, 149
 - thermal reactions, 149
 - Price makers, 105
 - Probabilistic energy flow model, 180
 - Probabilistic methods, 331
 - analytical approaches (*see* Analytical methods, probabilistic techniques)
 - PDFs, 263
 - simulation-based analysis (*see* Monte Carlo simulation (MCS))
 - Probability density functions (PDFs)
 - analytical approaches, 266
 - approximate-based techniques, 266
 - PEM, 266–268
 - scenario-based method, 268, 269
 - UT method, 268
 - linearization, 265
 - MCS, 264
 - normal PDF, 269
 - Rayleigh PDF, 269
 - RO, 276
 - Weibull PDF, 269
 - Procedural uncertainty, 261
 - Proposed BD method, 173
 - Proton exchange membrane (PEM), 148
 - Pseudo-sequential MCs, 263, 264
- R**
- Ramp-up/down limit, 182
 - RCGA-AFSA method, 169, 170
 - Reactive power service
 - participation, 101
 - service payments, 101
 - technical requirements, 101
 - Real power balance constraint, 162
 - Real-time pricing (RTP), 30
 - Regional energy system, 144
 - Reliability index, 216
 - Renewable energy, 209–211, 225, 231, 258, 331
 - biomass energy, 6, 7
 - economics, 2
 - fuel costs, 2
 - geothermal energy, 4, 5
 - solar energy, 3, 4
 - wind energy, 4, 5
 - Renewable generation, 196
 - Renewable heat incentives (RHIs), 114, 115
 - Renewable obligation certificates (ROCs), 108
 - Reserve provision, 89
 - Reservoir storage capacity restrictions, 165, 170
 - Residential gas loads, 185, 187
 - Resilient optimization, 275
 - Risk-based robust energy management, 280
 - River transport, 169
 - Robust optimization (RO), 275, 276
 - Robust optimization approach (ROA), 276, 293, 321
- S**
- Scenario-based approach, 196
 - Scenario-based decision-making, 268, 269
 - Scenario-based stochastic model, 144
 - SCENRED tool, 189
 - Scheduling period, 169
 - Second-order cone programming, 179
 - Sequential Monte Carlo (SMC) techniques, 263
 - Short-range hydro scheduling, 159
 - Short-term scheduling horizon, 161
 - Single input-multi-output (SIMO), 21
 - Single input-single output (SISO), 21
 - Sinusoidal component, 162
 - Sliding-pressure operation, 147
 - Small-scale CAES unit, 147
 - Smart buildings, 211
 - Smart energy, 196
 - Smart energy hub (SEH), 121
 - Smart energy management system, 63
 - Smart grid (SG), 121, 195
 - SNOPT-NLP, 169
 - SNOPT solver, 169, 170
 - Soft worst case approach, 276
 - Solar, 196
 - Solar energy, 3, 4
 - Solar production unit
 - efficiency, 66, 67
 - photovoltaic systems, 67

Solid oxide electrolysis cell (SOEC), 148
 Soyster's method, 276
 Spot market, 94
 Standard GBD method, 164
 State sampling approach, 263
 Stochastic optimization
 CCHP systems, 206
 Stochastic scheduling
 electricity-gas networks, 180
 Storage systems, 68, 69
 Subjective judgment uncertainty, 259
 Subproblems, 164, 165
 Supercritical compressed air energy storage (SC-CAES), 147
 Sustainable energy, 328
 System marginal price (SMP), 92
 Systematic errors, 259

T

Tabu search (TS), 61
 Tariffs, 114
 Taxes, 107, 110, 118
 Taylor series, 265
 Thermal demand response program (TDRP), 269, 331
 Thermal energy storages (TESs), 149, 237
 Thermal generation system
 economic dispatch (ED), 159
 Thermal loads, 212
 Thermal network, 209
 Thermal plants, generation, 159
 Thermal storage, 213, 216, 218, 219, 229–231
 storage capacity, 358
 storage/release heat, 358
 Time-based demand response programs, 32
 Time-varying acceleration coefficient (TVAC), 49
 Tradable white certificate (TWC), 113, 114
 Transmission system (TSO), 20
 Transmission system use-of-system (TSUoS) charges, 106, 110, 118
 Trigenation, 210
 Trigenation unit, 198
 Turbine vs. wind speed, 213, 214
 Two-stage unit commitment scheduling method, 144

U

Ultimate reservoir storage capacity restrictions, 165
 Uncertainty
 categories based on sources, 259
 context and framing, 260

decision, 261
 description, 259
 environmental, 259
 ignorance, 262
 knowledge/epistemic, 259
 linguistic, 260
 model uncertainty, 260 (*see also* Model uncertainty)
 parametric, 259
 procedural, 261
 rate of effectiveness, 261
 types and subcategories, 261
 variability/aleatory/random/stochastic, 260
 Uncertainty-accommodating flexibility, 327
 Uncertainty-handling methods, 48–50
 Uncertainty modeling
 applications in EH operation, 281
 arithmetic and pessimistic preference order, 197, 198
 data modeling, 262
 EH (*see* Energy hubs (EHs))
 hybrid approaches
 decision maker, 273
 EV (electrical vehicle), 272
 grid power, 272
 multi-energy systems, 273
 possibilistic Monte Carlo approach, 274
 possibilistic scenario-based approach, 274
 renewable generators, 273
 transformer, 272
 IGDT (*see* Information-gap decision theory (IGDT))
 interval analysis method, 280, 327
 interval-based optimization, 199
 interval numbers, 197, 198
 interval optimization, 196
 management framework, 196
 planning and management stage, systems, 262
 possibilistic method (*see also* Probabilistic methods)
 classical probability theory, 270
 fuzzy type 1 (T1), 270, 271
 fuzzy type 2 (T2), 271, 272
 possibilistic variables, 269
 possibilistic/fuzzy logic, 270
 power systems, 270
 RO, 275, 276
 types, 262
 Z-number, 275
 Uncertainty uncertain variables, 259
 Uncertainty variables, 259
 United States Department of Energy (DOE), 4
 Unscented transformation (UT) method, 268

Use of system (UoS) charges

BSUoS, 106, 107

DNUoS, 106, 110

markets/services, 105

TSUoS, 106, 110

types, 106

U.S. Energy Information Administration

(EIA), 340

Use-of-system cost (USC), 93

V

Vagueness uncertainty, 260

Valve-point effects, 162

Valve-point loading effects, 164

Ventilating technologies, 14

W

Warm home discount (WHD), 111

Water heating load profile, 221, 222

Water hub, 196

Water release, 159

Wholesale markets, 91

Wholesale trading market, 90, 108, 109

Wind, 196

Wind energy, 4, 5

benefits, 179

deployment, 179

Wind farms, 144

Wind generation, 204

Wind power and electrical load intervals, 204

Wind power generation, 269, 282, 283, 297,
300, 318

Wind production unit, 64, 65

Wind turbine, 213, 214, 224, 226, 227

Wind uncertainty

electricity and gas networks, 180, 189

optimal scheduling, 180

optimization method, 181

Worst-case optimization, 204

Z

Z-number, 275